Gerald R. Hintz

Orbital Mechanics and Astrodynamics

Techniques and Tools for Space Missions

Springer

Orbital Mechanics and Astrodynamics

Gerald R. Hintz

Orbital Mechanics and Astrodynamics

Techniques and Tools for Space Missions

Springer

Gerald R. Hintz
Astronautical Engineering Department
University of Southern California
Los Angeles, CA, USA

ISBN 978-3-319-09443-4 ISBN 978-3-319-09444-1 (eBook)
DOI 10.1007/978-3-319-09444-1
Springer Cham Heidelberg New York Dordrecht London

Library of Congress Control Number: 2014945365

© Springer International Publishing Switzerland 2015
This work is subject to copyright. All rights are reserved by the Publisher, whether the whole or part of the material is concerned, specifically the rights of translation, reprinting, reuse of illustrations, recitation, broadcasting, reproduction on microfilms or in any other physical way, and transmission or information storage and retrieval, electronic adaptation, computer software, or by similar or dissimilar methodology now known or hereafter developed. Exempted from this legal reservation are brief excerpts in connection with reviews or scholarly analysis or material supplied specifically for the purpose of being entered and executed on a computer system, for exclusive use by the purchaser of the work. Duplication of this publication or parts thereof is permitted only under the provisions of the Copyright Law of the Publisher's location, in its current version, and permission for use must always be obtained from Springer. Permissions for use may be obtained through RightsLink at the Copyright Clearance Center. Violations are liable to prosecution under the respective Copyright Law.
The use of general descriptive names, registered names, trademarks, service marks, etc. in this publication does not imply, even in the absence of a specific statement, that such names are exempt from the relevant protective laws and regulations and therefore free for general use.
While the advice and information in this book are believed to be true and accurate at the date of publication, neither the authors nor the editors nor the publisher can accept any legal responsibility for any errors or omissions that may be made. The publisher makes no warranty, express or implied, with respect to the material contained herein.

Printed on acid-free paper

Springer is part of Springer Science+Business Media (www.springer.com)

To: My wife
Mary Louise Hintz

Preface

This book is based on my work as an engineer and functional area manager for 37 years at NASA's Jet Propulsion Laboratory (JPL) and my teaching experience with graduate-level courses in Astronautical Engineering at the University of Southern California (USC).

At JPL, I worked on the development and flight operations of space missions, including Viking I and II (two orbiters and two landers to Mars), Mariner 9 (orbiter to Mars), Seasat (an earth orbiter), Voyager (for the Neptune encounter), Pioneer Venus Orbiter, Galileo (probe and orbiter to Jupiter), Ulysses (solar polar mission), Cassini-Huygens (orbiter to Saturn and lander to Titan), and Aquarius (an earth orbiter). I provided mission development or operation services to space missions that traveled to all the eight planets, except Mercury. These missions furnish many of the examples of mission design and analysis and navigation activities that are described in this text. The engineering experience at JPL has furnished the set of techniques and tools for space missions that are the core of this textbook.

I am an adjunct professor at USC, where I have taught a graduate course in Orbital Mechanics since 1979, plus three other graduate courses that I have initiated and developed. This teaching experience has enabled me to show that the techniques and tools for space missions have been developed from the basic principles of Newton and Kepler. The book has been written from my class notes. So, in a sense, I have been writing it for 35 years and I am very proud to see it in print.

The reason for writing this book is to put the results from these experiences together in one presentation, which I will continue to use at USC and share with my students and colleagues. The reader can expect to find an organized and detailed study of the controlled flight paths of spacecraft, including especially the techniques and tools used in analyzing, designing, and navigating space missions.

In academia, this book will be used by graduate students to study Orbital Mechanics or to do research in challenging endeavors such as the safe return of humans to the moon. (See Chaps. 6 and 7.) It will also serve well as a textbook for an Orbital Mechanics course for upper-division undergraduate and other advanced undergraduate students. Professional engineers working on space missions and people who are interested in learning how space missions are designed and navigated will also use the book as a reference.

This presentation benefits significantly from the many references listed in the back of the book. The list includes excellent textbooks by Marshall H. Kaplan, John E. Prussing and Bruce A. Conway, Richard H. Battin, and others and a technical report by Paul A. Penzo for the Apollo missions. Papers include those by Leon Blitzer, John E. Prussing, and Roger Broucke. Finally, there is the contribution of online sources, such as Eric Weisstein's "World of Scientific Biography," JPL's Near-Earth Objects and Solar System Dynamics, and the Rocket & Space Technology websites. To all these sources and the many others cited in the text, I express my gratitude.

My gratitude is also extended to my wife, Mary Louise Hintz, and our three children, JJ, Tana, and Kristin, for their support.

Los Angeles, CA, USA Gerald R. Hintz

Contents

Introduction

Our objective is to study the controlled flight paths of spacecraft, especially the techniques and tools used in this process. The study starts from basic principles derived empirically by Isaac Newton, that is, Newton's Laws of Motion, which were derived from experience or observation. Thus, we develop the relative 2-body model consisting of two particles, where one particle is more massive (the central body) and the other (the spacecraft) moves about the first, and the only forces acting on this system are the mutual gravitational forces. Kepler's Laws of Motion are proved from Newton's Laws. Solving the resulting equations of motion shows that the less-massive particle moves in a conic section orbit, i.e., a circle, ellipse, parabola, or hyperbola, while satisfying Kepler's Equation. Geometric properties of conic section orbits, orbit classification, and types of orbits are considered with examples. Astronomical constants needed in this study are supplied, together with several tables of geometric formulas for elliptic orbits.

After the orbit determination analyst estimates the spacecraft's orbit, trajectory correction maneuvers (TCMs) are designed to correct that estimated orbit to the baseline that satisfies mission and operational requirements and constraints. Such TCMs correct statistical (usually small) errors, while other maneuvers make adjustments (usually large) such as insertion of the spacecraft into an orbit about a planet from a heliocentric trajectory. Maneuver strategies considered include the optimal 2-maneuver Hohmann transfer and the optimal 3-maneuver bi-elliptic transfer with examples for comparison purposes. The design of TCMs determines the amount of velocity change required to correct the trajectory. The Rocket Equation is then used to determine the amount of propellant required to achieve the required change in velocity. Various fuel and oxidizer combinations are considered that generate the specific impulse, the measure of a propellant's capability, required to implement the orbit correction.

Gravity assists obtained when flying by planets in flight to the target body (another planet, comet or asteroid, or the sun) can produce a large velocity change with no expenditure of onboard propellant. Types and examples of interplanetary missions and the targeting space used in designing the required trajectories are described.

Techniques of Astrodynamics include algorithms for propagating the spacecraft's trajectory, Keplerian orbit elements which describe the orbit's size,

shape, and orientation in space and the spacecraft's location in the orbit, and Lambert's Problem, which is used to generate mission design curves called "pork chop plots". Other models advance our study to treat n bodies and distributed masses instead of just two point masses, and measure time, which is fundamental to our equations.

Non-Keplerian motion takes into account perturbations to the Keplerian model, such as oblateness of the central body, gravitational forces of other bodies ("3rd body effects"), solar wind and pressure, and attitude correction maneuvers. The study identifies the primary perturbations for an earth-orbiting vehicle, resolves a satellite orbit paradox, and considers "zero G" (or is it "zero W"?).

A strategy for rendezvousing a spacecraft with other vehicles such as the International Space Station is described with examples. One example is rendezvous of the Apollo 11 Lunar Excursion Module with the Command Module. One strategy is intended to avoid an unintentional rendezvous by placing the spacecraft in a standoff position with respect to another vehicle to, for example, allow the astronauts to sleep in safety.

Navigation techniques and tools include a TCM design tool and two methods for designing free-return circumlunar trajectories for use in returning humans to the moon safely. Launching into a free-return trajectory will ensure that the spacecraft will return to a landing site on the earth without the use of any propulsive maneuvers in case of an accident such as the one experienced by Apollo 13. After the spacecraft is determined to be in good working condition, it can be transferred from the free-return trajectory into one favorable for injection into a lunar orbit.

Chapter 8 discusses opportunities for further study in navigation, mission design and analysis, and related topics. Appendix A gives a brief review of vector analysis, which is especially important for students who are returning to academia after a long absence. Appendix B defines projects the students can perform to test and strengthen their knowledge of Astrodynamics and the techniques and tools for space missions. Appendix C provides additional parameters for use in designing free-return circumlunar trajectories.

There are exercises at the end of each of Chaps. 1–7 for use in strengthening and testing the students' grasp of the technical material. To aid the students in this process, numerical answers with units are supplied in the back of the book for selected exercises.

References for the material covered are listed at the end of the book. References are also listed at the end of Chaps. 1–7 and at selected points within these chapters, where they are identified by the names of the authors (or editors). In the case of authors who provided multiple sources, the year or year and month of the reference is (are) given. The students can then check the list in the back of the book to obtain the complete bibliographic information for identifying the particular source. Chapter 8 gives complete bibliographic information for the references it cites as sources of material for further study. The references in Chapter 8 are not repeated in the list at the end of the book.

Many terms are used in discussing Orbital Mechanics and Astronautics. The definitions of terminology used in this textbook are called out as "Def.:" followed by the definition with the term being defined underlined for clarity. Acronyms and abbreviations are defined at their first use and included in a list in the back of the book. Finally, an index is also provided to aid the reader in finding the various terms and topics covered in this text.

Fundamentals of Astrodynamics

1

1.1 Introduction

One of the most important uses of vector analysis (cf. Appendix A) is in the concise formulation of physical laws and the derivation of other results from these laws. We will develop and use the differential equations of motion for a body moving under the influence of a gravitational force only. In Chap. 5, we will add other (perturbing) forces to our model.

There are related disciplines, which are part of Flight Dynamics.

Def.: Celestial Mechanics is the study of the natural motion of celestial bodies.

Def.: Astrodynamics is the study of the controlled flight paths of spacecraft.

Def.: Orbital Mechanics is the study of the principles governing the motion of bodies around other bodies under the influence of gravity and other forces.

These subjects consider translational motion in a gravity field.

Attitude Dynamics and Attitude Control consider the spacecraft's rotational motion about its center of mass.

Def.: Spacecraft attitude dynamics is the applied science whose aim is to understand and predict how the spacecraft's orientation evolves.

In spacecraft mission activities, there is a coupling between satellite translation (the orbital variables) and spacecraft rotation (the attitude variables). In spite of the coupling effects, much of orbital mechanics proceeds by largely ignoring the effects of spacecraft attitude dynamics and vice versa. The field of Flight Dynamics, however, considers 6 degrees of freedom (DOF), consisting of 3 DOF from Orbital Mechanics and 3 DOF from Attitude Dynamics.

An example of an essentially 6DOF problem is: EDL (entry, descent, and landing), e.g., the landing of the Phoenix spacecraft on Mars 5/25/08. More information on the Phoenix mission can be found at the Phoenix Mars Mission Website at http://phoenix.lpl.arizona.edu/.

© Springer International Publishing Switzerland 2015

G.R. Hintz, *Orbital Mechanics and Astrodynamics*,
DOI 10.1007/978-3-319-09444-1_1

Parallel disciplines that must be part of spacecraft mission analyses include:

Orbital Mechanics	Attitude Dynamics
Orbit Determination	Attitude Determination
Flight Path Control	Attitude Control

Of these six disciplines, we consider primarily Orbital Mechanics plus related issues in Flight Path Control. Hence, our objective is to study the controlled flight paths of spacecraft, viz., Astrodynamics.

1.2 Mathematical Models

Use of Mathematical Models to Solve Physical Problems

Figure 1.1 describes the procedure for using a mathematical model to solve a physical problem.

In engineering, we make simplifying assumptions in our mathematical model to:

1. Get a good approximation to a solution
2. Gain insight into the problem
3. Get a good starting point for a more accurate numerical solution
4. Reduce computing time and costs.

Example: Archimedes

The king told Archimedes that he had given the goldsmith gold to make a crown for him. However, he suspected that the goldsmith had kept some of the gold and added a baser metal in its place. So his task for Archimedes was to determine whether or not his new crown was made of pure gold. Archimedes thought about this problem until one day when he was in the public bath and he saw water splashing out of a bathtub. Then, he yelled "Eureka" and ran to his working area to demonstrate the answer to the problem.

He placed the crown in a vat filled with water with a basin below the vat to catch the overflow. He obtained the amount of gold that equaled the volume of water that overflowed the vat. Then he placed this amount of gold on one side of a lever and the crown on the other side as shown in Fig. 1.2. The end of the lever with the gold descended, indicating that the crown was not pure gold. After Archimedes reported his findings to the king, the goldsmith did not cheat any more kings.

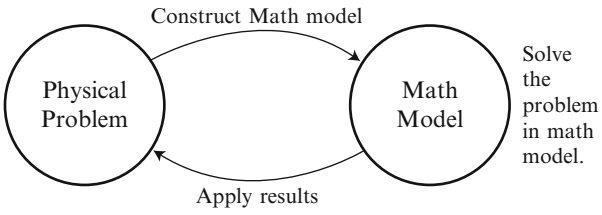

Fig. 1.1 Using a mathematical model to solve physical problems

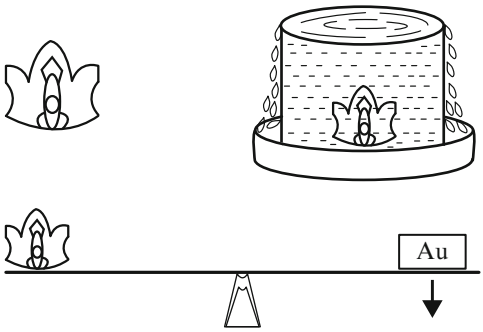

Fig. 1.2 Archimedes' Gold Experiment

Dynamics, including Astrodynamics, is a deductive discipline, which enables us:

1. To describe in quantitative terms how mechanical systems move when acted on by given forces or
2. To determine which forces must be applied to a system to cause it to move in a specified manner.

A dynamics problem is solved in two major steps:

1. Formulation of the equation of motion (EOM), the math model, and
2. Extraction of information from the EOM.

Optimization of rocket trajectories is usually accomplished by analytical and numerical approaches in a complimentary fashion. Dereck Lawden (cf. reference for Lawden) says; "... by making suitable simplifying assumptions, the actual problem can be transformed into an idealized problem whose solution is analytically tractable, then this latter solution will often provide an excellent substitute for the optimal motor thrust programme in the actual situation. All that then remains to be done is to recompute the trajectory employing this programme and taking account of the real circumstances. Further, it is only by adopting the analytical approach in any field of research, that those general principles, which lead to a real understanding of the nature of the solutions, are discovered. Lacking such an appreciation, our sense of direction for the numerical attack will be defective and, as a consequence, computations will become unnecessarily lengthy or even quite ineffective."

The analytical solution provides insight into how to approach a problem. It also enables you to verify that your solution is plausible and correct. You do not want to put yourself in the position of having your boss tell you that the results you have presented violate a basic principle and then be forced to say, "But the computer said . . . ." Another reason for looking at an idealized problem is that the insight gained can be used for mission planning and design purposes or feasibility studies for which exact values are not available.

High-precision software run in land-based computers or powerful real-time onboard computing provide precision numerical results and ultimately the commands to be executed by the spacecraft's onboard subsystems.

Coordinate Systems

To study motion, we need to set up a reference frame because we need to know "motion with respect to what?"

Inertial frames are "fixed with respect to the fixed stars," i.e., non-rotating and non-accelerating with respect to the fixed (from our perspective) stars, which is an imaginary situation. Practically speaking, an inertial system is moving with essentially constant velocity.

Example Geocentric equatorial system or Earth-centered Inertial (ECI) coordinate system

Use: To study orbital motion about the Earth

Definition:

- Origin at the center of the earth
- X-axis pointing to the first point of Aries, i.e., the vernal equinox. The vernal equinox direction is a directed line from the earth to the sun at the instant the sun passes through the earth's equatorial plane at the beginning of spring.
- Z-axis—normal to the instantaneous equatorial plane
- Y satisfies $\mathbf{Y} = \mathbf{Z} \times \mathbf{X}$, which completes the right-handed coordinate system

Example Heliocentric-ecliptic system

Use: for example to study orbital motion in interplanetary (I/P) flight

Definition:

- Origin at the center of mass of the sun
- The fundamental (XY) plane is the mean plane of the earth's orbit, called the ecliptic plane.
- The reference (X) direction is again the vernal equinox, where the X axis is the intersection of these two fundamental planes and points to the sun when it crosses the equator from south to north in its apparent annual motion along the ecliptic.

The directions of the vernal equinox and the earth's axis of rotation shift slowly in ways to be discussed later (Chap. 5). Therefore, we will refer to X, Y, Z coordinates for the equator and equinox of a particular year or date, e.g., equator and equinox of 2000.0 or "of date." We will consider measures of time in Chap. 4. For now, we will not consider this level of precision, ignoring perturbations such as

the precession of the earth. We consider an inertial system that is fixed with respect to the fixed stars as Newton did. For more information on coordinate systems, see for example Sect. 2.2 of the reference by Bate, Mueller, and White (BMW).

Non-inertial systems are rotating or accelerating. For example, a system that is fixed to the earth is rotating and, therefore, non-inertial. Such a coordinate system is chosen as the one that is natural for a particular type of problem.

1.3 Physical Principles

Tycho Brahe (1546–1601), a Danish astronomer, took accurate observations of the position of Mars before the telescope was invented. Brahe used a quadrant circle to sight the planets and stars. His large, accurate instruments yielded measurements that were accurate to within 4 min of arc. Brahe hired Kepler as an assistant to analyze the vast bulk of data that he had collected.

Johannes Kepler (1571–1630), an Austrian mathematician and astronomer, worked briefly with Tycho Brahe and inherited his data books after Brahe's death in 1601. Kepler devoted many years to intense study of these data to determine a mathematical description of the planetary motion described by the data. He derived a set of three empirical laws that describe planetary motion and led to our current understanding of the orbital motion of planets, moons, asteroids, and comets as well as artificial satellites and spacecraft.

Empirical laws are known from experience or observation. We derive results from these laws. In particular, we will derive the equations of motion from Newton's Laws of Motion and his Universal Law of Gravitation.

Kepler's Laws

Kepler's Laws are:

1. The orbit of each planet is an ellipse with the sun at a focus.
2. The line joining the planet to the sun sweeps out equal areas inside the ellipse in equal time intervals.

   Therefore, the velocity at closest approach is greater than the velocity at the furthest distance from the sun. Kepler's Second Law is illustrated in Fig. 1.3.
3. The square of the period of a planet is proportional to the cube of its mean distance from the sun. That is,

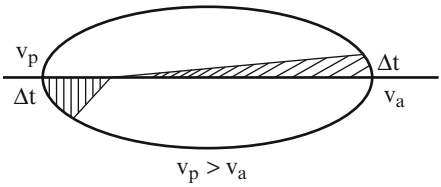

Fig. 1.3 Kepler's Second Law

$$\tau^2_{\text{planet}} \propto (\text{mean distance from sun})^3$$

where the symbol τ denotes the period (duration) of an orbit.

Johannes Kepler (1571–1630), an Austrian mathematician and astronomer, pursued his scientific career with extraordinary enthusiasm and diligence despite several hardships. His hands were crippled and his eyesight impaired from smallpox as a boy. He suffered from religious persecution for his protestant beliefs. He lost his first wife and several children. Often in desperate financial difficulties, he endured a bare subsistence livelihood. He even had to defend his mother from a charge of witchcraft.

Kepler, as Imperial Mathematician in Prague, published his third law in *Harmonice Mundi* (The Harmony of the World) in 1619, 10 years after the appearance of his first two laws in *Astronomia Nova De Motibus Stellae Martis*, known as *Astronomia Nova*.

Newton's Laws

Sir Isaac Newton[1] (1642–1727) defined the forces at work in *Philosophiae Naturalis Principia Mathematica* (The Mathematical Principles of Natural Philosophy), usually called the *Principia,* 1687. Kepler's Laws must follow. Newton determined why the planets move in this manner. Newton's Laws apply only to particles moving in an inertial reference frame.

Newton's Laws of Motion are:

1. Principle of Inertia: Every body is at rest or in uniform motion along a straight line unless it is acted on by a force.
2. Principle of Momentum: The rate of change of linear momentum is equal to the force impressed and is in the same direction as that force. That is,

[1] Isaac Newton (1642–1727) is generally regarded as one of the greatest mathematicians of all time. He entered Trinity College, Cambridge, in 1661 and graduated with a BA degree in 1665. In 1668, he received a master's degree and was appointed Lucasian Professor of Mathematics, one of the most prestigious positions in English academia at the time. In his latter years, Newton served in Parliament and was warden of the mint. In 1703, he was elected president of the Royal Society of London, of which he had been a member since 1672. Two years later, he was knighted by Queen Anne.

Newton is given co-credit, along with the German Wilhelm Gottfried von Leibnitz, for the discovery and development of calculus-work that Newton did in the period 1664–1666 but did not publish until years later, thus laying the groundwork for an ugly argument with Leibnitz over who should get credit for the discovery. In 1687, at the urging of the astronomer Edmund Halley, Newton published his ground-breaking compilation of mathematics and science, *Principia Mathematica,* which is apparently the first place that the root-finding method that bears his name appears, although he probably had used it as early as 1669. This method is called "Newton's Method" or "the Newton–Raphson Method."

$$\mathbf{F} = \frac{d}{dt}(m\mathbf{v}) \tag{1.1}$$

where **v** denotes the velocity vector and m denotes the mass.

Therefore,

$$\mathbf{F} = m\mathbf{a} \tag{1.2}$$

if the mass m is constant and **a** is the acceleration of m with respect to an inertial frame.

3. Principle of Action–Reaction: For every applied force, there is an equal and opposite reaction force. Therefore, all forces occur in pairs.

Newton's Law of Universal Gravitation:
Any two particles attract each other with a force of magnitude

$$F = G\frac{m_1 m_2}{r^2} \tag{1.3}$$

where m_1, m_2 = masses of the two particles,
r = distance between the particles,
G = universal constant of gravitation
We will refer to these three empirical laws as "NI," "NII," and "NIII," respectively.
Actually, NII implies NI because, if we set

$$m\mathbf{a} = m\frac{d^2 r}{dt^2} = 0$$

and integrate this equation, we obtain

$$\mathbf{v} = \mathbf{c}$$

which implies NI: v = 0 for a particle at rest or moving at constant velocity, if $\mathbf{v} \neq \mathbf{0}$.

Work and Energy

If the force **F** acting on a particle moves through a distance $\Delta\mathbf{r}$, the work done is equal to the scalar product $\mathbf{F} \cdot \Delta\mathbf{r}$. Hence, we define the total work done in going from $\mathbf{r_1}$ to $\mathbf{r_2}$, where $\mathbf{r_1} = \mathbf{r}(t_1)$ and $\mathbf{r_2} = \mathbf{r}(t_2)$, as follows.

Def.: Work (a scalar quantity) is the line integral along a path

$$W_{12} = \int_{\mathbf{r}_1}^{\mathbf{r}_2} \mathbf{F} \cdot d\mathbf{r} \tag{1.4}$$

between positions $\mathbf{r_1}$ and $\mathbf{r_2}$ where $\mathbf{F}$ is the force applied to a particle of mass m.

Show: The work $W_{12} = \Delta KE$, where KE denotes "kinetic energy."

Proof:
Let m = constant mass.

$$W_{12} \equiv \int_{\mathbf{r_1}}^{\mathbf{r_2}} \mathbf{F} \cdot d\mathbf{r} = m\int_{t_1}^{t_2} \mathbf{a} \cdot \mathbf{v} dt = m\int_{t_1}^{t_2} \frac{d\mathbf{v}}{dt} \cdot \mathbf{v} dt = \frac{m}{2}\int_{t_1}^{t_2} \frac{d}{dt}(\mathbf{v} \cdot \mathbf{v}) dt$$

$$= \frac{m}{2}\int_{t_1}^{t_2} \frac{d(v^2)}{dt^2} dt = \frac{1}{2}mv^2\Big|_{v_1}^{v_2} = \frac{1}{2}mv_2^2 - \frac{1}{2}mv_1^2 = \Delta KE. \text{ QED}$$

Def.: The force $\mathbf{F}$ is said to be conservative iff the integral of $\mathbf{F} \cdot d\mathbf{r}$ is zero over all closed paths.

Notation: We write $\oint \mathbf{F} \cdot d\mathbf{r} = 0$
where the symbol $\oint$ denotes integration over all closed paths.

Show: For a conservative force, the work to go from one point to another is independent of the path taken.

Proof:
Let $\mathbf{F}$ be a conservative force (Fig. 1.4).

Then $\int_{\substack{r_1 \\ \text{path a}}}^{r_2} \mathbf{F} \cdot d\mathbf{r} + \int_{\substack{r_2 \\ \text{path b}}}^{r_1} \mathbf{F} \cdot d\mathbf{r} = 0$ by definition of a conservative force

$$\int_{\substack{r_1 \\ \text{path a}}}^{r_2} \mathbf{F} \cdot d\mathbf{r} = -\int_{\substack{r_2 \\ \text{path b}}}^{r_1} \mathbf{F} \cdot d\mathbf{r} = \int_{\substack{r_1 \\ \text{path b}}}^{r_2} \mathbf{F} \cdot d\mathbf{r} \text{ for all paths a and b}$$

Therefore, the result follows. QED

Remark Properties p and q are equivalent iff property p is valid implies property q is valid and vice versa.

We have shown that $\oint \mathbf{F} \cdot d\mathbf{r} = 0$ implies that work is independent of path. The reverse of the argument is valid also. Therefore, the property for a force $\mathbf{F}$ that

$$\oint \mathbf{F} \cdot d\mathbf{r} = 0$$

for all closed paths is equivalent to the property that the work to go from one point to another is independent of the path taken. Therefore, the latter property could be used as the definition of a conservative force as is done in the reference by W. T. Thomson.

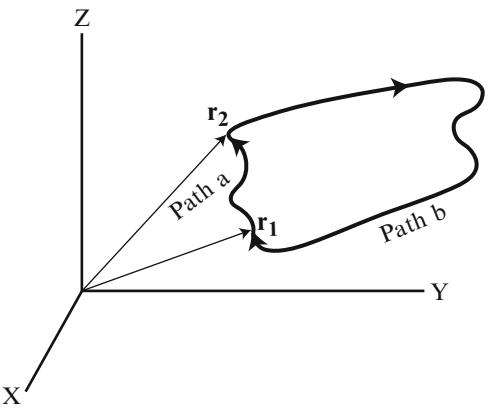

Fig. 1.4 Paths between positions $\mathbf{r_1}$ and $\mathbf{r_2}$

Def.: Potential energy $V(\mathbf{r_1})$ is the work done by a conservative force in going from point $\mathbf{r_1}$ to some reference point $\mathbf{r_0}$, i.e.,

$$V(\mathbf{r}_1) = \int_{\mathbf{r}_1}^{\mathbf{r}_0} \mathbf{F} \bullet d\mathbf{r} + V(\mathbf{r}_0) \tag{1.5}$$

Thus, every point in space can be assigned a scalar potential $V(\mathbf{r})$, which depends on the reference point.

Show: For a conservative force $\mathbf{F}$,

$$W_{12} = -\Delta PE. \tag{1.6}$$

Proof:
Since $\mathbf{F}$ is conservative,

$$W_{12} \equiv \int_{\mathbf{r}_1}^{\mathbf{r}_2} \mathbf{F} \bullet d\mathbf{r} = \int_{\mathbf{r}_1}^{\mathbf{r}_0} \mathbf{F} \bullet d\mathbf{r} + \int_{\mathbf{r}_0}^{\mathbf{r}_2} \mathbf{F} \bullet d\mathbf{r} \text{ from independence of path}$$

$$= \left[\int_{\mathbf{r}_1}^{\mathbf{r}_0} \mathbf{F} \bullet d\mathbf{r} + V(\mathbf{r}_0)\right] - \left[\int_{\mathbf{r}_2}^{\mathbf{r}_0} \mathbf{F} \bullet d\mathbf{r} + V(\mathbf{r}_0)\right]$$

$= V(\mathbf{r_1}) - V(\mathbf{r_2})$ by the definition of potential energy
$= -(V(\mathbf{r_2}) - V(\mathbf{r_1})) = -\Delta PE$. QED

Show: For a conservative force $\mathbf{F}$,

$$\mathbf{F} = -\nabla V(\mathbf{r}). \tag{1.7}$$

Proof:

$$W_{12} \equiv \int_{\mathbf{r}_1}^{\mathbf{r}_2} \mathbf{F} \bullet d\mathbf{r} = V(\mathbf{r}_1) - V(\mathbf{r}_2) \text{ from the argument above}$$

$$= -\int_{\mathbf{r_1}}^{\mathbf{r_2}} \mathrm{dV}$$

Therefore, $\int_{\mathbf{r_1}}^{\mathbf{r_2}} \mathbf{F} \bullet \mathrm{d}\mathbf{r} = -\int_{\mathbf{r_1}}^{\mathbf{r_2}} \mathrm{dV}$

Therefore, $\mathbf{F} \bullet \mathrm{d}\mathbf{r} = -\mathrm{dV}$ everywhere.

Therefore, $\mathbf{F} = -\left(\frac{\partial \mathrm{V}}{\partial \mathrm{x}}, \frac{\partial \mathrm{V}}{\partial \mathrm{y}}, \frac{\partial \mathrm{V}}{\partial \mathrm{z}}\right) = -\nabla \mathrm{V}(\mathbf{r})$. QED

Remark Since the reference point is arbitrary, we will select a reference point such that $\mathrm{V}(\mathbf{r_0}) = 0$.

Def.: If a force over a given region S of space can be expressed as the negative gradient of a scalar function ϕ, i.e., as

$$\mathbf{F} = -\nabla\phi = -\mathrm{grad}\phi,$$

we call ϕ a scalar potential.

The scalar potential describes the force by one function instead of three. A scalar potential is only determined up to an additive constant, which can be chosen to adjust its origin.

Remark Properties (statements) p, q, and r are equivalent means that p is valid iff q is valid and q is valid iff r is valid and r is valid iff p is valid. To demonstrate that these three properties are valid, it is sufficient to show p is valid implies q is valid and q is valid implies r is valid and r is valid implies p is valid or p is valid implies r is valid and r is valid implies q is valid and q is valid implies p is valid.

The following three relations are equivalent for a force $\mathbf{F}$ over a given region S of space:

1. The force $\mathbf{F}$ can be expressed as the negative gradient of a scalar function ϕ, i.e., as $\mathbf{F} = -\nabla\phi$.
2. $\nabla \times \mathbf{F} = 0$
3. $\oint \mathbf{F} \bullet \mathrm{d}\mathbf{r} = 0$ over every closed path in the region S.

For a proof of this equivalence, see pp. 66f of the reference by Arfken and Weber.

Law of Conservation of Total Energy

Let $\mathrm{KE_i}$ = kinetic energy at point i and $\mathrm{PE_i}$ = potential energy at point i for i = 1, 2. We have shown that $\mathrm{W_{12}} = \mathrm{KE_2} - \mathrm{KE_1} = \mathrm{PE_1} - \mathrm{PE_2}$

Therefore,

$$KE_2 + PE_2 = KE_1 + PE_1 = \text{Total Energy}$$

This equation gives the reason why the force **F** is said to be "conservative."

Examples We will find that gravity is a conservative force. However, atmospheric drag and friction are not conservative.

Angular Momentum

Consider the inertial X, Y, Z and moving x, y, z coordinate systems displayed in Fig. 1.5 and the linear momentum $m\dot{\mathbf{R}}$ in the inertial frame. The vector **r** is the position of the mass m in the moving x, y, z coordinate system.

Def.: The angular momentum (moment of momentum) $\mathbf{h}_0$ of the mass m about a point O is defined as

$$\mathbf{h}_0 = \mathbf{r} \times m\dot{\mathbf{R}} \tag{1.8}$$

This definition implies that $\mathbf{h_0}$ is perpendicular to **r** and $m\dot{\mathbf{R}}$.

An alternate definition is $\mathbf{h}_0 = \mathbf{r} \times m\dot{\mathbf{r}}$. The definition of angular momentum in terms of the inertial velocity vector as is Eq. (1.8) is used in the references by Kaplan and Thomson.

Rate of change of $\mathbf{h_0}$:

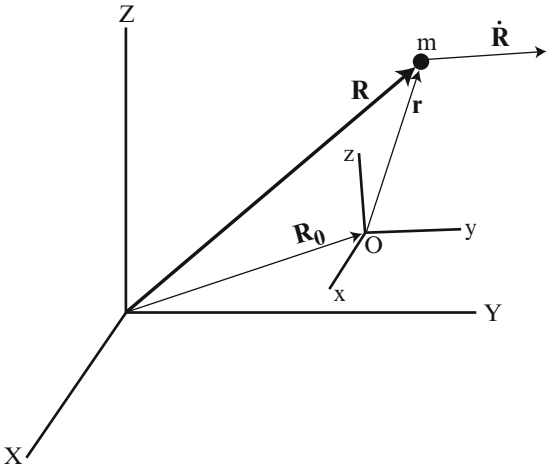

Fig. 1.5 Position of the mass m in a moving x, y, z coordinate system

Since $\mathbf{R} = \mathbf{R_0} + \mathbf{r}$, the derivative $\dot{\mathbf{R}} = \dot{\mathbf{R}}_0 + \dot{\mathbf{r}}$. Therefore,

$$\mathbf{h}_0 = \mathbf{r} \times m\dot{\mathbf{R}} = \mathbf{r} \times m\left(\dot{\mathbf{R}}_0 + \dot{\mathbf{r}}\right) = \mathbf{r} \times m\dot{\mathbf{r}} + \mathbf{r} \times m\dot{\mathbf{R}}_0$$

where the first term is the apparent angular momentum in the moving frame and the second term is the correction due to the motion of point O.

$$\begin{aligned}\dot{\mathbf{h}}_0 &= \frac{d}{dt}(\mathbf{r} \times m\dot{\mathbf{r}}) + \mathbf{r} \times m\ddot{\mathbf{R}}_0 + \dot{\mathbf{r}} \times m\dot{R}_0 \\ &= \frac{d}{dt}(\mathbf{r} \times m\dot{\mathbf{r}}) - \ddot{\mathbf{R}}_0 \times m\mathbf{r} - \dot{\mathbf{R}}_0 \times m\dot{\mathbf{r}}\end{aligned} \tag{1.9}$$

where the first term is the rate of change of apparent angular momentum in the moving frame at point O, the second term is the effect of the acceleration of point O, and the third is the effect of the velocity of point O.

Such a rate of change of $\mathbf{h_0}$ could be related to an applied torque about O.

Def.: The torque, or moment, of a force **F** acting on the mass m about the point O is defined as

$$\mathbf{M_0} = \mathbf{r} \times \mathbf{F} \tag{1.10}$$

Then $\mathbf{M_0}$ is orthogonal to **F** and **r.**

In Fig. 1.6, $x = r\sin\phi$, which implies that

$$\mathbf{M}_0 = Fr\sin\phi\hat{\mathbf{M}}_0 \tag{1.11}$$

Therefore, the magnitude of the torque $\mathbf{M_0}$ is the product of the magnitude of the force **F** and the perpendicular distance from the point O to the line of action of the force.

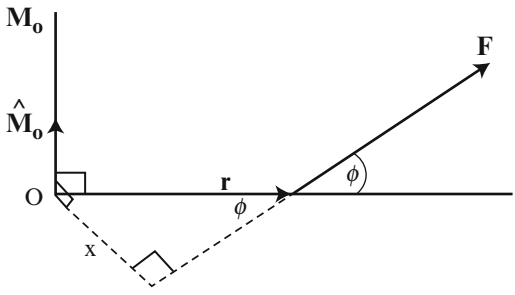

Fig. 1.6 Torque, or moment, of a force **F**

$$\mathbf{M}_O = \mathbf{r} \times \mathbf{F} = \mathbf{r} \times m\ddot{\mathbf{R}} = \mathbf{r} \times m\left(\ddot{\mathbf{R}}_0 + \ddot{\mathbf{r}}\right)$$
$$= \left(\mathbf{r} \times m\ddot{\mathbf{R}}_0\right) + (\mathbf{r} \times m\ddot{\mathbf{r}})$$

But $\frac{d}{dt}(\mathbf{r} \times m\dot{\mathbf{r}}) = (\dot{\mathbf{r}} \times m\dot{\mathbf{r}}) + (\mathbf{r} \times m\ddot{\mathbf{r}})$, where the first term is zero.

Therefore,

$$\mathbf{M_O} = \dot{\mathbf{h}}_\mathbf{0} + \dot{\mathbf{R}}_\mathbf{0} \times m\dot{\mathbf{r}} = \dot{\mathbf{h}}_\mathbf{0} \tag{1.12}$$

if O is fixed in space, i.e., $\dot{\mathbf{R}}_\mathbf{0} = \mathbf{0}$, or $\mathbf{r}$ is constant.

Therefore, if the applied torque $\mathbf{M_O}$ is zero, then $\dot{\mathbf{h}}_\mathbf{0} = \mathbf{0}$ so that $\mathbf{h_0}$ is constant, which implies that the angular momentum of a system is conserved if there are no external torques acting on the system,

This fact does not depend on whether the system is a single particle, a collection of particles, or a continuous body.

1.4 Fundamental Transformations

Transformations Between Coordinate Systems

Consider the two coordinate systems whose axes are shown in Fig. 1.5. For this discussion, the X, Y, Z frame could be any fixed system. In the fixed frame,

$$\mathbf{R} = \mathbf{R}_0 + \mathbf{r} = X\hat{\mathbf{I}} + Y\hat{\mathbf{J}} + Z\hat{\mathbf{K}}$$

and, in the moving frame,

$$\mathbf{r} = x\hat{\mathbf{i}} + y\hat{\mathbf{j}} + z\hat{\mathbf{k}}$$

The inertial position X, Y, Z can be written in terms of the x, y, z components in the moving frame as

$$X = \mathbf{R} \cdot \hat{\mathbf{I}} = (\mathbf{R}_0 + \mathbf{r}) \cdot \hat{\mathbf{I}} = X_0 + x\hat{\mathbf{I}} \cdot \hat{\mathbf{i}} + y\hat{\mathbf{I}} \cdot \hat{\mathbf{j}} + z\hat{\mathbf{I}} \cdot \hat{\mathbf{k}}$$

Similarly,

$$Y = Y_0 + x\hat{\mathbf{j}} \cdot \hat{\mathbf{i}} + y\hat{\mathbf{J}} \cdot \hat{\mathbf{j}} + z\hat{\mathbf{J}} \cdot \hat{\mathbf{k}}$$
$$Z = Z_0 + x\hat{\mathbf{K}} \cdot \hat{\mathbf{i}} + y\hat{\mathbf{K}} \cdot \hat{\mathbf{j}} + z\hat{\mathbf{K}} \cdot \hat{\mathbf{k}}$$

The dot products in these three equations are the nine direction cosines for the axes of one reference frame in terms of the other reference frame.

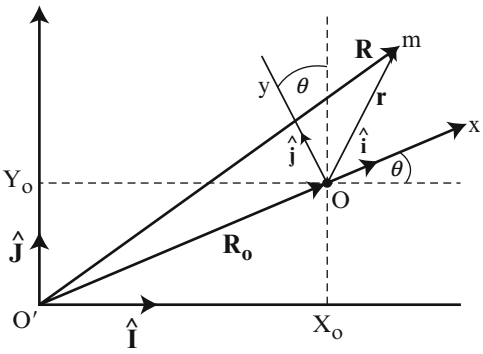

Fig. 1.7 Coordinate transformation in two-dimensional

Notation: In subsequent text, the "∧" over the unit reference vectors will be omitted for simplicity.

Thus, we write

$$\begin{bmatrix} X \\ Y \\ Z \end{bmatrix} = \begin{bmatrix} X_0 \\ Y_0 \\ Z_0 \end{bmatrix} + \begin{bmatrix} \mathbf{I} \cdot \mathbf{i} & \mathbf{I} \cdot \mathbf{j} & \mathbf{I} \cdot \mathbf{k} \\ \mathbf{J} \cdot \mathbf{i} & \mathbf{J} \cdot \mathbf{j} & \mathbf{J} \cdot \mathbf{k} \\ \mathbf{K} \cdot \mathbf{i} & \mathbf{K} \cdot \mathbf{j} & \mathbf{K} \cdot \mathbf{k} \end{bmatrix} \tag{1.13}$$

Now, consider the two-dimensional transformation as shown in Fig. 1.7.

In two-dimensions, the direction cosines reduce to the following.

$$\begin{aligned} \mathbf{I} \cdot \mathbf{i} &= (1)(1)\cos\theta = \mathbf{J} \cdot \mathbf{j} \\ \mathbf{I} \cdot \mathbf{j} &= (1)(1)\cos\left(\theta + \frac{\pi}{2}\right) = -\sin\theta \\ \mathbf{J} \cdot \mathbf{i} &= (1)(1)\cos\left(\frac{\pi}{2} - \theta\right) = \sin\theta \end{aligned}$$

Therefore,

$$X - X_O = x\mathbf{I} \cdot \mathbf{i} + y\mathbf{I} \cdot \mathbf{j} = x\cos\theta - y\sin\theta$$

Similarly,

$$Y - Y_O = x\sin\theta + y\cos\theta$$

Therefore,

$$\begin{bmatrix} X - X_0 \\ Y - Y_0 \end{bmatrix} = \begin{bmatrix} \cos\theta & -\sin\theta \\ \sin\theta & \cos\theta \end{bmatrix} \begin{bmatrix} x \\ y \end{bmatrix} \tag{1.14}$$

$$\begin{bmatrix} x \\ y \end{bmatrix} = \begin{bmatrix} \cos\theta & \sin\theta \\ -\sin\theta & \cos\theta \end{bmatrix} \begin{bmatrix} X - X_0 \\ Y - Y_0 \end{bmatrix}, \tag{1.15}$$

where the matrix in this equation is the inverse of the matrix in the previous equation as will be shown in Exercise 1.4(a).

Note that, in converting between the fixed and moving reference frames, the terms $X - X_0$ and $Y - Y_0$ provide the translation of the origin to the point O and the matrix provides the rotation.

Orthogonal Transformations

Notation: The matrix

$$\alpha = \begin{bmatrix} \alpha_{11} & \alpha_{12} & \alpha_{13} \\ \alpha_{21} & \alpha_{22} & \alpha_{23} \\ \alpha_{31} & \alpha_{32} & \alpha_{33} \end{bmatrix}.$$

with column vectors $\mathbf{c_i} = (\alpha_{1i}, \alpha_{2i}, \alpha_{3i})$, $i = 1, 2, 3$.

Theorem 1.1 *Any non-singular ($det\boldsymbol{\alpha} \neq 0$) matrix $\boldsymbol{\alpha}$ defines a linear transformation as $\boldsymbol{x}' = \boldsymbol{\alpha x}$.*

Def.: The Kronecker delta function is defined as

$$\partial_{jk} = \begin{cases} 1 \text{ if } j = k \\ 0 \text{ if } j \neq k \end{cases}, j, k = 1, 2, 3$$

i.e., $[\partial_{jk}] = I_3$, where I_3 denotes the 3×3 identity matrix.

Def.: Any linear transformation, $\mathbf{x}' = \boldsymbol{\alpha}\, \mathbf{x}$, that has the property

$$\sum_{i=1}^{3} \alpha_{ij}\alpha_{ik} = \delta_{jk} \;\; j, \; k \; = \; 1, \; 2, \; 3 \tag{1.16}$$

is called an orthogonal transformation.

Properties that are equivalent (shown in Exercise 1.1) to the defining property for an orthogonal transformation:

1. $\boldsymbol{\alpha}^{-1} = \boldsymbol{\alpha}^{T}$

Def.: A matrix $\boldsymbol{\alpha}$ that satisfies the condition $\boldsymbol{\alpha}^{-1} = \boldsymbol{\alpha}^{T}$ is called an orthogonal matrix.

2. The column vectors of the $\boldsymbol{\alpha}$ matrix are orthogonal unit vectors.

Example:

$$\alpha = \begin{bmatrix} \cos\theta & \sin\theta \\ -\sin\theta & \cos\theta \end{bmatrix}$$

Properties of orthogonal matrices (without proof):

1. Rotation matrices are orthogonal.
2. A product of orthogonal matrices is an orthogonal matrix.

Euler Angles

Leonhard Euler (1707–1783) was the first to use mathematical rather than geometrical methods for addressing problems in dynamics and, therefore, is considered the "father of analytical dynamics." Indeed, Euler applied mathematics to study the entire realm of physics. He pursued mathematics and completed his work at the Swiss University of Basel, near his birthplace, at the age of 15. He studied there under John Bernoulli. As a measure of his dauntless spirit, several of his books and approximately 400 of his papers were written during the last 17 years of his life when he was totally blind. Leonhard Euler ranks with Archimedes, Newton, and Gauss, and was the key mathematician and theoretical physicist of the eighteenth century. His name is everywhere in mathematics: Euler's constants, Eulerian integrals, Euler's formulas, Euler's theorems, Euler angles, Euler parameters, Euler axes, ...

We will see later that the Euler angles uniquely determine the orientation of an elliptical orbit (see Kepler's Laws) in space. For now, we consider the orientation of a body in space through the same series of three rotations **δ, γ,** and **β,** which produces an orthogonal transformation. We start by assuming the X, Y, Z and body-fixed frames coincide and perform a series of three two-dimensional rotations as shown in Fig. 1.8.

These three rotations are orthogonal transformations as defined by the following equations:

Rotation through Ψ about the third axis Z:

$$\begin{bmatrix} \xi' \\ \eta' \\ \zeta' \end{bmatrix} = \begin{bmatrix} \cos\Psi & \sin\Psi & 0 \\ \sin\Psi & \cos\Psi & 0 \\ 0 & 0 & 1 \end{bmatrix} \begin{bmatrix} X \\ Y \\ Z \end{bmatrix} = \delta \begin{bmatrix} X \\ Y \\ Z \end{bmatrix}$$

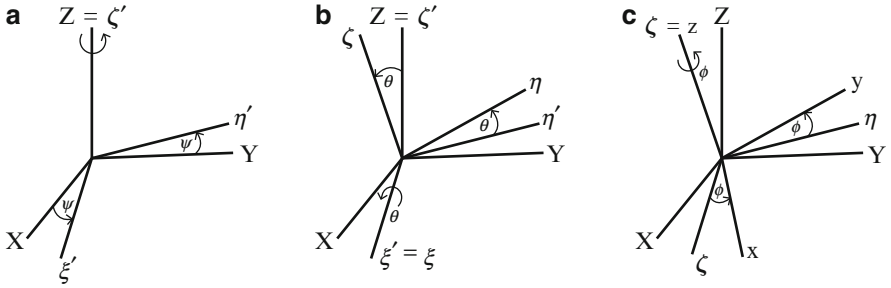

Rotation through ψ about the Z axis

Rotation through θ about the ξ'-axis

Rotation through ϕ about the ζ-axis

Fig. 1.8 Three rotations through the Euler angles

Rotation through θ about the first axis ξ':

$$\begin{bmatrix} \xi \\ \eta \\ \zeta \end{bmatrix} = \begin{bmatrix} 1 & 0 & 0 \\ 0 & \cos\theta & \sin\theta \\ 0 & -\sin\theta & \cos\theta \end{bmatrix} \begin{bmatrix} \xi' \\ \eta' \\ \zeta' \end{bmatrix} = \gamma \begin{bmatrix} \xi' \\ \eta' \\ \zeta' \end{bmatrix}$$

Rotation through ϕ about the third axis ζ:

$$\begin{bmatrix} \mathrm{x} \\ \mathrm{y} \\ \mathrm{z} \end{bmatrix} = \begin{bmatrix} \cos\phi & \sin\phi & 0 \\ -\sin\phi & \cos\phi & 0 \\ 0 & 0 & 1 \end{bmatrix} \begin{bmatrix} \xi \\ \eta \\ \zeta \end{bmatrix} = \beta \begin{bmatrix} \xi \\ \eta \\ \zeta \end{bmatrix}$$

Thus,

$$\begin{bmatrix} \mathrm{x} \\ \mathrm{y} \\ \mathrm{z} \end{bmatrix} = \beta\gamma\delta \begin{bmatrix} \mathbf{X} \\ \mathbf{Y} \\ \mathbf{Z} \end{bmatrix} = \alpha \begin{bmatrix} \mathrm{X} \\ \mathrm{Y} \\ \mathrm{Z} \end{bmatrix}, \tag{1.17}$$

where we have defined the matrix $\boldsymbol{\alpha} = \boldsymbol{\beta\gamma\delta}$.

Note that matrix multiplication is not commutative, so the order of multiplying these matrices must be maintained.

Multiplying the three matrices gives

$$\alpha = \begin{bmatrix} \mathrm{c}\phi\mathrm{c}\Psi - \mathrm{s}\phi\mathrm{c}\theta\mathrm{s}\Psi & \mathrm{c}\phi\mathrm{s}\Psi + \mathrm{s}\phi\mathrm{c}\theta\mathrm{c}\Psi & \mathrm{s}\phi\mathrm{s}\theta \\ -\mathrm{s}\phi\mathrm{c}\Psi - \mathrm{c}\phi\mathrm{c}\theta\mathrm{s}\Psi & -\mathrm{s}\phi\mathrm{s}\Psi + \mathrm{c}\phi\mathrm{c}\theta\mathrm{c}\Psi & \mathrm{c}\phi\mathrm{s}\theta \\ \mathrm{s}\theta\mathrm{s}\Psi & -\mathrm{s}\theta\mathrm{c}\Psi & \mathrm{c}\theta \end{bmatrix} \tag{1.18}$$

where c denotes the cosine and s denotes the sine function. Multiplying by the $\boldsymbol{\alpha}$ matrix transforms vectors in X, Y, Z coordinates to x. y, z coordinates as follows:

$$\begin{bmatrix} \mathrm{X} \\ \mathrm{Y} \\ \mathrm{Z} \end{bmatrix} = \alpha^{-1} \begin{bmatrix} \mathrm{x} \\ \mathrm{y} \\ \mathrm{z} \end{bmatrix} = \alpha^{\mathbf{T}} \begin{bmatrix} \mathrm{x} \\ \mathrm{y} \\ \mathrm{z} \end{bmatrix} \tag{1.19}$$

because $\boldsymbol{\alpha}$ is orthogonal as will be shown in Exercise 1.4(b).

Def.: The line of nodes is the intersection of the X, Y and x, y plane.

Def.: The rotation angles ψ, θ, and ϕ are called Euler angles.

The angles ψ, θ, and ϕ considered above are called the "3 − 1 − 3 Euler angles."

Relative Motion and Coriolis Acceleration

Def.: Absolute motion is movement of a point with respect to an inertial frame.

Def.: Relative motion is movement of a point with respect to a non-inertial frame.

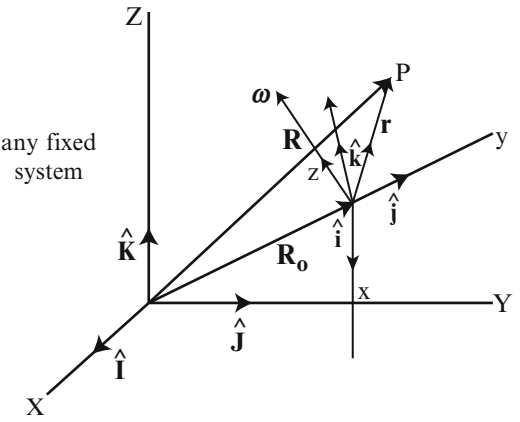

Fig. 1.9 Motion of an object with respect to a moving frame, rotating about **ω**

We now express the motion of an object with respect to a moving frame for which **ω** denotes the instantaneous angular velocity of the rotating frame with respect to the fixed frame as shown in Fig. 1.9.

Consider the motion of point P with respect to the x, y, z frame. The inertial position and absolute velocity P are, respectively,

$$\mathbf{R} = \mathbf{R_0} + \mathbf{r}$$
$$\dot{\mathbf{R}} = \dot{\mathbf{R}}_\mathbf{0} + \dot{\mathbf{r}}$$

where the dot denotes differentiation with respect to the fixed system. But

$$\dot{\mathbf{R}} = \dot{X}\,\mathbf{I} + \dot{Y}\,\mathbf{J} + \dot{Z}\,\mathbf{K}$$
$$\dot{\mathbf{R}}_0 = \dot{X}_0\mathbf{I} + \dot{Y}_0\mathbf{J} + \dot{Z}_0\mathbf{K}$$
$$\dot{\mathbf{r}} = \frac{d}{dt}(x\mathbf{i} + y\mathbf{j} + z\mathbf{k}) = \dot{x}\,\mathbf{i} + \dot{y}\,\mathbf{j} + z\mathbf{k} + x\,\dot{\mathbf{i}} + y\,\dot{\mathbf{j}} + z\,\dot{\mathbf{k}}$$

The question now is: "What are the terms $\dot{\mathbf{i}}$, $\dot{\mathbf{j}}$, and $\dot{\mathbf{k}}$?

In Fig. 1.10, $u = \sin\phi$, and $s = u\Delta\theta = (\sin\phi)\Delta\theta$ denotes arclength.

The $\dot{\mathbf{i}}$ is the rate of change of **i** introduced by the rotation ω. That is,

$$\dot{\mathbf{i}} = \text{velocity of}\,\mathbf{i} = \lim_{\Delta t\to 0}\frac{\Delta\mathbf{i}}{\Delta t} = \left(\lim_{\Delta t\to 0}\left(\frac{s}{\Delta t}\right)\right)\mathbf{u}_\perp = \frac{d\theta}{dt}\,\sin\phi\mathbf{u}_\perp = \omega\sin\phi\mathbf{u}_\perp = \omega\,x\mathbf{i}$$

where $\hat{\mathbf{u}}_\perp$ denotes a unit vector orthogonal to **u**.

By the same argument,

$$\dot{\mathbf{j}} = \omega \times \mathbf{j} \text{ and } \dot{k} = \omega \times \mathbf{k}$$

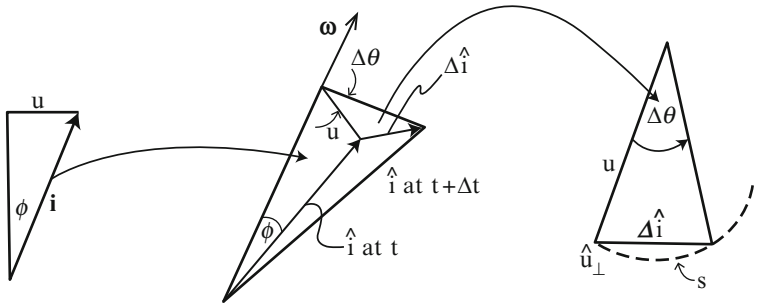

Fig. 1.10 Rotation about **ω**

Therefore,

$$\dot{\mathbf{r}} = \left[\frac{d\mathbf{r}}{dt}\right]_b + \boldsymbol{\omega} \times \mathbf{r}$$

where $\left[\frac{d\mathbf{r}}{dt}\right]_b = \dot{x}\,\mathbf{i} + \dot{y}\,\mathbf{j} + \dot{z}\,\mathbf{k}$ is the derivative of **r** in the rotating coordinate system

Thus, we obtain the following theorem, which provides the relation between the derivative of position in inertial coordinates and the derivative of position in rotating coordinates.

Theorem 1.2 For any vector **r** in a rotating frame, the derivative of **r** in inertial coordinates

$$\dot{\mathbf{r}} = \left[\frac{d\mathbf{r}}{dt}\right]_b + (\omega \times \mathbf{r}) \tag{1.20}$$

where $\left[\frac{d\mathbf{r}}{dt}\right]_b$ denotes the derivative of **r** in the rotating (or body-fixed) coordinate system and **ω** denotes the instantaneous angular velocity of the rotating system.

Since $\dot{\mathbf{R}} = \dot{\mathbf{R}}_o + \dot{\mathbf{r}}$,

$$\dot{\mathbf{R}} = \dot{\mathbf{R}}_0 + \left[\frac{d\mathbf{r}}{dt}\right]_b + \omega \times \mathbf{r}$$

where the term on the left-hand side denotes the absolute velocity of P, the first term on the right-hand side denotes the absolute velocity of the origin of the moving system, the second term denotes the derivative of **r** in the rotating system, and the third the apparent motion due to rotation (**ω**).

Acceleration of P with respect to the inertial frame

Notation: The velocity and acceleration of $\mathbf{r}$ in the rotating system are denoted, respectively, as

$$\dot{\mathbf{r}}_b = \left[\frac{d\mathbf{r}}{dt}\right]_b = \dot{x}\,\mathbf{i} + \dot{y}\,\mathbf{j} + \dot{z}\,\mathbf{k}$$
$$\ddot{\mathbf{r}}_b = \ddot{x}\,\mathbf{i} + \ddot{y}\,\mathbf{j} + \ddot{z}\,\mathbf{k}$$

Using Theorem 1.2, we obtain:

$$\ddot{\mathbf{r}} = \ddot{\mathbf{r}}_b + (\dot{\boldsymbol{\omega}} \times \mathbf{r}) + 2(\boldsymbol{\omega} \times \dot{\mathbf{r}}_b) + (\boldsymbol{\omega} \times (\boldsymbol{\omega} \times \mathbf{r})) \tag{1.21}$$

See the reference by BMW, page 92 for a proof. Also,

$$\ddot{\mathbf{R}} = \ddot{\mathbf{R}}_0 + \ddot{\mathbf{r}} \tag{1.22}$$

Combining Eqs. (1.21) and (1.22), we obtain

$$\ddot{\mathbf{R}} = \ddot{\mathbf{R}}_0 + \ddot{\mathbf{r}}_b + 2(\boldsymbol{\omega} \times \dot{\mathbf{r}}_b) + (\dot{\boldsymbol{\omega}} \times \mathbf{r}) + (\boldsymbol{\omega} \times (\boldsymbol{\omega} \times \mathbf{r})) \tag{1.23}$$

where

$\ddot{\mathbf{R}}_0$ = absolute acceleration of the origin of the moving frame
$\ddot{\mathbf{r}}_b$ = relative (apparent) acceleration of P in the moving frame
$2(\boldsymbol{\omega} \times \dot{\mathbf{r}}_b)$ = Coriolis acceleration due to motion of P in x, y, z frame, where $\boldsymbol{\omega}$ = angular velocity
$\dot{\boldsymbol{\omega}} \times \mathbf{r}$ = acceleration of P due to $\boldsymbol{\omega}$ change, i.e., due to angular acceleration, where $\dot{\boldsymbol{\omega}}$ = angular acceleration
$(\boldsymbol{\omega} \times (\boldsymbol{\omega} \times \mathbf{r}))$ = centripetal (center-seeking) acceleration which depends on the position of P with respect to the axis of rotation

Coriolis acceleration causes a particle moving along the Earth's surface (in a tangent plane) to drift to the right in the Northern Hemisphere and to the left in the Southern Hemisphere. This acceleration determines the sense of the rotation of cyclones. For more information on Coriolis acceleration, see the reference by Linn and two by Van Domelen.

References for this chapter: Arfken and Weber; Bate, Mueller, and White; Battin 1999; Kane and Levinson; Kaplan; Lawden; Linn; Schaub and Junkins; Thomson; Van Domelen, dvandom.com and eyrie.org Websites; Weisstein; and Wiesel.

Exercises.

1.1 Recall the defining property for an orthogonal matrix $\boldsymbol{\alpha}$ as defined in Eq. (1.16). Prove that the defining property and the following two properties are equivalent:
(i) The matrix $\boldsymbol{\alpha}$ satisfies the equation $\boldsymbol{\alpha}^{-1} = \boldsymbol{\alpha}^{\mathrm{T}}$.
(ii) The column vectors of the matrix $\boldsymbol{\alpha}$ are orthogonal, unit vectors.

1.2 Which, if any, of the following matrices, $\boldsymbol{\alpha}$ and $\boldsymbol{\beta}$, is (are) orthogonal? Explain.

$$\alpha = \begin{bmatrix} 0 & 1 & 0 \\ 4/5 & 0 & 3/5 \\ 3/5 & 0 & -4/5 \end{bmatrix}, \quad \beta = \begin{bmatrix} 0 & 1 & 0 \\ 4/5 & 0 & 3/5 \\ 3/5 & 0 & 4/5 \end{bmatrix}$$

1.3 Which, if any, of the matrices, $\boldsymbol{\alpha}$ and $\boldsymbol{\beta}$, defined in Exercise 1.2 define(s) a linear transformation? Explain.

1.4 (a) Show that the transformation defined by

$$\begin{bmatrix} \mathrm{x} \\ \mathrm{y} \end{bmatrix} = \alpha \begin{bmatrix} \mathrm{X} \\ \mathrm{Y} \end{bmatrix}.$$

is orthogonal for

$$\alpha = \begin{bmatrix} \cos\theta & \sin\theta \\ -\sin\theta & \cos\theta \end{bmatrix}$$

(b) Show that the transformation defined by

$$\begin{bmatrix} \mathrm{x} \\ \mathrm{y} \\ \mathrm{z} \end{bmatrix} = \alpha \begin{bmatrix} \mathrm{X} \\ \mathrm{Y} \\ \mathrm{Z} \end{bmatrix}$$

is orthogonal for the matrix $\boldsymbol{\alpha}$ defined in Eqs. (1.17) and (1.18) as the product $\boldsymbol{\beta\gamma\delta}$ of three rotation matrices.

1.5 Determine the inertial components of the point (5, 10, 15) in the rotating x, y, z coordinate system when the Euler angles $\psi = 60°$, $\theta = 45°$, and $\phi = 30°$.

1.6 Consider the point whose inertial components are $\mathrm{X} = 5$ km, $\mathrm{Y} = 10$ km, and $\mathrm{Z} = 15$ km. Determine the components of this point in a rotating frame when the Euler angles $\psi = 30°$, $\theta = 60°$, and $\phi = 45°$.

Keplerian Motion

2

2.1 Introduction

Orbital Mechanics Versus Attitude Dynamics

In studying the motion of a spacecraft, we consider it to be a rigid body and rely on a basic theorem.

Def.: A rigid body is a system of particles whose relative distances are fixed.

Theorem (which we take to be evident):
The motion of a rigid body can be described in terms of:

(a) Translations of its center of mass (Orbital Mechanics).
(b) Rotations about the center of mass (Attitude Dynamics).

Reducing a Complex Problem to a Simplified Problem

We seek to describe the flight path (translational motion) of a spacecraft through interplanetary space or of a celestial body through the universe. Imagine a spacecraft in orbit about the moon, which is in orbit about the earth, which is in orbit about the sun, which is in orbit about the center of the Milky Way Galaxy, which is in orbit about the Local Cluster of galaxies, etc. How can we describe the flight path or trajectory of the spacecraft? In this flight, the spacecraft experiences gravitational attraction from all the bodies of the universe plus non-gravitational forces (to be discussed in Chap. 5). This is a complicated problem. We will simplify the mathematical model to get the most important features and then add perturbations to the nominal or reference trajectory in Chap. 5.

© Springer International Publishing Switzerland 2015

G.R. Hintz, *Orbital Mechanics and Astrodynamics*,
DOI 10.1007/978-3-319-09444-1_2

2.2 Two-Body Problem

Derivation of the Equation of Motion: The Mathematical Model

We develop the equation of motion (the math model) for a satellite experiencing gravitational forces only. Other forces and all torques are assumed to be zero.

Consider an X, Y, Z inertial system. Figure 2.1 shows the positions $\mathbf{r_1}$ and $\mathbf{r_2}$ of the two masses, m_1 and m_2, respectively, the position $\mathbf{r_c}$ of the center of mass (cm), and the position $\mathbf{r} = \mathbf{r_1} - \mathbf{r_2}$ of m_1 with respect to (wrt) m_2.

Def.: The center of mass for the 2-body system in the X, Y, and Z frame is

$$r_c = \frac{m_1 r_1 + m_2 r_2}{m_1 + m_2} \tag{2.1}$$

where $m_1 + m_2 =$ the total mass of the system.

Assume:

1. The bodies of mass m_1 and m_2 are point masses or are spherically symmetric.
2. The particles m_1 and m_2 never touch.
3. No forces are acting on m_1 and m_2 other than the gravitational ones between m_1 and m_2. These forces act along the line joining the two centers of mass.

Assumptions (1) and (2) imply that we can treat m_1 and m_2 as particles located at their centers of mass. We refer to the motion of the two masses as "2-body mechanics" or "Keplerian motion."

By rearranging Eq. (2.1), we obtain

$$\mathbf{r}_1 - \mathbf{r}_c = \frac{m_2 \mathbf{r}}{m_1 + m_2} \tag{2.2}$$

which gives the distance from m_1 to the center of mass of the 2-body system. By solving this equation for $\mathbf{r_1}$ and differentiating with respect to t twice, we obtain the acceleration of mass m_1

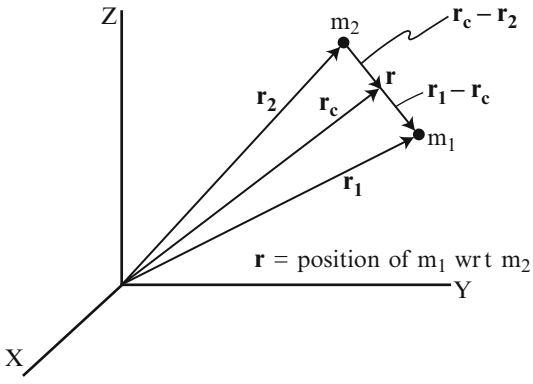

Fig. 2.1 Two-body system in inertial coordinates

$$\ddot{\mathbf{r}}_1 = \ddot{\mathbf{r}}_e + \frac{m_2}{m_1 + m_2}\ddot{\mathbf{r}} \tag{2.3}$$

Similarly, we obtain

$$r_2 - r_c = -\frac{m_1 r}{m_1 + m_2} \tag{2.4}$$

which gives the distance from m_2 to the center of mass of the 2-body system, and the acceleration of m_2

$$\ddot{\mathbf{r}}_2 = \ddot{\mathbf{r}}_c - \frac{m_1}{m_1 + m_2}\ddot{\mathbf{r}} \tag{2.5}$$

Let $F_1 =$ the force acting on m_1 and $F_2 =$ the force acting on m_2. Then, from Eqs. (1.2) and (2.3),

$$\begin{aligned} \mathbf{F}_1 &= m_1\ddot{\mathbf{r}}_1 \\ &= m_1\ddot{\mathbf{r}}_c + \frac{m_1 m_2}{m_1 + m_2}\ddot{\mathbf{r}} \end{aligned} \tag{2.6}$$

and similarly

$$\mathbf{F_2} = m_2\ddot{\mathbf{r}}_2 = m_2\ddot{\mathbf{r}}_c - \frac{m_1 m_2}{m_1 + m_2}\ddot{\mathbf{r}}. \tag{2.7}$$

NIII implies that

$$\mathbf{F}_1 = -\mathbf{F}_2 \tag{2.8}$$

Combining Eqs. (2.6)–(2.8), we obtain the equation

$$m_1\ddot{\mathbf{r}}_c = -m_2\ddot{\mathbf{r}}_c$$

which implies that

$$(m_1 + m_2)\ddot{\mathbf{r}}_c = 0$$

Therefore, $\ddot{\mathbf{r}}_c = 0$ because $m_1 + m_2 \neq 0$.

Hence, we have the following

Result: The center of mass never accelerates and $\dot{\mathbf{r}}_c =$ constant.

Therefore,

$$\mathbf{F}_1 = \frac{m_1 m_2}{m_1 + m_2}\ddot{\mathbf{r}} \tag{2.9}$$

from Eq. (2.6).

Newton's Universal Law of Gravitation is

$$\mathbf{F_1} = -\frac{Gm_1m_2}{r^2}\left(\frac{\mathbf{r}}{r}\right)$$

Equating the two expressions for $\mathbf{F_1}$, we obtain the following equation.

(Differential) Equation of Motion for the Two-body System

$$\frac{d^2\mathbf{r}}{dt^2} + \frac{\mu}{r^2}\mathbf{r} = \mathbf{0} \tag{2.10}$$

where

$$\mu = G(m_1 + m_2)$$

Given a new equation, it is often productive to see what you can observe from it. We observe the following:

Properties of the EOM:

1. The equation relates relative motion, i.e., motion of m_1 with respect to m_2, not motion of r_1 or r_2 in the inertial system.
2. Given position $\mathbf{r}$, we know the acceleration $\ddot{\mathbf{r}}$ and vice versa.
3. There are no velocity terms.
4. The vector equation is equivalent to three scalar equations:

$$\ddot{x} + \mu\frac{x}{r^3} = 0$$
$$\ddot{y} + \mu\frac{y}{r^3} = 0$$
$$\ddot{z} + \mu\frac{z}{r^3} = 0$$

5. By writing the equation as

$$\ddot{\mathbf{r}} = -\frac{\mu}{r^2}\hat{\mathbf{r}}$$

   we see that

$$\ddot{r} \propto \frac{1}{r^2}$$

   From this relationship, we see that acceleration decreases with the area of the surface of a sphere, $S = 4\pi r^2$.
6. The equation is a nonlinear (non-constant coefficient because of the $1/r^2$), second-order vector differential equation.

7. An alternate form of the equation is as a set of first order differential equations:

$$\begin{bmatrix} \mathbf{v} \\ \dot{\mathbf{v}} \end{bmatrix} = \begin{bmatrix} \dot{\mathbf{r}} \\ -\dfrac{\mu}{r^3}\mathbf{r} \end{bmatrix}$$

8. There are at least 6 constants of integration:

$$\mathbf{r_0} = (x_0, y_0, z_0) \text{ where } \mathbf{r_0} = \mathbf{r}(\mathbf{t_0})$$
$$\mathbf{v_0} = (\dot{x}_0, \dot{y}_0, \dot{z}_0) \text{ where } \mathbf{v_0} = \mathbf{v}(\mathbf{t_0})$$

9. The equation is unchanged if $\mathbf{r}$ is replaced by $-\mathbf{r}$, so the equation gives the motion of m_2 with respect to m_1 and m_1 with respect to m_2.

Even though the second-order vector differential equation governing the relative motion of two bodies is nonlinear, we will find that the equation does have a completely general analytical solution. The solution of the differential equation is expedited by some ad hoc vector operations applied to the equation of motion. These vector manipulations produce transformed versions of the equation of motion that are perfect differentials and, hence, immediately integrable.

Solution of the Equation of Motion

1. Cross $\mathbf{r}$ with the equation of motion and, by integrating, obtain the constant of integration $\mathbf{h} = \mathbf{r}$ x $\mathbf{v}$.

$$\mathbf{r} \times \left(\frac{d^2\mathbf{r}}{dt^2} + \frac{\mu}{r^3}\mathbf{r} \right) = 0$$

$$\left(\mathbf{r} \times \frac{d^2\mathbf{r}}{dt^2} \right) = 0 \text{ because } \mathbf{r} \times \mathbf{r} = \mathbf{0} \text{ from Eq. (A.8)}$$

$$\text{But } \frac{d}{dt}\left(\mathbf{r} \times \frac{d\mathbf{r}}{dt} \right) = \left(\frac{d\mathbf{r}}{dt} \times \frac{d\mathbf{r}}{dt} \right) + \mathbf{r} \times \frac{d^2\mathbf{r}}{dt^2} = \mathbf{r} \times \frac{d^2\mathbf{r}}{dt^2}$$

$$\text{Therefore, } \frac{d}{dt}(\mathbf{h}) = \frac{d}{dt}\left(\mathbf{r} \times \frac{d\mathbf{r}}{dt} \right) = \mathbf{0}$$

Def.: The vector $\mathbf{h} = \mathbf{r} \times d\mathbf{r}/dt = \mathbf{r} \times \mathbf{v}$ is the angular momentum per unit mass (or specific angular momentum).

We will call $\mathbf{h}$ the "angular momentum." (We have used this term for $\mathbf{h_O}$.) The vector $\mathbf{h}$ is interpreted as a massless angular momentum.

By integrating the equation

$$\frac{d\mathbf{h}}{dt} = \mathbf{0}$$

we see that $\mathbf{h}$ is a constant vector. That is, angular momentum is conserved in 2-body motion.

Since $\mathbf{h} = \mathbf{r} \times \mathbf{v}$, $\mathbf{r}$ is orthogonal to $\mathbf{h}$ and $\mathbf{v}$ is orthogonal to $\mathbf{h}$ where $\mathbf{h}$ is a constant vector, which implies that $\mathbf{h}$ is orthogonal to a plane that always contains $\mathbf{r}$ and $\mathbf{v}$. Therefore, the motion takes place in the plane $\mathbf{h} \bullet \mathbf{r} = 0$. Hence, the plane of motion is fixed in inertial space. We call this plane the "orbit plane."

2. Cross the equation of motion with $\mathbf{h}$ and, by integrating, obtain the constant of integration $\mathbf{e}$.

$$\frac{d^2\mathbf{r}}{dt^2} \times \mathbf{h} = -\frac{\mu}{r^3}\mathbf{r} \times \mathbf{h} = -\frac{\mu}{r^3}[\mathbf{r} \times (\mathbf{r} \times \mathbf{v})] = -\frac{\mu}{r^3}((\mathbf{r} \bullet \mathbf{v})\mathbf{r} - (\mathbf{r} \bullet \mathbf{r})\mathbf{v})$$

from the vector triple product expansion in Eq. (A.12)

$$-\frac{\mu}{r^3}\left(\left(\mathbf{r} \bullet \frac{d\mathbf{r}}{dt}\right)\mathbf{r} - (\mathbf{r} \bullet \mathbf{r})\frac{d\mathbf{r}}{dt}\right) = -\mu\frac{\left(\frac{dr}{dt}\mathbf{r} - r\frac{d\mathbf{r}}{dt}\right)}{r^2} \text{ from Exercise A.8 and Eq. (A.3)}$$

$$= \mu\frac{d}{dt}\left(\frac{\mathbf{r}}{r}\right)$$

Therefore,

$$\frac{d^2\mathbf{r}}{dt^2} \times \mathbf{h} = \mu\frac{d}{dt}\left(\frac{\mathbf{r}}{r}\right)$$

where $\mathbf{h}$ is a constant vector.

Integrating this last equation obtains

$$d\mathbf{r}/dt \times \mathbf{h} = \mu(\mathbf{r}/r + \mathbf{e}) = (\mu/r)(\mathbf{r} + r\mathbf{e})$$

where $\mathbf{e}$ = a constant vector of integration called the eccentricity vector.

3. Dot the equation in $\mathbf{e}$ with $\mathbf{h}$.

$$\left(\frac{d\mathbf{r}}{dt} \times \mathbf{h}\right) \bullet \mathbf{h} = \frac{\mu}{r}(\mathbf{r} + re) \bullet \mathbf{h}$$

By interchanging the dot and cross product as in Eq. (A.14), we obtain

$$\frac{d\mathbf{r}}{dt} \bullet (\mathbf{h} \times \mathbf{h}) = \frac{\mu}{r}\mathbf{r} \bullet \mathbf{h} + \mu\mathbf{e} \bullet \mathbf{h} = 0$$

because $\mathbf{h} \times \mathbf{h} = \mathbf{0}$.

$$-\frac{\mu}{r}\mathbf{r} \bullet \mathbf{h} + \mu\mathbf{e} \bullet \mathbf{h} = 0$$

because $\mathbf{r} \bullet \mathbf{h} = 0$

Therefore, $\mathbf{e} \bullet \mathbf{h} = 0$.

Therefore, $\mathbf{e} \perp \mathbf{h}$, so that the vector $\mathbf{e}$ lies in the orbit plane. We will use the orientation of $\mathbf{e}$ as a reference direction.

4. Dot **r** with the equation in **e**.

$$\mathbf{r} \bullet \left(\frac{d\mathbf{r}}{dt} \times \mathbf{h} \right) = \frac{\mu}{r} (\mathbf{r} + r\mathbf{e}) \bullet \mathbf{r}$$

$$\left(r \times \frac{d\mathbf{r}}{dt} \right) \bullet \mathbf{h} = \frac{\mu}{r} r^2 + \frac{\mu}{r} r\mathbf{e} \bullet \mathbf{r}$$

$$h^2 = \mathbf{h} \bullet \mathbf{h} = \mu (r + \mathbf{e} \bullet \mathbf{r})$$

$$\frac{h^2}{\mu} = r + \mathbf{e} \bullet \mathbf{r} = r + er\cos\theta$$

where $\theta = \angle(e, r)$ from Exercise A.1.

$$r = \frac{h^2/\mu}{1 + e\cos\theta}$$

where $\theta = \angle(\mathbf{e}, \mathbf{r})$. We call this equation the "Conic Equation."

But this equation for r is the general polar equation for a conic section with origin at a focus. Therefore, the relative position **r** travels through a conic section orbit. QED

There are four conic sections: circle, ellipse, parabola, and hyperbola.
Conic Equation:

$$r = \frac{h^2/\mu}{1 + e\cos\theta} \tag{2.11}$$

$$r_{min} = \frac{(h^2/\mu)}{1 + e} = r \text{ at } \theta = 0 \text{ deg}$$

Therefore, **e** is parallel to the direction of **r** that has the minimum magnitude of **r**.

The KE of the 2-body problem is

$$KE \equiv \frac{1}{2}\left[m_1 v_1^2 + m_2 v_2^2\right] = \frac{1}{2}(m_1 + m_2)\, \dot{\mathbf{r}}_\mathbf{c} \bullet \dot{\mathbf{r}}_\mathbf{c} + \frac{1}{2}\left(\frac{m_1 m_2}{m_1 + m_2}\, \dot{\mathbf{r}} \bullet \dot{\mathbf{r}} \right)$$

from Exercise 2.1.

Def.: The angle θ between the position vector **r** and the eccentricity vector **e** is known as the true anomaly.

The word "anomaly" goes back to Ptolemy, who said: "Any angle that does not increment uniformly in time is wrong or anomalous." Hence, the angle θ is an anomaly.

An Application: Methods of Detecting Extrasolar Planets

Scientists have studied the motion of stars to detect the existence of planets outside of the solar system. Consider a star that has a massive planet—say Jupiter-sized. Its motion about the center of mass (barycenter) of the system can be observed,

indicating the existence of the planet, by measuring Doppler shifts in the star's light caused by motion toward and away from us. This technique is sometimes called the "radial velocity method" or the "wobble method."

Methods of Detecting Extrasolar Planets:

1. Astrometry involves measuring the precise motions of a star on the sky as an unseen planet tugs the star back and forth.
2. Radial velocity detects the wobble of a star by measuring Doppler shifts in the star's light caused by motion toward and away from us.
3. The transit method looks for dips in a star's brightness as orbiting planets pass by and block the light from the star.

2.3 Central Force Motion

Another Simplifying Assumption

For the problem of a spacecraft moving about a planet or a planet moving about the sun, one mass is much greater than the other. Hence, we assume

4. $m_2 >> m_1$.

Then the motion of m_1 is essentially the motion of a particle in an inertially fixed field centered at m_2 because $\mathbf{r_c} = \mathbf{r_2}$. Strictly speaking, this model is the "relative 2-body problem," because we solve for the motion of the satellite relative to the central body. However, as we will learn later, this is the only n-body problem, for any n, that can be solved analytically in closed form. So there is no confusion introduced by referring to it as the "2-body problem," as is often done (Fig. 2.2).

Recall that the cm of a 2-body system never accelerates. For example, the earth has eccentricity $e > 0$ but small, which implies that the cm does accelerate slightly. However, a system centered at the cm of the earth is "inertial enough," i.e., it is close enough to being inertial.

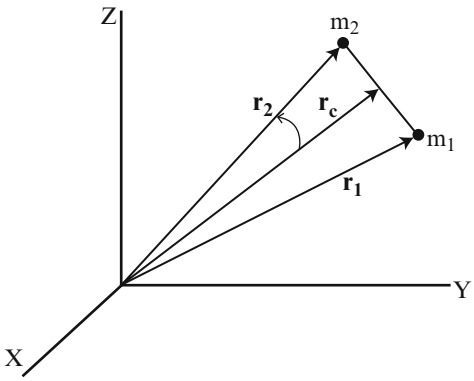

Fig. 2.2 Moving the center of motion for the two-body system

Def.: A force whose line of action always passes through a fixed point O in inertial space and whose magnitude is a function only of the distance r from the fixed point O is called a central force.

Def.: A central force is attractive or repulsive according to as it is directed toward or away from the fixed point O.

Def.: An inverse square force is a central force whose magnitude is inversely proportional to the distance squared (r^2) from O.

We are interested in the gravitational force **F** in Newton's Law of Universal Gravitation:

$$\mathbf{F} = -\frac{Gm_1m_2}{r^2}\frac{\mathbf{r}}{r}$$

which is an attractive central force.

Since $m_2 >> m_1$,

$$\mu = G(m_1 + m_2) \cong Gm_2$$

i.e., m_1 is negligible.

Modeling Assumptions:

1. $\dot{\mathbf{r}}_2 = \dot{\mathbf{r}}_c = 0$
2. $r_2 = r_c$ as in Fig. 2.3
3. $m_1 + m_2 = m_2$

If $m_2 >> m_1$, $KE = \frac{1}{2}m_1(\dot{\mathbf{r}} \bullet \dot{\mathbf{r}})$ from Exercise 2.2.

Central force motion results in a conic section orbit of the form

$$r = \frac{h^2/\mu}{1 + e\cos\theta}$$

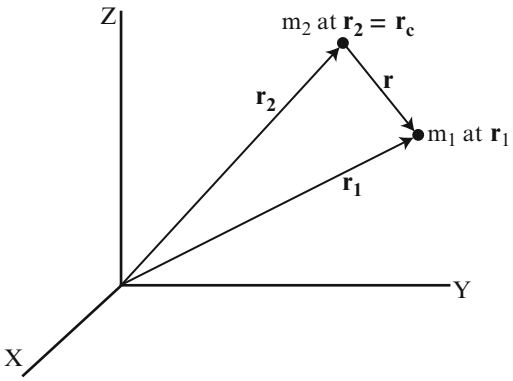

Fig. 2.3 Two-body system with center of motion at m_2

with the focus at the center of motion, m_2, and $\mu = Gm_2$. Thus, we have proved Kepler's first law (KI) from Newton's Laws. In the process, we have extended KI to include circles, parabolas and hyperbolas in addition to ellipses (as in KI).

We drop the subscript on m_2 so that $\mu = Gm$. where m = mass of the central body. Therefore, the conic equation is independent of the mass of the orbiting body. We have normalized the gravitational force by dividing out the mass m_1 of the smaller body to obtain

$$\mathbf{F} = -\frac{Gm_2}{r^2}\frac{\mathbf{r}}{r} = -\frac{\mu}{r^2}\frac{\mathbf{r}}{r}, \mu = Gm_2$$

Dropping the subscript 2, we have

$$\mathbf{F} = -\frac{Gm_2}{r^2}\frac{\mathbf{r}}{r} = -\frac{\mu}{r^2}\frac{\mathbf{r}}{r}, \mu = Gm$$

Let

$$U = U(r) = \frac{\mu}{r}$$

Then

$$\mathbf{F} = \nabla U \tag{2.12}$$

and $\mathbf{F}$ is conservative from Exercise 2.14. The function $U \equiv U(r)$ is called the "gravitational potential" and is equal to the negative of the potential energy, $U = -PE$, from the property shown in Chap. 1 that $U = \nabla V(\mathbf{r})$ where $V(\mathbf{r}) = PE$ by definition.

If $\mathbf{F}$ is conservative, then the Law of Conservation of Total Energy applies, so that

$$\mathscr{E} = \frac{KE}{\text{unit mass}} + \frac{PE}{\text{unit mass}} = T - U = \frac{m_1 \dot{\mathbf{r}} \bullet \dot{\mathbf{r}}}{2m_1} - \frac{\mu}{r}$$

That is,

$$\mathscr{E} = \frac{v^2}{2} - \frac{\mu}{r} = \text{constant} \tag{2.13}$$

which we call the "Energy Equation."

One author said of this equation "If this – were absent, then water would flow uphill" without further remarks. I thought this comment was unusual, until I realized that he means that water would flow uphill in the model. The term μ/r decreases as r increases, which implies that moving to lower PE would occur as r increases, i.e., as water flows uphill. We have $-\mu/r$, which decreases as r increases. The author is teasing us.

In the future, when we say "KE" or "PE," we will be referring to the normalized KE and normalized PE, respectively.

Remarks:

1. In potential theory, we consider a force field, i.e., a region in space in which a force **F** is defined at every point. For our application, the field is gravitational with **F**(x, y, z) being the force acting on a unit mass at each point (x, y, z). The force **F** experienced by a unit test body of the appropriate nature is called the field intensity.
2. The amount of work that must be done when a unit test body is moved along an arbitrary curve in the force field defined by the vector function **F** is the line integral of the tangential component of **F**, i.e.,

$$W = \int_{\mathbf{r}_1}^{\mathbf{r}_2} \mathbf{F} \bullet d\mathbf{r}$$

as defined in Chap. 1. If there is no dissipation of energy through friction or similar effects, then the force **F** is conservative and is the gradient of the scalar function

$$U(x, y, z) = \int_{\mathbf{r}_1}^{\mathbf{r}_2} \mathbf{F} \bullet d\mathbf{r}$$

The function U is called the "potential function of the field." We call U the "gravitational potential."
3. A gravitational field is conservative. That is, an object moving under the influence of gravity alone does not lose or gain mechanical energy but only exchanges one form of energy, kinetic, for another, potential energy.
4. We choose the zero reference for PE at infinity. The price we pay for this simplification is that the PE of a satellite is always negative.

Velocity Vector

This subsection describes properties of the velocity vector for use in the continuing development.

The velocity vector

$$\mathbf{v} \equiv \frac{d\mathbf{r}}{dt} \equiv \lim_{\Delta t \to 0} \frac{\mathbf{r}(t + \Delta t) - \mathbf{r}(t)}{\Delta t} = \lim_{\Delta t \to 0} \frac{\Delta \mathbf{r}}{\Delta s} \frac{\Delta s}{\Delta t} = \frac{ds}{dt} \hat{\mathbf{r}}_T$$

where $\hat{\mathbf{r}}_T$ denotes a unit vector tangent to the flight path at point P (as shown in Fig. 2.4) and $\frac{ds}{dt}$ is the rate of change of arc length. Therefore, the velocity vector **v** is the rate of change of arc length traveled and is always tangent to the path of the particle.

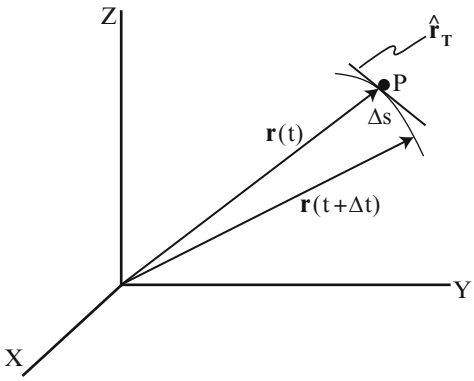

Fig. 2.4 Defining the velocity vector

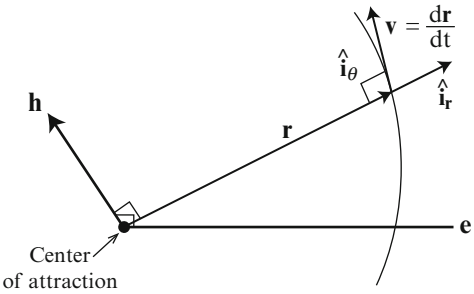

Fig. 2.5 Radial and transverse components of the velocity vector

Let $\mathbf{i_r}$ denote a unit reference vector along the radial direction and $\mathbf{i_\theta}$ a unit reference vector along the transverse that is in the orbit plane and along the direction of spacecraft motion as shown in Fig. 2.5. The center of attraction is at center of an inertial system, but the coordinate system having $\mathbf{i_r}$ and $\mathbf{i_\theta}$ as reference vectors is non-inertial, because it is rotating. We now decompose the velocity vector into two orthogonal components.

$$\mathbf{r} = r\mathbf{i_r}$$

$$\mathbf{v} \equiv \frac{dr}{dt} = \frac{d}{dt}(r\mathbf{i_r}) = \dot{r}\,\mathbf{i_r} + r\frac{d}{dt}(\mathbf{i_r}) = \dot{r}\,\mathbf{i_r} + r\left(\left[\frac{d\mathbf{i_r}}{dt}\right]_b + (\boldsymbol{\omega} \times \mathbf{i_r})\right)$$

by Theorem 2

But $\left[\frac{d\mathbf{i_r}}{dt}\right]_b = 0$ because it is the derivative of a constant vector and

$\boldsymbol{\omega}\mathbf{x}\mathbf{i_r} = \dot{\theta}\hat{\mathbf{h}}\,\mathbf{x}\,\mathbf{i_r} = \dot{\theta}\,\sin\frac{\pi}{2}\mathbf{i}_\theta$ so that

$$\mathbf{v} = \dot{r}\,\mathbf{i_r} + r\,\dot{\theta}\,\mathbf{i}_\theta \tag{2.14}$$

where the first term is the "radial component of **v**" and the second term is the "transverse component of **v.**"

From Eq. (2.14), we obtain

$$\mathrm{KE} = \frac{\mathrm{v}^2}{2} = (\dot{\mathrm{r}})^2 + \mathrm{r}^2\left(\dot{\theta}\right)^2 \tag{2.15}$$

and

$$\mathbf{h} \equiv \mathbf{r}\,\mathbf{x}\,\mathbf{v} = \mathbf{r}\,\mathbf{x}\left(\dot{\mathrm{r}}\,\mathbf{i}_{\mathrm{r}} + \mathrm{r}\,\dot{\theta}\,\mathbf{i}_{\theta}\right) = \mathbf{r}\,\mathrm{x}\,\mathrm{r}\,\dot{\theta}\,\mathbf{i}_{\theta} = \mathrm{r}^2\,\dot{\theta}\,\sin\frac{\pi}{2}\hat{\mathbf{h}}$$

From the latter equation, we obtain

$$\mathrm{h} = \mathrm{r}^2\,\dot{\theta} \tag{2.16}$$

Def.: The parameter or semilatus rectum p is

$$\mathrm{p} = \mathrm{h}^2/\mu \tag{2.17}$$

Combining Eqs. (2.11) and (2.17), we obtain an alternate form of the Conic Equation:

$$\mathrm{r} = \frac{\mathrm{p}}{1 + \mathrm{e}\cos\theta} \tag{2.18}$$

At $\theta = \pm\pi/2$, $\mathrm{r} = \mathrm{p}$.

The magnitude of the eccentricity vector

$$\mathrm{e} = \sqrt{1 + \frac{2\mathrm{p}}{\mu}\mathscr{E}} \tag{2.19}$$

where

$$\mathrm{e} = \sqrt{\mathbf{e} \bullet \mathbf{e}}$$

and **e** denotes the eccentricity vector. We know from analytic geometry that e indicates the orbit shape.

Energy Equation

From Exercise 2.6, we obtain the (very important) Energy Equation:

$$\mathscr{E} = \frac{\mathrm{v}^2}{2} - \frac{\mu}{\mathrm{r}} = -\frac{\mu}{2\mathrm{a}} \tag{2.20}$$

where a denotes the semimajor axis of the conic section orbit

$\mathscr{E}$ is constant at all positions in the orbit. $\mathscr{E}$ is called the "specific mechanical energy (of the satellite)." We usually just call it the "energy."

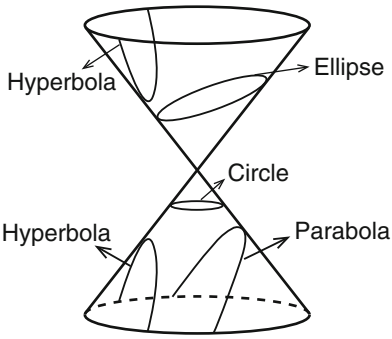

Fig. 2.6 Conic sections

An alternate form of the Energy Equation is obtained from Eq. (2.14) as

$$\frac{(\dot{\mathrm{r}})^2 + \left(\mathrm{r}\dot{\theta}\right)^2}{2} - \frac{\mu}{\mathrm{r}} = -\frac{\mu}{2\mathrm{a}} \tag{2.21}$$

Remarks:

1. The energy $\mathscr{E}$ is independent of the eccentricity e. That is, the energy depends on the size of the orbit, but not on the shape of the orbit.
2. Fix r. As v increases, the energy increases and, therefore, a increases.

Vis-Viva Equation

Solving the Energy Equation for v^2, we obtain the Vis-Viva Equation:

$$\mathrm{v}^2 = \mu\left(\frac{2}{\mathrm{r}} - \frac{1}{\mathrm{a}}\right) \tag{2.22}$$

Geometric Properties of Conic Sections

The circle, ellipse, parabola, and hyperbola are often called "conic sections" because they can be obtained as sections cut (sliced) from a right circular cone by a plane as in Fig. 2.6. The type of conic depends on the angle between the cutting plane and the base of the cone. If the plane section is parallel to the base, the conic is a circle. If the plane is inclined to the base at an angle less than that between the lines that generate the cone and its base, the section is an ellipse. If the cutting plane is parallel to one of the generators, the section is a parabola. Finally, if the plane is inclined to the base at a still greater angle, the plane will also cut the cone formed by the extension of the generators. The section consisting of these two parts is a hyperbola.

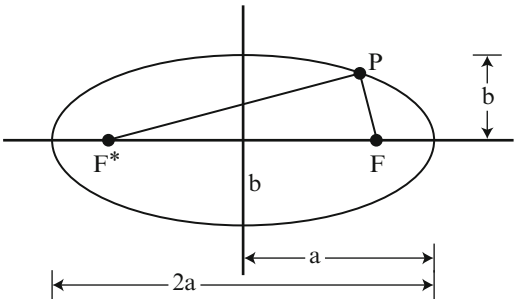

Fig. 2.7 An ellipse

Although conic sections were known to the ancient Greeks, the simplest proof, which relates the geometrical property to the focal definition of the ellipse, was supplied in 1822 by the Belgian mathematician Germinal P. Dandelin (1794–1847).

Reference: Richard H. Battin, 1999.

We consider each conic section in turn.

1. Ellipse ($a > 0$)

   Def.: An ellipse is the locus of all points, the sum of whose distances from two fixed points (the foci) is constant.

   That is, as indicated in Fig. 2.7, an ellipse is the set of all points P such that

$$PF + PF^* = 2a$$

   where F and F* are the foci. The central body is located at F, while F* is called the "vacant focus."

   The following formulas are available from analytic geometry.

$$e = \left(a^2 - b^2\right)^{1/2}/a$$

$$b = a\left(1 - e^2\right)^{1/2}$$

$$p = a\left(1 - e^2\right)$$

   where a is the semimajor axis, b is the semiminor axis, and p is the semilatus rectum.

2. Hyperbola ($a < 0$)

   Def.: A hyperbola is the locus of all points, the difference of whose distances from two fixed points (the foci) is constant.

   That is, as indicated in Fig. 2.8, a hyperbola is the location of all points P and P* such that

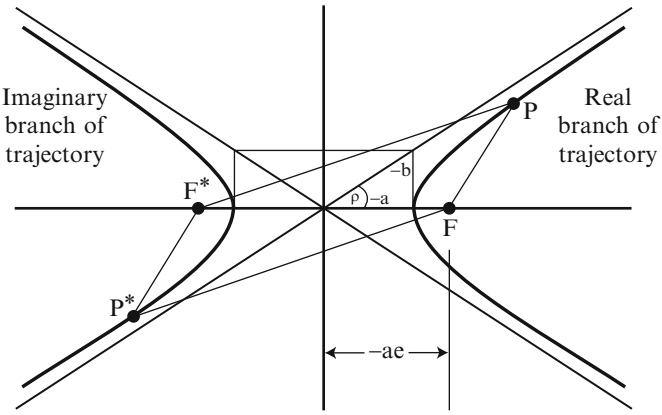

Fig. 2.8 A Hyperbola

$$PF^* - PF = -2a \text{ (real branch)}$$

$$P^*F - P^*F^* = -2a \text{ (imaginary branch)}$$

The spacecraft travels along the real branch.
The following formulas are available from analytic geometry.

$$e = \left(a^2 + b^2\right)^{1/2}/(-a)$$

$$b = a\left(e^2 - 1\right)^{1/2}$$

$$p = a\left(1 - e^2\right)$$

We follow the convention that $a < 0$ and $b < 0$. Be aware that some authors do not follow this convention.

3. Parabola

Def.: A parabola is the locus of all points whose distance from a fixed point (the focus) is equal to the distance from a fixed straight line (the directrix).

That is, as indicated in Fig. 2.9, a parabola is the set of all points P that satisfy the following equation:

$$PF = PN$$

where N denotes the directrix N.

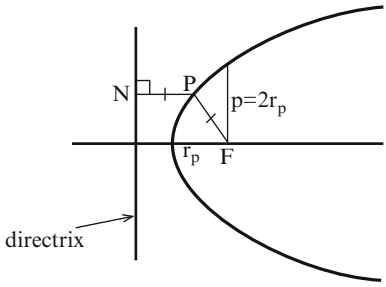

Fig. 2.9 A parabola

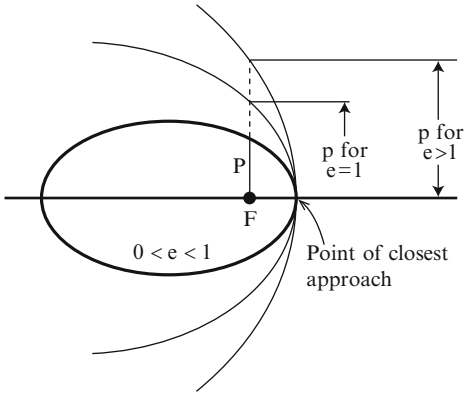

Fig. 2.10 Conic section orbits for $e > 0$

Formulas:

$$e = 1$$

$$p = 2r_p$$

where r_p denotes the radius at periapsis The value of p can be determined from the Conic Equation by evaluating r at 0° true anomaly to obtain $r_p = p/2$.

Orbit Classification: Conic Section Orbits

Figure 2.10 displays the categories of conic section orbits for $e > 0$. The point of closest approach on any conic section orbit has several names: periapsis, periapse, perifocus, plus names that are used for specific central bodies. For example, the periapsis of an orbit about the sun is called "perihelion", about the earth "perigee," about Jupiter "perijove," about Saturn "perichrone," and about the moon of the earth "perilune."

The energy $\mathscr{E}$ for each type of conic section orbit can be deduced from Eq. (2.19). For example, the energy of an ellipse must be negative for the radicand in Eq. (2.19) to be non-negative.

Range of e	Orbit shape	Energy $\mathscr{E}$
0	Circle	<0
$0 < e < 1$	Ellipse	<0
1	Parabola	0
>1	Hyperbola	>0

When my children were in elementary school, I conducted a Math and Science club after school, meeting about once per month. In one of these meetings, I told a story to describe the motion of a spacecraft at launch. Since I wanted to pick someone in the class who had a good arm, I asked if the pitcher from the baseball team was in the room. The answer was "No." So I asked if the catcher was in the classroom, knowing that she was there because she was my daughter, Tana. Tana raised her hand. (I was very proud. By the way, I could have picked her twin sister, Kristin, who was the shortstop and backup catcher. But I continued the story with Tana.) Then I asked, "What is the tallest building in the world and we agreed that it was the Sears Building in Chicago. Then I said that Tana took her baseball to the top of the Sears Building and throw the ball off the building. The ball fell to the ground. She was not happy with that flight so she retrieved her baseball and threw it harder a second time. The ball traveled further from the building but fell to the ground. It took the same length of time to hit the ground because the force of gravity was the same. Again she was not happy. So she retrieved her baseball and wound up and threw it even harder. This time the ball fell at the rate of the curvature of the earth, moving in a circle about the earth. Each time Tana threw the ball I drew the path in Fig. 2.11 on the board in the classroom. Tana put on her glove and walked to the other side of the building and caught the ball. She threw the ball again still harder so that the ball traveled higher than the last time. But eventually the force of gravity pulled the ball down as it moved around the earth. It moved in an ellipse until it arrived back where Tana caught it. Then she threw it harder so that the ball escaped the pull of gravity, moving along a curved path called a "parabola." Throwing the ball still harder sent it on another path called a "hyperbola," which I drew on the board, as shown in Fig. 2.11. At this point, I said, "You know that a baseball cannot be launched this way." I said that we really use a spacecraft to launch our payload as shown in the bottom of Fig. 2.11, which I drew on the board. I said the spacecraft travels at about 8,000 miles per hour so that it will fall at the rate of the curvature of the earth.

One question that remains is: "What keeps the spacecraft in orbit from falling?" The answer is: "Nothing." If the spacecraft were not falling, then, by Newton's First Law of Motion, it would continue flying in a straight line as shown in the upper right of Fig. 2.12. But it is falling at the rate of curvature of the earth, so it travels in a circular path around the earth.

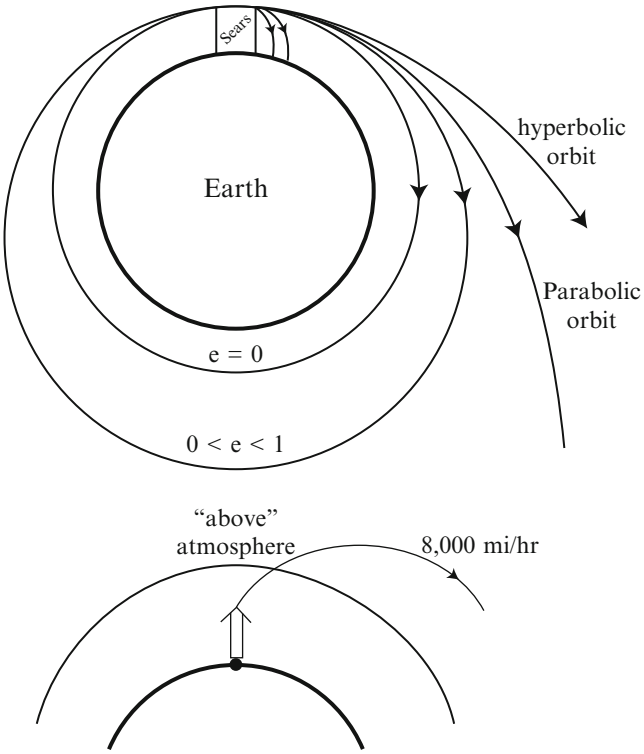

Fig. 2.11 Tana throws her baseball

Fig. 2.12 What keeps the spacecraft in orbit from falling?

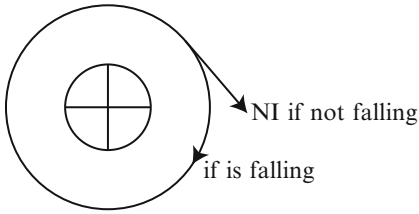

Types of Orbits

We consider various types of orbits that satellites or spacecraft might travel in around a central body.

Def.: A satellite is any object in orbital motion.

Natural satellites are those objects that were not sent into space by humans. An artificial satellite or spacecraft is a machine sent into space by humans.

Time is a fundamental parameter in the analysis of orbits. As humans improved their ability to measure time, they noticed that the time of day as measured by a

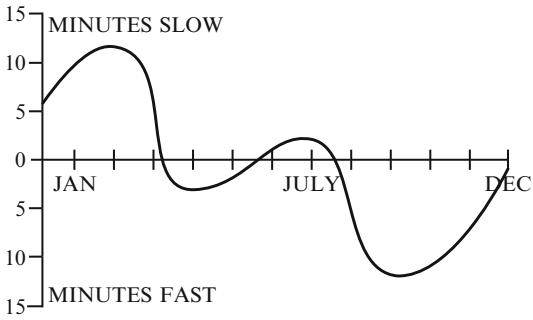

Fig. 2.13 Variations in the length of a day

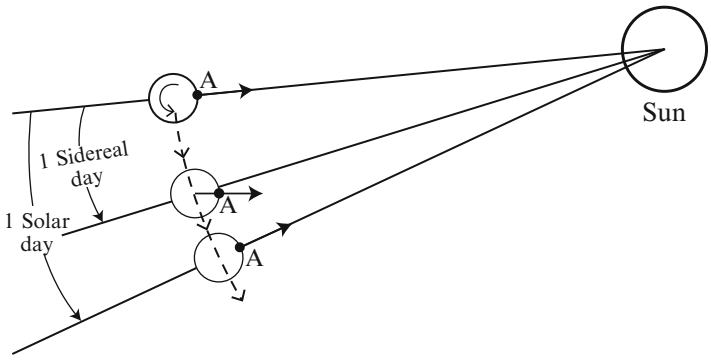

Fig. 2.14 Solar and sidereal day

sundial could vary from the norm (average) by as much as 15 min. in February and November as shown in Fig. 2.13, which shows the minutes slow or fast compared to the average solar day.

Reference: Jesperson and Fitz-Randolph, reprinted with permission of Dover Publications, Inc.

Def.: A solar day is the time interval between two successive "high noons" or upper transits of the sun.

Def.: A mean solar day is the average length of the individual solar days throughout the year.

We break up a mean solar day into 24 h.

Def.: A sidereal day is the time interval between two successive high transits of a star. That is, a sidereal day is the time required for the earth to rotate once on its axis relative to the stars.

If, in Fig. 2.14, you follow the point A fixed to the surface of the earth, you will see that it is initially subsolar and points to stars beyond the sun, then, as the earth turns about its axis and revolves about the sun, A is again lined up with the same

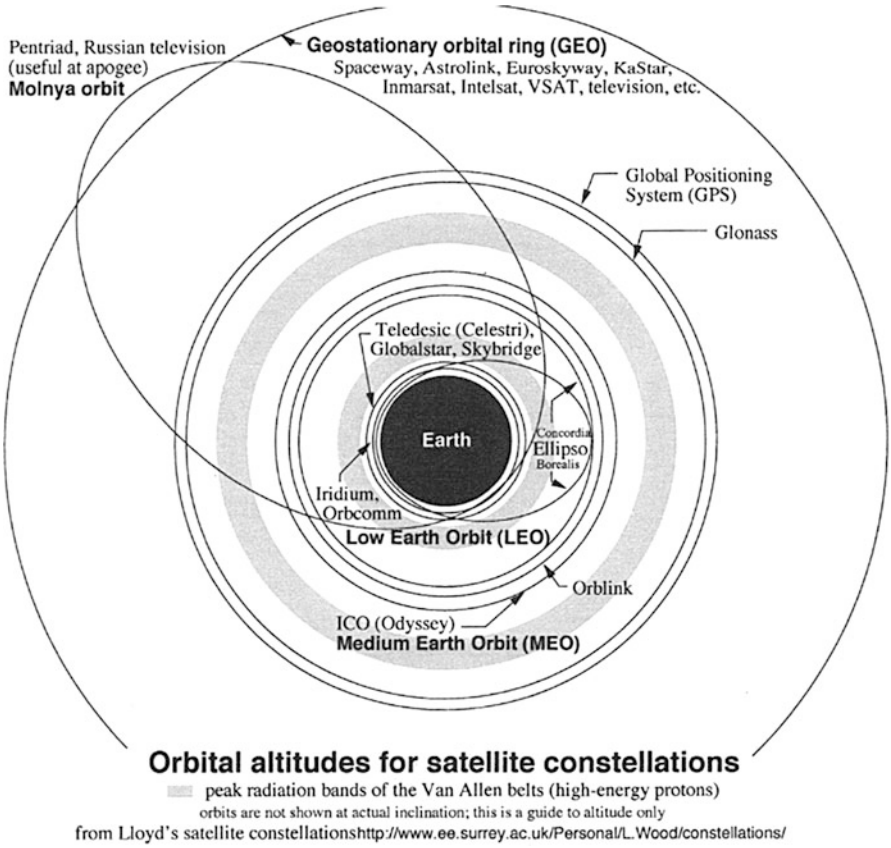

Fig. 2.15 Orbital altitudes for spacecraft [Published with the permission of Lloyd Wood. accessed 1/10/2014]

stars, but not with the sun, and eventually points to the sun again. The point A lines up with the stars after one sidereal day and with the sun after one solar day. A sidereal day is shorter than a mean solar day because, during one revolution of the earth about its axis, the earth moves some distance in its orbit about the sun. One sidereal day is 23 h:56 min: 4 s of mean solar time.

Reasons for variations in the length of a day:

1. The earth's orbit is an ellipse.
2. The earth's axis is tilted at ~23.5° with respect to the ecliptic plane.

For a sidereal day, these factors are not important at stellar distances.

Figure 2.15 displays several examples of orbits. The actual orbits are not in the same plane, but are shown as coplanar for comparison purposes. We consider the following types of orbits:

1. Low Earth Orbit (LEO)
   A LEO orbit is above the thickest part of the atmosphere and below one of different altitudes above the surface of the earth, depending on who is discussing the matter. So LEO satisfies

   ~100 mi (161 km) < altitude < ~1500 km, ~2000 km, or ~3000 km
   Note that altitude $= r - R_{\oplus}$, where $R_{\oplus}$ = the mean equatorial radius of the earth
   Such orbits have $\tau \sim 90$ min. with 16–17 orbits/day and usually are almost circular with $e < 0.03$.
   Examples: ISS and a parking orbit about the earth
   Example: Aura: A Mission to Understand and Protect the Air We Breathe

$$\text{Altitude} = 705\ \text{km} \quad \text{Launch Date}: \ \text{July 10, 2004}$$

   Reference: http://aura.gsfc.nasa.gov/
2. Polar Orbit
   A polar orbit travels over (or possibly nearly over) the North and South Poles.
   Objective: Global coverage
3. Geosynchronous Earth Orbit (GEO)

   Def.: A geosynchronous orbit (GEO) is an earth orbit that has a period equal to one sidereal day.

   Def.: A geostationary orbit (GEO) is a circular, geosynchronous orbit in the earth's equatorial plane.

   A spacecraft that is in a geostationary orbit will hover over a fixed point on the earth's equator.
4. Medium Earth Orbit (MEO)
   Examples:
   GPS (aka NAVSTAR)
   24 active satellites in four planes of six satellites each
   Glonass (Russian System)
   24 satellites with 8 satellites in each of 3 planes
   Galileo (European System) In development
5. HEO
   Highly Elliptical Orbit, e.g., Molnya orbit
   High Earth Orbit, e.g., GEO
6. Molnya Orbits
   "Molnya" is Russian for "lightning."
   $\tau \cong 12$ h (semisynchronous). Other orbit parameters will be defined later.
   The apogee and perigee are fixed.
   The spacecraft speeds through perigee (recall KII) and then spends most of its time over Northern Europe or North America.
   Applications: Such orbits were developed during the Cold War so the USSR could spy on us. Now they are used for high latitude communication.

Fig. 2.16 GTO

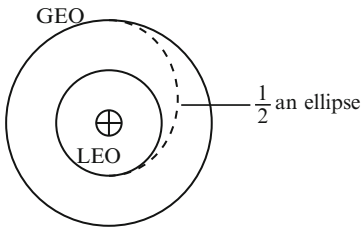

7. Geosynchronous Transfer Orbit (GTO)
   In a GTO, the spacecraft travels through one-half of an ellipse that connects the LEO and GEO as is shown in Fig. 2.16
8. Frozen Orbit
   Characteristics: Minimizes changes in a set of orbit parameters (to be defined later)
9. Sun Synchronous Orbit (SSO)
   Characteristics: The orbit rotates so as to maintain approximately constant orientation (to be defined later) with respect to the sun.
10. Repeating Ground Track
    Characteristic: Subsatellite ground track repeats.
    Example: Aquarius/SAC-D where the Aquarius experiment was supplied by NASA and SAC-D experiments by CONAE (Space Agency of Argentina).
    Orbit characteristics: Frozen orbit, SSO, repeating ground track, nearly polar, and LEO at 705-km altitude above the earth
    Examples: The A-Train is a precession of 4 (was 5) earth-orbiting satellites, Aqua, CloudSat, CALIPSO, and Aura. Parasol moved out of the A-Train on December 2, 2009 to 3.9 km below the altitude of the A-Train.
    Reference: Aviation Week, June 14, 2004
11. Interplanetary Trajectories are heliocentric orbits (to be defined later).

Flight Path Angle

Recall the following definition.

Def.: The velocity vector (aka velocity) is the rate of change of position.

The velocity vector is a directed quantity.

Recall that the velocity vector **v** is the rate of change of arc length traveled and is always tangent to the path of the particle.

The velocity vector is

$$\mathbf{v} = \dot{\mathrm{r}}\,\mathbf{i}_{\mathbf{r}} + \mathrm{r}\,\dot{\theta}\,\mathbf{i}_{\theta}$$

with magnitude

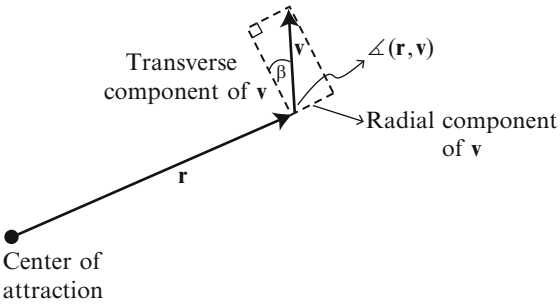

Fig. 2.17 Definition of flight path angle

$$v = \sqrt{(\dot{r})^2 + (r\dot{\theta})^2}$$

As shown in Fig. 2.17, we define

Def.: The flight path angle β is the angle between the velocity vector **v** and the local horizontal (i.e., the direction perpendicular to **r** along the direction of motion) with positive values corresponding to **v** above (with respect to the center of attraction) the horizontal direction.

The flight path angle gives the orientation of the velocity vector in the orbit plane. The magnitude of the Radial component of the velocity vector is

$$\dot{r} = \frac{dr}{dt} = v\cos(\angle(\mathbf{r}, \mathbf{v})) = v\sin\beta \tag{2.23}$$

The magnitude of the transverse component of the velocity vector is

$$r\dot{\theta} = v\sin(\angle(\mathbf{r}, \mathbf{v})) = v\cos\beta \tag{2.24}$$

We consider values of the flight path angle for each of the conic sections.

1. Circle $e = 0$
   As is shown in Fig. 2.18a, $\beta \equiv 0^\circ$ for circular orbits.
2. Ellipse $0 < e < 1$
   As is shown in Fig. 2.18b,

$$\begin{aligned} 0 < \theta < \pi \text{ iff } \quad \beta > 0 \\ \pi < \theta < 2 \text{ iff } \quad \beta < 0 \end{aligned} \tag{2.25}$$

   $\beta = 0$ at periapsis and apoapsis
   Also,

$$\begin{aligned} &\text{Radial component of } \mathbf{v} = \dot{r} \;=\; 0 \text{ at periapsis and apoapsis} \\ &\text{Transverse component of } \mathbf{v} = r\dot{\theta} \;=\; v \text{ at periapsis and apoapsis} \end{aligned}$$

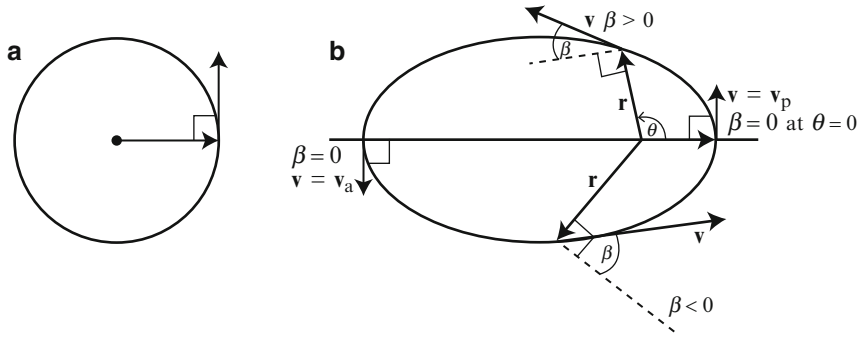

Fig. 2.18 (**a**) Flight path angle for circles. (**b**) Flight path angle for ellipses

3. and 4. Parabola and Hyperbola

$$\begin{aligned} \beta &= 0 \text{ at periapsis} \\ \dot{r} &= 0 \text{ at periapsis} \\ r\dot{\theta} &= v \text{ at periapsis} \end{aligned}$$

We proceed now to derive an identity relating β and θ:

$$v\sin\beta = \dot{r} = \frac{dr}{d\theta}\frac{d\theta}{dt} = \frac{dr}{d\theta}\frac{h}{r^2} \text{ from Eq. (2.16)}$$

$$= -\frac{d}{d\theta}\left(\frac{\mu(1+e\cos\theta)}{h}\right) = \frac{\mu}{h}e\sin\theta$$

Therefore,

$$v\sin\beta = \frac{\mu}{h}e\sin\theta \tag{2.26}$$

2.4 Position Versus Time in an Elliptical Orbit

Kepler's Equation

Let $0 < e < 1$ (Fig. 2.19).

Objective: To determine how long it takes to move from one position, e.g., periapsis, to another position at θ in orbit along an elliptical orbit. That is, we convert from θ to time.

At first, we determine t_p from θ and then we generalize to determining Δt_p from Δθ.

One might approach this problem by separating variables and integrating as follows.

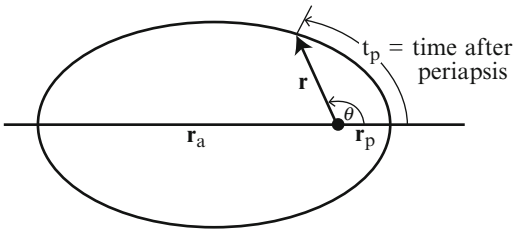

Fig. 2.19 Determining the time after periapsis from the true anomaly

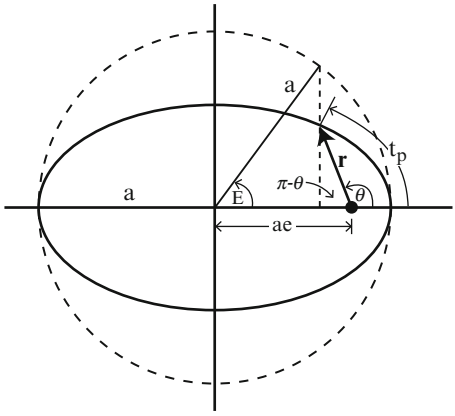

Fig. 2.20 Defining the eccentric anomaly

$$h = r^2 \frac{d\theta}{dt}$$

$$hdt = r^2 d\theta$$

$$\int_0^{t_p} dt = \int_0^{\theta} \frac{d\theta}{(1 + e\cos\theta)^2}$$

$$t_p = f(\theta)$$

Then we could use a table of integrals to obtain a function of θ, depending on the value of e. Instead of deriving such functions of θ, we proceed to obtain a simpler, classic result, Kepler's Equation.

In Fig. 2.20, consider a position **r** at true anomaly θ and construct a vertical line from the axis up through the point at the position **r** to the circumscribing circle of radius a. Then construct a line from the center of the ellipse to the point of intersection on the circle. The angle E between this line and the axis is called the "eccentric anomaly." The eccentric anomaly E satisfies the equation

$$\cos E = \frac{ae + r\cos\theta}{a} \tag{2.27}$$

But, from the Conic Equation by solving for cosθ, we obtain

$$\cos\theta = \frac{p - r}{er}$$

Therefore,

$$\cos E = \frac{ae + r\frac{p-r}{er}}{a} = \frac{a - r}{ae} \tag{2.28}$$

after substituting $p = a(1 - e^2)$. Solving for r in Eq. (2.28), we obtain

$$r = a(1 - e\cos E) \tag{2.29}$$

Differentiating Eq. (2.29), using the chain rule, we obtain

$$\dot{r} = (ae\sin E)\dot{E} \tag{2.30}$$

Note that we have the magnitude r as a function of θ in the Conic Equation and now we have r as a function of the eccentric anomaly E.

Starting from the alternate form of the Energy Equation in Eq. (2.21) and, using the equations. Equations (2.16), (2.17) and $p = a(1 - e^2)$, we derive the equation

$$\frac{ar^2(\dot{r})^2}{\mu} = a^2e^2 - (a - r)^2 = a^2e^2\left(1 - \left(\frac{a - r}{ae}\right)^2\right) = a^2e^2\sin^2\theta \tag{2.31}$$

Using Eqs. (2.30) and (2.31) and simplifying the resulting equation gives

$$r\dot{E} = \frac{\mu}{a} = \text{constant} \tag{2.32}$$

Using Eq. (2.32) and separating variables gives

$$rdE = \sqrt{\frac{\mu}{a}}dt$$

Substituting for r using Eq. (2.29) and integrating gives

$$\sqrt{\frac{a^3}{\mu}}\int_0^E (1 - e\cos E)dE = \int_0^{t_p} dt$$

where the limits of the integrations can be determined from Fig. 2.20.
The integrations obtain Kepler's Equation:

$$t_p = \sqrt{\frac{a^3}{\mu}}(E - e\sin E) \tag{2.33}$$

Proving Kepler's Laws from Newton's Laws

Setting $E = 2\pi$ in Kepler's Equation (2.33), we obtain

$$\tau = 2\pi\sqrt{\frac{a^3}{\mu}} \tag{2.34}$$

This equation proves Kepler's Third Law, which states that

$$\tau^2 \propto (\text{mean radius})^3$$

For Kepler, $a = (r_p + r_a)/2$
Reference: Prussing, 1977

Def.: The mean motion or average angular velocity is

$$n = \sqrt{\frac{\mu}{a^3}} \tag{2.35}$$

The mean motion is $2\pi/\tau$ in radians/s.
Now Kepler's equation can be written as

$$nt_p = E - e\sin E$$

During the period from 1618 to 1621, Kepler published a seven-volume work entitled *Epitome Astronomiae Copernicanae*. Kepler's Equation appears for the first time in Book V of this work.

So we are able to relate E to t_p. But suppose we are given θ and need to know the time it takes to go from periapsis to the position at θ. How can we compute E from θ?

$$\begin{aligned} \sin E &= \frac{(1 - e^2)^{1/2} \sin\theta}{1 + e\cos\theta} \\ \cos E &= \frac{e + \cos\theta}{1 + e\cos\theta} \\ \tan\frac{E}{2} &= \left(\frac{1 - e}{1 + e}\right)^{1/2} \tan\frac{\theta}{2} \end{aligned} \tag{2.36}$$

from Exercise 2.17. The last identity is a very useful relationship between θ and E because θ/2 and E/2 are always in the same quadrant. Now we can compute E from θ and then t_p using Kepler's Equation.

Question: For an elliptical orbit having values a and e, how long will it take to travel from $\theta = \theta_1$ to $\theta = \theta_2$?

Solution is as shown in Fig. 2.21:

Compute $E_1 = E(\theta_1)$ and $E_2 = E(\theta_2)$ from Eq. (2.36).

Compute t_{p_1} and t_{p_2} from Kepler's Equation.

Compute $\Delta t_p = t_{p_2} - t_{p_1}$.

To compute θ from E, use

$$\sin\theta = \frac{(1 - e^2)^{1/2} \sin E}{1 - e\cos E} \tag{2.37}$$

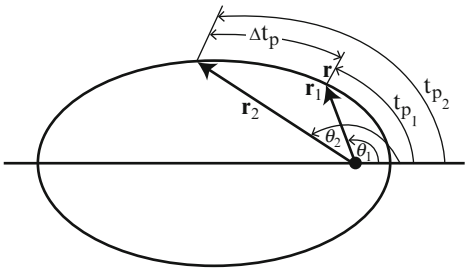

Fig. 2.21 Computing Δt_p

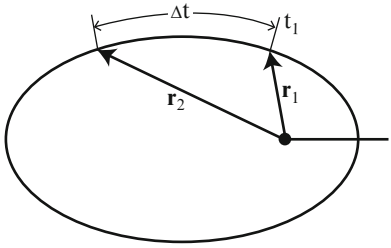

Fig. 2.22 Computing position $\mathbf{r_2}$ from Δt

$$\cos\theta = \frac{\text{cosE} - \text{e}}{1 - \text{ecosE}}$$

which can be derived as Exercise 2.18.

Def.: The mean anomaly is

$$\text{M} = n(\text{t} - \text{t}_\text{v}) = n\text{t}_\text{p}$$

The mean anomaly is the central angle the satellite would be at if $\dot{\theta}$ were constant. Measuring n in rad/s and t_p in s gives M in rad. Here we call M an "anomaly" even though it is linear in time, so it is an "anomalous anomaly."

So far we have considered:

Orbit size parameters: a, τ, and E,
Orbit shape parameter: e
Shape/size parameters: r_p, r_a, p, and h
Location-in-orbit parameters: θ, t_p, M, and E

We need three independent parameters to describe an orbit. For example, the set {a, e, θ} is acceptable, but the set {a, τ, θ} is not, because a and τ are not independent.

Remarks:

(1) There are parabolic and hyperbolic forms of Kepler's Equation (see Chap. 4).
(2) Kepler's Equation and these other forms of the equation can be used to determine the position at a specified later time (see Chap. 4). That is, as shown in Fig. 2.22, we can compute the position $\mathbf{r_2}$ at time $t_1 + \Delta t$.

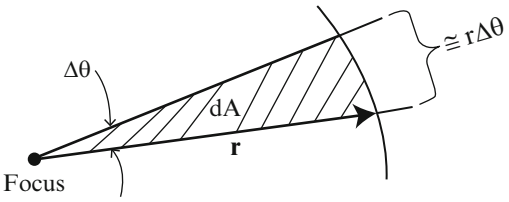

Fig. 2.23 Areal velocity

Def.: The areal velocity is the rate area is swept out by the radius vector.

As shown in Fig. 2.23,

$$dA \cong \frac{r^2}{2} d\theta = \text{area of a triangle} \qquad \frac{dA}{dt} = \frac{r^2}{2}\frac{d\theta}{dt} = \frac{r^2}{2}\dot{\theta} = \frac{h}{2} = \text{constant}$$

from Eq. (2.16). This argument proves KII from Newton's Laws.

2.5 Astronomical Constants

In-plane Parameters for Elliptic Orbits of the Planets and Pluto

See Exercise 2.3(a).

Body Gm and Radius of the Planets, Pluto, Sun, Selected Moons

See Exercise 2.3(b).

Astrodynamic Constants

See Exercise 2.3(c).

For more astronomical data, see the Solar System Dynamics Website at http://ssd.jpl.nasa.gov

2.6 Geometric Formulas for Elliptic Orbits

This section provides several formulas for use in analyzing elliptic orbits. Given the values of two parameters, we can determine other parameters using these formulas (Table 2.1).

Reference: Nelson and Loft

The reference provides similar formulas for hyperbolic orbits. However, in using the hyperbolic formulas, one must make adjustments for the fact that the authors do not follow the convention that the parameters a and b are negative. To use the

Table 2.1 Geometric formulas for elliptic orbit parameters

$a = \dfrac{b}{(1-e^2)^{1/2}}$ $= \dfrac{b^2}{p}$ $= \dfrac{p}{1-e^2}$ $= \dfrac{r_a}{1+e}$ $= \dfrac{r_p}{1-e}$ $= \dfrac{r_p + r_a}{2}$ $= \dfrac{b^2 + r_a^2}{2r_a}$ $= \dfrac{b^2 + r_p^2}{2r_p}$ $= \dfrac{r_a^2}{2r_a - p}$ $= \dfrac{r_p^2}{2r_p - p}$	$b = a(1-e^2)^{1/2}$ $= (ap)^{1/2}$ $= \dfrac{p}{(1-e^2)^{1/2}}$ $= r_a\left(\frac{1-e}{1+e}\right)^{1/2}$ $= r_p\left(\frac{1+e}{1-e}\right)^{1/2}$ $= \left(r_p r_a\right)^{1/2}$ $= \left(2ar_a - r_a^2\right)^{1/2}$ $= \left(2ar_p - r_p^2\right)^{1/2}$ $= r_a\left(\frac{p}{2r_a - p}\right)^{1/2}$ $= r_p\left(\frac{p}{2r_p - p}\right)^{1/2}$	$e = \left(1 - \left(\dfrac{b}{a}\right)^2\right)^{1/2}$ $= \left(1 - \dfrac{p}{a}\right)^{1/2}$ $= \left(1 - \left(\dfrac{p}{b}\right)^2\right)^{1/2}$ $= \dfrac{r_a}{a} - 1$ $= 1 - \dfrac{r_p}{a}$ $= \dfrac{r_a - r_p}{r_a + r_p}$ $= \dfrac{r_a^2 - b^2}{r_a^2 + b^2}$ $= \dfrac{b^2 - r_p^2}{b^2 + r_p^2}$ $= 1 - \dfrac{p}{r_a}$ $= \dfrac{p}{r_p} - 1$
$p = \dfrac{b^2}{a}$ $= a(1-e^2)$ $= b(1-e^2)^{1/2}$ $= r_a(1-e)$ $= r_p(1+e)$ $= \dfrac{2r_p r_a}{r_p + r_a}$ $= \dfrac{2b^2 r_a}{b^2 + r_a^2}$ $= \dfrac{2b^2 r_p}{b^2 + r_p^2}$ $= 2r_a - \dfrac{r_a^2}{a}$ $= 2r_p - \dfrac{r_p^2}{a}$	$r_a = \dfrac{p}{1-e}$ $= 2a - r_p$ $= \dfrac{b^2}{r_p}$ $= r_p\dfrac{1+e}{1-e}$ $= \dfrac{pr_p}{2r_p - p}$ $= a + \left(a^2 - b^2\right)^{1/2}$ $= a(1+e)$ $= b\left(\dfrac{1+e}{1-e}\right)^{1/2}$ $= a\left(1 + \left(1 - \dfrac{p}{a}\right)^{1/2}\right)$ $= \dfrac{b^2}{p}\left\{1 + \left[1 - \left(\dfrac{p}{b}\right)^2\right]^{1/2}\right\}$	$r_p = \dfrac{p}{1+e}$ $= 2a - r_a$ $= \dfrac{b^2}{r_a}$ $= r_a\dfrac{1-e}{1+e}$ $= \dfrac{pr_a}{2r_a - p}$ $= a - \left(a^2 - b^2\right)^{1/2}$ $= a(1-e)$ $= b\left(\dfrac{1-e}{1+e}\right)^{1/2}$ $= a\left[1 - \left(1 - \dfrac{p}{a}\right)^{1/2}\right]$ $= \dfrac{b^2}{p}\left\{1 - \left[1 - \left(\dfrac{p}{b}\right)^2\right]^{1/2}\right\}$

formulas, it is necessary to make the required changes in sign to have the analysis be consistent with our approach.

References for this chapter: Arfken and Weber; Aura Website; BMW; Battin, 1999; Bond and Allman; Chamberlin; Jesperson and Fitz-Randolph; Kaplan; Lee; Mecham; Nelson and Loft; Pierce (revised by Foster); Prussing 1977; Thomson; Weisstein; Wertz and Larson, 1999; Wiesel; Wood; and Wylie and Barrett

Exercises

2.1 Show that, for the 2-body problem,

$$KE \equiv \frac{1}{2}\left[m_1 v_1^2 + m_2 v_2^2\right] = \frac{1}{2}(m_1 + m_2)\dot{\mathbf{r}}_{\mathbf{c}} \bullet \dot{\mathbf{r}}_{\mathbf{c}} + \frac{1}{2}\left(\frac{m_1 m_2}{m_1 + m_2}\,\dot{\mathbf{r}} \bullet \dot{\mathbf{r}}\right)$$

2.2 Show that, for the 2-body problem, if $m_2 >> m_1$,

$$KE = \frac{1}{2} m_2 \left(\dot{\mathbf{r}} \bullet \dot{\mathbf{r}}\right)$$

2.3 Refer to the Solar System Dynamics Website at
http://ssd.jpl.nasa.gov
to complete the following three tables.

(a) In-plane Orbit Parameters for the Planets and Pluto

Body	a (AU)	e (unitless)
Mercury		
Venus		
Earth		
Mars		
Jupiter		
Saturn		
Uranus		
Neptune		
Pluto		

(b) Body Gm and Radius

Body	Gm (km^3/s^2)	Mean equatorial radius (km)
Mercury	22,032.080	
Venus	324,858.599	
Earth	398,600.433	
Mars	42,828.314	
Jupiter	126,712,767.858	
Saturn	37,940,626.061	
Uranus	5,794,549.007	
Neptune	6,836,534.064	
Pluto	981.601	
Body	Gm (km^3/s^2)	Mean radius (km)
Sun	132,712,440,017.987	6.96×10^5
Moon	4,902.801	1,737.5
Io		
Europa		
Ganymede		
Callisto		
Titan		

(c) Astrodynamic constants

Constant	Value
Length of a Julian year (days)	
Mean sidereal day (h:min:s)	
Gravitational constant ($km^3/kg\ s^2$)	
Astronomical unit distance (km)	
Speed of light (km/s)	

2.4 Prove that

$$e = (1/\mu)\ [(v^2 - (\mu/r))\ \mathbf{r} - (\mathbf{r} \bullet \mathbf{v})\mathbf{v}]$$

where e denotes the eccentricity vector, **r** the position vector, and **v** the velocity vector.

2.5 Show that the eccentricity can be obtained as

$$e\ =\ (1\ +\ 2\mathscr{E}p/\mu)^{1/2}$$

2.6 Prove that the energy

$$\mathscr{E} = -\frac{\mu}{2a}$$

Note that $\mathscr{E}$ is a constant that depends only on the size (semimajor axis, a) of the orbit and not on its shape (eccentricity, e).

2.7 Consider a spacecraft moving in an orbit having

$$r_p\ =\ 2R_\oplus \text{and}\ r_a\ =\ 4R_\oplus,$$

where $R_\oplus$ denotes the mean equatorial radius of the earth.

(a) Graph the energy, kinetic energy, and potential energy for this orbit as a function of true anomaly, $0° \leq \theta \leq 360°$.

(b) What happens to the energy, kinetic energy, and potential energy as $r_a \rightarrow \infty$ holding r_p fixed at $2R_\oplus$? Show your work or explain your results.

2.8 (a) Derive a formula for computing circular orbit speed from the orbital radius.

(b) For two spacecraft in circular orbits about a central body, the higher one has greater energy $\mathscr{E}$. Why does this higher spacecraft have a lower speed?

2.9 A spacecraft is tracked by ground stations and determined to have an altitude of 800 km and velocity vector whose radial and transverse components are −3.5 km/s and 8.0 km/s, respectively, at a specified time $t = t_0$.

(a) What type of conic section orbit is the spacecraft in? Explain your answer.

(b) Compute the true anomaly at the time t_0.

2.10 For elliptical orbits ($0 < e < 1$), show that
(a) $r_p = p/(1+e) = a(1-e)$
(b) $r_a = p/(1-e) = a(1+e)$
(c) $h = (\mu r_p(1+e))^{1/2} = (a\mu(1-e^2))^{1/2}$

2.11 Consider a satellite in an elliptical orbit about the earth.
(a) Draw a figure that shows this elliptical orbit and label the following parameters: p, a, b, ae, θ, **r** (vector), and perigee.
(b) Determine the value of the magnitude r of the position vector at the semiminor axis in terms of a, e, and p.
(c) Determine the corresponding value of θ in terms of a, e, and p.
(d) Determine the spacecraft's angular momentum at the semiminor axis in terms of μ, a, e, and p.
(e) What fraction of the orbital period is required to travel from perigee to the semiminor axis in terms of μ, a, e, and p.

2.12 Complete the following table by computing the missing entries.

Spacecraft	Body central	a (km)	τ	e (unitless)	p (km)	r_p (km)	r_a (km)
SEASAT-A	Earth	7,168		0.0008			
GPS satellite	Earth			0.0	26,561.7		
Pioneer Venus Orbiter	Venus		24 h	0.843			
Viking	Mars		24.6 h		4,900		
Cassini	Saturn		116 days			80,680	

2.13 Prove that the eccentricity e satisfies the following equation:

$$e^2 = (X_0 - 1)^2 \cos^2\beta_0 + \sin^2\beta_0$$

where $X_0 = r_0 v_0^2/\mu$ and r_0, v_0, and β_0 denote the magnitude of the radius (position) vector, speed, and flight path angle, respectively, at a specified time t_0.

2.14 The gravitational force **F** for central force motion in an inverse square field is

$$\mathbf{F} = \frac{\mu}{r^2}\frac{\mathbf{r}}{r}$$

with the gravitational potential

$$U = U(r) = \frac{\mu}{r}$$

where $\mu = Gm$ and m is the mass of the central body.
Prove that:
(a) $\mathbf{F} = \nabla U$
(b) **F** is a conservative force.

2.15 At burnout of the upper stage of the launch vehicle, a spacecraft is at an altitude of 622 km above the earth with a transverse velocity component of 7.0 km/s and a radial velocity component of 4.0 km/s.
(a) Compute the flight path angle and true anomaly at burnout.
(b) Compute the semimajor axis, period, eccentricity, radius at apogee, and angular momentum of the achieved orbit.

2.16 At 02:00:00 UTC on December 25, 2004, the Cassini spacecraft delivered the Huygens Probe to Titan from the following position and velocity vectors:

$$\mathbf{r} = (-2684153.865, \ -1666234.282, \ 663859.755) \ (\text{km})$$

$$\mathbf{v} = (-0.39769724, \ -1.75237359, \ 0.85252714) \ (\text{km/s})$$

in the Saturn-centered, inertial, ecliptic of 2000 coordinate system.
(a) Calculate the flight path angle β_0 at probe release in degrees and the magnitude of the radial and transverse components of **v**.
(b) Calculate the radial and transverse component vectors of the velocity vector **v**.
(c) Calculate the following orbital (size and shape) parameters: a, e, p, r_p, r_a, and τ (in days).
(d) Calculate the true, eccentric, and mean anomalies at probe release in degrees.
(e) Calculate the time t_p after periapsis and the length of time (duration) to the next periapsis passage in days.

2.17 Derive Eqs. (2.36).

2.18 Derive Eqs. (2.37)

2.19 Prove that the angular momentum

$$h = rv_\theta$$

where r is the magnitude of the position vector and v_θ is the transverse component of the velocity vector.

2.20 The Space Shuttle used to orbit the earth in about 90 min. A low-altitude orbit about either of the inner planets Mercury and Venus takes about 1½ h. An orbit about Mars takes about the same amount of time. Why are these orbit periods all about the same? Explain your answer.

Orbital Maneuvers

3

3.1 Introduction

A spacecraft performs propulsive maneuvers to correct or adjust the size, shape, or orientation (to be considered later) of its orbit. Thus, we define:

Def.: An orbital maneuver is the transfer of a spacecraft from one orbit into another orbit via a change in the velocity vector.

Such orbital maneuvers fall into two general categories:

1. Statistical—usually small maneuvers that correct for orbit determination and maneuver execution errors and small forces experienced in flight.
2. Deterministic—usually large maneuvers to adjust or transfer into another orbit, e.g., an orbit insertion into a orbit about a planet.

Deterministic maneuvers are implemented with a statistical part that corrects the errors accumulated by the time the maneuver is designed.

The first category consists of by far the greatest number of maneuvers so we consider them first.

3.2 Statistical Maneuvers

Trajectory Correction Maneuvers

Statistical maneuvers are usually called "trajectory correction maneuvers", but also have other names.

Def.: A trajectory correction maneuver (TCM) is an orbital maneuver performed by a spacecraft to correct the spacecraft's flight path. A TCM may also be called a trim maneuver, a trim, an orbit trim maneuver (OTM), an orbit correction maneuver

© Springer International Publishing Switzerland 2015

G.R. Hintz, *Orbital Mechanics and Astrodynamics*,
DOI 10.1007/978-3-319-09444-1_3

(OCM), or a midcourse maneuver. (The term "midcourse maneuver" is usually applied to interplanetary corrections.)

Statistical maneuvers are performed to remove the effects of orbit determination and execution errors experienced at previous TCMs or the launch and other small errors (cf. Chap. 5). Methods for estimating the trajectory and computing the associated covariance matrix, which describes dispersions statistically, are treated in the reference by Tapley, Schutz, and Born (TSB). Maneuver execution errors are described in terms of the Gates Model (defined in the reference by Gates), which accounts for four independent error sources: fixed- and proportional-magnitude- and fixed- and proportional-pointing errors. The word "fixed" does not mean that the errors are constant, but rather refers to the independence of the two fixed errors with respect to the magnitude of the Δv vector being implemented. "Proportional" means that the dispersions of these two are proportional to the magnitude of the Δv. Each of the four sources is assumed to have a Gaussian distribution with a zero mean. The reference by Goodson documents the evolution of the execution error model parameters for the TCMs performed by the Cassini–Huygens spacecraft, along with the analyses, procedures, and software associated with the model development.

The opportunity to perform maneuvers to correct for statistical errors is planned in the mission schedule and the onboard sequence of events. As the time of the statistical TCM draws near, the Navigation Team estimates the trajectory and compares it to the desired trajectory to see if a TCM is required. The nominal or expected value of the Δv for such a maneuver is small or even zero and some of these statistical maneuvers are not performed because the expected miss distance is within the uncertainties or allowable tolerances.

For example, one or two statistical TCMs are often performed after launch to remove the launch errors. The 1σ value for the first TCM, if performed at 10 days after launch, is referred to as the launch vehicle's "figure of merit" (FOM) and is used as a measure of the vehicle's performance.

Selecting a spacecraft maneuver strategy usually involves tradeoffs of many competing factors. The reference by Hintz and Chadwick describes such a tradeoff process. The method uses parametric data to cope with targeting requirements, thruster configuration and performance, hardware constraints, operational considerations, propellant optimization demands, and expected maneuver execution and orbit determination errors, while remaining flexible to react to new conditions.

Maneuver Implementation

To make trim maneuvers, the spacecraft must carry propellant and oxidizer or a monopropellant onboard. There have been spacecraft that did not have a propulsion system.

Example 1: The Galileo probe after release from the orbiter vehicle 150 days before arrival at Jupiter did not have the ability to adjust its trajectory, so it was necessary to deliver the probe within specified targeting conditions at probe release.

Reference: Hintz and Longuski

Example 2: The Swift spacecraft was launched on November 20, 2004 without a propulsion system. It did not need to refine its trajectory to look for Gamma Ray Bursts (GRB).

Performing a TCM usually involves:

1. Turning the spacecraft to point the thrusters in the correct direction to make the velocity change Δv. The thrusters must point in the direction opposite the Δv vector so that the thrust will be applied in the correct direction by means of NIII. The thrust is usually performed in a fixed direction in inertial space. An exception was implemented by the Cassini spacecraft at Saturn Orbit Insertion (SOI) on July 1, 2004, when the spacecraft turned at a constant rate during the burn.
2. Igniting the engine at the correct time, equivalently location in orbit.
3. Imparting the Δv. An accelerometer is often used onboard to determine autonomously when the correct Δv has been imparted. A timer is used as a backup to end the burn at a specified later time in case the accelerometer fails to terminate the burn.
4. Turning back usually to earth pointing for communications. This turn back may also be called a "rewind" or an "unwind."

No turns maneuvers are sometimes used to avoid pointing away from the earth for safety purposes. These maneuvers are implemented by burning more than one thruster. Neither thruster may point in the direction of the desired Δv vector, but the sum of the two Δv vectors will as shown in Fig. 3.1.

Burn Models

These models are:

1. Finite burn—high precision trajectory integration of the equation of motion, including the acceleration due to the maneuver. The EOM is:

$$\ddot{\mathbf{r}} = -\frac{\mu}{r^3}\mathbf{r} + \mathbf{a_p}$$

where the first term on the right-hand side of the equation is the acceleration from two-body motion and the second term is the sum of perturbations

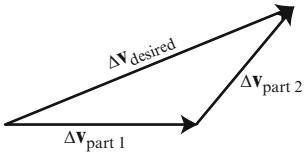

Fig. 3.1 No turns Δvs

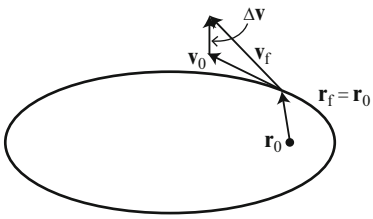

Fig. 3.2 Impulsive burn model

(see Chap. 5) to two-body motion. This model is required for precision calculations such as those to determine the maneuver parameters that will be sent to the spacecraft and executed to obtain a trajectory correction.

2. Impulsive burn in which we set

$$\begin{aligned} &\mathbf{r_f} = \mathbf{r_0} \\ &\mathbf{v_f} = \mathbf{v_0} + \mathbf{\Delta v} \\ &\text{Burn duration} = 0\,\text{s} \end{aligned} \tag{3.1}$$

where $\mathbf{r_o}$ and $\mathbf{v_o}$ denote the pre-maneuver position and velocity vectors, respectively, and $\mathbf{r_f}$ and $\mathbf{v_f}$ denote the post-maneuver position and velocity vectors, respectively. See Fig. 3.2.

This impulsive model is acceptable for analysis purposes if the distance traveled during the thrusting is negligible when compared to the magnitude of the radius vector. It is not used to determine maneuver parameters that are to be sent to the spacecraft.

We will use the impulsive burn model in our analyses.

Note that $\mathbf{v_f}$ is determined by a vector addition. Therefore, in general,

$$v_f \neq v_0 + \Delta v$$

There is equality, if the vectors are collinear and have the same direction. If they are directed in the opposite directions, then

$$v_f = v_o - \Delta v$$

3.3 Determining Orbit Parameters

Parameter Estimation

Before we perform a TCM, we need to know well enough where the spacecraft is. An orbit determination analysis uses tracking data from ground stations and telemetry data from sensors onboard the spacecraft to provide the position vector = (x, y, z), velocity vector = ($\dot{x}$, $\dot{y}$, $\dot{z}$), and other "solved for" parameters.

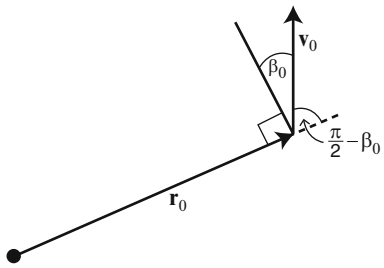

Fig. 3.3 Computing angular momentum

From the position and velocity vectors, we compute r_0, v_0, and β_0 at $t = t_0$, using Eqs. (A.1), (2.23), and (2.24). The time t_0 is chosen when the spacecraft is acted on by gravity alone, i.e., essentially no drag, thrusting, or other forces.

Analytical Computations

In the following computations, we start with r_0, v_0, and β_0 and then compute other parameters that can be compared to desired values. If necessary, we perform a maneuver (fire thrusters) to adjust the orbit.

1. Compute angular momentum h.
   Since h is constant, we have

$$h = |\mathbf{r}_0 \times \mathbf{v}_0| = r_0 v_0 \sin\left(\frac{\pi}{2} - \beta_0\right) = r_0 v_0 \cos\beta_0 \tag{3.2}$$

   from Eq. (A.6). See Fig. 3.3.
2. Compute e, which describes the orbit shape, as in

$$e^2 = \cos^2\beta_0 \left(\left(\frac{r_0 {v_0}^2}{\mu}\right) - 1\right)^2 + \sin^2\beta_0$$

   from Exercise 2.13. An alternate form of this equation is

$$e^2 = \cos\beta_0 (X_0 - 1)^2 + \sin^2\beta_0 \tag{3.3a}$$

   where

$$X_0 = \frac{r_0 v_0^2}{\mu} \tag{3.4}$$

   The computation of e is simpler if it is made at periapsis or apoapsis, since $\beta_0 = 0$ at these points. Therefore,

$$e = \left| \frac{r_p v_p^2}{\mu} - 1 \right| = \left| \frac{r_a v_a^2}{\mu} - 1 \right| \tag{3.3b}$$

3. Compute θ_0 as follows. Solve the Conic Equation (2.11) for $\cos\theta_0$ to obtain

$$\begin{aligned} \cos\theta_0 &= \frac{1}{e}\left(\frac{h^2}{\mu r_0} - 1\right) \\ &= \frac{X_0 \cos^2\beta_0 - 1}{\sqrt{(X_0 - 1)^2 \cos^2\beta_0 + \sin^2\beta_0}} \end{aligned} \tag{3.5}$$

from Eqs. (3.2) and (3.3a). Using the identity in Eq. (2.26), we obtain

$$\sin\theta_0 = \frac{h v_0}{\mu e}\sin\beta_0 = \frac{X_0 \cos\beta_0 \sin\beta_0}{\sqrt{(X_0 - 1)^2 \cos^2\beta_0 + \sin^2\beta_0}} \tag{3.6}$$

from Eqs. (3.2) and (3.4). Therefore,

$$\begin{aligned} \tan\theta_0 &= \frac{X_0 \sin\beta_0 \cos\beta_0}{X_0 \cos^2\beta_0 - 1} \\ \text{where } X_0 &= \frac{r_0 v_0^2}{\mu} \end{aligned} \tag{3.7}$$

which gives the location in terms of r_0, v_0, and β_0.

Solving Eq. (3.7) for X_0, we obtain

$$X_0 = 1/\left(\cos^2\beta_0 - (\sin\beta_0 \cos\beta_0 / \tan\theta_0)\right)$$

which gives X_0 as a function of β_0 for constant θ_0. Fixing e and solving for X_0 in the equation for e^2, we obtain

$$X_0 = 1 \pm \sqrt{1 - \frac{1 - e^2}{\cos^2\beta_0}}$$

which gives X_0 as a function of β_0 for constant e. Also,

$$\cos\beta_0 = \pm\sqrt{\frac{1 - e^2}{2X_0 - X_0^2}}$$

Graphical Presentation of Elliptical Orbit Parameters

These results are displayed parametrically in Fig. 4.13.2 of the reference by Thomson, together with a comparable display for hyperbolic orbits in Fig. 4.13.3. Thus, we obtain two methods of solution: analytically using the equations and graphically using the parametric display in Fig. 3.4.

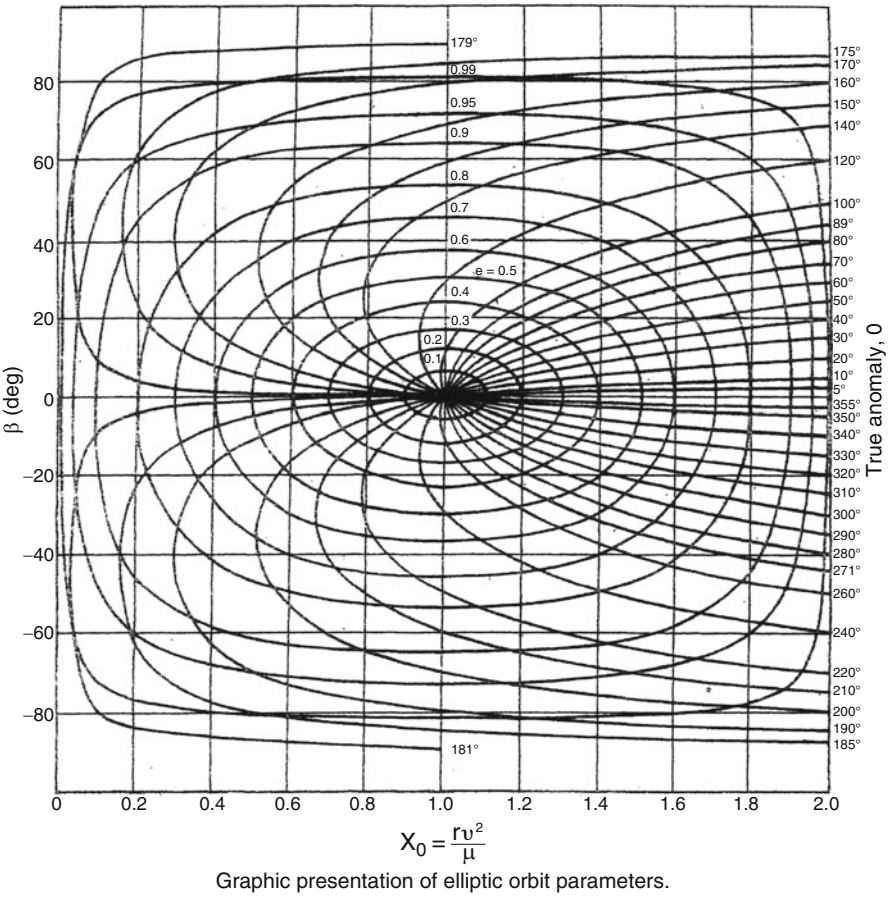

Fig. 3.4 β versus X_0 with e and θ as parameters for elliptic orbits. Reference: Thomson, 1986 [Figure published with the permission of Dover Publications, Inc.]

Properties of the parametric display:

1. The same figure can be used for any central body.
2. The figure displays all possible combinations of e, θ_0, β_0, and X_0 for elliptic orbits. At this point, it is not clear that the range for X_0 is as shown in Fig. 3.4. However, this point will be clarified below.
3. The figure can be used for graphical determination of any two parameters if the other two are known, except for the ambiguity case.

Example 1: Suppose r_0, v_0, and β_0 produce the values $X_0 = 1.0$ and $\beta_0 = 30°$ from Eq. (3.4). By examining the parametric display in Fig. 3.4, we determine that $e = 0.5$ and $\theta_0 = 120°$. Note that we find the intersection of the vertical line

$X_0 = 1$ and the horizontal line for $\beta_0 = 30^\circ$ and then move along the θ curve to read the value $\theta = 120^\circ$ along the vertical axis on the right-hand side of Fig. 3.4.

Example 2 (Ambiguity Case): Consider the values $e = 0.5$ and $X_0 = 1$. By examining Fig. 3.4, we obtain two points: $\beta_0 = 30^\circ$ and $\theta_0 = 120^\circ$ where the spacecraft is leaving periapsis and $\beta_0 = -30^\circ$ and $\theta_0 = 240^\circ$ where the spacecraft is approaching periapsis. The two points are symmetric about the periapsis.

By multiplying the Energy Equation in the form

$$\mathscr{E} = \frac{v_0^2}{2} - \frac{\mu}{r_0}$$

by $2r_0/\mu$ and solving for X_0, we obtain the equation

$$X_0 = \frac{2r_0}{\mu}\mathscr{E} + 2$$

Therefore,

$$0 \leq X_0 = \frac{2r_0}{\mu}\mathscr{E} + 2 \leq 2$$

because the energy is negative for elliptical orbits. Equality occurs for $e = 1$ because $\mathscr{E} = 0$ for parabolas. Note that this inequality shows that the range of values for X_0 is as shown in Fig. 3.4.

To study the figure, we consider the following cases.

Case 1: $X_0 = 2$
This value for X_0 is along the right-hand edge of the figure and, as discussed above, represents parabolic (escape) trajectories. Setting the Energy Equation equal to zero and solving for v_0, we obtain

$$v_0 = \sqrt{\frac{2\mu}{r_0}} = v_{esc}$$

where v_{esc} denotes escape velocity.

Case 2: $X_0 = \frac{r_0 v_0^2}{\mu} = 1$
Solving for v_0 obtains

$$v_0 = \sqrt{\frac{\mu}{r_0}} = v_c$$

where v_c denotes circular orbit speed. But the orbit is circular only if $\beta_0 = 0$. Therefore, the condition $v_0 = v_c$ is necessary but not sufficient for the orbit to be circular.

Case 3: $\beta_0 = 0$, which implies one of three situations: elliptical orbit at periapsis, elliptical orbit at apoapsis, or circular orbit

If $\beta_0 = 0$,

$$e^2 = (X_0 - 1)^2$$

$e = |X_0 - 1|$ from Eq. 3.3 and

$$\tan\theta_0 = \frac{X_0 \sin\beta_0 \cos\beta_0}{X_0 \cos^2\beta_0 - 1} = \frac{0}{X_0 - 1}$$

This situation has four subcases:

1. For $0 \leq X_0 < 1$, $\tan\theta_0 = 0$, which implies that $\theta_0 = 0$ or 180° because the tangent function has period of 180°, but Fig. 3.4 shows that θ_0 must then be 180°.
2. For $X_0 = 1$, $e = 0$ because $|X_0 - 1|$, which implies that θ_0 is indeterminate and the orbit is circular.
3. For $1 < X_0 < 2$, $\tan\theta_0 = 0$, which implies that $\theta_0 = 0$ or 180°, but Fig. 3.4 shows that $\theta_0 = 0^\circ$.
4. For $X_0 = 2$, $e = 1$ so the orbit is parabolic and $\tan\theta_0 = 0$ implies $\theta_0 = 0$.

Example (To study β):

Suppose the spacecraft is in an orbit with $e = 0.8$.

The first column of Table 3.1 gives the true anomaly in deg; the second the flight path angle in deg as read from Fig. 3.4; and the third the flight path angle in deg as determined from the identity in Eq. (2.26). The flight path angle data from Fig. 3.4 is graphed in Fig. 3.5. The remainder of the function is symmetric about the value at apoapsis.

Figure 3.5b gives plots of the flight path angle as a function of true anomaly for eccentricity $e = 0.3$, 0.6, and 0.9 made using the identity in Eq. (2.26).

Properties of β for $0 < e < 1$ as deduced from Figs. 3.4 and 3.5b:

1. $\beta = 0$ at $\theta = 0^\circ$ and 180°
2. $\beta > 0$ for $0 < \theta < 180^\circ$
3. $\beta < 0$ for $180^\circ < \theta < 360^\circ$
4. $|\beta(\theta)|$ increases as e increases
5. $\beta \equiv 0$ if $e = 0$

In Exercise 3.4, it is left to the reader to complete column 2 of Table 3.1, using Fig. 3.4, and column 3, using the identity in Eq. 2.26. Then make a MATLAB plot of both columns of data to show the accuracy of the parametric tool given in Fig. 3.4.

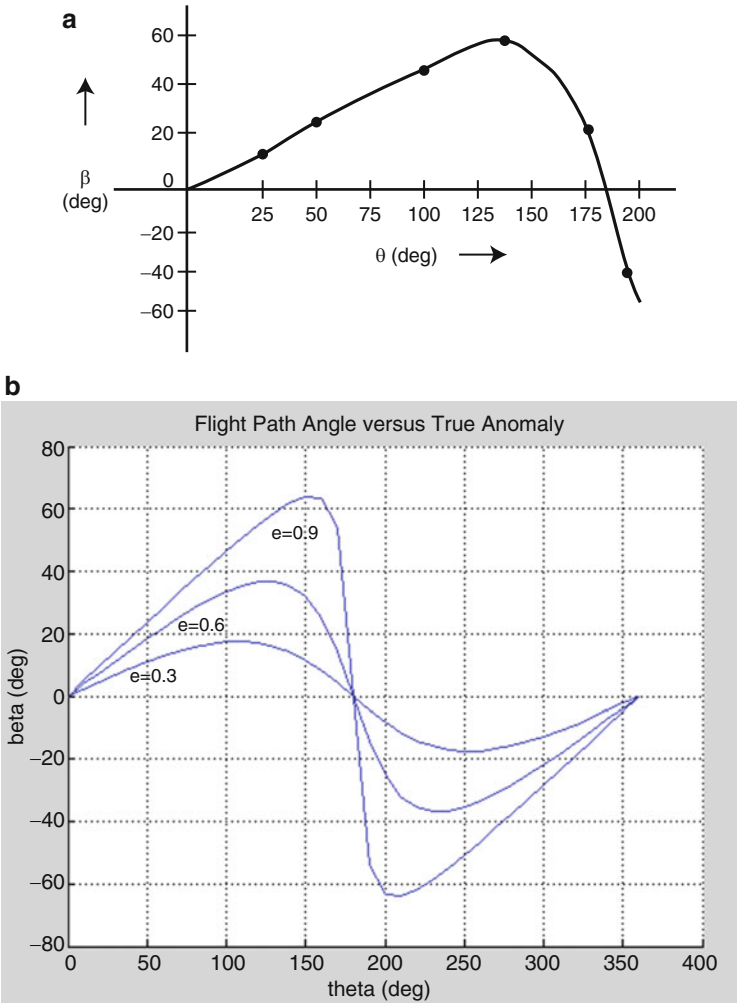

Fig. 3.5 (**a**) Graph of data from Fig. 3.4. (**b**) Flight path angle versus true anomaly

Table 3.1 Beta values from Fig. 3.4 and identity

Theta (°)	Beta (°) (from figure)	Beta (°) (from identity)
0	0	0
25	10	11
50	21	22
100	43	42.5
150	53	52.5
175	18	19
180	0	0
200	−48	−48

Circular Orbits

For circular orbits,

$\beta \equiv 0^\circ$ and $e = 0$

$r = p = a$ (former from Conic Equation and latter from Energy Equation and Exercise 2.8a)

$$v = v_c = \sqrt{\frac{\mu}{r}} = \text{constant because } r = a.$$

Slightly Eccentric Orbits

Suppose the target orbit is circular with

$$r = r_{target}$$

Suppose we achieve

$$\beta_0 \neq 0, \text{ but small}$$
$$v - v_c \neq 0, \text{ but small}$$

Assume r_0 is exact. (Select one of the two points in the orbit where $r = r_{target}$.) Obtain e from Eq. (3.3a) and θ_0 from Eq. (3.7). Then, from Eq. (3.2), the Conic Equation, and Exercise 2.8a, we obtain

$$e \cos\theta_0 = \frac{{v_0}^2 \cos^2\beta_0}{{v_c}^2} - 1 \tag{3.8}$$

and, from Eqs. (2.26), (3.3a), (3.7), and Exercise 2.8a, that

$$e \sin\theta_0 = \frac{{v_0}^2}{{v_c}^2} \cos\beta_0 \sin\beta_0 \tag{3.9}$$

So far, we have not used the facts that β_0 and $v_0 - v_c$ are small. From Eq. (3.8) and a Taylor series expansion for the cosine function, we obtain

$$e \cos\theta_0 = \frac{(v_c + (v_0 - v_c))^2}{{v_c}^2} \left(1 - \frac{{\beta_0}^2}{2} + \ldots\right)^2 - 1$$

But, because the product of small values is negligible, all terms after the first in the Taylor series expansion are essentially zero, so

$$e \cos\theta_0 \cong \frac{2(v_0 - v_c)}{v_c} \tag{3.10}$$

after using again that the product of small values is negligible. By a similar argument,

$$e \sin \theta_0 = \beta_0 \tag{3.11}$$

Therefore, from Eqs. (3.10) and (3.11), we obtain

$$\tan \theta_0 = \frac{\beta_0 v_c}{2(v_0 - v_c)} \tag{3.12}$$

which gives the location in the orbit, and

$$e = \sqrt{4\left(\frac{v_0 - v_c}{v_c}\right)^2 + {\beta_0}^2} \quad \text{(small)} \tag{3.13}$$

which gives the shape of the orbit.

The effect of $v_0 - v_c$ on a is

$$\frac{\partial a}{a} = 2\frac{\partial v}{v} \tag{3.14}$$

Proof:
Assume r is fixed.

By differentiating the Energy Equation and multiplying by $1/v^2$, we obtain

$$\frac{\partial v}{v} = \frac{\mu \partial a}{2a^2 v^2} = \frac{\mu \partial a}{2a\mu} = \frac{\partial a}{2a}$$

from Exercise 2.8a and the fact that the orbit is approximately circular.
Therefore,

$$\frac{\partial a}{a} = \frac{2\partial v}{v} \quad \text{QED}$$

Similarly, using Eq. (2.34), we obtain

$$\frac{\partial \tau}{\tau} = 3\frac{\partial v}{v} \tag{3.15}$$

Therefore, an excess of launch velocity over v_c increases a and energy (from the Energy Equation). Increasing a increases τ from Eq. (2.34).

3.4 Orbit Transfer and Adjustment

We first treat deterministic maneuvers for which the direction of the angular momentum vector, **h**, is fixed. That is, we consider maneuvers that do not change the orbit plane.

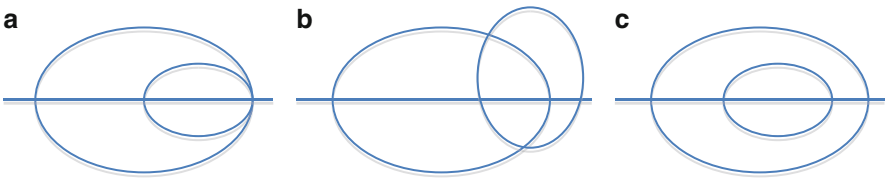

Fig. 3.6 Coplanar orbits. (**a**) One intersection. (**b**) Two intersections. (**c**) No intersections

Single Maneuver Adjustments

From the Energy Equation and Eq. (2.19), we see that energy and e are functions of the velocity magnitude. Therefore, maneuvers made in the orbit plane can change the energy and eccentricity of the orbit.

We call an orbital maneuver that does not change the plane of the spacecraft's orbit an "in-plane maneuver." As shown in Fig. 3.2, an in-plane maneuver can change the magnitude of the velocity vector, so it can change the magnitude of the angular momentum vector $\mathbf{h} = \mathbf{r} \times \mathbf{v}$. However, it cannot change the direction of **h**, which is orthogonal to the orbit plane. Recall that we are discussing impulsive maneuvers, not finite burns.

One restriction for a single-maneuver adjustment: The new (post-maneuver) orbit must intercept the old (pre-maneuver) orbit at the maneuver point.

Mathematical Fact: Two confocal ellipses intersect in 0, 1, or 2 points.

Figure 3.6 shows the three different intersection situations for two confocal ellipses. A spacecraft could transition from one of the ellipses in Fig. 3.6a to the other by performing a maneuver at the intersection point. A spacecraft could move from one ellipse in Fig. 3.6b to the other by performing a maneuver at either of the two intersection points. However, a spacecraft cannot move from one orbit to the other as shown in Fig. 3.6c by performing only a single maneuver. One could draw two ellipses that intersect in four points, but the ellipses would not be confocal.

We often target a value for the period $\tau = \tau_f$, which corresponds to a value $a = a_f$. For example, PVO was positioned in an orbit with $\tau_f = 24$ h to synchronize with tracking stations on the earth. Viking maintained $\tau_f = 24.6$ h = 1 Mars day, which is called a "sol."

Once a maneuver location has been selected (by a method such as one that uses the tool described in Sect. 7.3), the magnitude r_0 of the position vector at the maneuver point can be calculated from the Conic Equation as

$$r_0 = \frac{p_0}{1 + e_0 \cos\theta_0}$$

where e_0 and p_0 are values for the initial (pre-maneuver) orbit. Note that in previous analyses we have only had one value for each of these parameters, but now we have different values for the initial and final orbit. If a target value τ_f is specified, then a_f

can be calculated using Eq. (2.34) and the required velocity at the maneuver point on the post-maneuver orbit can be calculated from the Vis-Viva Equation as

$$v_f = \sqrt{\frac{2\mu}{r_f} - \frac{\mu}{a_f}}$$

Now a_f is known, but what is the value of r_f? Recall the impulsive burn model, which assumes that $r_f = r_0$, so r_f is known and v_f can be computed.

Hohmann Transfer

Walter Hohmann (1880–1945), a German engineer, first published his result for a Hohmann transfer as a conjecture in a monograph entitled *Die Erreichbarkeit der Himmelskörper* [The Attainability of Celestial Bodies] in 1925. NASA published an English translation in NASA Technical Translations F-44, 1960. A rigorous, analytic proof of the optimality of such a transfer for a 2-impulse sequence was not available until 1963.

Problem: To transfer a spacecraft between two coplanar, circular orbits about the same central body by using the minimum $\Delta v_{Total} = \Delta v_1 + \Delta v_2$ for a 2-maneuver sequence.

Notation: The Δv_1 denotes the magnitude of the velocity increment for the first maneuver of the 2-maneuver sequence and Δv_2 denotes the magnitude of the second velocity increment.

Outward Hohmann Transfer Profile

Consider two coplanar, circular orbits about a central body. Denote the inner circle as C_1 and its radius as r_p. Denote the outer circle as C_2 with radius r_a. The transfer orbit has r_p as the radius at periapsis and r_a as the radius at apoapsis. When moving in the inner circle, the spacecraft has circular orbit speed, v_{c1}. The first maneuver applies Δv_1 along the velocity vector to move the spacecraft into the transfer orbit by giving the spacecraft the velocity v_p at periapsis on an ellipse. The second maneuver is performed at the apoapsis of the transfer orbit by adding Δv_2 to the velocity v_a at apoapsis to obtain v_{c2}, the speed of the outer circle (Fig. 3.7).

Note: The $\mathbf{v_{c1}}$ and $\mathbf{\Delta v_1}$ are collinear and $\mathbf{v_{c2}}$ and $\mathbf{\Delta v_2}$ are collinear. Also the semimajor axis of the transfer ellipse is

$$a = \frac{r_p + r_a}{2}$$

Example: Recall from Fig. 2.16 that, if C_2 is a GEO, then the transfer orbit is called a GTO, a geosynchronous transfer orbit.

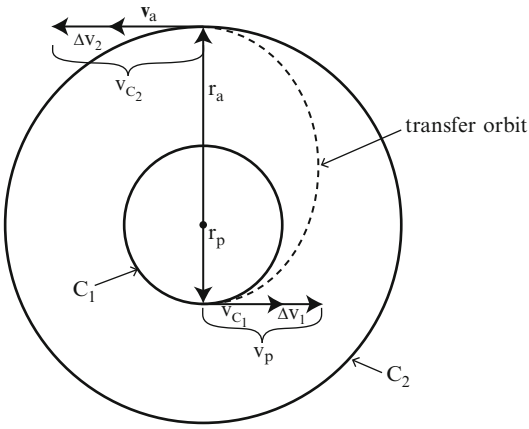

Fig. 3.7 Outward Hohmann transfer

Calculation of Δv_1:

$$\Delta v_1 = v_p - v_{c_1} = \sqrt{\frac{2\mu}{r_p} - \frac{2\mu}{r_p + r_a}} - \sqrt{\frac{\mu}{r_p}}$$

$$= \sqrt{\frac{\mu}{r_p}}\left[\sqrt{\frac{2\frac{r_a}{r_p}}{1+\frac{r_a}{r_p}}} - 1\right] \tag{3.16}$$

Calculation of Δv_2:

$$\mathbf{h} = \mathbf{r} \times \mathbf{v} = \text{constant vector}$$

At periapsis, $h = r_p v_p \sin\frac{\pi}{2} = r_p v_p$

At apoapsis, $h = r_a v_a \sin\frac{\pi}{2} = r_a v_a$

Therefore, conservation of angular momentum implies that

$$h = r_p v_p = r_a v_a \tag{3.17}$$

Therefore,

$$\Delta v_2 = v_{c_2} - v_a = \sqrt{\frac{\mu}{r_a}} - \frac{r_p}{r_a}\sqrt{\frac{2\mu}{r_p} - \frac{2\mu}{r_p + r_a}}$$

$$= \sqrt{\frac{\mu}{r_a}}\left[1 - \sqrt{\frac{2}{1+\frac{r_a}{r_p}}}\right] \tag{3.18}$$

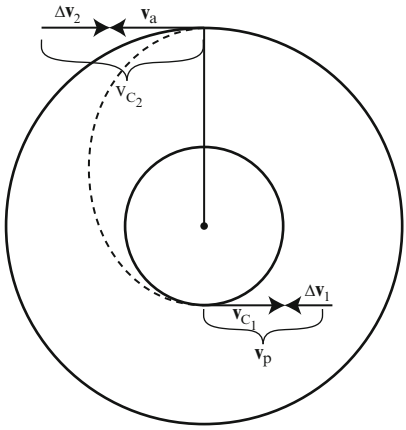

Fig. 3.8 Inward Hohmann transfer

The total Δv required for the Hohmann transfer is

$$\Delta v_{Total} = \Delta v_1 + \Delta v_2 = \sqrt{\frac{\mu}{r_p}}\left[\sqrt{\frac{2\frac{r_a}{r_p}}{1+\frac{r_a}{r_p}}}\left(1-\frac{r_p}{r_a}\right) + \sqrt{\frac{r_p}{r_a}} - 1\right] \tag{3.19}$$

Inward Hohmann Transfer

In Fig. 3.8, we are still calling the velocity increment performed on the outer circle Δv_2 to keep the notation the same as for the outward transfer.

As above,

$$\Delta v_{Total} = \Delta v_1 + \Delta v_2 \quad \text{(scalars)}$$

The energy is reduced twice.

Remarks:

1. To transfer between two circular, coplanar orbits about the same body, the Hohmann transfer requires the minimum total impulsive Δv for a two-maneuver sequence. In fact, each maneuver provides the minimum Δv to achieve the required energy change to reach the other circular orbit. We will not prove this statement of the optimality of the Hohmann transfer, but rather cite the following references with respect to the topic. In particular, the references by Barrar and Prussing 1992 give such proofs.

   References: Barrar, Hohmann, Lawden, and Prussing 1992

2. If $r_a > 11.94\, r_p$, there is a slightly more efficient three-maneuver transfer, called a "bi-elliptic transfer," which is discussed in the next subsection.

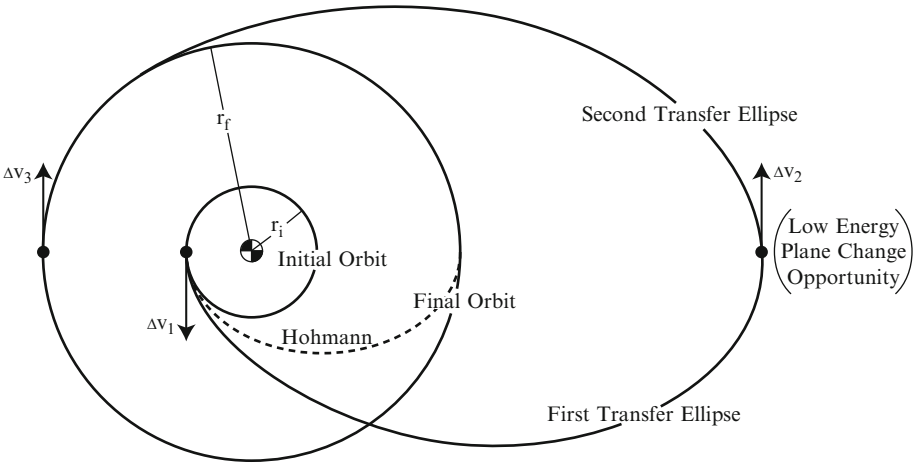

Fig. 3.9 Bi-elliptic transfer

3. Going to a higher number of impulses does not reduce the total Δv required for impulsive maneuvers. That is, if $r_a \leq 11.94\ r_p$, the Hohmann transfer requires the least total impulsive Δv for an n-maneuver sequence for any n. If $r_a > 11.94\ r_p$, the bi-elliptic transfer requires the least total impulsive Δv for an *n*-maneuver sequence.

   Reference: Ting

4. The effects of finite thrust on the results obtained from the impulsive model are treated in the reference by Zee.
5. For other information on optimal transfer between coplanar orbits, see the reference by Broucke and Prado. Also, see some of the many references cited therein for transfer between either coplanar or non-coplanar orbits.

Bi-elliptic Transfer

Notation: Let "OMi" denote orbital maneuver number i.

As shown in Fig. 3.9, the bi-elliptic transfer maneuvers are:

(a) OM1, which moves the spacecraft onto a transfer ellipse that travels well beyond the radius of the outer orbit.
(b) OM2, which raises the periapsis of the first transfer ellipse to equal the radius of the outer circle.
(c) OM3, which reduces the radius at apoapsis of the second transfer ellipse to equal the radius of the outer circle.

The Δv_{TOTAL} for the three maneuvers of a bi-elliptic transfer sequence is

$$\begin{aligned}\Delta v_{TOTAL} &= \Delta v_1 + \Delta v_2 + \Delta v_3 \\ &= \left(\sqrt{\frac{2\mu}{r_1} - \frac{2\mu}{r_1 + r_2}} - \sqrt{\frac{\mu}{r_1}}\right) + \left(\frac{r_f}{r_2}\sqrt{\frac{2\mu}{r_f} - \frac{2\mu}{r_f + r_2}} - \frac{r_1}{r_2}\sqrt{\frac{2\mu}{r_1} - \frac{2\mu}{r_1 + r_2}}\right) \\ &\quad - \left(\sqrt{\frac{\mu}{r_f}} - \sqrt{\frac{2\mu}{r_f} - \frac{2\mu}{r_f + r_2}}\right) \\ &= \sqrt{\frac{\mu}{r_1}}\left[\sqrt{\frac{2\frac{r_2}{r_1}}{1 + \frac{r_2}{r_1}}} - 1\right] + \sqrt{\frac{\mu}{r_2}}\left[\sqrt{\frac{2}{1 + \frac{r_2}{r_f}}} - \sqrt{\frac{2}{1 + \frac{r_2}{r_1}}}\right] + \sqrt{\frac{\mu}{r_f}}\left[\sqrt{\frac{2\frac{r_2}{r_f}}{1 + \frac{r_2}{r_f}}} - 1\right]\end{aligned} \tag{3.20}$$

where r_1 denotes the radius of the inner circular orbit, r_f the radius of the outer circular orbit, and r_2 the radius at apoapsis of the transfer ellipses from Exercise 3.12.

Example: The Δv savings for Bi-elliptic Transfer versus a Hohmann Transfer

Consider a spacecraft in a circular orbit about the earth at 200-km altitude. Compute the Δv savings for a transfer to a coplanar, circular orbit with 30 times the radius of the initial orbit if the bi-elliptic sequence transfers the spacecraft to an intermediate ellipse having a radius at apoapsis of 50 times the radius of the initial orbit.

Required data:

$r_1 = R_\oplus + 415$ km $= 6{,}793.14$ km (Approximate radius of the ISS on 5/19/2014).
$r_2 = 50 r_1$ km $= 339{,}657.00$ km.
$r_f = 30 r_1$ km $= 203{,}794.20$ km.
Gm of the earth $= 398{,}600.433$ km^3/s^2 from Exercise 2.3b.

From Eq. (3.20), the Δv values for the three maneuvers of the bi-elliptic transfer are:

$\Delta v_1 = 3.0662$ km/s
$\Delta v_2 = 0.7236$ km/s
$\Delta v_3 = 0.1651$ km/s

and the total

$\Delta v_{TOTAL} = 3.9549$ km/s

From Eq. (3.19), the Δv values for the two maneuvers of the Hohmann transfer are:

$\Delta v_1 = 2.9968$ km/s
$\Delta v_2 = 1.0433$ km/s

and the total

$\Delta v_{TOTAL} = 4.0401$ km/s,

providing a meager savings of 0.0852 km/s = 85.2 m/s.

Heuristic argument for the optimality of the bi-elliptic transfer over the Hohmann transfer if $r_a > 11.94 r_p$: When r_a/r_p is large, $\Delta v_1 \cong \Delta v_{esc}$. Once at a point whose distance is much greater than the r_a of Hohmann transfer, the corresponding Δv to raise periapsis is small. Therefore, the final reverse Δv plus the extra Δv applied to the first maneuver may be less than the Δv required to raise the periapsis to r_a in the second burn of Hohmann transfer (for impulsive Δvs).

For a proof of the optimality of the bi-elliptic transfer, we cite the reference by Hoelker and Silber.

The major disadvantage of the bi-elliptic transfer is that the transfer time is more than twice the Hohmann transfer time, while the Δv saving is modest. Increasing the transfer time increases operational costs. When the initial and final orbits are not in the same plane, significant Δv savings can be realized as discussed in Sect. 3.6.

Examples: Hohmann Transfer

Comparison of a Hohmann Transfer to Escape from a Low-Altitude Circular Orbit

An escape trajectory will take the spacecraft out of the gravitational field of one central body and into the gravitational field of another. For example, a spacecraft in orbit about the earth may be moved into a heliocentric orbit by increasing its speed with respect to the earth to escape speed, i.e., moving it into a parabolic orbit with respect to the earth as shown in Fig. 3.10. Therefore, escape velocity v_{esc} satisfies the Energy Equation for energy = 0. That is,

$$\frac{v_{esc}^2}{2} - \frac{\mu}{r} = 0$$

for any value of r. Solving this equation for the velocity of escape, we obtain

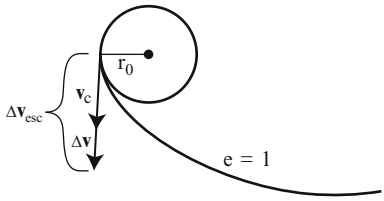

Fig. 3.10 Escape trajectory

$$v_{esc} = \sqrt{\frac{2\mu}{r_p}} = \sqrt{2}v_C \tag{3.21}$$

where r_p denotes the radius at closest approach on the parabolic orbit. Therefore, the velocity increment required to escape is

$$\Delta v_{esc} = v_{esc} - v_c = \left(\sqrt{2} - 1\right)\sqrt{\frac{\mu}{r_p}} \tag{3.22}$$

because $\mathbf{v_{esc}}$ and $\mathbf{v_c}$ are collinear.

If this amount of energy is used to raise the spacecraft to another orbit via a Hohmann transfer, its final radius is determined by equating

$$\Delta v_{esc} = \Delta v_1 + \Delta v_2$$

$$\left(\sqrt{2} - 1\right)\sqrt{\frac{\mu}{r_p}} = \sqrt{\frac{\mu}{r_p}}\left[\sqrt{\frac{2\frac{r_a}{r_p}}{1 + \frac{r_a}{r_p}}\left(1 - \frac{r_p}{r_a}\right)} + \sqrt{\frac{r_p}{r_a}} - 1\right]$$

and solving for r_a, as

$$r_a = 3.4\, r_p$$

If $r_a \geq 3.4\ r_p$, it takes less Δv for escape than to make a Hohmann transfer to a circular orbit of radius r_a.

Remarks:

(a) For an earth orbiter, "escape" refers to escaping the pull of earth's gravity, which means that the spacecraft goes into a heliocentric orbit (an orbit about the sun).

(b) A spacecraft in an elliptical orbit must still achieve

$$\frac{v^2}{2} - \frac{\mu}{r} = 0$$

to escape. That is,

$$\frac{v_{esc}^2}{2} = \frac{\mu}{r}$$

$$v_{esc} = \sqrt{2}v_c$$

Therefore,

$$\Delta v_{esc} = v_{esc} - v_r$$

if the $\mathbf{\Delta v}$ is applied to be collinear with $\mathbf{v_r}$.

(c) The escape condition has no restriction on the flight path angle β. A particle that is traveling at any angle whatever with the velocity v_{esc} or greater will escape

the parent body if it does not impact the central body or a satellite. Circular orbit conditions, on the other hand, cannot be achieved without realizing a specific angle $\beta = 0^\circ$ and a specific velocity $v = v_c$.

A Series of Comparisons with a Hohmann Transfer
For each example in the following series, the initial orbit is a circular earth orbit at 200-km altitude.

(a) Hohmann transfer to a geosynchronous orbit

$$r_p = 200\,\text{km} + R_\oplus = 6,578.14\,\text{km}$$

$$\tau_{GEO} = 2\pi\sqrt{\frac{{r_{GEO}}^3}{\mu}} = 23\ \text{h}\ 56\,\text{min}\ 4\,\text{s}$$

because $r = a$ if $e = 0$. Solving for the radius, we obtain

$$r_{GEO} = 42,164\,\text{km}$$

Using Eq. (3.19), we determine the Δv required to transfer from a 200-km altitude orbit about the earth to GEO is:

$$\Delta v_{TOTAL} = \Delta v_1 + \Delta v_2 = 2.45\,\text{km/s} + 1.48\,\text{km/s} = 3.93\,\text{km/s}$$

(b) Translunar injection
For translunar injection $r_a = r_M = 384{,}400$ km, the mean distance between the earth and the moon (Fig. 3.11). Using Eq. (3.16), we obtain

$$\Delta v_1 = 3.13\,\text{km/s} < 3.93\,\text{km/s (GTO)}$$

Therefore, the injection Δv that is capable of placing a payload (PL) into a GEO could send a more massive PL to the moon.

(c) Escape trajectory

$$\Delta v_{esc} = v_{esc} - v_c = \left(\sqrt{2} - 1\right)\sqrt{\frac{\mu}{r_p}} = 3.22\,\text{km/s} < 3.93\,\text{km/s (GTO)}$$

which implies that we can send a more massive PL into a heliocentric orbit than we can transfer to GEO.

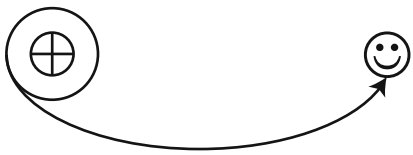

Fig. 3.11 Translunar injection

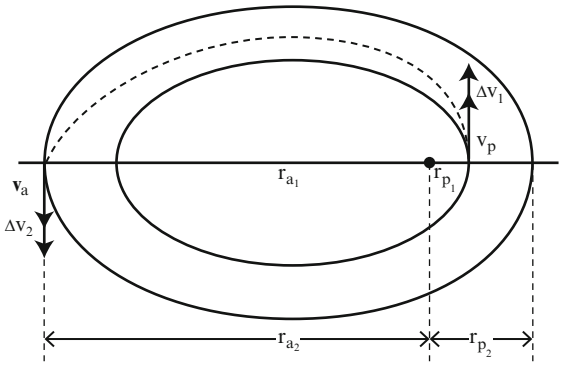

Fig. 3.12 Transfer between coplanar coaxial elliptical orbits

General Coplanar Transfer Between Circular Orbits

I encourage the student to read pp. 166–169 of the text by Bate, Mueller and White as an exercise for learning about the general coplanar transfer between circular orbits. We will discuss transfer trajectories other than the Hohmann transfer in Chap. 4 and the material in BMW may be helpful for understanding the approach.

Transfer Between Coplanar Coaxial Elliptical Orbits

We consider the transfer from periapsis on the inner ellipse shown in Fig. 3.12 to the apoapsis of the outer elliptical orbit. The total velocity for the two-impulse sequence is

$$\Delta v_{\text{Total}} = \Delta v_1 + \Delta v_2$$

where

$$\Delta v_1 = v_{p_t} - v_{p_1} = \sqrt{\frac{2\mu}{r_{p_1}} - \frac{2\mu}{r_{p_1} + r_{a_2}}} - \sqrt{\frac{2\mu}{r_{p_1}} - \frac{2\mu}{r_{p_1} + r_{a_1}}}$$

$$\Delta v_2 = v_{a_2} - v_{a_t} = \sqrt{\frac{2\mu}{r_{a_2}} - \frac{2\mu}{r_{p_2} + r_{a_2}}} - \sqrt{\frac{2\mu}{r_{a_2}} - \frac{2\mu}{r_{p_1} + r_{a_2}}}$$

and parameters for the inner ellipse are labeled with a subscript "1", those for the outer ellipse with a subscript "2" and the transfer ellipse with a subscript "t." Such a transfer is also called a "Hohmann transfer."

Now let us consider a thought exercise. We consider an alternate maneuver sequence as shown in Fig. 3.13. In this sequence, the first maneuver is performed at apoapsis of the inner ellipse to increase the height at periapsis to that of the outer orbit and then the second maneuver is performed at the periapsis of the outer orbit to raise the height at apoapsis to match that for the outer ellipse. Let us call the Δv

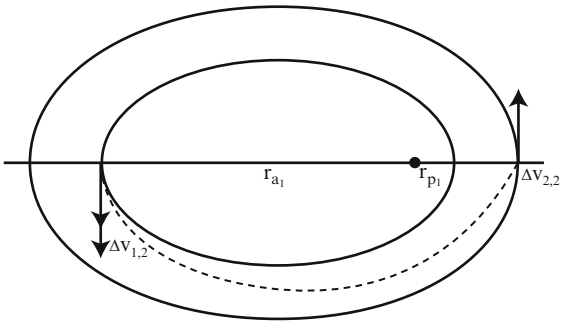

Fig. 3.13 Alternate maneuver sequence

changes $\Delta v_{1,2}$ and $\Delta v_{2,2}$ to stand for the first and second Δv, respectively. Call the total for this second maneuver strategy

$$\Delta v_{TOTAL2} = \Delta v_{1,2} + \Delta v_{2,2}$$

My question is: How does this second total compare to the first? Is

$$\Delta v_{TOTAL2} > \Delta v_{TOTAL}$$
$$\Delta v_{TOTAL2} = \Delta v_{TOTAL}$$
$$\Delta v_{TOTAL2} < \Delta v_{TOTAL}$$

Explain your answer. (See Exercise 3.19.)

3.5 Interplanetary Trajectories

In this section, we study two types of interplanetary trajectories. For a flyby mission, Fig. 3.14 shows that the spacecraft has been launched into a circular parking orbit about the earth. From there, the craft performs a propulsive maneuver to transfer into a hyperbolic trajectory about the earth. When it moves into the sun's gravity field, it transfers into an elliptical orbit about the sun. As it approaches Venus, it enters a hyperbola about that planet. When it leaves Venus, it enters another heliocentric ellipse that is not the same one as it traveled in before Venus encounter. So Venus has changed the spacecraft's trajectory. For the orbiter mission, the trajectory is the same until arrival at Venus, when a Venus Orbit Insertion (VOI) is performed. This maneuver decreases the spacecraft's energy with respect to Venus so that the spacecraft inserts into an elliptical orbit about the planet.

Hyperbolic Trajectories

Let $e > 1$.

As shown in Fig. 3.15, the spacecraft travels along the incoming asymptote until it is attracted by the gravitational force of the large body at F, which causes it to

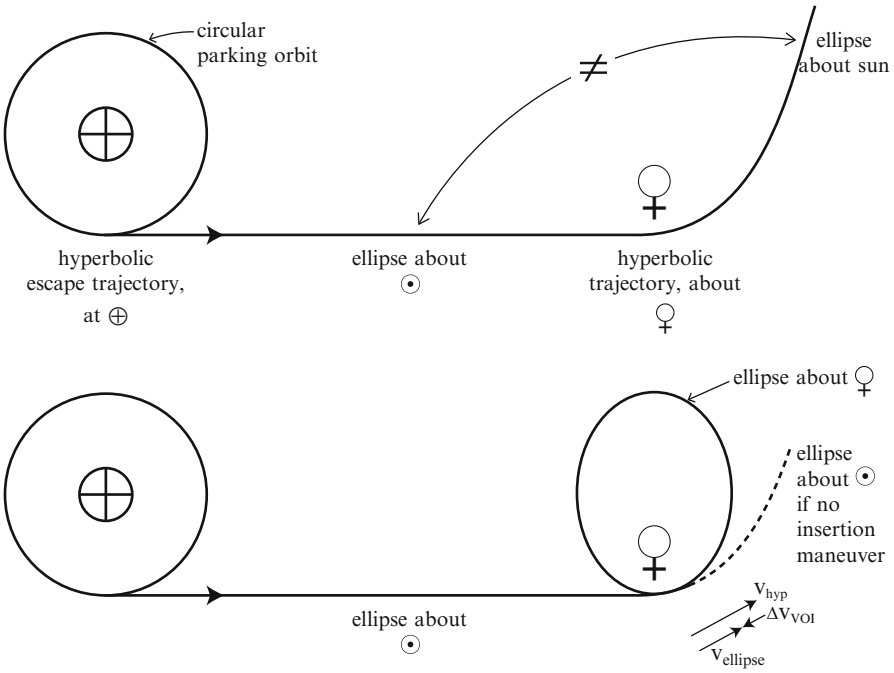

Fig. 3.14 Interplanetary trajectories. *Upper panel*: Flyby mission. *Lower panel*: Orbiter mission

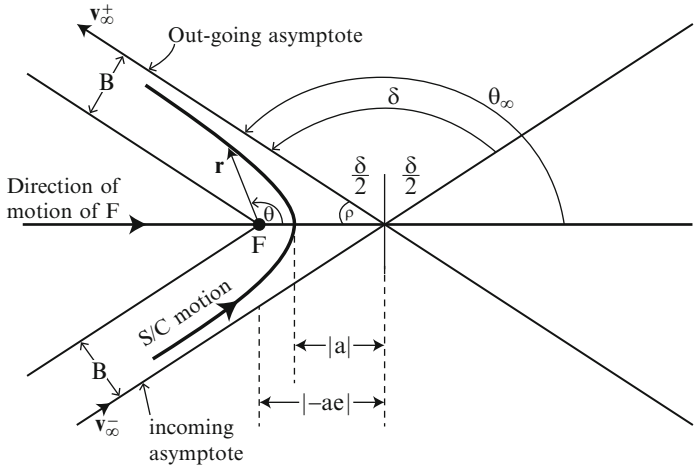

Fig. 3.15 Hyperbolic trajectory

swing around the center axis and approach the outgoing asymptote after the flyby of the central body. The point where $\theta = 0$ is called the "point of closest approach" or the "encounter point."

Consider what happens in the limit as r approaches infinity.

$$\lim_{r\to\infty} \mathscr{E} = \lim_{r\to\infty} \left(\frac{v^2}{2} - \frac{\mu}{r}\right) = -\frac{\mu}{2a}$$

But $-\mu/r$ approaches 0 and the energy is constant, so v must approach a limit which we denote as $\mathbf{v}_\infty{}^+$. Therefore,

$$\lim_{r\to\infty} \mathscr{E} = \frac{\left(v_\infty^+\right)^2}{2} = -\frac{\mu}{2a}$$

Similarly, imagine that the spacecraft travels backwards to $-\infty$, so that we would obtain

$$\lim_{r\to-\infty} \mathscr{E} = \frac{\left(v_\infty^-\right)^2}{2} = -\frac{\mu}{2a}$$

Since these two limits are equal, we define v_∞ such that

$$v_\infty^- = v_\infty^+ = v_\infty \tag{3.23}$$

Define

B = the distance between the focus F and the asymptotes (This parameter will be introduced later as the "impact parameter.")
θ_∞ = the true anomaly of the (outgoing) asymptote
$\mathbf{v}_\infty^-$ = the hyperbolic approach velocity vector
$\mathbf{v}_\infty^+$ = the hyperbolic departure velocity vector
δ = the deflection angle of the $\mathbf{v}_\infty$ = the angle between the incoming and outgoing asymptotes = (aka) the turn angle = the amount the $\mathbf{v}_\infty$ is turned during the flyby
ρ = the hyperbolic asymptote angle

Def.: The hyperbolic excess velocity (v_∞) is the speed that a vehicle on an escape trajectory has in excess of escape speed. This residual is the speed the vehicle would have even at infinity. That is,

$$v_\infty = \lim_{r\to\infty} (v)$$

where v denotes the velocity magnitude and r denotes the magnitude of the position vector.

Therefore, the energy equation can be written for hyperbolic trajectories as follows:

$$\frac{v^2}{2} - \frac{\mu}{r} = \frac{v_\infty^2}{2} = -\frac{\mu}{2a} \tag{3.24}$$

Solving Eq. (3.24) for a, we obtain

$$a = -\frac{\mu}{v_\infty^2} \tag{3.25}$$

which is a function of v_∞. Note that a is negative. Also,

$$r_p = a(1 - e) \tag{3.26}$$

by the same argument used in proving this result for elliptical orbits in Exercise 2.10a. Solving this equation for e and substituting for a using Eq. (3.25), we obtain

$$e = 1 - \frac{r_p}{a} = 1 + \frac{r_p v_\infty^2}{\mu} \tag{3.27}$$

which is a function of r_p and v_∞, the fundamental parameters for flyby analyses.

At periapsis, the Energy Equation gives

$$\frac{v_p^2}{2} - \frac{\mu}{r_p} = \frac{v_\infty^2}{2}$$

Solving this equation for v_p, we obtain

$$v_p = \sqrt{v_\infty^2 + \frac{2\mu}{r_p}} \tag{3.28}$$

which gives v_p as a function of the fundamental parameters.

Determine θ_∞, δ, and ρ. Each of these parameters is a measure of the bending of a hyperbolic trajectory. Solving the Conic Equation for $\cos\theta$ and taking the limit as r approaches infinity, we obtain

$$\cos\theta_\infty = \lim_{r\to\infty}\left[\frac{1}{e}\left\{\frac{p}{r} - 1\right\}\right] = -\frac{1}{e} \tag{3.29}$$

Therefore,

$$\theta_\infty = \cos^{-1}\left(-\frac{1}{e}\right) \tag{3.30}$$

It is geometrically obvious that

$$\theta_\infty = \frac{\delta}{2} + \frac{\pi}{2} \tag{3.31}$$

From Eqs. (3.30) and (3.31), we obtain

$$\frac{1}{e} = \sin\left(\frac{\delta}{2}\right) \tag{3.32}$$

Solving for δ,

$$\delta = 2\sin^{-1}\left(\frac{1}{e}\right) \tag{3.33}$$

It is geometrically obvious that

$$\rho = \frac{\pi}{2} - \frac{\delta}{2} \tag{3.34}$$

From Eqs. (3.32) and (3.34)

$$\cos\rho = \frac{1}{e} \tag{3.35}$$

$$\rho = \cos^{-1}\left(\frac{1}{e}\right) \tag{3.36}$$

Angular momentum:

From Eqs. (3.17), (3.26), and (3.28),

$$h = r_p v_p = r_p\sqrt{v_\infty^2 + \frac{2\mu}{r_p}} = \sqrt{a^2(1-e)^2 v_\infty^2 + 2\mu a(1-e)}$$

$$= \sqrt{\left(\frac{-\mu}{v_\infty^2}\right)^2 (1-e)^2 v_\infty^2 + 2\mu\left(\frac{-\mu}{v_\infty^2}\right)(1-e)}$$

and simplifying this result gives

$$h = \frac{\mu}{v_\infty}\sqrt{e^2 - 1} \tag{3.37}$$

Def.: The impact vector **B** is the vector from the center of mass of the target body to the incoming asymptote that is orthogonal to the incoming asymptote. We call the magnitude of the **B** the "impact parameter."

Notice that B is the distance from F to the incoming asymptote, not the distance to the trajectory (Fig. 3.16).

From Exercise 3.10 and a formula for the semiminor axis,

$$B = -b = -a\sqrt{e^2 - 1}$$

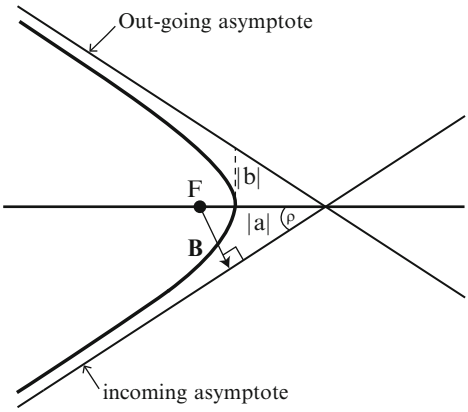

Fig. 3.16 Impact vector **B**

Multiplying this equation by v_∞ and using Eq. (3.25), we obtain

$$h = v_\infty B = v_\infty |b| = \frac{\mu}{v_\infty}\sqrt{(e^2 - 1)} \tag{3.38}$$

Recall that, from Eq. (3.27),

$$e = 1 + \frac{r_p}{\mu} v_\infty^2$$

So the shape of the hyperbolic trajectory depends on the closest approach distance r_p, the speed at ∞, and the Gm of the planet.

Recall that

$$\frac{1}{e} = \sin\left(\frac{\delta}{2}\right)$$

from Eq. (3.32). From this equation we see that a large value of e implies a small δ. Therefore, a large e implies little bending.

Small μ (i.e., small target body mass) implies large e, which implies little bending. That is, there is a small attraction from gravity.

Large r_p implies large e, which implies little bending. That is, the spacecraft is too far away to sense the mass of the body.

Large v_∞ implies large e, which implies little bending. That is, the spacecraft is moving too fast to sense the body.

If the v_∞ and r_p are known, then the other parameters (a, e, $\mathscr{E}$, θ_∞, δ, and h) can be computed from these equations. The v_∞ is determined by the interplanetary flight path and the injection vehicle capability.

Gravity Assist

Consider a spacecraft that is in orbit about the primary body and has an encounter with a secondary body, e.g., primary body is the sun and the secondary is a planet.

Define:
$\mathbf{v}^-$, $\mathbf{v}^+$ = the inertial spacecraft (absolute) velocity vectors with respect to the primary body before and after the flyby of the secondary body, respectively.
$\mathbf{v}^-_{\infty/\mathbf{sec}}, \mathbf{v}^+_{\infty/\mathbf{sec}}$ = the spacecraft velocity vectors at infinity with respect to the secondary body before (incoming $\mathbf{v}_\infty$) and after (outgoing $\mathbf{v}_\infty$) the flyby, respectively.
$\mathbf{v}_{\text{sec}}$ = the secondary body's inertial velocity vector with respect to the primary body at the time of the encounter. (In the example, $\mathbf{v}_{\text{sec}}$ is the planet's heliocentric velocity vector.)

The spacecraft travels along a heliocentric trajectory to approach the target secondary body. The absolute velocity vector on approach is $\mathbf{v}^-$ and the incoming $\mathbf{v}_\infty$ with respect to the secondary body is $\mathbf{v}^- - \mathbf{v}_{\mathbf{sec}}$ as shown in Fig. 3.17a. The spacecraft encounters the secondary body and, after the flyby, its relative velocity vector approaches the outgoing velocity vector $\mathbf{v}_{\infty/\mathbf{sec}}{}^+$. The outgoing absolute velocity vector is $\mathbf{v}^+ = \mathbf{v}^+_{\infty/\mathbf{sec}} + \mathbf{v}_{\mathbf{sec}}$.

During the encounter the $\mathbf{v}_{\infty/\mathbf{sec}}$ is rotated through δ deg as shown in Fig. 3.17b. Its magnitude does not change because energy is conserved with respect to the secondary body (2-body mechanics). However, there is a change in the magnitude and/or direction of the $\mathbf{v}$ with respect to the primary body. This change adds a $\Delta\mathbf{v}_{\mathbf{GA}} = \mathbf{v}^+ - \mathbf{v}^-$ to the spacecraft's velocity as shown in Fig. 3.17b.

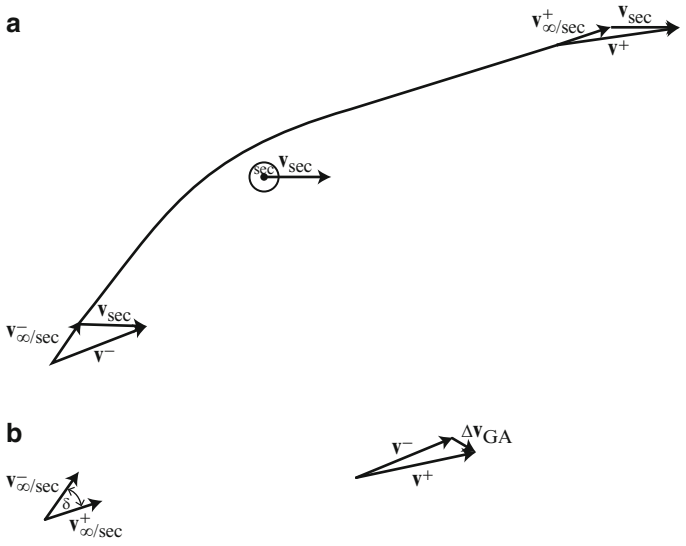

Fig. 3.17 (**a**) Gravity assist flyby. (**b**) Effects of gravity assist

The change in spacecraft energy with respect to the primary is provided through an exchange of energy with the secondary body, i.e., from the angular momentum of the secondary in orbit about the primary to the spacecraft. Since the secondary body is many times more massive than the spacecraft, the velocity change of the secondary is insignificant.

Thus, we have the following equations.

Relative approach velocity:

$$\mathbf{v}_{\infty/\,\mathrm{sec}}^{-} = \mathbf{v}^{-} - \mathbf{v}_{\mathrm{sec}} \tag{3.39}$$

Absolute approach velocity:

$$\mathbf{v}^{-} = \mathbf{v}_{\mathrm{sec}} + \mathbf{v}_{\infty/\,\mathrm{sec}}^{+} \tag{3.40}$$

Absolute departure velocity:

$$\mathbf{v}^{+} = \mathbf{v}_{\mathrm{sec}} + \mathbf{v}_{\infty/\,\mathrm{sec}}^{+} \tag{3.41}$$

Note the assumption that $\mathbf{v}_{\mathrm{sec}}$ and $\mathbf{r}_{\mathrm{sec}}$ are constant during the flyby. This is similar to the impulsive maneuver assumption and is based on the fact that the duration of the flyby is much less than the period of the secondary.

The change in absolute velocity is

$$\Delta\mathbf{v}_{\mathrm{GA}} = \mathbf{v}^{+} - \mathbf{v}^{-} = \mathbf{v}_{\infty/\,\mathrm{sec}}^{+} - \mathbf{v}_{\infty/\,\mathrm{sec}}^{-} \tag{3.42}$$

Note: This equation is a vector subtraction.

Def.: The use of a celestial body to change the velocity of a spacecraft during a flyby is called the gravity assist technique of navigation.

Figure 3.18a displays the hyperbolic trajectory for a spacecraft that passes in front of the secondary body. Figure 3.18b displays the vector diagram for this trajectory. Note that the $\mathbf{v}^{+}{}_{\infty/\mathbf{sec}}$ and $\mathbf{v}^{-}{}_{\infty/\mathbf{sec}}$ shown in Fig. 3.18b are drawn parallel to the corresponding vectors in Fig. 3.18a. Figure 3.19a exhibits the hyperbolic trajectory for passage behind the secondary body and Fig. 3.19b gives the corresponding vector diagram. The v_∞ vectors in Fig. 3.19b are also parallel to the v_∞ vectors in Fig. 3.19a. Note that Figs. 3.15 and 3.19a show the special case in which the $\mathbf{r_p}$ is along the $\mathbf{v_{sec}}$. Also, the secondary body is designated as F in these figures.

By selecting the spacecraft's trajectory to pass in front of or behind the secondary body, the orbital energy of the spacecraft can be decreased or increased, respectively. This fact can be seen by observing that, in the vector diagram Fig. 3.18, the magnitude of the incoming v_∞ vector is greater than the magnitude of the outgoing vector and that the reverse is true in Fig. 3.19b. Figures 3.18 and 3.19b display the result given in Eq. (3.42).

The concept of gravity assist was documented as early as the late 1700s by D'Alembert and Laplace. Specific applications of the gravity assist technique are considered in Subsect. 3.5, "Types and Examples of Interplanetary Missions".

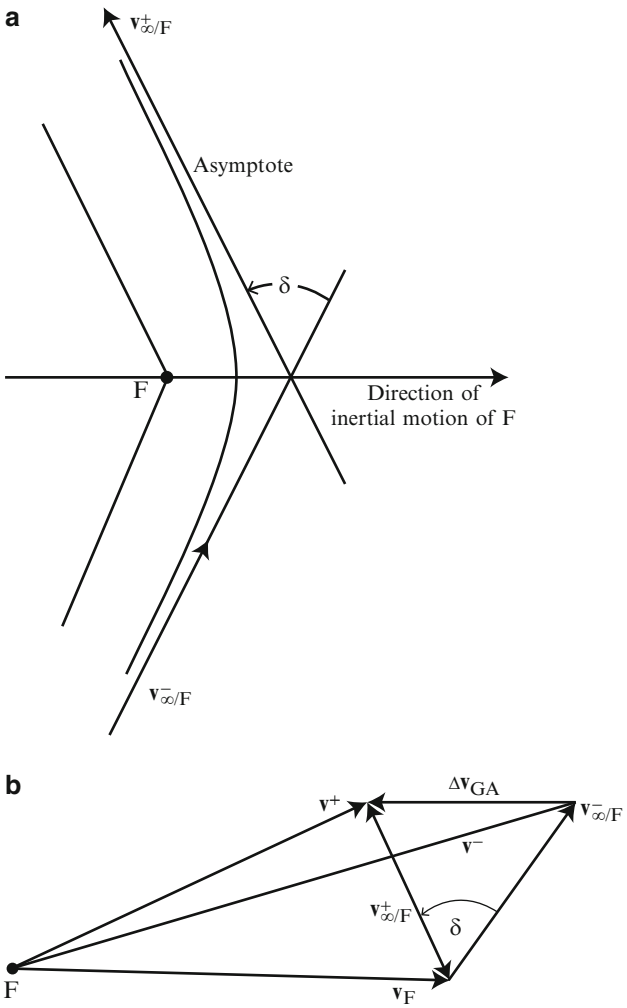

Fig. 3.18 Vector diagram for passage in front of the secondary body

References for Gravity Assist: Brouke 2001; Cesarone; Diehl and Nock; Doody; Kaplan; Strange and Longuski; Uphoff, Roberts, and Friedman

Patched Conics Trajectory Model

We look at an interplanetary trajectory model that consists of:

1. An escape trajectory along a hyperbola at earth.
2. A transfer trajectory—a heliocentric ellipse.

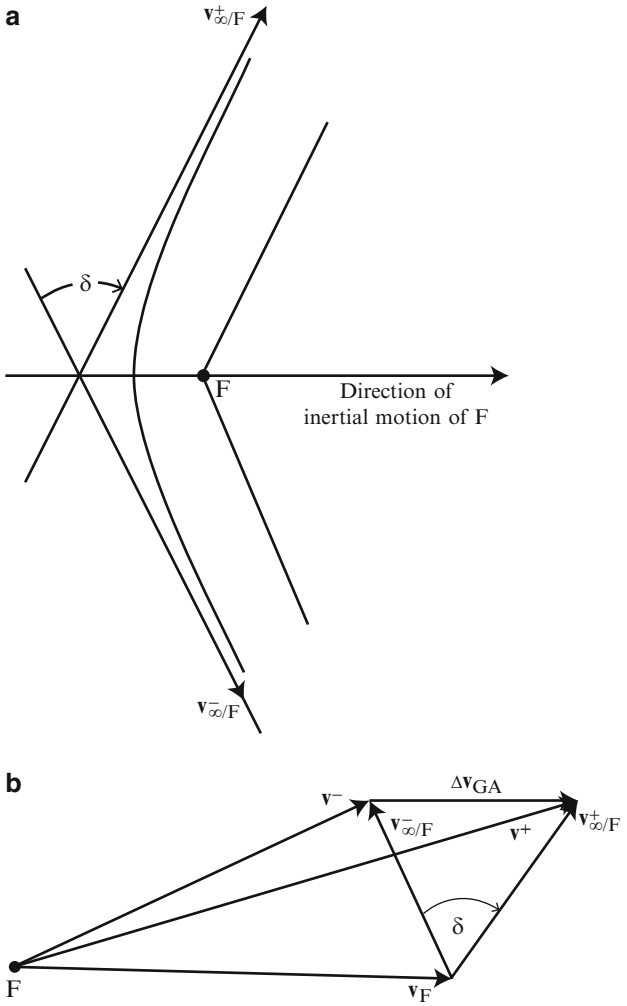

Fig. 3.19 (**a**) Hyperbolic passage behind the secondary body. (**b**) Vector diagram for passage behind the secondary body

3. An approach trajectory—a hyperbola at the target body.
4. Another heliocentric ellipse.

This model uses 2-body mechanics in each of four conic segments that are patched together in the position vector and the velocity vector. The spacecraft is one of the two bodies in each segment.

Example (Venus Flyby)
Consider a Hohmann transfer from a 200-km-altitude, circular, earth orbit to pass at a 500-km altitude on the sunlit side of Venus. The spacecraft would leave a LEO parking orbit on a hyperbolic escape trajectory, then travel on a heliocentric trajectory to a Venus hyperbolic flyby and continue on into a different heliocentric ellipse.

Comments:
1. Each segment is a 2-body problem. In each segment, we use the μ (Gm) of the central body for that phase and the distance r to the center of that central body. The Gm values are available from Exercise 2.3b.
2. We use an inward Hohmann transfer ellipse with Venus at periapsis ($r_p = r_{♀}$)and the earth at apoapsis ($r_a = r_{⊕}$) as shown in Fig. 3.20. Of course we do not insist that a transfer from earth to another planet always be done via a Hohmann transfer. But, by looking at a Hohmann transfer, we know we need at least the amount of Δv determined for this transfer.
3. We assume the motion of Venus and the spacecraft are in the ecliptic plane. (But the method can be applied to more general cases.) We assume all the orbits are coplanar.
4. We assume the orbits of the earth and Venus and the parking orbit are circular.
5. Def.: The sphere of influence of a celestial body is the region in three-dimensional space in which its gravitational force is the dominant gravitational force.

Def.: A zero sphere of influence means that the gravitational force is modeled as being applied impulsively at the celestial body.

The Venus-flyby example uses the zero sphere of influence assumption at earth and Venus to include the effects of the masses of these bodies on the trajectory.

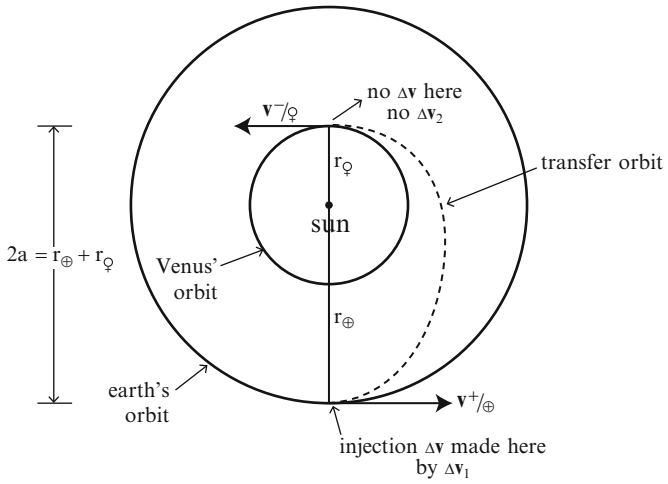

Fig. 3.20 Inward Hohmann transfer to Venus

6. Some terminology is appropriate here

General term	Sun	Earth
Periapsis	Perihelion	Perigee
Apoapsis	Aphelion	Apogee

7. "Sunlit side" and "sunny side" refer to the side of the secondary body towards the sun, the dayside. That is, the spacecraft is passing between the sun and the secondary. "Dark side" refers to the side of the secondary opposite the sun, the night side. "In front of" means that the spacecraft passes through the path of the secondary in front of the secondary, i.e., before the secondary gets to the point in the orbit where the spacecraft crosses the secondary's orbit. "Passing behind" refers to crossing the orbit of the secondary after the secondary has gone through that point in its orbit. So, as a word of caution, "sunlit side" does not refer to passage in front of the secondary and "dark side" does not refer to passage behind the secondary. (That information is the answer to a FAQ.)

Hyperbolic Escape from Earth

1. Velocities at Escape from Earth
   The absolute velocity of the spacecraft as it escapes the earth $\mathbf{v}^+ =$ the aphelion velocity of the Hohmann transfer ellipse. The spacecraft must leave the earth with escape velocity (speed) = aphelion velocity (speed) of the transfer ellipse. For the spacecraft's transfer trajectory,

$$\mathscr{E} = \frac{v_a^2}{2} - \frac{\mu_\odot}{r_p} = \frac{-\mu_\odot}{2a_t} \tag{3.43}$$

   where $v_a = v^+$ outgoing from the earth and $r_a = r_\oplus = 1$ AU. Thus,

$$\mathscr{E} = \frac{(v^+)^2}{2} - \frac{\mu_\odot}{r_\oplus} = \frac{-\mu_\odot}{2a_t}$$

   where $a_t = (r_\oplus + r_\varphi)/2 = 1.289 \times 10^8$ km and r_φ denotes the mean distance between Venus and the sun. Therefore,

$$v^+ = \sqrt{\mu_\odot \left(\frac{2}{r_\oplus} - \frac{1}{a_t}\right)} = 27.286\,\text{km/s} \tag{3.44}$$

   outgoing from the earth. The orbital velocity of the earth is

$$v_\oplus = \sqrt{\frac{\mu}{r_\oplus}} = 29.785\,\text{km/s} \tag{3.45}$$

   which is the velocity of the spacecraft when it is sitting on the surface of the earth. Since $v_\oplus > v^+$, earth escape must be opposite $\mathbf{v}_\oplus$ as shown in Fig. 3.21.

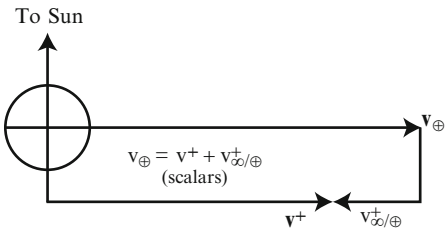

Fig. 3.21 Determining the $\mathbf{v}_\infty{}^+$ at earth escape

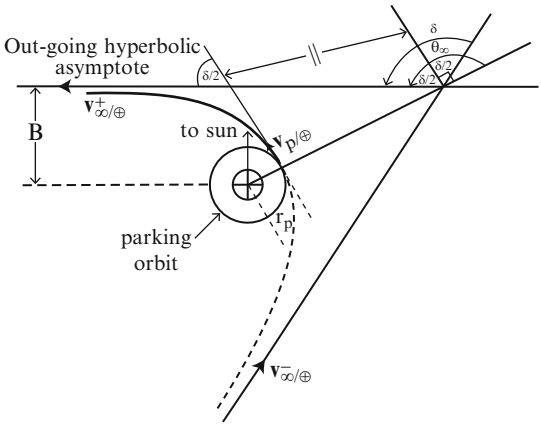

Fig. 3.22 Hyperbolic escape from the earth

The v^+ is determined by subtracting part of the spacecraft's velocity, which equals the earth's velocity. $v_\infty{}^+$ is the speed relative to the earth after escape, which must be $|\mathbf{v}_\oplus - \mathbf{v}^+|$ for the spacecraft to reach Venus at periapsis.

That is,

$$\left|\mathbf{v}^+_{\infty/\oplus}\right| = |\mathbf{v}_\oplus - \mathbf{v}^+| \tag{3.46}$$

(Helpful Hintz: Use the ABS function in MATLAB to evaluate this absolute value so you can use the same computer code for both inward and outward transfers.) For transfer to Venus,

$$\left|\mathbf{v}^+_{\infty/\oplus}\right| = \mathbf{v}_\oplus - \mathbf{v}^+ = 2.499\,\mathrm{km/s}$$

$\mathbf{v}_{\infty/\oplus}{}^+$ is the speed relative to the earth after escape.

2. Hyperbolic Escape Path

The hyperbolic escape path from the parking orbit is obtained by reducing the speed of the spacecraft so it drops behind the earth and moves toward the sun along the transfer ellipse as shown in Fig. 3.22.

Solving the Energy Equation for the required perigee velocity, we obtain

$$v_{p/\oplus} = \sqrt{\left(v_{\infty/\oplus}\right)^2 + \frac{2\mu}{r_{p/\oplus}}} = 11.289\,\text{km/s} \tag{3.47}$$

where $r_{p/\oplus} = R_\oplus + h_p = 6{,}578.14$ km. This value is the velocity at perigee of the escape hyperbola after applying the Δv_{inj} to enable the spacecraft to just reach the orbit of Venus. The value of this injection Δv is

$$v_{inj} = v_{p/\oplus} - \sqrt{\frac{\mu_\oplus}{r_{p/\oplus}}} = (11.289 - 7.784)\,\text{km/s} = 3.504\,\text{km/s} \tag{3.48}$$

This injection Δv is supplied by the upper (usually the third) stage of the launch vehicle.

For a hyperbolic trajectory, the shape of the orbit is given as

$$e = 1 + \frac{r_{p/\oplus} v_{\infty/\oplus}^2}{\mu} = 1.103 > 1.0 \tag{3.49}$$

Also,

$$\theta_{\infty/\oplus} = \cos^{-1}\left(-\frac{1}{e}\right) = 155.0^\circ \tag{3.50}$$

The deflection of the velocity vector between $\mathbf{v}_{\mathbf{p}/\oplus}$ and $\mathbf{v}_{\infty/\oplus}$ is

$$\delta/2 = \theta_\infty - 90^\circ = 65.0^\circ \tag{3.51}$$

The escape path is displaced toward the sun by

$$B = \frac{\mu_\oplus}{v_\infty^2}\sqrt{e^2 - 1} = 2.97 \times 10^4\,\text{km} \tag{3.52}$$

Therefore, the actual aphelion of transfer is slightly less than $r_\oplus$. There are two approaches to this situation. The reference by BMW takes this effect into account. However, Kaplan chooses to assume that the difference is negligible because $B \ll r_p$. We will ignore the difference for simplicity. I encourage you to consider both of these models to determine the significance of this approximation.

After earth escape, the heliocentric transfer begins along an ellipse about the sun. We make the escape trajectory at earth produce the heliocentric ellipse. That is, we patch together a hyperbola about the earth and a heliocentric ellipse, which has the velocity vector needed to arrive at Venus.

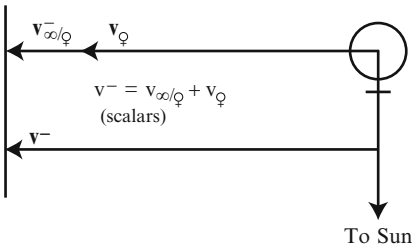

Fig. 3.23 Vector diagram at the approach to Venus

Hyperbolic Approach at Venus

1. Velocities at Venus Approach

   At Venus, the spacecraft is moving faster at the periapsis of its orbit than Venus. This trajectory is an inward Hohmann transfer without the Δv performed at Venus. The velocity at Venus, ignoring the presence of Venus, is $\mathbf{v}^-$ = the absolute (inertial) velocity at approach to Venus.

   From the conservation of angular momentum, Eq. (3.17),

$$h_t = r_\oplus v^+ = r_♀ v^- \tag{3.53}$$

   where the v^+ is at earth and the v^- is at Venus and $r_♀$ is the mean distance between Venus and the sun. Therefore,

$$v^- = \frac{r_\oplus}{r_♀} v^+ = 37.740\ \text{km/s} \quad v_♀ = \sqrt{\frac{\mu_\odot}{r_♀}} = 35.029\ \text{km/s} \tag{3.54}$$

   Hence, $v^- > v_♀$ as expected for the inward Hohmann transfer. Therefore, the vector diagram for the approach to Venus is as displayed in Fig. 3.23.

   In this figure, we see that

$$v_{\infty/♀} = v^- - v_♀ = (37.740 - 35.029)\,\text{km/s} = 2.711\,\text{km/s} \tag{3.55}$$

   We again recommend using the ABS function in MATLAB to compute

$$v_{\infty/♀} = \text{ABS}(v^- - v_♀)$$

   so that your MATLAB software will cover both inward and outward Hohmann transfers.

2. Hyperbolic Approach Path

   The shape of the approach conic hyperbolic orbit is

$$e = 1 + \frac{r_{p_♀} v^2_{\infty/♀}}{\mu_♀} = 1.148 > 1 \tag{3.56}$$

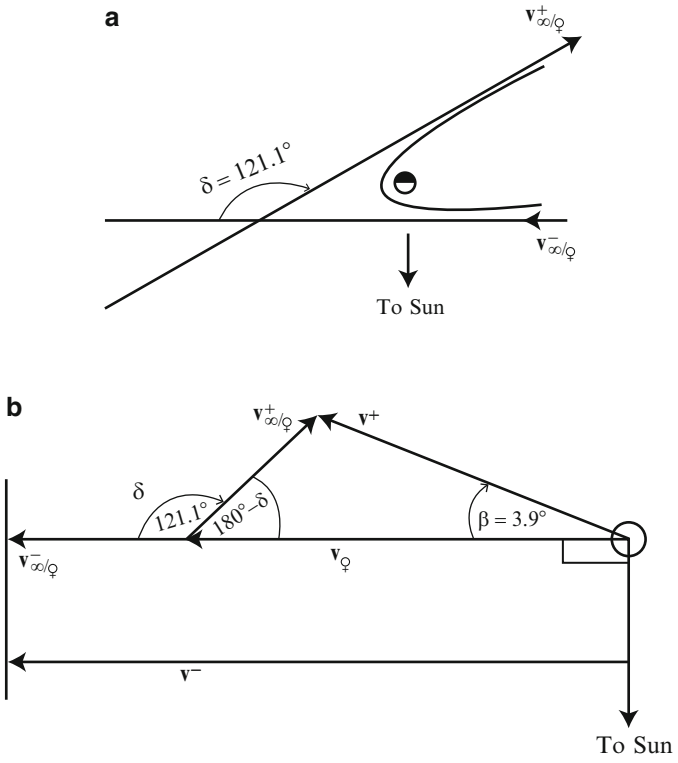

Fig. 3.24 (**a**) Hyperbolic passage at venus. (**b**) Gravity assist vector diagram at venus encounter

where

$$r_{p_\varphi} = \left(R_\varphi + 500\right) \text{ km} = 6,551.9 \text{km and } v_{\infty/\varphi} = 2.711 \text{km/s}$$

Therefore, the deflection of $\mathbf{v}_{\infty/\varphi}$ is

$$\delta = 2 \sin^{-1}\left(\frac{1}{e}\right) = 121.1° \tag{3.57}$$

which provides the gravity assist diagram in Fig. 3.24a.

The corresponding gravity assist vector diagram is shown in Fig. 3.24b.

Note: The Venus velocity vector is orthogonal to Venus's position vector relative to the sun because of the assumption that Venus's orbit is circular. Therefore, the angle between $\mathbf{v}_\varphi$ and $\mathbf{v}^+$ in Fig. 3.24b is the flight path angle β.

Given that δ, v_∞ and v_φ are known, we can now use the Law of Cosines to compute

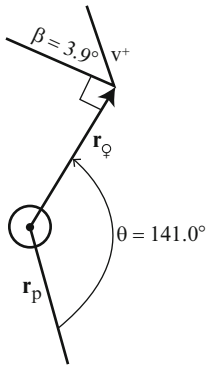

Fig. 3.25 Location in post-Venus elliptical orbit

$$(v^+)^2 = v_{\infty/♀}^2 + v_♀^2 - 2v_{\infty/♀}v_♀ \cos(180° - \delta) = 1,136.2\,\text{km}^2/\text{s}^2$$
$$v^+ = 33.707\,\text{km/s}$$

Using the Law of Cosines again and solving for β, we compute

$$\beta = (\text{sgn}\beta)\cos^{-1}\left(\frac{v_♀^2 + (v^+)^2 - v_{\infty/♀}^2}{2v_♀v^+}\right) = 3.9°$$
$$\text{where sgn}\beta = \begin{cases} +1 \text{ if } \beta > 0 \\ -1 \text{ if } \beta < 0 \end{cases}$$

When the spacecraft passes on the sunlit side of Venus, as in our example, sgn β = + 1.

Elliptical Post-Venus Helicentric Orbit

$$r \cong r_♀ = 1.0821 \times 10^8\,\text{km}$$
$$v = v^+ = 33.707\,\text{km/s}$$
$$\beta = 3.9°$$

From Eq. (3.3a),

$$e^2 = (X_0 - 1)^2\cos^2\beta + \sin^2\beta = 0.0102$$
$$\text{where } X_0 = \frac{rv^2}{\mu_\odot} = 0.9260 < 1.0$$

Then, the shape parameter e = 0.101 < 1 for an elliptical orbit. The location in orbit (Fig. 3.25) is given by

$$\tan\theta = \frac{X_0 \sin\beta\cos\beta}{X_0\cos^2\beta - 1} = -0.8109$$

$$\theta = 141.0^\circ \text{ or } 321.0^\circ$$

$\beta > 0$ implies that $0^\circ < \theta < 180^\circ$ from Eq. (2.25)

so that $\theta = 141.0^\circ$

Also,

$$r_{p_\odot} = \frac{h^2/\mu_\odot}{1+e} = 9.05 \times 10^7 \text{ km}$$

where $h = rv\cos\beta = 3.6378 \times 10^9$ km^2/s^2 from Eq. (3.2).
Using Eq. (2.17) and the equation $p = a(1-e^2)$, we solve for a to obtain

$$a = \frac{h^2}{\mu_\odot(1-e^2)} = 1.007 \times 10^2 \text{ km}$$

$$\tau = 2\pi\sqrt{\frac{a^3}{\mu_\odot}} = 201.73 \text{ days}$$

Therefore, the post-Venus elliptical orbit is nearly circular with period close to Venus's 224.7-day orbit. A Venus year = 224.7 earth days and a Venus day = 243 earth days. So a Venus day is longer than a Venus year.

Summary Remarks on the Patched Conics Model:

1. For Venus and Mercury, $v^+ < v_\oplus$ at departure from the earth and $v^- > v_{TB}$ at arrival at the target body (TB). Recall the inward Hohmann transfer conditions. The inward trajectory is shown in Fig. 3.26a, the vector diagram for the escape trajectory at the earth in Fig. 3.26b, and the vector diagram for the arrival at the target body in Fig. 3.26c.
2. For Mars through Neptune, $v^+ > v_\oplus$ at departure and $v^- < v_{TB}$ at arrival. Recall the outward Hohmann transfer. Trajectory and vector diagrams for outward patched conics are given in Fig. 3.27.

References for the Patched Conics Trajectory Model: BMW, Battin 1999, Chobotov, and Kaplan

Types and Examples of Interplanetary Missions

Types:

1. A flyby of a planet in a hyperbolic orbit.

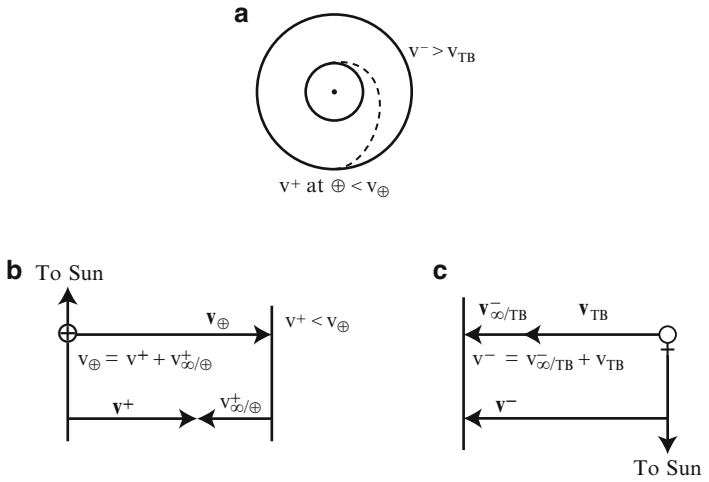

Fig. 3.26 Patched conics for inward transfer. (**a**) Inward Hohmann transfer. (**b**) Vector diagram for departure from earth. (**c**) Vector diagram for arrival at target body

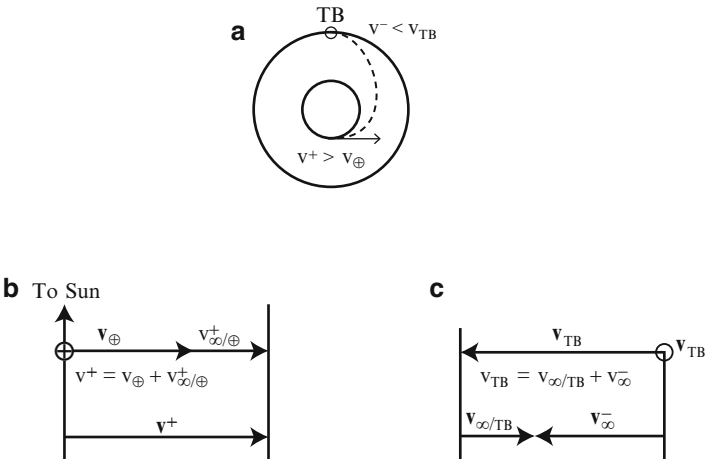

Fig. 3.27 Patched conics for outward transfer. (**a**) Outward Hohmann transfer. (**b**) Vector diagram for departure from earth. (c) Vector diagram for arrival at target body

2. An orbiter makes a hyperbolic approach and applies a $\Delta\mathbf{v}$ to reduce its energy (speed) to enter an elliptic orbit about the target body.
3. Soft landers are sent to the surface of target body, e.g., Viking, Phoenix and MSL to the surface of Mars, NEAR (later called "NEAR-Shoemaker") to the asteroid Eros.

Fig. 3.28 Mariner 10 to Venus and Mercury. Reference: http://www.jpl.nasa.gov/missions/missiondetails.cfm?mission=Mariner10

4. Probes, hard landers, e.g., Pioneer Venus Multiprobes to Venus and the Galileo Probe to Jupiter.

Examples of Gravity Assist Missions:

Example 1: Mariner Venus Mercury aka Mariner 10 (1973)
Mariner 10 made the first application of gravity assist in mission navigation. One gravity assist flyby of Venus and three of Mercury reduced the energy of the spacecraft's orbit (Fig. 3.28).

Example 2: The Grand Tour
A favorable configuration of four planets, Jupiter, Saturn, Uranus, and Neptune, occurs every 179 years. The most recent opportunity occurred in 1975–1981 and the next will be in 2154. (The last occurrence before 1975 happened during the administration of Thomas Jefferson, but he passed up the opportunity in favor of the expedition of Lewis and Clark.) Grand tour trajectories are shown parametrically in launch year in Fig. 3.29.

Example 3: Pioneer X (1972) and XI (1973)
The Pioneer X and XI spacecraft received gravity assists that will send them out of the Solar System.

Example 4: Voyager I (1977) and II (1977)
Voyager I and II received gravity assists that will send them out of the solar system and, in fact, Voyager I has been determined to have left the solar system. Both

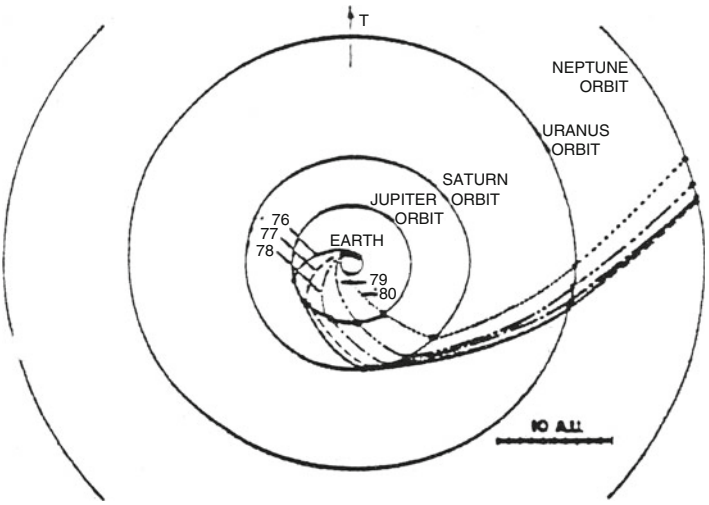

Fig. 3.29 Grand Tour trajectories

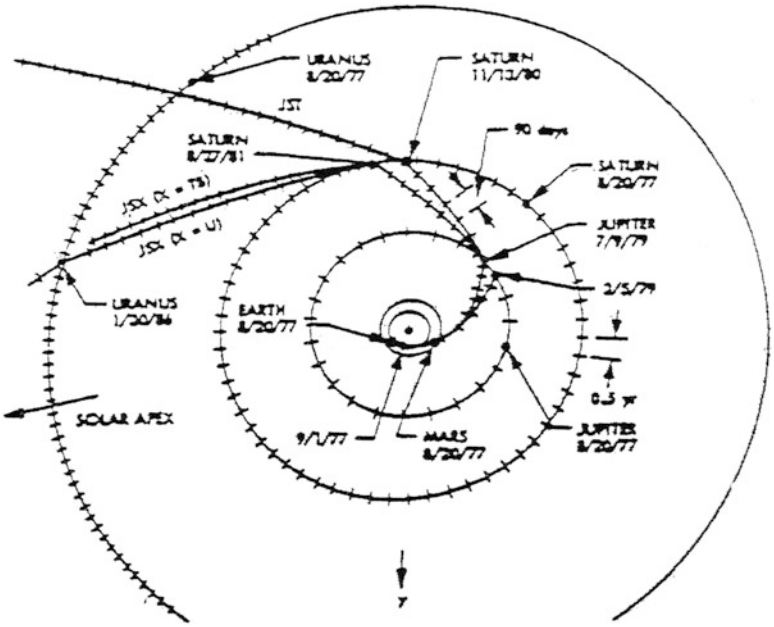

Fig. 3.30 Ecliptic-plane view of Voyager II trajectories

spacecraft were originally targeted to flyby Titan, a moon of Saturn. After, Voyager I flew successfully past Titan, Voyager II was retargeted to Uranus and onward to complete the Grand Tour. Notice in Fig. 3.30 that Voyager II was originally called

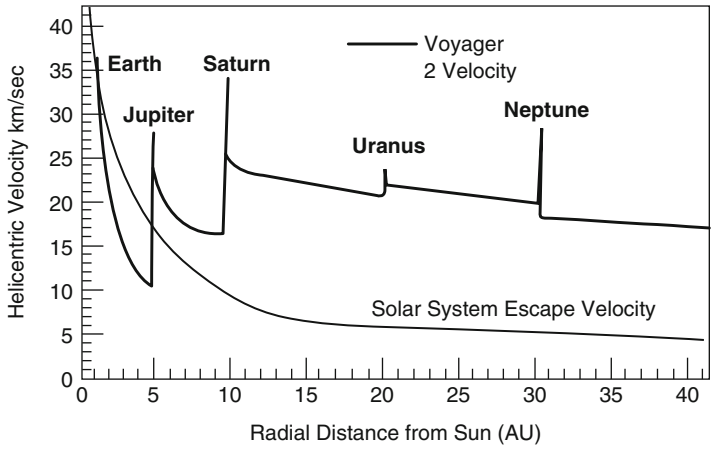

Fig. 3.31 Voyager II gravity assist velocity changes

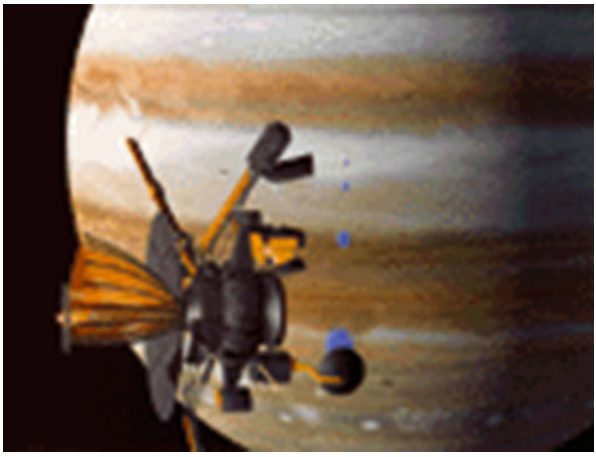

Fig. 3.32 The Galileo spacecraft

JSX, where the J denoted Jupiter, S Saturn, and the X either stood for Titan, if Voyager was unsuccessful, or Uranus otherwise.

Figure 3.31 shows the Gravity-Assist Velocity changes for Voyager II at Jupiter, Saturn, Uranus, and Neptune. Notice that Voyager II's velocity was increased enough at Jupiter to escape the solar system (SS), because its velocity exceeded the escape velocity. Its speed was increased again at Saturn and Uranus and then decreased at Neptune, but remained sufficient for SS escape.

Example 5: Galileo (1989)
Figure 3.32 gives an artist's picture of the Galileo spacecraft at Jupiter. Figure 3.33 shows Galileo's Venus–Earth–Earth Gravity Assist (VEEGA) trajectory to Jupiter. Note that Galileo flew by Venus once and the earth twice to gain enough energy to

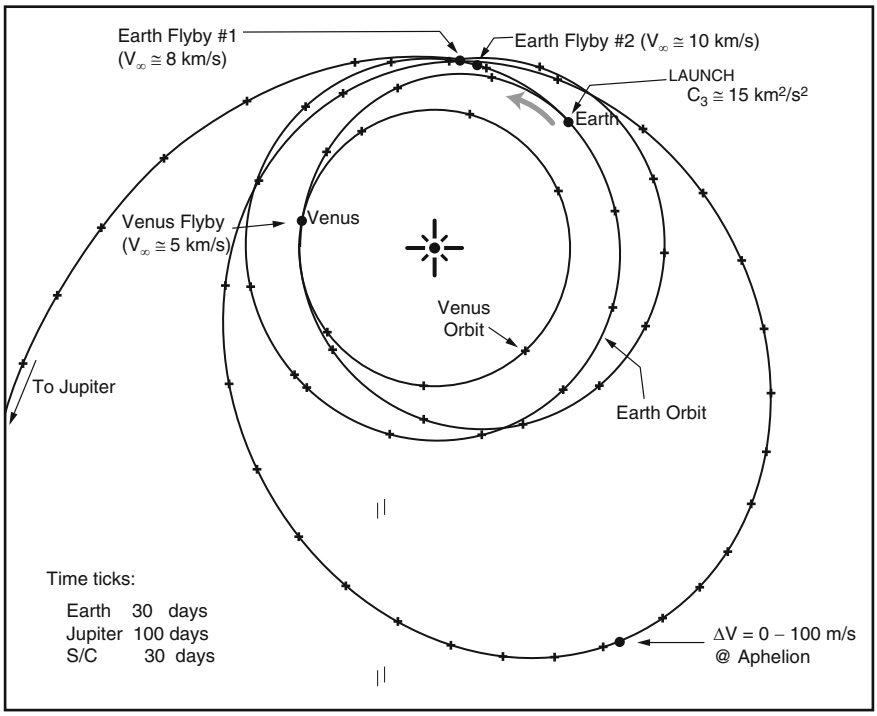

Fig. 3.33 Galileo's VEEGA trajectory to Jupiter

reach Jupiter. (The original plan was for Galileo to fly a direct (no gravity assists) trajectory to Jupiter. But, after the Challenger disaster, which occurred on the launch immediately before Galileo's launch, NASA decided that it was not safe for the astronauts to fly with so much liquid propellant onboard. So the Galileo could not rely on a liquid upper stage. But a solid rocket could not fly a direct trajectory. Roger Diehl, at JPL, discovered the VEEGA trajectory, which Galileo did fly.)

Example 6: Ulysses (1990)
Figure 3.34 provides an artist's concept of the Ulysses spacecraft.

Reference: http://www.jpl.nasa.gov/missions/missiondetails.cfm?mission=Ulysses

Figure 3.35 shows a typical overview of the trajectory. Note that the orbits of the earth and Jupiter appear to be elliptical because they are rotated so that the trajectory of the spacecraft is in the plane of the picture. The gravity assist at Jupiter performed a plane change that moved the spacecraft out of the ecliptic plane and up to 80° latitude with respect to the sun.

Example 7: Cassini–Huygens (1997)
The Cassini–Huygens spacecraft flew a VVEJGA interplanetary trajectory, receiving gravity assists at Venus twice, the earth, and Jupiter (Fig. 3.36). After performing its Saturn Orbit Insertion maneuver, the orbiter sent the Huygens probe to Titan from the elliptical orbit.

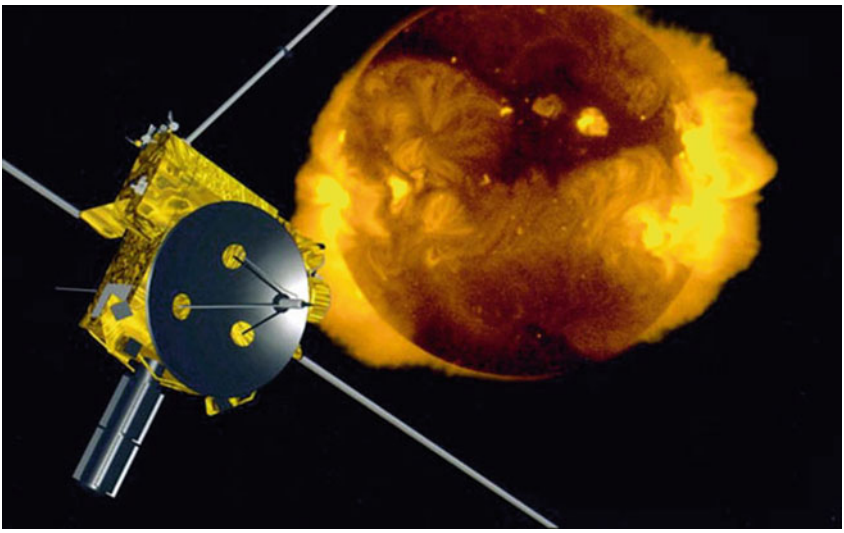

Fig. 3.34 Ulysses Solar Polar Mission

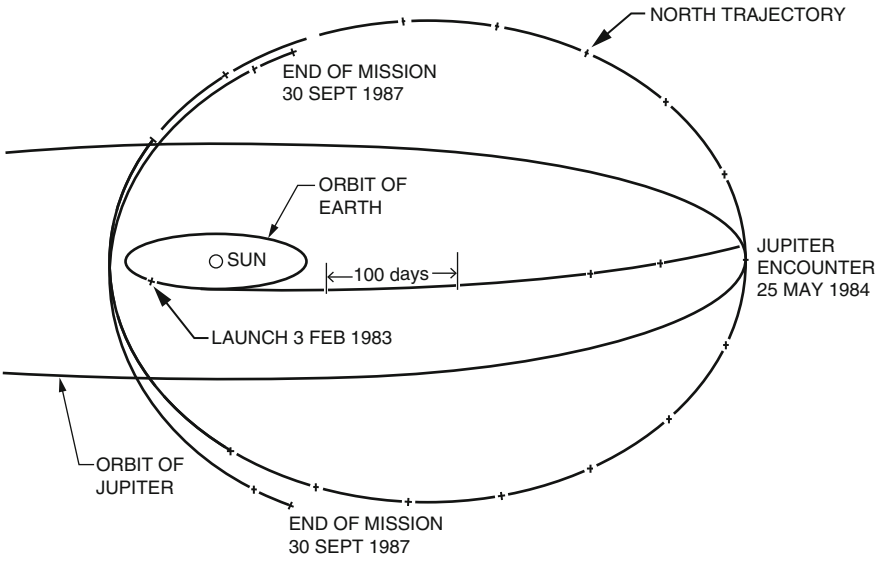

Fig. 3.35 Ulysses trajectory overview

Example 8: First Commercial Gravity Assist Mission (1998)
A satellite that was intended for a geostationary orbit over Asia was left stranded in an unusable orbit at launch on December 25, 1997. Since the spacecraft was in good condition with 3,700 lbs of propellant, Hughes Global Services performed a series

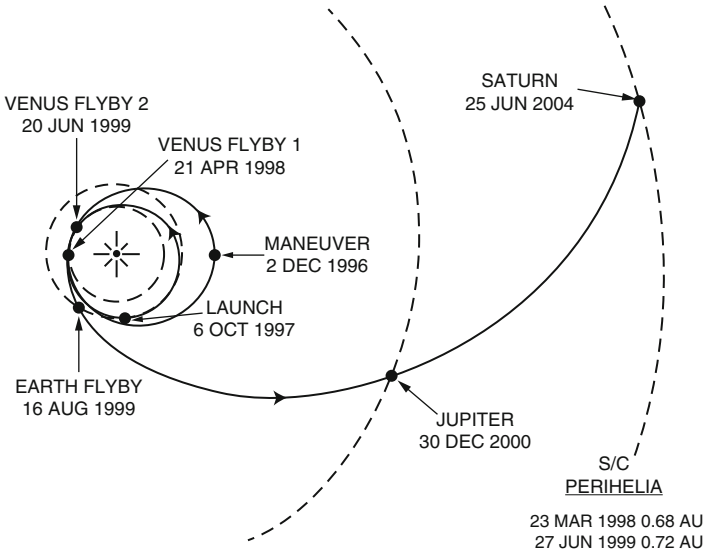

Fig. 3.36 Cassini–Huygens VVEJGA trajectory

of maneuvers to raise the apoapsis of the spacecraft to produce a lunar swingby on May 13, 1998, followed by another lunar swingby on June 6, 1998. On June 14, 1998, the spacecraft was inserted into a geostationary orbit of the earth.

Example 9: HAYABUSA nee MUSES-C (2003)

Objective: To make observations and collect samples of asteroid Itokawa (nee 1998SF36) for return to earth.

HAYABUSA made an earth gravity assist (EGA) in the spring of 2004 and arrived at the asteroid in the summer of 2005. The original plan was to depart in the winter of 2005, but it actually returned to earth in the summer of 2007, arriving at the earth on June 14, 2010.

Reference: JAXA's Website at http://www.jaxa.jp/projects/index_e.html

JAXA denotes the Japanese Aerospace Exploration Agency (Japanese Space Agency).

Example 10: Messenger (2004)

A launch slip changed Messenger's trajectory from V^3M^2 (Venus three times-Mercury twice) to EV^2M^3 (earth-Venus twice-Mercury three times as shown in Fig. 3.37). Notice the introduction here of five Deep Space Maneuvers (DSM), which usually are large maneuvers performed at a long distance from any celestial bodies to set up a gravity assist flyby.

Gravity assist trajectories provide energy changes without using propellant, which reduces the mass launch requirements. However, there is a disadvantage because such trajectories delay the arrival at the mission destination, which increases operations costs.

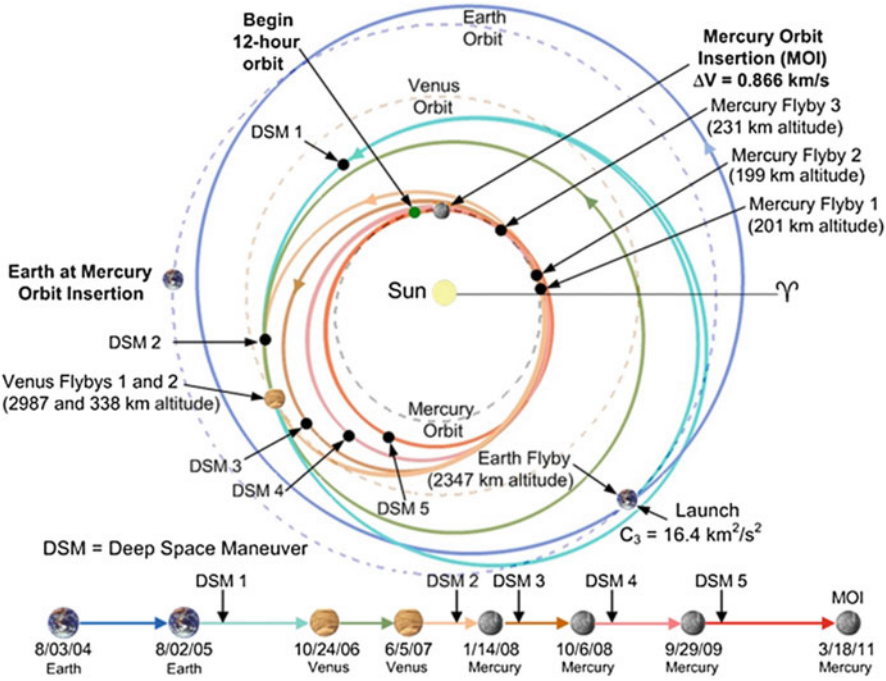

Fig. 3.37 Messenger's EV^2M^3 trajectory. Reference: http://messenger.jhuapl.edu/the_mission/trajectory.html

Target Space

To aim our trajectory so the spacecraft will encounter our target body successfully, we define the encounter aiming plane or B plane shown in Fig. 3.38 as follows.

Def.: The B plane with R, T, S axes is defined so that the RT plane is orthogonal to the incoming asymptote at the target body. The T axis is parallel to a reference plane (e.g., the equator of the target body or the ecliptic plane); the S axis is along the direction of the incoming asymptote; and the R axis completes the right-handed coordinate system.

Def.: The impact vector **B** is the vector in the B plane from the center of mass of the target body to the intersection of the spacecraft's incoming asymptote with the B plane. We call the magnitude of the B vector the "impact parameter."

Note: The "tip" of the B vector is the point where the incoming asymptote pierces the B-plane, not the trajectory.

Figure 3.39 shows the relative size of the interplanetary aiming zones for several NASA missions. Since the missions considered in this figure have been completed, the aiming (success) zones have shrunk drastically.

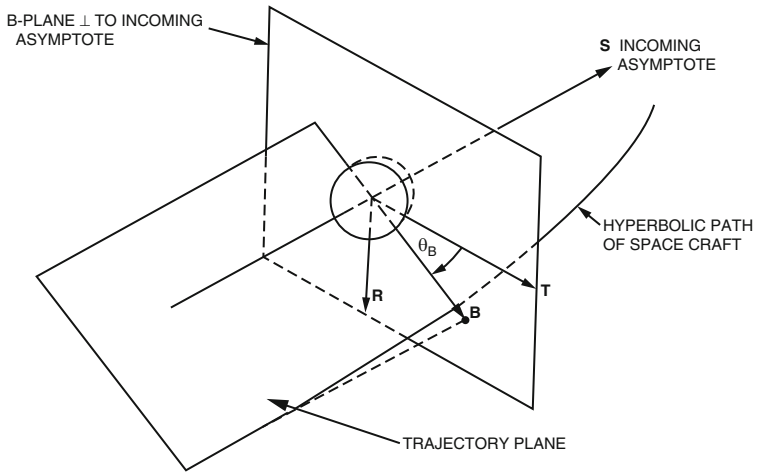

Fig. 3.38 Encounter aiming plane (the B plane)

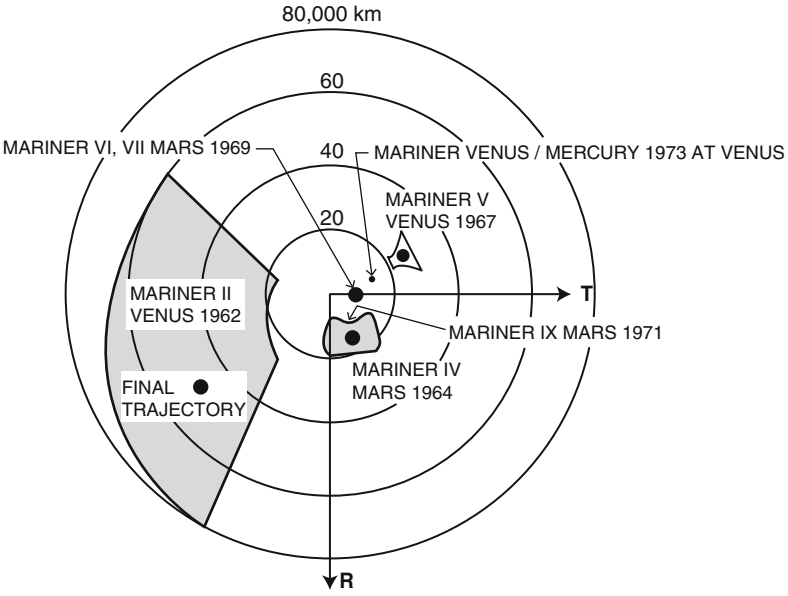

Fig. 3.39 Relative size of interplanetary aiming zones

Now imagine that you are working on the Navigation Team for a space mission. You have to consider three trajectories as shown in Fig. 3.40. First, there is the nominal or reference trajectory which would impact the B plane at the desired point. Then there is the estimated trajectory that members of your team have determined using orbit determination software. You, as the maneuver analyst (flight

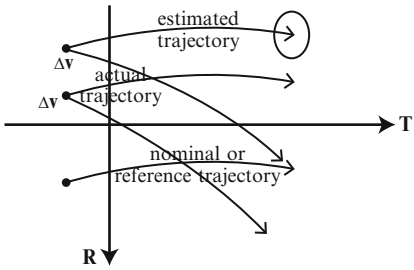

Fig. 3.40 Three trajectories

path control member) of your team, will use the estimated trajectory to compute TCM parameters that will move the spacecraft from the estimated trajectory to the nominal impact point in the B plane. Finally, there is the actual trajectory that we will never know exactly, although we will get better and better solutions for it as we reconstruct the trajectory. The maneuver will be applied to the actual trajectory. We will not achieve the nominal impact point exactly because of the OD errors experienced when estimating the trajectory and maneuver execution errors experienced in executing the TCM, plus other errors we will discuss in Chap. 5.

The reasons for using the B plane in these analyses are:

1. It provides an initial guess for the $\mathbf{\Delta v}$ that leads to rapid convergence to the final velocity correction, using precision software.
2. Errors experienced at the TCM can be mapped linearly to delivery errors in the B-plane for analyzing and comparing OD solutions. (We state this result without proof, leaving the derivation to an OD course that uses a textbook such as TSB.)

   An analog to the B plane is used for Rutherford scattering, which is an inverse square central force, but is a repulsive force.

   Let

$$\mathbf{B} = \left(\mathbf{B} \cdot \hat{\mathbf{T}}\right)\hat{\mathbf{T}} + \left(\mathbf{B} \cdot \hat{\mathbf{R}}\right)\hat{\mathbf{R}}$$

   Suppose you have determined that the miss in the B space is

$$\mathbf{m} = (\Delta\mathbf{B} \cdot \mathbf{R}, \Delta\mathbf{B} \cdot \mathbf{T}, \Delta\text{LTF})$$

   Therefore, you must introduce a change in the B space of **–m**. So you set

$$-\mathbf{m} = \mathbf{K}\mathbf{\Delta v}$$

where

$$\mathbf{K} = \frac{\partial \mathbf{m}}{\partial \mathbf{v}} = \begin{bmatrix} \frac{\partial \mathbf{B}\cdot\mathbf{R}}{\partial v_1} & \frac{\partial \mathbf{B}\cdot\mathbf{R}}{\partial v_2} & \frac{\partial \mathbf{B}\cdot\mathbf{R}}{\partial v_3} \\ \frac{\partial \mathbf{B}\cdot\mathbf{T}}{\partial v_1} & \frac{\partial \mathbf{B}\cdot\mathbf{T}}{\partial v_2} & \frac{\partial \mathbf{B}\cdot\mathbf{T}}{\partial v_3} \\ \frac{\partial \mathrm{LTF}}{\partial v_1} & \frac{\partial \mathrm{LTF}}{\partial v_2} & \frac{\partial \mathrm{LTF}}{\partial v_3} \end{bmatrix}$$

Therefore,

$$\Delta \mathbf{v} = -\mathbf{K}^{-1}\mathbf{m} \quad \text{if } K^{-1} \text{ exists.} \tag{3.58}$$

The linearized time of flight LTF = the time to go from the spacecraft's location directly to the center of the target body. The spacecraft is not going to fly to the center of the target body. But this variable has a very desirable characteristic. This parameter is orthogonal to the B-plane so TCMs designed to correct B-plane errors leave LTF unchanged and vice versa. The LTF can be written as

$$\mathrm{LTF} = T_{CA} - \frac{\mu}{2v_\infty^2} \ln\left(1 + \frac{B^2 v_\infty^4}{\mu^2}\right) \tag{3.59}$$

where T_{CA} = the time to closest approach from the spacecraft's location. (We state this result without proof.) The quantity we take the natural logarithm of in Eq. (3.59) is the square of the eccentricity written in terms of the impact parameter B as seen in Exercise 3.18.
Reference: Kizner

Interplanetary Targeting and Orbit Insertion Maneuver Design Technique

Selecting a planetary encounter aimpoint and a spacecraft propulsive maneuver strategy usually involves tradeoffs of many competing factors. The reference by Hintz 1982 describes such a tradeoff process and its applications to the Pioneer Venus Orbiter mission. This method uses parametric data spanning a region of acceptable targeting aimpoints in the delivery space, plus geometric considerations. Trajectory redesign features exercised in flight illustrate the insight made available in solving the interplanetary targeting and orbit insertion maneuver (OIM) problems. Real-time maneuver adjustments accounted for known attitude control errors, orbit determination updates, and late changes in a targeting specification. An elementary maneuver reconstruction technique is also considered.

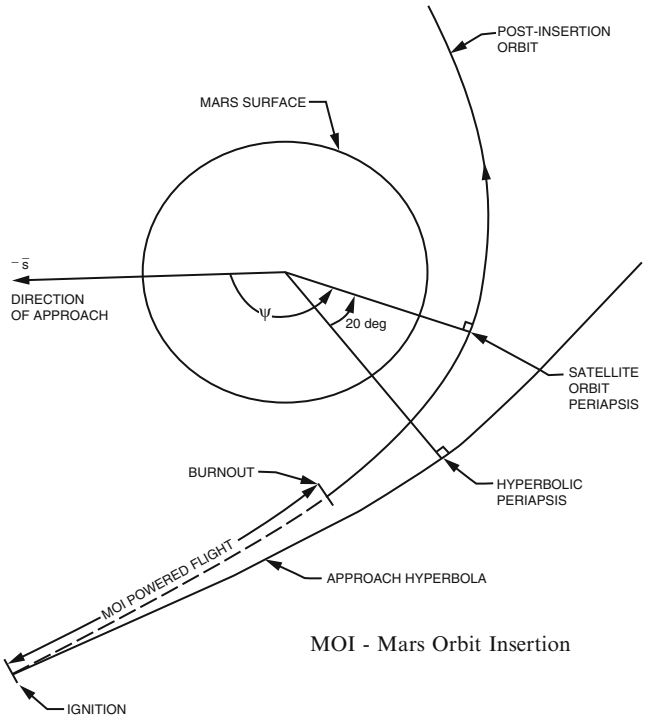

Fig. 3.41 Orbit insertion geometry for a large positive apsidal rotation

3.6 Other Spacecraft Maneuvers

We have looked at in-plane maneuvers between elliptic orbits. Next, we will consider an in-plane maneuver from a hyperbolic trajectory to an elliptical one.

Orbit Insertion

Figure 3.41 shows a 40-min powered flight from the approach hyperbolic trajectory into an elliptical trajectory about Mars. In performing this maneuver, the line of apsides on the hyperbola is rotated 20° to the line of apsides on the ellipse. Notice that our impulsive burn model will not accurately model this MOI maneuver. In our exercises, we will simplify our model so that there is no apsidal rotation and the maneuver is impulsive.

Examples:

1. Viking (1975)
   $\Delta v_{MOI} \cong 1{,}100$ mps and the duration of the burn $\cong$40 min. Therefore, we needed a finite burn model in our software.

2. Pioneer Venus Orbiter (1978)
   $\Delta v_{VOI} \cong 1{,}100$ mps and the duration of the burn was ≅30 s. Why so large a difference in burn duration? Ans.: We used a solid rocket for the VOI. (We will discuss rockets and propellants in Sect. 3.7.)
3. Mars Odyssey (2001)
   Figure 3.42a shows the sequence of events in performing the MOI for the 2001 Mars Odyssey spacecraft. Times are given relative to the start of MOI. Figure 3.42b shows how the trajectory was viewed from earth, whereas Fig. 3.42a is rotated to show all the events. Notice that the spacecraft disappeared from our view during the burn and completed the burn during the occultation. The engineers working in Mars Odyssey operations did not know if the burn had been performed nominally until after the end of the occultation, a DSN antenna acquired the spacecraft, and the OD data were processed on earth.

   The measure of the price we pay for needing to perform finite burns instead of impulsive maneuvers is the gravity losses, which are defined as follows.

Def.: Gravity losses (or finite burn losses) = finite burn Δv − impulsive Δv.

There are two kinds of finite burn losses during an insertion burn:

1. The Δv is not applied exactly at periapsis on the hyperbolic trajectory.
2. The $\mathbf{\Delta v}$ is not applied exactly along the velocity vector.

The $\mathbf{\Delta v}$ is usually fixed in inertial space. An exception was the SOI performed at Saturn by Cassini, which rotated during the burn to reduce the offset of the $\mathbf{\Delta v}$ from the velocity vector. Thus, the finite burn losses were reduced.

Example (impulsive Δv computation for orbit insertion):

In Exercise 3.16, you will compute the magnitude of the impulsive $\mathbf{\Delta v}$ that would transfer the spacecraft from the hyperbolic approach trajectory to an elliptical orbit about the target body. This transfer is accomplished by subtracting the $\mathbf{\Delta v}$ from the velocity vector on the approach trajectory at periapsis to acquire the elliptical orbit as shown in Fig. 3.43.

Plane Rotation

So far we have looked at maneuvers that are in the orbit plane. Next we will add a $\mathbf{\Delta v}$ that is not in the orbit plane so that the spacecraft will move into another orbit plane. We begin by making the following definition.

Def.: A pure rotation maneuver is a spacecraft maneuver that changes the orbit plane without changing the orbit shape or energy.

In a pure rotation maneuver, all the velocity change goes into plane change, just as before when all of the velocity change produced in-plane changes of energy or shape. By defining such a maneuver, we are able to produce orthogonal vectors that will add to achieve both the required in-plane and out-of-plane changes.

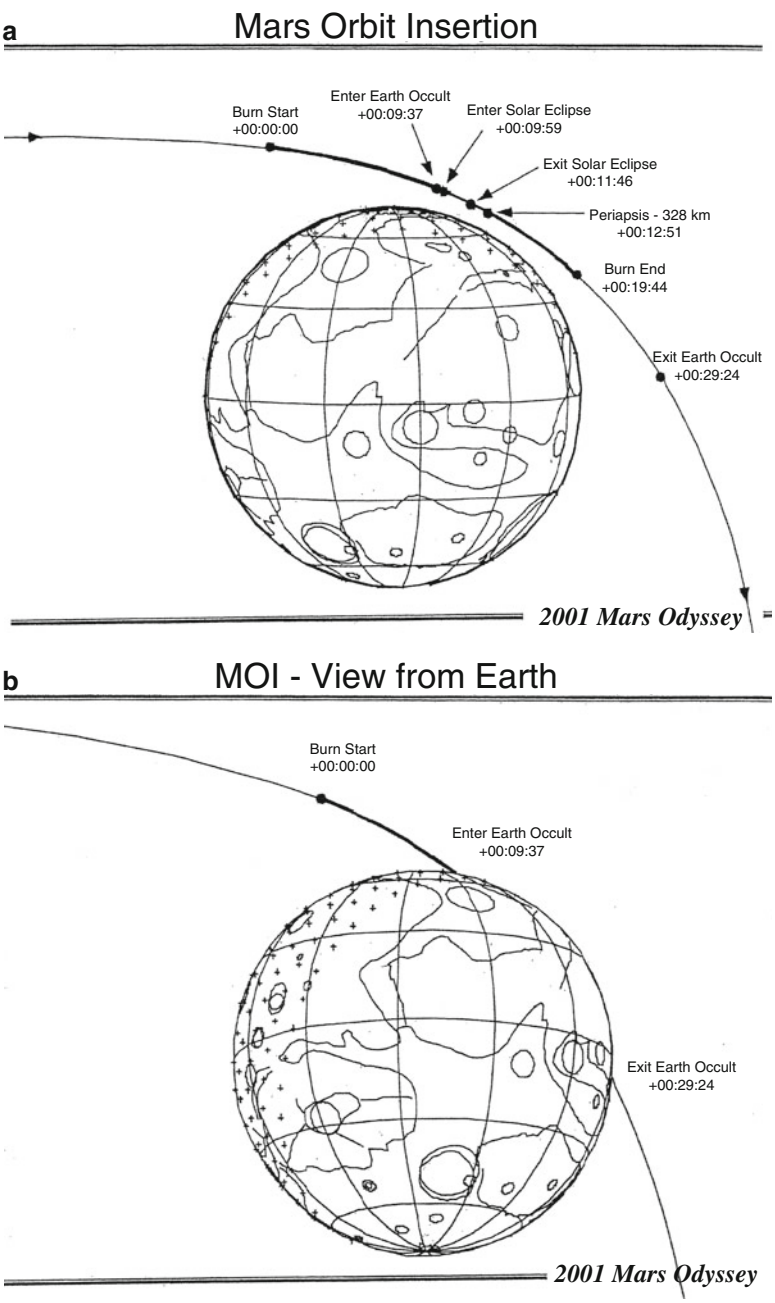

Fig. 3.42 MOI for 2001 mars odyssey. (**a**) Sequence of events at MOI. (**b**) MOI as seen from the earth

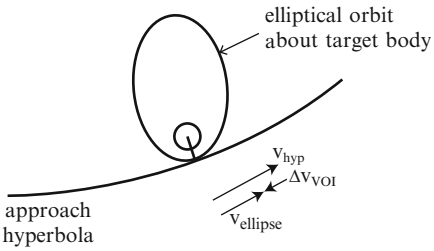

Fig. 3.43 Impulsive orbit insertion

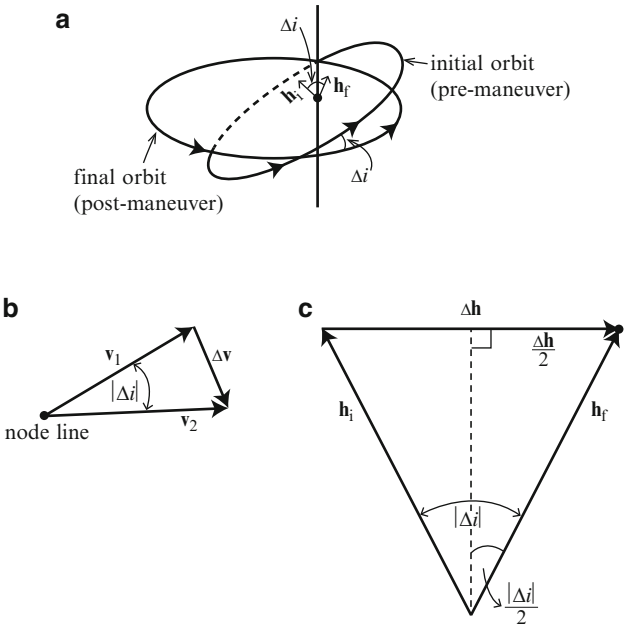

Fig. 3.44 Plane rotation. (**a**) Δi. (**b**) $\Delta \mathbf{v}$. (**c**) $\Delta \mathbf{h}$

The Δi is the angle between the tangents (velocity vectors) to the two orbits at the node line as shown in Fig. 3.44b. Therefore, it is the angle between the angular momentum vectors for the two (pre-maneuver and post-maneuver) orbits as shown in Fig. 3.44a. Let $\mathbf{h_i}$ denote the angular momentum vector for the pre-maneuver orbit and $\mathbf{h_f}$ denote the angular momentum vector for the post-maneuver orbit.

For a pure rotation $h_i = h_f \equiv h$ by definition. From Fig. 3.44c, we see that

$$\Delta h = 2h \sin\left(\frac{|\Delta i|}{2}\right)$$

Recall, from Eq. (1.10), that

$$\mathbf{M}_0 = \mathbf{rxF}$$

where

$$\mathbf{F} = \mathrm{m}\,\ddot{\mathbf{r}}$$
$$\mathbf{h}_0 = \mathbf{r}\mathrm{x}\mathrm{m}\mathbf{v}$$
$$\mathbf{M}_\mathrm{O} = \dot{\mathbf{h}}_0$$

if O is not moving, from Eq. (1.12). For normalized unit mass,

$$\mathbf{M} = \dot{\mathbf{h}}$$

and the applied torque is M = Fr. Let r = the orbit radius at the node line. Then

$$\Delta \mathrm{h} = \frac{\Delta \mathrm{h}}{\Delta \mathrm{t}}\Delta \mathrm{t} \cong \dot{\mathrm{h}}\,\Delta \mathrm{t} = \mathrm{M}\Delta \mathrm{t} = \mathrm{Fr}\Delta \mathrm{t} = \mathrm{r}\Delta \mathrm{v}$$

Therefore,

$$\Delta \mathrm{v} = \frac{\Delta \mathrm{h}}{\mathrm{r}} = \frac{2\mathrm{h}\sin\frac{|\Delta i|}{2}}{\mathrm{r}} = 2\mathrm{v}_\theta \sin\left(\frac{|\Delta i|}{2}\right)$$

because $\mathrm{h} = \mathrm{rv}\,\cos\beta = \mathrm{rv}_\theta$ from Exercise 2.19. Therefore, the magnitude of the velocity change required for a pure rotation maneuver is

$$\Delta \mathrm{v} = 2\mathrm{v}_\theta \sin\left(\frac{|\Delta i|}{2}\right) \tag{3.60}$$

where v_θ = the transverse component of **v** at the node line and Δi denotes the required change in inclination (the tilt of the orbit or slope of the orbit plane). (Note: $\mathrm{v}_\theta \neq \mathrm{v}$ in general.) Using a small angle approximation, we obtain the following expression for the magnitude of the velocity increment required for a pure rotation maneuver:

$$\Delta \mathrm{v} = \mathrm{v}_\theta |\Delta i| \tag{3.61}$$

where v_θ = the transverse component of **v** at the node line and Δi denotes the change in inclination.

For e = 0,

$$\begin{aligned} v_\theta &= v_c = \sqrt{\frac{\mu}{r}} \\ \Delta v &= v_\theta |\Delta i| = v_c |\Delta i| = |\Delta i| \sqrt{\frac{\mu}{r}} \end{aligned} \tag{3.62}$$

For $0 < e < 1$,

$$\begin{aligned} \Delta v &= v_\theta |\Delta i| \\ v_\theta &= r\dot{\theta} = \frac{h}{r} \end{aligned}$$

where we have used Eq. (2.16). So

$$\Delta v = \frac{h}{r} |\Delta i| \tag{3.63}$$

Therefore, Δv is minimized at the crossing point on the node line where r is larger. Therefore, Δv is less at the node line crossing point closer to apoapsis than at the only other candidate maneuver point.

Combined Maneuvers

We can obtain a plane change and in-orbit parameter change by one maneuver as a vector sum of $\Delta \mathbf{v}$s as shown in Fig. 3.45. The in-plane $\Delta \mathbf{v}$ will change the size and/or shape of the orbit. The out-of-plane $\Delta \mathbf{v}$ will change the plane of the orbit.

If both a plane change and a large in-plane correction are required, the spacecraft can perform the combined $\Delta \mathbf{v}$, which is not much more than the out-of-plane $\Delta \mathbf{v}$.

Example: Recall the bi-elliptic transfer described in Fig. 3.9. The Δv savings are modest for an inplane bi-elliptic transfer. The bi-elliptictransfer may provide significant propellant savings if the initial and final orbits are not coplanar because the required plane change can be accomplished at a larger radius and, therefore, for a lower Δv. An application of the bi-elliptic transfer with orbit plane change is launching from Cape Canaveral into a geostationary orbit. The plane-change would decrease the inclination of the orbit obtained at launch by about 28.5°.

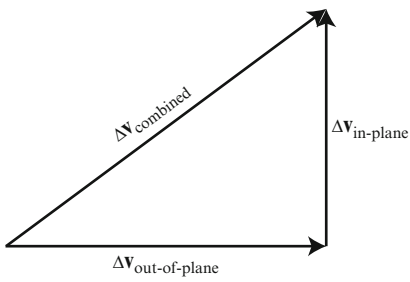

Fig. 3.45 Combined maneuvers

"The minimum total velocity increment required for bi-elliptic transfer between non-coplanar circular orbits" is given as an iterative solution in the reference by Roth. The Δv-optimization of bi-elliptic transfer between non-coplanar elliptical orbits is given as a series of three plane change maneuvers performed along the line of nodes of the initial and final orbits in the reference by Kamel.

References for Sect. 3.6: C. Brown, Edelbaum, Kamel, Prussing 1992, and Roth

3.7 The Rocket Equation

The "cost" of orbital maneuvers has been measured so far in terms of the amount of Δv required to implement a trajectory correction maneuver, transfer or adjustment. The cost in terms of resources is the amount of propellant used to implement the Δv. In this section, we will learn how to convert Δv into the amount of propellant by using the Rocket Equation.

A rocket can be regarded as a jet engine that carries its own oxidizer. Like any other kind of engine, a rocket is a device for converting one form of energy into another, and so it must be provided with a source of energy. This energy source may be chemical, nuclear, or electrical and rocket engines are often distinguished accordingly.

Def.: The reaction force produced on a rocket as a result of the exhaust of the high-velocity exhaust gas is called the thrust.

The faster the exhaust gas flows out of the back of the rocket, the greater is the thrust of the rocket forward.

Thrust is generally stated in pounds of force. To lift a spacecraft off the ground, the number of pounds of thrust by the launch vehicle must be greater than the number of pounds the launch vehicle/payload combination weights. For example, as Tony Simon wrote when referring to the launch of Apollo, "the ground shook, and for rules around everyone felt the thunderous power of Saturm V as its 7,500,000 grounds of thrust lifted 6,500,000 pounds of weight".

In Field-Free Space

Modeling assumptions:

1. *Environment*: We consider a rocket moving in a vacuum in "gravity-free" space, in which the only force acting is rocket thrust. This model is a useful approximation for "high thrust" engines, i.e., engines that provide thrust acceleration magnitudes that are significantly higher than the local gravitational acceleration.
2. *Thrust model*: Let the thrust, assumed constant, act continuously in one direction. The rocket works by ejecting part of its mass at a high velocity; in assuming its thrust to be constant, we also assume the mass ejected per second and the exhaust velocity (measured with respect to the vehicle) to be constant.

The rocket mass is not constant during an engine burn. It decreases because some mass is expelled out of the rocket nozzle to provide thrust, which is the

reaction force in the opposite direction as predicted by Newton's Third Law of Motion. According to NII,

$$F = d(mv)/dt = mdv/dt + vdm/dt = ma$$

if m is constant. But, during a burn, $dm/dt \neq 0$ so $F \neq ma$ during maneuvers.

From the conservation of linear momentum, we can equate the spacecraft momentum plus the momentum of the exhaust particles at time $t + \Delta t$ to the momentum of the system at t to get

$$(m + dm)(v + dv) + (v - v_e)(-dm) = mv$$

where $v - v_e$ is the velocity of the exhaust particles and $-dm > 0$. Simplifying and noting that dmdv is a product of smalls so it is negligible, we obtain

$$mdv + v_e dm = 0$$

Separating variables and integrating, we obtain

$$mdv = -v_e dm$$
$$\int_{t_0}^{t_f} dv = -\int_{t_0}^{t_f} \frac{v_e}{m} dm$$

The result is the Rocket Equation:

$$\Delta v = v_f - v_0 = v_e \ln \frac{m_0}{m_f}$$

where v_f denotes the velocity attained at the final time $t = t_f$, v_0 the initial velocity, m_0 the initial mass, and m_f the final mass.

Def.: The exhaust velocity v_e is the velocity of the expelled particles relative to the rocket.

The exhaust velocity v_e depends on the heat liberated per pound and on the molecular weight. We want the heat liberated to be large and the molecular weight to be small.

The value of the thrust is dependent mainly on the product of the rate at which the exhaust gasses are expelled, expressed as the mass per unit time, and the exhaust velocity. While thrust is generally stated in pounds of force, it may be stated in Newtons (N), where

$1\ N = 1\ kg\ m/s^2$

Def.: The specific impulse I_{sp} is

$$I_{sp} = \frac{v_e}{g_\oplus}$$

where $g_\oplus$ is earth gravity at sea level.

This parameter is equal to

$$\frac{v_e \dot{m}}{g_\oplus \dot{m}} = \frac{\text{thrust}}{\text{gravity} \times \text{fuel mass flow rate}} = \frac{\text{thrust}}{\text{weight} - \text{flow} - \text{rate}}$$

because

$$\text{thrust} = bv_e + A_e[P_e - P_a] \cong bv_e$$

where A_e is the nozzle exit area, P_e is the gas pressure at the nozzle exit, and P_a is the ambient pressure and we have used the fact that $A_e[P_e - P_a]$ is much smaller than bv_e in the approximation. If A_e is measured in m^2, then P_e and P_a are in N/m^2. Note that we consider the ratio of thrust to weight flow rate because the term in the numerator and that in the denominator can be measured accurately in the laboratory (error $<1\%$).

Properties:

1. The specific impulse of a rocket propellant combination (fuel plus oxidizer) is the number of seconds a pound of the propellant will produce a pound of thrust.
2. The parameter I_{sp}, usually quoted in seconds, is a measure of a propellant's performance.

Thus, we obtain the Rocket Equation in the form

$$\Delta v = g_\oplus I_{sp} \ln \frac{m_0}{m_f} \tag{3.64}$$

where
$m_0 =$ spacecraft mass at the beginning of the burn
$m_f =$ spacecraft mass at the end of the burn
$g_\oplus =$ (constant) earth's gravity at sea level $= 0.00980665$ km/s$^2 = 9.80665$ m/s^2
$I_{sp} =$ (constant) specific impulse.

Note: This is the form of the Rocket Equation that we will usually use in this book.

The rocket equation was published by Konstantin Tsiolkovsky in 1903. Konstantin Tsiolkovsky (1857–1935) was a Russian physicist and the theoretical father of rocketry.

Tsiolkovsky was the son of a Polish deportee to Siberia. Tsiolkovsky was an inventor and aviation engineer who was also an insightful visionary. As early as 1894, he designed a monoplane, which subsequently flew in 1915. He also built the first Russian wind tunnel in 1897. In 1903, as part of a series of articles in a Russian aviation magazine, Tsiolkovsky published the rocket equation, and in 1929, a theory of multistage rockets. Tsiolkovsky was also the author of *Investigations of Outer Space by Rocket Devices* (1911) and *Aims of Astronauts* (1914).

One of Tsiolkovsky's many memorable and inspiring quotes is "Mankind will not forever remain on Earth, but in the pursuit of light and space will first timidly emerge

Table 3.2 Examples of specific impulse, s

Fuel	Oxidizer	Specific impulse s at sea level
Liquid hydrogen	Liquid oxygen	381
Liquid methane	Liquid oxygen	299
Kerosene	Liquid oxygen	289
Hydrazine	Liquid oxygen	303
Hydrazine	Nitrogen tetroxide	286
Monomethyl hydrazine (MMH)	Nitrogen tetroxide	280
Unsymmetrical dimethyl hydrazine (UDMH)	Nitrogen tetroxide	277
Hydrazine	Hydrogen peroxide (85 % concentration)	269

from the bounds of the atmosphere, and then advance until he has conquered the whole of circumsolar space" (1911). Tsiolkovsky's most famous quote is, "Earth is the cradle of humanity, but one cannot remain in the cradle forever."

Reference: Eric W. Weisstein, Eric Weisstein's World of Scientific Biography, http://scienceworld.wolfram.com/biography

Def.: The fraction m_0/m_f is called the mass ratio where m_0 denotes the initial mass and m_f denotes the final mass.

Specific impulse is characteristic of the type of propellant; however, its exact value will vary to some extent with the operating conditions, design of the rocket engine, and the oxidizer used.

Examples (Propellants) (Table 3.2):

Reference: Rocket & Space Technology Website at http://www.braeunig.us/space/propel.htm [accessed 1/2/2014]

This reference provides a list of 27 I_{sp} values for various combinations of fuel and oxidizer, together with information about liquid, solid, and hybrid propellants; properties of rocket propellants (chemical formula, molecular weight, density, melting point, and boiling point); rocket propellant performance (whether or not it is hypergolic, mixture ratio (of oxidizer to fuel), specific impulse, and density impulse); propellants for selected rockets (Atlas/Centaur, Titan II, Saturn V, Space Shuttle, and Delta II). For example, the Atlas/Centaur propellants are:

> Stage 0 has a Rocketdyne YLR89-NA7 (X2) engine, which uses LOX/RP-1 propellant with $I_{sp} = 259$ s sl and 292 s in vacuum; stage 1 has a Rocketdyne YLR105-NA7 engine, which uses LOX/RP-1 propellant with $I_{sp} = 220$ s sl and 309 s in vacuum; and stage 2 has a P&W RL-10A-3.3 (X2) engine, which uses LOX/LH_2 propellant with $I_{sp} = 444$ s in vacuum. LOX (or LO_2) is liquid oxygen, which is the oxidizer, RP-1 is highly refined kerosene, LH_2 is liquid hydrogen, and "sl" denotes "sea level."

NASA has relied on the efficient but highly toxic, flammable, and corrosive hydrazine to power satellites and manned spacecraft for decades. But NASA may replace hydrazine with a green fuel, called AF-M315E, which has nearly 50 % better performance and is far more benign than hydrazine. The propellant is an

energetic ionic liquid that evaporates more slowly and requires more heat to ignite than hydrazine, making it more stable and much less flammable. Its main ingredient is hydroxyl ammonium nitrate, and when it burns, it gives off nontoxic gasses like water vapor, hydrogen, and carbon dioxide. Importantly, M315E is safe enough to be loaded into a spacecraft before it goes to the launch pad, which would cut the time and cost of ground processing for a vehicle headed for space. However, M315E burns so hot that it would damage current rocket engines, requiring development of engines that can survive the intense heat.

References: Megan Gannon, "NASA's Quest for Green Rocket Fuel Passes Big Test," 7/11/2013, available at http://www.livescience.com/38120-nasa-green-rocket-fuel-test.html [accessed 1/2/2014]; Jullian Scharr, "New Rocket Fuel Helps NASA 'Go Green'," 5/16/2013, available at http://www.technewsdaily.com/18090-new-rocket-fuel-helps-nasa-go-green.html [accessed 1/2/2014].

Consider the Rocket Equation in the form of Eq. (3.64).

Given I_{sp}, m_0, and m_f, we can compute the Δv directly.

Given I_{sp}, m_0, and the required Δv, we can solve for m_f as

$$m_f = m_0 e^{\frac{-\Delta v}{g_\oplus I_{sp}}} \tag{3.65}$$

Then, we compute the required amount of propellant as

$$\Delta m = m_0 - m_f = m_0 \left(1 - e^{\frac{-\Delta v}{g_\oplus I_{sp}}}\right) \tag{3.66}$$

Example: Consider a two-maneuver series, Δv_1, Δv_2, performed in orbit. Let $m_{0,1}$, $m_{f,1}$ denote the initial and final mass for Δv_1, respectively, and $m_{0,2}$, $m_{f,2}$ denote the initial and final mass for Δv_2, respectively. Then

$$\begin{aligned}
\Delta m &= (m_{0,1} - m_{f,1}) + (m_{0,2} - m_{f,2}) \\
&= m_{0,1} - m_{f,2} \\
&= m_{0,1} - m_{0,2} e^{\frac{-\Delta v_2}{g_\oplus I_{sp}}} \\
&= m_{0,1} - m_{0,1} e^{\frac{-\Delta v_1}{g_\oplus I_{sp}}} e^{\frac{-\Delta v_2}{g_\oplus I_{sp}}} \\
&= m_{0,1} \left(1 - e^{\frac{-(\Delta v_1 + \Delta v_2)}{g_\oplus I_{sp}}}\right)
\end{aligned}$$

where we have used the fact that $m_{f,1} = m_{0.2}$ and Eq. (3.65) twice. Similarly, for any number n of maneuvers,

$$\Delta m_{TOT} = m_0 \left(1 - e^{\frac{-\sum_{i=1}^{n} \Delta v_i}{g_\oplus I_{sp}}}\right) \tag{3.67}$$

or

$$\Delta m_{TOT} = m_0 \left(1 - e^{\frac{-\Delta v_{TOT}}{g_{\oplus} I_{sp}}} \right) \tag{3.68}$$

where m_0 denotes the initial mass before the first maneuver.

Note (Helpful Hintz): We do not need to compute each of the Δm_i and add $\sum_{i=1}^{n} \Delta m_i$ to get Δm_{TOT}. We only need to add $\sum_{i=1}^{n} \Delta v_i$ and compute Δm_{TOT} as in Eq. (3.68).

In the derivation of Eqs. (3.67) and (3.68), we have assumed there are no other changes in mass, such as dropping tanks, between or during the maneuvers. For the injection of a spacecraft into a heliocentric orbit, the initial mass consists of the structure of and propellant in the upper stage of the launch vehicle, plus the payload (spacecraft, including its propellant). The I_{sp} for injection is the I_{sp} of the propellant for the upper stage. The structure of the upper stage is jettisoned after the injection, so it is not part of the initial mass for the orbital maneuvers.

Remarks:

1. A high thrust chemical engine has:
   - A moderate exhaust velocity (v_e)
   - A high mass flow rate ($\dot{m}$) because of the large amount of combustion exhaust products flowing out of the nozzle.
2. A low thrust engine, e.g., an ion engine, has:
   - A very high specific impulse because ions are expelled at tremendously high speeds (v_e) and
   - A low thrust because the rate mass is expelled ($\dot{m}$) is extremely low.

Example 1: Hayabusa (nee MUSES-C) used high-performance electric propulsion engines continuously in flight.

Example 2: Deep Space 1 (DS1) used ion propulsion that provided 90 mN = 1/50 lb. of thrust with I_{sp} = 2,500–3,500 s.

Example 3: NASA's Evolutionary Xeon thruster (NEXT) developed by NASA Glenn to provide a 7-kW ion thruster.

3. Chemical rockets have demonstrated fuel efficiencies up to 35%; ion thrusters have demonstrated fuel efficiencies over 90%.
4. Ion thrusters must be used in a vacuum to operate at the available power levels.
5. Ion thrusters cannot be used for launch because large amounts of thrust are needed to escape the earth's gravity and atmosphere.

In a Gravitational Field at Launch

For launch, using a simplified model that omits forces such as atmospheric drag, the Rocket Equation becomes:

$$mdv = -v_e dm - mgdt$$

$$dv = -v_e \frac{dm}{m} - gdt$$

By integrating, we obtain:

$$\Delta v = v_e \ln \frac{m_0}{m} - \int_0^t g(h)dt$$

where h is the rocket's height above a reference point. For constant g, this result is:

$$\Delta v = v_e \ln \frac{m_0}{m} - gt \tag{3.69}$$

The last term on the right-hand side of this equation is called a gravity loss term, because it represents a decrease in the velocity change due to the gravitational force compared with the value for field-free space. The size of the gravity loss depends on the burn time. For a given thrust maneuver, the burn time may be quite short for a very high-thrust engine, in which case the gravity loss is small and perhaps negligible compared with a lower-thrust engine that must burn for a longer time to perform the same velocity change.

For information about rocket payloads and staging and how to optimize the allocation of mass among launch vehicle stages, see Sects. 5.5 and 5.6 of the reference by Prussing and Conway.

References for this chapter: Barrar; Brouke, 2001; Broucke and Prado; C. Brown; Cesarone; Chobotov; Diehl and Nock; Doody; Edelbaum; Federation of American Scientists; Gannon; Gates; Glasstone; Hintz and Chadwick; Hintz, Farless, and Adams; Hintz and Longuski; Hoelker and Silber; Hohmann; Kaplan; Kizner; Lawden; Logsdon; Pisacane and Moore; Prussing, 1992; Prussing and Conway; Rocket & Space Technology Website; Scharr; Simon; Spaceflight Now Website; Strange and Longuski; Stricherz; TSB; Thomson, 1961; Thomson, 1986; Ting; Uphoff, Roberts, and Friedman; Wagner and Goodson; Weisstein; Wertz and Larson; Wylie and Barrett; and Zee.

Exercises

3.1 The upper stage of a launch vehicle has placed its payload in an orbit having $v_0 = 9$ km/s, $r_0 = 7{,}500$ km, and $\beta_0 = 0°$.
   (a) Did this launch achieve a circular orbit? Explain.
   (b) Where is the spacecraft in its orbit? Explain.

(c) What are the values of $\mathscr{E}$ (energy), a, p, and h for this orbit?
(d) Do 3.1(a–c) again, using MATLAB.

3.2 A spacecraft was launched from the Cape with booster burn-out occurring at an altitude of 500 km with a velocity $v_0 = 9.25$ km/s and flight path angle $\beta_0 = 20°$ at the time $t = t_0$.
(a) Determine θ_0, e, a, r_p, and r_a.
(b) At apogee, the spacecraft's engine is fired to circularize its orbit. However, due to errors in the maneuver execution, the resulting velocity was inaccurate by 2% and $\beta = 5°$ at the end of the thrusting. The resulting value of the eccentricity e is small, but non-zero. What is this value of e?
(c) Could this maneuver be performed at perigee? Why or why not?

3.3 An earth-orbiting satellite is determined to have parameters $r_0 = 7{,}000$ km, $v_0 = 7.55$ km/s, and $\beta_0 = 20°$ at time $t = t_0$.
(a) Approximate e, θ_0, $\mathscr{E}$ (energy), a, r_p, r_a, and E (eccentric anomaly) for these conditions.
(b) At time $t = t_0$, a TCM is performed to adjust the eccentricity to 0.5 without rotating the line of apsides. (Def.: The line of apsides is the line through periapsis and apoapsis.) Approximate β and v just after applying the impulsive maneuver.
(c) Sketch the original and new orbits, showing the point at which the orbit changes and the pre- and post-maneuver flight path angles.
(d) What will happen to the satellite?

3.4 Complete column 2 of Table 3.1, using Fig. 3.4, and column 3, using the identity in Eq. (2.26). Then make a MATLAB plot of both columns of data to show the accuracy of the parametric tool given in Fig. 3.4.

3.5 Use MATLAB to plot the flight path angle versus true anomaly for $e = 0.3$, 0.6, and 0.9 as in Fig. 3.5b.

3.6 A spacecraft is moved from a circular LEO having a 200-km altitude to a circular 18-h orbit via a Hohmann transfer. Calculate the:
(a) Eccentricity of the Hohmann transfer ellipse.
(b) Total required velocity increment Δv_T.

3.7 The UCLA spacecraft is moving in a circular orbit about the earth of radius r_{UCLA}, while the USC spacecraft is moving in a circular orbit of radius r_{USC}, where $r_{UCLA} < r_{USC}$.
(a) Which spacecraft has the greater orbital velocity? Explain.
(b) Which spacecraft has the greater orbital period? Explain.
(c) Which spacecraft has the higher energy? Explain.

3.8 Assuming a one-impulse transfer from a 200-km-altitude LEO, which flight requires less impulsive Δv a Venus flyby or a Mars flyby? Explain your answer.

3.9 (a) A spacecraft is in a circular parking orbit in the ecliptic plane at an altitude of 200 km around the earth. What is the minimum Δv required to send this spacecraft out of its parking orbit and into a Hohmann transfer to Jupiter? Assume the earth and Jupiter have circular heliocentric orbits in the ecliptic plane.

(b) What is the angular distance around the earth from perigee to escape from the earth, θ_∞?

3.10 Prove that the magnitude of the impact parameter B equals the length |b| of the hyperbolic semiminor axis.

3.11 The Pioneer X spacecraft flew by Jupiter and on to solar system escape. During the planning phase for this mission, the possibility of using a Hohmann transfer to Jupiter was considered. No Δv was to be imparted to the spacecraft after leaving the parking orbit, except for small midcourse corrections. Determine whether or not the spacecraft could achieve enough energy via a Hohmann transfer and Jupiter flyby to escape the solar system.

3.12 Show that the Δv_{TOTAL} for the three maneuvers of a bi-elliptic transfer sequence is

$$\begin{aligned}\Delta v_{TOTAL} &= \Delta v_1 + \Delta v_2 + \Delta v_3 \\ &= \left(\sqrt{\frac{2\mu}{r_1} - \frac{2\mu}{r_1 + r_2}} - \sqrt{\frac{\mu}{r_1}}\right) + \left(\frac{r_f}{r_2}\sqrt{\frac{2\mu}{r_f} - \frac{2\mu}{r_f + r_2}} - \frac{r_1}{r_2}\sqrt{\frac{2\mu}{r_1} - \frac{2\mu}{r_1 + r_2}}\right) \\ &\quad - \left(\sqrt{\frac{\mu}{r_f}} - \sqrt{\frac{2\mu}{r_f} - \frac{2\mu}{r_f + r_2}}\right) \\ &= \sqrt{\frac{\mu}{r_1}}\left[\sqrt{\frac{2\frac{r_2}{r_1}}{1+\frac{r_2}{r_1}}} - 1\right] + \sqrt{\frac{\mu}{r_2}}\left[\sqrt{\frac{2}{1+\frac{r_2}{r_f}}} - \sqrt{\frac{2}{1+\frac{r_2}{r_1}}}\right] + \sqrt{\frac{\mu}{r_f}}\left[\sqrt{\frac{2\frac{r_2}{r_f}}{1+\frac{r_2}{r_f}}} - 1\right]\end{aligned}$$

where r_1 denotes the radius of the inner circular orbit, r_f the radius of the outer circular orbit, and r_2 the radius at apoapsis of the transfer ellipses.

3.13 A spacecraft is sent on a Mars flyby mission via a direct Hohmann heliocentric transfer orbit from a 200-km-altitude, circular parking orbit about the earth. Assume that the earth and Mars have circular heliocentric orbits in the ecliptic plane and that the spacecraft's parking orbit is in the ecliptic plane.

(a) Compute the parameters e, δ, and θ_∞ for a passage at 590 km above the Martian surface.

(b) Draw a diagram that shows the hyperbolic passage and a vector diagram that shows the vectors $\mathbf{v}_\infty^-$, $\mathbf{v}_\infty^+$, $\mathbf{v}^-$, and $\mathbf{v}_{\mathbf{Mars}}$, if the spacecraft passes on the sunny side of Mars. Indicate the direction to the sun in each of these figures.

(c) Draw the same two diagrams as in part (b), if the spacecraft passes on the dark side of Mars. Show the direction to the sun in each of these figures.

3.14 (a) Compute the following parameters for the heliocentric orbit that is achieved by the lit-side passage considered in Exercise 3.13(b): e, θ, h, r_p, a, and τ.

(b) Compute the same parameters as in part (a) for the dark-side passage considered in Exercise 3.13(c).

(c) How does the orbit obtained in part (b) differ from the orbit obtained in part (a)?

3.15 A GEO spacecraft crosses the earth's equatorial plane when its true anomaly is 30°. The eccentricity of the orbit is 0.1 and its initial inclination is 5° with respect to the equator. What minimum velocity increment is required to transfer this GEO to an equatorial orbit?

3.16 On July 1, 2004, the Cassini spacecraft approached Saturn with hyperbolic excess velocity $V_\infty = 5.5$ km/s to swing by the planet at the closest approach distance $r_p = 80{,}680$ km. Compute the impulsive ΔV magnitude required for a maneuver performed at the closest approach to Saturn to transfer the Cassini spacecraft into a 116-day elliptical orbit having the same periapsis point as the approach (hyperbolic) trajectory.

3.17 Prove that the velocity v_p of a spacecraft at closest approach to a central body is

$$v_p = \sqrt{\frac{\mu}{r_p}}(1+e) \quad \text{for all } e > 0,$$

where μ denotes the gravitational constant of the central body in km^3/s^2,
e denotes the eccentricity of the spacecraft's orbit, and
r_p denotes the radial distance in km at closest approach.

3.18 Prove that, for a hyperbolic trajectory,

$$e^2 = 1 + \frac{B^2 v_\infty^4}{\mu^2}$$

where B is the impact parameter, v_∞ the hyperbolic excess velocity, and
μ denotes the gravitational constant of the central body in km^3/s^2.

3.19 What is your answer to the thought exercise proposed at the end of Sect. 3.4? Is the Δv_{TOTAL2} for the maneuver sequence described in Fig. 3.13 greater than, equal to, or less than the Δv_{TOTAL} for the maneuver sequence described in Fig. 3.12? Explain why your answer is correct.

3.20 A spacecraft's initial mass is 10,000 kg when its engine ejects mass at a rate of 30 kg/s with an exhaust velocity of 3,100 m/s. The pressure at the nozzle exit is 5,000 N/m^2 and the exit area is 0.7 m^2.

(a) What is the thrust of the engine in a vacuum?

(b) What is the magnitude of the $\mathbf{\Delta v}$ in km/s if the spacecraft's engine burns for 1 min?

3.21 A spacecraft is injected from a 200-km-altitude parking orbit about the earth into a transfer orbit to flyby Mars as described in Exercise 3.8. Immediately before injection, the spacecraft's wet mass is 4,000 kg and its dry mass is 1,000 kg. How much propellant is used in the injection maneuver if the launch vehicle is an Atlas/Centaur? Assume that the wet mass of the Centaur upper stage is 30,000 lbs., including the Centaur's structure and propellant. [Reference: Federation of American Scientists].

3.22 The Cassini spacecraft used a bipropellant of nitrogen tetroxide (NTO) oxidizer and monomethyl hydrazine (MMH) fuel for the insertion into orbit about Saturn. The wet mass prior to the insertion burn was 4,532 kg and the specific impulse in a vacuum was 306 s. Compute the amount of propellant that would have been consumed by the impulsive orbit insertion maneuver computed in Exercise 3.16. (Actually, a finite burn was performed centered on the periapsis passage of the hyperbolic trajectory and the spacecraft rotated at a constant rate during the maneuver to reduce finite burn losses.)

3.23 Derive a formula for the gravity assist velocity increment ΔV_{GA} in terms of the magnitude of the spacecraft's incoming (before flyby) and outgoing (after flyby) inertial velocity vectors and the magnitude of the secondary body's inertial velocity vector.

FAQ:

I have a question regarding problem 3.13 that you went over in class this past week. You drew the relation of the hyperbolic flyby of Mars with the light side passage and the dark side passage.

My question is, when you drew it you had the S/C coming in from left to right on the page and the velocity of Mars in the left direction (all relative to the page). If you are doing a Hohmann transfer where the Earth is at r_p at the "south side" of the orbit (wrt to the paper calling North up) and the S/C arrived at Mars when Mars was in the "north side" of its orbit, how could the S/C have incoming velocity vector from the left to right, which is opposite the velocity of Mars? Assuming all orbits are counterclockwise wouldn't the S/C approach Mars from right to left and $\mathbf{V}_{\infty}^{-}$ be added to the velocity of Mars to get V_{-}? I'm a little confused.

A: The reason why the spacecraft is shown entering from the left is that the planet is moving faster than the spacecraft. So the S/C is moved into position in front of the planet and the planet overtakes the S/C. If the S/C were to travel behind the planet, the S/C would not be able to catch up to the planet and pass it. The figure that shows the S/C traveling to the right is the picture of the 2-body model with the S/C in a hyperbolic trajectory about the planet. The motion in that picture is wrt the planet. Recall that we break the patched conic trajectory model into four segments. The picture you are looking at is the third segment, which shows motion wrt the target planet. It does not show motion wrt the sun, which would be much different.

Techniques of Astrodynamics

4

4.1 Introduction

We now consider techniques used in the study of the controlled flight paths of human-made vehicles, beginning with algorithms for propagating the spacecraft's trajectory and then defining Keplerian parameters, which describe the orbit's size, shape, and orientation. Lambert's Problem is used to generate mission design curves, called "pork chop plots." Other models advance our study to treat n bodies and distributed masses instead of just two point masses. Lastly, we consider how to measure time, which is fundamental to the equations of motion.

4.2 Orbit Propagation

Position and Velocity Formulas as Functions of True Anomaly for Any Value of e

Consider a spacecraft in a conic section trajectory as shown in Fig. 4.1. Define a unit reference vector $\mathbf{i_p}$ along the periapsis vector and an orthogonal vector $\mathbf{i_q}$ that is positive in the direction of spacecraft motion. The origin of the coordinate system is at the center of mass of the central body. The position vector can be written in the p–q space, using the Conic Equation, as

$$\mathbf{r} = r\cos\theta\mathbf{i}_p + r\sin\theta\mathbf{i}_q = \frac{p}{1+e\cos\theta}\left(\cos\theta\mathbf{i}_p + \sin\theta\mathbf{i}_q\right) \tag{4.1}$$

By differentiating Eq. (4.1) and simplifying, we obtain the velocity vector

© Springer International Publishing Switzerland 2015
G.R. Hintz, *Orbital Mechanics and Astrodynamics*,
DOI 10.1007/978-3-319-09444-1_4

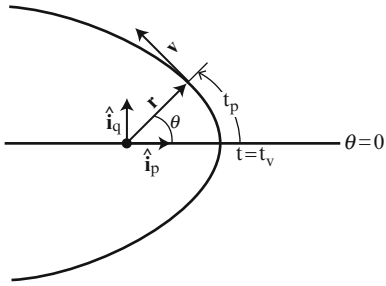

Fig. 4.1 Position vector in p–q space

$$\mathbf{v} = \sqrt{\frac{\mu}{p}}\left[-\sin\theta\mathbf{i}_p + (e + \cos\theta)\mathbf{i}_q\right] \tag{4.2}$$

as in Exercise 4.1. The Eqs. (4.1) and (4.2) are valid for all values of e.

Deriving and Solving Barker's Equation

Objective: Given t_p, find θ, **r** and **v** for a parabolic orbit.
Since $e = 1$, the Conic Equation, the half-angle formula for the cosine, and two trigonometric identities give

$$r = \frac{p}{1 + \cos\theta} = \frac{p}{2\cos^2\frac{\theta}{2}} = \frac{p}{2}\left[\frac{\cos^2\frac{\theta}{2} + \sin^2\frac{\theta}{2}}{\cos^2\frac{\theta}{2}}\right] = \frac{p}{2}\left[1 + \tan^2\frac{\theta}{2}\right] = \frac{p}{2}\sec^2\frac{\theta}{2}$$

Therefore,

$$r^2 = \frac{p^2}{4}\sec^4\frac{\theta}{2}$$

Since $h = r^2\frac{d\theta}{dt} = \sqrt{\mu p}$, $r^2 = \sqrt{\mu p}\frac{dt}{d\theta}$

Equating these two expressions for r^2 and separating variables provides the following differential equation

$$4\sqrt{\frac{\mu}{p^3}}dt = \sec^4\frac{\theta}{2}d\theta$$

which can be integrated, using the integration formula

$$\int \sec^n x dx = \frac{\tan x \sec^{n-2} x}{n-1} + \frac{n-2}{n-1}\int \sec^{n-2} x dx$$

Thus we obtain Barker's Equation:

$$2\sqrt{\frac{\mu}{p^3}}t_p = \tan\left(\frac{\theta}{2}\right) + \frac{1}{3}\tan^3\left(\frac{\theta}{2}\right) \tag{4.3}$$

This cubic equation is the parabolic form of Kepler's equation. In some references, this equation is written in the following alternate form:

$$t_p = \frac{1}{\sqrt{\mu}}\left(\frac{p}{2}D + \frac{D^3}{6}\right)$$

where

$$D = \sqrt{p}\tan\frac{\theta}{2}$$

We set the mean motion $n = \mu^{1/2}$ for parabolic orbits.

Solution of Barker's Equation:

Let $\tan\frac{\theta}{2} = \lambda - \frac{1}{\lambda}$. Then

$$2\sqrt{\frac{\mu}{p^3}}t_p = \tan\frac{\theta}{2} + \frac{1}{3}\tan^3\frac{\theta}{2} = \left(\lambda - \frac{1}{\lambda}\right) + \frac{1}{3}\left(\lambda - \frac{1}{\lambda}\right)^3 = \frac{1}{3}\left(\lambda^3 - \frac{1}{\lambda^3}\right)$$

Let $\lambda = -\tan w$ and $\lambda^3 = -\tan s$ which implies that $\tan^3 w = \tan s$. So

$$\lambda^3 - \frac{1}{\lambda^3} = -\tan s + \frac{1}{\tan s} = -\frac{1}{\cot s} + \cot s = \frac{\cot^2 s - 1}{\cot s} = 2\cot 2s$$

from the multiple angle formula for cot 2s. Therefore,

$$2\sqrt{\frac{\mu}{p^3}}t_p = \frac{1}{3}\left(\lambda^3 - \frac{1}{\lambda^3}\right) = \frac{1}{3}(2\cot 2s)$$

$$3\sqrt{\frac{\mu}{p^3}} = \cot 2s$$

Thus, we have determined the following procedures.

Procedure for Solving Barker's Equation

To find θ on a parabolic orbit for given t_p, we:

1. Compute s from

$$\cot(2s) = 3\sqrt{\frac{\mu}{p^3}}t_p \tag{4.4}$$

2. Solve for tan(w) from

$$\tan^3(w) = \tan(s) \tag{4.5}$$

3. Solve for θ in

$$\tan\left(\frac{\theta}{2}\right) = -\tan(w) + \frac{1}{\tan(w)} \tag{4.6}$$

Procedure for Propagating a Parabolic Orbit

Given the length of time since periapsis passage t_p on a parabolic orbit, we can now:

1. Compute θ at t_p by following the procedure given above for solving Barker's Equation.
2. Compute

$$\mathbf{r} = \frac{p}{1 + \cos\theta}\left[\cos\theta \mathbf{i}_p + \sin\theta \mathbf{i}_q\right]$$

$$\mathbf{v} = \sqrt{\frac{\mu}{p}}\left[-\sin\theta \mathbf{i}_p + (1 + \cos\theta)\mathbf{i}_q\right]$$

So we know $\mathbf{r} = \mathbf{r}(\mathbf{t})$ and $\mathbf{v} = \mathbf{v}(\mathbf{t})$ for any time t on a parabolic orbit in terms of the reference vectors $\mathbf{i}_p$ and $\mathbf{i}_q$.

Orbit Propagation for Elliptic Orbits: Solving Kepler's Equation

Consider $0 < e < 1$

Problem: If the state $(\mathbf{r_0}, \mathbf{v_0})$ is known at some time t_0, what is the state $(\mathbf{r}(t), \mathbf{v}(t))$ at any later time t? That is, given the initial conditions

$\mathbf{r}_0 = (\mathbf{x}_0, \mathbf{y}_0, \mathbf{z}_0)$ and $(\dot{\mathbf{x}}_0, \dot{\mathbf{y}}_0, \dot{\mathbf{z}}_0)$ at the initial time t_0, determine the position and velocity vectors at a later time $t = t_0 + \Delta t$ as shown in Fig. 4.2.

From Eqs. (4.1) and (4.2) and Exercises 4.3(a) and 4.3(b),

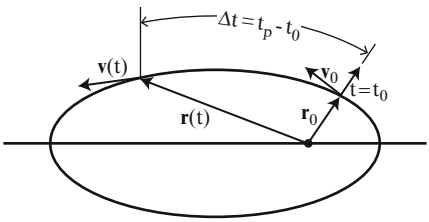

Fig. 4.2 Orbit propagation for elliptic trajectories

$$\begin{aligned}\mathbf{r} &= a(\cos E - e)\mathbf{i}_p + \sqrt{ap}\sin E\mathbf{i}_q \\ \mathbf{v} &= \dot{\mathbf{r}} = \left(-\frac{\sqrt{\mu a}}{r}\sin E\right)\mathbf{i}_p + \left(\frac{\sqrt{\mu p}}{r}\cos E\right)\mathbf{i}_q\end{aligned} \tag{4.7}$$

in terms of the eccentric anomaly E, where we have again discontinued showing the cap notation for unit vectors.

Problem: To determine the position and velocity vectors in terms of the given initial values.

Assume that $\mathbf{r} = \mathbf{r}_0$, $\mathbf{v} = \mathbf{v}_0$, and $E = E_0$ at $t = t_0$. Note that t_0 is not necessarily the time t_v of periapsis passage. Hence, at $t = t_0$, we have

$$\begin{aligned}\mathbf{r}_0 &= a(\cos E_0 - e)\mathbf{i}_p + \sqrt{ap}\sin E_0\mathbf{i}_q \\ \mathbf{v}_0 &= \left(-\frac{\sqrt{\mu a}}{r_0}\sin E_0\right)\mathbf{i}_p + \left(\frac{\sqrt{\mu p}}{r_0}\cos E_0\right)\mathbf{i}_q\end{aligned}$$

by using Eq. (4.7) at time t_0. Solve these two equations, as in Exercise 4.3(c), to obtain:

$$\begin{aligned}\mathbf{i}_p &= \frac{\cos E_0}{r_0}\mathbf{r}_0 - \sqrt{\frac{a}{\mu}}\sin E_0\mathbf{v}_0 \\ \mathbf{i}_q &= \sqrt{\frac{a}{p}}\frac{\sin E_0}{r_0}\mathbf{r}_0 + \frac{a}{\sqrt{\mu p}}(\cos E_0 - e)\mathbf{v}_0\end{aligned} \tag{4.8}$$

A good practice is to verify your work when possible. Let us perform the following check.

If $t_0 = t_v$, then, from Eq. (4.8),

$$\begin{aligned}\mathbf{i}_p &= \frac{\mathbf{r}_0}{r} \\ \mathbf{i}_q &= \frac{a}{\sqrt{\mu p}}(1-e)\mathbf{v}_0 = \frac{1}{\sqrt{\dfrac{\mu p}{a^2(1-e)^2}}}\mathbf{v}_0 = \frac{\mathbf{v}_0}{\sqrt{\dfrac{\mu}{r_p}(1+e)}} = \frac{\mathbf{v}_0}{v_0}\end{aligned}$$

because $v_p = \sqrt{\frac{\mu}{r_p}(1+e)}$ from Exercise 3.17. Thus, we have verified that the Eq. (4.8) are correct at $t = t_v$, which is an indication (not a guarantee) that we derived those equations correctly.

Substitute Eq. (4.8) into the position formula in Eq. (4.7) to obtain

$$\begin{aligned}\mathbf{r}(t) = \frac{a}{r_0}[\cos(E - E_0) - e\cos(E_0)]\mathbf{r}_0 \\ + \sqrt{\frac{a^3}{\mu}}[\sin(E - E_0) - e(\sin(E) - \sin(E_0))]\mathbf{v}_0\end{aligned} \tag{4.9}$$

where we have used trigonometric identities for $\sin(E - E_0)$ and $\cos(E - E_0)$ to write the equation in terms of the angle $\Delta E = E - E_0$. Then differentiate Eq. (4.9) and use Eq. (2.32) to obtain

$$\mathbf{v}(\mathbf{t}) = -\frac{\sqrt{\mu a}}{r r_0}\sin(E - E_0)\mathbf{r}_0 + \frac{a}{r}[\cos(E - E_0) - e\cos(E)]\mathbf{v}_0 \tag{4.10}$$

Thus, we see that we need E to compute $\mathbf{r}$ and $\mathbf{v}$ from these two equations. The functional relationship between the given t_p and E is given by Kepler's equation. We solve Kepler's equation in a form that includes the initial conditions at $t = t_0$. Thus, we evaluate Kepler's equation at E and E_0 and subtract to obtain

$$\begin{aligned}\sqrt{\frac{\mu}{a^3}}(t_p - t_{p_0}) &= E - E_0 - e(\sin E - \sin E_0)\\ &= E - E_0 + e\sin E_0(1 - \cos(E - E_0))\\ &\quad - e\cos E_0 \sin(E - E_0)\end{aligned} \tag{4.11}$$

where

$$e\cos E_0 = 1 - \frac{r_0}{a} \text{ from Eq.(2.29)}$$
$$e\sin E_0 = \frac{\dot{r}_0}{a\dot{E}_0} \text{ from Eq.(2.30)}$$

But

$$e\sin E_0 = \frac{\mathbf{r}_0 \bullet \mathbf{v}_0}{\sqrt{a\mu}}$$

from Eq. (2.32) and Exercise A-8. Therefore,

$$\begin{aligned}e\cos(E_0) &= 1 - \frac{r_0}{a}\\ e\sin(E_0) &= \frac{\mathbf{r}_0 \bullet \mathbf{v}_0}{\sqrt{a\mu}}\end{aligned} \tag{4.12}$$

Thus, Eq. (4.11) can be written as

$$\begin{aligned}\sqrt{\frac{\mu}{a^3}}(t - t_0) &= E - E_0 + \frac{\mathbf{r}_0 \bullet \mathbf{v}_0}{\sqrt{a\mu}}(1 - \cos(E - E_0))\\ &\quad - \left(1 - \frac{r_0}{a}\right)\sin(E - E_0)\end{aligned} \tag{4.13}$$

In Eq. (4.13), we know t, t_0, and the initial conditions r_0, and v_0 and a can be computed from the Energy Equation. To determine how to find E, we begin by showing that there exists a unique solution for E in Kepler's Equation.

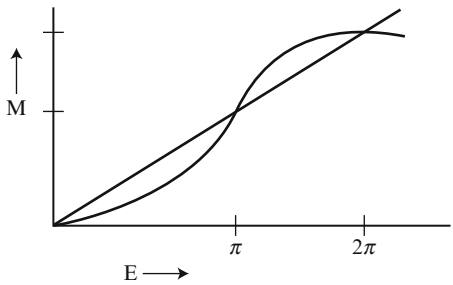

Fig. 4.3 Mean anomaly versus eccentric anomaly

Kepler's equation can be written in terms of the mean anomaly M (shown in Fig. 4.3) as

$$n t_p = M = E - e \sin(E) \tag{4.14}$$

Differentiating Eq. (4.14) with respect to E, we obtain

$$\frac{dM}{dE} = 1 - e \cos E > 0$$

which shows that M is monotonically increasing. Since M is unbounded, there is one and only one solution for E for a given t_p. QED

Given E, it is easy to obtain M. That is, given location, find time.

Given M, we need to solve for E. That is, given time, find the location. There are hundreds of methods for solving this equation. Four general classes of these methods are:

1. Graphical methods,
2. Closed form approximations,
3. Iterative methods, and
4. Series expansions.

Example (type 2) (See page 196 of Battin [1999] for a sketch of a proof of this solution of Kepler's equation.):

A good approximation for E is obtained for e small as follows:

$$E = M + \frac{e \sin M}{1 - e \cos M} - \frac{1}{2}\left(\frac{e \sin M}{1 - e \cos M}\right)^3 \tag{4.15}$$

if fourth and higher powers of e are neglected.

Example (type 3) Newton's method

(Newton's method is the classic algorithm for finding roots of functions. The method is sometimes called Newton–Raphson in honor of Joseph Raphson, who published the idea before Newton did.)

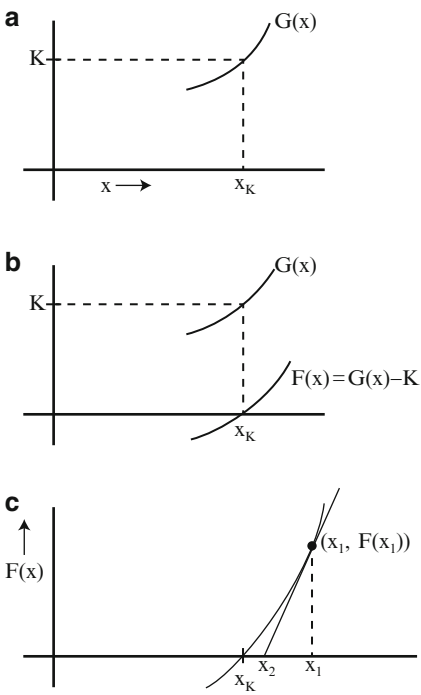

Fig. 4.4 Employing Newton's method. (**a**) Function G(x). (**b**) Function F(x). (**c**) First iteration

Suppose we need to find $x = x_K$ such that a function G(x) satisfies

$$G(x_K) = K$$

(see Fig. 4.4a). Consider the function $F(x) = G(x) - K$. Then we need to find x_K such that $F(x_K) = 0$, as shown in Fig. 4.4b.

Select an initial guess x_1 as shown in Fig. 4.4c. If $F(x_1) = 0$, we are finished. Hence, we suppose $F(x_1) \neq 0$ and proceed as follows.

The slope of the tangent line at $x = x_1$ is

$$F'(x_1) \cong \frac{F(x_1) - 0}{x_1 - x_2}$$

Solving for x_2 obtains

$$x_2 = x_1 - \frac{F(x_1)}{F'(x_1)}$$

Continue with

$$x_{n+1} = x_n - \frac{F(x_n)}{F'(x_n)}$$

Then $x_1, x_2, \ldots, x_n, \ldots \rightarrow x_K$ until $|x_n - x_{n+1}| < \varepsilon_{tol} \Rightarrow$ convergence, where ε_{tol} is an input tolerance parameter.

For more information on Newton's Method, see, for example, the reference by Epperson.

Application of Newton's method to Kepler's equation:

$$M = E - e \sin E = \sqrt{\frac{\mu}{a^3}} t_p$$

That is, $M = G(E) = K$.

Define

$$F(E) = E - e\sin E - M$$

and solve for E with M (equivalently t_p) given. Then

$$F'(E) = 1 - e \cos E$$

How do we obtain the initial guess x_1?

The reference by Smith provides a table of initial guesses that include the following:

$$\begin{aligned} E_1 &= M \\ E_1 &= M + e \\ E_1 &= M + e \sin M \\ E_1 &= M + \frac{e \sin M}{1 - \sin(M + e) + \sin M} \end{aligned} \tag{4.16}$$

The author demonstrates that the last of this set is the most efficient one computationally, but the others can also be used effectively.

Hyperbolic Form of Kepler's Equation

Consider $e > 1$.

Remarks

1. Our procedure is analogous to that for elliptic orbits.
2. We substitute an area for the eccentric anomaly E.
3. This area is based on a reference geometric shape, the equilateral hyperbola.

In the hyperbolic case, we make use of hyperbolic functions such as sinhx, coshx, and tanhx, which are treated in, for example, the references *CRC Standard Mathematical Tables* handbook and *Handbook of Mathematical Functions with Formulas, Graphs, and Mathematical Tables*, edited by Milton Abramowitz and Irene A. Stegun.

The sinhx and coshx are odd and even functions, respectively.

Def.: Let f(x) be a real-valued function of a real variable. Then f is even iff the following equation holds for all real x:

$$f(-x) = f(x)$$

Geometrically, an even function is symmetric with respect to the y-axis. The designation "even" is due to the fact that the Taylor series of an even function includes only even powers. For example,

$$\cosh x = 1 + \frac{x^2}{2!} + \frac{x^4}{4!} + \ldots + \frac{x^{2n}}{(2n)!} + \ldots, \quad |x| < \infty$$

Def.: Let f(x) be a real-valued function of a real variable. Then f is odd iff the following equation holds for all real x:

$$f(-x) = -f(x)$$

Geometrically, an odd function is symmetric with respect to the origin. The designation "odd" is due to the fact that the Taylor series of an odd function includes only odd powers. For example,

$$\sinh x = x + \frac{x^3}{3!} + \frac{x^5}{5!} + \ldots + \frac{x^{2n+1}}{(2n+1)!} + \ldots, \quad |x| < \infty$$

Reference: www.wordiq.com/definition/odd_function [Retrieved 9/29/13].

Cartesian equation for a hyperbola:

$$\frac{x^2}{a^2} - \frac{y^2}{b^2} = 1$$

$a = b$ for an equilateral hyperbola.

Define H such that

$$X = CR = |a|\cosh H$$

$$Y = PR = |b|\sinh H$$

Then a hyperbolic identity implies that

$$\frac{x^2}{a^2} - \frac{y^2}{b^2} = \frac{(CR)^2}{a^2} - \frac{(PR)^2}{b^2} = \cosh^2 H - \sinh^2 H = 1$$

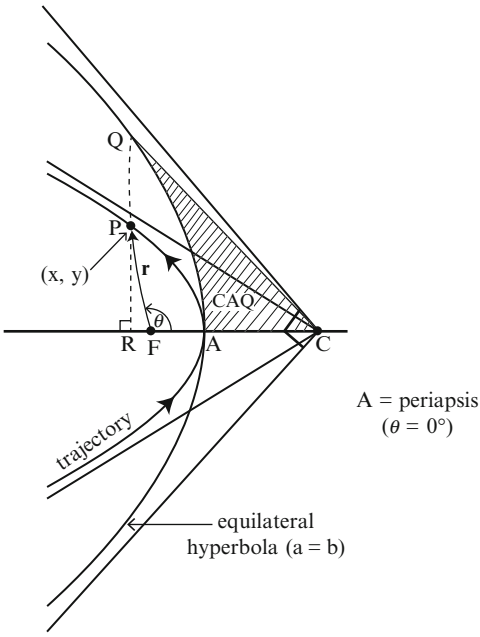

Fig. 4.5 Hyperbolic trajectory and the equilateral hyperbola

Def.: The hyperbolic anomaly is the parameter H in the parametric equations of a hyperbola given as follows:

$$x = |a|\cosh H$$

$$y = |b|\sinh H$$

The parameter H is the hyperbolic analog of the eccentric anomaly.

The hyperbolic anomaly

$$H = \frac{2}{a^2}\text{area}(CAQ) \tag{4.17}$$

where CAQ denotes the shaded region designated in Fig. 4.5 as shown in Exercise 4.5.

For hyperbolic motion, the magnitude of the radius vector

$$r = a(1 - e\cosh H) \tag{4.18}$$

as a function of the hyperbolic anomaly H, as shown in Exercise 4.6.

The following identities that relate the parameter H to the true anomaly θ are obtained by comparing this equation for r as a function of H to the conic equation that gives r as a function of θ:

$$\begin{aligned}
\cos\theta &= \frac{e - \text{coshH}}{e\text{coshH} - 1} \\
\sin\theta &= \frac{\sqrt{e^2 - 1}\,\text{sinhH}}{e\text{coshH} - 1} \\
\text{coshH} &= \frac{e + \cos\theta}{1 + e\cos\theta} \\
\text{sinhH} &= \frac{\sqrt{e^2 - 1}\sin\theta}{1 + e\cos\theta} \\
\tanh\frac{H}{2} &= \sqrt{\frac{e-1}{e+1}}\tan\frac{\theta}{2}
\end{aligned} \tag{4.19}$$

Def.:

$$N = \sqrt{\frac{\mu}{(-a)^3}}t_p \tag{4.20}$$

The parameter N is analogous to the mean anomaly of elliptic motion.

Then the hyperbolic form of Kepler's equation is given as

$$N = e\text{sinhH} - H \tag{4.21}$$

or

$$t_p = \sqrt{\frac{(-a)^3}{\mu}}(e\text{sinhH} - H) \tag{4.22}$$

where

$$\text{sinhH} = \frac{\mathbf{r} \bullet \mathbf{v}}{e}\sqrt{\frac{1}{-a\mu}} \tag{4.23}$$

$$\text{coshH} = \frac{a - r}{ae} \tag{4.24}$$

$$H = \ln(\text{sinhH} + \text{coshH}) \tag{4.25}$$

The hyperbolic form of Kepler's equation can be obtained formally from the elliptic form by setting

$E = -iH$ and $M = iN$

where $i = \sqrt{-1}$

For a derivation of the hyperbolic form of Kepler's equation, see the reference: Battin 1999.

Given the state vector of the spacecraft as (**r**, **v**), a hyperbolic set of orbital elements can be obtained by the algorithm described in the reference: Llanos, Miller, and Hintz Aug 2012.

By an argument similar to the one used for elliptical orbits, we can obtain expressions for **r**(**t**) and **v**(**t**) as follows:

$$\mathbf{r}(\mathbf{t}) = \left\{1 + \frac{a}{r_0}[\cosh(H - H_0) - 1]\right\}\mathbf{r}_0 + \left\{t - \frac{\sinh(H - H_0) - (H - H_0)}{\sqrt{\mu/(-a)^3}}\right\}\mathbf{v}_0 \tag{4.26}$$

$$\mathbf{v}(\mathbf{t}) = -\frac{\sqrt{-\mu a}}{r r_0}\sinh(H - H_0)\mathbf{r}_0 + \left\{1 + \frac{a}{r}[\cosh(H - H_0) - 1]\right\}\mathbf{v}_0 \tag{4.27}$$

where $(H - H_0)$ is obtained from the equation

$$\sqrt{\frac{\mu}{-a^3}}(t - t_0) = -(H - H_0) + \frac{\mathbf{r}_0 \bullet \mathbf{v}_0}{\sqrt{-\mu a}}[\cosh(H - H_0) - 1] + \left(1 - \frac{r_0}{a}\right)\sinh(H - H_0) \tag{4.28}$$

Orbit Propagation for All Conic Section Orbits with e > 0: Battin's Universal Formulas

We have seen how to propagate a trajectory from initial conditions $\mathbf{r_0}$ and $\mathbf{v_0}$ at $t = t_0$ for parabolic, elliptic and hyperbolic orbits. Now we use a set of universal formulas to obtain **r** and **v** for any of the three conic shapes without knowing which conic orbit we have. The problem is, given initial position and velocity vectors, determine **r** and **v** at some specified later time t. Notice the result: given six numbers, we know the state (position and velocity vectors) at any time for Keplerian motion.

Define the Stumpff functions (aka C and S functions) as

$$S(x) = \frac{1}{3!} - \frac{x}{5!} + \frac{x^2}{7!} - \ldots = \begin{cases} \dfrac{\sqrt{x} - \sin\sqrt{x}}{(\sqrt{x})^3}, x > 0 \\ 1/6,\ x = 0 \\ \dfrac{\sinh\sqrt{-x} - \sqrt{-x}}{(\sqrt{-x})^3}, x < 0 \end{cases} \tag{4.29}$$

$$C(x) = \frac{1}{2!} - \frac{x}{4!} + \frac{x^2}{6!} - \ldots = \begin{cases} \dfrac{1 - \cos\sqrt{x}}{x}, x > 0 \\ 1/2, x = 0 \\ \dfrac{\cosh\sqrt{-x} - 1}{-x}, x < 0 \end{cases} \tag{4.30}$$

Suggestions:

1. Use the definition in terms of trigonometric and hyperbolic functions, not the series definitions.
2. In your programming code, define S(x) and C(x) as:
   (a) in Eqs. (4.29) and (4.30), for $x > 0$, if $x > 10^{-7}$
   (b) in Eqs. (4.29) and (4.30), for $x < 0$, if $x < -10^{-7}$
   (c) $S(x) = 1/6$ and $C(x) = ½$, if $-10^{-7} < x < 10^{-7}$

We can determine the following identities for the C and S functions:

$$\begin{aligned} \frac{dS}{dx} &= \frac{1}{2x}[C(x) - 3S(x)], x \neq 0 \\ \frac{dC}{dx} &= \frac{1}{2x}[1 - xS(x) - 2C(x)], x \neq 0 \\ [1 - xS(x)]^2 &= C(x)[2 - xC(x)] = 2C(4x) \end{aligned} \tag{4.31}$$

Given initial conditions $\mathbf{r_0}$ and $\mathbf{v_0}$, compute the magnitudes r_0 and v_0 and define

$$\begin{aligned} \alpha_0 &\equiv \frac{2}{r_0} - \frac{v_0^2}{\mu} = \frac{1}{a}, \; e \neq 1 \\ \alpha_0 &\equiv 0, \; e = 1 \end{aligned}$$

Using the variable α instead of a avoids the discontinuity in a at $e = 1$.

Theorem 4.1: Set

$$x = \begin{cases} \dfrac{E - E_0}{\sqrt{\alpha_0}} & \text{for elliptic orbits} \\ \dfrac{H - H_0}{\sqrt{-\alpha_0}} & \text{for hyperbolic orbits} \\ \sqrt{p}\left[\tan\dfrac{\theta}{2} - \tan\dfrac{\theta_0}{2}\right] & \text{and } \alpha_0 = 0 \text{ for parabolic orbits} \end{cases} \tag{4.32}$$

Then Kepler's Equation becomes the "universal Kepler's Equation":

$$\sqrt{\mu}(t - t_0) = \frac{\mathbf{r_0} \bullet \mathbf{v_0}}{\sqrt{\mu}} x^2 C(\alpha_0 x^2) + (1 - r_0\alpha_0)x^3 S(\alpha_0 x^2) + r_0 x \tag{4.33}$$

for all three conic section orbits, $e > 0$.

Proof (Sketch):
Let $0 < e < 1$. Substitute in Eq. (4.33) for x the ratio $(E - E_0)/\sqrt{\alpha_0}$ to obtain Kepler's Equation in terms of $E - E_0$ as in Exercise 4.7. Similarly for $e > 1$ and $e = 1$. QED

To solve the universal Kepler's Equation, denote the right-hand side of Eq. (4.33) as G(x) and the left-hand side of Eq. (4.33) as K. Then, following the procedure described in Fig. 4.4, set $F(x) = G(x) - K$ so that

$$F'(x) = \frac{\mathbf{r}_0 \bullet \mathbf{v}_0}{\sqrt{\mu}}\left[x - \alpha_0 x^3 S\left(\alpha_0 x^2\right)\right] + (1 - r_0\alpha_0)x^2 C\left(\alpha_0 x^2\right) + r_0 \tag{4.34}$$

Set $x_1 =$ an initial guess. See the reference P&C on pages 39–41 or the reference Bergen and Prussing for candidate initial guesses. Then use Newton's Method to solve for x. That is,

$$x_2 = x_1 - \frac{F(x_1)}{F'(x)}$$

and continue with

$$x_{n+1} = x_n - \frac{F(x_n)}{F'(x_n)}$$

so that $x_1, x_2, \ldots, x_n, \ldots, \rightarrow x_K$, where convergence has occurred when $|x_n - x_{n+1}| < \varepsilon_{tol}$, an input tolerance parameter.

Then compute

$$\mathbf{r}(t) = \left[1 - \frac{x^2}{r_0} C\left(\alpha_0 x^2\right)\right]\mathbf{r}_0 + \left[\Delta t - \frac{x^3}{\sqrt{\mu}} S\left(\alpha_0 x^2\right)\right]\mathbf{v}_0 \tag{4.35}$$

where $\Delta t = t - t_0$.

$$\mathbf{v}(t) = \frac{\sqrt{\mu}}{r r_0}\left[\alpha_0 x^3 S\left(\alpha_0 x^2\right) - x\right]\mathbf{r}_0 + \left[1 - \frac{x^2}{r} C\left(\alpha_0 x^2\right)\right]\mathbf{v}_0 \tag{4.36}$$

Equations (4.35) and (4.36) are derived from the identities in Eq. (4.31).

Reference: P&C, pp 36ff

Procedure for Propagating an Orbit from an Initial Time $t = t_0$ to a Later Time $t > t_0$ for All Values of $e > 0$

Given $\mathbf{r_0}$ and $\mathbf{v_0}$ at t_0 and a desired time t, a computer program can be formulated to:

1. Compute

$$\alpha_0 = \frac{2}{r_0} - \frac{v_0^2}{\mu} \tag{4.37}$$

2. Determine x from the "universal" Kepler's equation, using an iterative routine such as Newton's method or the Laguerre algorithm.

3. Compute $S(\alpha_0 x^2)$ and $C(\alpha_0 x^2)$ from the definitions of the S and C functions in Eqs. (4.29) and (4.30), respectively.
4. Compute $\mathbf{r}(t)$ and $\mathbf{v}(t)$ from the formulas for the "universal" position and velocity vectors in Eqs. (4.35) and (4.36), respectively.

Note Bene (Caution):
We do not use the definition of x given in Eq. (4.32) to determine x. We use an iterative procedure to obtain x and, from x and α_0, we determine $\mathbf{r}(t)$ and $\mathbf{v}(t)$ at $t > t_0$.

Another method for computing $\mathbf{r}(t)$, $\mathbf{v}(t)$ without needing to use iterations:

Let $0 < e < 1$. Denote the coefficient of $\mathbf{r_0}$ in Eq. (4.9) as a function f and the coefficient of $\mathbf{v_o}$ as a function g. Then

$$\mathbf{r}(t) = f(t, t_0, \mathbf{r}_0, \mathbf{v}_0)\mathbf{r}_0 + g(t, t_0, \mathbf{r}_0, \mathbf{v}_0)\mathbf{v}_0$$
$$\mathbf{v}(t) = \dot{f}(t, t_0, \mathbf{r}_0, \mathbf{v}_0)\mathbf{r}_0 + \dot{g}(t, t_0, \mathbf{r}_0, \mathbf{v}_0)\mathbf{v}_0$$

These coefficients are called the "f and g functions." A series expansion in terms of the elapsed time $\Delta t = t - t_0$ gives the f, g series solutions for the f and g functions.

This method due to Gauss eliminates iteration. Unfortunately, the truncation error for the series increases with increasing elapsed time $\Delta t = t - t_0$ and the radius of convergence of the series is finite, so the use of series is limited to moderate values of elapsed time.

Reference: P&C

References for Sect. 4.1: Battin 1999; Battin 1964; Bergam and Prussing; Broucke 1980; Epperson; Kaplan; Llanos, Miller, and Hintz Aug 2012; Prussing and Conway; Smith.

4.3 Keplerian Orbit Elements

Definitions

Recall the Euler angles considered in Chap. 1 and set $\psi = \Omega$, $\theta = i$, and $\phi = \omega$. Thus we obtain the three orientation angles shown in Fig. 4.6. These angles are called:

Ω = right ascension of ascending node, $0° \le \Omega \le 360°$
ω = argument of periapsis, $0° \le \omega \le 360°$
i = inclination, $0° \le i \le 180°$

These parameters are inertial, because they are defined with respect to an inertial X, Y, Z frame. In particular, Ω is not the "longitude of the ascending node." Longitude is an earth-fixed (non-inertial) parameter.

Five parameters are needed to define a Keplerian, i.e., 2-body mechanics, orbit uniquely.

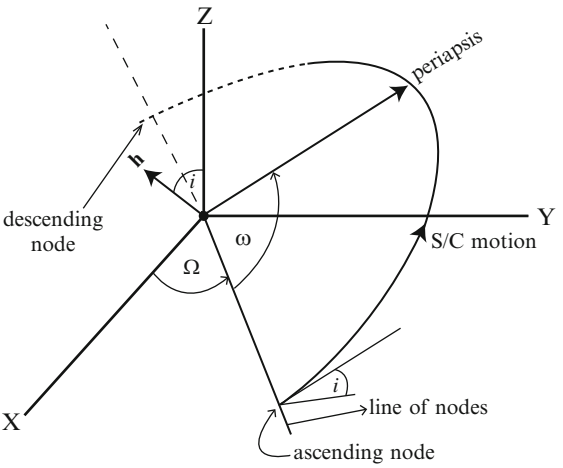

Fig. 4.6 Classical orientation angles

Two in-plane size and shape parameters:

$$\{a,\ e\} \Leftrightarrow \{e,\ p\} \overset{\text{ellipse}}{\Leftrightarrow} \{\tau, r_p\}$$

Three classical orientation angles ≡ Euler angles:

Ω, ω, *i*

To determine the location in orbit, add one of the following parameters:

$$\theta \overset{\text{ellipse}}{\Leftrightarrow} t_p \Leftrightarrow E \Leftrightarrow M$$

to this list of parameters.

Terminology: The expression "in-plane" means "in the orbit plane."

The parameter ω is the in-plane orientation angle.

The true classical element set is:

a, e, *i*, Ω, ω, time of perifocal passage

The modified classical element set (aka Keplerian elements) consists of:

a, e, *i*, Ω, ω, and θ or M or t_p or $(\theta + \omega)$

We use the modified classical element set to avoid the complications involved in keeping track of time.

We have shown that six numbers are sufficient to determine the location of a satellite at any time in 2-body mechanics (Keplerian motion). We now have a set of six elements or parameters, which provide a description of the orbit. The set has been selected to be independent so we have a complete set of six orbit elements.

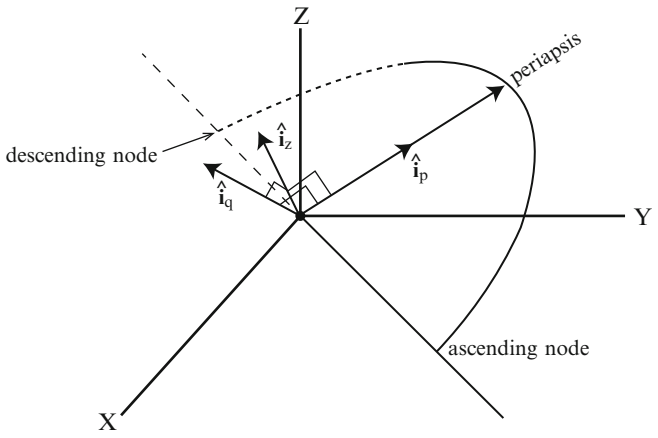

Fig. 4.7 Periapsis set of unit reference vectors

Def: The argument of latitude is the central angle in the orbit plane measured from the ascending node (positive in the direction of spacecraft motion).

If $e = 0$, replace θ by the argument of latitude, $\theta + \omega$.

Def: A posigrade orbit (aka direct orbit) is an orbit whose inclination i satisfies $0^\circ \leq i < 90^\circ$, a polar orbit $i = 90^\circ$, and a retrograde orbit $90^\circ < i \leq 180^\circ$.

Often an orbit that is nearly, i.e., $i \cong 90^\circ$, is said to be "polar."

Transformations Between Inertial and Satellite Orbit Reference Frames

1. Define the unit reference vectors shown in Fig. 4.7 as

$$\mathbf{i}_p = \hat{e}$$

$$\mathbf{i}_z = \hat{\mathbf{h}}$$

$$\mathbf{i}_q = \mathbf{i}_z \times \mathbf{i}_p$$

Recall the matrix $\boldsymbol{\alpha}$, which is defined in Chap. 1 as the product $\boldsymbol{\alpha} = \boldsymbol{\beta\gamma\delta}$, where the three matrices $\boldsymbol{\beta}$, $\boldsymbol{\gamma}$, and $\boldsymbol{\delta}$ define rotations through the three Euler angles. Setting the three Euler angles $\psi = \Omega$, $\theta = i$, and $\phi = \omega$, we can now write $\boldsymbol{\alpha}$ as

$$\alpha = \begin{bmatrix} c\omega c\Omega - s\omega cis\Omega & c\omega s\Omega + s\omega cic\Omega & s\omega si \\ -s\omega c\Omega - c\omega cis\Omega & -s\omega s\Omega + c\omega cic\Omega & c\omega si \\ sis\Omega & -sic\Omega & ci \end{bmatrix} \tag{4.38}$$

where c denotes the cosine function and s denotes the sine function. This matrix gives a rotation through Ω, i, and ω and, therefore, it is an orthogonal matrix.

$$\begin{array}{lll} \alpha : X, Y, Z & \rightarrow & \mathbf{i}_p, i_q, i_z \\ \text{inertial} & \rightarrow & \text{satellite orbit} \\ \text{system} & & \text{reference frame} \end{array}$$

Also

$$\begin{array}{lll} \alpha^T : \mathbf{i}_p, \mathbf{i}_q, \mathbf{i}_z & \rightarrow & X, Y, Z \\ \text{satellite orbit} & \rightarrow & \text{inertial} \\ \text{reference frame} & & \text{system} \end{array}$$

In particular,

$$\begin{aligned} \hat{i}_p &= \overline{\alpha}^T(1,0,0) \\ \hat{i}_q &= \overline{\alpha}^T(0,1,0) \\ \hat{i}_z &= \overline{\alpha}^T(0,0,1) \end{aligned} \tag{4.39}$$

give the unit reference vectors of the satellite orbit frame in the inertial reference frame.

Note that $\alpha^T = \alpha^{-1}$ because $\boldsymbol{\alpha}$ is an orthogonal matrix.

2. Define the radial set of unit reference vectors shown in Fig. 4.8 as

$$\begin{aligned} \hat{i}_r &= \hat{r} \equiv \left(\frac{\overline{r}}{r}\right) \\ \hat{i}_z &= \hat{h} \\ \hat{i}_\theta &= \hat{i}_z \times \hat{i}_r \end{aligned}$$

For this set, the first reference vector is along the radial direction and the rotation matrix is $\boldsymbol{\alpha}^*$. The matrix $\boldsymbol{\alpha}^*$ is the same as the matrix $\boldsymbol{\alpha}$, except that the argument of periapsis ω is replaced by the argument of latitude, $\theta^* \equiv \omega + \theta$.

Conversion from Inertial Position and Velocity Vectors to Keplerian Orbital Elements

A spacecraft is in orbit about a central body with $\mu = Gm$. Consider a X, Y, Z inertial frame whose origin is at the center of mass of the central body and has unit reference vectors **I**, **J**, **K**. Suppose the spacecraft's position and velocity vectors in

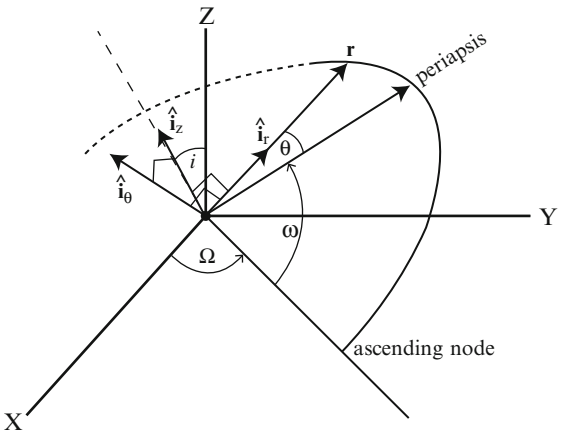

Fig. 4.8 Radial set of unit reference vectors

this inertial frame are $\mathbf{r_0}$ and $\mathbf{v_0}$. We derive expressions for Ω, ω, i from the Cartesian vectors $\mathbf{r_0}$ and $\mathbf{v_0}$.

Objective: To convert from Cartesian coordinates ($\mathbf{r}(\mathbf{t_0})$, $\mathbf{v}(\mathbf{t_0})$) to classical orientation parameters, Ω, ω, and i.

Note: Then we will be able to convert from Cartesian coordinates to (modified) classical coordinates because we already know how to compute size, shape, and location parameters from $\mathbf{r}(\mathbf{t})$ and $\mathbf{v}(\mathbf{t})$. See Exercises 2.16 and 4.8.

Inclination i:

$$\hat{\mathbf{h}} = \frac{\hat{\mathbf{r}}_0 \times \hat{\mathbf{v}}_0}{\hat{\mathbf{r}}_0 \times \hat{\mathbf{v}}_0} \qquad \mathbf{K} = (0, 0, 1)$$

$$\cos i = \hat{\mathbf{h}} \bullet \hat{\mathbf{K}}$$

$$i = \cos^{-1}(\mathrm{h}(3)) \tag{4.40}$$

Right Ascension of the Ascending Node Ω:

Define the vector

$$\hat{\mathbf{N}} = \frac{\mathbf{K}\mathbf{x}\hat{\mathbf{h}}}{\mathbf{K}\mathbf{x}\hat{\mathbf{h}}} \tag{4.41}$$

along the line of nodes. This vector is in the X, Y plane and in the orbit plane.

Therefore,

$$\cos \Omega = \hat{\mathbf{N}} \bullet \hat{\mathbf{I}}$$

so that

$$\Omega = \cos^{-1}\left(\hat{\mathbf{N}}(\mathbf{1})\right) \tag{4.42}$$

If $\hat{\mathbf{N}}(\mathbf{2}) > 0$, then Ω is in the first or second quadrant, so Ω is found as $\cos^{-1}\left(\hat{\mathbf{N}}(\mathbf{1})\right)$. If $\hat{\mathbf{N}}(\mathbf{2}) < 0$, replace Ω by $360^\circ - \Omega$.

Argument of Periapsis ω:
For ω,

$$\cos\omega = \frac{\mathbf{e} \bullet \hat{\mathbf{N}}}{e}$$

so that

$$\omega = \cos^{-1}\left(\frac{\mathbf{e} \bullet \hat{\mathbf{N}}}{e}\right) \tag{4.43}$$

where

$$\mathbf{e} = (1/\mu)\left[(v_0{}^2 - (\mu/r_0))\,\mathbf{r_0} - (\mathbf{r_0} \bullet \mathbf{v_0})\mathbf{v_0}\right] \text{ from Exercise 2.4}$$

and

$$0^\circ < \omega < 180^\circ \text{ if } \mathbf{e}(3) > 0$$
$$180^\circ < \omega < 360^\circ \text{ if } \mathbf{e}(3) < 0.$$

In MATLAB, we write

```
lomega = acosd((dot(e,Nhat))/norm(e))
if e(3) < 0
        lomega = 360 - lomega
end
```

Conversion from Keplerian Elements to Inertial Position and Velocity Vectors in Cartesian Coordinates

Objective: Given the values of the modified classical element set

$$\{a,\ e, i,\ \Omega,\ \omega,\ \theta\},$$

obtain the Cartesian (inertial) position and velocity vectors, **r** and **v**.
Procedure:

1. Compute the parameter p as

$$p = a\left(1 - e^2\right)$$

and the magnitude of **r** from the Conic Equation as

$$r = \frac{p}{1 + e\cos\theta}$$

2. Write the position **r** and velocity **v** vectors in the periapsis-based orbital frame as follows:

$$\begin{aligned} \mathbf{r}_{\text{orbital}} &= r\cos\theta\mathbf{i}_p + r\sin\theta\mathbf{i}_q \\ &= (r\cos\theta, r\sin\theta, 0.0) \end{aligned} \tag{4.44}$$

$$\begin{aligned} \mathbf{v}_{\text{orbital}} &= \sqrt{\frac{\mu}{p}}(-\sin\theta\mathbf{i}_p + (e + \cos\theta)\mathbf{i}_q) \\ &= \sqrt{\frac{\mu}{p}}(-\sin\theta, (e + \cos\theta), 0.0) \end{aligned} \tag{4.45}$$

3. Rotate $\mathbf{r}_{\text{orbital}}$ and $\mathbf{v}_{\text{orbital}}$ from the periapsis-based orbital frame to the inertial frame as:

$$r_{\text{inertial}} = \alpha^T r_{\text{orbital}}$$

$$v_{\text{inertial}} = \alpha^T v_{\text{orbital}}$$

where

$$\alpha^T = \begin{bmatrix} c\omega c\Omega - s\omega c i s\Omega & -s\omega c\Omega - c\omega c i s\Omega & s\Omega s i \\ c\omega s\Omega + s\omega c i c\Omega & -s\omega s\Omega + c\omega c i c\Omega & -s i c\Omega \\ s\omega s i & c\omega s i & c i \end{bmatrix} \tag{4.46}$$

where s denotes the sine function and c denotes the cosine function.

Alternative Orbit Element Sets

We have considered the modified classical element set: a, e, i, Ω, ω, and θ. Sometimes, alternative sets of parameters are useful. For example, if the eccentricity is near zero, the periapsis is not well defined, especially in the presence of small perturbations, which make the orbit non-Keplerian. If the inclination is near zero, the line of nodes is not well defined.

To remove the singularities encountered at $e = 0$ and/or $i = 0^\circ$ or 180°, we often use equinoctial elements, consisting of six elements that are defined in terms of the Keplerian elements that are used for elliptical orbits. Two references are: Broucke and Cefola, Battin 1999. An alternate form of the equinoctial element set is defined in the reference by Nacozy and Dallas.

A set of modified equinoctial orbit elements is introduced in the references: Walker, Ireland and Owens 1985 and 1986. Modified equinoctial elements remove singularities for all eccentricities and inclinations, including hyperbolic and parabolic orbits.

There are more element sets. The survey provided in the reference Hintz 2008 discusses 22 element sets plus variations.

References for Keplerian Elements: BMW; Battin 1999; Broucke and Cefola; Hintz 2008; Kaplan; Nacozy and Dallas; Pisacane and Moore, eds.; Walker, Ireland, and Owens 1985, 1986.

4.4 Lambert's Problem

Problem Statement

We have looked at the problem of determining the position and velocity vectors at a specified time t, given a set of initial conditions $\mathbf{r}_0$ and $\mathbf{v}_0$. In the relative 2-body problem, the six numbers in $\mathbf{r}_0$ and $\mathbf{v}_0$ completely determine $\mathbf{r}(t)$ and $\mathbf{v}(t)$ for all t. We now look at the problem of determining flight paths about a central body of attraction and between two given points. For example, one point might be at the earth (representing the injection point) and the other at another planet (representing the target body) as in Fig. 4.9. We determine families of heliocentric orbits that could be followed. The selection of an orbit depends on energy considerations for the launch vehicle at one end and planetary approach considerations, e.g., science requirements, at the other.

Problem: To determine a Keplerian orbit, having a specified flight time and connecting two position vectors. Lambert's Problem is the 2-point boundary value problem with a specified time of flight for the relative 2-body problem. This method was first stated and solved by Johann Heinrich Lambert (1728–1779).

Application: To obtain mission design curves, called "pork chop plots," used to design trajectories that satisfy launch energy constraints and target body requirements.

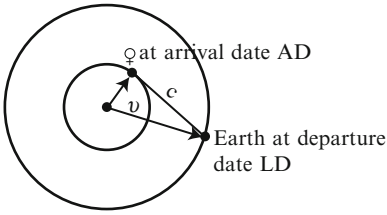

Fig. 4.9 Boundary points in Lambert's problem

A Mission Design Application

Interplanetary mission design:

1. In the Patched Conics Example, using a Hohmann transfer required that the flight time = 146 days and we assumed that Venus is in the ecliptic plane and used the zero sphere of influence model. The conic segments fit together in position and velocity vectors in an interplanetary trajectory model.
2. In the Mission Design Curves, we assume massless planets, which implies that we have only one conic that goes from the center of one planet to the center of the other. However, we do not assume the target planet is in the ecliptic plane.

The energy at injection into the interplanetary elliptic trajectory about the sun is

$$\mathscr{E}_I = \frac{v_\infty^2}{2} = \frac{v_I^2}{2} - \frac{\mu}{R_I} \tag{4.47}$$

We define the launch energy

$$C_3 = C3 = 2\ \mathscr{E}_I = {v_\infty}^2 = v_I^2 - \frac{2\mu}{R_I} \tag{4.48}$$

where v_I = conic injection velocity and R_I = the magnitude of the radius vector at injection.

Additional parameters that will be used in the following discussion are:

VHP = the arrival v_∞ at the target body,
DLA = declination of the launch azimuth,
TTIME = TFL = time of flight, and
υ = HCA = heliocentric angle between the two boundary vectors.

We also define the following trajectory types.

Def.: A Type I trajectory is a trajectory from the earth to a target body that satisfies

$$0 < \text{HCA} < 180^\circ$$

Def.: A Type II trajectory is a trajectory from the earth to a target body that satisfies

$$180^\circ < \text{HCA} < 360^\circ$$

We now consider mission design curves known as "pork chop plots," which are contours of trajectory performance and geometry data as a function of launch and arrival between two bodies orbiting the sun. Data types that are available include C3, VHP, and DLA. The C3 is the launch energy required for the spacecraft to

travel from the earth on the launch date (LD) to the target body on the arrival date (AD); TFL is the time between LD and AD; VHP denotes the arrival velocity at the target body; and DLA describes the launch direction when combined with the right ascension of the launch azimuth.

In Fig. 4.10, the horizontal axis shows launch dates (LD) and the vertical axis arrival dates (AD). In Fig. 4.10a, the blue contours are the LD/AD points that require the C3 indicated and points inside the contour require less than that C3 to reach Venus from the earth. Note that the C3 contours become very steep nearing the Hohmann transfer. This extremely large Δv at injection into the heliocentric transfer trajectory is required because of the large velocity change required to change the orbit plane from ecliptic to the Venus orbit plane. The red lines denote the time of flight (TFL).

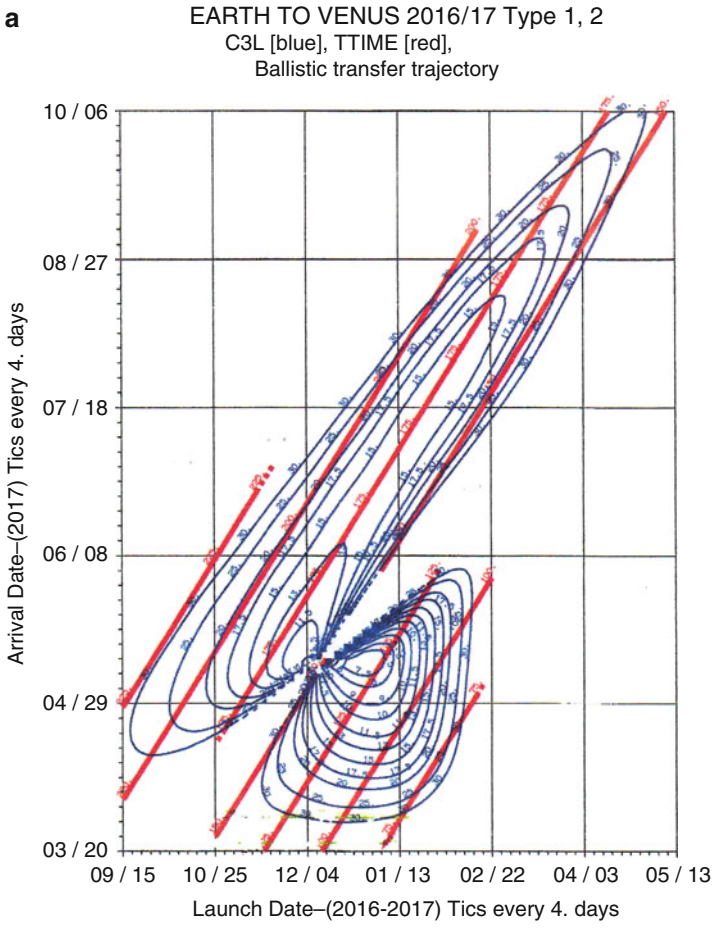

Fig. 4.10 (**a**): Pork chop plot of Earth–Venus trajectories for 2016–2017: C3 and TFL. (**b**) Pork chop plot of Earth–Venus trajectories for 2016–2017: C3, VHP, and TFL. (**c**): Pork chop plot of Earth–Venus trajectories for 2016–2017: C3, DLA, and TFL

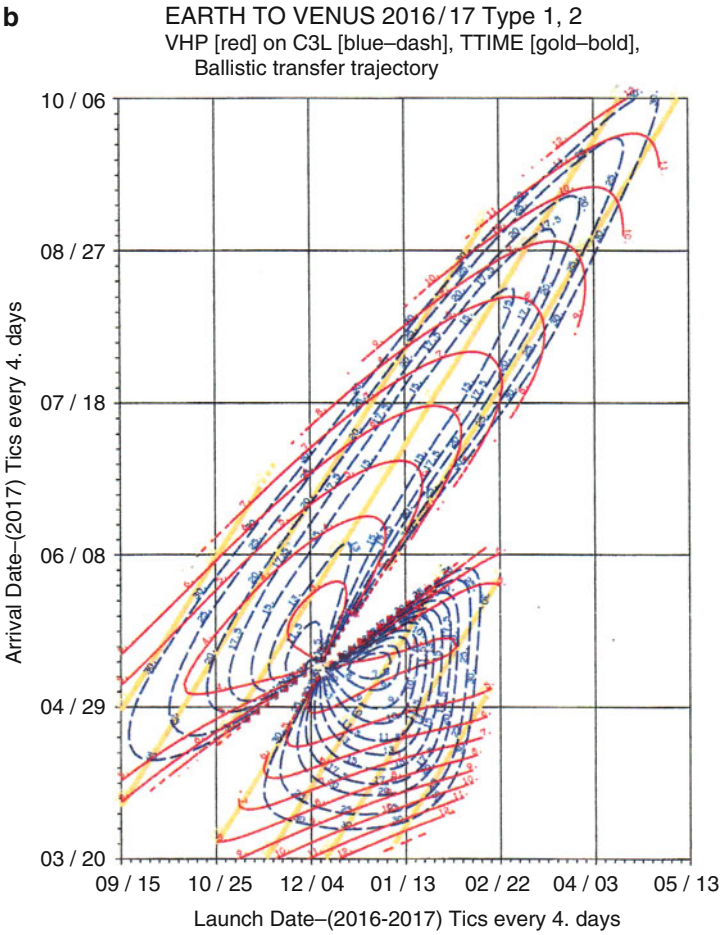

Fig. 4.10 (continued)

Figure 4.10b displays the VHP contours in red, C3L in dashed blue curves, and TTIME in gold lines. Figure 4.10c gives the DLA curves in red, C3L in dashed blue curves, and TTIME in bold gold lines.

Example (C3, VHP, TFL):

What are the C3, VHP, and TFL for LD = 1/13/2017 and AD = 4/29/2017?

Answer: Fig. 4.10a shows that C3 = 10 km^2/s^2 and Fig. 4.10b shows VHP = 4.9 km/s. The TFL = 107 days.

Example (constraints):

Which regions in Fig. 4.10b satisfy the constraints C3 $\leq$ 13.0 km^2/s^2 and VHP $\leq$ 5.0 km/s?

Answer: See Exercise 4.10.

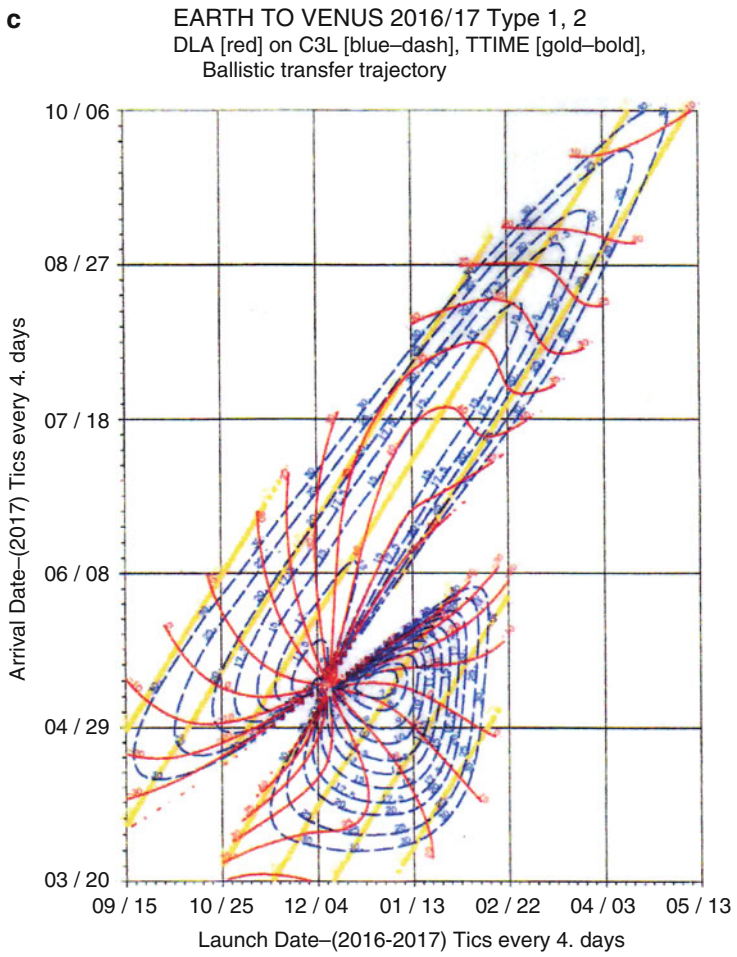

Fig. 4.10 (continued)

Launch constraints may restrict the region of LD/AD pairs that are acceptable for a mission. For example, launches to the ISS require a DLA less than approximately 50°. See Exercise 4.10.

People often confuse the "launch period" and "launch window." They are different as indicated in the following two definitions.

Def: The launch period is the set of contiguous days the LV can be launched to its target within mission and launch vehicle performance constraints.

Def: The launch window is the duration within each day of the launch period in which the launch can be executed within mission and launch vehicle performance constraints.

The launch window is typically 0–60 min, depending on LV performance capability.

The launch period is typically 20–30 days to allow for delays such as bad weather. The nominal launch day may be chosen on a C3 curve that satisfies the launch energy constraint on C3 as, for example, a spacecraft which provides $C3 = 15\ km^2/s^2$ for a nominal LD = 12/4/2016 and AD = 6/8/2017. Then, for each day the launch is postponed, the LD is delayed 1 day, but the AD is held fixed. Thus, the C3 decreases as the launch moves into the launch period. (This requirement also accommodates the scientists because they have scheduled science-data-taking at the target body that is time-dependent.) Note that this strategy gives the spacecraft a launch period of 25 days that satisfy a requirement of $C3 \leq 15\ km^2/s^2$ as on the nominal launch day.

Thus, pork chop plots are employed for many mission planning purposes, including:

1. To determine the launch date.
2. To determine the arrival date at the target body.
3. To provide a preliminary estimate of the amount of propellant to be carried onboard the spacecraft. This estimate dictates the launch vehicle to be used and/or the use of navigation and mission design strategies such as aerobraking at a target body that has an atmosphere.
4. To provide information on the capture orbit when the spacecraft arrives at the target body. This information enables selecting the arrival date that minimizes the amount of propellant used to brake the spacecraft's speed to allow it to be captured into orbit. It is also important to the scientists for meeting data-taking requirements.
5. To verify that launch constraints such as the DLA requirement for launching to the ISS are met.
6. To select a LD/AD pair for which the launch period is acceptable.

How do we obtain these parametric plots?

For each LD and AD pair, we know:

Distance between sun and earth at departure
Distance between sun and Venus at arrival
Distance between earth at launch and Venus at arrival
$\upsilon = \Delta$ heliocentric true anomaly = heliocentric angle (HCA)
Flight time = arrival time − departure time

Trajectories/Flight Times Between Two Specified Points

Survey of all Possible Flight Paths for any Flight Time:

Without loss of generality (wolog), we assume $r_1 < r_2$. We will consider an example about how we cope with the reverse inequality. The given data for

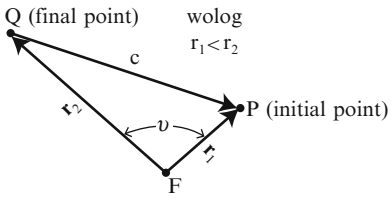

Fig. 4.11 Given values in Lambert's problem

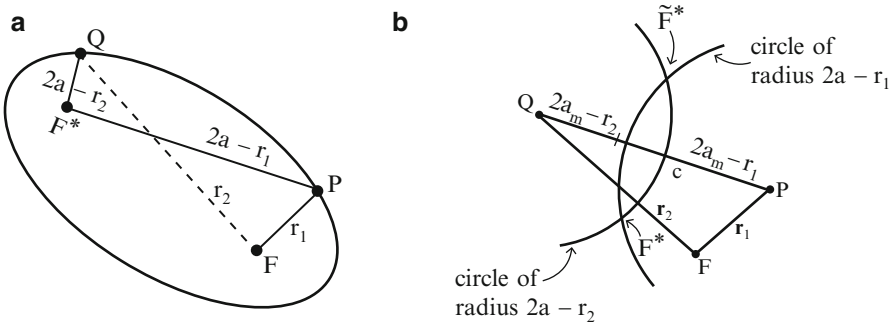

Fig. 4.12 Location of F* for elliptical orbits from point P to point Q. (**a**) Elliptical orbit from point P to point Q. (**b**) Vacant foci F*

Lambert's Problem are shown in Fig. 4.11. Note that we do not know where the vacant focus F* is in this figure.

We determine all conic section flight paths through P and Q. In the Mission Design Application, flight time is known. We are not saying that we know the flight time here as we do in generating the mission design curves. We survey all possible flight paths between P and Q for all flight times and then throw away the trajectories we do not need.

1. Elliptic Orbits
   Let a = the semimajor axis of such an elliptic orbit. Then, as shown in Fig. 4.12a,
   $PF^* + PF = PF^* + r_1 = 2a$ and $QF^* + QF = QF^* + r_2 = 2a$
   so that

$$PF* = 2a - r_1 \quad \text{and} \quad QF* = 2a - r_2 \tag{4.49}$$

   Since the vacant focus must satisfy both equations, each vacant focus is at the intersection of two circles—one circle of radius $2a - r_1$ centered at the initial point P and the other of radius $2a - r_2$ centered at the final point Q, as shown in Fig. 4.12b. We consider all vacant foci F* for different values of the semimajor axis a.

The Minimum Energy Transfer Ellipse

There is a minimum a—call it a_m—such that the two circles are tangent along the chord c. For $a < a_m$, the energy is too small for an elliptic orbit to reach Q from P. The value a_m satisfies the equation

$$\min \mathscr{E} \equiv \mathscr{E}_m = -\mu/(2a_m)$$

Notation:

e_m = eccentricity of minimum energy ellipse
p_m = parameter of minimum energy ellipse
s = semiperimeter of the triangle FPQ, i.e.,
$s = (r_1 + r_2 + c)/2$

Then

$$(2a_m - r_2) + (2a_m - r_1) = c$$

$$a_m = (1/4)(r_1 + r_2 + c)$$

Therefore,

$$2a_m = s \tag{4.50}$$

Consider the triangle PQF as shown in Fig. 4.13. Let the angle between the sides PQ and FQ be denoted as ψ. Then the lengths of the sides of the triangle are as shown. In particular,

$QF_m^* = 2a_m - r_2 = s - r_2$
$PF_m^* = 2a_m - r_1 = s - r_1$
$FF_m^* = 2a_m e_m$
υ = HCA

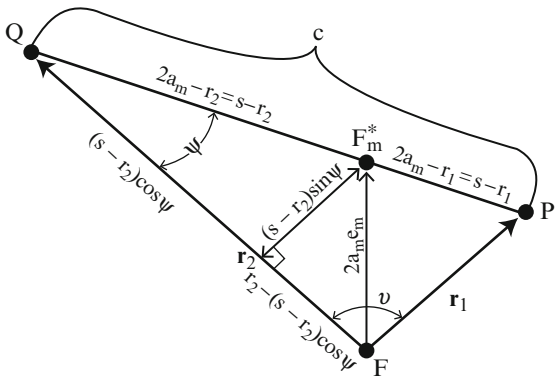

Fig. 4.13 Triangle PQF

From the Law of Cosines, we determine that

$$\cos\psi = \frac{2s(s - r_1)}{r_2 c} - 1 \tag{4.51}$$

Therefore,

$$\begin{aligned}(2e_m a_m)^2 = \left(FF_m^*\right)^2 &= [(s - r_2)\sin\psi]^2 + [r_2 - (s - r_2)\cos\psi]^2 \\ &= s^2 - \frac{4s}{c}(s - r_1)(s - r_2)\end{aligned}$$

after using Eq. (4.51), which gives one expression for $(2e_m a_m)^2$. Since $p = a(1 - e)^2$, $a - p = ae^2$. So we obtain

$$(2a_m e_m)^2 = 4a_m(a_m - p_m) = s^2 - 2sp_m$$

from Eq. (4.50).

Equating the two expressions for $(2a_m e_m)^2$, and solving for p_m, we obtain

$$p_m = -\frac{2}{c}(s - r_1)(s - r_2) = \frac{r_1 r_2}{c}(1 - \cos(\upsilon)) \tag{4.52}$$

from the Law of Cosines. Using $p_m = a_m(1 - e_m{}^2)$ and Eq. (4.50) again and solving for $e_m{}^2$, we obtain

$$e_m^2 = 1 - \frac{2p_m}{s} \tag{4.53}$$

Therefore, the size (a_m) and shape (e_m) of the minimum energy transfer ellipse are known immediately.

For $a > a_m$, there are two possible vacant foci, $F^*, \tilde{F}^*$, for two different ellipses for the same a.

$$\begin{aligned}&FF^* = 2ae < F\tilde{F}^* = 2a\tilde{e} \\ &\text{so } e < \tilde{e} \text{ and } p > \tilde{p}\end{aligned}$$

What is the set of all F^* for all a, $\{F^* | \text{ for all a}\}$?

Subtracting the two equations in Eq. (4.49) gives

$$PF^* - QF^* = r_2 - r_1 = \text{constant} > 0$$

because $r_1 < r_2$ by assumption. Therefore, by the definition of a hyperbola (see Fig. 2.8), the set $\{F^*\}$ of all vacant foci for all semimajor axis lengths is a hyperbola with P and Q as foci and $r_2 - r_1 = -2a_H$, where a_H denotes the semimajor axis of this hyperbola. (Recall $r_1 < r_2$ so $r_2 - r_1 > 0$). This hyperbola bends around Q.

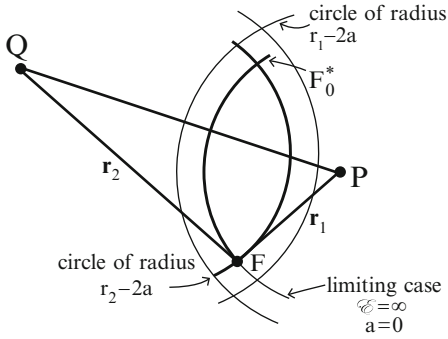

Fig. 4.14 Location of F* for hyperbolic trajectories and the limiting case

2. Hyperbolic Paths between P and Q:
From the definition of a hyperbola,

$$PF^* - PF = QF^* - QF = -2a > 0$$

Hence,

$$PF^* = r_1 - 2a \geq r_1$$
$$QF^* = r_2 - 2a \geq r_2$$
$$QF^* - PF^* = r_2 - r_1$$

Limiting case: $a = 0$ ($\mathscr{E} = \infty$)

The circles for this limiting case pass through F. Denote the upper intersection point as F_0^* (Fig. 4.14).

$$\{F^*\} = \{F^* | QF^* - PF^* = r_2 - r_1 = \text{constant} > 0\}.$$

Therefore, the set of all vacant foci for all semimajor axis lengths (a) is a hyperbola that bends around P minus the arc between F and F_0*.

3. Parabolic Orbits:
There are two possibilities as shown in Fig. 4.15. The reference by Kaplan provides a geometric argument that the values of the parameter p for these two trajectories are:

$$p = \frac{4(s - r_1)(s - r_2)}{c^2}\left(\sqrt{\frac{s}{2}} \pm \sqrt{\frac{s - c}{2}}\right) \tag{4.54}$$

Also, $e = 1$ and $a = \infty$. The times of flight, TFL1 and TFL2, from P to Q along the two parabolic orbits are different as will be shown by Eqs. (4.63a,b).

We now obtain p for $e \neq 1$. Denote the magnitude of the position as r_1 and the true anomaly as θ_1 for the point P and correspondingly r_2 and θ_2 at Q (Fig. 4.16). By solving the Conic Equation for $\cos\theta$, we obtain

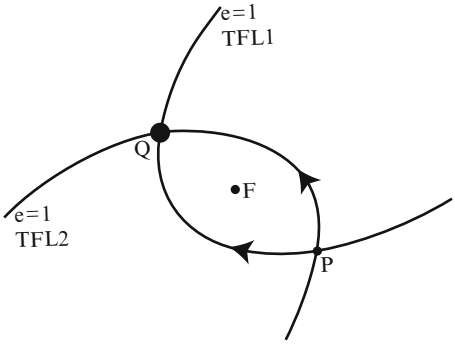

Fig. 4.15 Parabolic trajectories from P to Q

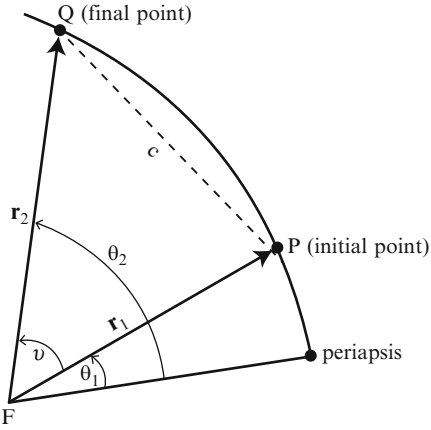

Fig. 4.16 Trajectories from P to Q for $e \neq 1$

$$\cos\theta_1 = \left(\frac{p}{r_1} - 1\right)/e$$

$$\cos\theta_2 = \cos(\theta_1 + \upsilon) = \left(\frac{p}{r_2} - 1\right)/e$$

Substituting these two expressions into the identity

$$\cos^2(\theta_1 + \upsilon) - 2\cos(\theta_1 + \upsilon)\cos\theta_1\cos\upsilon + \cos^2\theta_1 - \sin^2\upsilon = 0$$

obtains a quadratic equation in p.

Define angles α, β, γ, and δ such that

$$\sin\left(\frac{\alpha}{2}\right) = \sqrt{\frac{s}{2a}} \quad \sin\left(\frac{\beta}{2}\right) = \sqrt{\frac{s-c}{2a}} \qquad (4.55a, b)$$

$$\sinh\left(\frac{\gamma}{2}\right) = \sqrt{\frac{s}{-2a}} \quad \sinh\left(\frac{\delta}{2}\right) = \sqrt{\frac{s-c}{-2a}} \tag{4.55c, d}$$

The two solutions for each of the quadratic equations are given as

$$p = \frac{4a(s-r_1)(s-r_2)}{c^2} \sin^2\left(\frac{\alpha \pm \beta}{2}\right) \text{ for } 0 < e < 1 \tag{4.56a$^+$, a$^-$}$$

and as

$$p = -\frac{4a(s-r_1)(s-r_2)}{c^2} \sinh^2\left(\frac{\gamma \pm \delta}{2}\right) \tag{4.56b$^+$, b$^-$}$$

for $e > 1$

Reference: John E. Prussing 1979

Lambert's Theorem: The transfer time between any two points on a conic orbit is a function of the sum of the distances of each point from the focus, the distance between the points, and the semimajor axis, i.e.,

$$t = t(r_1 + r_2, c, a) \tag{4.57}$$

Proof (sketch):
For $0 < e < 1$, let E_1, E_2 = eccentric anomalies of P, Q, respectively.

1. Kepler's Equation implies

$$t = 2\sqrt{\frac{a^3}{\mu}}\left(\frac{E_2 - E_1}{2} - e \sin\frac{E_2 - E_1}{2} \cos\frac{E_2 + E_1}{2}\right)$$

2. Consider two identities:

$$c^2 = 2a^2 \sin^2\left(\frac{E_2 - E_1}{2}\right)\left(1 - e^2 \cos^2\left(\frac{E_2 + E_1}{2}\right)\right)$$
$$r_1 + r_2 = 2a\left(1 - e\cos\frac{E_2 + E_1}{2} \cos\frac{E_2 - E_1}{2}\right)$$

3. Solve these two equations for

$$e\cos\left(\frac{E_2 + E_1}{2}\right) \text{ and } \frac{E_2 - E_1}{2} \text{ in terms of a, } r_1 + r_2, \text{ and c.}$$

4. Substitute the results into the equation in (1) to show that t depends only on a, $r_1 + r_2$, c.

Similar arguments imply the result for parabolic and hyperbolic orbits. QED

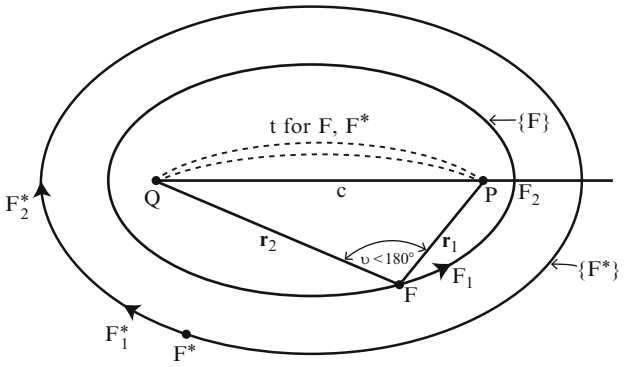

Fig. 4.17 Elliptic orbits with fixed time of flight from P to Q

Lambert conjectured this theorem. Lagrange proved it analytically 1 year before Lambert died.

Note that t is independent of e.

Formulas for the flight time t:

Case 1 (E1):

1. Elliptic arc from P to Q.
2. F* is on the lower branch of the hyperbola of {F*}
3. $\upsilon < 180°$ (Type I trajectory)

Mathematical device:
Lambert's Theorem implies that the shape of the elliptical path from P to Q may be changed by moving F, F* without changing t provided $r_1 + r_2$, c, and a are held constant.

The set of permissible $F = \{F \mid r_1 + r_2 = \text{constant}\}$ is an ellipse with foci at P and Q and $2a_F = r_1 + r_2$.

The set $\{F^*\} = \{F^* \mid PF^* + QF^* = 4a - (r_1 + r_2) = \text{constant}\}$ is an ellipse with foci at P and Q and $2a_{F^*} = 4a - (r_1 + r_2)$ (Fig. 4.17).

$F^* \not\subset$ sector PQF for $\upsilon < 180°$. Moving F to F_1 and F* to F_1* implies a new elliptic path from P to Q with the same t. Moving F to F_2 and F* to F_2* in the limiting case implies that the transfer ellipse flattens to the chord c, i.e., the orbit assumes rectilinear motion, a mathematical device that enables computing t simply. See Fig. 4.17.

Rectilinear orbits are straight lines on the major axis, so they are one-dimensional. They satisfy the following properties:

1. $e = 1$ for rectilinear ellipses, parabolas, and hyperbolas.
2. $h = 0$ because the position and velocity vectors are parallel or antiparallel, so $p = 0$.
3. $r_p = 0$.

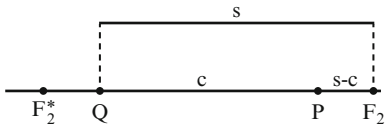

Fig. 4.18 Integration interval for Case E1

For more information on rectilinear orbits, see the references Roy 1988 and Roy 2004.

Rectilinear Motion

$v = dr/dt$ along the line PQ

$$\frac{dr}{dt} = \sqrt{\mu\left(\frac{2}{r} - \frac{1}{a}\right)} \text{ from the Vis-Viva Equation}$$

$$dt = \frac{rdr}{\sqrt{\mu}\left(\sqrt{2r - \frac{r^2}{a}}\right)}$$

Integration from P to Q along the line PQ according to Fig. 4.18 gives

$$t_{E1} = \frac{1}{\sqrt{\mu}} \int_{s-c}^{s} \frac{rdr}{\sqrt{2r - \frac{r^2}{a}}}$$

Let $r = a(1 - \cos\sigma)$. Then $dr = a(\sin\sigma)d\sigma$ and

$\sigma = \beta$ for $r = s - c$ from Eq. (4.55b) and
$\sigma = \alpha$ for $r = s$ from Eq. (4.55a).

Thus, we obtain

$$t_{E1} = \sqrt{\frac{a^3}{\mu}} \int_{\beta}^{\alpha} (1 - \cos\sigma)d\sigma = \frac{\tau}{2\pi}[(\alpha - \sin\alpha) - (\beta - \sin\beta)] \qquad (4.58)$$

Note: $t_{E1} = t_{E1}(r_1 + r_2, c, a)$ as in Lambert's Theorem because a, α, β are functions of $r_1 + r_2$, c, and a. The parameter p is computed from Eq. (4.56a$^+$).

Case 2 (E2):

1. Elliptic arc from P to Q.
2. F* is on the upper branch of the hyperbola of {F*}
3. $\upsilon < 180°$ (Type I trajectory)

The argument is similar to that for Case E1, except each ellipse passes through apoapsis and F* ⊂ sector PQF if HCA < 180°, as shown in Fig. 4.17. Therefore,

$$t_{E2} = t_{E1} + 2(\text{time from Q to } F_2{}^*) = t_{E1} + \frac{2}{\sqrt{\mu}}\int_s^{2a} \frac{rdr}{\sqrt{2r - \frac{r^2}{a}}}$$

so that

$$t_{E2} = \tau - \frac{\tau}{2\pi}[(\alpha - \sin\alpha) + (\beta - \sin\beta)] \tag{4.59}$$

The parameter p is computed from Eq. (4.56a$^-$).

Therefore, for elliptic orbits with $\upsilon < 180°$, t is obtained from t_{E1} or t_{E2}, depending on which vacant focus is selected.

Minimum Energy Transfer

Recall that $s = 2a_m$ so that, from Eq. (4.55a),

$$\sin\frac{\alpha_m}{2} = 1$$

$$\alpha_m = \pi$$

and

$$\tau_m = \pi\sqrt{\frac{s^3}{2\mu}}$$

Therefore, from Eq. (4.58),

$$t_m = \frac{\tau_m}{2\pi}[\pi - \beta_m + \sin\beta_m]$$

where

$$\sin\frac{\beta_m}{2} = \sqrt{\frac{s-c}{s}} \tag{4.60}$$

Case 3 (H1):

1. Hyperbolic path from P to Q (see Fig. 4.19a)
2. F* on upper branch of {F*} (see Fig. 4.14)

From an argument analogous to that for E1, except replace α, β by γ, δ and use Eq. (4.55c,d), we obtain

$$t_{H1} = \sqrt{\frac{-a^3}{\mu}}[(\sinh\gamma - \gamma) - (\sinh\delta - \delta)] \tag{4.61}$$

The parameter p is computed from Eq. (4.56b$^+$).

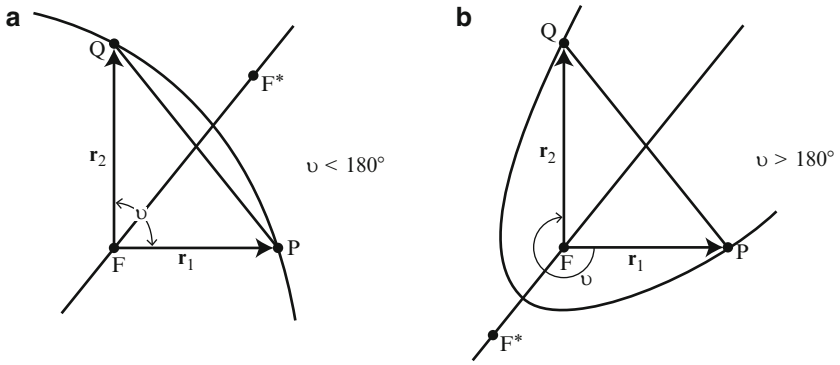

Fig. 4.19 Hyperbolic paths from P to Q. (**a**) Hyperbolic path from P to Q for $\upsilon < 180°$. (**b**) Hyperbolic path from P to Q for $\upsilon > 180°$

Case 4 (H2):

1. Hyperbolic path from P to Q (see Fig. 4.19b)
2. F* along lower branch of {F*} (see Fig. 4.14)

$$t_{H2} = \sqrt{\frac{-a^3}{\mu}}[(\sinh\gamma - \gamma) - (\sinh\delta - \delta)] \tag{4.62}$$

The parameter p is computed from Eq. (4.56b$^-$).

Case 5 (P1) and Case 6 (P2): parabolic paths

$$\begin{aligned} t_{P1} &= \lim_{-a\to\infty} t_{H1} = \frac{1}{3}\sqrt{\frac{2}{\mu}}\left[s^{3/2} - (s-c)^{3/2}\right] \\ t_{P2} &= \lim_{-a\to\infty} t_{H2} = \frac{1}{3}\sqrt{\frac{2}{\mu}}\left[s^{3/2} + (s-c)^{3/2}\right] \end{aligned} \tag{4.63a, b}$$

The parameter p is computed from Eq. (4.54).

Case 7: (E3): Same as E1, except $\upsilon > 180°$

$$t_{E3} = \tau - t_{E1} \tag{4.64}$$

See Fig. 4.20.
The parameter p is computed from Eq. (4.56a$^+$).

Case 8 (E4): Same as E2, except $\upsilon > 180°$

$$t_{E4} = \tau - t_{E2} \tag{4.65}$$

The parameter p is computed from Eq. (4.56a$^-$).

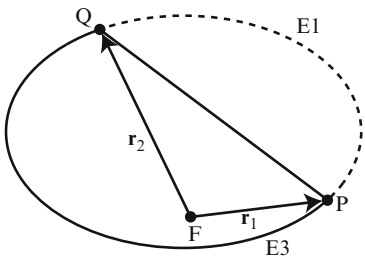

Fig. 4.20 Elliptic path from P to Q for $\upsilon > 180°$, Case 7

For more information on the conic transfer from P to Q, see the references by Kaplan and Thomson.

Let $\mathbf{r}_1$ and $\mathbf{r}_2$ denote the position vectors at P and Q, respectively. What is $\mathbf{v}_1$, the velocity at P?

Exercise 4.13 shows that

$$\mathbf{r}_2 = \left[1 - \frac{r_2}{p}(1 - \cos\upsilon)\right]\mathbf{r}_1 + \left[\frac{r_1 r_2}{\sqrt{\mu p}} \sin\upsilon\right]\mathbf{v}_1 \tag{4.66}$$

Solving Eq. (4.66) for $\mathbf{v_1}$ determines the velocity vector at P in terms of $\mathbf{r}_1$ and $\mathbf{r}_2$ as

$$\mathbf{v}_1 = \frac{\sqrt{\mu p}}{r_1 r_2 \sin\upsilon}\left\{\mathbf{r}_2 - \left[1 - \frac{r_2}{p}(1 - \cos\upsilon)\right]\mathbf{r}_1\right\} \tag{4.67}$$

which is the velocity at P for a trajectory that will pass through Q.

If $\mathbf{v}_P$ (velocity at P) $\neq \mathbf{v}_1$, then we make a $\Delta\mathbf{v}$ correction with

$$\Delta\mathbf{v} = \mathbf{v}_1 - \mathbf{v}_P$$

if the (impulsive) maneuver is performed at P.

Mission Design Application (Continued)

Procedure for obtaining a parametric tool for solving Lambert's Problem:

1. Injection is in the direction of the earth's velocity vector so we delete some of the t formulas for this application.
2. Def.: A trajectory that satisfies the condition $0° < \upsilon < 180°$ for points P and Q is called a Type I trajectory; a trajectory that satisfies $180° < \upsilon < 360°$ is a Type II trajectory; $360° < \upsilon < 540°$ is Type III; and so forth.
3. For a specific departure date/arrival date point in the mission design plots,

$$\begin{aligned} t(r_1 + r_2, c, a) &= \text{arrival time-departure time} \\ &= \text{time of flight} \end{aligned}$$

is solved iteratively for a and then we compute C_3, VHP, etc. Finally, a contour plotter is used to plot the contours of C_3, VHP, etc. in departure date versus arrival date space, producing pork chop plots.

4. Alternately, we use a parametric solution tool and technique to determine the semimajor axis a for elliptic trajectories between P and Q as described in the following subsection.

Parametric Solution Tool and Technique

Define the following non-dimensional parameters:

$$\mathscr{E}* = \mathscr{E} / \mid \mathscr{E}_{\mathrm{m}} \mid = -\mathrm{a_m}/\mathrm{a} \tag{4.68}$$

$$\mathrm{K} = 1 - \mathrm{c}/\mathrm{s} \tag{4.69}$$

where c = length of chord = distance from P to Q and s = semiperimeter

$$\mathrm{T}^* = n_{\mathrm{m}}\mathrm{t} \tag{4.70}$$

where $n_{\mathrm{m}} = \sqrt{\dfrac{\mu}{\mathrm{a}_{\mathrm{m}}^3}}$

A parametric display of possible transfers between two points is given in Fig. 4.21.

Assumption: We ignore the effects of planetary attraction on flight time.

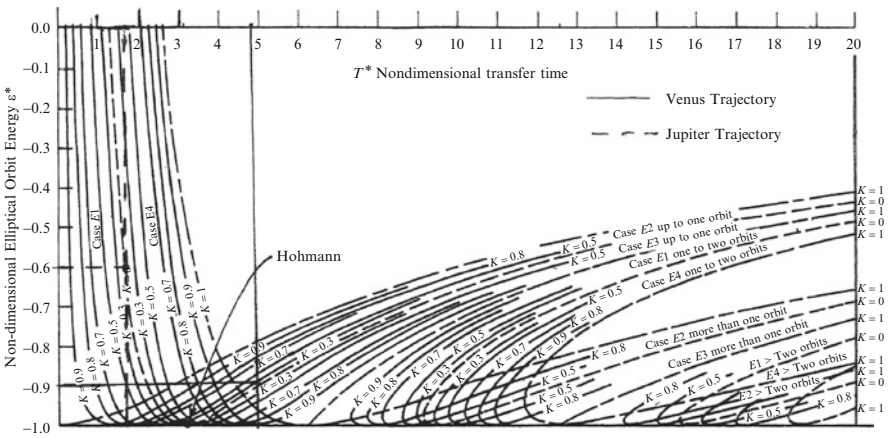

Fig. 4.21 Possible elliptic transfers between two points as in Lambert's problem with the Cassini Earth-to-Venus and an Earth-to-Jupiter examples

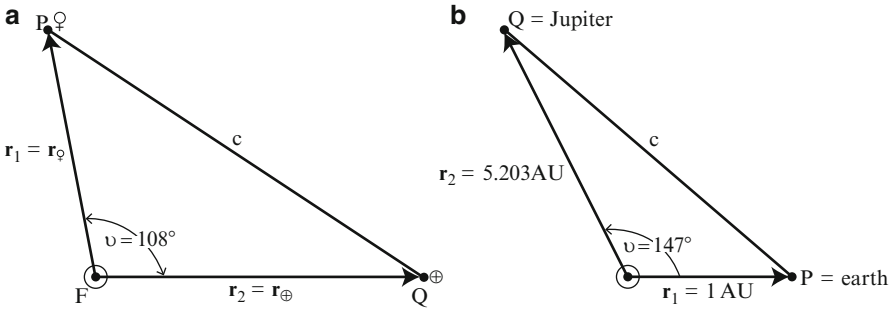

Fig. 4.22 (**a**) PQF diagram for Cassini transfer from Earth to Venus. (**b**) PQF diagram for mission to Jupiter

Example (Cassini transfer from Earth to Venus):

We consider the flight of the Cassini spacecraft, which was launched on 10/15/1997 to transfer to Venus for its first gravity assist flyby on 4/26/1998. For this LD/AD pair, the flight time was:

$$t = TFL = AD - LD = 193 \text{ days}.$$

Ephemeris software can be used to generate the sun–earth vector at launch and the sun–Venus vector at arrival. Then the angle between these two vectors is computed as $\upsilon = 108^\circ$

Relevant data for this transfer is displayed in Fig. 4.22a. Note that the diagram has been labeled for a launch from Venus to satisfy our assumption that $r_1 < r_2$. This is just a matter of labeling.

We compute the non-dimensional parameters K and T* as follows.

$$r_1 = r_♀ = 0.723 \text{ AU from Exercise 2.3.}$$
$$r_2 = r_⊕ = 1 \text{ AU} = 1.496 \times 10^8 \text{km}$$
$$\upsilon = 108 \text{ deg}$$
$$c = 1.403 \text{ AU from the Law of Cosines}$$
$$s = \frac{(r_1 + r_2 + c)}{2} = 1.563 \text{ AU}$$
$$K = 1 - \frac{c}{s} = 0.1$$
$$a_m = \frac{s}{2} = 0.782 \text{ AU} = 116927840 \text{ km}$$
$$n_m = \sqrt{\mu_⊙ / a_m^3} = 2.881 \times 10^{-7} \text{ rad/s}$$
$$T^* = n_m t = 4.80$$

Next, we use Fig. 4.21 to determine values of $\mathscr{E}^*$ by scanning down the vertical line at $T^* = 4.80$, as in the example in that figure, for intersections with parametric

curves for K = 0.1. Thus, candidate values for $\mathscr{E}^*$ are located. Then values of the semimajor axis of the candidate trajectories are computed from Eq. (4.68). Each of these candidates has a different launch time and required Δv_{inj}. Consider the case of an E2 elliptic trajectory of less than one orbit where

$\mathscr{E}^* = -0.9 = -1.169 \times 10^8/a$ so that $a = 1.299 \times 10^8$ km, which determines the size of the orbit.

Then, from Eq. (4.55a,b),

$$\sin\frac{\alpha}{2} = \sqrt{\frac{s}{2a}} = 0.9487 => \alpha = 143.1^\circ$$
$$\sin\frac{\beta}{2} = \sqrt{\frac{s-c}{2a}} = 0.3033 => \beta = 35.3^\circ$$

From Eq. (4.56a$^-$), p = 81,530,756.2 km.

Since $p = a(1 - e^2)$,

$$e = \sqrt{1 - \frac{p}{a}} \tag{4.71}$$

= 0.6103, which determines the shape of the orbit.

One can complete the example by:

1. Computing the magnitude v_2,
2. Determining the angle between the velocity of the earth and $\mathbf{v}_2$,
3. Drawing a vector diagram that includes the velocity vector for the earth, $\mathbf{v}_2$, and $\mathbf{v}_\infty{}^+$ (with respect to the earth),
4. Computing the v_∞ of the escape trajectory, and
5. Computing the Δv required to inject the spacecraft into an interplanetary trajectory from a low parking orbit about the earth.

Example (Transfer from Earth to Jupiter):
Consider the example of a Mariner spacecraft as described in Exercise 4.12. Figure 4.22b displays relevant data. Note that, for planets outside the earth in their orbits about the sun, the spacecraft launches from the earth to travel to the target body as shown in Fig. 4.22b, whereas, for Venus and Mercury, the spacecraft launches from the target body to travel to the earth (in the model) as shown in Fig. 4.22a.

For this exercise, the reader will compute the non-dimensional parameters K = 0.01 and T* = 1.67 and then use Fig. 4.21 to determine the third non-dimensional parameter $\mathscr{E}^* = -0.6$. Refer to the Jupiter example exhibited in Fig. 4.21 as you solve for the semimajor axis a and complete this exercise.

Summary of the use of Fig. 4.21:

We used the parametric figure that gives a summary of possible transfers between two points as shown in Fig. 4.23.

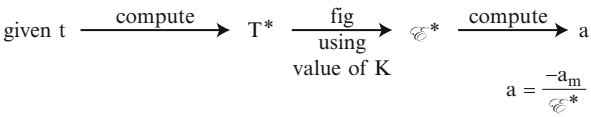

Fig. 4.23 Using the parametric plot to compute the semimajor axis

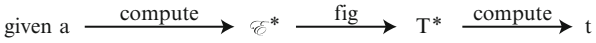

Fig. 4.24 Using the parametric plot to compute flight time t

The computations for obtaining T* are:

$$s = \frac{(r_1 + r_2 + c)}{2}$$
$$K = 1 - \frac{c}{s}$$
$$a_m = \frac{s}{2}$$
$$n_m = \sqrt{\frac{\mu}{a_m}}$$
$$T^* = n_m t$$

We started with t, r_1, r_2, υ and computed c from the Law of Cosines. In the example, we are given transfer time t as AD – LD.

A different way to use the parametric figure is shown in Fig. 4.24. In this application, we are given the semimajor axis a and we obtain the transfer time t.

The computations for $\mathscr{E}^*$ are:

$$s = \frac{(r_1 + r_2 + c)}{2}$$
$$a_m = \frac{s}{2}$$
$$\mathscr{E}* = -a_m/a$$

To be able to use Fig. 4.21, we also need:

$$K = 1 - \frac{c}{s}$$

Computation of t:

$$n_m = \sqrt{\frac{\mu}{a_m^3}}$$
$$t = T^*/n_m$$

A Fundamental Problem in Astrodynamics

The problem of determining a Keplerian orbit, having a specified flight time and connecting two position vectors, is frequently referred to as Lambert's[1] Problem, which is a fundamental problem in astrodynamics. It is also called the Gauss problem by some authors. R. Battin considers several methods of solving this problem in *An Introduction to the Mathematics and Methods of Astrodynamics* (Chap. 7) and in his earlier book *Astronautical Guidance* (Chap. 3).

One of these methods is Gauss's method. In fact, the first real progress in the solution of Lambert's Problem was made by Carl Friedrich Gauss[2] in his book *Theoria Motus Corporum Coelestium in Sectionibus Coicis Colem Ambientium* (Theory of the Motion of the Heavenly Bodies Moving about the Sun in Conic Sections) or *Theoria Motus*.

R. Battin and R. Vaughan have developed a new (improved) method from Gauss' method, which appears in the reference:

Richard H. Battin and Robin M. Vaughan, "An Elegant Lambert Algorithm," *Journal of Guidance*, *Control*, *and Dynamics*, Vol. 7, November–December 1984.

This algorithm accomplishes two improvements:

1. It moves a singularity for a transfer angle of 180°.
2. It drastically improves the convergence for the entire range of transfer angles between 0° and 360°.

References for Lambert's Problem: BMW; Battin 1999; Battin 1964; Battin and Vaughan; Bell; Breakwell, Gillespie, and Ross; Kaplan; Lancaster and Blanchard; NASA's Mars Exploration Website; Prussing 1979; Roy; Schaub and Junkins; Weisstein

4.5 Celestial Mechanics

In previous chapters, the central mass behaves like a particle, i.e., it is either a point mass or a body of uniform density. But, in the current discussion, we enhance our mathematical model by considering a distributed mass that is not of uniform

[1] Johann Heinrich Lambert (1728–1777), a German mathematician, proved that π is irrational and introduced hyperbolic functions (sinh, cosh, tanh, csch, sech, coth). When asked by Frederick II in which science he was most proficient, Lambert replied "All."

[2] Carl Friedrich Gauss (1777–1855) was born in Brunswick, Germany. He taught himself to read and to calculate before he was 3 years old. A list of Gauss' contributions to mathematics and mathematical physics is almost endless. By the time of his death at the age of 78, his contemporaries hailed him as the "Prince of Mathematicians." For more information about Gauss, see the reference:

Eric Temple Bell, "The Prince of Mathematicians," *The World of Mathematics*, Vol. 1, Part II, Chapter 11, pp. 291-332, Tempus Books, 1988.

density. In previous analysis, we considered 2-body (Keplerian) motion, but, in this section, we consider the n-body problem.

As part of the discussion of a distributed mass, we study Legendre polynomials, which provide the mathematical model of the central body.

Legendre Polynomials

The Binomial Expansion is:

$$(a+b)^n = a^n + na^{n-1}b + \frac{n(n-1)}{2}a^{n-2}b^2 + \ldots \tag{4.72}$$

Take $n = -1/2, a = 1, b = \beta^2 - 2\alpha\beta = \beta(\beta - 2\alpha)$
to obtain

$$\begin{aligned}
&\left(1+\beta^2-2\alpha\beta\right)^{-1/2} = (1+\beta(\beta-2\alpha))^{-1/2} \\
&= 1 + (-1/2)\beta(\beta-2\alpha) + \frac{(-1/2)(-3/2)}{2}\beta^2(\beta-2\alpha)^2 + \ldots \\
&= 1 + \alpha\beta^1 + \left(-\frac{1}{2} + \frac{3}{8}4\alpha^2\right)\beta^2 + \ldots \\
&= \sum_{n=0}^{\infty} P_n(\alpha)\beta^n, \quad |\,\beta\,| < 1 \text{ for convergence}
\end{aligned}$$

where

$P_0(\alpha) = 1$
$P_1(\alpha) = \alpha$
$P_2(\alpha) = (3/2)\,\alpha^2 - (1/2)$
. . .

Now take $\beta = x$ and $\alpha = \cos\gamma$ to obtain

$$\left(1 + x^2 - 2x\cos\gamma\right)^{-1/2} = \sum_{n=0}^{\infty} x^n P_n(\cos\gamma) \tag{4.73}$$

Def.: The functions P_n are called the Legendre polynomials.

This is one way of getting these polynomials. It is the way Legendre got them.

Def.: The function $(1 - 2\alpha x + x^2)^{-1/2}$ is called the generating function for the Legendre polynomials $P_n(\alpha)$ or the Legendre generating function.

The functions $P_n(\alpha)$ are defined as the coefficients of the power series expansion

$$\left(1 - 2\alpha x + x^2\right)^{-1/2} = \sum_{n=0}^{\infty} P_n(\alpha)x^n$$

From the identity

$$\left(1 - 2(-\alpha)x + x^2\right)^{-1/2} = \left(1 - 2\alpha(-x) + (-x)^2\right)^{-1/2}$$

we can deduce the property

$$P_n(-\alpha) = (-1)^n P_n(\alpha) \text{ for } n = 0, 1, \ldots$$

This equation shows that $P_n(\alpha)$ is an odd function of α for odd n (symmetric with respect to the origin) and an even function of α for even n (symmetric with respect to the y-axis).

By differentiating both sides of the expansion of the generating function with respect to x, multiplying through by $(1 - 2\alpha x + x^2)$, and equating coefficients of x^n, we can derive the following recursion formula for the Legendre polynomials

$$nP_n(\alpha) - (2n - 1)\alpha P_{n-1}(\alpha) + (n - 1)P_{n-2}(\alpha) = 0, \; n \geq 2 \tag{4.74a}$$

Therefore,

$$P_n(\alpha) = \left(\frac{2n - 1}{n}\right)\alpha P_{n-1}(\alpha) - \left(\frac{n - 1}{n}\right)P_{n-2}(\alpha), \; n \geq 2 \tag{4.74b}$$

The above recursion formula for the Legendre polynomials can be used to complete the following table

$$\begin{aligned}
P_0(\alpha) &= 1 \\
P_1(\alpha) &= \alpha \\
P_2(\alpha) &= (1/2)(3\alpha^2 - 1) \\
P_3(\alpha) &= (1/2)(5\alpha^3 - 3\alpha) \\
P_4(\alpha) &= (1/8)(35\alpha^4 - 30\alpha^2 + 3) \\
P_5(\alpha) &= (1/8)\left(63\alpha^5 - 70\alpha^3 + 15\alpha\right) \\
P_6(\alpha) &= (1/16)\left(231\alpha^6 - 315\alpha^4 + 105\alpha^2 - 5\right) \\
P_7(\alpha) &= (1/16)\left(429\alpha^7 - 693\alpha^5 + 315\alpha^3 - 35\alpha\right) \\
P_8(\alpha) &= (1/128)\left(6435\alpha^8 - 12012\alpha^6 + 6930\alpha^4 - 1260\alpha^2 + 35\right)
\end{aligned} \tag{4.75}$$

Remarks:

The Legendre polynomials in algebraic form satisfy the orthogonality relations

$$\int_{-1}^{1} P_m(\alpha)P_n(\alpha)d\alpha = \left\{ \begin{array}{ll} 0 & m \neq n \\ \dfrac{2}{2n + 1} & m = n \end{array} \right\} \tag{4.76}$$

In trigonometric form, the Legendre polynomials satisfy the orthogonality relations

$$\int_0^{\pi} P_m(\cos\gamma)P_n(\cos\gamma)\sin\gamma d\gamma = \left\{ \begin{array}{ll} 0 & m \neq n \\ \dfrac{2}{2n+1} & m = n \end{array} \right\} \tag{4.77}$$

Reference: Wylie and Barrett

Def.: The associated Legendre functions of the first kind of degree k and order j are given by

$$P_k^j = \left(1 - v^2\right)^{j/2} \frac{d^j}{dv^j} P_k(v) \tag{4.78}$$

Note that the Legendre function of the first kind of degree k and order 0 is equal to the P_k Legendre function because

$$P_k^0(v) = \left(1 - v^2\right)^0 \frac{d^0}{dv^0} P_k(v) = P_k(v) \tag{4.79}$$

which is the P_k Legendre polynomial.

Adrien-Marie Legendre (1752–1833) was a French mathematician and a disciple of Euler and Lagrange. He published a classic work on geometry, *Élements de géométrie*. He also made significant contributions in differential equations, calculus, function theory, number theory in *Essai sur la théorie des nombres* (1797–1798), and applied mathematics. He expanded his three-volume treatise *Exercises du calcul intégral* (1811–1819) into another three volume work, *Traité des fonctions elliptiques et des intégrales eulériennes* (1825–1832). He invented the Legendre polynomials in 1784 while studying the attraction of spheroids. His work was important for geodesy. In number theory, he proved the insolvability of Fermat's last theorem for $n = 5$.

References: Weisstein; Wylie and Barrett

Gravitational Potential for a Distributed Mass

Let B denote a distributed mass.

Let dm_2 denote a typical volume element of the body B and m_1 a particle of mass attracted by B, as shown in Fig. 4.25. From Newton's Universal Law of Gravitation, the force due to dm_2 on m_1 is

$$d\mathbf{F} = -Gm_1 \frac{\mathbf{r}_{12}}{r_{12}^3} dm_2$$

So

$$\mathbf{F} = -Gm_1 \int_B \frac{\mathbf{r}_{12}}{r_{12}^3} dm_2$$

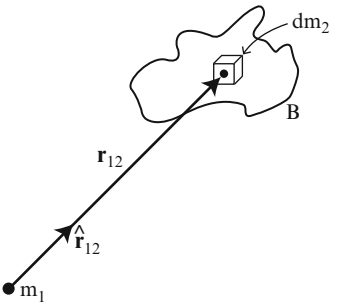

Fig. 4.25 Gravitational potential of a distributed mass

Def.: The gravitational field at any point (or gravitational field intensity) is the force (a vector) acting on a unit mass at that point.

"Field" is a physics term for a region that is under the influence of a force that can act on matter within that region. For example, the sun produces a gravitational field that attracts the planets in the solar system and thus influences their orbits.

Calculating gravitational field intensities is hard because we integrate vectors. It is usually easier to integrate scalar functions. So we look at the gravitational potential.

Properties of the gravitational potential of a distributed mass:

(1) Scalar function $U = U(\mathbf{r})$ of position
(2) Used to describe the attraction properties of a distributed mass.

We convert to spherical polar coordinates because they are convenient when we work with bodies that are nearly spherical.

In the inverse square field of 2-body mechanics,

$$U(r) = \frac{\mu}{r} = \text{a constant on a sphere}$$

In this discussion, the central body is not a point mass, but rather a distributed mass. We will show that

$$U(\mathbf{r}) \neq \text{ constant on a sphere}$$

but rather is a function of position and magnitude.

Let P denote the vector giving the position of a point in the gravitational field of body B expressed in a right-handed coordinate system. The Cartesian elements of P measure distances along each of the three X, Y, and Z coordinate axes. Vector P can also be expressed as spherical elements.

Spherical coordinate elements are defined as a radius and two angles. The radius measures the length of the vector P. In the standard definition for spherical elements, the first angle ϕ is the angle from the +Z axis to the P vector. The second angle θ is the angle from the X-axis to the projection of P on the XY plane measured

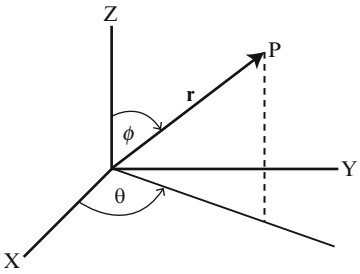

Fig. 4.26 Spherical coordinate elements for point P

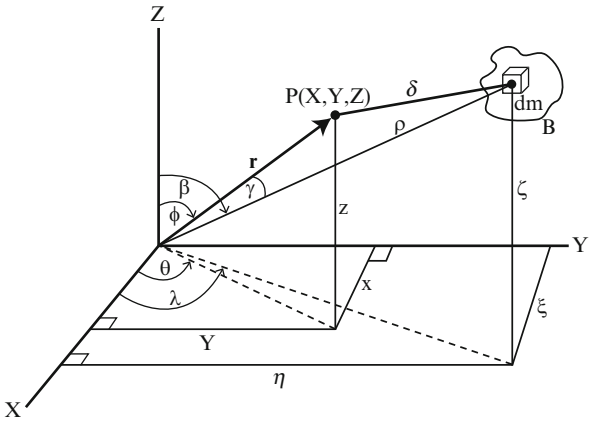

Fig. 4.27 Conversion from inertial to spherical coordinates

positive counterclockwise around the Z-axis. Thus, the position of an arbitrary point P is determined by an ordered triplet of numbers (r, ϕ, θ), where r = the magnitude of the position vector, and ϕ denotes the colatitude and θ the longitude of the point P as shown in Fig. 4.26.

We consider the gravitational potential at P. Points (X, Y, Z) outside of B are converted to r,ϕ,θ (fixed) and points (ξ,η,ζ) inside body B to (ρ,β,λ), as shown in Fig. 4.27.

Spherical polar coordinates:

$$\begin{aligned} \xi &= \rho \sin\beta \cos\lambda \\ \eta &= \rho \sin\beta \sin\lambda \\ \zeta &= \rho \cos\beta \end{aligned} \tag{4.80}$$

One more fact about Legendre polynomials is the

Addition Theorem for Legendre Polynomials:

If γ is the angle between the two directions specified by the spherical polar angles (ϕ, θ) and (β, λ), then

$$P_k(\cos\gamma) = \sum_{j=0}^{k} K_k^j \cos\left(j(\theta - \lambda)\right) P_k^j(\cos\phi) P_k^j(\cos\beta) \tag{4.81}$$

where

$K_k{}^j = 1$ if $j = 0$ and

$$K_k^j = \frac{2(k-j)!}{(k+j)!} \text{ if } j \neq 0$$

A proof of this theorem is available in the reference Battin 1999, Chapter 8.

The potential at point P(X, Y, Z) due to the attraction of the element dm is

$$dU(X,\ Y,\ Z) = G\frac{dm}{\delta} = \frac{G}{(r^2 + \rho^2 - 2r\rho\cos\gamma)^{1/2}}dm$$

from the Law of Cosines

$$= G\frac{dm}{r}\sum_{k=0}^{\infty}\left(\frac{\rho}{r}\right)^k P_k(\cos\gamma) \quad \text{if } \rho < r$$

from Eq. (4.73), since the fraction is the Legendre generating function with $x = \rho/r$, after factoring out 1/r. Convergence is guaranteed outside the smallest sphere that circumscribes the body if the origin of the inertial X, Y, Z coordinate system is placed at the center of mass of the body B.

Therefore, the potential at P(X, Y, Z) due to the entire body B is

$$\begin{aligned} U &= \int_B dU = \frac{G}{r}\int_B \sum_{k=0}^{\infty}\left(\frac{\rho}{r}\right)^k P_K(\cos\gamma)dm \\ &= \frac{G}{r}\sum_{k=0}^{\infty}\int_B \left(\frac{\rho}{r}\right)^k P_k(\cos\gamma)dm \\ &= \frac{G}{r}\sum_{k=0}^{\infty}\int_B \left(\frac{\rho}{r}\right)^k \left[\sum_{j=0}^{k} K_k^j \cos(j(\theta-\lambda))P_k^j(\cos\phi)P_k^j(\cos\beta)dm\right] \end{aligned}$$

by the Addition Theorem for Legendre Polynomials

$$= \sum_{k=0}^{\infty}\sum_{j=0}^{k}\frac{G}{r}\int_B \left(\frac{\rho}{r}\right)^k K_k^j \cos(j(\theta-\lambda))P_k^j(\cos\phi)P_k^j(\cos\beta)dm \tag{4.82}$$

$$\begin{aligned} &\equiv \sum_{k=0}^{\infty}\sum_{j=0}^{k} U_{kj} \\ &= (U_{00}) + (U_{10} + U_{11}) + (U_{20} + U_{21} + U_{22}) + \ldots \end{aligned}$$

where we have defined U_{kj} accordingly.

In practice, we cannot perform the integration over B, but we write the expression for U in a useful form. We look at specific terms.

$k = 0, j = 0$:

$$U_{00} = \frac{Gm}{r} = \frac{\mu}{r}$$

where $m =$ mass of B.

$k = 1, j = 0$:

$$U_{10} = \frac{G}{r}\int_B \frac{\rho}{r}\cos\phi\cos\beta dm = \frac{G}{r^2}\cos\phi\int_B \rho\cos\beta dm = \frac{G}{r^2}\cos\phi\int_B \zeta dm$$

We now select the origin of our coordinate system to be at the center of mass of B. Then

$$U_{10} = \frac{G}{r^2}\cos\phi(\text{first moment of mass about X, Y plane}) = 0 \tag{4.83}$$

from dynamics

Exercise 4.15: Show that $U_{11} = 0$ if the origin is at the center of mass.

This is as far as we can go in general without knowing the distribution of the mass. But we can look at the character of the general term.

k,j term:

$$\begin{aligned}
U_{kj} &= \frac{G}{r}\int_B \left(\frac{\rho}{r}\right)^k K_k^j \cos(j(\theta-\lambda))P_k^j(\cos\phi)P_k^j(\cos\beta)dm \\
&= \frac{G}{r^{k+1}}P_k^j(\cos\phi)K_k^j\int_B \rho^k P_k^j(\cos\beta)[\cos(j\theta)\cos(j\lambda) + \sin(j\theta)\sin(j\lambda)]dm \\
&= \frac{G}{r^{k+1}}P_k^j(\cos\phi)\left[\cos j\theta K_k^j\int_B \rho^k P_k^j(\cos\beta)\cos j\lambda dm + \sin j\theta K_k^j\int_B \rho^k P_k^j(\cos\beta)\sin j\lambda dm\right] \\
&= \frac{G}{r^{k+1}}P_k^j(\cos\phi)\left[A_k^j\cos j\theta + B_k^j\sin j\theta\right] = \frac{Gm}{r^{k+1}}P_k^j(\cos\phi)R_e^k\left[C_k^j\cos j\theta + S_k^j\sin j\theta\right]
\end{aligned} \tag{4.84}$$

where we have defined

$$\begin{aligned}
A_k^j &= K_k^j\int_B \rho^k P_k^j(\cos\beta)\cos j\lambda dm \\
B_k^j &= K_k^j\int_B \rho^k P_k^j(\cos\beta)\sin j\lambda dm \\
C_k^j &= \frac{A_k^j}{mR_e^k} \text{ and } S_k^j = \frac{B_k^j}{mR_e^k}
\end{aligned}$$

and $R_e =$ the mean equatorial radius of the distributed mass B. The coefficients $A_k{}^j$ and $B_k{}^j$ are divided by $mR_e{}^k$ to obtain dimensionless quantities $C_k{}^j$ and $S_k{}^j$. The values for R_e are given in Table 4.1 for the planets, Pluto, the sun, and the moon.

References: Bills and Ferrari, Seidelmann et al., Tholen and Buie.

Table 4.1 Mean equatorial radius values

Body	Mean equatorial radius (km)
Mercury	2,439.7
Venus	6,051.8
Earth	6,378.14
Mars	3,396.19
Jupiter	71,492
Saturn	60,268
Uranus	25,559
Neptune	24,764
Pluto	1,151
Sun	696,000.
Moon	1,737.5

Thus,

$$U_{kj} = \frac{Gm}{r^{k+1}} P_k^j(\cos\phi) R_e^k \left[C_k^j \cos j\theta + S_k^j \sin j\theta \right]$$

where R_e = the mean equatorial radius.

$$\begin{aligned} C_k^j &= \frac{K_k^j}{mR_e^k} \int_B \rho^k P_k^j(\cos\beta) \cos j\lambda \, dm \\ &= \frac{K_k^j}{mR_e^k} \iiint_B \rho^k P_k^j(\cos\beta) \cos j\lambda \left[\rho^2 \sin\beta \Gamma(\rho,\beta,\lambda) d\rho d\beta d\lambda \right] \\ S_k^j &= \frac{K_k^j}{mR_e^k} \int_B \rho^k P_k^j(\cos\beta) \sin j\lambda \, dm \\ &= \frac{K_k^j}{mR_e^k} \iiint_B \rho^k P_k^j(\cos\beta) \sin j\lambda \left[\rho^2 \sin\beta \Gamma(\rho,\beta,\lambda) d\rho d\beta d\lambda \right] \end{aligned}$$

where

$$\Gamma(\rho,\beta,\lambda) = \text{density at } \rho,\beta,\lambda$$

and the quantity in brackets is the Jacobian of spherical coordinates.

Therefore, $U = U(r, \phi, \theta)$ is a scalar function of position (r = distance, ϕ = colatitude, and θ = longitude) with

$$U(r,\phi,\theta) = \frac{Gm}{r} \left[1 + \sum_{k=2}^{\infty} \sum_{j=0}^{k} \left(\frac{R_e}{r} \right)^k P_k^j(\cos\phi) \left\{ C_k^j \cos j\theta + S_k^j \sin j\theta \right\} \right] \quad (4.85)$$

where the origin of our coordinate system is at the center of mass of the central body and the C_k^j and S_k^j are the *Stokes coefficients* of the potential. This is the form in which we represent the external potential for all celestial bodies. The Cs and Ss are determined experimentally from spacecraft data.

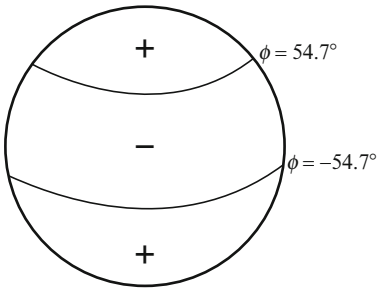

Fig. 4.28 J2 zonal harmonic

Def.: The functions $\cos j\theta P_k^j(\cos\phi)$ and $\sin j\theta P_k^j(\cos\phi)$ are called spherical harmonics.

The spherical harmonics are periodic on the surface of a unit sphere. Specifically, the indices j and k determine lines on the sphere along which the functions vanish.

1. Zonal harmonics (aka "zonals"): $j = 0$
   The zonals are $C_k^j P_k^j(\cos\phi)$ because $\cos(j\theta) = 1$ and $\sin(j\theta) = 0$.
   Since $j = 0$, the dependence on longitude vanishes and the field is axisymmetric. The Legendre polynomials $P_k^j(\cos\phi)$ are periodic on the surface of a unit sphere and there are k circles of latitude along which $P_k^0 = 0$. Therefore, there are $(k + 1)$ zones in which the function is alternately positive and negative, which is the reason behind the name "zonals."

   Example:

$$P_2(\alpha) = \frac{3}{2}\alpha^2 - \frac{1}{2}$$
$$P_2(\cos\phi) = \frac{3}{2}\cos^2\phi - \frac{1}{2} = \frac{1}{4}(3\cos 2\phi + 1) = 0$$
$$\text{iff } \phi = \pm 54.7\text{deg}$$

   as shown in Fig. 4.28.

   Def.: The zonal harmonic coefficients (zonals) of the gravitational potential function are

$$J_k = -C_k^0$$

   Thus,

$$U = U(r, \phi, \theta) = \frac{Gm}{r}\left[1 - \sum_{k=2}^{\infty}\left(\frac{R_e}{r}\right)^k J_k P_k(\cos\phi) + \sum_{k=2}^{\infty}\sum_{j=1}^{k}\left(\frac{R_e}{r}\right)^k P_k^j(\cos\phi)\left\{C_k^j \cos j\theta + S_k^j \sin j\theta\right\}\right] \tag{4.86}$$

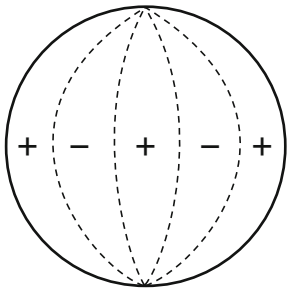

Fig. 4.29 2j "Orange-slice" sectors

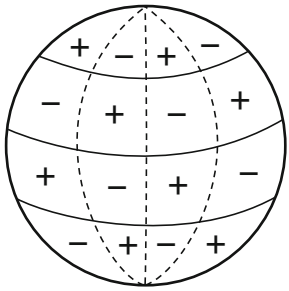

Fig. 4.30 Tesseral harmonics

Remarks:

(a) The J_2 term describes oblateness, i.e., the flattening at the poles.
(b) The zonal harmonics depend on latitude only.

2. Sectorial harmonics: $j = k$

Def.: The functions $\cos j\theta P_k{}^k(\cos\phi)$ and $\sin j\theta P_k{}^k(\cos\phi)$ are called sectorial harmonics.

Def.: The coefficients of the sectorial harmonics are called sectorial coefficients.

It turns out that the polynomials $P_k{}^k(\cos\phi)$ are zero only at the poles ($\phi = 0°$, 180°). The factors $\cos j\theta$ and $\sin j\theta = 0$ for 2j different values of θ. Hence, the lines along which $\cos j\theta P_k{}^k(\cos\phi)$ and $\sin j\theta P_k{}^k(\cos\phi) = 0$ are meridians of longitude, producing 2j "orange-slice" sectors in which the harmonics are alternately positive and negative. The similarity to orange slices has motivated the name "sectorial harmonics" as shown in Fig. 4.29.

3. Tesseral harmonics: $j \neq k$

Def.: The functions $\cos j\theta P_k{}^j(\cos\phi)$ and $\sin j\theta P_k{}^j(\cos\phi)$ for $j \neq k$ are called tesseral harmonics.

Def.: The coefficients of the tesseral harmonics are called tesseral coefficients.

Tesseral harmonics produce a checkerboard pattern in which the harmonics are alternately positive and negative as shown in Fig. 4.30.

Example: $\cos(4\theta)P_7^4(\cos\phi)$

There are other forms of U in the literature. One form writes U in terms of latitude instead of co-latitude, replacing $P_k^j(\cos\phi)$ with P_k^j (sin(LAT)).

Comments:

1. We have the 2-body problem iff all Js, Cs, Ss = 0 so $U = U(r, \phi, \theta) = Gm/r$.
2. Since we cannot evaluate an infinite series, we truncate the infinite series. The truncation errors are distributed over the coefficients that are kept in the expansion. To show hills and valleys in the potential function, we increase the number of terms used to get a finer grid.
3. The Js, Cs, and Ss are definite integrals, but the integrations cannot be performed because the density function $\Gamma(\rho, \beta, \lambda)$ is unknown.
4. Values of the coefficients can be determined from spacecraft observations. We use a least squares method to solve for the Cs and Ss as described in the reference TSB.
5. The moon has MASCONS, large concentrations of mass near the surface. The earth does not have these large-scale anomalies. Some analysts have modeled the MASCONS and solved for their positions because of the computational problems in solving for all the coefficients in the spherical harmonic expansion. Supercomputers now make such attempts unnecessary.
6. If $r >> R_e$, the effects of these anomalies are reduced. Only low orbits experience the effects of the higher degree terms in a harmonic expansion of U. For such low altitude orbits, it is said that the spacecraft is "buffeted by the harmonics."
7. Some of the Js, Cs, and Ss for the earth are estimated as in Table 4.2. Note that $J_2 \geq 3$ orders of magnitude larger than the other values.
   Remarks about the Table of Spherical Harmonic Coefficients for the Earth:
   (a) Data is from the NASA-NIMA Earth Gravity Model EGM96
   (b) EGM96 is a 360×360 Earth Gravity Field Model
   (c) For this model, Gm is 398,600.4415 km^3/s^2 and the mean equatorial radius of the earth is 6,378.1363 km.
8. Some texts assume that $C_2^1 = S_2^1 = 0$. Thus, they assume that the offset of the principal axis and the rotational axis is zero. This offset is very small, but it is not zero. The assumption that these offsets are zero is not always done in practice; in fact, the analyst may solve for C_2^1 and S_2^1 and use the values obtained as verification that the results are correct. Obtaining larger values than expected for C_2^1 and S_2^1 is an indication that something is wrong. Getting small values helps to verify the results.
9. The spherical harmonics are orthogonal. This property makes the spherical harmonics the natural means for general (unique) representation of a function over a spherical surface.
10. For numerical reasons, it is convenient to normalize the coefficients as discussed in the reference by Kaula.
11. There is a solution for the Venus gravity field that involves the spherical harmonic coefficients to degree and order 180 or 33,000 coefficients. The

Table 4.2 Spherical harmonic coefficients for the Earth

$J(2) = 1{,}082.6267 \times 10^{-6}$
$J(3) = -2.5327 \times 10^{-6}$
$J(4) = -1.6196 \times 10^{-6}$
$J(5) = -0.2273 \times 10^{-6}$
$J(6) = 0.5407 \times 10^{-6}$
$J(7) = -0.3524 \times 10^{-6}$
$J(8) = -0.2048 \times 10^{-6}$
$J(9) = -0.1206 \times 10^{-6}$
$J(10) = -0.2411 \times 10^{-6}$
$C(2,1) = -0.00024 \times 10^{-6}$
$C(2,2) = 1.57446 \times 10^{-6}$
$C(3,1) = 2.19264 \times 10^{-6}$
$C(3,2) = 0.30899 \times 10^{-6}$
$C(3,3) = 0.10055 \times 10^{-6}$
$C(4,1) = -0.50880 \times 10^{-6}$
$C(4,2) = 0.07842 \times 10^{-6}$
$C(4,3) = 0.05921 \times 10^{-6}$
$C(4,4) = -0.00398 \times 10^{-6}$
$C(5,1) = -0.05318 \times 10^{-6}$
$C(5,2) = 0.10559 \times 10^{-6}$
$C(5,3) = -0.01493 \times 10^{-6}$
$C(5,4) = -0.00230 \times 10^{-6}$
$C(5,5) = 0.00043 \times 10^{-6}$
$S(2,1) = 0.00154 \times 10^{-6}$
$S(2,2) = -0.90380 \times 10^{-6}$
$S(3,1) = 0.26842 \times 10^{-6}$
$S(3,2) = -0.21144 \times 10^{-6}$
$S(3,3) = 0.19722 \times 10^{-6}$
$S(4,1) = -0.44914 \times 10^{-6}$
$S(4,2) = 0.14818 \times 10^{-6}$
$S(4,3) = -0.01201 \times 10^{-6}$
$S(4,4) = 0.006526 \times 10^{-6}$
$S(5,1) = -0.08086 \times 10^{-6}$
$S(5,2) = -0.05233 \times 10^{-6}$
$S(5,3) = -0.00710 \times 10^{-6}$
$S(5,4) = 0.00039 \times 10^{-6}$
$S(5,5) = -0.00165 \times 10^{-6}$
where $J(n) = J_n$; $C(n,m) = C_n^m$; $S(n,m) = S_n^m$

coefficients were solved for in three different sets with a maximum of 15,000 coefficients solved for at one time, using a least squares estimation procedure. See the reference by Konopliv, Banerdt, and Sjogren. Lunar gravity models are presented in the reference by Konopliv, Asmar, Carranza, Sjogren, and Yuan.

A Martian gravity field model of degree and order 75 is available in the reference by Yuan, Sjogren, Konopliv, and Kucinskas.

12. To prepare for the NEAR landing on the asteroid Eros, an ellipsoidal expansion of the potential function was used to increase the region of convergence to be everywhere outside a circumscribing ellipsoid about the irregularly shaped asteroid. It was important to know the gravitational potential to avoid a spacecraft collision caused by the gravitational attraction. See the references by Garmier and J. P. Barriot; Garmier, Barriot, Konopliv, and Yeomans; Konopliv, Miller, Owen, Yeomans, and Giorgini; Miller, Konopliv, Antreasian, Bordi, Chesley, Helfrich, Owen, Wang, Williams, and Yeomans.
13. The characteristics of the various Math models are:

Spherical harmonics—unstable inside a circumscribing sphere (Brillouin sphere)
Ellipsoidal—better, but tough to get higher order terms
Polyhedral—better, but tough to put in density variations, coupled to shape model; lots of calculations
Surface Integration—few calculations, accurate, updatable independent of shape model; stable very close to body. In surface integration, use Green's Theorem to replace the volume integral by a surface integral.

Reference: Weeks and Miller.

The n-Body Problem

Consider n particles $P_1, P_2, \ldots, P_n$ of mass $m_1, m_2, \ldots, m_n$, respectively.
Let $\mathbf{F_i}$ = gravitational force of attraction on P_i of the other $(n-1)$ particles.
Let $\mathbf{r}_i = X_i\mathbf{I} + Y_i\mathbf{J} + Z_i\mathbf{K}$ denote the inertial position of P_i, $i = 1, \ldots, n$.

Def.: $\mathbf{r_{ij}} = \mathbf{r_i} - \mathbf{r_j}$

Then $r_{ij} = \sqrt{r_i^2 + r_j^2 - 2r_i r_j \cos\gamma_{ij}}$ where γ_{ij} is the angle between r_i and r_j as shown in Fig. 4.31. The force

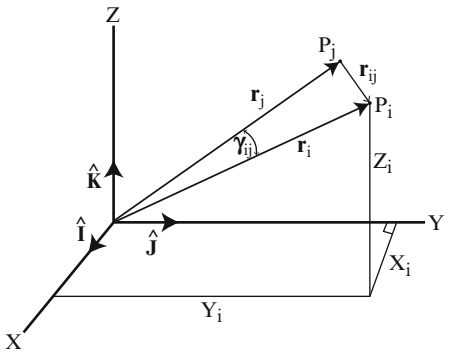

Fig. 4.31 The n-body problem

$$\mathbf{F}_i = -Gm_i \sum_{\substack{j=1 \\ j \neq i}}^{n} \frac{m_j}{r_{ij}^3} \mathbf{r}_{ij}, i = 1, \ldots, n \tag{4.87}$$

$\mathbf{F_i}$ is conservative from Exercise 4.16. From NII,

$$\mathbf{F}_i = m_i \frac{d^2 \mathbf{r}_i}{dt^2}$$

Equating the two expressions for $\mathbf{F_i}$ produces n vector differential equations

$$\frac{d^2 \mathbf{r}_i}{dt^2} = -G \sum_{\substack{j=1 \\ j \neq i}}^{n} \frac{m_j}{r_{ij}^3} \mathbf{r}_{ij}, i = 1, \ldots, n \tag{4.88}$$

as the EOM of the system of n mass particles.

Def.: The gravitational potential U_i at (X_i, Y_i, Z_i) is

$$U_i = G \sum_{\substack{j=1 \\ j \neq i}}^{n} \frac{m_j}{r_{ij}} \tag{4.89}$$

The potential function depends only on the distances to the other particles so the choice of axes is independent.

$\nabla U_i =$ the force of attraction on a particle of unit mass at (X_i, Y_i, Z_i)

Therefore,

$$\mathbf{F}_i = m_i \nabla U_i \tag{4.90}$$

which follows from Exercise 4.17.

Def.:

$$U = \frac{1}{2} \sum_{k=1}^{n} m_i U_i = \frac{G}{2} \sum_{k=1}^{n} \sum_{\substack{j=1 \\ j \neq i}}^{n} \frac{m_k m_j}{r_{kj}} \tag{4.91}$$

Then

$$\mathbf{F}_i = \nabla_i U \quad \text{where} \quad \nabla_i = \mathbf{I} \frac{\partial \bullet}{\partial X_i} + \mathbf{J} \frac{\partial \bullet}{\partial Y_i} + \mathbf{K} \frac{\partial \bullet}{\partial Z_i} \tag{4.92}$$

Properties of U:

1. U can be thought of as being the total work done by gravitational forces in assembling the n particles from a state of infinite dispersion to a given configuration.
2. PE of system $= -U$
3. U is the gravitational potential function of n bodies.

The idea that force can be derived from a potential function was used by Daniel Bernoulli in *Hydrodynamics* (1738). The Bernoulli family tree included brothers Johann Bernoulli (1667–1748) aka John I. Bernoulli and Jakob Bernoulli (1654–1705). The sons of Johann were Daniel Bernoulli (1700–1782) and Nicholas Bernoulli (1695–1726). Daniel Bernoulli was a Swiss mathematician, who showed that as the velocity of a fluid increases, the pressure decreases, a statement known as the Bernoulli principle. He won the annual prize of the French Academy ten times for work on vibrating strings, ocean tides, and the kinetic theory of gases. For one of these victories, he was ejected from his jealous father's house, because his father had also submitted an entry for the prize.

A complete solution of the n-body problem requires that we solve for 6n quantities: three components of position and three components of velocity for each of n particles referred to an inertial reference frame. But only ten integrals are known for use in reducing the order of the system of differential equations of motion to be solved. Recall that, in Chap. 2, we solved the relative 2-body problem, which is often referred to as the "2-body problem." Jules Henri Poincare (1854–1912), a French mathematician, proved that there are no more of these constants.

The ten integrals are obtained as six from the conservation of total linear momentum, three from the conservation of total angular momentum, and one from the conservation of total energy. See the reference by Kaplan, pp. 283–285.

Jules Henri Poincare (1854–1912) was a French mathematician who did important work in many different branches of mathematics. However, he did not stay in any one field long enough to round out his work. He had an amazing memory and could state the page and line of any item in a text he had read. He retained his memory all his life. His normal work habit was to solve a problem completely in his head, then commit the completed problem to paper. Poincare did fundamental work in celestial mechanics in his treatises *Les Methodes Nouvelles de la Mecanique Celeste* (1892, 1893, 1899) and *Lecons de Mecanique Celeste* (three volumes, 1905–1910). In these works, he attacked the 3-body problem.

Disturbed Relative 2-Body Motion

Since the n-body problem cannot be solved analytically, we consider disturbed relative 2-body motion to introduce the gravitational effects of a third body.

Def.: Third body effects are the gravitational effects on a satellite produced by a body other than the central body.

Example (Pioneer Venus Orbiter): The Keplerian orbital parameters for PVO were: $\tau = 24$ h, $h_p \approx 200$ km (However, the spacecraft did go as low as about 140 km in altitude on the night side and as low as about 150 km on the day side so we could study the atmosphere of Venus by determining its effect on the spacecraft's orbit.), $i = 105°$, $\Omega = 22.8°$, and $\omega = 160.7°$ with respect to mean ecliptic and equinox of 1950.0 coordinates. (See the reference by Shapiro et al.)

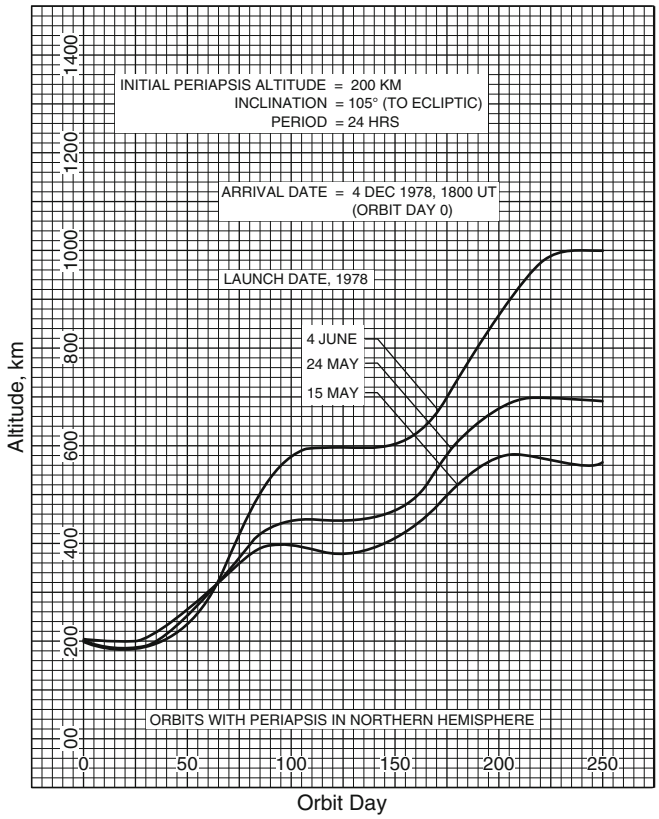

Fig. 4.32 Parametric display of orbital altitude drift for PVO

The dominant perturbation to 2-body (Keplerian) motion for PVO was solar gravity (third body effect of the sun). Figure 4.32 shows the spacecraft's altitude as a function of days from entry into orbit about Venus. This figure is a parametric display for three different launch dates, June 4, May 24, and May 16 in 1978. (PVO was launched on May 20, 1978.) This figure assumes no trim maneuvers to correct for the increasing altitude. In reality, the altitude was decreased as illustrated in Fig. 4.33. Note that the altitude drift was over-corrected to reduce the number of TCMs required to keep the altitude within tolerances.

We look at relative 2-body motion with other bodies disturbing the motion as illustrated in Fig. 4.34. We consider n-bodies $P_1, P_2, \ldots, P_n$ with masses $m_1, m_2, \ldots, m_n$, respectively and ask the question: What is the motion of P_2 with respect to P_1, given gravitational disturbances by P_j, $j = 3, \ldots, n$?

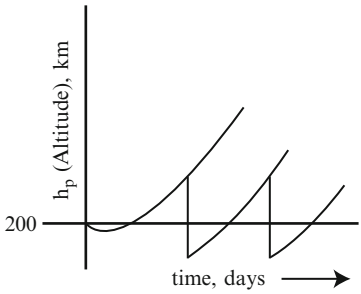

Fig. 4.33 PVO corrections for altitude drift

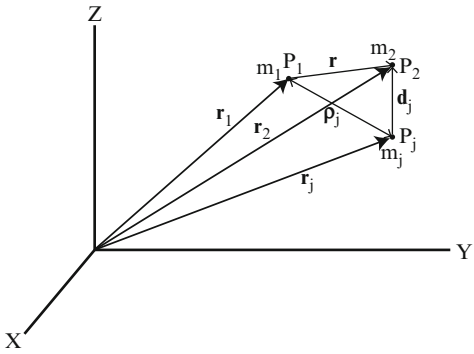

Fig. 4.34 Motion of body P_2 about primary body P_1 given disturbances by other bodies $P_j = 3, 4, \ldots, n$

Examples:
Planetary theory: $P_1 =$ sun, $P_2 =$ a specific planet, $P_j =$ the other planets

Lunar (satellite) theory; $P_1 =$ earth, $P_2 =$ moon (spacecraft), Pj = the sun and other planets

Def.:

$$\begin{aligned} \mathbf{r} &= \mathbf{r}_2 - \mathbf{r}_1 \\ \rho_{\mathbf{j}} &= \mathbf{r}_j - \mathbf{r}_1 \\ \mathbf{d}_j &= \mathbf{r} - \rho_{\mathbf{j}} = \mathbf{r}_2 - \mathbf{r}_j \end{aligned} \tag{4.93}$$

Let $\mathbf{F_i} =$ force of attraction on P_i. Then, from NII and the Universal Law of Gravitation,

$$\mathbf{F}_i = m_i \frac{d^2\mathbf{r}_i}{dt^2} = G\sum_{\substack{j=1 \\ j\neq i}}^{n} \frac{m_i m_j}{r_{ij}^3}\left(\mathbf{r}_j - \mathbf{r}_i\right),\ i = 1, \ldots, n \tag{4.94}$$

For $i = 1$ $(j \neq 1)$

$$\frac{\mathbf{F}_1}{m_1} = \frac{d^2\mathbf{r}_1}{dt^2} = \frac{Gm_2}{r_{12}^3}(\mathbf{r}_2 - \mathbf{r}_1) + G\sum_{j=3}^{n} \frac{m_j\left(\mathbf{r}_j - \mathbf{r}_1\right)}{r_{1j}^3}$$

For $i = 2$ $(j \neq 2)$

$$\frac{\mathbf{F}_2}{m_2} = \frac{d^2\mathbf{r}_2}{dt^2} = \frac{Gm_1}{r_{21}^3}(\mathbf{r}_1 - \mathbf{r}_2) + G\sum_{j=3}^{n} \frac{m_j(\mathbf{r}_j - \mathbf{r}_2)}{r_{2j}^3}$$

Subtracting these two equations, we obtain

$$\frac{d^2\mathbf{r}}{dt^2} + \frac{\mu}{r^3}\mathbf{r} = -G\sum_{j=3}^{n}\left(\frac{m_j}{d_j^3}\mathbf{d}_j + \frac{m_j\rho_j}{\rho_j^3}\right) = G\sum_{j=3}^{n} m_j \nabla\left(\frac{1}{d_j} - \frac{\mathbf{r}\bullet\rho_j}{\rho_j^3}\right) \tag{4.95}$$

where $\mu = G(m_1 + m_2)$ and $\nabla =$ gradient operator with respect to the components of $\mathbf{r}$ from Exercise 4.18.

Define the $n-2$ scalar quantities

$$D_j = Gm_j\left(\frac{1}{d_j} - \frac{1}{\rho_j}\mathbf{r}\bullet\rho_j\right),\ j = 3, \ldots, n \tag{4.96}$$

D_j is called the disturbing function associated with the disturbing body P_j.

Then the basic (differential) equation of the relative motion of P_2 with respect to P_1 in the presence of a disturbing potential due to $n-2$ other particles is

$$\frac{d^2\mathbf{r}}{dt^2} + \frac{\mu}{r^3}\mathbf{r} = \nabla\left(\sum_{j=3}^{n} D_j\right) \tag{4.97}$$

where $\nabla =$ the gradient operator with respect to the components of the vector $\mathbf{r}$.

Note that $D_j = 0$, $j = 3, \ldots, n \Leftrightarrow$ 2-body problem (Keplerian motion)

Example:

For an earth satellite perturbed by the sun, the disturbing function is

$$D = (Gm_\odot/\rho)\left(1 + \sum_{k=2}^{\infty}(r/\rho)^k P^k(\cos\alpha)\right) \tag{4.98}$$

where α is the angle between the earth-to-sun and earth-to-satellite vectors from Exercise 4.19.

Sphere of Influence

In what region of space is one body the primary attracting mass and another the disturbing mass?

Let $P_1, P_3 =$ attracting bodies acting on P_2 with $m_1 << m_3$ as shown in Fig. 4.35.

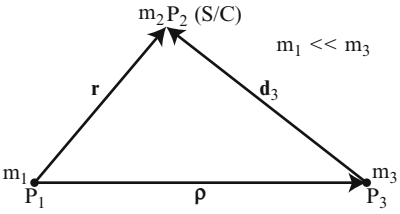

Fig. 4.35 Two attracting bodies for one spacecraft

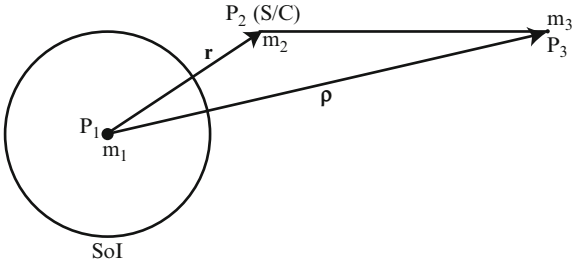

Fig. 4.36 Sphere of influence

Example:

$P_1 =$ earth
$P_2 =$ spacecraft
$P_3 =$ sun
$\rho \cong 1$ AU

When considering the disturbed motion of one body of mass m_2 in the presence of two bodies of mass m_1 and m_3, it is important for numerical computation to select the appropriate body to which the motion of the body of mass m_2 is to be referred.

The dividing surface is defined as the locus of points at which the ratio between the force with which the body of mass m_3 perturbs the motion of the body at P_2 and the force of attraction of the body of mass m_1 is equal to the ratio between the perturbing force of the mass m_1 and the force of attraction of the body of mass m_3. It happens that the surface boundary over which these two ratios are equal is almost spherical if r is considerably smaller than ρ as shown in Fig. 4.36.

Sphere of influence (SoI) = sphere about P_1 of radius

$$r \cong \rho \left(\frac{m_1}{m_3} \right)^{2/5} \tag{4.99}$$

where ρ denotes the distance between P_1 and P_3. See the 1999 reference by Battin on pages 395–396 or the reference by Kaplan on pages 287–289 for a proof. The planetary spheres of influence are given in Table 4.3.

Table 4.3 Planetary and Pluto's spheres of influence

Planet or Pluto system	Mass ratio (Sun or planetary system)	Average distance to Sun (10^5 km)	Radius of SOI (10^5 km)
Mercury	6,023,600	579.1	1.12
Venus	408,523.71	1,082	6.16
Earth + Moon	328,900.56	1,496	9.29
Mars system	3,098,708	2,279.4	5.77
Jupiter system	1,047.3486	7,785	482.19
Saturn system	3,497.898	14,294	546.55
Uranus system	22,902.98	28,709.9	517.70
Neptune system	19,412.24	45,040	867.70
Pluto system	1.35E + 08	59,135.2	33.09

Inside this sphere of influence for P_1, the motion of the spacecraft at P_2 is considered to be dominated by m_1 and only perturbed by m_3. Then P_1 is used as the origin of the inertial coordinates. When P_2 is outside this sphere, the coordinate system is centered at P_3.

The concept of sphere of influence originated with Pierre-Simon de Laplace when he was studying the motion of a comet that passed near Jupiter. In his orbit determination calculations, he searched for a logical criterion for choosing the origin of his coordinate system during various phases of the motion.

The sphere of influence for the planets and Pluto are given in Table 4.3.

Battin [1999] says the following about Laplace:

Pierre-Simon de Laplace (1749–1827), mathematician and French politician during the Napoleonic era, made many important discoveries in mathematical physics and chemistry but most of his life was devoted to celestial mechanics. His *Mecanique celeste*, consisting of five volumes, published between 1799 and 1825, was so complete that his immediate successors found little to add. Unfortunately, his vanity kept him from sufficiently crediting the works of those whom he considered rivals. Laplace was the originator of that troublesome phrase, which continues to plague students of mathematics: "It is easy to see that . . ." when, in fact, the missing details are anything but obvious.

Example (Solar system)

$$r_{SoI} \cong \left(\frac{m_1}{m_3}\right)^{2/5} \rho = \left(0.0304 \times 10^{-4}\right)^{2/5} \left(1.496 \times 10^{8} \text{km}\right) = 9.29 \times 10^{5} \text{km}$$

Example (Earth–Moon system)

$Gm_M = 4{,}902.801\ km^3/s^2$

Moon's average distance from earth = 384,400 km

$m_M/m_\oplus = 1/81.30059$

$R_\oplus = 6{,}378.14$ km

Moon's $r_{SoI} = \rho\left(\frac{m_M}{m_\oplus}\right)^{2/5} = 66,183\text{km} \cong 10R_\oplus$ in the literature.

The derivation of r_{SoI} given in the reference by Walter says:

$$r_{SoI} = \frac{\rho}{(m_1/m_3)^{-2/5} + 1}$$

But the 1 is not negligible for the moon because

$$(m_M/m_\oplus)^{-2/5} = 5.808.$$

Therefore, for the moon,

$$r_{SoI} = \frac{\rho}{(m_M/m_\oplus)^{-2/5} + 1} = 56,462\text{km} \cong 9R_\oplus$$

Reference: Walter
Example (Jovian system)
Radius of Io $R_{Io} = 1{,}821.6$ km, Distance between Jupiter and Io = 421,600 km

$$\frac{\text{mass of Io}}{\text{mass of Jupiter}} = 4.7 \times 10^{-5}$$

Therefore, for Io, $r_{SoI} = 4.3\ R_{Io}$

References for Sect. 4.5: Battin 1999; Battin 1964; Bills and Ferrari; Hobson; Kaplan; Kaula; Konopliv, Banerdt, and Sjogren; Konopliv, Asmar, Carranza, Sjogren, and Yuan; Seidelmann et al.; Tholen and Buie; Walter; Weisstein; Wylie and Barrett; and ssd.jpl.nasa.gov Website.

4.6 Time Measures and Their Relationships

Introduction

Time is a fundamental parameter in the equations of motion. To establish a system of time, one must define two quantities: the unit of duration (e.g., the second or day), and the epoch, or zero, of the chosen time. In physics and astronomy, there are four types of time systems in common use. Broadly speaking, they are the following:

1. Universal time, in which the unit of duration is the (mean) solar day, defined to be as uniform as possible, despite variations in the rotation of the earth (see Fig. 2.14).
2. Atomic time, in which the unit of duration corresponds to a defined number of wavelengths of radiation of a specified atomic transition of a chosen isotope.

3. Dynamical time, in which the unit of duration is based on the orbital motion of the earth, moon, and planets.
4. Sidereal time, in which the unit of duration is the period of the earth's rotation with respect to a point nearly fixed with respect to the stars.

Universal Time

Effects of Changes in Earth's Rotation Rate

Astronomers saw that the moon and planets did not appear where they were expected. These discrepancies are introduced by variations in the translational and rotational motion of the earth, on which time systems have traditionally been based. The eccentricity of the earth's orbit about the sun introduces translational variations. Earth's rotation is not uniform for various reasons:

1. Earth's rotation is gradually slowing down from tidal friction of the moon on the earth's oceans. (See Sect. 5.7.)
2. The positions of the North and South Poles wander around by a few meters from 1 year to the next due to seasonal effects and rearrangements in the internal structure of the earth (implies maybe a 30 ms change).
3. There are also changes in the spin rate of the earth, causing variations in the length of the day as described in the article located at the Website: http://www.jpl.nasa.gov/earth/features/longdays.html

This variation is about 1 ms over a year, increasing gradually over the winter for the Northern Hemisphere and decreasing during the summer. "There are also longer patterns of changes in the length of day that last decades, even centuries."

Introduction of Universal Time

These irregularities cause the earth to be a somewhat irregular clock. Therefore, three different scales of time called "universal time" (UT0, UT1, and UT2) have been developed as follows:

1. UT0 is the scale generated by the mean solar day. Thus, UT0 corrects for the tilted earth moving around the sun in an elliptical orbit.
2. UT1 (a more uniform scale) is UT0 corrected for the polar motion of the earth. (We use UT1.)
3. UT2 is UT1 corrected for the regular slowing down and speeding up of the earth's spin rate in winter and summer.

Universal time is the mean solar time at Greenwich, England, defining the zero epoch from which UT is measured.

Atomic Time

International Atomic Time (TAI)
Atomic time is based on the Système International (SI) second (atomic second), which is defined as the elapsed time of 9,192,631,770 "oscillations of the undisturbed cesium atom." Atomic time is equal to a count of atomic seconds (SI) since the astronomically determined instant of midnight January 1, 1958 00:00:00 at the Royal Observatory in Greenwich, England. TAI is kept by the International Earth Rotation Service (IERS—formerly the Bureau International L'Heure, BIH) in Paris, France. Practically speaking, this time is updated as a weighted average of many atomic clocks corrected to sea level around the world.

Coordinated Universal Time (UTC)
Atomic time is regular. So the irregularity of the earth's rotation rate implies that UT and TAI will get out of step. Therefore, the "leap second" was invented in 1972. UTC is always to be within 0.9 s of UT1. IERS notifies the world when a leap second is to be added or subtracted (always added so far) at the end of June or December.

Notice that the acronym for Coordinated Universal Time is "UTC". This order of the letters was chosen to be no one's acronym, so people will not be jealous because the acronym is not from their language as in the French acronyms "SI" and "TAI."

Dynamical Time

Ephemeris Time
In 1952, the International Astronomical Union (IAU) introduced Ephemeris Time (ET), based on the occurrence of astronomical events, to cope with the irregularities in the earth's rotation that affected the flow of mean solar time. The uniform time scale ET is the independent variable (dynamical time) in the differential equations of motion of the planets, the sun, and moon. In 1976, the IAU introduced two dynamical times that are often called ephemeris time:

(a) Barycentric Dynamical Time (BDT) used when describing the motion of bodies with respect to the solar system barycenter.
(b) Terrestrial Dynamical Time (TDT) used when describing the motion of objects near the earth.

Relativistic Time Scales
While time is an absolute quantity in the context of Newtonian physics, which does not depend on the location and the motion of the clock, the same is no longer true in a general relativistic framework. Instead, different proper times apply for clocks that are related to each other by a four-dimensional space-time transformation. Geocentric Coordinate Time (TCG) represents the time coordinate of a four-dimensional reference system.

Sidereal Time

Apart from the inherent motion of the equinox due to precession and nutation, sidereal time is a direct measure of the diurnal rotation of the earth. In general terms, sidereal time is the hour angle of the vernal equinox, i.e., the angle between the mean vernal equinox of date and the Greenwich meridian. Observatories measure sidereal time by observing celestial objects. The observation data are used to solve for UT1. Apparent sidereal time is the hour angle of the true equinox (the intersection of the true equator of date with the ecliptic plane), which is affected by the earth's nutation. Mean sidereal time is measured to the mean equinox of date, which is affected by precession.

Julian Days

The Julian day system provides a unique number to all days that have elapsed since a selected standard reference day, January 1, 4713 B.C., in the Julian calendar. The days are in mean solar measure. The Julian day (JD) numbers are never repeated and are not partitioned into weeks or months. Therefore, the number of days between two dates can be obtained by subtracting Julian day numbers.

There are 36,525 mean solar days in a Julian century and 86,400 s in a day. The Julian century does not refer to a particular time system; but rather is merely a count of a fixed number of days. Ephemeris calculations are done in Julian days and Julian centuries.

A Julian day starts at noon UT instead of midnight, an astronomical custom that is followed to avoid having the day number change during a night's observations. Julian days can be calculated from calendar dates between the years 1901 A.D. and 2099 A.D. as follows:

$$\begin{aligned} \mathrm{J} \;=\; & 367\mathrm{Y} - \mathrm{int}\left[7\left(\frac{\mathrm{Y} + \mathrm{int}((\mathrm{M}+9)/12)}{4}\right)\right] + \mathrm{int}\left(\frac{275\mathrm{M}}{9}\right) + \mathrm{D} \\ & + 1,721,013.5 \end{aligned} \tag{4.100}$$

where J denotes the Julian day number, Y (expressed as yyyy) the calendar year, M the calendar month number, D the calendar day and fraction, and int denotes the greatest integer in the argument.

For more information on time and time scales, see the references: Jespersen and Fitz-Randolph, and Seidelmann.

What Time Is It in Space?

Keeping tabs on a spacecraft way out at Saturn can get complicated. Unless otherwise noted, all times in this subsection have been converted to US Pacific

Time—the time zone of Cassini mission control at NASA's Jet Propulsion Laboratory (JPL) in Pasadena, California. Here are some definitions to help you keep tabs on mission time:

Coordinated Universal Time (UTC): The worldwide scientific standard of timekeeping

It is based upon carefully maintained atomic clocks and is highly stable. The addition or subtraction of leap seconds, as necessary, at two opportunities every year adjusts UTC for irregularities in Earth's rotation.

Spacecraft Event Time (SCET): The time something happens at the spacecraft, such as a science observation or engine burn.

One-Way Light Time (OWLT): The time it takes for a signal—which moves at the speed of light through space—to travel from the spacecraft to Earth. From Saturn, one-way light time can range from about 1 h and 14 min to 1 h and 24 min.

Earth Received Time (ERT): The time the spacecraft signal is received at mission control on Earth (the Spacecraft Event Time plus One-Way Light Time).

Local Time: Time adjusted for locations around the Earth. This is the time most people use to set watches and alarm clocks.

For example, Cassini began transmitting data from its very first close Titan flyby at 00:16 SCET on Oct. 27. The first signal arrived at Earth 1 h and 14 min later at 01:30 SCET on Oct. 27.

Adjusting for local time, the signals arrived on the screens at mission control in Pasadena, California at 6:30 p.m. PDT (or 9:30 p.m. EDT for folks tuned in at NASA headquarters in Washington, D.C.)

You can use a time zone converter or the chart in Table 4.4 to figure out when Cassini's signals would reach your house.

Table 4.4 Time zone converter chart

Time zone	Relative time (from UTC)
Atlantic Daylight	Subtract 3 h
Atlantic Standard	Subtract 4 h
Eastern Daylight	Subtract 4 h
Eastern Standard	Subtract 5 h
Central Daylight	Subtract 5 h
Central Standard	Subtract 6 h
Mountain Daylight	Subtract 6 h
Mountain Standard	Subtract 7 h
Pacific Daylight	Subtract 7 h
Pacific Standard	Subtract 8 h
Alaska Daylight	Subtract 8 h
Alaska Standard	Subtract 9 h
Hawaii–Aleutian Daylight	Subtract 9 h
Hawaii–Aleutian Standard	Subtract 10 h
Samoa Standard	Subtract 11 h

Reference: http://saturn.jpl.nasa.gov/mission/saturntourdates/saturntime/ [accessed 1/10/2014]

References for this chapter: BMW; Battin 1964; Battin 1999; Battin and Vaughan; Bell; Bergam and Prussing; Bills and Ferrari; Breakwell, Gillespie, and Ross; Broucke 1980; Broucke and Cefola; Cassini Equinox Mission Website; Cassini Solstice Mission Website; C. Brown; Epperson; Escobal; Hintz 2008; Hobson; Jespersen and Fitz-Randolph; Kaplan; Kaula; Konopliv, Banerdt, and Sjogren; Konopliv, S. W. Asmar, E. Carranza, W. L. Sjogren, and D. N. Yuan; Lancaster and Blanchard; Llanos, Miller, and Hintz 2012; Montenbruck and Gill; Nacozy and Dallas; NASA's Mars Exploration Program Website; Official US Time Website; Pisacane and Moore; Prussing 1979; Prussing and Conway; Roy 1988 and 2004; Seidelmann; Seidelmann et al.; Smith; ssd.jpl.nasa.gov Website; Tholen and Buie; Vallado; Walker, Ireland, and Owens 1985 and 1986; Walter; Weisstein; and Wylie and Barrett

Exercises

4.1 Derive Eq. (4.2).

4.2 A non-periodic comet approaches the sun in a parabolic orbit and reaches perihelion $r_p = 2$ AU at time $t = t_0$.

(a) Determine the true anomaly in this parabolic orbit exactly 10 days after perihelion.

(b) What are the position and velocity vectors at the time $t = t_0 + 10$ days in terms of the unit reference vectors $\mathbf{i}_\xi$ and $\mathbf{i}_\eta$ defined at perihelion.

4.3 Prove that, for an elliptic orbit,

(a) $\mathbf{r} = a(\cos E - e)\,\hat{\mathbf{i}}_p + \sqrt{ap}\sin E\hat{\mathbf{i}}_q$

(b) $\mathbf{v} = -\dfrac{\sqrt{\mu a}}{r}\sin E\hat{\mathbf{i}}_p + \dfrac{\sqrt{\mu p}}{r}\cos E\hat{\mathbf{i}}_q$

(c) $\hat{\mathbf{i}}_q = \dfrac{\cos E_0}{r_0}\mathbf{r_0} - \sqrt{\dfrac{a}{\mu}}\sin E_0\mathbf{v_0}$

$$\mathbf{i}_q = \sqrt{\frac{a}{p}}\frac{\sin E_0}{r_0}\mathbf{r}_0 + \frac{a}{\sqrt{\mu p}}(\cos E_0 - e)\mathbf{v}_0$$

4.4 (a) Construct MATLAB M-file(s) for the patched conic model of the interplanetary flight from a circular parking orbit at earth to a flyby of any other planet. Use input commands to supply all of the input data (altitude of parking orbit, Gm parameters, flyby altitude, etc.). In the comments to your MATLAB program,

- Give the name of each variable/constant and describe it as appropriate when it is initialized and give its unit(s).
- Describe the input and output with units.
- Describe what the program does and the computations.

Then submit your well-commented code.

(b) Run your M-file(s) to generate the numerical results for the:

- Venus flyby example we discussed in class
- Mars flyby example you computed for dark-side passage in Exercises 3.13(c) and 3.14(b).

Then submit your printout for each run from the MATLAB command window and construct a table containing the following output data with units:

- Δv for injection
- Post-flyby values of the scalars r, v, and β
- Post-flyby heliocentric ellipse values of e, θ, h, r_p, a, and τ.

4.5 Prove that the hyperbolic anomaly

$$H = \frac{2}{a^2}\text{area}(CAQ)$$

where CAQ denotes the shaded region designated in Fig. 4.5.

4.6 Prove that, for hyperbolic motion, the magnitude of the radius vector

$$r = a(1 - e\cosh H)$$

as a function of the hyperbolic anomaly H.

4.7 Complete the proof of Theorem 4.1 for elliptic orbits.

4.8 Recall that Exercise 2.16 included computing the Keplerian elements a, e, and θ for the orbit of the Huygens Probe at Titan from position and velocity vectors. Complete the conversion from the Cartesian position and velocity vectors to the modified classical element set by computing the orientation angles i, Ω, and ω in degrees.

4.9 At April 10.5 TDB, the Keplerian orbital elements for the asteroid 2005 GL were:

$$\begin{aligned} a &= 1.05448404728002 \text{ AU} \\ e &= 0.305256235263636 \\ \omega &= 265.1060039173237^\circ \\ \Omega &= 43.72082802193163^\circ \\ i &= 15.8687544967489^\circ \\ M &= 227.1876710870660^\circ \end{aligned}$$

in (inertial) heliocentric ecliptic of J2000 coordinates.

(a) Compute the true anomaly at this point.

(b) Compute the asteroid's position and velocity vectors at this point in the (inertial) heliocentric ecliptic of J2000 coordinate frame.

4.10 (a) Use the mission design plot in Fig. 4.10b to determine which launch date/arrival date combinations for the opportunities for launches to Venus satisfy the constraints

$$C_3 \leq 15 \text{ km}^2/\text{s}^2 \text{ and VHP} \leq 5 \text{ km/s}$$

Shade in the two regions in the plot and label the region for Type I ($0° \leq \upsilon \leq 180°$) trajectories with "I" and label the region for Type II ($180° < \upsilon < 360°$) trajectories with "II".

(b) Does a launch constraint of DLA $< 50°$ restrict the region of acceptable LD/AD pairs obtained in part (a)? Justify your answer by using the appropriate pork chop plot. It is important to check this constraint when designing a launch, especially a launch to the ISS.

4.11 Consider Lambert's Problem for a trip from earth to a newly discovered planet. The relevant data are:

$$\text{Gm of the sun} = 3 \times 10^{-4} \text{ AU}^3/\text{day}^2$$
$$r_1 = 1 \text{ AU}$$
$$r_2 = 2 \text{ AU}$$
$$\upsilon = 60°$$

with the earth at the initial point P, the planet at the final point, and the sun at the focus F.

(a) Compute the values of a, n (mean motion), and t (transfer time) for minimum energy transfer.

(b) If the transfer time is specified to be 500 days, determine the smallest appropriate value of the semimajor axis for the transfer trajectory.

(c) If the semimajor axis a = 2.0 AU for the transfer path, calculate the minimum time to make this transfer.

4.12 NASA considered sending a Mariner spacecraft to fly by Jupiter and Uranus. It would have been launched on November 3, 1979, to arrive at Jupiter 523 days later on April 10, 1981, at a flyby radius of 5.5 Jupiter radii. Using a Jupiter gravity assist to accelerate and turn the trajectory, the spacecraft would then proceed to encounter Uranus in July 1985.

(a) Determine the semimajor axis of a transfer trajectory from the earth to Jupiter that satisfies all of the above conditions, given that the angle between the sun-to-earth vector at launch and the sun-to-Jupiter vector at arrival was 147°. Assume that the earth and Jupiter are massless as an approximation.

(b) In which case of trajectories does the trajectory chosen as the answer to part (a) appear? Explain.

(c) Determine the eccentricity of the transfer trajectory considered in part (a) of this problem. Give the values of any angles in degrees.

4.13 Let $\mathbf{r_1}$ and $\mathbf{r_2}$ denote the position vectors of the initial point P and final point Q, respectively, and $\mathbf{v_1}$ denote the velocity vector at P for elliptic orbits in Lambert's Problem and show that

$$\mathbf{r}_2 = \left[1 - \frac{r_2}{p}(1 - \cos \upsilon)\right]\mathbf{r}_1 + \left[\frac{r_1 r_2}{\sqrt{\mu p}} \sin \upsilon\right]\mathbf{v}_1$$

4.14 (a) Derive the Legendre polynomials $P_3(\alpha)$ and $P_4(\alpha)$.
(b) Use MATLAB to plot the Legendre Polynomials $P_1(\alpha)$, $P_2(\alpha)$, $P_3(\alpha)$, and $P_4(\alpha)$ over the interval $-1 \leq \alpha \leq 1$ in the same figure. Label each of the curves in the figure to identify the polynomial being plotted, give a title to the figure, and label the horizontal and vertical axes. Use the grid command. Submit a copy of your MATLAB code with your figure.

4.15 Show that U_{11} in the infinite series expansion of the potential at P(X,Y,Z) due to the body B satisfies $U_{11} = 0$, if the origin of the inertial X,Y,Z coordinate system is at the center of mass of the body B.

4.16 Show that the force $\mathbf{F_i}$ in Eq. (4.87) is conservative.

4.17 Derive Eq. (4.90).

4.18 Derive Eq. (4.95).

4.19 Derive the disturbing function D for an earth satellite perturbed by the sun as shown in Eq. (4.98).

4.20 (a) Compute the sphere of influence of Jupiter relative to the sun.
(b) Compute the sphere of influence of Mercury relative to the sun.
(c) Compute the sphere of influence of Titan relative to Saturn.

4.21 (a) Compute the Julian day corresponding to the calendar date May 14, 2013 at 9:00 pm PST.
(b) What is the elapsed time between October 4, 1957 UT 19:26:24 (the launch date of the first satellite, Sputnik I, made by humans) and the date considered in part (a) of this problem? The Julian day number of the launch of Sputnik I is JDI = 2,436,116.3100.

Non-Keplerian Motion 5

5.1 Introduction

We have emphasized the relative 2-body solution to the trajectory problem for four reasons:

1. Only the relative 2-body problem can be solved analytically.
2. It is often a good approximation to the real solution, because the gravitational force of the central body is much greater than perturbing forces.
3. It provides an understandable and illustrative picture of the situation, which can be used in feasibility studies and verification of results.
4. It can be used as a reference trajectory for precise trajectory determination techniques.

But forces other than the central body's gravitational force act on the satellite to perturb it away from the Keplerian orbit, giving non-Keplerian motion. In this chapter, we transition from Keplerian motion to non-Keplerian by identifying types of perturbations, using perturbation techniques, and drawing from the astrodynamics techniques described in Chap. 4. We study the effects of the oblateness of the central body on a spacecraft's orbit, using the potential function of an oblate body as described in Chap. 4. An important mission application is the sun synchronous orbit. Finally, we culminate our study of non-Keplerian motion by considering the satellite orbit paradox and its applications to atmospheric drag, libration of 24-h, nearly circular equatorial satellites, and the fact that the moon is slowly moving away from the earth, plus a discussion of "zero G."

5.2 Perturbation Techniques

We consider methods for including perturbations to Keplerian motion in our analyses.

© Springer International Publishing Switzerland 2015

G.R. Hintz, *Orbital Mechanics and Astrodynamics*,
DOI 10.1007/978-3-319-09444-1_5

Perturbations

Def.: Perturbation forces are forces acting on an object other than those that cause it to move along a reference trajectory.

Def.: A perturbation is a deviation from the normal or expected motion.

The expected motion is conic (relative 2-body) motion.

Def.: Changes to a trajectory produced by perturbation forces are known as trajectory perturbations.

Def.: The trajectory that results from perturbation forces is called a perturbed trajectory or a non-Keplerian trajectory.

Def.: The reference trajectory or expected motion is referred to as an unperturbed trajectory or a Keplerian trajectory.

Examples of perturbation forces:

1. Gravitational forces of other attracting bodies ("3rd body effects), e.g., solar 3rd body effects on PVO as shown in Fig. 4.32.
2. Gravitational forces resulting from the asphericity and non-uniform density of the central body as discussed under the "Gravitational Potential of a Distributed Mass" in Chap. 4.
3. Surface forces resulting from atmospheric lift and drag.
4. Surface forces resulting from solar wind and pressure.
5. Thrusting from spacecraft engines.
   (a) Trajectory corrections—TCMs.
   (b) Attitude corrections—Attitude correction maneuvers (ACMs) are designed to correct the spacecraft's attitude, but may also produce translational motion.

The resulting perturbations can be significant, especially over a long time.

Def.: The solar wind is a gale of low-energy atomic particles (a plasma) that streams out radially from the sun.

The solar wind:

(a) Has an average speed of 300–700 km/s.
(b) Slows to much less than 20 km/s in the termination shock.
(c) Reaches a maximum every 11 years with the solar activity cycle.

Data from the Hinode (Mission to the Sun) satellite show that magnetic waves play a critical role in driving the solar wind into space. The solar wind is a stream of electrically charged gas that is propelled away from the sun in all directions at speeds of almost 1 million miles per hour. Better understanding of the solar wind may lead to more accurate prediction of damaging radiation waves before they reach satellites. Findings by American-led international teams of researchers appear in the Dec. 7, 2007 issue of the journal *Science*.

Hinode was launched in September 2006 to study the sun's magnetic field and how its explosive energy propagates through the different layers of the solar atmosphere. It is a collaborative mission between NASA and the space agencies of Japan, the UK, Norway, and Europe and Japan's National Astronomical Observatory. Marshall manages science operations and managed the development of the scientific instrumentation provided for the mission by NASA, industry and other federal agencies. The Lockheed Martin Advanced Technology Center, Palo Alto, Calif., is the lead US investigator for the Solar Optical Telescope. The Smithsonian Astrophysical Observatory in Cambridge, Massachusetts is the lead US investigator for the X-Ray Telescope.

To view images about these findings and learn more about Hinode, visit: http://www.nasa.gov/mission_pages/solar-b/.

Reference: Brown and Morone.

Def.: Solar radiation pressure (SRP) is the force produced by the transfer of momentum through impact, reflection, absorption, and re-emission of photons from the sun.

The earth is another perturbation source through reflected solar radiation and emitted radiation as shown in Fig. 5.1. At times, the moon looks bright in the area illuminated by the sun and dark, but not black, in the rest. The question is: where does the light come from that partially illuminates this dark region. It is not due to light refraction by an atmosphere because the moon's atmosphere is extremely thin. The answer is that the light comes from earthshine.

Recall, from Chap. 1, the definition of a conservative force and the three equivalent properties for this definition. We say that a perturbing force $\mathbf{F_p}$ is conservative if it is derivable from a scalar function, i.e.,

$$\mathbf{F_p} = \nabla \mathrm{U}(\mathrm{r})$$

Recall the gravitational potential U(**r**) of the earth considered in Sect. 4.4. The perturbing forces caused by third bodies are conservative field forces. There are also non-conservative perturbing forces such as atmospheric drag.

In the case of geostationary orbits, solar pressure tends to change the eccentricity (shape) of the orbit. Atmospheric drag is pertinent to low-altitude orbits about the earth. Such forces tend to decrease the major axis (size) of the orbit, eventually causing a satellite to fall back to the earth's surface.

Two categories of perturbation techniques, i.e., methods for solving the equations of motion with perturbations, are:

1. Special perturbations, which use direct numerical integration of the equations of motion, including all necessary perturbing accelerations.

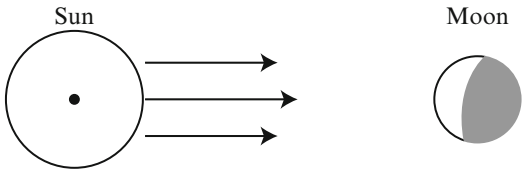

Fig. 5.1 Earthshine on the Moon

2. General perturbations, which use analytic integration of series expansions of the perturbing accelerations in the variational equations of orbit elements.

Special Perturbations

We consider the following three methods for incorporating perturbations into our analyses:

1. Cowell's method integrates the sum of all accelerations numerically

$$\frac{d^2\mathbf{r}}{dt^2} + \frac{\mu}{r^3}\mathbf{r} = \mathbf{a_p} \tag{5.1}$$

where $\mathbf{a_p}$ = the sum of accelerations due to all disturbing forces. (Recall the disturbed 2-body problem.)

The advantages of this method are:

(a) Its simplicity.
(b) It obtains the vectors **r** and **v** directly.

However, it is not easy to see the resulting changes in classical orbit elements, i.e., changes caused by perturbations.

Remark: Philip Herbert Cowell (1870–1949) used this method to predict the return of Halley's Comet in 1910.

2. Encke's method integrates the differential accelerations instead of the total accelerations, omitting the gravitational acceleration of the central body.

The advantages of this method are:

(a) It is quicker than Cowell's method.
(b) It obtains the vectors **r** and **v** directly.

However, it is not easy to see resulting changes in classical orbital elements.

Remarks about Johann Franz Encke (1791–1865):
His education, though interrupted twice by military service during the Wars of Liberation, was guided by Gauss. His work on the computation of the orbit of a comet with a period of 3.3 years brought him promotions and fame. The comet was later called Encke's comet.
Remark:
Either of these methods works if formulated correctly. However, it is appropriate to use Cowell's method because of its simplicity and the speed of modern computers, which allows us to do so. Here, we work with the Cartesian state.

3. Variation of Parameters considers the influence of perturbing forces on the Keplerian elements directly as we will see in the following discussion.

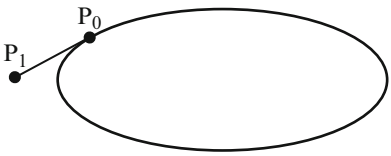

Fig. 5.2 Osculating ellipse

The advantages for this method are as follows:

(a) It provides analytic description of rates of change of Keplerian elements—thus, we obtain direct information on how a particular force affects the orbital elements.
(b) It provides physical insight.
(c) It becomes the starting point to develop averaging techniques.

Its disadvantage is that it does not extract **r** and **v** directly in the process (However, it is possible to compute **r**(t) and **v**(t) from the Keplerian elements as in Sect. 4.3, Eqs. (4.44)–(4.46).)

Osculating Ellipse

For Keplerian motion, the six elements (a, e, t_p, Ω, ω, *i*) are uniquely related to the six state components $\left(X,\ Y,\ Z,\ \dot{X},\ \dot{Y},\ \dot{Z}\right)$ at any instant of time and may be considered to be the six constants of integration of the equation of motion. In the presence of perturbing forces, the orbit is not Keplerian.

Def.: The osculating ellipse at a specified time t is the path the particle would follow if the perturbing forces were suddenly removed at the time t.

At P_0 (as shown in Fig. 5.2), the osculating ellipse has Keplerian elements: are:

$$
\begin{aligned}
a_0 &= a_0(x_0, y_0, z_0, \dot{x}_0, \dot{y}_0, \dot{z}_0; t_0)\\
e_0 &= e_0(x_0, y_0, z_0, \dot{x}_0, \dot{y}_0, \dot{z}_0; t_0)\\
i_0 &= i_0(x_0, y_0, z_0, \dot{x}_0, \dot{y}_0, \dot{z}_0; t_0)\\
\Omega_0 &= \Omega_0(x_0, y_0, z_0, \dot{x}_0, \dot{y}_0, \dot{z}_0; t_0)\\
\omega_0 &= \omega_0(x_0, y_0, z_0, \dot{x}_0, \dot{y}_0, \dot{z}_0; t_0)
\end{aligned}
$$

At P_1, the osculating ellipse has Keplerian elements are:

$$
\begin{aligned}
a_1 &= a_1(x_1, y_1, z_1, \dot{x}_1, \dot{y}_1, \dot{z}_1; t_1)\\
e_1 &= e_1(x_1, y_1, z_1, \dot{x}_1, \dot{y}_1, \dot{z}_1; t_1)\\
i_1 &= i_1(x_1, y_1, z_1, \dot{x}_1, \dot{y}_1, \dot{z}_1; t_1)\\
\Omega_1 &= \Omega_1(x_1, y_1, z_1, \dot{x}_1, \dot{y}_1, \dot{z}_1; t_1)\\
\omega_1 &= \omega_1(x_1, y_1, z_1, \dot{x}_1, \dot{y}_1, \dot{z}_1; t_1)
\end{aligned}
$$

The differences

$$\begin{aligned}\Delta a &= a_1 - a_0\\ \Delta e &= e_1 - e_0\\ \Delta i &= i_1 - i_0\\ \Delta\Omega &= \Omega_1 - \Omega_0\\ \Delta\omega &= \omega_1 - \omega_0\end{aligned}$$

are the perturbations in elements during the time interval $\Delta t = t_1 - t_0$.

Note that, while X, Y, Z, $\dot{X}$, $\dot{Y}$, and $\dot{Z}$ change rapidly, the osculating elements change slowly due to the perturbations only. The Keplerian elements a, e, i, Ω, ω, which do not change without perturbations, are called "slow variables." The variables θ, t_p, M, which do change without perturbations, are called "fast variables."

5.3 Variation of Parameters Technique

Basically, we find analytic expressions for the rate of change of elements $\left(\dot{a}, \dot{e}, \dot{i}, \dot{\Omega}, \dot{\omega}\right)$ resulting from perturbations and then integrate. A perturbation force could be in any direction. We decompose perturbation velocity impulses in a three-dimensional velocity space to study their effects on orbital elements.

In-Plane Perturbation Components

We first consider perturbations in the orbit plane.

We denote velocity components in the tangential and orthogonal direction as shown in Fig. 5.3 as follows:

$f_t dt$ = tangential velocity change = v_t
$f_n dt$ = inward normal velocity change

where f_t, f_n = accelerations (forces/unit mass) so that $f_t dt$, $f_n dt$ = velocity perturbations.

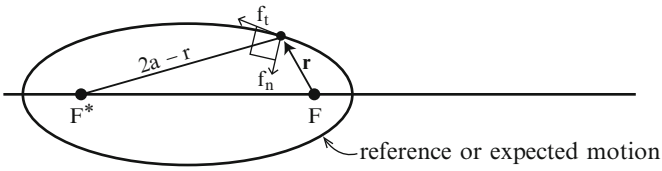

Fig. 5.3 In-plane perturbation components

The perturbing accelerations are small compared to the gravitational acceleration by the central body.

Consider $v_t = f_t dt$:

The Energy Equation says

$$\mathscr{E} = \frac{v^2}{2} - \frac{\mu}{r} = \frac{-\mu}{2a}$$

where we consider r to be fixed. So a change in velocity magnitude will change the energy and a according to

$$d\mathscr{E} = vdv = \frac{\mu}{2a^2} da = vdv$$

so that

$$\frac{da}{dv} = \frac{2va^2}{\mu} > 0 \tag{5.2}$$

Therefore, a increases as v is increased and, therefore, τ increases as v is increased.

For $v_n = f_n dt$, the velocity increment is perpendicular to **v** so that the increment vector does not change v or r to first order so that the increment does not change $\mathscr{E}$ or a or τ. But it does change the direction of the vector **v**. The reference by Kaplan provides geometric and small angle approximations that demonstrate that

$$\dot{e} = \frac{2f_t}{v}(\cos\theta + e) - \frac{f_n}{v}\frac{r}{a}\sin\theta \tag{5.3}$$

$$\dot{\omega} = \frac{2f_t}{ve}\sin\theta + \frac{f_n}{v}\left(2 + \frac{r}{ae}\cos\theta\right) + f_L(\theta) \tag{5.4}$$

where we have added a third component that is in the out-of-plane direction. We offer no analytic formula for this third component, but will provide a graphical display of this component for an example in Sect. 7.3.

Out-of-Plane (or Lateral) Perturbation Component

Consider the third orthogonal component f_L along the vector **h**. The acceleration f_L rotates the orbit plane about the radius vector, so that f_L does not change a, τ, or e but it does change the orientation parameters Ω and i. In particluar,

$$\frac{di}{dt} = \frac{f_L}{v_\theta}\cos\theta^* \tag{5.5}$$

$$\dot{\Omega} = \frac{f_L}{v_\theta}\frac{\sin\theta^*}{\sin i} \tag{5.6}$$

$$\dot{\theta} \;=\; \frac{h}{r^2} \;-\; \dot{\Omega}\cos i \tag{5.7}$$

where

$$\theta^* \;=\; \theta + \omega$$

Summary

To first order:

Only f_t changes a, τ, $\mathscr{E}$.
Only f_t, f_n change e, $r_{p.}$
Only f_L changes i, Ω.
All three (f_t, f_n, f_L) change ω.

5.4 Oblateness Effects: Precession

Potential Function for an Oblate Body

Recall that the potential function for a distributed mass is

$$U(r,\phi,\theta) \;=\; \frac{Gm}{r}\left[1 - \sum_{k=2}^{\infty}\left(\frac{R_e}{r}\right)^k J_k P_k(\cos\phi) + \sum_{k=2}^{\infty}\sum_{j=1}^{k}\left(\frac{R_e}{r}\right)^k P_k^j(\cos\phi)\left\{C_k^j\cos j\theta + S_k^j\sin j\theta\right\}\right]$$

from Eq. (4.86). If the mass distribution of the central body is symmetric about the z axis, then the body is an oblate attracting body so that the density function $\Gamma = \Gamma(\rho,\beta)$. Since the density function is independent of longitude, λ, the coefficients

$$C_k^j = \frac{A_k^j}{mR_e^k} = (\text{constant})\int_0^{2\pi}\cos(j\lambda)d\lambda\iint_B(\ldots)d\rho d\beta = 0$$

because

$$\int_0^{2\pi}\cos(j\lambda)d\lambda = 0$$

and similarly $S_k{}^j = 0$ for all $j \geq 1$. Therefore, for the oblate earth model,

Table 5.1 Zonal harmonic coefficients for the Earth

$J(2) = 1{,}082.6267 \times 10^{-6}$	$J(16) = 0.0181 \times 10^{-6}$
$J(3) = -2.5327 \times 10^{-6}$	$J(17) = -0.1169 \times 10^{-6}$
$J(4) = -1.6196 \times 10^{-6}$	$J(18) = -0.0309 \times 10^{-6}$
$J(5) = -0.2273 \times 10^{-6}$	$J(19) = 0.0203 \times 10^{-6}$
$J(6) = 0.5407 \times 10^{-6}$	$J(20) = -0.1424 \times 10^{-6}$
$J(7) = -0.3524 \times 10^{-6}$	$J(21) = -0.0385 \times 10^{-6}$
$J(8) = -0.2048 \times 10^{-6}$	$J(22) = 0.0763 \times 10^{-6}$
$J(9) = -0.1206 \times 10^{-6}$	$J(23) = 0.1551 \times 10^{-6}$
$J(10) = -0.2411 \times 10^{-6}$	$J(24) = -0.0053 \times 10^{-6}$
$J(11) = 0.2444 \times 10^{-6}$	$J(25) = -0.0229 \times 10^{-6}$
$J(12) = -0.1886 \times 10^{-6}$	$J(26) = -0.0368 \times 10^{-6}$
$J(13) = -0.2198 \times 10^{-6}$	$J(27) = -0.0206 \times 10^{-6}$
$J(14) = 0.1307 \times 10^{-6}$	$J(28) = 0.0687 \times 10^{-6}$
$J(15) = -0.0082 \times 10^{-6}$	$J(29) = 0.0382 \times 10^{-6}$
	$J(30) = -0.0471 \times 10^{-6}$

where $J(n) = J_n$.

$$U_{\oplus}(r, \phi) = \frac{Gm}{r}\left[1 + \sum_{k=2}^{\infty}\left(\frac{R_e}{r}\right)^k J_k P_k(\cos\phi)\right] \tag{5.8}$$

since all the sectorial and tesseral terms are zero.

By consulting Table 5.1, we see that $J_2 \approx 3$ orders of magnitude larger than other coefficients, so that J_2 is the only term of interest here. Therefore,

$$\begin{aligned} U_{\oplus}(r, \phi) &= \frac{\mu}{r}\left[1 - \left(\frac{R_{\oplus}}{r}\right)^2 J_2\left(\left(\frac{3}{2}\right)\cos^2\phi - \frac{1}{2}\right)\right] \\ &= \frac{\mu}{r}\left[1 - \left(\frac{R_{\oplus}}{r}\right)^2 J_2\left(\frac{3}{2}\sin^2(\text{LAT}) - \frac{1}{2}\right)\right] \\ &= \frac{\mu}{r}\left[1 - \left(\frac{R_{\oplus}}{r}\right)^2 J_2\left(\frac{3}{2}\left(\frac{z}{r}\right)^2 - \frac{1}{2}\right)\right] \end{aligned} \tag{5.9}$$

Because $\cos\phi = \sin(90^\circ - \phi) = \sin(\text{LAT}) = \frac{z}{r}$, where LAT denotes latitude as seen in Fig. 5.4.

Oblateness

The earth is not a perfect sphere. We now use an oblate spheroid model that is obtained by revolving an ellipse about the earth's axis of rotation. In this model, cross sections parallel to the equator are circles of constant latitude and meridians of constant longitude are ellipses as shown in Fig. 5.5 with

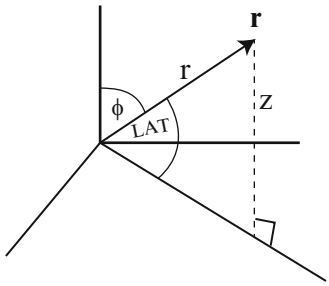

Fig. 5.4 Latitude and co-latitude of position

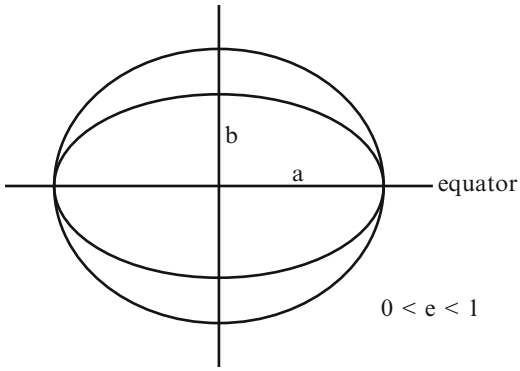

Fig. 5.5 Oblate body

$a = R_{\oplus} =$ mean equatorial radius of the earth
$b =$ polar radius of the earth

However, we will continue to say $r = R_{\oplus} +$ altitude for the orbit radius of a spacecraft.

Oblateness was caused by centrifugal acceleration

$$\boldsymbol{\omega} \times (\boldsymbol{\omega} \times \mathbf{r}),\ \omega = \text{spinrate}$$

when the earth was molten. Oblateness introduces the J_2 term in the potential function U.

Def.: The flattening f of a body is the difference between the semimajor and semiminor axes of the ellipse of revolution divided by the semimajor axis, i.e.

$$f = \frac{a - b}{a} \tag{5.10}$$

Therefore,

$$f = 1 - \frac{b}{a} = 1 - \sqrt{1 - e^2}$$

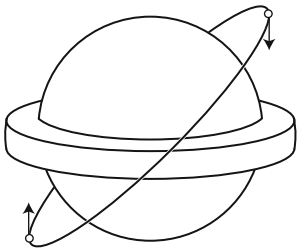

Fig. 5.6 Earth's equatorial bulge. Reference: BMW [Figure published with the permission of Dover Publications, Inc.]

Solving this equation for e^2, we obtain

$$e^2 = 2f - f^2 \tag{5.11}$$

where e = eccentricity of the ellipse of revolution, i.e., a meridian of longitude.

Examples: For the World Geodetic Survey (WGS-84), $f_{\oplus} = 1/298.25722 = 0.00335$ and $e = 0.0818191$. For comparison, the flattening for Jupiter is $f_{Jupiter} = 0.065$.

These arguments apply to bodies other than the earth.

Examples (J_2):

Venus: $J_2 = 6 \times 10^{-6}$
Earth: $J_2 = 1{,}082.63 \times 10^{-6}$
Jupiter: $J_2 = 14{,}696.43 \times 10^{-6}$
Saturn: $J_2 = 16{,}290.71 \times 10^{-6}$

So we see, for example, that the J_2 for Jupiter is much larger than the earth's J_2.

Additional data on Outer Planet Gravity Fields are available online at http://ssd.jpl.nasa.gov/?gravity_fields_op [Accessed 10/14/13]

Precession of the Line of Nodes

See Figure 3.1-4 in the Bate–Mueller–White text and shown here as Fig. 5.6.

The earth's equatorial bulge provides a slight torque on an earth-orbiting spacecraft about the center of the earth so the spacecraft's orbit plane precesses just as a gyroscope would under a similar torque. The result is that the line of nodes moves eastward or westward depending on the inclination of the orbit.

Lagrange's Planetary Equations can be used to show that

$$\frac{d\Omega}{dt} = -3\pi J_2 \left(\frac{R_{\oplus}}{p}\right)^2 n \cos(i) \tag{5.12}$$

Reference: Battin 1999, p 483.

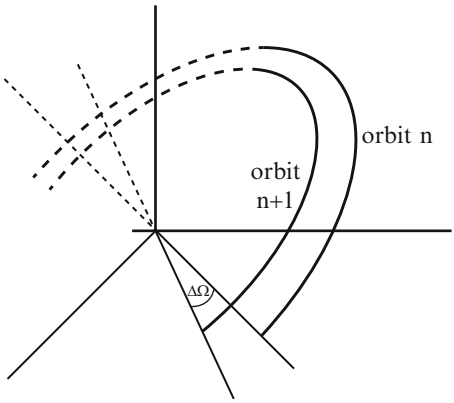

Fig. 5.7 Precession of Line of Nodes for $0 < i < 90°$

By multiplying this equation by τ and simplifying the result, we obtain

$$\left(\frac{d\Omega}{dt}\right)_{av} = -3\pi J_2 \left(\frac{R_\oplus}{p}\right)^2 \cos(i) \tag{5.13}$$

which is the change $\Delta\Omega$ per orbit in radians. Hence, the orbit precesses as shown in Fig. 5.7.

Similarly,

$$\frac{d\omega}{dt} = \frac{3}{2} J_2 \left(\frac{R_\oplus}{p}\right)^2 n \left(2 - \left(\frac{5}{2}\right) \sin^2 i\right) \tag{5.14}$$

Therefore,

$$\left(\frac{d\omega}{dt}\right)_{av} = \tau \frac{d\omega}{dt} = 3\pi J_2 \left(\frac{R_\oplus}{p}\right)^2 \left(2 - \left(\frac{5}{2}\right) \sin^2 i\right) \tag{5.15}$$

which is the change $\Delta\omega$ per orbit in radians.

Similarly,

$$\left(\frac{di}{dt}\right)_{av} = \left(\frac{dh}{dt}\right)_{av} = \left(\frac{de}{dt}\right)_{av} = \left(\frac{da}{dt}\right)_{av} = 0 \tag{5.16}$$

Therefore, only Ω and ω are affected to first order by J_2. Note that the effect is a function of the inclination for Ω and ω.

Def.: A critical inclination orbit is an orbit that has an inclination for which

$$\left(\frac{d\omega}{dt}\right)_{av} = 0.$$

The critical values of inclinations are determined in Exercise 5.3a.

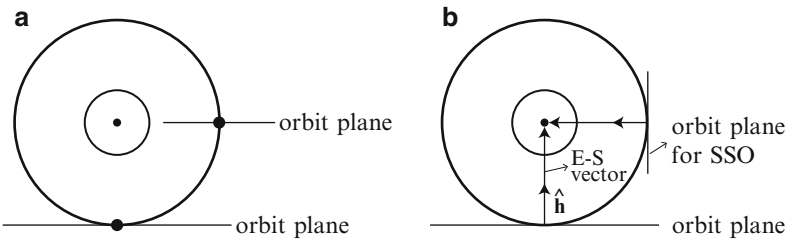

Fig. 5.8 Orbit plane for an earth orbiter. (**a**) Relative two-body motion, (**b**) SSO

Example (precession of the line of nodes)

Relative two-body motion occurs in a fixed orbit plane in inertial space as in Fig. 5.8a.

Def.: A sun synchronous orbit (SSO) is an orbit that maintains a constant angle between the earth–sun vector and the normal (**h**) to the orbit plane.

Figure 5.8b shows a SSO that has a fixed angle between the angular momentum vector and the earth–sun vector of 0°.

In a sun synchronous orbit, the satellite plane remains approximately fixed with respect to the sun. We introduce this relationship by matching the nodal precession rate (the secular variation in the right ascension of the ascending node) to the earth's mean orbital rate around the sun (0.986°/day). That is, we set

$$\begin{aligned}\frac{2\pi \text{ rad}}{365.25 \text{ day}} &= \left(\left(\frac{d\Omega}{dt}\right)_{av} \frac{\text{rad}}{\text{rev}}\right)\left(\frac{\#\text{revs}}{\text{day}}\right) \\ &= \left(-3\pi\left(\frac{R_\oplus}{p}\right)^2 J_2 \cos i\right)\left(\frac{(3600)24\,\text{s/day}}{\tau}\right) \\ &= -3J_2\left(\frac{R_\oplus}{a(1-e^2)}\right)^2 \left(\frac{12(3600)}{\sqrt{a^3/\mu}}\right)\cos i \,\text{rad/day}\end{aligned} \tag{5.17}$$

where τ is in seconds. This form is a function of a and e times cos *i*. Therefore, we need select the size, shape, and inclination of the orbit. Usually, some of these parameters are specified by mission requirements.

A sun synchronous orbit might be selected, for example, to produce the same lighting conditions along the ground track all year long, to avoid pointing a radiator at the sun, or to avoid entering the earth's shadow for thermal or power reasons. A SSO provides global coverage at all latitudes, except a few degrees from the North and South Pole. The reference by Boain considers the "A-B-Cs of Sun-Synchronous Orbit Mission Design."

Examples of SSO missions are:

1. Radarsat-1, launched 11/4/1995, was Canada's first commercial earth-observation satellite with an orbit at 798-km altitude and $i = 98.6°$.
2. Aquarius/SAC-D, launched on 6/10/11, was a joint effort between NASA and CONAE (Comision Nacional de Actividades Espaciales, Argentina's Space Agency) with 657-km altitude and $i = 98°$ providing 7-day global coverage.
3. NPOESS Preparatory Project (NPP), where NPOESS stands for "National Polar-orbiting Operational Environmental Satellite System," is in an 824-km altitude SSO, orbiting the earth 16 times/day and observing nearly the entire surface of the earth.
4. Afternoon Constellation (A-Train) 705-km altitude, $i = 98$, circular orbits consisting of.
   (a) Aqua—launched 5/4/2002
   (b) CloudSat—launched 4/28/2006 in dual launch with CALIPSO
   (c) CALIPSO—launched 4/28/2006 in dual launch with CloudSat
   (d) PARASOL—launched from Kourou, French Guiana on 12/18/2004 for CNES (French Agency)
   (e) Aura—launched 7/15/2004

For these spacecraft, the normal altitude is 705 km and $i = 98$. Each satellite completes 14.55 orbits/day. However, PARASOL was maneuvered out of the A-Train on 12/2/2009 and dropped 4 km below the other satellites by early January 2010.

5.5 An Alternate Form of the Perturbation Equations

RTW (Radial, Transverse, and Out-of-Plane) Coordinate System

Components of a perturbation force per unit mass can be considered in the RTW coordinate system such that

$\hat{\mathbf{R}}$ is in the radial direction pointing outward from the central body.

$\hat{\mathbf{W}}$ is in the out-of-plane direction for the instantaneous orbit plane, i.e., parallel to the instantaneous angular momentum vector.

$\hat{\mathbf{T}}$ completes the right-handed coordinate system, i.e., along the transverse direction.

In this system, the three components of perturbing accelerations are denoted as f_R, f_T, and f_W with corresponding velocity impulses $f_R dt$, $f_T dt$, and $f_W dt$. (This reference frame is often called the RTN or radial-transverse-normal system.) The perturbing accelerations are small compared to the central gravitational acceleration.

Perturbation Equations of Celestial Mechanics

The perturbation equations of celestial mechanics give the rates of change induced by perturbation forces on the Keplerian orbital elements of an elliptical orbit. The rates of change are given in terms of the components of the applied force in the RTW coordinate system. The differential equations for changes to the Keplerian elements are given by the Gaussian-Lagrange planetary equations, which can be found in the reference by Pisacane and Moore, ed. In this reference, the components of force f_R, f_T, and f_W are denoted as R, T, and W, respectively.

An elementary derivation of these perturbation equations is given in the reference by Burns. The method of proof in this reference is to write the orbital elements in terms of the orbital energy $\mathscr{E}$ and angular momentum h and then differentiate the resulting equations with respect to time to determine the effect on the orbital elements of small changes in $\mathscr{E}$ and h. The perturbation equations in terms of disturbing force components are then derived by computing the manner in which perturbing forces change $\mathscr{E}$ and h.

5.6 Primary Perturbations for Earth-Orbiting Spacecraft

The primary perturbations for earth-orbiting spacecraft are:

(a) Gravitational forces of the sun and moon
(b) Gravitational forces of the non-spherical earth
(c) Atmospheric drag
(d) Solar radiation pressure (SRP).

The perturbations (a) and (d) affect high altitude orbits the most, while (b) and (c) affect low orbits the most. For example, Exercise 5.5 considers the effects of the J_2 perturbation, a gravitational force of the non-spherical earth.

Reference: Wertz and Larson (ed.), pp. 141 ff.

5.7 Satellite Orbit Paradox

Introduction

The fact that atmospheric drag produces an increase in average speed and KE of a satellite is called the "satellite drag paradox." To explain this paradox, we return to considering an unperturbed Keplerian orbit, then determine the effect of a disturbing impulse on orbit characteristics, and lastly consider three applications of this analysis.

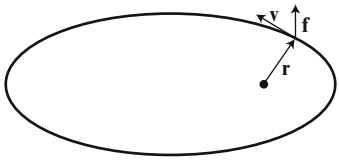

Fig. 5.9 Disturbing force **f**

Keplerian Orbit

For an unperturbed elliptical orbit,

$$\begin{aligned}
\mathscr{E} &= -\frac{\mu}{2a} \\
(\mathrm{PE})_{\mathrm{av}} &= -\frac{\mu}{a} \\
(\mathrm{KE})_{\mathrm{av}} &= \frac{\mu}{2a} \\
\tau &= \frac{2\pi a^{3/2}}{\sqrt{\mu}} \\
n &= \frac{2\pi}{\tau} = \frac{\sqrt{\mu}}{a^{3/2}} \\
(v^2)_{\mathrm{av}} &= \frac{\mu}{a} = 2(\mathrm{KE})_{\mathrm{av}}
\end{aligned} \tag{5.18}$$

where averages are taken with respect to time. If we know any of the above parameters, we know them all.

We derive the formula for $(\mathrm{PE})_{\mathrm{av}}$:

$$(\mathrm{PE})_{\mathrm{av}} = \frac{\oint (\mathrm{PE})\mathrm{dt}}{\tau} = \frac{1}{2\pi\sqrt{\frac{a^3}{\mu}}} \int_0^{2\pi} \left(-\frac{\mu}{r}\right) \frac{\mathrm{dE}}{\dot{\mathrm{E}}} = \frac{-\mu\sqrt{\frac{\mu}{a^3}}}{2\pi} \int_0^{2\pi} \frac{\mathrm{dE}}{\sqrt{\frac{\mu}{a}}} = -\frac{\mu}{a}$$

from Eq. (2.32). The proof for $(\mathrm{KE})_{\mathrm{av}}$ is similar and left as Exercise 5.6.

Orbit Paradox

Consider a disturbing force **f** as in Fig. 5.9, where

$$\dot{f} << \frac{\mu}{r^2}$$

The force **f** is a succession of infinitesimal impulses. The work done by **f** is

$$\Delta\mathscr{E} = \Delta W = \mathbf{f}\cdot\mathbf{\Delta s} = \mathbf{f}\cdot\mathbf{v}\Delta t = f_T v\Delta t$$

where $\mathbf{\Delta s}$ is the displacement by **f**, $\mathbf{f}\bullet\mathbf{v}$ is the component of **f** along **v**, and f_T is the tangential component of **f**.

The $\Delta\mathscr{E}$ produces changes in the other parameters as follows:

$$\begin{aligned}
\Delta a &= \left(\frac{2a^2}{\mu}\right)\Delta\mathscr{E}\\
\Delta(PE)_{av} &= 2\Delta\mathscr{E}\\
\Delta(KE)_{av} &= -\Delta\mathscr{E}\\
\Delta\tau &= \left(\frac{3a\tau}{\mu}\right)\Delta\mathscr{E}\\
\Delta n &= \frac{-3an}{\mu}\Delta\mathscr{E}\\
\Delta v_{av} &= -\left(\frac{a}{\mu}\right)^{1/2}\Delta\mathscr{E}
\end{aligned} \tag{5.19}$$

From Eqs. (5.19), we deduce Table 5.2.

Assume $e = 0$. Then

$$v = v_c = \sqrt{\frac{\mu}{a}}$$

$$\Delta v = \frac{-\sqrt{\mu}}{2a^{3/2}}\Delta a = \frac{-\sqrt{\mu}}{2a^{3/2}}\frac{2a^2}{\mu}\Delta\mathscr{E} = \frac{-a^{1/2}}{\mu^{1/2}}\Delta\mathscr{E} = \frac{-a^{1/2}}{\mu^{1/2}}f_T v\Delta t$$

Therefore,

$$\frac{\Delta v}{\Delta t} = -f_T$$

which is an apparent contradiction of NII, which is a paradox.

Explanation: The perturbation f is not the total force. The total force, gravitational force plus f, obeys NII.

From Table 5.2, an enlargement of the orbit ($\Delta a > 0$) implies an average increase in $PE = 2\Delta\mathscr{E}$ and average loss in $KE = \Delta\mathscr{E}$. A shrinking of the orbit ($\Delta a < 0$) implies an average decrease in $PE = 2\Delta\mathscr{E}$ and an average gain in $KE = \Delta\mathscr{E}$. In each case, there is a net change in orbital energy $\Delta\mathscr{E}$ = work done by an impulsive force.

Table 5.2 Effect of disturbing impulse on orbit characteristics

Parameter	For $\Delta\mathscr{E} > 0$ (positive thrust)	For $\Delta\mathscr{E} < 0$ (negative thrust)
a	Increase	Decrease
$(PE)_{av}$	Increase	Decrease
$(KE)_{av}$	Decrease	Increase
τ	Increase	Decrease
n	Decrease	Increase
v_{av}	Decrease	Increase

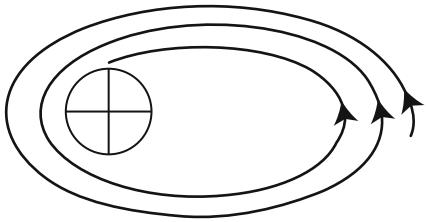

Fig. 5.10 Effect of atmospheric drag on the spacecraft's orbit

Applications

Example 1: Atmospheric Drag
In the presence of atmospheric drag, the disturbing force **f** is directly opposed to **v**, which produces $\Delta\mathscr{E} < 0$ at all times. From Table 5.2, we see that a and τ decrease monotonically and the average velocity increases. The drag is greatest at perigee where velocity and atmospheric density are greatest, which produces the greatest energy drain at perigee and minimum at apoapsis. Therefore, the orbit becomes more circular as it shrinks, so that the spacecraft spirals inward as shown in Fig. 5.10 until it burns up or impacts the surface.

Example 2: Libration of 24-Hour, Nearly Circular, Equatorial Satellite
Initially, we modeled the earth as a point mass, then as a sphere, then as an oblate spheroid, and now as a triaxial ellipsoid. The last three models are shown in Fig. 5.11. The equations of the last three models are:

$$\frac{x^2}{a^2}+\frac{y^2}{a^2}+\frac{z^2}{a^2}=1$$
$$\frac{x^2}{a^2}+\frac{y^2}{a^2}+\frac{z^2}{b^2}=1$$
$$\frac{x^2}{a^2}+\frac{y^2}{b^2}+\frac{z^2}{c^2}=1$$

for a Cartesian coordinate system whose origin is at the center of mass of the earth.

Figure 5.12 shows the earth's equator, which is an ellipse with the difference between major and minor axes approximately equal to 130 m with the long axis at

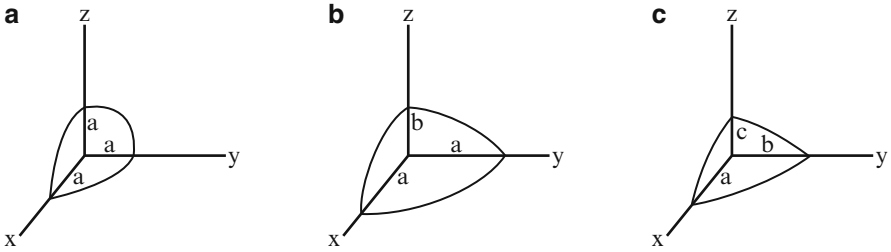

Fig. 5.11 Earth models. (**a**) Sphere, (**b**) oblate spheroid, (**c**) triaxial ellipsoid

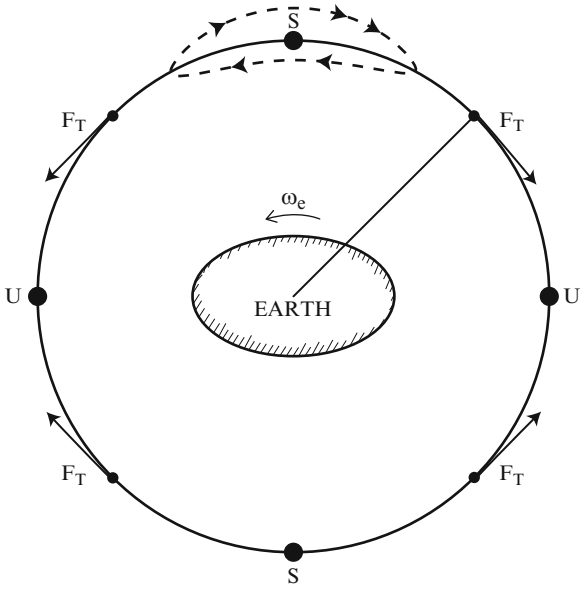

Fig. 5.12 Equatorial section of the Earth (looking south along the polar axis)

15°W longitude. The dashed curve in Fig. 5.12 shows the libration path of a spacecraft in a coordinate system that is rotating with the earth. The satellite is shown librating about a stable equilibrium point S. (Points marked "U" are unstable equilibrium points.) Consider the spacecraft at a point in its orbit to the right of the point S and beyond the earth's orbit. The satellite is actually rotating about the earth in an orbit that is slightly further away from the earth than S. At this point, the gravitational tug of the mass bulge of the earth on the right-hand side is greater than the force from the left-hand bulge, so the net force is a retarding force, which reduces a. The satellite moves to the right away from the earth because it is in a larger orbit so it is moving slower than the earth. The satellite's orbit shrinks until it is inside the earth's orbit when it begins to speed up relative to the earth. The satellite eventually overtakes the earth so that the equatorial bulge on the left has a

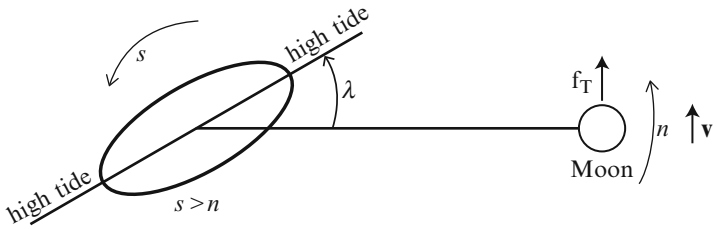

Fig. 5.13 High tides caused by the Moon's gravity

stronger tug and provides a net positive force, increasing a and the velocity of the spacecraft. Eventually the spacecraft moves outside the earth's orbit and begins slowing down and moving to the right to repeat the libration.

Librations with periods of approximately 2.1 years have been observed on a Syncom satellite librating around the S point near 105°W longitude over Brazil.

Example 3: Secular Acceleration of a Moon

Let $n =$ the secondary's orbital angular momentum and $s =$ the primary's rotational angular momentum. For the earth's moon, $s > n$.

The force of the moon's gravity decreases with the inverse square of distance according to Newton's Universal Law of Gravity. Therefore, the moon tugs on the water closer to it more than on the earth so there is a high tide on the right-hand side as shown in Fig. 5.13. (The reader might wonder why there is a high tide on the other side of the earth. There is no force to the left pulling on the water. Since the gravitational force of the moon decreases with distance, the moon pulls the earth away from the water on the left side.)

Since the bulge on the right is closer to the moon than the one on the left, there is a net tangential force f_T along the moon's velocity vector, providing $\Delta \mathscr{E} > 0$ to the moon's energy. From Table 5.2, we know that a and τ increase and the average linear and angular velocity decrease. Therefore, the moon is receding from the earth and the length of the month is increasing. With no external torques acting on the earth–moon system, the total angular momentum is a constant and as the moon's angular momentum increases the earth's spin momentum decreases due to friction on the ocean floor (which causes the high tide to be ahead of the direction to the moon as shown in Fig. 5.13). Therefore, the day is getting longer. Eventually, the length of the day would equal the length of the month if tidal drag were allowed to run its course. However, the sun will become a red giant long before that happens, engulfing the earth.

If $s < n$ as for Phobos, a moon of Mars, and Triton, a satellite of Neptune, then the situation is as shown in Fig. 5.14. Here the tidal forces withdraw energy and angular momentum from the orbit of the moon so the orbit collapses and usually circularizes.

References for Sect. 5.6: Blitzer; Burns; Murray and Dermott.

Material from the reference by Leon Blitzer was reproduced with permission from the Am. J. Phys. 39, 882 (1971). Copyright 1971. American Association of Physics Teachers.

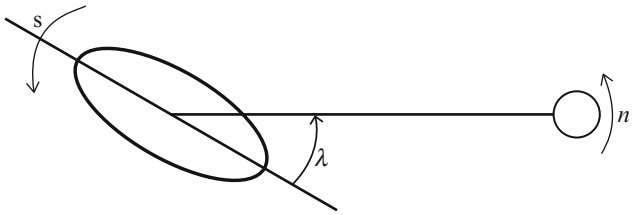

Fig. 5.14 High tides if $s < n$ as for Phobus and Triton

5.8 "Zero G"

When I prepared my "Tana Throws Her Baseball" talk, I found the book *Weight and Weightlessness* by Franklyn Branley in the juvenile section of our local library. This book discusses how a spacecraft is launched into an orbit in which it falls at the rate of the curvature of the earth. So there is gravity that is causing the spacecraft to fall, not zero G. Then he draws a cartoon of a young boy standing on a scale, which shows that his weight is 60 lb. The scale measures the force it must apply to prevent the boy from falling to the floor. By NIII, that force is equal and opposite to the gravitational force of the boy, i.e., his weight. By NII, his gravitational force is

$$F = ma = mg_{\oplus}$$

where $g_{\oplus}$ denotes the earth's gravity.

The author says to imagine that someone suddenly digs a hole under the boy that goes straight down to the center of the earth. Then a cartoon shows that the scale, which the boy is still standing on as he falls, registers 0 lb. So the situation is not one of "zero G," as we often say, but one of "zero W," i.e., "zero weight."

Reference for Sect. 5.8: Branley.

References for this chapter: Blitzer; Boain; Bond and Allman; Branley; Brown and Morone; Burns; Chao; Chobotov; Cutting, Born, and Frautnick; Kaplan; Murray and Dermott; NASA website; Pisacane and Moore; Sidi; Wertz and Larson.

Exercises

5.1 A spacecraft is in a 24-h earth orbit when the Mission Design Team determines that the period must be increased to 24.5 h. The only criterion in determining the ΔV-maneuver to achieve this period change is that the ΔV must be minimized to save spacecraft propellant.

(a) At what true anomaly should this (impulsive) maneuver be performed? Explain.

(b) The velocity correction vector can be described in terms of three components.

$\Delta V_t = f_t dt$, the tangential component.

$\Delta V_n = f_n dt$, the inward normal component.
$\Delta V_L = f_L dt$, the lateral, or out-of-plane, component.
What is the lateral component ΔV_L of the minimum ΔV maneuver determined in part (a)? Explain.

5.2 (a) For what inclinations is $(d\Omega/dt)_{av} = 0$?
(b) For what inclinations will the line of nodes precess, i.e., rotate, to the west?

5.3 (a) For what inclinations is $(d\omega/dt)_{av} = 0$? These values are called the "critical values" of the inclination.
(b) For what inclinations is $(d\omega/dt)_{av} < 0$?

5.4 Consider a spacecraft in an earth orbit having

$$r_p = 6{,}700 \text{ km and } r_a = 7{,}300 \text{ km}.$$

(a) Use MATLAB as described below to plot $(d\Omega/dt)_{av}$ in degrees as a function of the orbit inclination in degrees.
(b) Use MATLAB as described below to plot $(d\omega/dt)_{av}$ in degrees as a function of the orbit inclination in degrees.
(c) Compute the daily change in ω if $i = 90°$.

In parts (a) and (b), use MATLAB's plot function, insert grid lines, use the xlabel command to label the x-axis as "Orbit Inclination (°)," use the ylabel command to give an appropriate label to the y-axis (including "deg" as the unit), and give each plot an appropriate title using the title command. Note that, in order to produce the two figures by the same execution of MATLAB, you will need to use a "figure" command to produce the second plot; otherwise, the second plot will overwrite the first plot.

5.5 Construct a table of values of the rate of change in Ω and ω in °/day for the ISS, SSO, GPS, Molnya, geosynchronous with $i = 60°$, and geostationary orbits by an oblate earth.

5.6 Derive the equation

$$(KE)_{av} = \frac{\mu}{2a}$$

where the average is taken with respect to time. (See Eqs. (5.18.)

5.7 In Sect. 5.4, we consider flatness of an oblate body. Consider the flatness of a triaxial body in the equatorial plane. Define this equatorial flatness parameter as:

$$f_e = \frac{b - c}{R_e}$$

where b–c denotes the difference between the maximum and minimum radius of the body in the equatorial plane and R_e denotes the mean equatorial radius of the body. Compute the value of the equatorial flatness f_e of the earth.

Spacecraft Rendezvous

6

6.1 Introduction

Consider the problem of spacecraft rendezvous, e.g., the return of the Lunar Excursion Module (LEM) to the Command Module (aka Command and Service Module or CSM) in orbit about the moon for the Apollo mission (see Fig. 6.1). Or consider the situation in which NASA's Space Shuttle (crewed), the European Space Agency's (ESA) Jules Verne Automated Transfer Vehicle (ATV, robotic), Russian Soyuz (crewed) or Progress (robotic), or Japanese H-II Transfer Vehicle (robotic) vehicle performs a rendezvous and docking with the International Space Station (ISS). For example, on March 27, 2008, the Jules Verne ATV conducted maneuvers "to guide the ship to an 'interface point' 24 miles behind and three miles below the station." Later, the ATV performed a rendezvous and docking with the ISS.

Rendezvous in space between two satellites is accomplished when both satellites attain the same position vector and velocity vector at the same time. However, at the time the rendezvous sequence is initiated, they may be very far apart, possibly with one satellite at liftoff.

The two parts in a rendezvous sequence are:

1. Phasing for rendezvous—performing the maneuvers in the timing sequence that will bring the two satellites into close proximity.
2. Terminal rendezvous—performing the maneuvers that induce the relative motion between the satellites that is required for rendezvous and docking, i.e., the motion of one satellite (chase or active vehicle) with respect to the other (target or passive) vehicle in a coordinate frame attached to one (target) of the satellites.

© Springer International Publishing Switzerland 2015

G.R. Hintz, *Orbital Mechanics and Astrodynamics*,
DOI 10.1007/978-3-319-09444-1_6

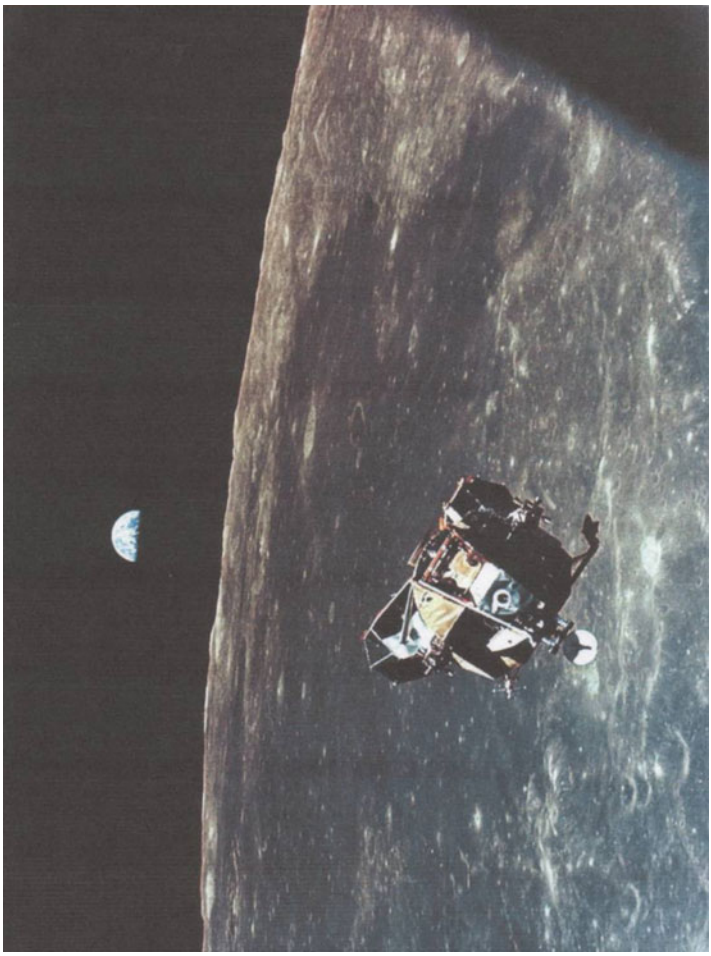

Fig. 6.1 Lunar module approaches the command module

Description of Fig. 6.1: With a half-earth in the background, the Lunar Module ascent stage with moon-walking Astronauts Neil Armstrong and Edwin Aldrin Jr. approaches for a rendezvous with the Apollo Command Module manned by Michael Collins. The Apollo 11 liftoff from the moon came early, ending a 22-h stay on the moon by Armstrong and Aldrin.

6.2 Phasing for Rendezvous

Phasing for rendezvous may be accomplished by the (optimal) Hohmann or bi-elliptic (with or without a plane change) transfer, either inward or outward as appropriate, as described in Sect. 3.4, or one of the following alternate transfer orbits.

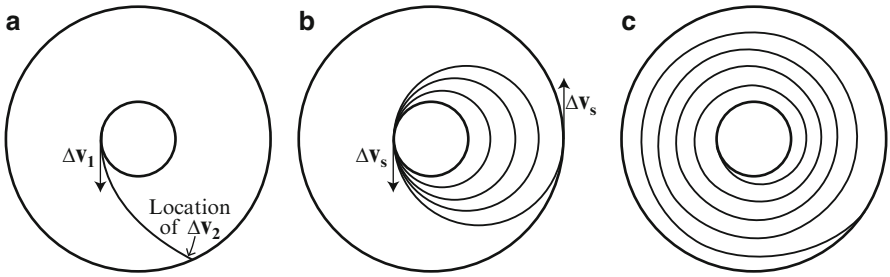

Fig. 6.2 Alternative transfer orbits. (**a**) High energy, (**b**) low thrust chemical, (**c**) electric propulsion

Alternative Transfer Orbits

High energy (Type I) orbits as in Fig. 6.2a would be used if the transfer time is critical, e.g., for military operations or for a human mission to Mars, requiring the use of more energy than is required for a Hohmann transfer.

Low-thrust chemical transfer would execute a series of burns around perigee and then one or two burns at apogee to reach the final orbit as shown in Fig. 6.2b.

Electric propulsion transfer as shown in Fig. 6.2c involves spiraling outward, requiring less total propellant because of electric propulsion's high I_{sp}. The direction of the $\Delta \mathbf{v}$ varies.

Reference: Wertz and Larson 1999, p 185.

6.3 Example: Apollo 11 Ascent from the Moon

The Apollo 11 powered ascent had two phases:

1. Vertical rise to achieve terrain clearance (clearing the descent stage).
2. Orbit insertion into a 9×45 n. mi. orbit at a true anomaly of 18° and an altitude of 60,000 ft (10 n. mi.) with nominal ascent burn time = 7 min 18 s ± 17 s (3σ) and $\Delta V = 6{,}056$ fps + contingencies.

The time of liftoff was chosen to provide the proper phasing for rendezvous. Target requirements were on the altitude, velocity, and orbit plane. The +X body axis jets fired for attitude control during ascent.

The ascent propulsion system (APS) provided a constant thrust of approximately 3,500 lb throughout the ascent. This thrust could be enhanced by approximately 100 lb by the reaction control system (RCS) attitude control.

Actual insertion time: 7 min 15 s from liftoff.

Resulting orbit after velocity residual trim:

Apolune altitude = 47.3 n. mi.
Perilune altitude = 9.5 n. mi.

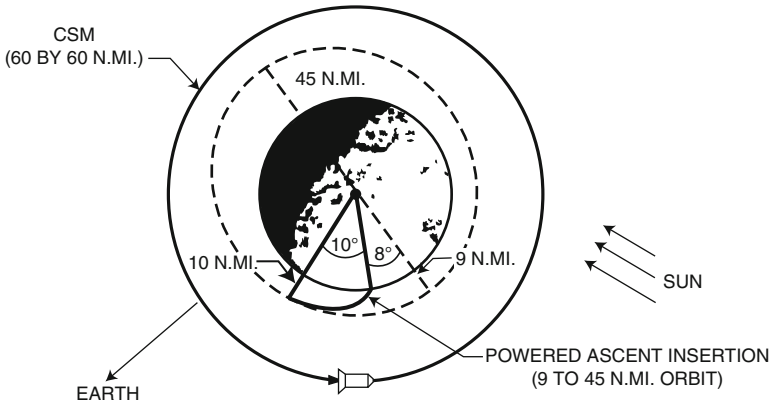

Fig. 6.3 Lunar module ascent

A sketch of the lunar module's ascent from the lunar surface is given in Fig. 6.3. Reference: Bennett.

6.4 Terminal Rendezvous

Consider the problem of spacecraft rendezvous in neighboring nearly circular orbits. It is convenient to consider relative motion between the two vehicles.

Equations of Relative Motion for a Circular Target Orbit

Consider the relative position between a target spacecraft and a chase vehicle over an interval of time (Fig. 6.4).

Let $\mathbf{r_1} = \mathbf{r_1}(t)$ denote the inertial position vector of the target vehicle at time t and $\mathbf{r_2} = \mathbf{r_2}(t)$ denote the inertial position of the chase vehicle at the same time.

Define $\boldsymbol{\rho}(t) = \mathbf{r_2}(t) - \mathbf{r_1}(t)$.

Assume $\boldsymbol{\tau_1} \cong \boldsymbol{\tau_2}$ and e_2 (small) $> e_1 = 0$.

Def.: The (rotating) local vertical coordinate frame or CW frame is defined such that the

x axis is directed along the radial direction to the target from the central body
y axis is along the target orbit path
z axis is normal to the target orbit (out-of-plane)

If this coordinate system is considered to be attached to the target vehicle and allowed to rotate with the orbit position, then the position of the chase satellite can be described with respect to the target. The relative position

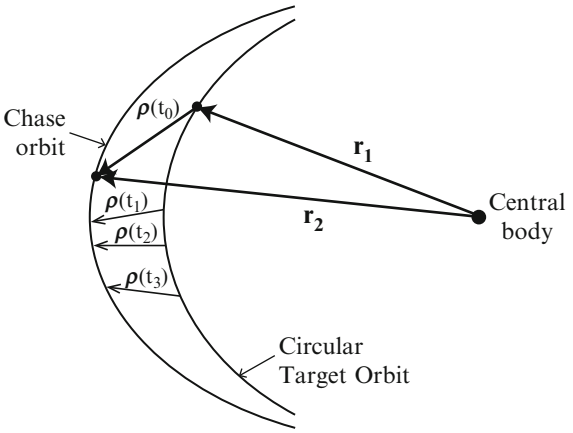

Fig. 6.4 Relative position of target and chase vehicles in an inertial reference frame

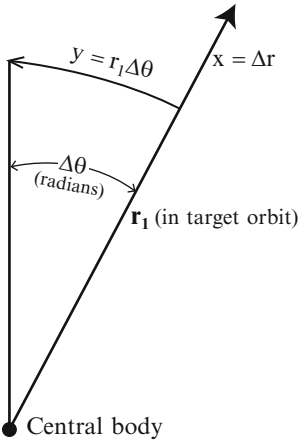

Fig. 6.5 y-Axis wrapped along the target orbit

$$\boldsymbol{\rho} = (\mathrm{x(t)},\ \mathrm{y(t)},\ \mathrm{z(t)})$$

with $\mathrm{x} = \mathrm{y} = \mathrm{z} = 0$ is like a bull's eye for the chase vehicle.

Consider y to be wrapped along the target orbit as is shown in Fig. 6.5 so that

$$\mathrm{y} \cong \mathrm{r}_1 \Delta\theta \tag{6.1}$$

For the target spacecraft (passive being chased):

$$\ddot{\mathbf{r}}_1 = -\mu \frac{\mathbf{r}_1}{\mathrm{r}_1^3} \tag{6.2}$$

and for the chase spacecraft (may be influenced by a perturbing force):

$$\ddot{\mathbf{r}}_2 = -\mu \frac{\mathbf{r}_2}{\mathrm{r}_2{}^3} + \mathbf{f} \tag{6.3}$$

where $\mathbf{f}$ is force/unit mass $= \mathbf{a_p}$, the sum of perturbing accelerations.

Define $\boldsymbol{\rho} = \mathbf{r_2} - \mathbf{r_1}$ and consider $\boldsymbol{\rho}$ such that

$$\rho = \sqrt{x^2 + y^2 + z^2} << r_1 \tag{6.4}$$

where slightly non-coplanar (i.e., $z \neq 0$, but small) orbits are allowed. Then

$$\begin{aligned} \ddot{\boldsymbol{\rho}} &= \frac{\mu}{{r_1}^3}\left[\mathbf{r}_1 - {r_1}^3 \frac{\mathbf{r}_2}{{r_2}^3}\right] + \mathbf{f} \\ &= n_1^2\left[\mathbf{r}_1 - {r_1}^3\left(\frac{\mathbf{r}_2}{{r_2}^3}\right)\right] + \mathbf{f} \end{aligned} \tag{6.5}$$

where

$$n_1 = \sqrt{\frac{\mu}{{r_1}^3}} = \text{mean motion of the target vehicle.} \tag{6.6}$$

Consider the Binomial Expansion:

$$\frac{1}{(1 \pm \varepsilon)^m} = 1 \mp m\varepsilon + \frac{m(m+1)}{2!}\varepsilon^2 + \ldots \tag{6.7}$$

where $\varepsilon^2 < 1$ for convergence.

A linear approximation is

$$\frac{1}{(1 \pm \varepsilon)^m} = 1 \mp m\varepsilon \tag{6.8}$$

But

$${r_2}^2 = {r_1}^2 + 2\rho \bullet \mathbf{r}_1 + \rho \bullet \rho \tag{6.9}$$

Therefore,

$$\frac{\mathbf{r}_2}{{r_2}^3} \cong \frac{\mathbf{r}_1 + \rho}{{r_1}^3\left(1 + \dfrac{2\mathbf{r}_1 \bullet \rho}{{r_1}^2}\right)^{3/2}} \text{ because } \rho << r_1$$

$$= \frac{\mathbf{r}_1 + \rho}{{r_1}^3}\left[1 - \frac{3}{2}\left(\frac{2\mathbf{r}_1 \bullet \boldsymbol{\rho}}{{r_1}^2}\right)\right] \text{ by a linear approximation to the binomial} \tag{6.10}$$

expansion. In this last step, we use the fact that

$$\varepsilon = \frac{2}{{r_1}^2} r_1 \rho \cos\left(\measuredangle(\mathbf{r}_1, \boldsymbol{\rho})\right) \leq \frac{2\rho}{r_1} << 1$$

implies that $\varepsilon^2 < 1$. Therefore,

$$\ddot{\rho} = {n_1}^2 \left[\mathbf{r_1} - {r_1}^3 \left(\frac{\mathbf{r}_2}{{r_2}^3}\right)\right] + \mathbf{f} \tag{6.11}$$

$$= {n_1}^2 \left(-\boldsymbol{\rho} + \frac{3\mathbf{r}_1 \bullet \rho}{r_1} \frac{\mathbf{r}_1}{r_1}\right) + \mathbf{f} \quad \text{from Eqs. (6.4) and (6.10)} \tag{6.12}$$

because

$$\left({n_1}^2/{r_1}^2\right)\rho(\mathbf{r}_1 \bullet \boldsymbol{\rho}) = \frac{\mu}{{r_1}^2} \frac{\rho \cos\left(\measuredangle(\mathbf{r}_1, \boldsymbol{\rho})\right)}{r_1} \frac{\rho}{r_1} \leq \frac{\mu}{r_1} \left(\frac{\rho}{r_1} \frac{\rho}{r_1}\right)$$

which is negligible because $\rho << r_1$.

Equation (6.12) provides one expression for $\ddot{\rho}$. From Theorem 1.2, we obtain a second expression as follows.

$$\ddot{\mathbf{r}}_2 = \ddot{\mathbf{r}}_1 + \ddot{\boldsymbol{\rho}}_b + 2\boldsymbol{\omega} \mathrm{x} \dot{\boldsymbol{\rho}}_b + \dot{\boldsymbol{\omega}}\, \mathrm{x}\boldsymbol{\rho} + \boldsymbol{\omega} \mathrm{x}(\boldsymbol{\omega} \mathrm{x} \boldsymbol{\rho})$$

Therefore,

$$\ddot{\boldsymbol{\rho}} = \ddot{\mathbf{r}}_2 - \ddot{\mathbf{r}}_1 = \ddot{\boldsymbol{\rho}}_b + 2\boldsymbol{\omega} \mathrm{x} \dot{\boldsymbol{\rho}}_b + \dot{\boldsymbol{\omega}}\, \mathrm{x}\boldsymbol{\rho} + \boldsymbol{\omega} \mathrm{x}(\boldsymbol{\omega} \mathrm{x} \boldsymbol{\rho}) \tag{6.13}$$

where $\omega = \dfrac{2\pi}{\tau} = \sqrt{\dfrac{\mu}{a^3}} = n_1$ and $\ddot{\boldsymbol{\rho}}_b$ is the relative acceleration of $\mathbf{r_2}$ with respect to $\mathbf{r_1}$ in a body-fixed system.

Consider terms on the right-hand side of this second expression for $\ddot{\boldsymbol{\rho}}$. In the x, y, z frame,

$$\boldsymbol{\rho} = \begin{bmatrix} \mathrm{x} \\ \mathrm{y} \\ \mathrm{z} \end{bmatrix} \quad \text{and} \quad \boldsymbol{\omega} = \begin{bmatrix} 0 \\ 0 \\ n_1 \end{bmatrix} \tag{6.14}$$

The vector derivatives of $\dot{\boldsymbol{\rho}}_b$ and $\ddot{\boldsymbol{\rho}}_b$ in the x, y, z frame are

$$\dot{\boldsymbol{\rho}}_b = \begin{bmatrix} \dot{\mathrm{x}} \\ \dot{\mathrm{y}} \\ \dot{\mathrm{z}} \end{bmatrix} \quad \text{and} \quad \ddot{\boldsymbol{\rho}}_b = \begin{bmatrix} \ddot{\mathrm{x}} \\ \ddot{\mathrm{y}} \\ \ddot{\mathrm{z}} \end{bmatrix} \tag{6.15}$$

because the derivatives are taken with respect to the frame in which the vectors are expressed. Then

$$\boldsymbol{\omega} \mathrm{x} \dot{\boldsymbol{\rho}}_{\mathrm{b}} = (0, 0, n_1)\, \mathrm{x}(, \dot{\mathrm{x}}, \dot{\mathrm{y}}, \dot{\mathrm{z}}) = (-n_1\, \dot{\mathrm{y}}, n_1\, \dot{\mathrm{x}}\,,\ 0) \tag{6.16}$$

Likewise,

$$\boldsymbol{\omega} \mathrm{x}(\boldsymbol{\omega} \mathrm{x} \boldsymbol{\rho}) = -{n_1}^2(\mathrm{x},\ \mathrm{y},\ 0) \tag{6.17}$$

Substituting the Eqs. (6.14) and (6.15) into Eq. (6.13), we obtain the expression

$$\ddot{\boldsymbol{\rho}} = (\ddot{\mathrm{x}}, \ddot{\mathrm{y}}, \ddot{\mathrm{z}}) + 2n_1(-\dot{\mathrm{y}}\,, \dot{\mathrm{x}}\,, 0) - {n_1}^2(\mathrm{x},\ \mathrm{y},\ 0) \tag{6.18}$$

After making similar simplifications for the expression in Eq. (6.12), that equation can be rewritten as

$$\ddot{\boldsymbol{\rho}} = -n^2(\mathrm{x}, \mathrm{y}, \mathrm{z}) + \left(3n^2\mathrm{x}, 0, 0\right) + \mathbf{f} \tag{6.19}$$

We now drop the subscript on n_1 and equate the two expressions in Eqs. (6.18) and (6.19) to obtain the following set of equations.

Hill's Equations

$$\begin{aligned} \ddot{\mathrm{x}} - 2n\,\dot{\mathrm{y}} - 3n^2\mathrm{x} &= \mathrm{f}_{\mathrm{x}} \\ \ddot{\mathrm{y}} + 2n\,\dot{\mathrm{x}} &= \mathrm{f}_{\mathrm{y}} \\ \ddot{\mathrm{z}} + n^2\mathrm{z} &= \mathrm{f}_{\mathrm{z}} \end{aligned} \tag{6.20}$$

where $n \equiv (\mu/{a_1}^3)^{1/2}$ denotes the mean motion of the target vehicle.

Hill's equations are also called the "Clohessy–Wiltshire (CW) equations." Hill's study in the nineteenth century described the motion of the moon relative to the earth. Clohessy and Wiltshire rediscovered these equations (in a paper in September 1960) in a study of the motion of a vehicle relative to a satellite in earth orbit. These two applications are quite different, but they both consider small displacements relative to a known reference motion. In Hill's application, the distance of the moon from the earth is small compared to the distance of the earth from the sun. In the Clohessy–Wiltshire application, the distance of the vehicle from the earth-orbiting satellite is small compared to the distance from the satellite to the center of the earth. That is, $\rho << \mathrm{r}_1$.

These equations are called the Euler–Hill[1] equations in the reference by Pisacane and Moore.

Remarks:

1. These equations can be used to study:
   (a) The forces required to perform an orbit rendezvous.
   (b) The displacements from a reference trajectory produced by maneuvers or other velocity changes.
   (c) The effects of perturbations on the displacements from a reference trajectory.
2. These are second-order differential equations with constant coefficients. The solution consists of:
   (a) The complementary solution (of the homogeneous equation, $\mathbf{f} \equiv \mathbf{0}$), which is independent of the accelerations and represents the effects of the initial conditions, and
   (b) A particular solution which represents the effects of the applied forces per unit mass.
3. These equations are valid for small displacements—a few tens of kilometers—in the radial (x) and out-of-plane (z) directions, but remain correct for an order of magnitude—a few hundreds of km—larger change in the down-track coordinate, y. The y component need not be small provided it is measured along the target trajectory.

Solutions for the Hill–Clohessy–Wiltshire Equations

1. Complementary Solutions ($\mathbf{f} = \mathbf{0}$)

By integrating the second equation in Eq. (6.20), we obtain

$$\dot{y} + 2nx = \dot{y}_0 + 2nx_0 \tag{6.21a}$$

[1] George William Hill (1838–1914) must be considered a mathematician, but his mathematics was entirely based on that necessary to solve his orbit problems.

In 1861, Hill joined the Nautical Almanac Office working in Cambridge, Massachusetts. After 2 years he returned to West Nyack, NY where he worked from his home. Except for a period of 10 years from 1882 to 1892 when he worked in Washington on the theory and tables for the orbits of Jupiter and Saturn, this was to be his working pattern for the rest of his life.

E. W. Brown wrote:

He was essentially of the type of scholar and investigator who seems to feel no need of personal contacts with others. While the few who knew him speak of the pleasure of his companionship in frequent tramps over the country surrounding Washington, he was apparently quite happy alone, whether at work or taking recreation.

From 1898 until 1901, Hill lectured at Columbia University, but "characteristically returned the salary, writing that he did not need the money and that it bothered him to look after it."

By rearranging the first equation in Eq. (6.20) and using Eq. (6.21a), we obtain

$$\ddot{x} + n^2 x = 2n(\dot{y}_0 + 2nx_0) \tag{6.21b}$$

Thus, we obtain linear, second order differential equations with constant coefficients.

By integrating Eq. (6.21) and the third equation in Eq. (6.20), we obtain the following set of equations. For the force-free case ($\mathbf{f} \equiv 0$),

$$\begin{aligned} x(t) &= (4 - 3\cos(nt))x_0 + \frac{\sin(nt)}{n}\dot{x}_0 + 2\left(\frac{1 - \cos(nt)}{n}\right)\dot{y}_0 \\ y(t) &= 6(\sin(nt) - nt)x_0 + y_0 - 2\left(\frac{1 - \cos(nt)}{n}\right)\dot{x}_0 + \left(\frac{4}{n}\sin(nt) - 3t\right)\dot{y}_0 \\ z(t) &= \cos(nt)z_0 + \frac{\sin(nt)}{n}\dot{z}_0 \end{aligned} \tag{6.22}$$

These three equations constitute the complementary solution of Hill's equations. Given initial conditions $x_0, y_0, z_0, \dot{x}_0, \dot{y}_0, \dot{z}_0$, Eq. (6.22) provide the complementary solution

$$\boldsymbol{\rho}(t) = (x(t), y(t), z(t)) \equiv (x, y, z)$$

Remarks:

1. All periodic terms are at orbital frequency n, the mean motion of the target vehicle.
2. There is a secular drift term $-(6nx_0 + 3\dot{y}_0)t$ in the along-track y(t) that grows linearly in time and can arise from either x_0 or $\dot{y}_0$.
3. The y-oscillation is a quarter period ahead of the x-oscillation with double the amplitude.
4. The third equation represents simple harmonic motion in the z direction, corresponding to a slight inclination difference between target and chase orbits. Also

$$z_0 = 0 = \dot{z}_0 \Rightarrow z \equiv 0$$

5. The oscillation in x represents a varying differential radius, ∂r, which describes a neighboring elliptic orbit.
6. The solution for y(t) has two parts:
   (a) A periodic component due to the oscillatory x-motion and
   (b) A term of the form $k_1 t + k_2$. The term $k_1 t$ is called secular and represents a steady drift along the y-axis whose direction is determined by the sign of k_1, which is determined by initial conditions x_0 and $\dot{y}_0$. The drift due to a nonzero value of k_1 describes a neighboring orbit of period slightly different from the target period. In the special case $k_1 = 0$, the periodic x and y motion

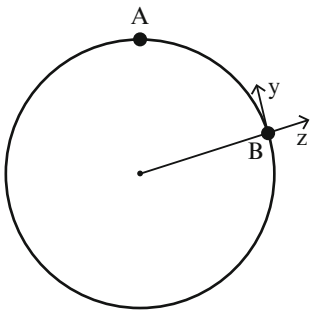

Fig. 6.6 Standoff position of chase vehicle relative to target spacecraft

(of the same period) represents a neighboring elliptic orbit with period equal to the target period.

7. The combined effects of relative motion in all components of the CW frame represents the general case of a neighboring orbit that is elliptic, inclined, and of different period than the target orbit.

Example: Standoff Position to Avoid Collision with the Target Vehicle

In Fig. 6.6, point A denotes the position of the chase spacecraft and B the position of the target vehicle, e.g., the ISS. The standoff position might be assumed prior to rendezvous to allow time, for example, for the astronauts to sleep, while avoiding a collision between the two vehicles. The initial conditions are $x_0 = 0$, $y_0 = y_0$, $z_0 = \dot{x}_0 = \dot{y}_0 = \dot{z}_0$ at time t_0. By substituting these initial conditions into Eq. (6.20), we obtain the solution

$$x(t) = 0, y(t) = y_0, z(t) = 0$$

for all values of $t \geq t_0$.

Spacecraft Intercept or Rendezvous with a Target Vehicle

By differentiating Eq. (6.22) with respect to time, the corresponding velocity components for the force-free case are obtained as:

$$\begin{aligned} \dot{x}(t) &= 3n \sin(nt) x_0 + \cos(nt)\dot{x}_0 + 2\sin(nt)\dot{y}_0 \\ \dot{y}(t) &= 6n(\cos(nt) - 1)x_0 - 2\sin(nt)\dot{x}_0 + (4\cos(nt) - 3)\dot{y}_0 \\ \dot{z}(t) &= -n \sin(nt) z_0 + cos(nt)\dot{z}_0 \end{aligned} \tag{6.23}$$

These three equations give the relative motion (relative velocity) between the chase and target vehicles.

General solution for the deviation in the state vector $\delta\mathbf{s}(\mathbf{t})$ of the chase vehicle relative to the target state:

$$\delta\mathbf{s}(\mathbf{t}) \;=\; \begin{bmatrix}\delta\mathbf{r}(\mathbf{t})\\ \delta\mathbf{v}(\mathbf{t})\end{bmatrix} \;=\; \begin{bmatrix}\mathrm{x}\\ \mathrm{y}\\ \mathrm{z}\\ \dot{\mathrm{x}}\\ \dot{\mathrm{y}}\\ \dot{\mathrm{z}}\end{bmatrix} \tag{6.24}$$

$$\delta\mathbf{s}(\mathbf{t}) \;=\; \Phi(\mathrm{t})\delta\mathbf{s}(\mathbf{0}),\quad \Phi(0) \;=\; \mathrm{I}_6 \tag{6.25}$$

where $\Phi(\mathrm{t})$ denotes the state transition matrix for the CW equations.

$$\Phi(\mathrm{t}) \;=\; \begin{bmatrix} (4-3\mathrm{c}) & 0 & 0 & \frac{\mathrm{s}}{n} & \frac{2}{n}(1-\mathrm{c}) & 0\\ 6(\mathrm{s}-n\mathrm{t}) & 1 & 0 & -\frac{2}{n}(1-\mathrm{c}) & \frac{4\mathrm{s}-3n\mathrm{t}}{n} & 0\\ 0 & 0 & \mathrm{c} & 0 & 0 & \frac{\mathrm{s}}{n}\\ 3n\mathrm{s} & 0 & 0 & \mathrm{c} & 2\mathrm{s} & 0\\ -6n(1-\mathrm{c}) & 0 & 0 & -2\mathrm{s} & (4\mathrm{c}-3) & 0\\ 0 & 0 & -n\mathrm{s} & 0 & 0 & \mathrm{c}\end{bmatrix} \tag{6.26}$$

where $\mathrm{s} \equiv \sin(n\mathrm{t})$ and $\mathrm{c} \equiv \cos(n\mathrm{t})$.

An advantage of the linearized, CW frame is that the standard orbital calculations are greatly simplified. Here we can evaluate $\Phi(\mathrm{t})$ and compute the deviation in the state vector by the equation

$$\delta\mathbf{s}(\mathrm{t}) = (\mathrm{t})\delta\mathbf{s}(0) \tag{6.27}$$

for any value of t.

The complementary (homogeneous) solutions to Hill's equations are useful for studying satellite maneuvering and rendezvous if the force applied is brief enough so that it can be treated as an impulse providing a change in velocity (the impulsive burn model).

We partition the 6×6 transition matrix into four 3×3 submatrices as denoted in

$$\Phi(\mathrm{t}) \;=\; \begin{bmatrix}\mathrm{M}(\mathrm{t}) & \mathrm{N}(\mathrm{t})\\ \mathrm{S}(\mathrm{t}) & \mathrm{T}(\mathrm{t})\end{bmatrix} \tag{6.28}$$

Then the relative position vector $\delta\mathbf{r}(\mathbf{t})$ is given by:

$$\delta\mathbf{r}(\mathbf{t}) \;=\; \mathrm{M}(\mathrm{t})\delta\mathbf{r}(\mathbf{0}) \;+\mathrm{N}(\mathrm{t})\delta\mathbf{v}(\mathbf{0}) \tag{6.29}$$

and the corresponding relative velocity vector $\delta\mathbf{v}(\mathbf{t})$ is:

$$\delta\mathbf{v}(\mathbf{t}) = S(t)\delta\mathbf{r}(\mathbf{0}) + T(t)\delta\mathbf{v}(\mathbf{0}) \tag{6.30}$$

The vectors $\delta\mathbf{r}(0)$ and $\delta\mathbf{v}(0)$ represent the six scalar constants that define the orbit relative to the origin of the CW frame. The equation for $\delta\mathbf{r}(t)$ is the linear analog of Kepler's equation because it gives the position $\delta\mathbf{r}$ at time t in terms of the state at the initial time $t_0 = 0$.

Recall Lambert's Problem, the orbital boundary problem in the inverse-square gravitational field. The linear analog of Lambert's problem is given by the above equation for $\delta\mathbf{r}(\mathbf{t})$ if $\delta\mathbf{r}(\mathbf{t})$ and $\delta\mathbf{r}(\mathbf{0})$ are specified and the unknown is the required initial value $\delta\mathbf{v}(\mathbf{0})$. Equation (4.67) gives the velocity vector required at the initial point P with position vector $\mathbf{r_1}$ for the spacecraft to arrive at the final point Q with position vector $\mathbf{r_2}$.

Assume the desired final state for the rendezvous is the origin of the CW frame. If the origin is in the space station, the chase vehicle is performing a rendezvous with the space station. Let $t_f =$ the specified final time. Then the desired final relative position is $\delta\mathbf{r}(t_f) = \mathbf{0}$. Thus, we have the following boundary value problem (Lambert's Problem):

Given the initial position $\delta\mathbf{r}(0)$, desired final position $\delta\mathbf{r}(t_f) = \mathbf{0}$, and specified transfer time t_f, determine the orbit that satisfies these conditions, including the required initial velocity vector.

For rendezvous at t_f, we have

$$\mathbf{0} = \delta\mathbf{r}(t_f) = M(t_f)\delta\mathbf{r}(0) + N(t_f)\delta\mathbf{v}(0) \tag{6.31}$$

Therefore, we can determine the necessary velocity vector at the initial time $t = 0$ as

$$\delta\mathbf{v}(\mathbf{0}) = -(N(t_f))^{-1}M(t_f)\delta\mathbf{r}(\mathbf{0}) \tag{6.32}$$

and the orbit that solves the boundary value problem is

$$\delta\mathbf{r}(t) = M(t)\delta\mathbf{r}(0) + N(t)\delta\mathbf{v}(0) = \left[M(t) - N(t)(N(t_f))^{-1}M(t_f)\right]\delta\mathbf{r}(0) \tag{6.33}$$

Note that

$$\delta\mathbf{r}(t) \to 0 \text{ as } t \to t_f$$

as required. However, $N(t_f)$ is not invertible if $t_f = k\pi$ for any integer k and certain other values such as 2.8135π and 4.8906π. So t_f must be selected to avoid these values.

In general, an (impulsive) thrust, a TCM, will be needed at t_0 to achieve the required $\delta\mathbf{v}(0)$. Let $\delta\mathbf{v}^+(0)$ denote the post-maneuver velocity vector, i.e.,

$$\delta\mathbf{v}^+(0) = -(N(t_f))^{-1}M(t_f)\delta\mathbf{r}(0) \tag{6.34}$$

Let $\delta\mathbf{v}^-(0) =$ the specified velocity vector before the impulsive $\Delta\mathbf{v}$ is added. Then the $\Delta\mathbf{v}_0$ provided by the thrust made at $t = 0$ is

$$\Delta\mathbf{v}_0 = \delta\mathbf{v}^+(0) - \delta\mathbf{v}^-(0) = -(N(t_f))^{-1}M(t_f)\delta\mathbf{r}(0) - \delta\mathbf{v}^-(0) \tag{6.35}$$

Executing this value of $\Delta\mathbf{v}_0$ via an (impulsive) TCM will produce intercept. To produce a rendezvous with $\mathbf{v}(t_f) = 0$, we continue as follows.

The relative velocity vector before the second thrusting maneuver made at t_f is

$$\begin{aligned}\delta\mathbf{v}^-(t_f) &= S(t_f)\delta\mathbf{r}(0) + T(t_f)\delta\mathbf{v}^+(0)\\ &= S(t_f)\delta\mathbf{r}(0) + T(t_f)\left(-(N(t_f))^{-1}M(t_f)\right)\delta\mathbf{r}(0)\\ &= \left[S(t_f) - T(t_f)(N(t_f))^{-1}M(t_f)\right]\delta\mathbf{r}(0)\end{aligned} \tag{6.36}$$

The final velocity vector must satisfy

$$\delta\mathbf{v}^+(t_f) = \delta v^-(t_f) + \Delta\mathbf{v}_f = 0 \tag{6.37}$$

Therefore,

$$\begin{aligned}\Delta\mathbf{v}_f &= \delta\mathbf{v}^+(t_f) - \delta\mathbf{v}^-(t_f)\\ &= -\left[S(t_f) - T(t_f)(N(t_f))^{-1}M(t_f)\right]\delta\mathbf{r}(0)\\ &= \left[T(t_f)(N(t_f))^{-1}M(t_f) - S(t_f)\right]\delta\mathbf{r}(0)\end{aligned} \tag{6.38}$$

because

$$\delta\mathbf{v}^+(t_f) = 0. \tag{6.39}$$

Therefore, for rendezvous,

$$\Delta v_{TOTAL} = |\Delta\mathbf{v}_0| + |\Delta\mathbf{v}_f| \tag{6.40}$$

where $\Delta\mathbf{v_0}$ and $\Delta\mathbf{v_f}$ are obtained from Eqs. (6.35) and (6.38), respectively.

Remark (word of caution):

Do not make the mistake of adding the vectors $\Delta\mathbf{v_0}$ and $\Delta\mathbf{v_f}$ and taking the magnitude of the sum of the vectors. The Δv_{TOTAL} is the sum of the magnitudes of two vectors, not the magnitude of the sum of two vectors.

The amount of propellant that is required to execute these two maneuvers can be computed using Eq. (3.66), given the value of the specific impulse of the propellant available onboard the spacecraft.

Summary of a Terminal Rendezvous Maneuver Sequence

1. The initial velocity change $\mathbf{\Delta V_0}$ places the chase vehicle on a trajectory that will intercept the origin at time t_f.
2. The final velocity change $\mathbf{\Delta V_f}$ cancels the arrival velocity vector of the chase vehicle at the origin of the CW frame to complete the rendezvous.

References for Sect. 6.4: Kaplan, Prussing and Conway, Weisstein.

[Eqs. (6.24)–(6.33) and (6.35)–(6.38) were reprinted from *Orbital Mechanics* by John E. Prussing and Bruce A. Conway, pp 149–152, by permission of Oxford University Press USA.]

6.5 Examples of Spacecraft Rendezvous

The two-maneuver, terminal rendezvous sequence described in Sect. 6.4 is analytically tractable and provides an estimate of the propellant requirements for implementing a rendezvous. This section considers variations to the rendezvous sequence that are incorporated when we must consider such factors as the safety of the astronauts and ways to enhance the delivery accuracy for accomplishing the rendezvous.

Space Shuttle Discovery's Rendezvous with the ISS

On the afternoon of 9/30/2009, a course correction burn moved Discovery to 8 n. mi. behind the ISS. At this point, Discovery performed an 11-s Terminal Initiation (TI) burn, followed by 3–4 very small correction maneuvers. The Shuttle moved to 725 ft below ISS along the position vector **r**, closing at 6 ft/s. (The announcer on NASA TV called the position vector "rbar.") Commander Rick Sturckow began flying Discovery manually, moving the spacecraft along rbar to 650 ft below ISS, closing at 0.4 ft/s with pulsed firings. Rendezvous pitch maneuvers (RPMs) implemented a "rotational back flip" that took 8.5 min, turning at the rate of ¾°/s. The objective was to enable two astronauts aboard ISS to take pictures of Discovery's landing gear, external tank, and heat shield. Digital cameras were used in this 90-s photo opportunity.

Maneuvers to move 400 ft ahead of ISS along its velocity vector and orient Discovery for mating to the ISS achieved orientation within 1.25° pitch out. (Rick Sturckow can easily correct pitch out in the final approach.) The shuttle proceeded to close in along the velocity vector at 0.2 ft/s and moved inch-by-inch within the cone of approach. The objective was to move the circular docking mechanism on springs on Discovery to contact the pressurized docking mechanism on ISS for link up.

Discovery braked to decrease the closing rate to 0.1 ft/s for contact and capture. The reduced pitch out was made precisely aligned within 30 ft of ISS. The post-contact thrust was armed 8 ft away from contact. Then there was contact and the

post-contact thrust was performed so the two docking mechanisms were firmly set against one another. Capture occurred over the Atlantic Ocean. The two vehicles were allowed to fly to allow damping and stabilization of relative motion between the two vehicles. ISS pulled Discovery into firm contact by performing ring retraction to get a hard mate between the Shuttle and ISS. The two crews performed leak checks for 1½ h. Then the hatches were opened for the crew greetings.

While the shuttle remained in contact with ISS, NASA examined the pictures that were taken during the final approach. The space agency began checking for damage to the shuttle's delicate heat shield after the 2003 Columbia disaster. A slab of fuel tank foam knocked a hole in Columbia's wing, which led to its destruction during re-entry. NASA's Mission Management Team said, "The Damage Assessment Team provided their final summary to the team (NASA's Mission Management Team) and declared that the TPS (thermal protection system) is acceptable for entry."

References: William Harwood, "Space shuttle's heat shield cleared for entry," story written for CBS News and appeared in Spaceflight Now.com; NASA TV.

Mars Sample Return

A proposed future mission will return a sample from Mars, In such a mission, a launcher will go to the surface of Mars, obtain a sample of Mars soil, rendezvous with an orbiter, and pass the soil sample to the orbiter for return to the earth.

6.6 General Results for Terminal Spacecraft Rendezvous

Particular Solutions ($\mathsf{f} \neq \mathbf{0}$)

In Sect. 6.4, we considered complementary solutions ($\mathbf{f} = \mathbf{0}$) for the Hill–Clohessy–Wiltshire equations Eq. (6.20). The particular solutions ($\mathbf{f} \neq \mathbf{0}$) of these equations are dependent on the nature of the perturbing accelerations, the forcing function $\mathbf{f}$. Decomposing the perturbations into constant and periodic functions, if possible, may make the analysis more tractable.

Target Orbits with Non-Zero Eccentricity

In Sect. 6.4, we considered circular target orbits. The case of elliptical target orbits is considered in the reference by Jones. This reference gives formulas "for the perturbation state transition matrix of the two-body problem" that "are valid for motion in the linear neighborhood of reference orbits with $0 \leq \mathsf{e} < 1. \ldots$ In addition to the general form, a simplified version, valid for small eccentricity orbits, is given."

Highly Accurate Terminal Rendezvous

Accuracy for terminal rendezvous is considered in the reference by Kechichian 1992.

"A highly accurate analytic two-impulse terminal rendezvous theory is presented. A first-order orbit theory is combined with the second-order conic approximation in order to create a highly accurate predictor valid for several revolutions. The resulting set of nonlinear equations of motion are solved via a Newton–Raphson iteration process after providing the initial guess for the components of the first velocity change from an analytic theory developed earlier. A computer code evaluates ΔV_1 with high accuracy resulting in negligible intercept or closure error at the specified final time."

A typical large transfer where the two vehicles are initially separated by 2,000 km is achieved with an interception error of 5 km.

General Algorithm

An algorithm for the two-impulse, time-fixed, noncoplanar rendezvous with drag and oblateness effects for the general elliptic orbit is given in the reference by Kechichian 1998.

References for this chapter: Bennett, Chobotov, Clohessy and Wiltshire, Fehse, Harwood, Hill, Jones, Kaplan, Kechichian 1992, Kechichian 1998, Prussing and Conway, Pisacane and Moore, Vallado with contributions by Wayne D. McClain, Weisstein, Wertz and Larson, and Wylie and Barrett.

Exercises

6.1 A chase satellite in a low earth orbit (LEO) at 200 km altitude performs a Hohmann transfer to phase for rendezvous with a coplanar target satellite at geosynchronous earth orbit (GEO). Compute the

$$\Delta V_{TOTAL} = \Delta V_1 + \Delta V_2,$$

where ΔV_1 and ΔV_2 are the magnitudes of the impulsive velocity corrections for this Hohmann maneuver sequence.

6.2 Consider a Hohmann transfer by a chase (active) vehicle in a circular orbit of radius r_i to rendezvous with a target (passive) satellite in a coplanar, circular orbit of radius r_f with $r_f > r_i$.

(a) Show that, at the time of the first maneuver of the Hohmann maneuver sequence, the target satellite must lead the chase satellite by an angle

$$\phi = \pi \left[1 - \left(\frac{r_i + r_f}{2r_f} \right)^{3/2} \right] \text{radians}.$$

(b) Compute the lead angle for the Hohmann transfer defined in Problem 6.1.

(c) A GPS satellite is in a MEO orbit at a mean radius of 26,560 km. A chase satellite in a 200-km-altitude LEO performs a Hohmann transfer to phase for rendezvous with the coplanar GPS satellite. Compute the lead angle for this Hohmann transfer in degrees.

6.3 Assume that the Space Shuttle's orbit is circular at an altitude of 200 km above a spherical earth. In this orbit, an astronaut will throw a baseball out of the shuttle's bay in the direction directly away from the center of the earth with a velocity relative to the shuttle of 1 m/s.

(a) Sketch the trajectory of the baseball relative to the shuttle.

(b) NASA has been asked to retrieve the baseball so that it can be placed in the Baseball Hall of Fame. What is the minimum number of maneuvers that the Space Shuttle will have to perform to retrieve the baseball? Explain.

6.4

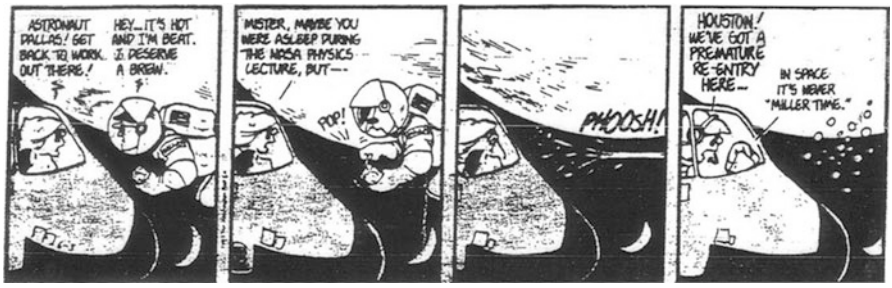

Contrary to the initial report, Astronaut Dallas will not reenter the earth's atmosphere. However, he has introduced a ΔV of 0.5 m/s in the direction directly toward the earth. So he has begun drifting away from the Space Shuttle, which is in a circular orbit at a 200-km altitude. The President is expected to call the astronauts in 15 min to congratulate them on a job well done. Will Astronaut Dallas be within the communication range of 1 km from the shuttle to answer the call on his cell phone?

6.5 Consider a spacecraft that is in a standoff position 2 km behind the International Space Station (ISS) when the ISS is at an altitude of 350 km. The spacecraft initiates a two-impulse rendezvous sequence to rendezvous with the ISS in 1.5 h.

(a) Compute the mean motion of the ISS to 6-digit accuracy.

(b) Compute the total delta-V requirement for the rendezvous.

(c) Submit a copy of your MATLAB code you used to solve part (b).

(d) Submit a copy of the equations you used to solve part (b). Write the equations in analytical form separate from your MATLAB code.

6.6 The Hubble Spacecraft was released from the Space Station, which was in a circular orbit at 590 km altitude. The relative velocity with respect to the Space Station of the injection was 0.1 m/s up, 0.04 m/s backwards, and 0.02 m/s to the right. These data are interpreted according to our relative motion definitions as

$$\dot{x}_0 = -0.1 \text{ m/s} \quad \dot{y}_0 = -0.04 \text{ m/s} \quad \dot{z}_0 = -0.02 \text{ m/s}$$

(a) Compute the position and velocity of the Hubble Space Telescope with respect to the Space Station 1 h after release.
(b) Submit a hard copy of the MATLAB code you used to solve part (a) of this problem.
(c) Submit a copy of the equations you used to solve this problem. Write the equations in analytical form separate from your MATLAB code.
(d) The altitude of the ISS given in this problem is not the current value. Bring us up to date by accessing the Heavens Above Website at http://www.heavens-above.com/ and clicking on the "Height of the ISS" link to determine the altitude of the ISS on the first day of the current month.

6.7 A chase/interceptor satellite is at a position $x_0 = 50$ km, $y_0 = 100$ km and $z_0 = 0$ km from a target spacecraft at the initial time $t_0 = 0$. The target spacecraft is in a circular earth orbit with a period of 88.8 min, which corresponds to an altitude of 222 km. The chase spacecraft performs a rendezvous with the first maneuver at the initial time and the final maneuver 22.2 min (one-quarter period) later.
(a) Plot the relative position of the chase vehicle in the CW frame. That is, plot the radial component x as the dependent variable versus the downtrack component y as the independent variable.
(b) Submit a hardcopy of the MATLAB code you used to solve this problem.

Navigation and Mission Design Techniques and Tools

7

7.1 Introduction

Online tools that can be used for background studies for small bodies are described in Sect. 7.2. A tool for use in designing orbital maneuvers is treated in Sect. 7.3, together with examples, the description of the computer algorithm, and a brief discussion of some maneuver constraints. Two methods for designing free-return circumlunar trajectories for use in ensuring as much as possible the safe return of humans to the moon are described in Sect. 7.4.

7.2 Online Ephemeris Websites

We start with the following definitions:

Def.: A tropical year equals 365.24219 days.

Def.: A Julian year equals 365.25 days.

Def.: A sidereal year equals 365.25636 days.

Each of these definitions of a year expresses one earth revolution about the sun with respect to a particular reference. A tropical year is from equinox to equinox and a sidereal year is from fixed star to fixed star. The length of a Julian year has been chosen as an even fixed value, while the other two definitions change slightly with time.

Def.: The apparent distance between two objects in space is the distance between one object and where the other object appears to be when light left the second object.

© Springer International Publishing Switzerland 2015

G.R. Hintz, *Orbital Mechanics and Astrodynamics*,
DOI 10.1007/978-3-319-09444-1_7

Def.: The geometric distance between two objects in space is the actual distance between the objects at a specified time.

The difference between these two distances is introduced by the finite speed of light.

Solar System Dynamics Website: ssd

The ssd Website is available at

http://ssd.jpl.nasa.gov/.

Example: Rise, Transit, and Set Times
The NASA Deep Space Network—or DSN—is an international network of antennas that supports interplanetary spacecraft missions and radio and radar astronomy observations for the exploration of the solar system and the universe. The network also supports selected earth-orbiting missions. The DSN currently consists of three deep-space communications facilities placed approximately 120° apart in longitude around the world: at Goldstone, CA in California's Mojave Desert; near Madrid, Spain; and near Canberra, Australia. This strategic placement permits continuous observation of spacecraft as the earth rotates. Thus, a spacecraft can have radio communication with one of the three DSN antennas, eventually move out of the 2-way communication range of that antenna and into the range of another antenna, and continuously repeat this process. To describe this process more carefully, we introduce additional definitions for an observer that is an earth-based (e.g., DSN) antenna. (For more information on the DSN, see the DSN Website at http://deepspace.jpl.nasa.gov/dsn/.)

Def.: An object is said to rise when it moves above the observer's local horizon.

Def.: The transit of an object is its crossing of the observer's local meridian or longitude, i.e., the point of highest possible elevation.

The word "transit" means to "go across." One definition of the verb "transit" in Webster's Dictionary is "to pass across (a meridian, a celestial body, or the field of view of a telescope)." So we also say that Venus made a transit of the sun on June 8, 2004, meaning that the planet (a smaller body) passed across the disk of the sun (a larger body) at an angle visible from the earth, for the first time in 122 years. Mercury made a transit of the sun on November 8, 2006 and makes approximately 13 per century.

Def.: An object is said to set when it moves below the observer's local horizon.

So the observer has radio communications from rise to set, minus any time of interference from local terrain surrounding the antenna, called the "mask."

Def.: The solar elongation of an object is the sun–earth–object angle.

Def.: When an object has a solar elongation of 180°, the object is said to be at opposition and the disk of the object is as large as possible.

The planets Mars through Neptune can be in opposition with the earth, but Mercury and Venus cannot. For example, Mars will be in opposition with the earth when the sun, earth, and Mars lie on a line in that order from the sun.

Directions for Obtaining Information About Rise, Transit, and Set Times:

1. Go to http://ssd.jpl.nasa.gov/.
2. Click on "HORIZONS."
3. Click on "Web Interface."
4. Click on "web-interface tutorial" for instructions.
5. Return to Web Interface to change the settings under the Ephemeris Type, Target Body, Observer Location, Time Span, and Table Settings links as necessary to obtain the information needed to answer the user's questions. For example, if the mask is to be taken as zero, select the RTS flag to be the True Visual Horizon and a time step interval of 1 minute for coverage from horizon at rise to horizon at set. Save your settings under each button by clicking on the "Use Selected Settings," "Use Settings Below," or other appropriate button.
6. Click on "Generate Ephemeris."
7. Answer such questions as: What was the solar elongation in degrees for Mars at the transit on April 1, 2013?

Example: JPL's HORIZONS Online Ephemeris Generation System

The JPL HORIZONS Online Solar System Data and Ephemeris Computation Service provides access to key solar system data and flexible production of highly accurate ephemerides for solar system objects (643,615 asteroids, 3,270 comets, 178 planetary satellites, 8 planets, the sun, L1, L2, select spacecraft, and system barycenters—data accessed on 6/1/14 at which time asteroids were being discovered at the rate of approximately 2,350 asteroids/month over the previous 7 months). The HORIZONS is provided by the Solar System Dynamics Group of the Jet Propulsion Laboratory and can be accessed at the Solar System Dynamics Website at

http://ssd.jpl.nasa.gov/?horizons

Instructions for how to generate an ephemeris and the HORIZONS User Manual are available at this Website.

Trojan Asteroids

The Trojan asteroids are in two groups of asteroids that revolve about the sun in the same orbit as Jupiter; one group is about 60° ahead of the planet in its orbit and the other is about 60° behind it. They are in orbits whose semimajor axis satisfies

$$5.05 \text{ AU} \leq a \leq 5.4 \text{ AU}$$

The first Jupiter Trojan asteroid, Achilles, was discovered in 1906. In 1990, a similar asteroid, Eureka, was found in the orbit of Mars. Others have been found in Neptune's orbit and are called "Neptune Trojans."

Directions for Finding Information about Trojan Asteroids:

1. Go to http://ssd.jpl.nasa.gov/?bodies.
2. Click on "Asteroids."
3. Click on "small body database search engine."
4. Provide data and select options as appropriate in steps 1 and 2 to get a list of Trojan asteroids that meet your specifications.
5. Save these options in step 3 by clicking the "Append Selected" button.
6. Click on "Generate Table."

Near Earth Objects Website: neo

The Near Earth Objects Website is available at

http://neo.jpl.nasa.gov/

Near-Earth Objects (NEOs) are comets and asteroids that have been nudged by the gravitational attraction of nearby planets into orbits that allow them to enter the earth's neighborhood. Composed mostly of water ice with embedded dust particles, comets originally formed in the cold outer planetary system while most of the rocky asteroids formed in the warmer inner solar system between the orbits of Mars and Jupiter. The scientific interest in comets and asteroids is due largely to their status as the relatively unchanged remnant debris from the solar system formation process some 4.6 billion years ago. The giant planets Jupiter, Saturn, Uranus, and Neptune formed from an agglomeration of billions of comets and the left over bits and pieces from this formation process are the comets we see today. Likewise, today's asteroids are the bits and pieces left over from the initial agglomeration of the inner planets that include Mercury, Venus, Earth, and Mars. As the primitive, leftover building blocks of the solar system formation process, comets and asteroids offer clues to the chemical mixture from which the planets formed some 4.6 billion years ago. If we wish to know the composition of the primordial mixture from which the planets formed, then we must determine the chemical constituents of the leftover debris from this formation process—the comets and asteroids.

Example: Visualize the Orbit of a Comet or Asteroid
Procedure:

1. Go to http://neo.jpl.nasa.gov/orbits/.
2. Enter the object name and click on the "Search" button.
3. Click on "Orbit Diagram."

4. Use buttons with double arrows for continuous motion and buttons next to those with the double arrows for changing position of the selected comet or asteroid 1 day at a time.
5. Use the scroll bars to rotate the viewing position of the comet or asteroid and planets, i.e., to rotate the orbit plane of the comet or asteroid.
6. Click the "Date" button to get a dialogue box for use in changing the date, if necessary to move to several years away.

Potentially Hazardous Asteroids

Directions for Finding Information about Potentially Hazardous Asteroids:

1. Go to http://neo.jpl.nasa.gov/.
2. Click on "NEO BASICS."
3. Click on "NEO Groups."
4. Then find or determine the answers to such questions as: What is a Potentially Hazardous Asteroid (PHA)?

Online ephemeris exercises, using the ssd and neo Websites, are defined as a project in Appendix B, section "Online Ephemeris Project on PHAs, NEOs and Other Celestial Objects".

References for Sect. 7.2: Deep Space Network Website; Infoplease/Encyclopedia Website; Near-Earth Objects Website; Seidelmann; Solar System Dynamics Website.

7.3 Maneuver Design Tool

Flight Plane Velocity Space (FPVS)

Figure 7.1 shows the unit reference vectors $\hat{\mathbf{V}}_{\mathbf{M}}$, $\hat{\mathbf{V}}_{\mathbf{G}}$, $\hat{\mathbf{V}}_{\mathbf{N}}$, which define the non-inertial Flight Plane Velocity Space (FPVS). Perturbations along these reference directions satisfy

$$\begin{aligned} \Delta V_M &= f_t dt \\ \Delta V_G &= -f_n dt \\ \Delta V_N &= f_L dt \end{aligned}$$

in terms of the perturbations $f_t dt$, $f_n dt$, and $f_L dt$ as defined in Chap. 5. The direction of the unit vectors change as a function of θ.

For example, Figs. 7.2, 7.3, 7.4, 7.5, and 7.6 show the gradients of orbit parameters in FPVS for the Pioneer Venus Orbiter in the Keplerian orbit about Venus defined as follows:

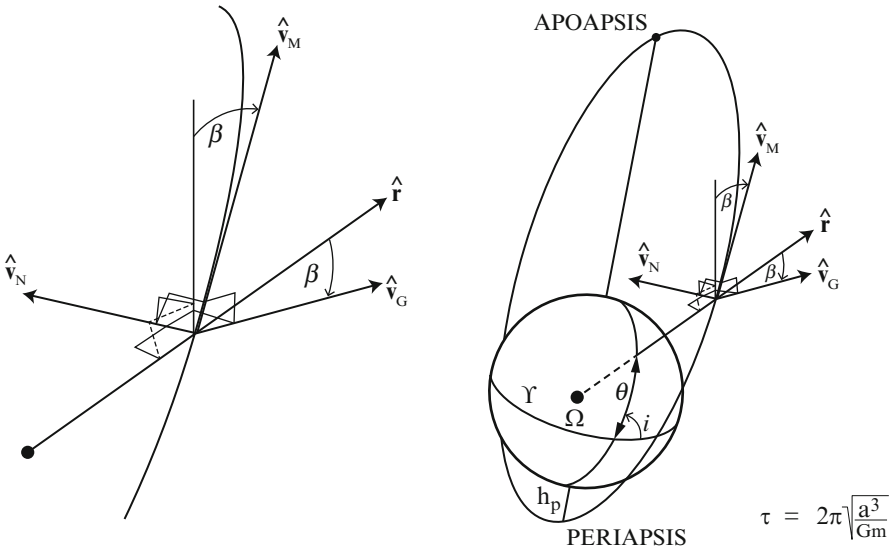

NOMENCLATURE

	τ	= Orbit period
	a	= Semimajor axis
	Gm	= Gravitational constant
	h_p	= Periapsis altitude
	β	= Flight path angle
	θ	= True anomaly
"Flight plane velocity space"	$\hat{\mathbf{v}}_M$	= Unit vector along nominal velocity vector
	$\hat{\mathbf{v}}_G$	= Unit vector normal to nominal velocity vector in orbit plane directed away from planet
	$\hat{\mathbf{v}}_N$	= Unit vector normal to orbit plane in momentum direction
	i	= Inclination
	Ω	= Longitude of ascending node
	ω	= Argument of periapsis

Fig. 7.1 Orbit geometry and Flight Plane Velocity Space

$$\tau = 24.0 \text{ h}$$
$$r_p = 6{,}252 \text{ km}$$
$$\Omega = 33.1^\circ$$
$$\omega = 147.2^\circ$$
$$i = 105.0^\circ$$

with respect to mean ecliptic and equinox of 1950.0 coordinates.

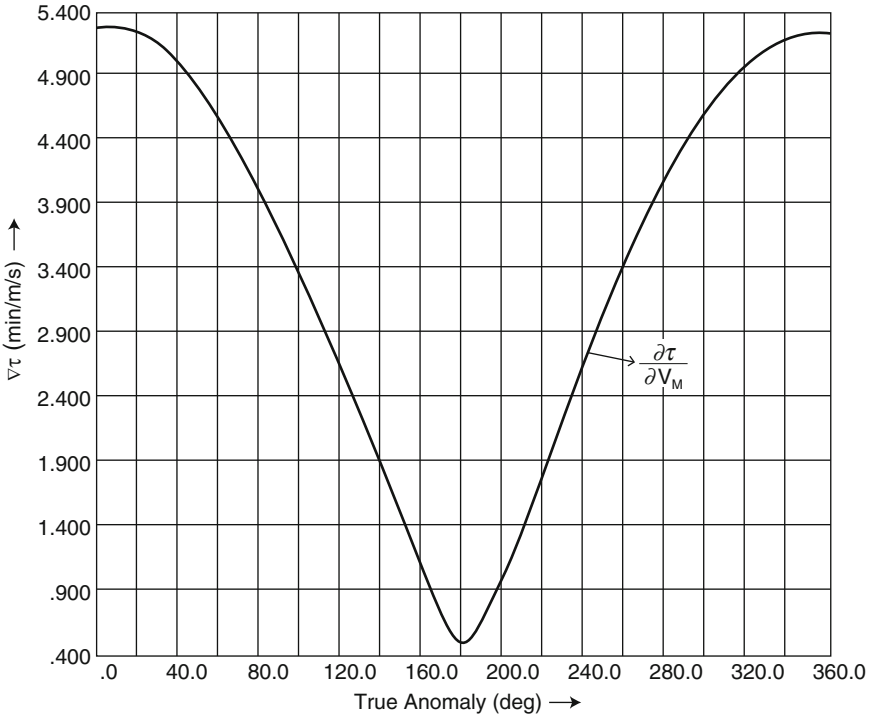

Fig. 7.2 Gradient of period in FPVS

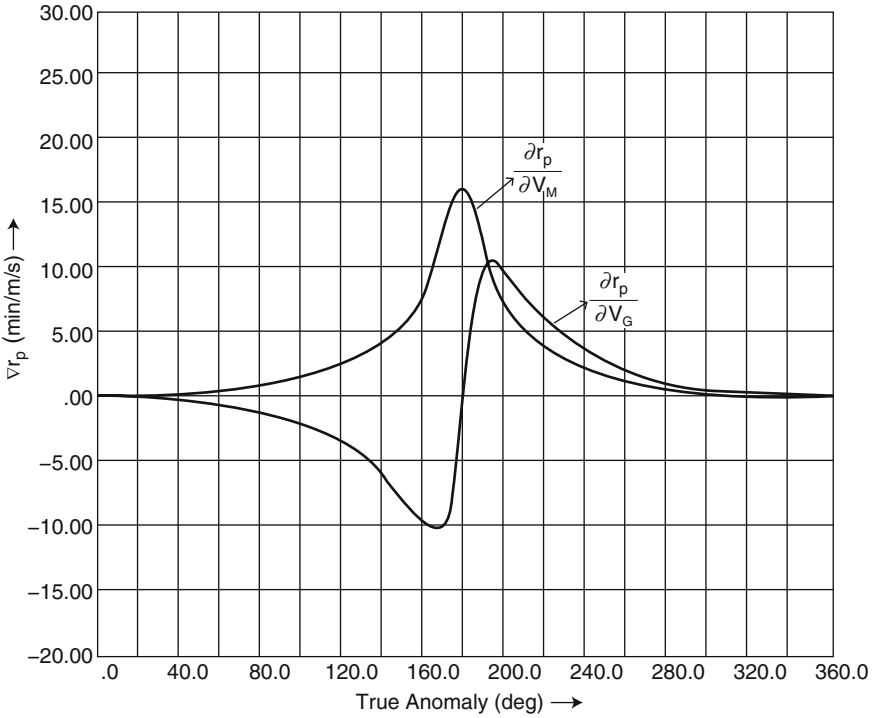

Fig. 7.3 Gradient of periapsis altitude in FPVS

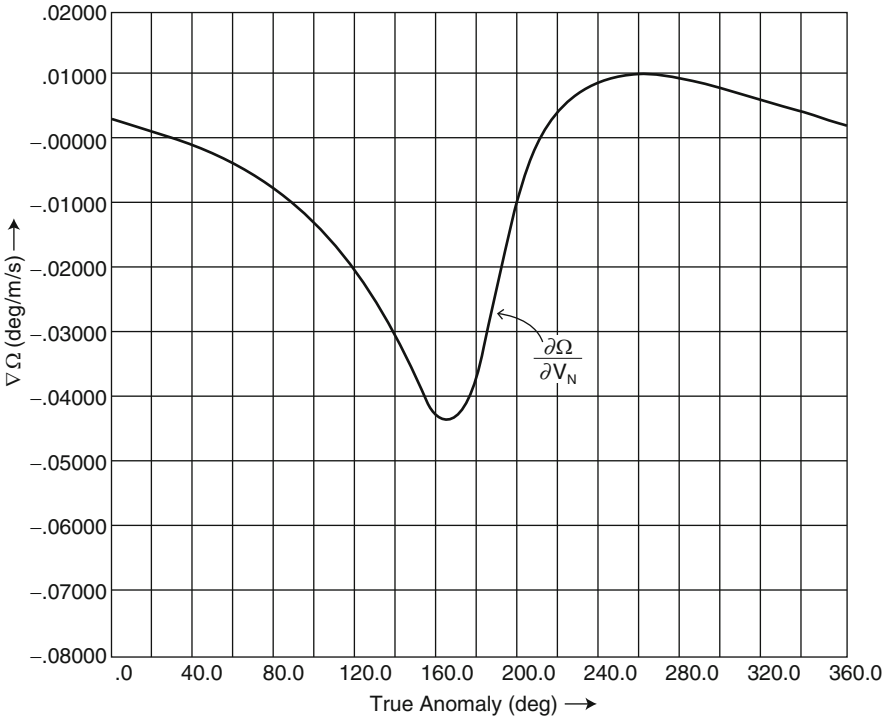

Fig. 7.4 Gradient of the right ascension of the ascending node in FPVS

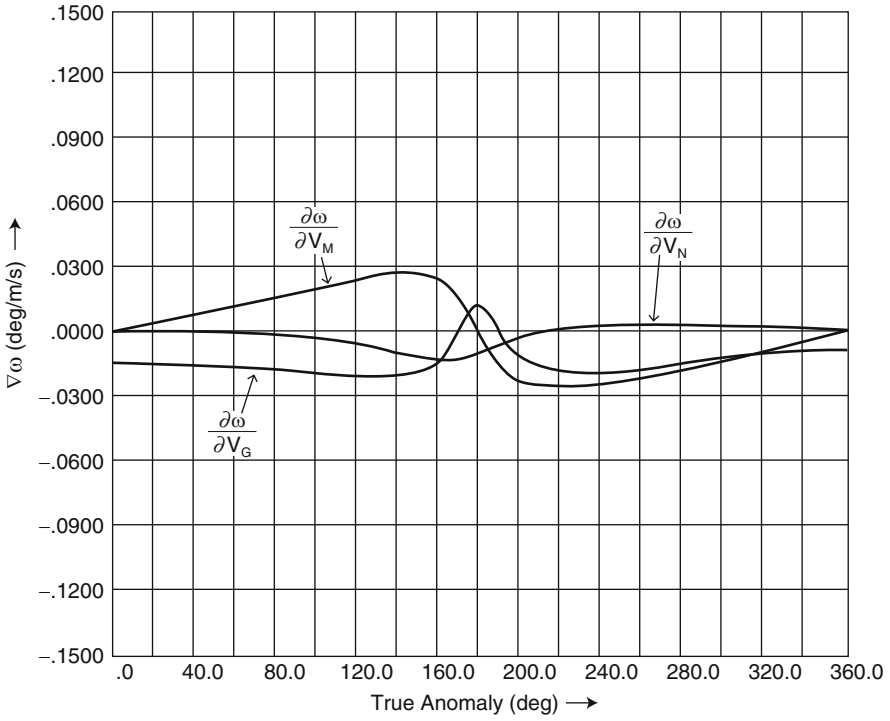

Fig. 7.5 Gradient of the argument of periapsis

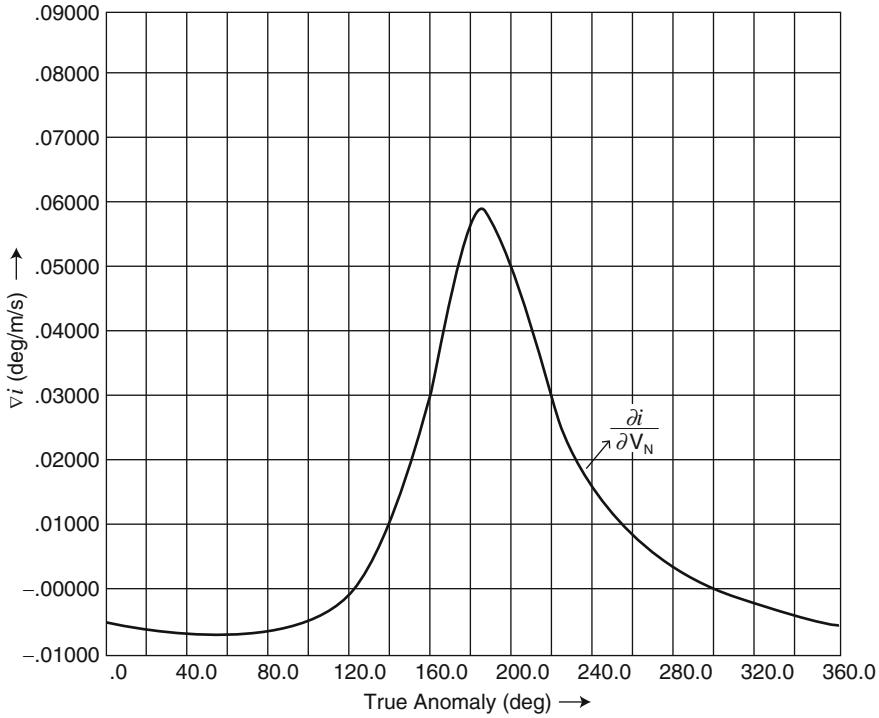

Fig. 7.6 Gradient of the inclination in FPVS

1. Period (τ)
   The partial derivative of period with respect to V_M is given analytically as

$$\frac{\partial \tau}{\partial V_M} = \frac{3av}{\mu}\tau \tag{7.1}$$

   from Exercise 7.1. Recall that the maximum value of velocity is at periapsis and the minimum value is at apoapsis from Kepler's Second Law. Therefore, this equation implies that the maximum value of $\partial\tau/\partial V_M$ is at periapsis and the minimum value is at apoapsis as can be seen in Fig. 7.2.

   For the other two components of the gradient of period in FPVS,

$$\frac{\partial \tau}{\partial V_G} \equiv \frac{\partial \tau}{\partial V_N} \equiv 0$$

2. Periapsis Radius (r_p)
   As seen in Fig. 7.3,

$$\frac{\partial r_p}{\partial V_M} = 0 \text{ at } \theta = 0^\circ$$

$$\frac{\partial r_p}{\partial V_M} = \max \text{ at } \theta = 180^\circ$$

The gradient of periapsis radius is

$$\nabla r_p = \left(\frac{\partial r_p}{\partial V_G}, \frac{\partial r_p}{\partial V_M}, \frac{\partial r_p}{\partial V_N} \right)$$

where $\hat{V}_G, \hat{V}_M, \hat{V}_N$ define a right-handed coordinate system and the third component

$$\frac{\partial r_p}{\partial V_N} \equiv 0$$

3. Right Ascension of the Ascending Node (Ω)

$$\frac{\partial \Omega}{\partial V_M} \equiv 0 \equiv \frac{\partial \Omega}{\partial V_G}$$

The remaining component is shown in Fig. 7.4.

4. Argument of Periapsis (ω)
See Fig. 7.5. None of the three components of the gradient is identically zero. Recall that, in the discussion of Eq. (5.4), we said, "We offer no analytic formula for this third component, but will provide a graphical display of this component for an example in Sect. 7.3." The curve in Fig. 7.5 marked "$\partial\omega/\partial V_N$" is the graphical display of the PVO example.
5. Inclination (i)
For the gradient of inclination,

$$\frac{\partial i}{\partial V_M} \equiv 0 \equiv \frac{\partial i}{\partial V_G}$$

and the third component is as shown in Fig. 7.6.

Maneuver Design Examples

Example 1 **(Period-change)** Compute the minimum ΔV for a period-change on the PVO mission.

As shown in Fig. 7.2, the ΔV for changing the period is minimized by performing the maneuver at periapsis along the velocity vector.

(a) $\Delta\tau = +10$ min.
This exercise changes the period from $\tau_0 = 24$ h. to $\tau_f = 24$ h 10 min.

Since $\Delta\tau = \dfrac{\partial \tau}{\partial V_M} \Delta V_M$,

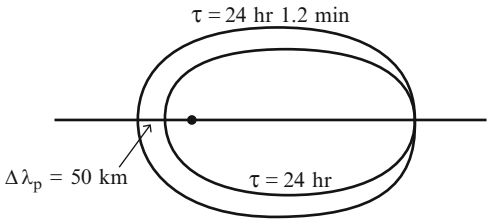

Fig. 7.7 Change in period from change in r_p

$$\Delta V = \Delta V_M = \frac{\Delta\tau}{\left.\frac{\partial\tau}{\partial V_M}\right|_{\theta=0^\circ}} = \frac{10\ \text{min}}{5.3\,\frac{\text{min}}{\text{m/s}}} = 1.9\ \text{m/s}$$

(b) $\Delta\tau = -10$ min
This exercise changes the period from $\tau_0 = 24$ h to $\tau_f = 23$ h 50 min.

$$\Delta V = \Delta V_M = \frac{\Delta\tau}{\left.\frac{\partial\tau}{\partial V_M}\right|_{\theta=0^\circ}} = \frac{-10\text{min}}{5.3\,\frac{\text{min}}{\text{m/s}}} = -1.9\text{m/s}$$

The minus sign means that the engine is fired in the opposite direction from that in part (a) to take energy out of the system. The amount of velocity change is

$$|\Delta V| = 1.9\text{m/s}$$

as in part (a).

Example 2 (**r_p-change**) Compute the minimum ΔV for a change in the altitude at periapsis passage and its effect on the period.

Fact (stated without proof): The ΔV for changing the radius at periapsis is minimized by applying the ΔV along the velocity vector at apoapsis.

(a) $\Delta r_p = 50\ \text{km} = \Delta h_p$
Here, we change $r_{p_0} = 6252$ km to $r_{p_0} + 50$ km $= 6302$ km

$$\Delta V = \Delta V_M = \frac{\Delta h_p}{\left.\frac{\partial r_p}{\partial V_M}\right|_{\theta=180^\circ}} = \frac{50\ \text{km}}{16\ \text{km/mps}} = 3.1\text{m/s}$$ from Fig. 7.3

(b) What change in τ will be produced by this maneuver? (Fig. 7.7)

$$\Delta\tau = \Delta V_M \left.\frac{\partial\tau}{\partial V_M}\right|_{\theta\,=\,180^\circ} = (3.1\text{m/s})\left(0.4\frac{\text{min}}{\text{m/s}}\right) = 1.2\ \text{min}$$ from Fig. 7.2.

Thus, period changes from $\tau_0 = 24$ h to $\tau_f = 24$ h 1.2 min.

Maneuver Considerations

Constraints
For example, the Navigation Team is often not allowed to perform a maneuver near periapsis to avoid interfering with science-data-taking activities. See Exercise 7.4. For Exercise 7.4, use the partial derivative of each of the parameters with respect to V_M at $\theta = 120°$.

There may be other constraints on the implementation of the maneuver such as not pointing optically—or thermally—sensitive instruments, e.g., a camera, at the sun or other bright body during the burn or during the turn to or from the burn direction. It is also desirable to avoid loosing communication with the spacecraft during the turns and burn, but this may be impossible to avoid. Some maneuvers are made in the blind. Sometimes they are made behind the target body, i.e., behind when viewed from the earth. An example of performing a maneuver in the blind is the orbit insertion burn for 2001 Mars Odyssey. (See Fig. 3.42.)

Controls
There are four controls, i.e., three components of the $\mathbf{\Delta V}$ and the time of ignition.

Targets
There are less than or equal to four specified target parameters and not all targets are independent, e.g., i and Ω. However, tolerances on the parameters may allow satisfying conditions on more than four parameters and on parameters that are not independent of each other.

Maneuver Strategies
A maneuver strategy is a sequence of interdependent maneuvers. Such a strategy might be designed to overfly a specified site on the central body as, for example, for Viking in orbit about Mars where the orbiters overflew the landers or to reduce the ΔV requirement to, for example, correct the r_p by performing a maneuver at or near apoapsis and the period by performing a maneuver at or near periapsis.

Reference: Hintz, Farless, and Adams

Algorithm for Computing Gradients in FPVS

We now define an algorithm for computing gradients in FPVS such as those given in Figs. 7.2, 7.3, 7.4, 7.5, and 7.6 for use in PVO flight operations (Fig. 7.8).

Input
Orbit parameters: $\tau, r_p, \Omega, \omega, i$ with respect to a specified inertial coordinate system

$\theta_{min},\ \Delta\theta,\ \theta_{max}$

$\Delta V_{G_p}, \Delta V_{M_p}, \Delta V_{N_p}$ = perturbations along $\hat{V}_G, \hat{V}_M, \hat{V}_N$, respectively

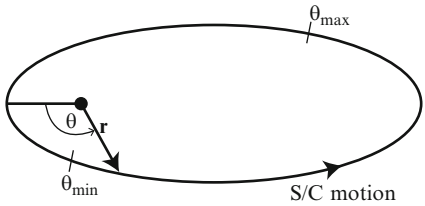

Fig. 7.8 Input to algorithm for computing gradients in FPVS

$\mu = Gm$ of central body
For Figs. 7.2, 7.3, 7.4, 7.5, and 7.6, $\theta_{min} = 0°$ and $\theta_{max} = 360°$.

Algorithm (for Each $\theta = \theta_{min}, \theta_{min} + \Delta\theta, \theta_{min} + 2\Delta\theta, \ldots, \theta_{max}$)

1. Convert the Keplerian elements $\tau, r_p, \Omega, \omega, i, \theta$ to the Cartesian position and velocity vectors, $\mathbf{r}(\theta)$ and $\mathbf{v}(\theta)$.
2. Compute the unit reference vectors in FPVS:

$$\hat{V}_M = \hat{V} = \frac{\bar{V}(\theta)}{V(\theta)} \quad \hat{V}_N = \frac{\bar{r}(\theta) x \bar{v}(\theta)}{|\bar{r}(\theta) x \bar{v}(\theta)|} = \hat{h} \quad \hat{V}_G = \frac{\hat{V}_M x \hat{V}_N}{|\hat{V}_M x \hat{V}_N|} \tag{7.2}$$

3. Convert the Cartesian position and velocity vectors, $\mathbf{r}(\theta), \mathbf{v}(\theta) + \Delta V_{M_p} \hat{V}_M = \left(1 + \Delta V_{M_p}\right)\mathbf{v}(\theta)$ to Keplerian orbit elements of the perturbed orbit. Denote these Keplerian elements as $\tau_M, r_{p_M}, \Omega_M, \omega_M, i_M$.
4. Compute partial derivatives for each Keplerian element as finite differences, i.e.,

$$\begin{aligned}
\frac{\partial \tau}{\partial V_M} &= \frac{\tau_M - \tau}{\Delta V_{M_p}} \\
\frac{\partial r_p}{\partial V_M} &= \frac{r_{p_M} - r_p}{\Delta V_{M_p}} \\
\frac{\partial \Omega}{\partial V_M} &= \frac{\Omega_M - \Omega}{\Delta V_{M_p}} \\
\frac{\partial \omega}{\partial V_M} &= \frac{\omega_M - \omega}{\Delta V_{M_p}} \\
\frac{\partial i}{\partial V_M} &= \frac{i_M - i}{\Delta V_{M_p}}
\end{aligned} \tag{7.3}$$

5. Do likewise to obtain partial derivatives with respect to V_N and V_G.

Example
Using the PVO orbit elements produced Figs. 7.2, 7.3, 7.4, 7.5, and 7.6.

Comments on This Algorithm

1. We assume Keplerian motion.
2. We assume the partial derivatives are constant over the duration of the maneuver. Therefore, the accuracy in computing the ΔV decreases as the size of the required parameter change increases.
3. We use the impulsive burn model.
4. Recall that we have an analytic formula for $\partial\tau/\partial V_M$. But the finite difference partial derivatives are acceptable and the algorithm is simpler if we use the finite differences for the partial derivatives of all orbital elements. Thus, the software is easier to maintain.

7.4 Free-Return Circumlunar Trajectory Analysis Techniques

Introduction

Ralph B. Roncoli's "Lunar Constants and Model's Document" supplies the constants and models to be used in the trajectory and navigation design of missions to orbit or land on the moon. It also gives the mission analyst some basic background information about the moon, its orbit, and the previous missions that have explored the moon. Table 7.1 provides some lunar, earth, and solar data for use in planning our return to the moon.

We need the following lunar terminology.

Def.: Apolune (aka apocynthion) is the point in a lunar orbit that is furthest from the moon.

Def.: A lunar orbit is an orbit about the moon.

Def.: Perilune (aka periselene or pericynthion) is the point in a lunar orbit that is closest to the moon.

Table 7.1 Lunar and related data

Parameter	Value	Unit	Remarks
Lunar data			
Mean radius	1,737.5	km	
Gm_M	4,902.801	km^3/s^2	
Ave. distance from earth	384,400	km	
Sphere of Influence	56,462	km	Approx. $9R_\oplus$
Earth data			
$Gm_\oplus$	398,600.433	km^3/s^2	
Mean equatorial radius $R_\oplus$	6,378.14	km	
Solar data			
$Gm_\odot$	132,712,440,017.987	km^3/s^2	
Mean radius	6.96E + 05	km	

Apollo Program

We begin this subsection with a brief discussion of selected Apollo lunar missions as an introduction to our quest to return to the moon. More information about all the Apollo missions is available at the National Space Science Data Center Website at nssdc.gsfc.nasa.gov.

That website provides the following description of the program:

> The Apollo program was designed to land humans on the Moon and bring them safely back to Earth. Six of the missions (Apollos 11, 12, 14, 15, 16, and 17) achieved this goal. Apollos 7 and 9 were Earth orbiting missions to test the Command and Lunar Modules, and did not return lunar data. Apollos 8 and 10 tested various components while orbiting the Moon, and returned photography of the lunar surface. Apollo 13 did not land on the Moon due to a malfunction, but also returned photographs. The six missions that landed on the Moon returned a wealth of scientific data and almost 400 kg of lunar samples. Experiments included soil mechanics, meteoroids, seismic, heat flow, lunar ranging, magnetic fields, and solar wind experiments.

The website continues with the following explanation:

> The Apollo mission consisted of a Command Module (CM) and a Lunar Module (LM). The CM and LM would separate after lunar orbit insertion. One crew member would stay in the CM, which would orbit the Moon, while the other two astronauts would take the LM down to the lunar surface. After exploring the surface, setting up experiments, taking pictures, collecting rock samples, etc., the astronauts would return to the CM for the journey back to Earth.

In particular, Apollo 11 was launched on 7/16/1969, landed in the Sea of Tranquility on 7/20/1969, and returned to the earth safely on 7/24/1969. The commander of the mission was Neil A. Armstrong, the lunar module "Eagle" pilot was Edwin Aldrin, Jr. (who later changed his name to Buzz Aldrin), and the command module "Columbia" was piloted by Michael Collins. Apollo 13 had a different adventure in which it was launched on 4/11/1970, performed a lunar flyby and return, but an explosion onboard forced cancellation of the lunar landing, and then the astronauts returned safely to earth on 4/17/1970. The commander of the Apollo 13 mission was James A. Lovell, the lunar module "Aquarius" pilot was Fred W. Haise, Jr, and the command module "Odyssey" pilot was John L. Swigert, Jr.

The Apollo 13 failure was caused by the explosion of cryogenic oxygen tank No. 2 55.9 h after launch. The LM had three propulsion systems: the Descent Propulsion System (DPS), the Ascent Propulsion System (APS), and the LM Reaction Control System (RCS). All three propulsion systems used nitrogen tetroxide and unsymmetrical dimethyl hydrazine hypergolic propellants. The DPS was used for three maneuvers (DPS-1, DPS-2, and MCC-5, Midcourse Correction 5) after the oxygen tank explosion. The APS was not used during the flight. The RCS provided attitude control of the LM/CSM stack for most of the mission following the explosion and performed the MCC-7 trajectory correction and SM separation maneuvers. ("CSM" denotes the "Command and Service Module.")

For more information on the GNC challenges, see the reference by Goodman, which says:

> After a mission abort was declared, four trajectory adjustment maneuvers were performed. The first placed the vehicle on a trajectory that would ensure return to Earth with appropriate trajectory conditions at Entry Interface (EI), that is, the arrival of the vehicle at an altitude 400,000 ft above an oblate earth, a point at which the, vehicle enters the sensible atmosphere. The second shortened the remaining flight time and moved the splashdown point from the Indian Ocean to the mid Pacific, the normal landing area for Apollo lunar missions. The third and fourth maneuvers were small trajectory adjustments to meet required EI conditions.

Reference: Goodman

Free-Return Circumlunar Trajectory Analysis Method 1

Our objective is to estimate circumlunar transfer parameters from a low-altitude circular parking orbit about the earth.

Modeling Assumptions
At periapsis, the energy equation is

$$\frac{v_p{}^2}{2} - \frac{\mu_\oplus}{r_p} = -\frac{\mu}{2a} \tag{7.4}$$

For lunar transfer, take $r_a \geq r_M$, the moon's average radial distance from the earth. Ignoring the mass of the moon, we compute

$$\Delta v = v_p - v_c = \sqrt{\frac{2\mu_\oplus}{r_p} - \frac{\mu_\oplus}{a}} - \sqrt{\frac{\mu_\oplus}{r_p}} \tag{7.5}$$

for a Hohmann transfer, where v_p is obtained by solving Eq. (7.4) for v_p. For the first maneuver of a Hohmann transfer, $\Delta v = 3.13$ km/s, as we determined in Sect. 3.3, and the time of transfer is:

$$t_{transfer} = \frac{\tau}{2} = \pi\sqrt{\frac{a^3}{\mu_\oplus}} \tag{7.6}$$

where

$$a = \frac{r_p + r_a}{2} \tag{7.7}$$

Based on the assumption that parking orbits have altitudes of only a couple hundred km, we consider a low-altitude parking orbit such that

$$r_p \cong 6600 \text{ km so that } h_p \cong 222 \text{ km}$$

Therefore, from Eq. (7.7), $a \cong 1.96 \times 10^5$ km, which implies that

$$t_{transfer} \cong 5.0\,\text{days}$$

From the first term in Eq. (7.5), $v_p = 10.90$ km/s, which implies that

$$h = r_p v_p = 7.2 \times 10^4\,\text{km}^2/\text{s} \tag{7.8}$$

A Hohmann transfer requires the least impulsive Δv, but its transfer time is longer than a Type I trajectory. Shorter transfer times to the moon are possible by using transfer orbits with apogee $r_a > r_M$, which requires extra Δv. However, the additional impulse applied at perigee above that of a Hohmann transfer is small. So h is not increased significantly above 7.2×10^4 km^2/s for higher energy transfers.

Alternately, we can consider the velocity vector at r_M, i.e.,

$$\mathbf{v} = v_r \mathbf{i}_r + v_\theta \mathbf{i}_\theta$$

Higher energy transfers have $v_r > 0$ at r_M instead of $v_r = 0$ as for a Hohmann transfer. But v_θ at r_M is just slightly greater than v_θ for the Hohmann transfer. Since

$$h = |\mathbf{r}x\mathbf{v}| = rv_\theta = r_M v_{\theta_M} \tag{7.9}$$

from Exercise 2.19, the assumption of constant angular momentum for all lunar transfers is valid within the approximation method employed here. Thus, we can assume a constant value of

$$v_{\theta_M} = \frac{h}{r_M} = 0.19\text{km/s} \tag{7.10}$$

at the moon's distance r_M.

However, we do not assume $v_r = 0$ at r_M. Once v_r at r_M is determined, the transfer ellipse parameters can be determined as follows. From Eqs. (2.17) and (2.19), Exercise 2.19, the Energy Equation, and simplifying the result, we obtain

$$e = \sqrt{\left(\frac{r_M v_\theta^2}{\mu_\oplus} - 1\right)^2 + \left(\frac{r_M v_\theta v_r}{\mu_\oplus}\right)^2} \tag{7.11}$$

which gives the shape of the transfer orbit. Also the semimajor axis of the transfer orbit is

$$a = \frac{p}{1 - e^2} = \frac{h^2/\mu}{1 - e^2} = \frac{r_M{}^2 v_\theta{}^2}{\mu(1 - e^2)} \tag{7.12}$$

from Eq. (2.17) and Exercise 2.19. From the Conic Equation, Exercise 2.19, and Eq. (7.11),

$$\cos\theta = \frac{1}{e}\left(\frac{h^2}{\mu r} - 1\right) = \left(\frac{r_M {v_\theta}^2}{\mu_\oplus} - 1\right) \Big/ \sqrt{\left(\frac{r_M {v_\theta}^2}{\mu_\oplus} - 1\right)^2 + \left(\frac{r_M v_\theta v_r}{\mu_\oplus}\right)^2} \tag{7.13}$$

which gives the true anomaly (location in orbit) at r_M. The time to transfer, ignoring lunar gravity effects, is

$$t_{transfer} = \frac{E - e\sin E}{n} \tag{7.14}$$

from Kepler's Equation, where the eccentric anomaly E is obtained from Eq. (2.27) and the mean motion

$$n = \sqrt{\mu/a^3}$$

from Eq. (2.35). The eccentricity for the Hohmann transfer is $e \cong 0.97$ from Exercise 7.6(a) and, for any higher energy transfer,

$$e \cong \sqrt{0.932 + 0.033 v_r} \tag{7.15}$$

from Exercise 7.6(b).

Based on this discussion, we can now say that the following set of assumptions are justified within the approximation model being used in this analysis:

1. The moon travels in a circular orbit about the earth that is approximately 384,400 km in radius.
2. Use of the patched conic model—Since the moon is relatively close to the earth and the two bodies actually travel around each other, the results are less accurate than those obtained for interplanetary transfer. The earth and moon move around a common center of mass, which is 4,670 km away from the geocenter and, thus, the position of the earth shifts considerably in the course of time. In fact, this approach is not satisfactory for calculation of earth return trajectories because of the manner in which lunar gravity is handled. Also, the perilune altitude cannot be accurately predicted. But the method is good for outbound Δv evaluations and provides insight into the problems of lunar transfer missions.
3. In adopting the patched conics model, we assume Keplerian motion, ignoring third body gravitational effects of, for example, the sun, and other perturbations, and modeling the earth and moon as perfect spheres.
4. The sphere of influence of the moon is ignored until conditions at the lunar distance have been established. (This zero sphere of influence model was also used in the interplanetary transfer analysis in the Venus flyby patched conics example.) However, the lunar SoI is not negligibly small compared to the earth–moon distance. The radius of the SoI is about 15 % of the earth–moon distance

even for the revised SoI discussed in Subsection 4.5. Therefore, the elliptic orbit is not a Hohmann trajectory to the moon.
5. The gravitational attraction of the moon is ignored in computing the Δv for injecting into the lunar transfer orbit.
6. The calculations are made for $r_p = 6{,}600$ km, which implies that the altitude of the parking orbit = 222 km. Thus, we assume that parking orbits have altitudes of only a couple hundred km. Hence, we also have $a \cong 1.96 \times 10^5$ km and, therefore, $t_{transfer} \cong 5.0$ days.
7. The transfer Δv is impulsive.
8. Assumption of constant angular momentum $h = r_M v_\theta = 7.2 \times 10^4$ km^2/s for all lunar transfers, including transfers with higher energy than a Hohmann trajectory.
9. Assumption of a constant value for $v_\theta = 0.19$ km/s at the moon's distance.

Trajectory Design Tool: Michielsen Chart

Michielsen devised a graphical display for all lunar transfer information, including passage effects, on a single plot. This chart is presented in Fig. 7.9 with an application to the Apollo 11 Mission. The v_r axis is calibrated in km/s, but is directly related to transfer time. Thus, each value of v_r associated with the transfer orbit corresponds to a unique value of transfer time. The two vertical lines marking the constant values of $v_\theta = \pm 0.19$ km/s at r_M are calibrated in days to reach r_M, i.e., the transfer time from earth to the moon. Transfers which have $v_\theta = +0.19$ km/s are direct and those with $v_\theta = -0.19$ km/s are retrograde.

The earth intercept zone connotes return to the earth without any thrusting maneuvers.

Note the moon's velocity vector $\mathbf{v_M}$. The magnitude

$$v_{\theta_M} = v_c = \sqrt{\frac{\mu_\oplus}{r_M}} = 1.02 \text{ km/s}$$

since the moon is assumed to be in a circular orbit about the earth. So the point $v_\theta \cong 1$ km/s, $v_r \cong 0$ is the orbital velocity of the moon with respect to the earth.

A probe's approach (v_θ, v_r) is specified by the transfer trajectory. Hyperbolic passage of the moon is handled in an analogous manner to that for planetary passage.

As the spacecraft reaches r_M, the earth's gravitational attraction is "turned off" (in the model) and the moon's gravity is "turned on" (in the model). The deflection angle δ measures the turning of the spacecraft's velocity in the moon-relative hyperbolic trajectory. A typical velocity vector diagram for lunar passage is shown in Fig. 7.10. Since the spacecraft passes in front of the moon, the turn angle δ is taken clockwise and geocentric energy is decreased via a gravity assist (see Fig. 3.18). These vector triangles predict the probe's departure velocity $\mathbf{v}^+$ from the moon.

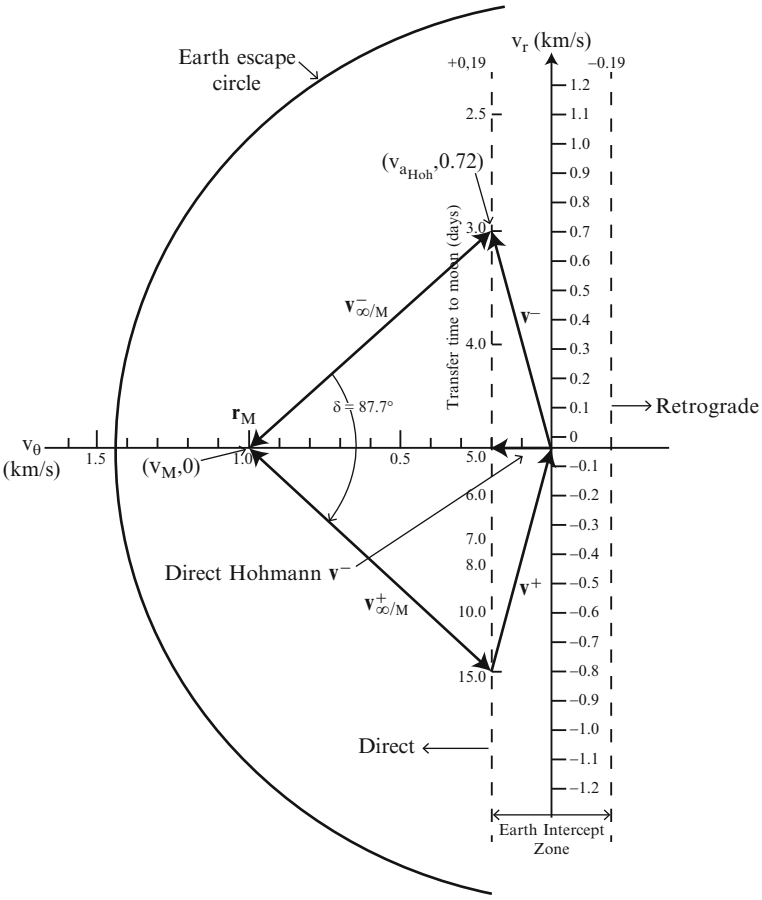

Fig. 7.9 Michielsen chart for lunar transfer on Apollo 11

The whole passage can be plotted on a Michielsen Chart. If the outgoing (post-flyby) velocity

$$v^+ > \sqrt{2}v_M = \sqrt{2}v_c \text{ (at the moon)} = v_{esc}$$

earth escape occurs. If v+ crosses the earth escape circle, then enough energy was added during passage to go into a heliocentric orbit. Note that energy is always added for a Hohmann transfer (see Michielsen Chart), since

$$v_{\theta_{Hoh}} = v_{a_{Hoh}} = \frac{r_p}{r_a} v_{p_{Hoh}} = 0.19 \text{ km/s}$$

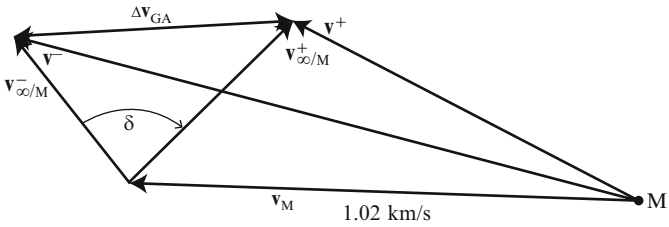

Fig. 7.10 Velocity diagram for hyperbolic passage of the moon

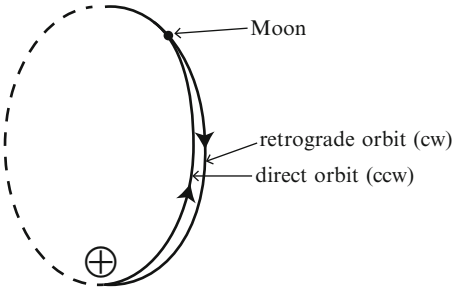

Fig. 7.11 Lunar transfer and return flight profile

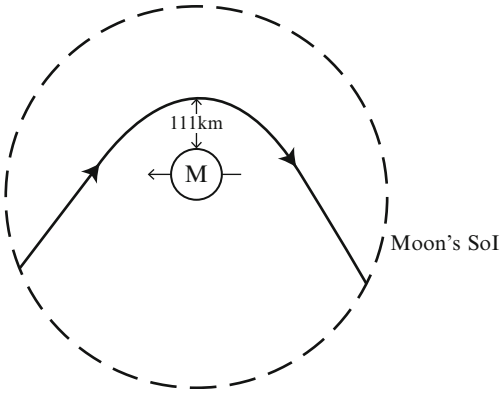

Fig. 7.12 Apollo 11's flyby of the moon at 111 km in moon-fixed coordinates

The Michielsen Chart (Fig. 7.9) represents the flight of Apollo 11 from a circular parking orbit on a high-energy, 3-day transfer trajectory. Since the spacecraft passed in front of the moon, δ is taken clockwise such that the spacecraft returns to low earth perigee. Figure 7.11 depicts the flight profile in an earth–moon fixed coordinate system. Figure 7.12 is an enlargement of the flyby trajectory in moon-fixed coordinates. Referring to the Michielsen Chart, the radial component of the probe's velocity $v_r^- = 0.72$ km/s at r_M and the transverse component $v_\theta^- = v_M - v_{\theta_M} = 0.81$ km/s. Thus, the magnitude of $v_{\infty/M} = 1.08$ km/s (hypotenuse of a right triangle.). If passage is specified to be within 111 km of the moon's

surface, the deflection of $v_{\infty/M}$ from the hyperbolic passage of the moon can be calculated from Eqs. (3.26) and (3.32) as follows:

$$e = 1 + \frac{r_p v_\infty{}^2}{\mu_M} = 1.44$$

where $r_p = R_M + 111$ km $= 1{,}848.5$ km and $\mu_M = 4902.801$ km^3/s^2.

Therefore,

$$\delta = 2\arcsin\left(\frac{1}{e}\right) = 87.7 \text{ deg.}$$

The $v_{\infty/M}{}^+$ is plotted on the Michielsen chart for a 3-day transfer to the moon. The deflection δ is taken clockwise because of the frontside passage. Given this deflection of the inbound asymptote, the vehicle's inertial velocity vector with respect to the earth outbound from the moon $\mathbf{v}^+$ can be plotted as in Fig. 7.9 and is seen to be approximately symmetric with respect to the incoming inertial velocity vector v−. The gravity assist Δv is

$$\Delta v_{GA} = |\mathbf{v}^+ - \mathbf{v}^-| = 1.2 \text{ km/s}$$

Note that

$$\Delta v_{GA} \neq v^+ - v^- = 0.08 \text{ km/s}$$

where v^+ and v^- are (scalar) magnitudes.

So we have performed a first order mission design of a circumlunar transfer. This method provides good outbound Δv evaluations, but is not sufficiently accurate in calculating earth return trajectories. So we do not proceed at this point to use r, v, and β to evaluate the trajectory parameters of the return trajectory as we have done in Chap. 3. However, we do proceed to consider the circumlunar trajectories used for the Apollo missions qualitatively.

Free-Return Circumlunar Trajectories and Applications to the Apollo Missions

Def.: A free-return circumlunar trajectory is a trajectory about the earth, which will fly by the moon and return to an earth reentry point without the assistance of any propulsive maneuvers after injection into the lunar transfer trajectory.

A free return to the earth is accomplished via a lunar gravity assist.

This type of transfer was very useful on the Apollo lunar flights. If the spacecraft rockets could not be fired for any reason upon reaching the moon, safe return to the earth was guaranteed. Early Apollo flights were injected into free return trajectories of the type shown in Fig. 7.13. Typically, the spacecraft was sent on a 3-day outbound leg to make a front-side passage such that it could enter a 3-day return leg if a failure occurred. The corresponding simplified (from Fig. 7.9) velocity vector diagram is shown in Fig. 7.14. With the proper approach velocity, the trajectory is deflected into a "figure 8" pattern for free return to earth as shown in Figs. 7.13 and 7.17 (reconstructed plot for Apollo 13).

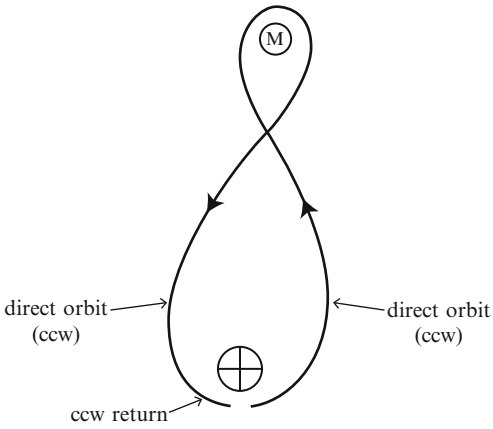

Fig. 7.13 Apollo type free-return trajectory in earth–moon centered coordinates

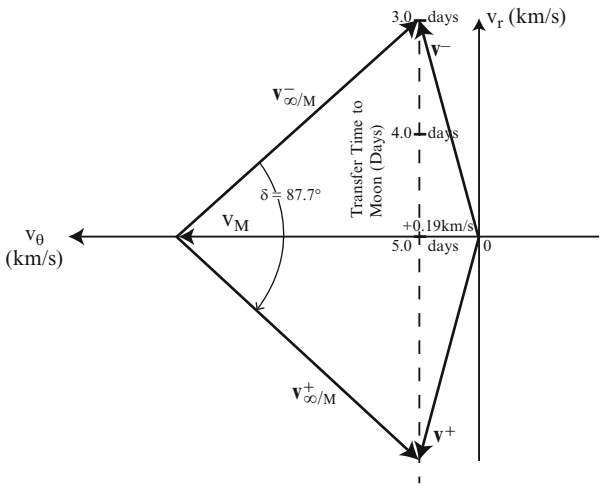

Fig. 7.14 Apollo mission free-return vector diagram

Direct Versus Retrograde Trajectories
Recall the definition of direct (or posigrade) orbits and retrograde orbits given in Sect. 4.3:

Orbits with $0° < i < 90°$ are direct (or posigrade)
Orbits with $90° < i < 180°$ are retrograde

as shown in Fig. 7.15.

Figure 7.13 shows a trajectory with a direct outbound leg and direct return leg. Figure 7.16 shows a trajectory with a direct outbound leg and a retrograde return

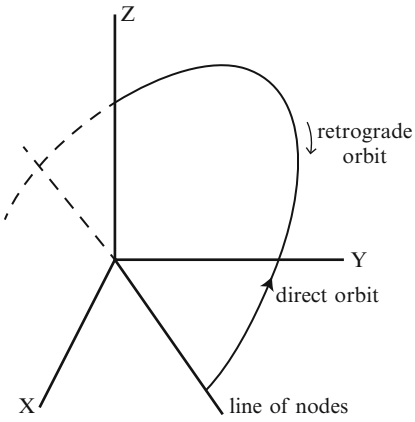

Fig. 7.15 Direct versus retrograde orbits

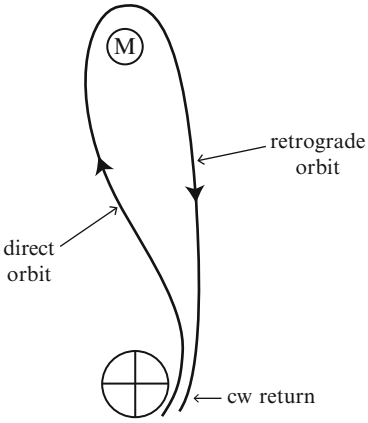

Fig. 7.16 Trajectory with direct outbound leg and retrograde return

leg. To change from a direct return leg to a retrograde return requires doing less bending in the hyperbolic trajectory at the moon. Recall, from Eq. (3.32), that large values of e imply little bending in the hyperbolic trajectory. From Eq. (3.27), we see that the eccentricity of the hyperbolic trajectory can be increased by increasing r_p or v_∞. Hence, the return leg can be changed from direct to retrograde by shortening the time of flight on the outbound leg to increase v_∞ and/or raising the altitude at closest approach at the moon. In Exercise 7.7, the reader will determine the value of the turn (deflection) angle δ and the closest approach distance r_p at the moon for an Apollo type free-return trajectory.

The reconstructed figure in the reference by Walter shows that the Apollo 11 free-return trajectory is symmetric and periodic and passes the surface of the moon at a minimum distance of 111 km, which corresponds exactly to the periselene (perilune) altitude of Apollo 8, 10, and 11. Later moon landing missions entered at this point into a circular moon orbit, from which it was possible to descend to the moon's surface. If the mission had to be aborted for any reason, the

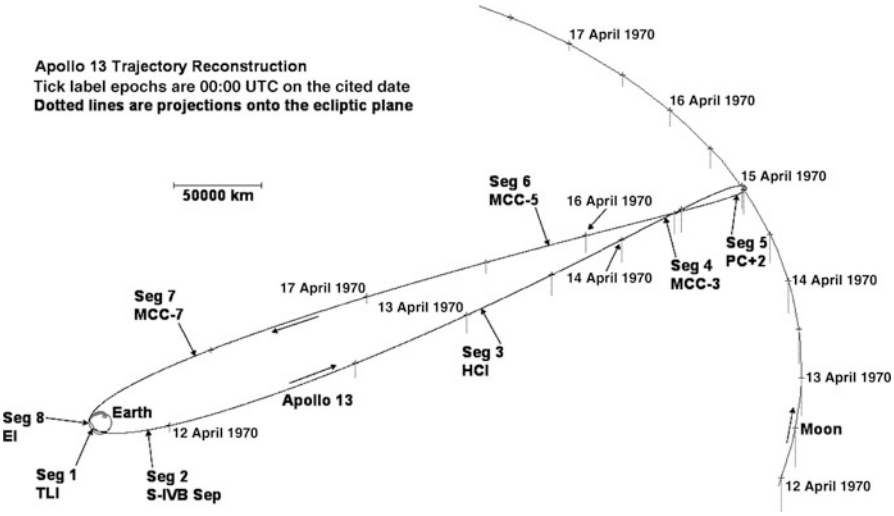

Fig. 7.17 Geocentric trajectory reconstruction plot for Apollo 13 [From "Apollo 13 Trajectory Reconstruction via State Transition Matrices" by Daniel R. Adamo, reprinted by permission of the American Institute of Aeronautics and Astronautics, Inc.]

engine ignition required for braking performed behind the moon into the circular moon orbit would not have happened and the astronauts would automatically have returned to the earth. This indeed happened for Apollo 13. The reference by Adamo provides an annotated geocentric plot, as shown in Fig. 7.17, of the reconstructed Apollo 13 trajectory accompanied by the moon's geocentric motion.

These references also say that, while the reconstructed trajectories are fully symmetric relative to the earth–moon connecting line, the actual trajectories of the Apollo missions were slightly asymmetric such that on return the spacecraft would touch the earth's atmosphere in order to guarantee an automatic re-entry. This asymmetry was achieved by a slight shift of the position of the periselene.

During the outward as well as the return flight, the free-return trajectory is clearly elliptical in the proximity of the earth, as the gravitational influence of the earth is dominating. Approaching the edge of the moon's SoI, the trajectory becomes more and more a straight line. Here the orbital velocity has already decreased considerably and the gravitational influence of the earth and moon plus centrifugal force just cancel each other. In this area, the real trajectory deviates utmost from the patched conics approximation. Near the moon, the trajectory is bent into a hyperbola.

As confidence in the Apollo CSM increased, the free-return trajectories were changed to accommodate lunar orbit entry parameters. Apollo 13 had made a midcourse correction to leave its free-return path before experiencing the failure, which aborted the lunar landing. The lunar module engines were used after the explosion in the CSM to modify their course to enable return to the earth re-entry altitude in a reasonable time.

We have applied the Michielsen Chart to circumlunar free-return trajectories. The reference by Kaplan provides information about more general applications of this chart.

We now consider a second method of free-return circumlunar analysis that is based on less restrictive modeling assumptions than those employed in the first analysis method.

Free-Return Circumlunar Trajectory Analysis Method 2

Introduction

The Apollo missions were injected from a parking orbit about the earth into a free-return circumlunar orbit, so that no major propulsive ΔV maneuvers were needed to return the spacecraft to atmospheric entry to achieve a specified landing site on the earth. The main content of the following analysis is a complete parametric representation of the outward and return orbital inclinations and times of flight with the pericynthion (periapsis of the lunar orbit) altitude at the moon and the position of the moon (from ephemeris input) in its eccentric orbit. We will use the parametric approach to obtain approximate values for:

(a) Injection conditions from the parking orbit about the earth into the outbound ellipse
(b) Approach conditions at the moon—the pericynthion distance
(c) Earth atmospheric entry and landing conditions.

These data could be used as first approximations in a precision trajectory search program, using linear search methods to solve for the corresponding exact trajectory. Thus, one could generate the nominal trajectory for a free-return circumlunar mission.

Some examples of the comparison of data obtained in generating the parametric plots to results obtained by running an integration program with a high-precision model are presented in the following analyses to determine the validity of the parametric model. But the focus of this presentation is the simplified gravitational model of the earth–moon system provided so that trajectories in this system can be studied qualitatively and the parametric plots used in the qualitative studies with examples of their use.

This study concentrates on the class of free-return circumlunar trajectories that are of interest to a crewed lunar program, i.e., injection from a circular parking orbit, a very close approach to the surface of the moon, and re-entry into the earth's atmosphere at a shallow angle. In addition, relationships are presented which tie the characteristics of such trajectories computed in an inertial coordinate system to the geographic position of the launch and landing sites in earth-fixed (non-inertial) coordinates.

The parametric plots considered here can be used for feasibility analyses, mission planning, and verification of results for lunar missions requiring free-return circumlunar trajectories.

Model Assumptions (Simplifications) for Free-Return Circumlunar Trajectory Parametric Plots

The parametric plots are developed utilizing the following simplified model of motion in the earth–moon system. The model on which the following analysis is based was first described by Egorov in 1956. (See reference by Egorov.)

Sphere of Influence

The simplified trajectory model is based on the sphere of influence concept where motion outside of this sphere (centered at the moon) is represented by an earth-influenced conic and motion within the sphere is a moon-influenced conic. The conics are chosen such that the position and velocity vectors match at the spherical boundary as well as satisfying other constraints. For the parametric plots we will consider, the sphere of influence is taken to be about 10 earth radii, $10R_{\oplus}$. (Note the improved model assumption versus the zero sphere of influence model considered for the Patched Conic example.) Thus, we obtain two earth-based ellipses and one moon-based hyperbola as shown in Fig. 7.18. These conics are such that the position and velocity vectors match at the earth-to-moon and moon-to-earth phase boundaries. The apparent discontinuity in the velocity in Fig. 7.18 is due to the moon's motion about the earth. This discontinuity is removed in the display by considering a rotating coordinate system fixed to the earth–moon system as we have done previously. Thus, we obtain a "figure-8" trajectory.

Moon's Orbit

The complex motion of the moon about the earth affects the behavior of circumlunar trajectories. Not only the moon's distance from the earth, which varies as

$$56\ R_{\oplus} < LD < 64R_{\oplus},$$

but also the path angle of its velocity vector greatly affects important parameters such as pericynthion distance, time of flight, etc. Therefore, this study has to include as a variable parameter the moon's distance together with some indication of the radial direction of the moon's motion in terms of the inclination i_M with respect to the earth's equatorial plane.

A first approximation to the moon's orbit would be an ellipse with a mean semimajor axis and eccentricity of

$$a_M = 60R_{\oplus} = 382,688\,\text{km} \quad \text{and} \quad e_M = 0.056$$

respectively. The inclination of the moon's orbit plane with respect to the earth's equatorial plane varies as

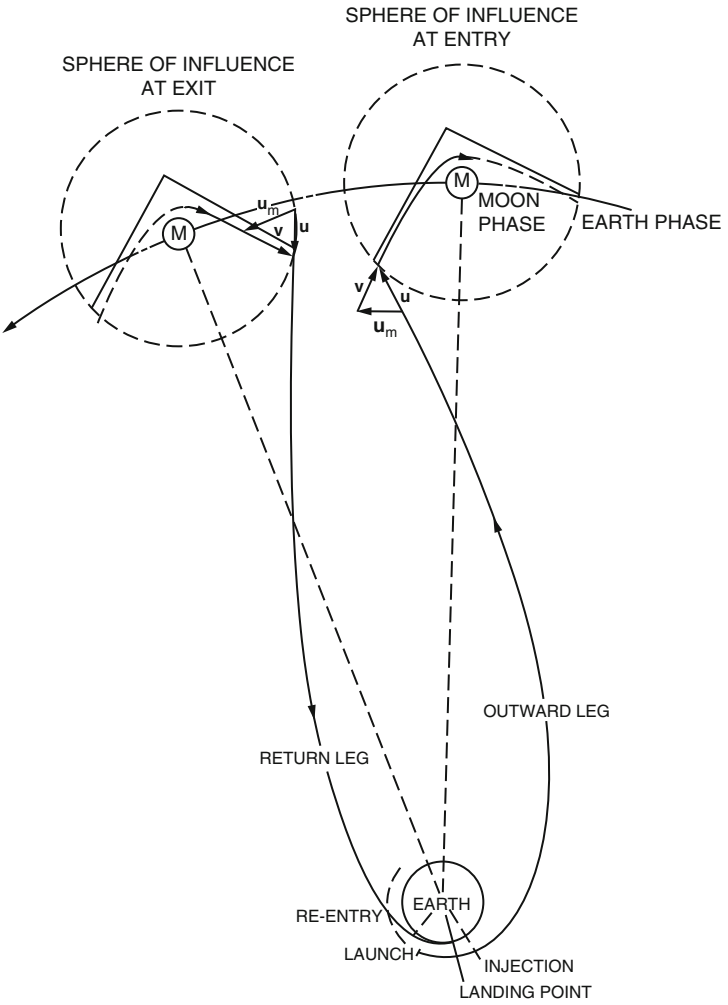

Fig. 7.18 Schematic of a circumlunar free-return trajectory

$$18.5^\circ \leq i_M \leq 28.5^\circ$$

and the node regresses with both conditions having a period of approximately 20 years. (In 1967, the inclination was near its maximum.) Further, the line of apsides advances at a rate of approximately 40° per year. All dependence on these angular variations is avoided if the circumlunar trajectories are referred to the moon's orbit plane. However, the mean ellipse is a poor approximation of the moon's in-plane motion. The moon's perigee varies by about 2.5 $R_\oplus$ and its apogee varies about $0.5R_\oplus$ as seen in the reference by Woolston. A cycle of this variation occurs in approximately 7 months.

Because of the large variation in the perigee, we will include trajectories for both extremes of this distance. Since the apogee variation is small, we assume it to be

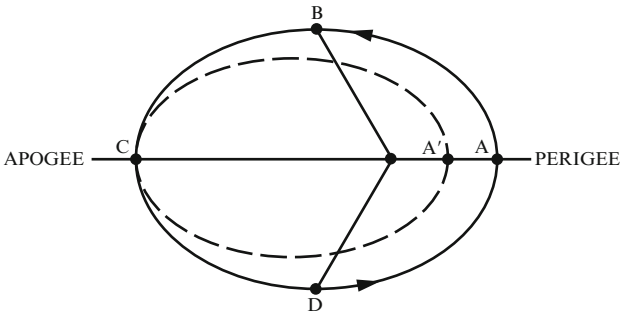

Fig. 7.19 Positions of the moon in its orbit about the earth

Table 7.2 Distance of the moon from the earth

Location	Distance (km)
Perigee A′	356,620
Perigee A	368,812
Position B	390,149
Position C (Apogee)	405,389
Position D	381,005
Average LD	384,400
a for Perigee A′	381,005
a for Perigee A	387,100.50

constant. The notation attached to the position of the moon in its orbit is the following set as illustrated in Fig. 7.19:

Position A: Moon at maximum perigee
Position A′: Moon at minimum perigee
Position B: Moon at its mean distance from the earth with its distance increasing
Position C: Moon at the apogee of its orbit
Position D: Moon at its mean distance from the earth with its distance decreasing

The moon's periapsis changes with time between when it is at A′ and when it is at A. The distance from these points to the earth and the values of the semimajor axis for the conics through points A and A′ are given in Table 7.2.

Fixed Conditions
The following conditions are known:

1. Cape Canaveral, which is at 28.5°N latitude and 80.6°W longitude, has been chosen as the launch site.
2. The moon's orbital inclination has been chosen near its maximum value of 28.5°, reflecting the value at the time of the early Apollo launches. This assumption permits launches from the Cape into the moon's orbit plane.

3. The powered flight angle and time were chosen as 30° and 10 min, respectively.
4. The circular parking orbit altitude was fixed at 600,000 ft (183 km) and the injection flight path angle at 90°.
5. Reflecting the desired value for crewed flights, the re-entry angle was chosen as 96° measured from the vertical (6° from horizontal) with a re-entry altitude of 400,000 ft (122 km). This altitude is the "entry interface (EI)" location.

Specifying the above launch and re-entry conditions is almost equivalent to fixing the perigee altitudes of the outward and return phases of the mission. The launch azimuth from the Cape determines the inclination of the outward phase and the inclination of the return phase is a separate input.

Additional Assumptions Used Selectively

Seven categories of parametric plots, listed as Categories (1)–(7), are considered below in the subsection entitled "Penzo Parametric Plots for Circumlunar Free-Return Trajectory Analyses." For the first three categories, no additional simplifying assumptions were made. However, additional assumptions had to be made to eliminate second order effects. For example, for the next three categories, it is assumed that the declination and right ascension of the spacecraft's entry and exit points at the SoI are equal to those of the moon at the time of the spacecraft's pericynthion passage. This assumption allows the generation of first order graphical data, which could not be done otherwise.

Free-Return Circumlunar Trajectory Selection Procedure

Since only conic motion is considered in the model, it is possible to program the equations to satisfy certain initial and terminal conditions. Utilizing an iterative scheme, it is possible to solve the boundary value problem.

The input quantities for this selection procedure are:

1. Day of launch
2. Launch azimuth
3. Powered flight angle from launch to burnout
4. Flight path angle at injection
5. Parking orbit altitude
6. Length of coast in the parking orbit
7. Time of flight to the moon
8. Clockwise or counterclockwise return trajectory to the earth
9. Re-entry flight path angle
10. Re-entry altitude
11. Re-entry maneuver downrange angle
12. Maneuver time to touchdown
13. Latitude of the landing site
14. Longitude of the landing site

The first seven quantities are required to determine the outward leg of the earth-phase trajectory. Thus, we calculate the time of launch, time (duration) of coast to the injection point in the parking orbit, conic elements, and the position, velocity and time of any point on the outward leg. The first aim point for this leg is the center of a massless moon. The successive aim points, calculated from the second iteration on, will be the entry point at the moon's sphere of influence with the mass of the moon considered.

The next six parameters, together with the moon-phase exit velocity magnitude from the sphere of influence (which equals the moon-phase entry velocity magnitude), are used to determine the earth-phase return leg of the trajectory. The solution of this phase requires an iterative procedure as shown in Fig. 7.20. The iterative procedure is needed to solve for the direction of the moon-phase exit velocity vector, which is unknown, so that the earth-phase energy is unknown. A first guess, such as assuming that the energy is equal to that of the outward leg, is made and successive iterations performed until the calculated earth-phase velocity at the exit point is consistent with the required moon-phase velocity. This iterative procedure produces a unique circumlunar trajectory.

After calculating the return phase conic, the exit velocity vector can be calculated. This velocity vector is found with respect to the moon by subtracting off the velocity vector $\mathbf{u_M}$ of the moon with respect to the earth at the time of exit as indicated in Fig. 7.18. An ephemeris file provides the exact position and velocity of the moon at any time.

The two moon-centered velocity vectors at entrance and exit of the sphere of influence (SoI) completely determine the moon-phase conic (see Exercise 7.11); the plane being determined by the cross-product of the two velocity vectors; and the conic (hyperbolic) elements, a and e. From the conic elements, the entry and exit positions at the sphere can be found. At this point, the calculated positions are compared with those found from the earth-phase conics. If they lie within specified tolerances, then the search is complete. If not, the old positions and times at the sphere are replaced by the new values just calculated and the process is repeated.

So far, we have not used the landing site longitude, because the conic calculated for the return phase is referenced to inertial space and is independent of any geographic position on the earth. The return phase conic and the time of landing, which is an output parameter, determine the landing site longitude. To obtain a desired longitude, the total time of circumlunar flight time must be altered, letting the earth obtain the correct orientation with respect to the moon at re-entry to obtain the desired landing longitude. The total time of flight is altered by changing the input time of flight to the moon in the launch phase. Once this is done, the entire circumlunar search process is repeated until the landing site longitude tolerance is met.

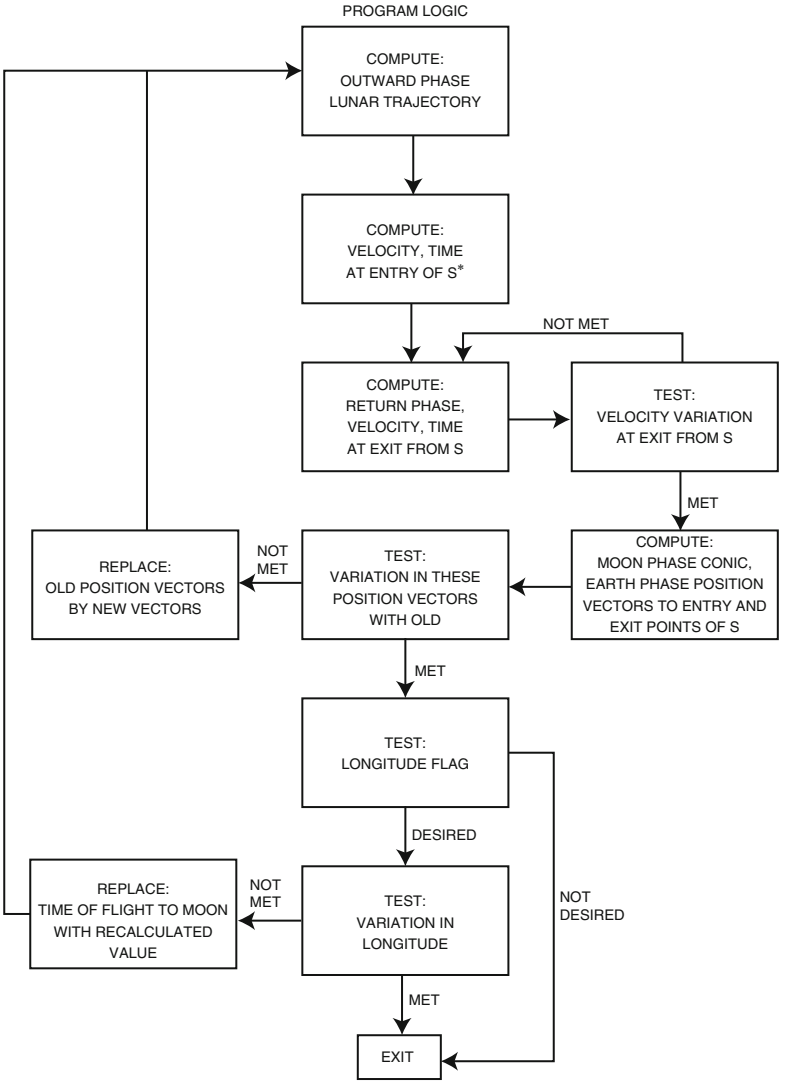

Notation: "S" denotes the sphere of influence of the moon.

Fig. 7.20 General logic block diagram

Trajectory Design Tool: Penzo Parametric Plots for Circumlunar Free-Return Trajectory Analyses

This subsection provides the Penzo parametric (P^2) plots, which display data with respect to the pericynthion distance, flight time, launch azimuth, and landing site location. The plots are treated below in seven categories:

1. Pericynthion Distance
2. Time of Flight

3. Fixed Pericynthion Altitude ($h_p = 100$ nm)
4. Azimuth and Inclination
5. Maneuver Angle and Touchdown Latitude
6. Touchdown Longitude
7. Some Additional Parameters

All of these plots were obtained from the reference:

Paul A. Penzo, "An Analysis of Free-Flight Circumlunar Trajectories," STL Report No. 8976-6010-RU-000, Space Technology Laboratories, Inc., Redondo Beach, CA, 1962.

This report was generated for the Jet Propulsion Laboratory.

Category (1): Pericynthion Distance

Figures 7.21, 7.22, 7.23, 7.24, 7.25, 7.26, 7.27, 7.28, 7.29, and 7.30 show the variation of the pericynthion distance with the inclination of the return phase conic for fixed times of flight T_o (in hours) to the moon. Also plotted on each graph are two curves for fixed return times T_r (in hours) from the moon.

Specifically, Figs. 7.21, 7.22, 7.23, 7.24, and 7.25 consider launches in the moon's orbit plane.

Example (Apollo): Launches in the moon's orbit plane were possible for the early Apollo missions because the moon's inclination with respect to the earth's equatorial plane was 28.5°, which equals the latitude of the launch site.

The first noticeable characteristic of these curves is that, for fixed outward flight times, the pericynthion altitude is greater for clockwise (cw) returns than for counterclockwise (ccw) returns. (See Fig. 7.13, which shows a direct outbound trajectory with a direct return, and Fig. 7.16, which shows a direct outbound trajectory with a retrograde return.) A similar characteristic is the fact that, for fixed return flight times, the pericynthion altitudes are greater for ccw return trajectories than for cw return trajectories.

Recall, from Eqs. (3.27) and (3.33), large e implies little bending so r_p small implies large bending as needed to achieve ccw return leg. Therefore, to change from a posigrade to a retrograde return leg, we must shorten TFL outward and/or raise periapsis at the moon.

Examples in Fig. 7.21:

$i_o = 0°$, $i_r = 70°$ (ccw), and $T_o = 60$ h
$\Rightarrow$ pericynthion altitude = 133 nm = 246 km
$i_o = 0°$, $i_r = 110°$ (cw), and $T_o = 60$ h
$\Rightarrow$ pericynthion altitude = 608 nm = 1126 km
$i_o = 0°$, $i_r = 70°$ (ccw), and $T_r = 70$ h
$\Rightarrow$ pericynthion altitude = 311 nm = 576 km
$i_o = 0°$, $i_r = 110°$ (cw), and $T_r = 70$ h
$\Rightarrow$ pericynthion altitude = 28 nm = 52 km

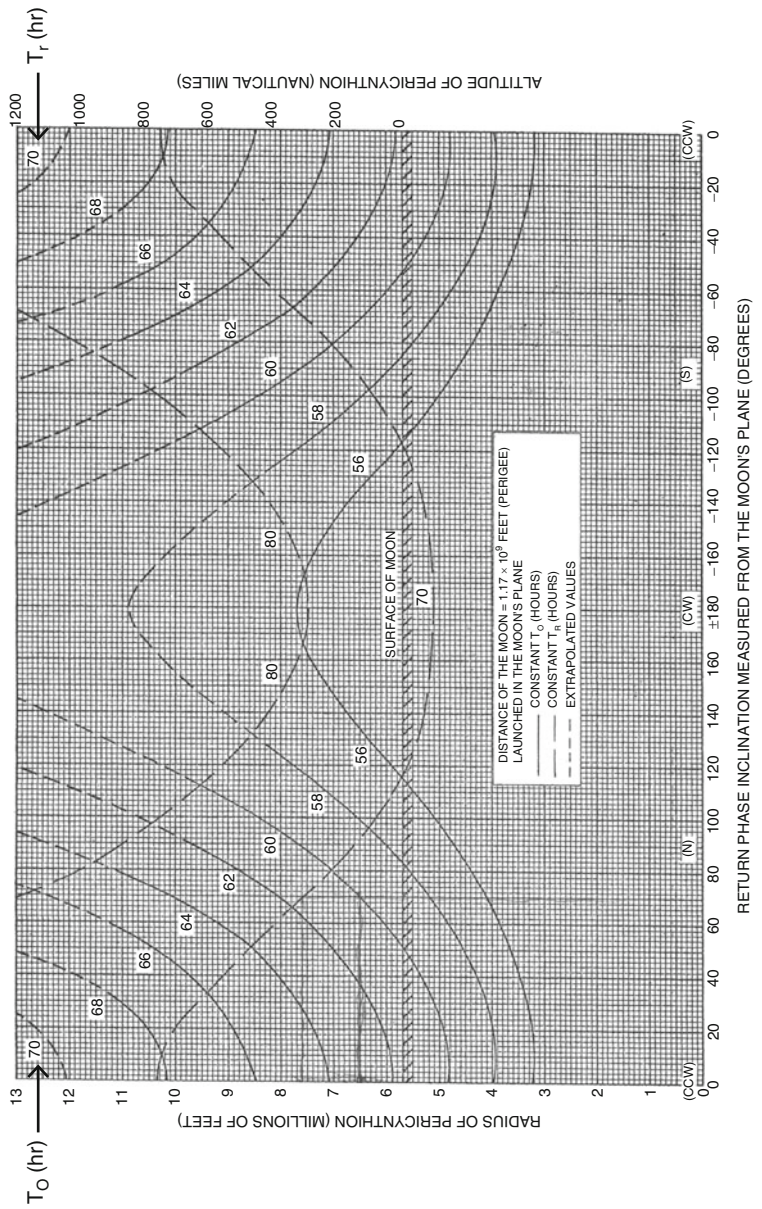

Fig. 7.21 The spacecraft's pericynthion distance versus the return phase inclination for constant outward phase flight times for position A′ if launched into the moon's orbit plane

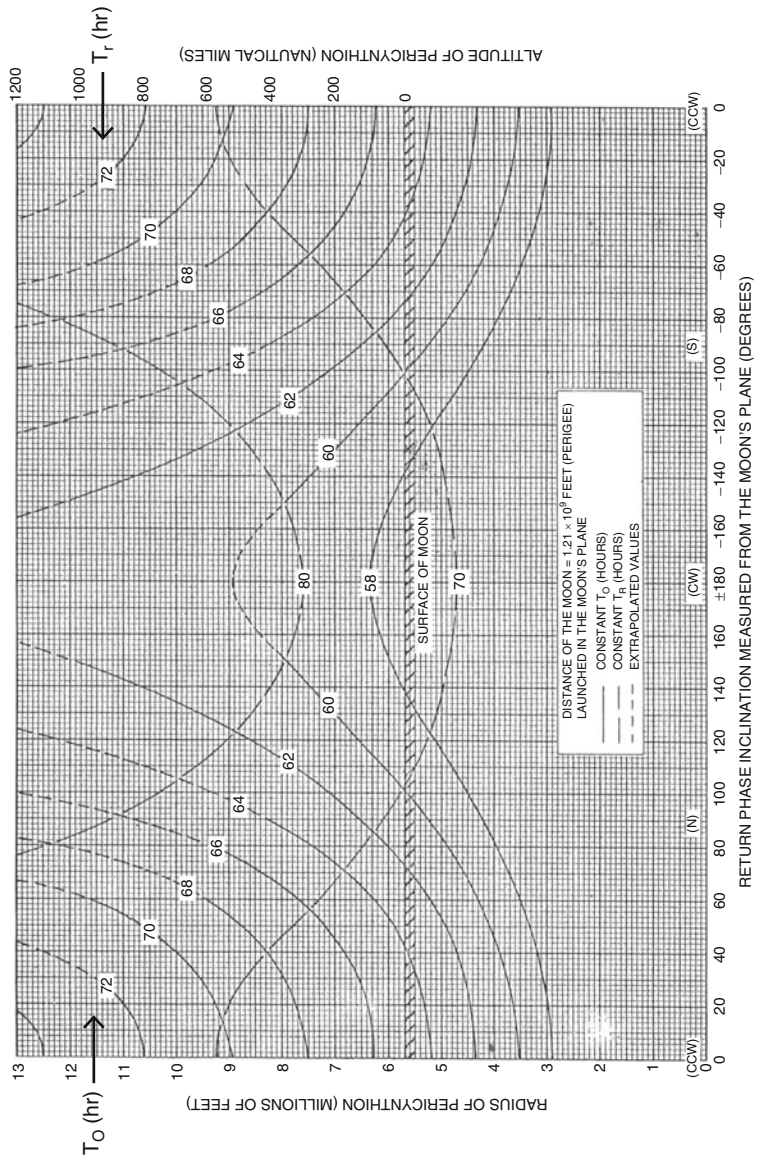

Fig. 7.22 The spacecraft's pericynthion distance versus the return phase inclination for constant outward phase flight times for position A if launched into the moon's orbit plane

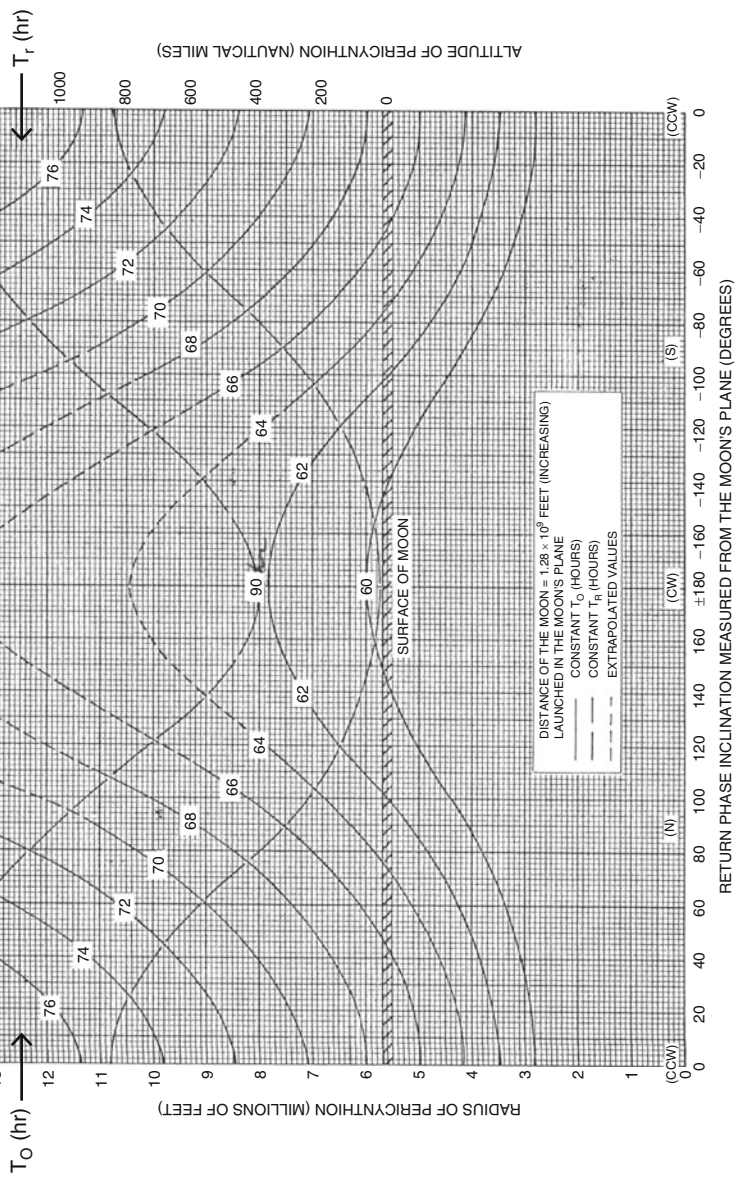

Fig. 7.23 The spacecraft's pericynthion distance versus the return phase inclination for constant outward phase flight times for position B if launched into the moon's orbit plane

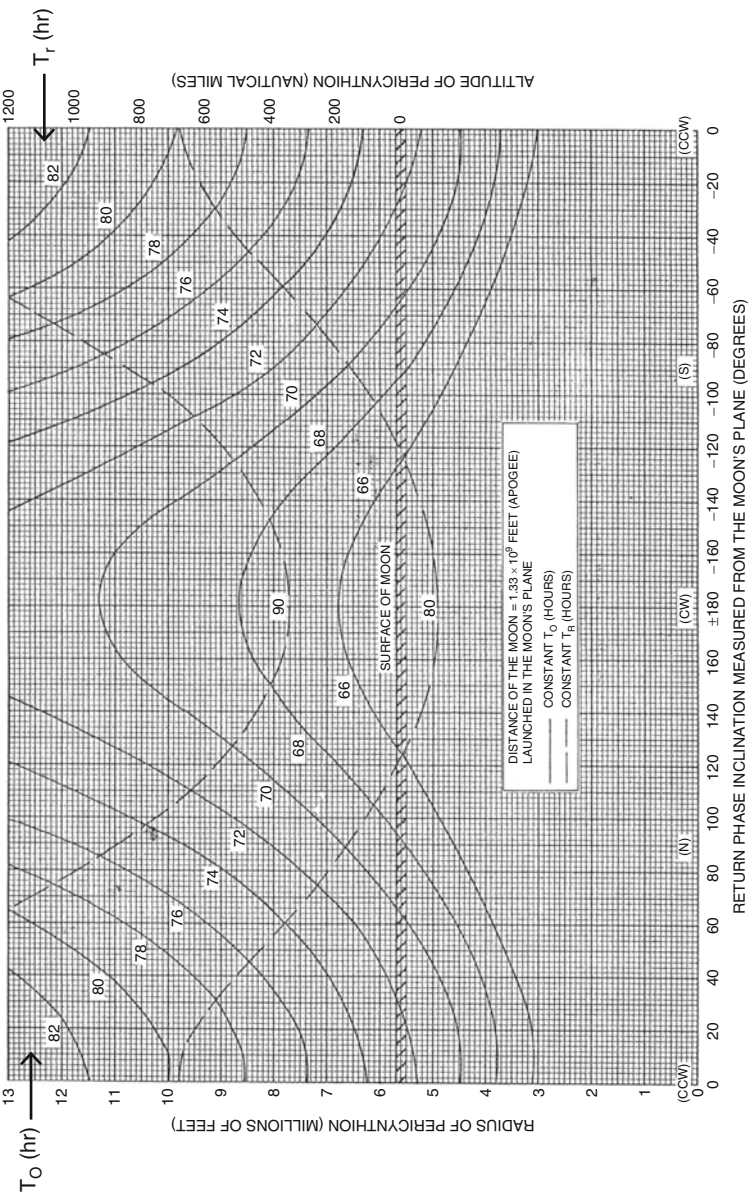

Fig. 7.24 The spacecraft's pericynthion distance versus the return phase inclination for constant outward phase flight times for position C if launched into the moon's orbit plane

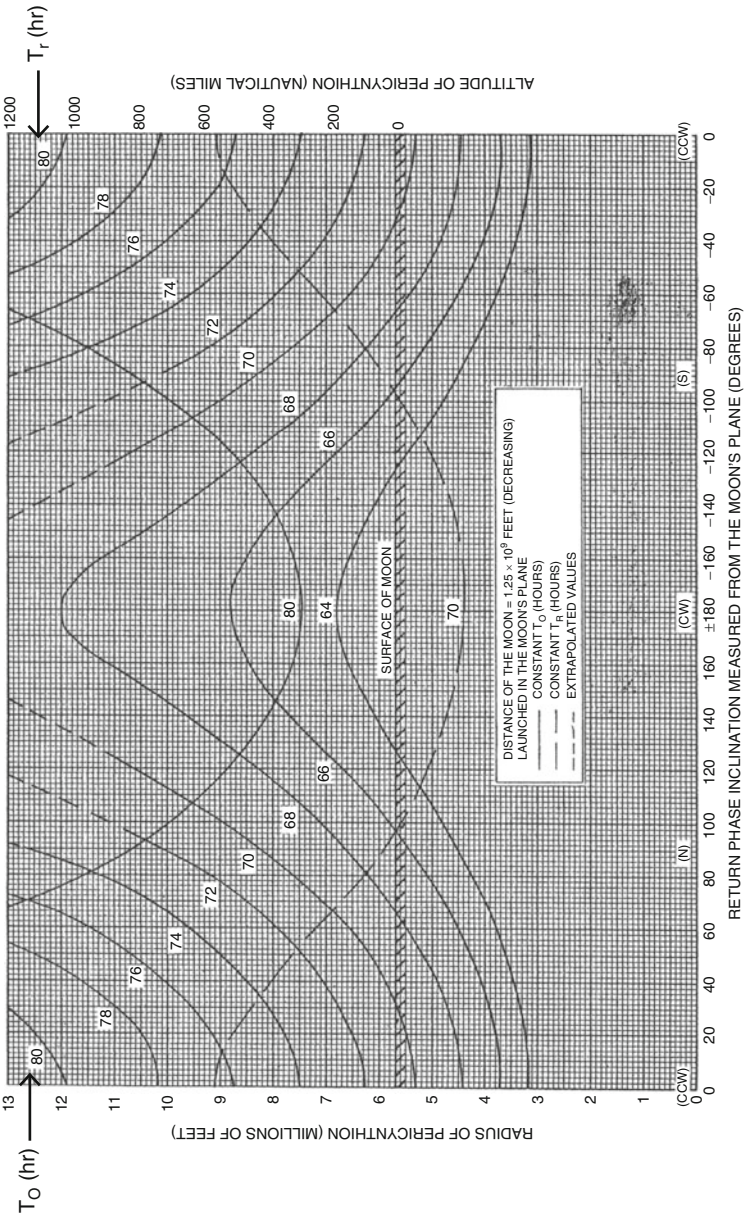

Fig. 7.25 The spacecraft's pericynthion distance versus the return phase inclination for constant outward phase flight times for position D if launched into the moon's orbit plane

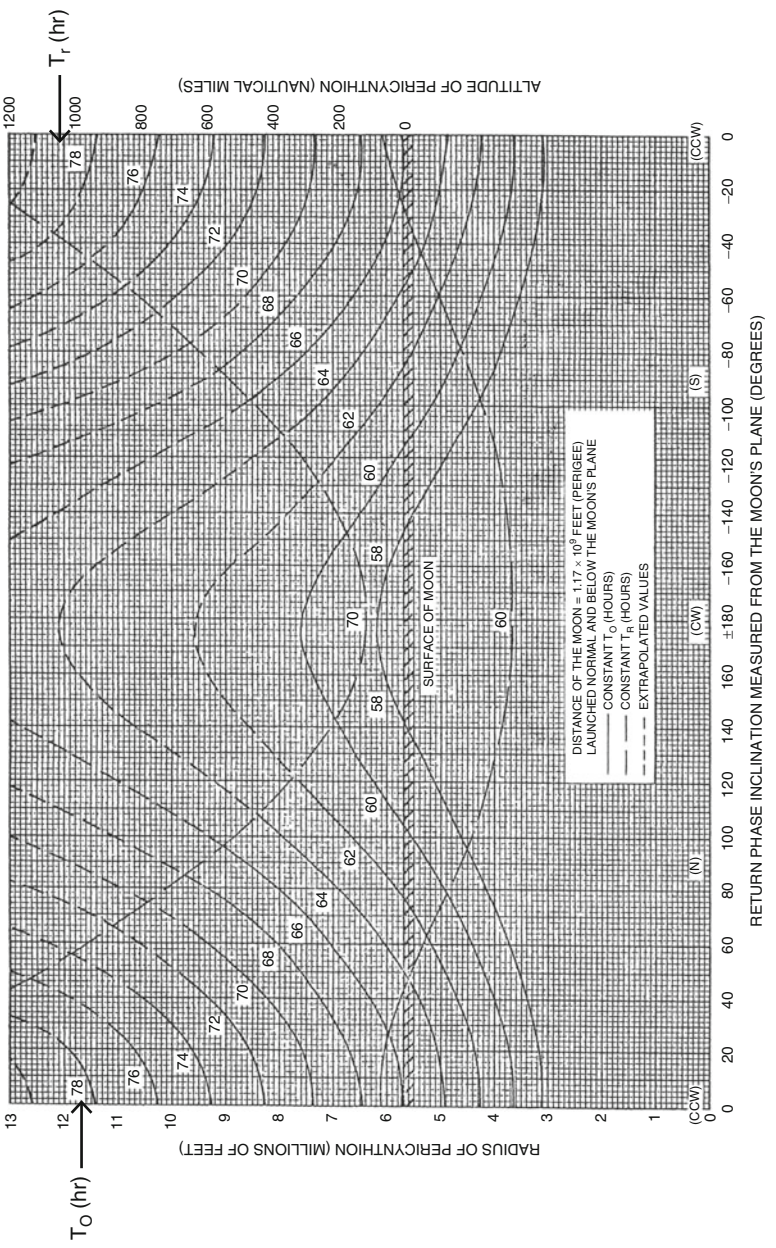

Fig. 7.26 The spacecraft's pericynthion distance versus the return phase inclination for constant outward phase flight times for position A′ if launched normal to and below the moon's orbit plane

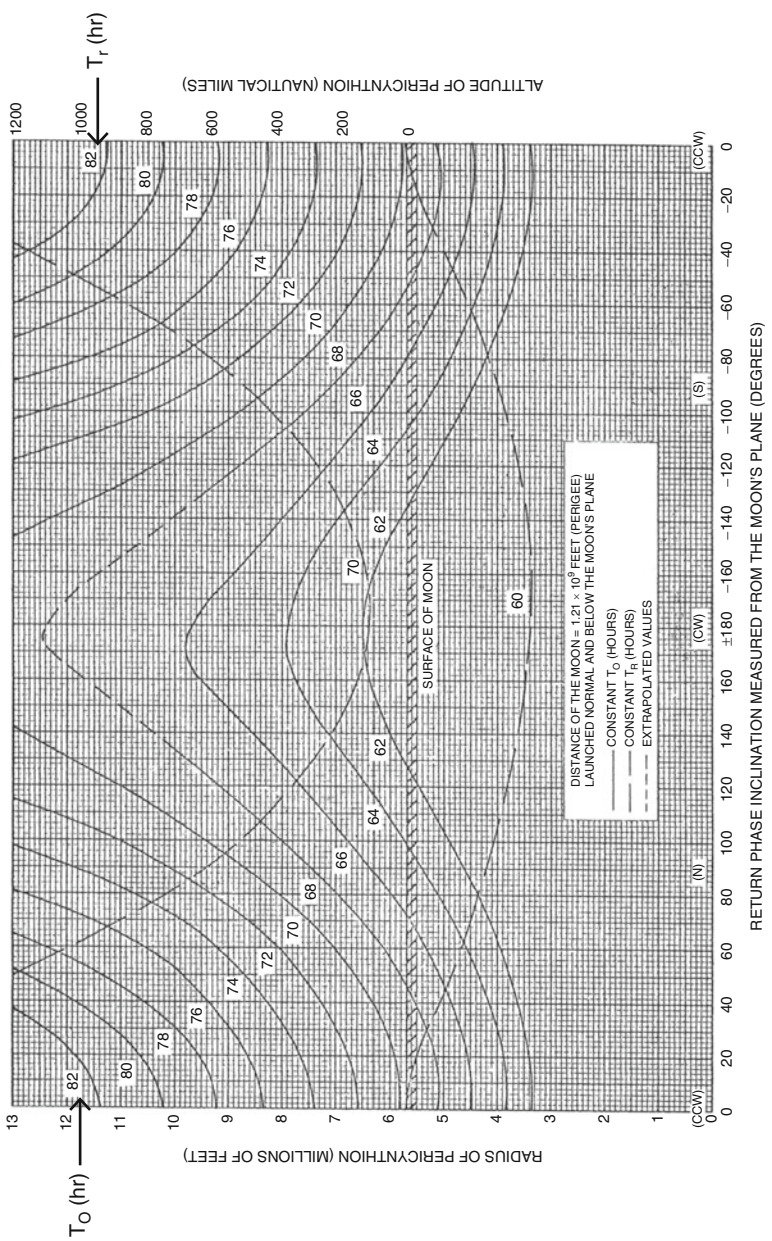

Fig. 7.27 The spacecraft's pericynthion distance versus the return phase inclination for constant outward phase flight times for position A if launched normal to and below the moon's orbit plane

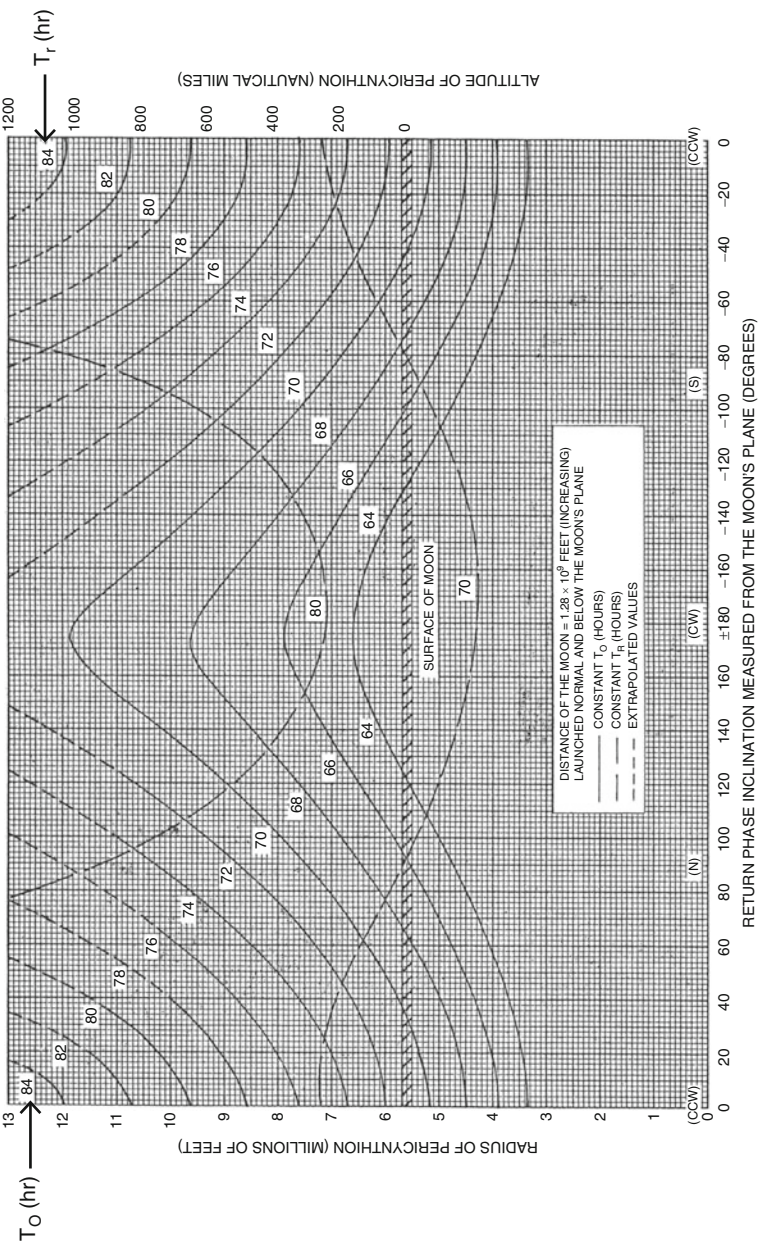

Fig. 7.28 The spacecraft's pericynthion distance versus the return phase inclination for constant outward phase flight times for position B if launched normal to and below the moon's orbit plane

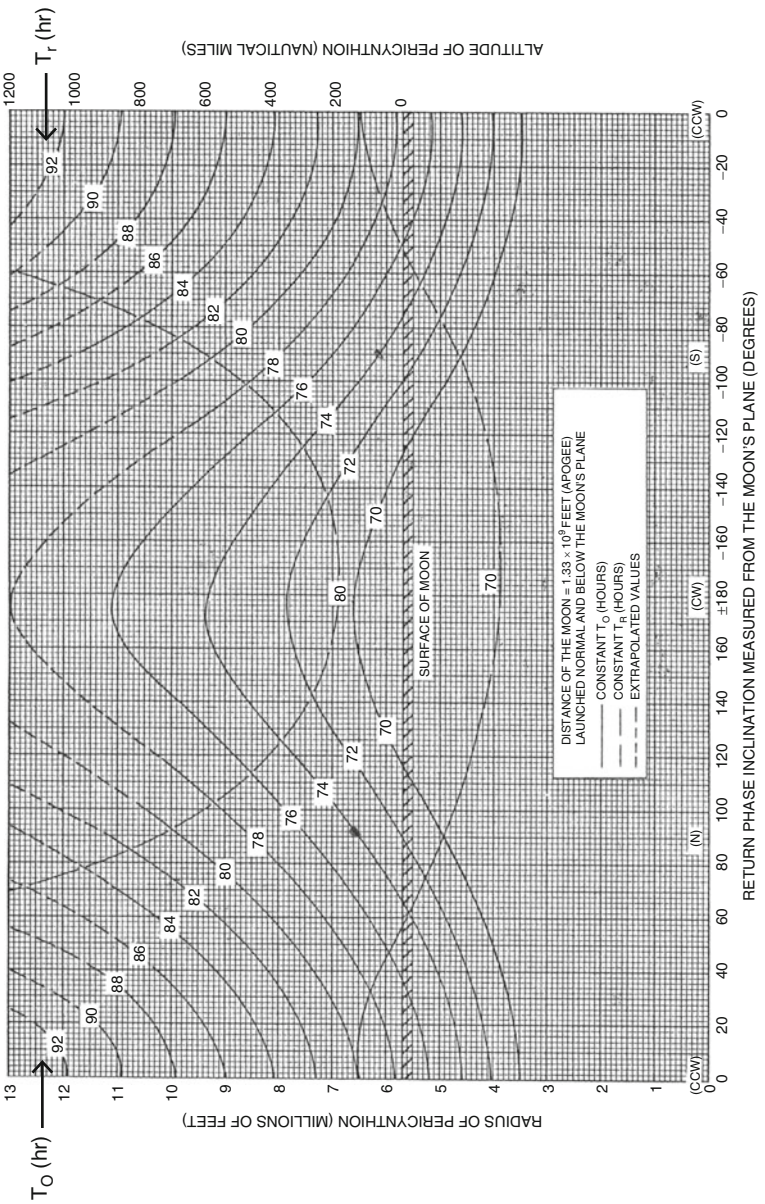

Fig. 7.29 The spacecraft's pericynthion distance versus the return phase inclination for constant outward phase flight times for position C if launched normal to and below the moon's orbit plane

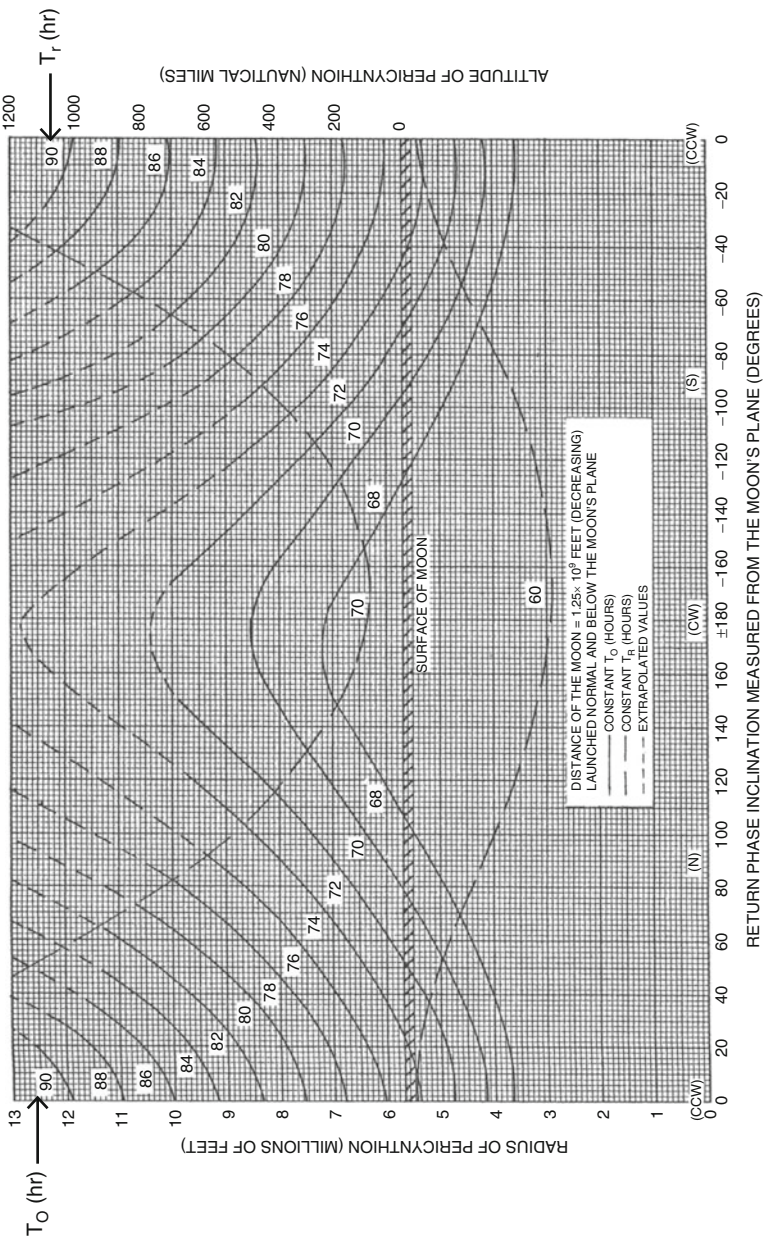

Fig. 7.30 The spacecraft's pericynthion distance versus the return phase inclination for constant outward phase flight times for position D if launched normal to and below the moon's orbit plane

We turn now to the effect of the moon's distance on the pericynthion altitude for a fixed flight time to the moon and fixed outward and return inclinations. Since the V_∞ at the moon must increase with increasing lunar distance, the pericynthion altitude must decrease to maintain the some bending of the hyperbolic trajectory for the spacecraft's return to this earth (see Eqs. 3.27 and 3.33). Similarly, this result also holds true for a fixed return flight time.

Example of moon's distance on pericynthion altitude for a fixed flight time to the moon and fixed outward and return inclinations:

$i_o = 0°$, $i_r = 60°$, and $T_o = 68$ h

Figure 7.22 (Position A) ⇒ pericynthion altitude = 620 nm = 1148 km
Figure 7.23 (Position B) ⇒ pericynthion altitude = 284 nm = 526 km

A final characteristic of these curves is the symmetry condition. As mentioned above, circumlunar trajectories are symmetric with respect to the moon's phase. Figures 7.21, 7.22, 7.23, 7.24, and 7.25 for which the outward phase lies in the moon's plane, i.e., the outward phase inclination is $i_o = 0°$, indicate this result since values for return phase inclinations i_r are equal to $-i_r$ values.

Examples in Fig. 7.21:

$i_o = 0°$, $i_r = 60°$ and $T_o = 62$ h
⇒ pericynthion altitude = 300 nm = 556 km
$i_o = 0°$, $i_r = -60°$ and $T_o = 62$ h
⇒ pericynthion altitude = 300 nm = 556 km

Figures 7.26, 7.27, 7.28, 7.29, and 7.30 are for launches normal to and below the moon's orbit plane, i.e., the outward phase inclination is $i_o = -90°$. A comparison of pericynthion altitude for return inclinations i_r with inclinations $-i_r$ (where i_r is positive) indicates that negative return inclinations result in lower pericynthion distances for a given outward phase flight time. This fact can be explained by means of the general observation that the angle through which the moon phase velocity vector must turn at entrance and exit of the moon's sphere of influence is greater for outward and return earth phases on the same side of the moon's orbit plane ($i_r = -90° < 0$ and $i_r < 0$) than for these phases on opposite sides of the moon's orbit plane ($i_r = -90° < 0$ and $i_r > 0$). Thus, for a fixed outward time of flight, which implies an essentially fixed moon phase velocity magnitude, the pericynthion distance must be less to achieve the required greater turning of the velocity vector for (in this case) negative return phase inclinations from Eqs. (3.27) and (3.33).

Examples in Fig. 7.26 (i_o):

$i_o = -90°$, $i_r = 60°$ and $T_o = 66$ h
⇒ pericynthion altitude = 224 nm = 415 km
$i_o = -90°$, $i_r = -60°$ and $T_o = 66$ h
⇒ pericynthion altitude = 150 nm = 278 km

Category (2): Time of Flight

The times of flight considered here are the times from injection to pericynthion, from pericynthion to re-entry, and the sum of these values, i.e., the total time of flight. For the fixed conditions listed above, specifying the outward and return inclinations and the outward time of flight determine a unique trajectory and, in particular, a specific return time of flight. Figures 7.31, 7.32, 7.33, 7.34, 7.35, 7.36, 7.37, 7.38, 7.39, and 7.40 present this return time versus the outward time for constant return phase inclinations with the moon's orbit plane. Each graph is drawn for an in-plane or normal firing with respect to the moon's orbit plane and for a particular position of the moon in its orbit. Constant total flight times are also plotted as indicated by the labels shown in the right-hand side of each figure.

In comparing these graphs, several observations can be made. The first observation is that launches in the moon's orbit plane produce equal or greater flight times in the return phase. Return flight times for launches normal to the moon's orbit plane are nearly symmetric with respect to 90° returns. Secondly, the difference in the outward and return times of flight may be considerable, as you will demonstrate in an exercise.

As indicated on all the time graphs, the dashed curves represent extrapolated values, i.e., values not obtainable with the simplified model in the parametric plots. There is no guarantee that these extrapolated trajectories exist and, in fact, some do not exist. In particular, there is a constraint cut off in the upper region of the cw return trajectories. These extrapolated values are verified in the next step of the trajectory design procedure, which is to run precision software after selecting the best opportunity available in the parametric plots.

Examples in Fig. 7.31 (Minimum Perigee Position A′):

Outward FT = 70 h and return $i_r = 0°$
$\Rightarrow$ Return FT = 72 h = 3 days
Outward FT = 65 h and return $i_r = 30°$
$\Rightarrow$ Return FT = 68.5 h

Category (3): Fixed Pericynthion Altitude

Consider free-return circumlunar trajectories that approach very close to the moon. This class of trajectories can be generated by cross-plotting Figs. 7.21, 7.22, 7.23, 7.24, 7.25, 7.26, 7.27, 7.28, 7.29, and 7.30. This cross-plotting was done for an altitude of 100 nautical miles to produce Figs. 7.41, 7.42, and 7.43. One may choose specific outward and return inclinations and then obtain a specific pericynthion distance by controlling the outward time of flight. This time of flight depends on the moon's distance from the earth as indicated in Fig. 7.41 (for launches in the moon's orbit plane) and Fig. 7.42 (for launches orthogonal to the moon's orbit plane) when the moon is at positions A, B, C, or D. The required outward time of flight decreases as the return inclinations go from 0° to 180°. However, the return time of flight increases. Recall that the pericynthion altitude is greater for cw returns than for ccw returns. Therefore, to decrease the pericynthion altitude for cw returns, holding the turning angle of the moon phase velocity nearly fixed, one must increase the

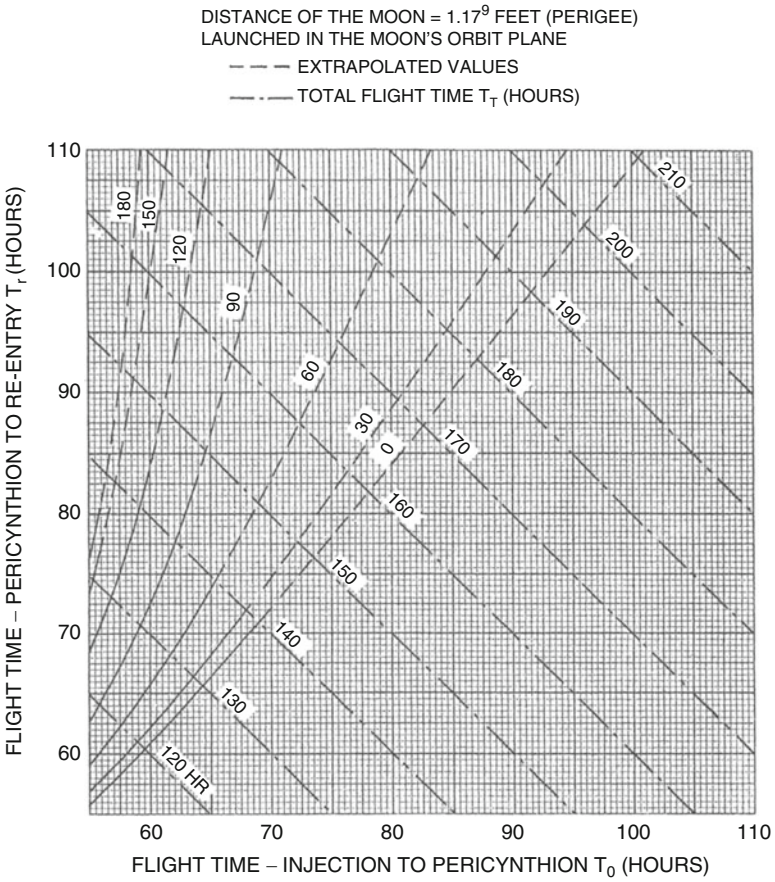

Fig. 7.31 The return flight time versus the outward flight time for constant return phase inclination for position A′ if launched into the moon's orbit plane

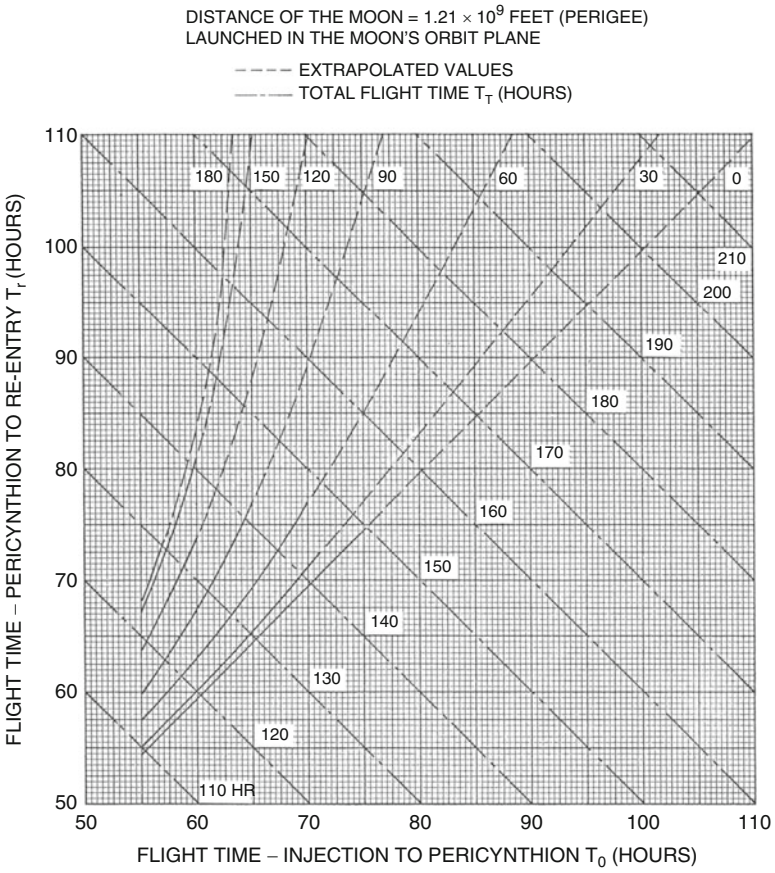

Fig. 7.32 The return flight time versus the outward flight time for constant return phase inclination for position A if launched into the moon's orbit plane

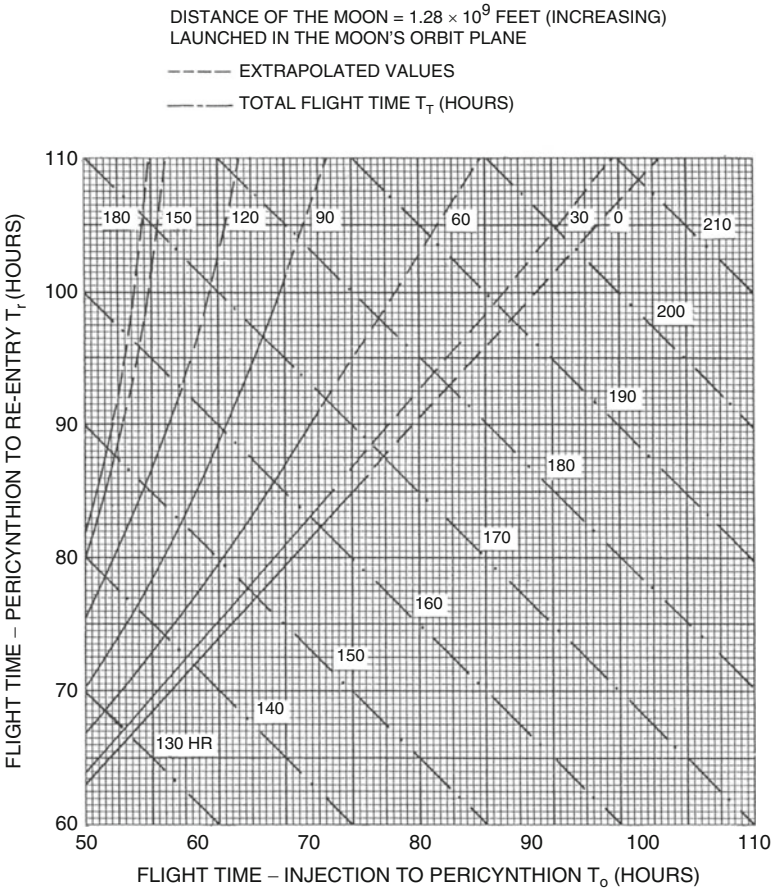

Fig. 7.33 The return flight time versus the outward flight time for constant return phase inclination for position B if launched into the moon's orbit plane

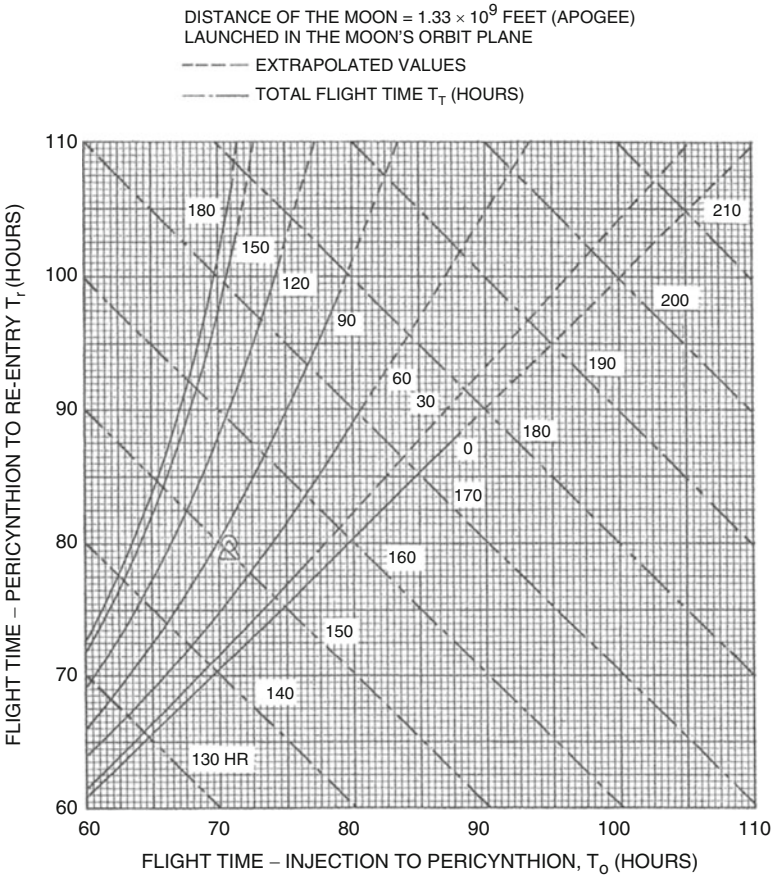

Fig. 7.34 The return flight time versus the outward flight time for constant return phase inclination for position C if launched into the moon's orbit plane

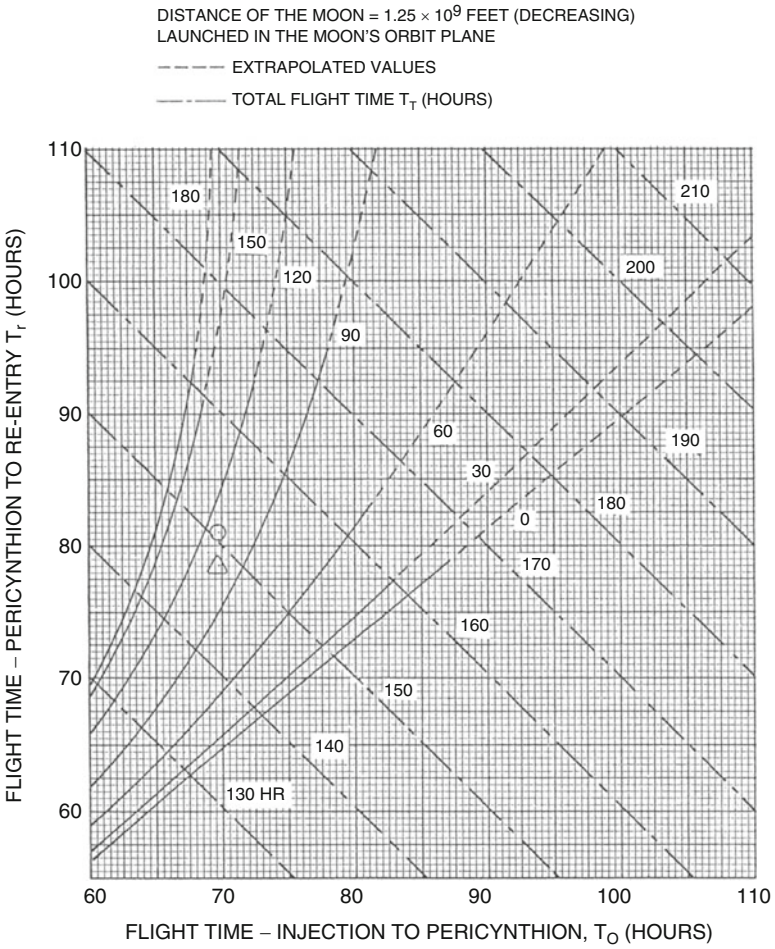

Fig. 7.35 The return flight time versus the outward flight time for constant return phase inclination for position D if launched into the moon's orbit plane

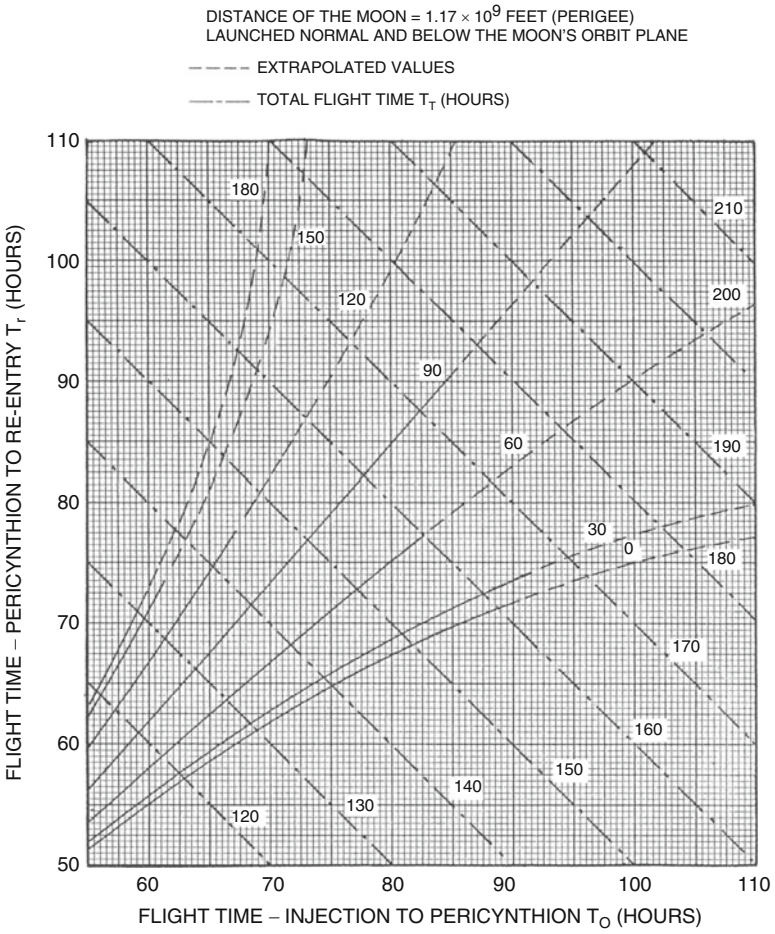

Fig. 7.36 The return flight time versus the outward flight time for constant return phase inclination for position A′ if launched normal to and below the moon's orbit plane

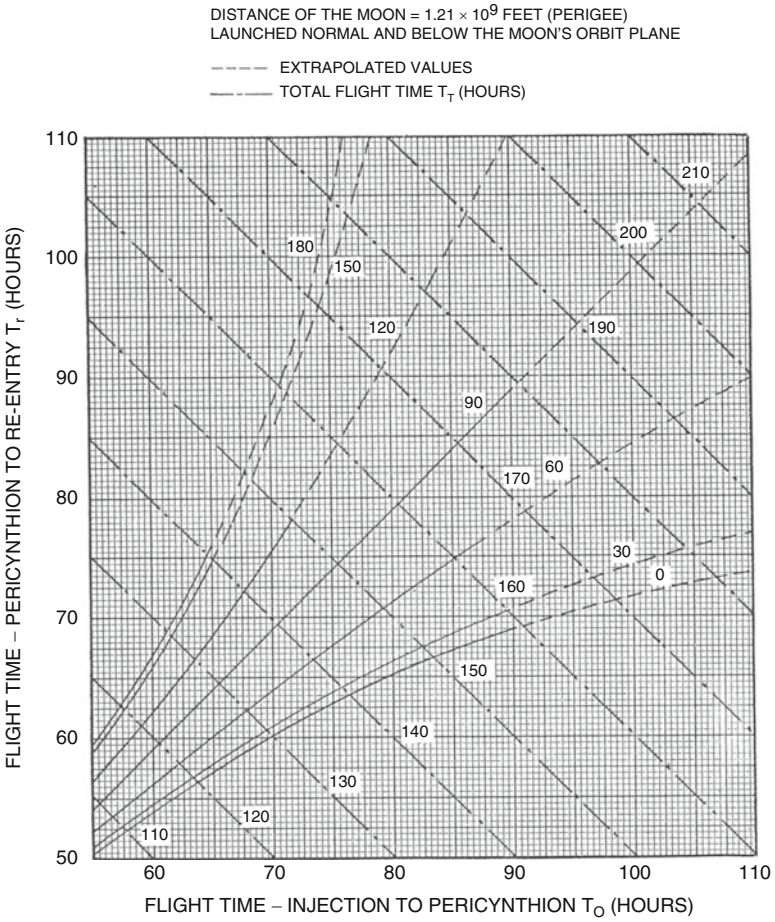

Fig. 7.37 The return flight time versus the outward flight time for constant return phase inclination for position A if launched normal to and below the moon's orbit plane

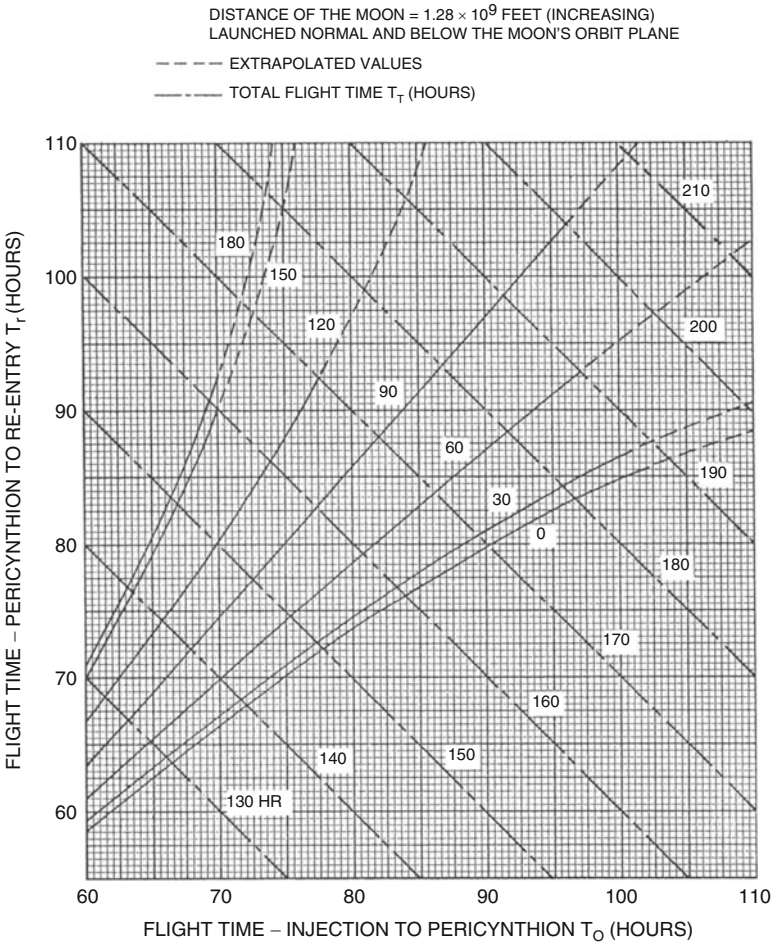

Fig. 7.38 The return flight time versus the outward flight time for constant return phase inclination for position B if launched normal to and below the moon's orbit plane

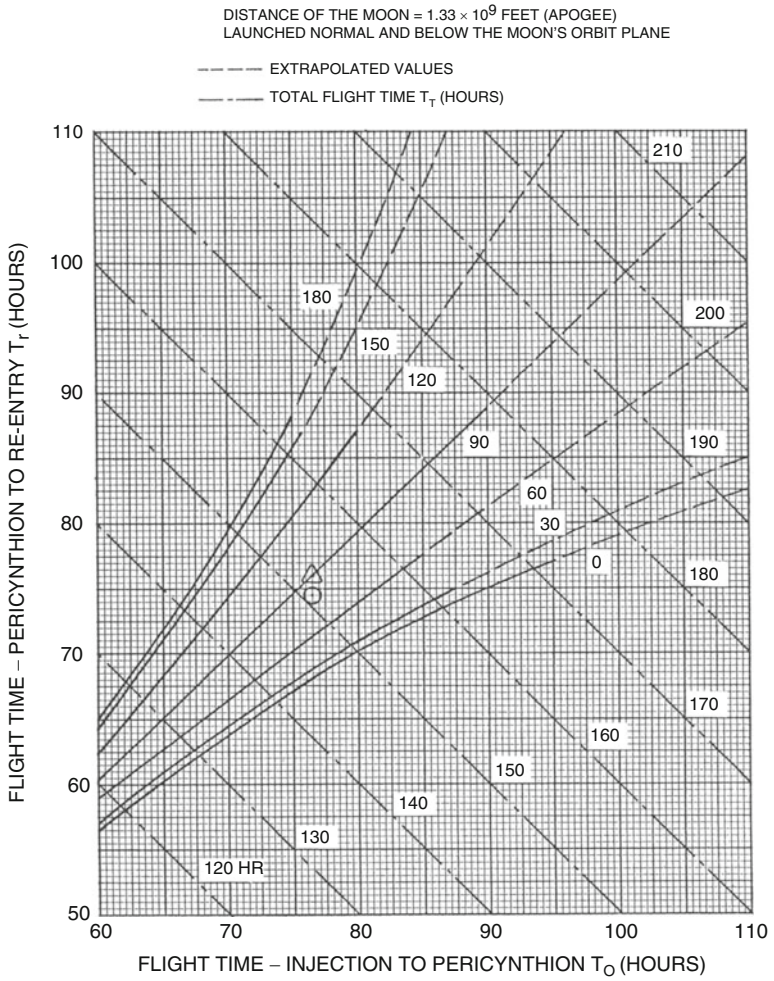

Fig. 7.39 The return flight time versus the outward flight time for constant return phase inclination for position C if launched normal to and below the moon's orbit plane

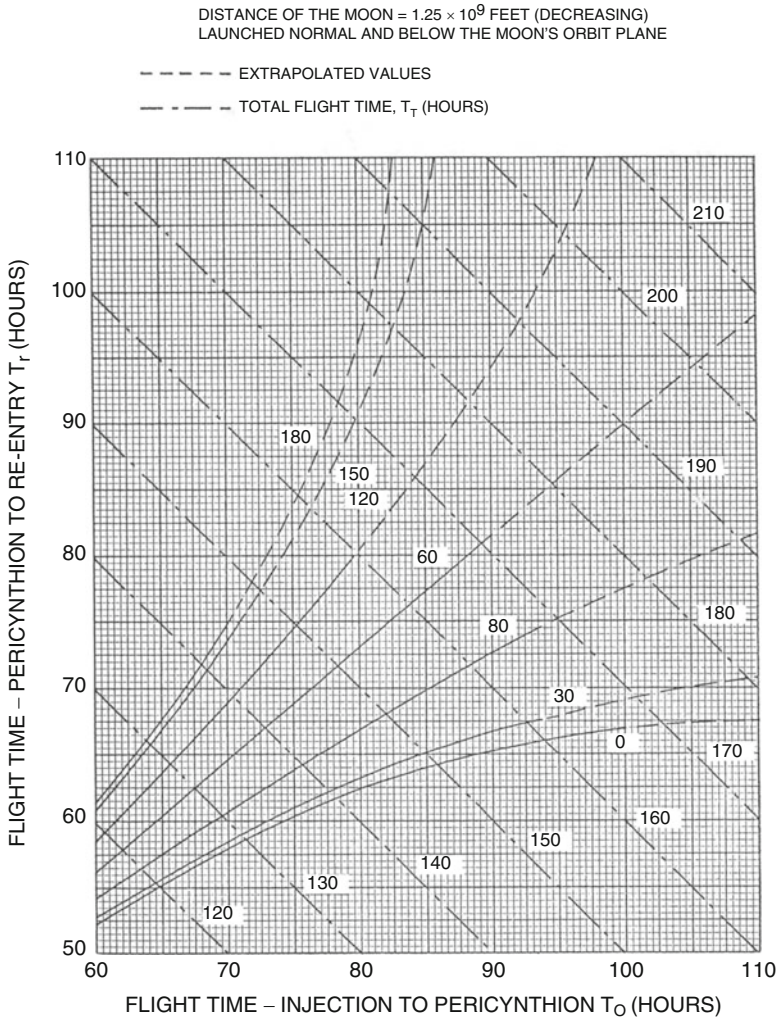

Fig. 7.40 The return flight time versus the outward flight time for constant return phase inclination for position D if launched normal to and below the moon's orbit plane

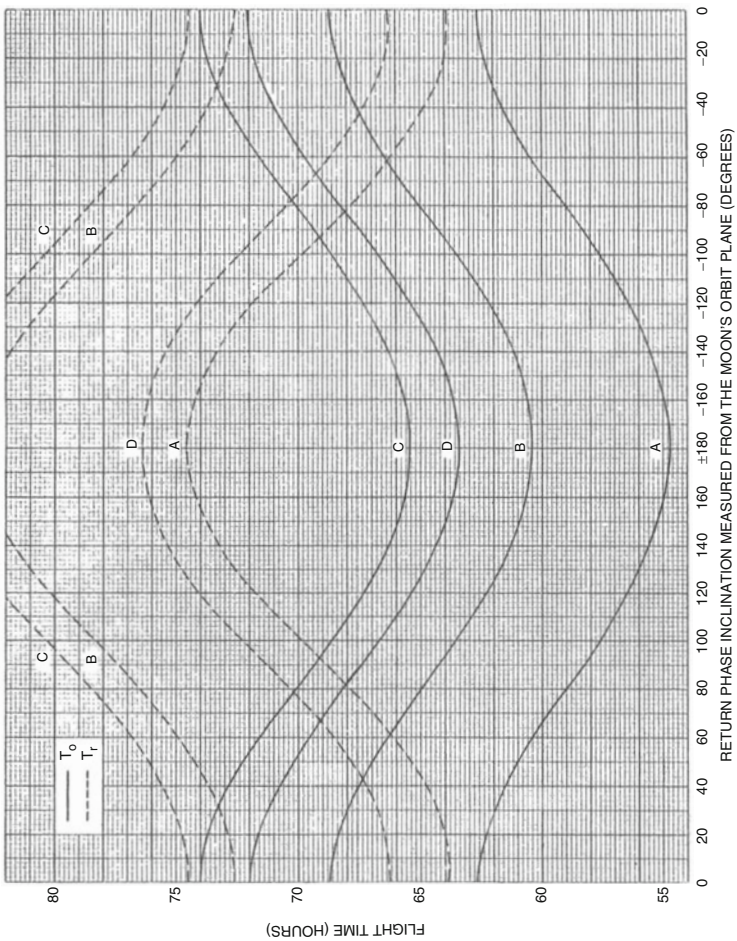

Fig. 7.41 Outward and return flight times versus the return phase inclination for various distances of the moon for launch in moon's orbit plane. The pericynthion altitude is fixed at 100 nautical miles

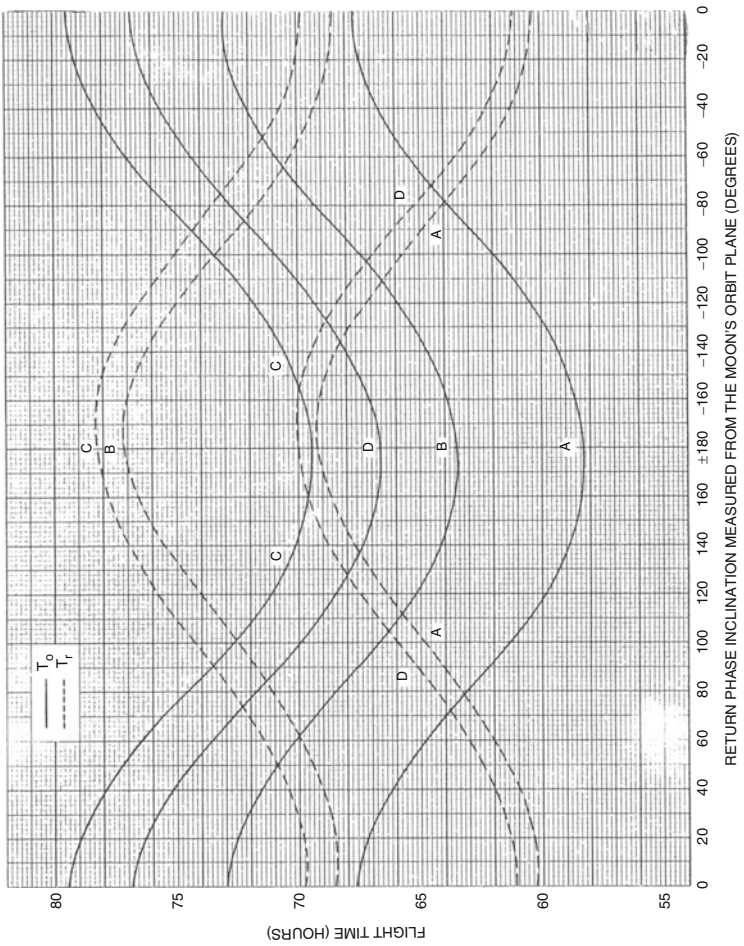

Fig. 7.42 Outward and return flight times versus the return phase inclination for various distances of the moon for launch orthogonal to moon's orbit plane from the south. The pericynthion altitude is fixed at 100 nautical miles

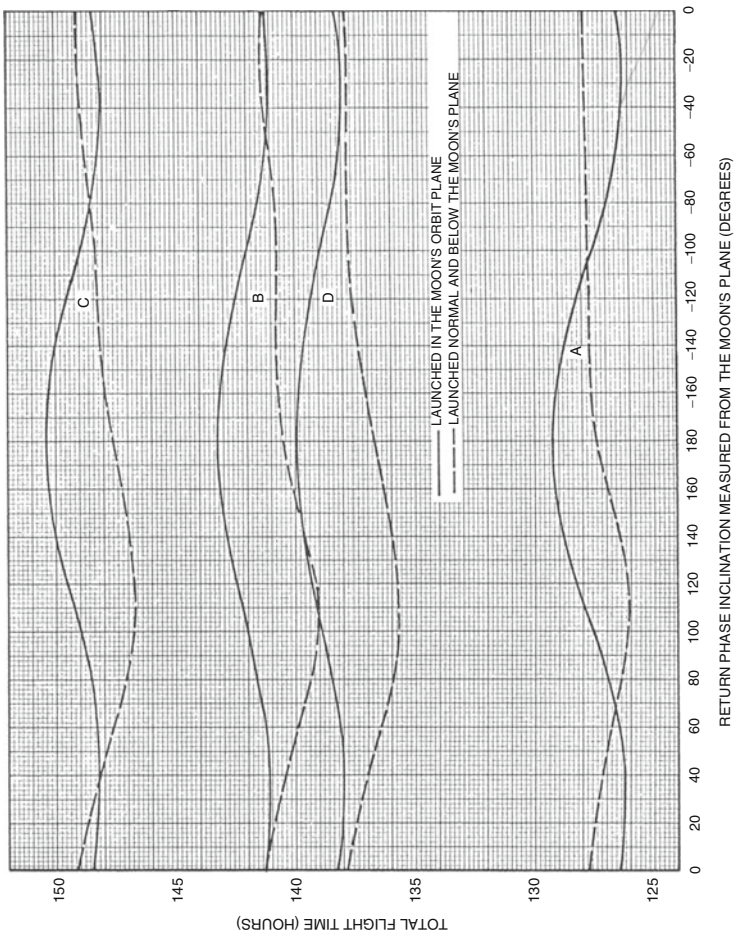

Fig. 7.43 Total flight time versus return phase inclination for various distances of the moon. Pericynthion altitude is fixed at 100 nautical miles

velocity magnitude, which is equivalent to decreasing the outward flight time. A similar argument can be used to explain the increase in the return flight time when going from ccw to cw returns. These variations in flight time are common to both Figs. 7.41 and 7.42 regardless of whether the spacecraft is launched in the moon's orbit plane or perpendicular to the moon's orbit plane. Figure 7.43 gives the total time of flight, which is strongly affected by the distance to the moon with variations over 20 km, but nearly constant otherwise.

Category (4): Azimuth and Inclination

Given that a specific circumlunar trajectory is to be generated, what launch azimuth from the Cape and what return inclination with respect to (wrt) the earth's equatorial plane are required? This situation would be for specific outward and return inclinations wrt the moon's orbit plane. First, it is clear that the launch azimuth, together with the declination of the Cape, will determine the outward phase inclination wrt the earth's equator. This relationship is shown in Fig. 7.46. The inclination i_{Mo} of this outward trajectory plane wrt the plane of the moon's orbit will in turn depend on the inclination i_o wrt the equatorial plane, the inclination i_M of the moon's orbit plane, and the declination δ_M of the moon, as shown in Fig. 7.44. Figures 7.47, 7.48, 7.49, 7.50, and 7.51 indicate the relationships between these parameters for several inclinations of the moon's orbit plane. These figures, together with Fig. 7.46, determine the launch azimuth from the Cape for a desired trajectory plane's inclination wrt the moon's orbit plane. Note that the inclinations are double valued and depend on the type of coast chosen.

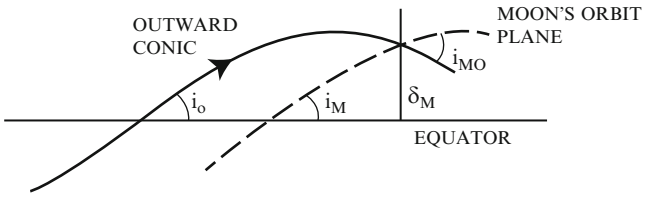

Fig. 7.44 Inclination relationships

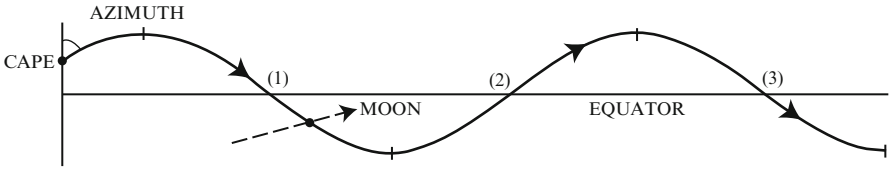

Fig. 7.45 Mercator projection of trajectory types

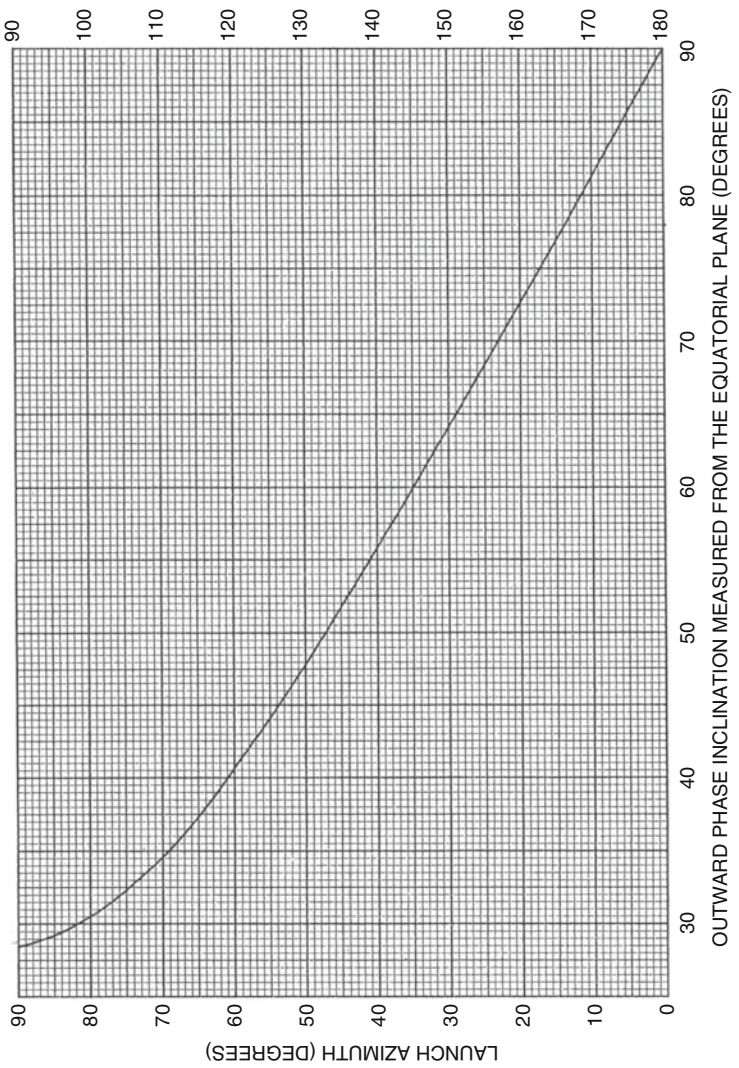

Fig. 7.46 Launch azimuth from Cape Canaveral versus the outward phase inclination

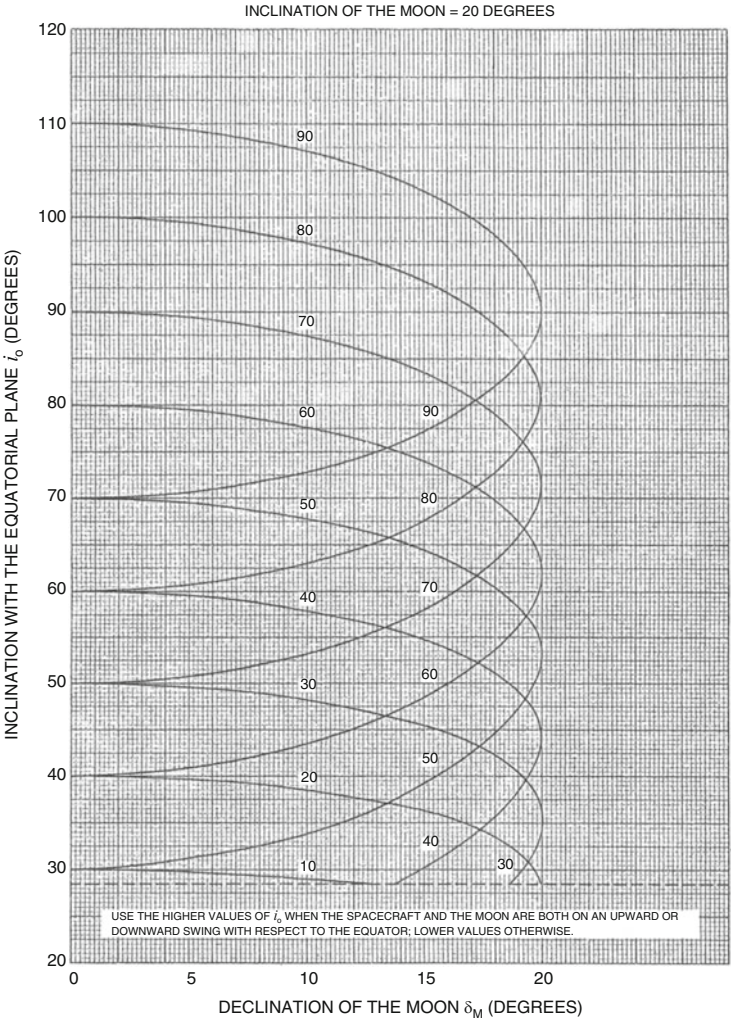

Fig. 7.47 Inclination wrt the equatorial plane versus the declination of the moon for constant inclinations wrt the moon's orbit plane: inclination of the moon = 20°

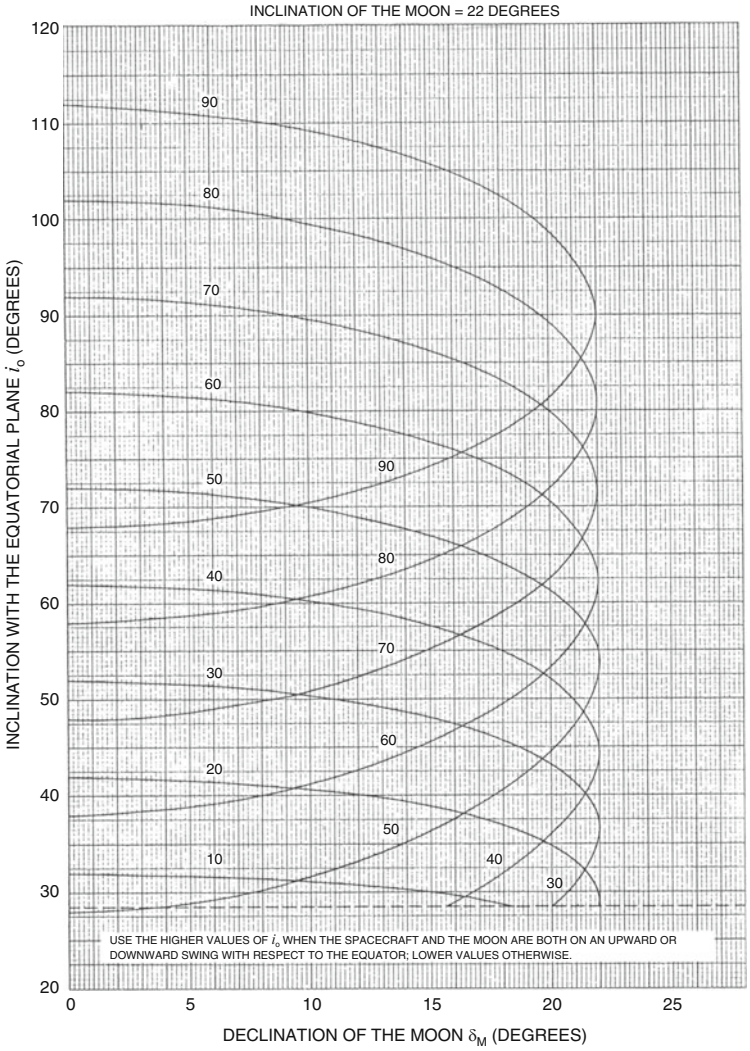

Fig. 7.48 Inclination wrt the equatorial plane versus the declination of the moon for constant inclinations wrt the moon's orbit plane: inclination of the moon = 22°

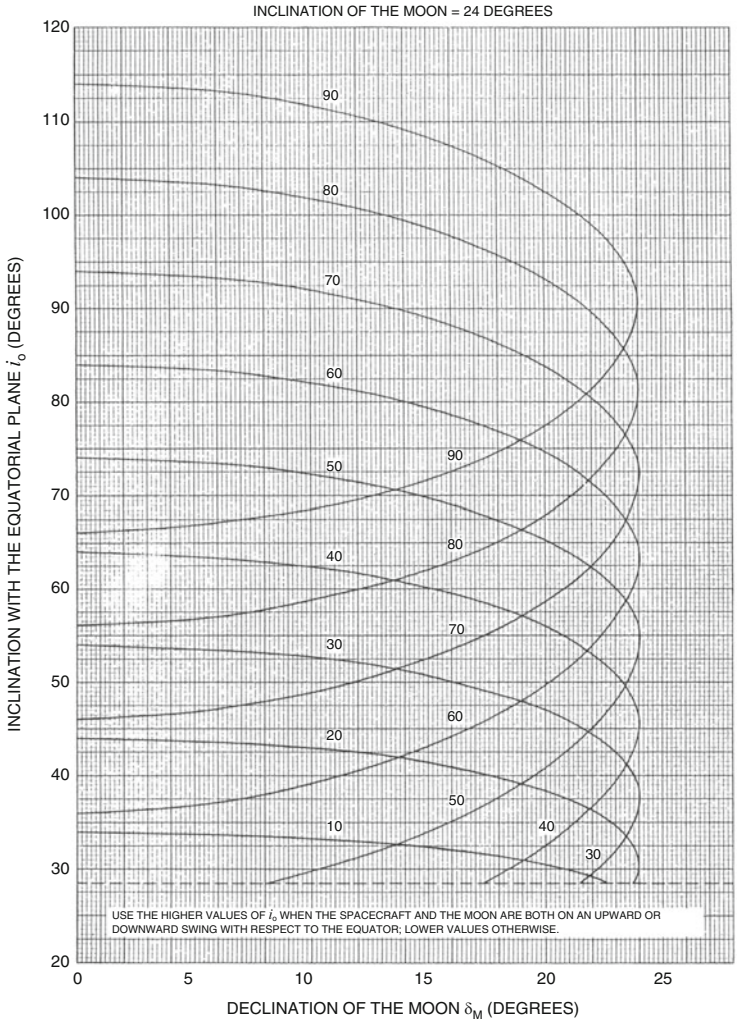

Fig. 7.49 Inclination wrt the equatorial plane versus the declination of the moon for constant inclinations wrt the moon's orbit plane: inclination of the moon = 24°

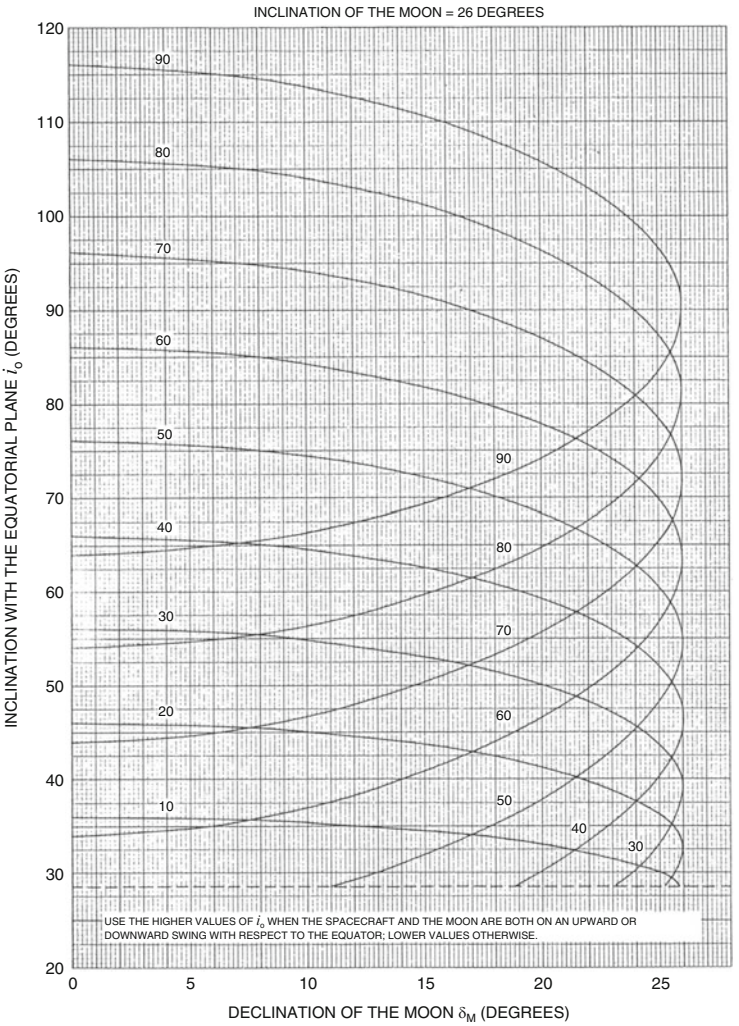

Fig. 7.50 Inclination wrt the equatorial plane versus the declination of the moon for constant inclinations wrt the moon's orbit plane: inclination of the moon = 26°

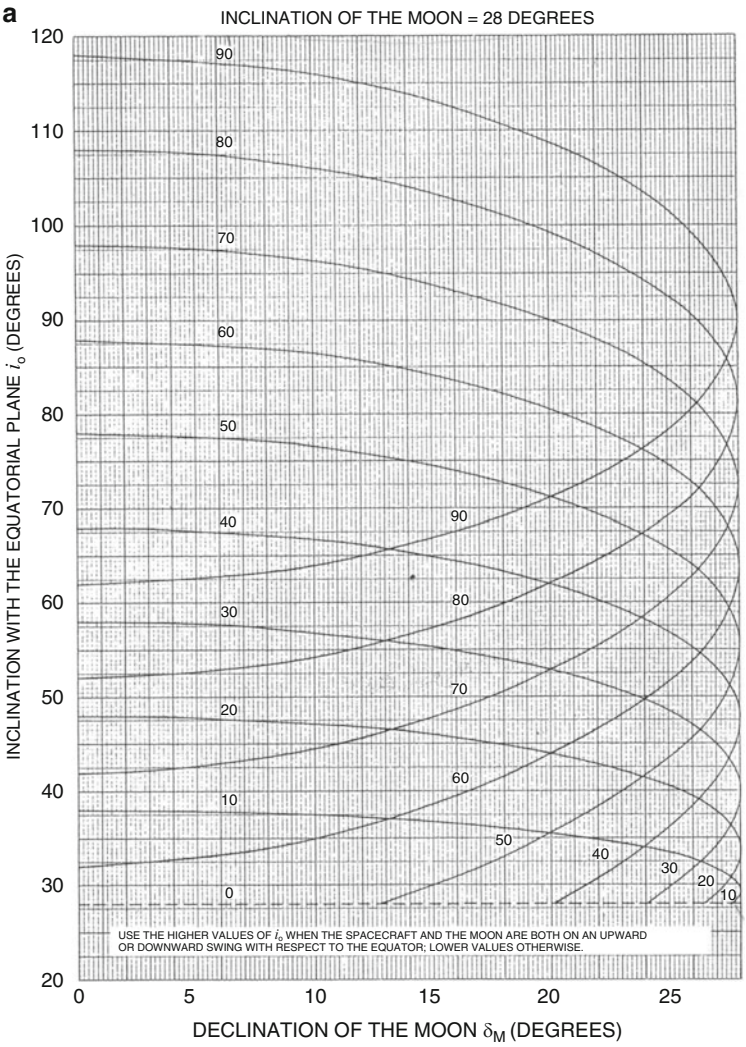

Fig. 7.51 (**a**) Inclination wrt the equatorial plane versus the declination of the moon for constant inclinations wrt the moon's orbit plane: inclination of the moon = 28°. (**b**) Inclination wrt the equatorial plane versus the declination of the moon for constant inclinations wrt the moon's orbit plane (complete for return trajectories)

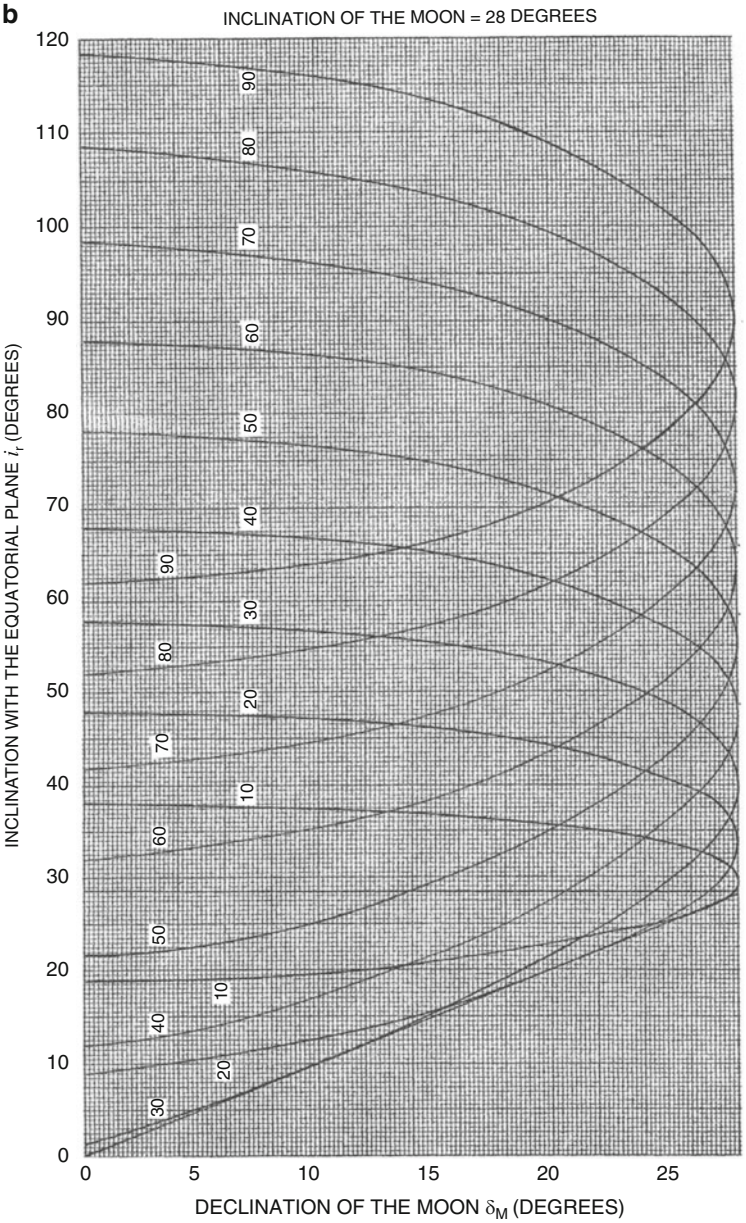

Fig. 7.51 (continued)

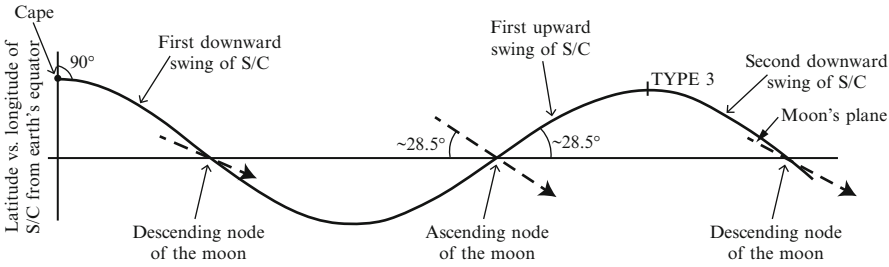

Fig. 7.52 Trajectory characteristics for launching in the moon's orbit plane

But, before we can use Figs. 7.47, 7.48, 7.49, 7.50, and 7.51, we must consider the classification of the types of coast trajectories. Since the complete trajectory from launch to arrival at the moon may produce an in-plane angle greater than 360°, Mercator projections such as Fig. 7.45 are very convenient. Figure 7.45 presents the three types of coasting orbits that we may encounter:

Type (1) is defined as the coasting orbit required to intercept the moon on the spacecraft trajectory's first downward swing.
Type (2) is the coast trajectory that will intercept the moon on the trajectory's next upward swing. This coast is the section labeled (2) in Fig. 7.45.
Type (3) is the coast trajectory that will intercept the moon on its next downward swing after the type (2) section.

It is possible that a Type (1) or (2) trajectory will not exist for a particular set of circumstances; however, a Type (3) will always exist. In all cases, the outward phase conic will consist of a launch powered flight arc, a coasting arc in the parking orbit, and a free-flight (post injection) arc.

The inclination of the return phase conic as a required input in the trajectory selection procedure must be referenced to the earth's equatorial plane. This input value may vary from −90° to 90°. The inclination is plus if the vehicle leaves the sphere of influence upward wrt the equatorial plane and negative otherwise.

Fig. 7.46 provides the launch azimuth from Cape Canaveral versus the outward phase inclination and, for the return phase, Figs. 7.47–7.51 present a direct relationship between the inclination wrt the moon's orbit plane and the inclination wrt the equatorial plane. For example, Figs. 7.46 and 7.51 show that, when the inclination i_M of the moon is 28°, it is possible to launch into the moon's orbit plane, using a 90°-launch azimuth from the Cape.

In the Mercator projection in Fig. 7.52, the trajectory follows a plane that is through the center of the earth; however, zero inclination wrt the moon is attained only if the trajectory motion of the spacecraft corresponds with the motion of the moon. This figure indicates that this correspondence occurs on the day when the moon is passing through its descending node. A Type (3) coast trajectory is necessary in the case considered in Fig. 7.52 because Type (1) is too short and Type (2) crosses the moon's plane with about a 57° inclination.

The next section relates the inclination to the re-entry (maneuver) angle.

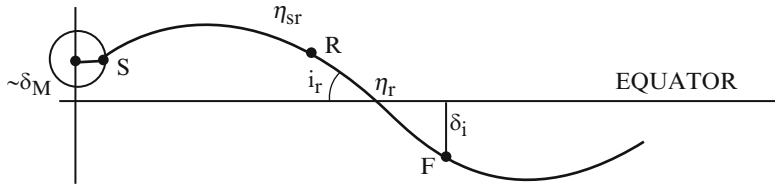

Fig. 7.53 Relation of the re-entry maneuver angle to the return phase geometry

Category (5): Maneuver Angle and Touchdown Latitude
Re-entry is described in terms of the maneuver angle or re-entry angle η_r, which is defined as follows.

Def.: The maneuver angle or re-entry angle η_r is the great circle arc required by the spacecraft in going from the re-entry point, at about 400,000 ft (122 km) altitude, to a specified landing site.

The maneuver angle is the downrange angle in the orbit plane from where the spacecraft entered the atmosphere to landing. It is assumed that, during this "maneuver," the spacecraft remains in the same plane as the return phase conic. The magnitude of this angle for crewed re-entry presently varies between 20° and 60°. Figure 7.53 is a Mercator projection of a possible return phase conic and maneuver angle, where δ_i is the desired latitude of the touchdown (TD) point. The declination of the spacecraft's exit point from the sphere of influence is approximately that of the moon when the vehicle is at pericynthion. (Examination of many runs indicates that the two declinations will be within 1.5° of each other.) Also, the in-plane angle η_{sr} measured from the sphere of influence S (or essentially the moon) to the re-entry point R depends essentially on the time of the return flight from pericynthion passage to re-entry and the re-entry (velocity) flight path angle. For a re-entry angle of 96°, an examination of trajectory computer runs indicates that this angle η_{sr} will be within 5° of 160° regardless of the time of flight and the distance of the moon. Figure 7.53 shows that the maneuver angle is a function only of the declination δ_M of the moon at the vehicle's pericynthion, the inclination i_r of the return phase conic, and the touchdown latitude F. The relations between these quantities are given in Figs. 7.54, 7.55, and 7.56 for three fixed values of the re-entry maneuver angle. It is interesting to note the limitations on the available touchdown latitudes for a maneuver angle of 20°. This limitation is caused by the fact that the total in-plane angle from the moon to touchdown adds up to 180°. Thus, for a given declination of the moon, the only available touchdown latitude is the negative of this declination, regardless of the return inclination. A maneuver angle of 40° will result in a total in-plane angle of $160° + 40° = 200°$. Thus, returning above the equator will cause the spacecraft to reach touchdown latitudes lower than the negative of the declination of the moon and returning below the equator will result in touchdown latitudes below that of the negative of the declination of the moon. This effect is even more pronounced in Fig. 7.56 where the maneuver angle is 60°. If maneuver angles greater than 60° are allowed, even greater ranges of touchdown latitudes will be produced.

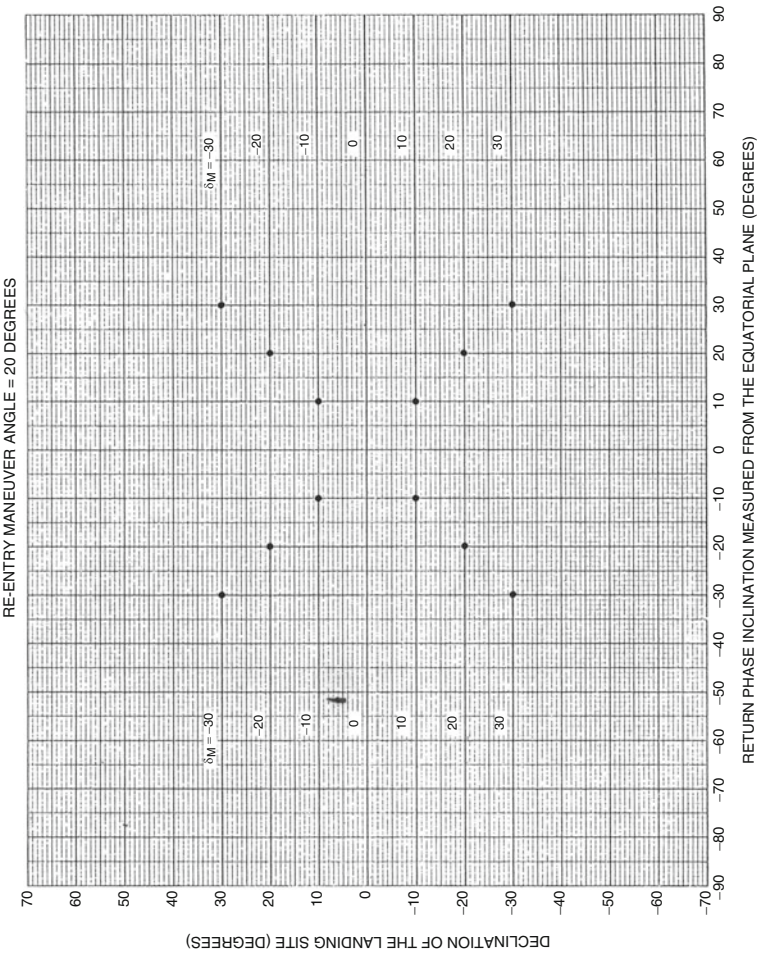

Fig. 7.54 Declination of the landing site versus the return phase inclination wrt the equatorial plane for fixed declinations of the moon: re-entry maneuver angle = 20°

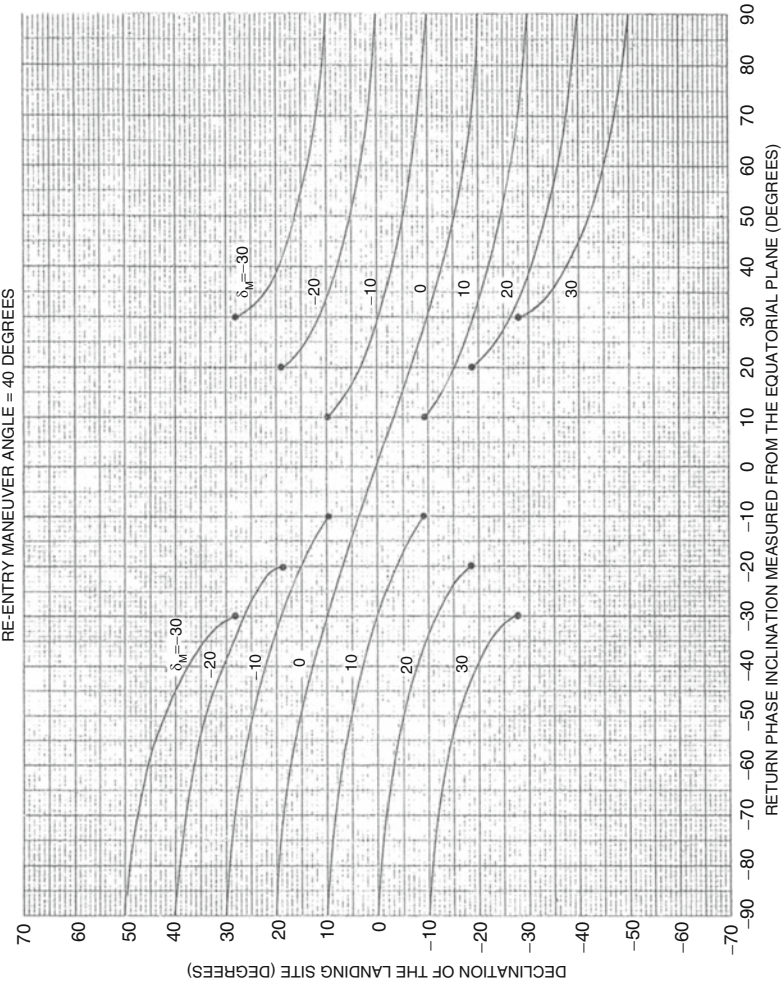

Fig. 7.55 Declination of the landing site versus the return phase inclination wrt the equatorial plane for fixed declinations of the moon: re-entry maneuver angle = 40°

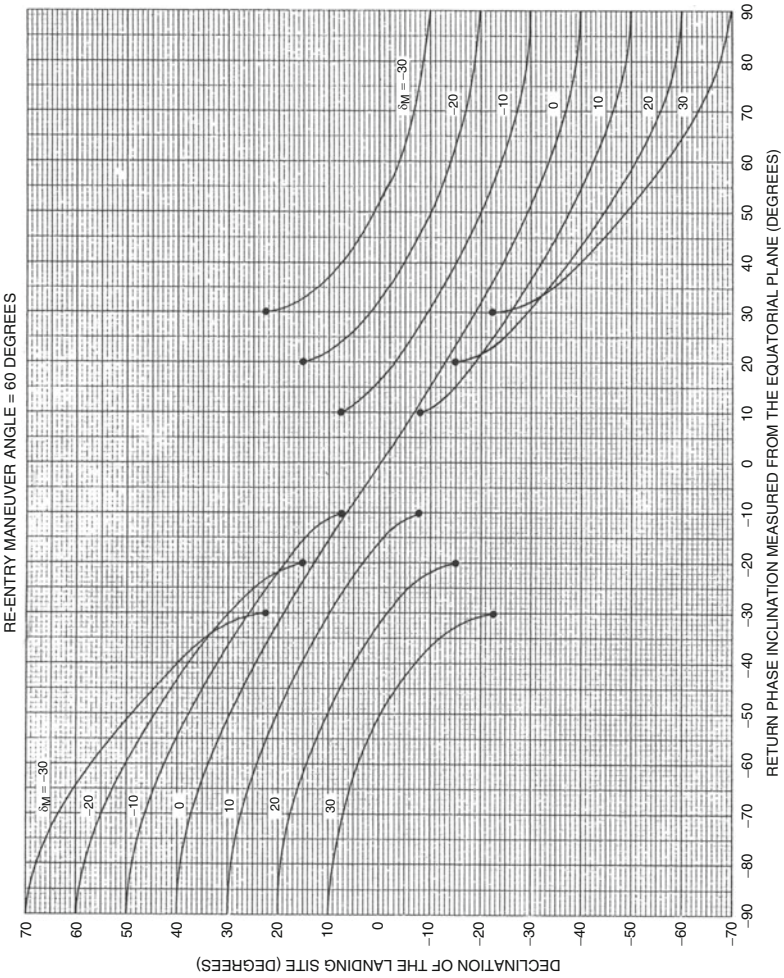

Fig. 7.56 Declination of the landing site versus the return phase inclination with the equatorial plane for fixed declinations of the moon: re-entry maneuver angle = 60°

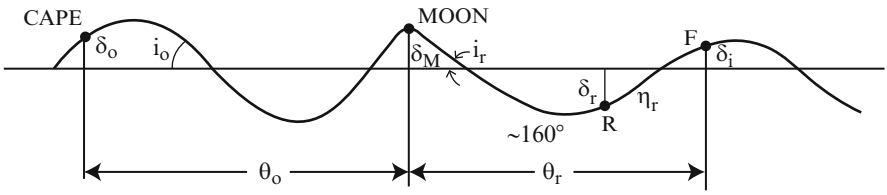

Fig. 7.57 Mercator projection of the outward and return phases neglecting the moon phase

Examples for Figs. 7.54, 7.55, and 7.56:

$\eta_r = 20°$ (see Fig. 7.54)
$\delta_M = 20° \Rightarrow$ TD latitude $= -20°$ for $i_r = -20°$
$\eta_r = 40°$ (see Fig. 7.55)
$\delta_M = 20° \Rightarrow -19° \leq$ TD latitude $\leq 0°$ for $-90° \leq i_r \leq -20°$
(returning below the earth's equator)
$-40° \leq$ TD latitude $\leq -19°$ for $20° \leq i_r \leq 90°$
(returning above the earth's equator)
$\eta_r = 60°$ Data from Exercise 7.16.

With the figures given here and those of the last section, it is possible to relate the re-entry maneuver angle and the latitude of the landing site to the inclination of the return phase wrt the moon's orbit plane. Thus, if one begins with a day of launch (a particular inclination and declination of the moon) and the spacecraft's inclination wrt the moon's orbit plane, as well as the touchdown latitude, then the re-entry maneuver angle and the inclination wrt the equatorial plane can be found. Also, it is interesting to note that fixing the spacecraft's inclination, re-entry angle and touchdown latitude determine a specific declination of the moon, which in turn will require a specific day of launch.

Category (6): Touchdown Longitude
Returning to the Free-Return Lunar Trajectory Selection Procedure, note that we have not included targeting to the longitude of the landing site. However, we did say earlier that the correct longitude is acquired by adjusting the input time of flight to the moon in the launch phase. Adjusting the outward flight time allows the earth to attain the desired orientation wrt the moon at the time of spacecraft re-entry. Figure 7.57 indicates the dependence of longitude on other parameters. The entry and exit points of the sphere of influence are within 3° of each other in right ascension and about 1.5° of each other in declination. This small difference in location implies that, as far as the earth is concerned, the circumlunar trajectory is

composed of two planar motions—the two earth phases—and the effect of the moon is to change only the orientation of the plane of motion and the energy of the orbit, not the position in inertial space.

In terms of right ascension and time, the longitude can be given by the following expressions,

$$L_o = \alpha_o - \omega_e t_o - \alpha_{go}$$
$$L_i = \alpha_i - \omega_e t_i - \alpha_{go}$$

where L_o, L_i are longitudes and α_o, α_i are right ascensions at launch and landing, respectively. The times t_o and t_i are measured from midnight of the day of launch and α_{go} is the right ascension of Greenwich (or sidereal time) at midnight on the day of launch. The constant ω_e is the spin rate of the earth. If differences are taken, then

$$L_i - L_o = (\alpha_i - \alpha_o) - \omega_e(t_i - t_0)$$

But, the difference in right ascension between touchdown and launch is approximately the sum of the angular differences θ_o and θ_i shown in Fig. 7.57, where θ_o denotes the outward phase longitude difference and θ_r the return phase longitude difference. Also, $(t_i - t_o)$ is the total time of flight. Then,

$$L_i = L_o + (\theta_o + \theta_r) - \omega_e T_T \tag{7.16}$$

where T_T denotes the total time of flight from injection to re-entry. The last two subsections have covered some aspects of the geometry of the outward and return phases. Specifically, for the outward phase, the latitude of the Cape and the launch azimuth determine the outward phase inclination. The coast Type and the position of the moon fix the orientation of the trajectory plane in space. Figure 7.58 presents the angular difference θ_o as a function of the inclination, Type, and declination of the moon.

For the return phase, it has been shown that the in-plane angle from the moon to touchdown is approximately 160° for a reentry angle of 96°. Fixing the position of the moon, the touchdown latitude and the reentry maneuver angle determine the orientation of the return phase in space and specifically the angle θ_r. Figures 7.59 and 7.60 present this angle for maneuver angles of 40° and 60°, respectively. The value of θ_r for a maneuver angle of 20° is 180° for all return inclinations since the in-plane angle is approximately this value.

Once θ_o and θ_r have been found and the total flight time T_T is known, Eq. (7.16) can be used to determine the touchdown longitude. Understand that this equation is approximate and that the greatest error is probably introduced by the flight time T_T. The rotation of the earth is about 15° per hour so that an error of 1 h in the flight time causes the landing longitude to be off by 15°. Figure 7.61 presents the relation

$$L = L_i - (\theta_o + \theta_r) = L_o - \omega_e T_T \tag{7.17}$$

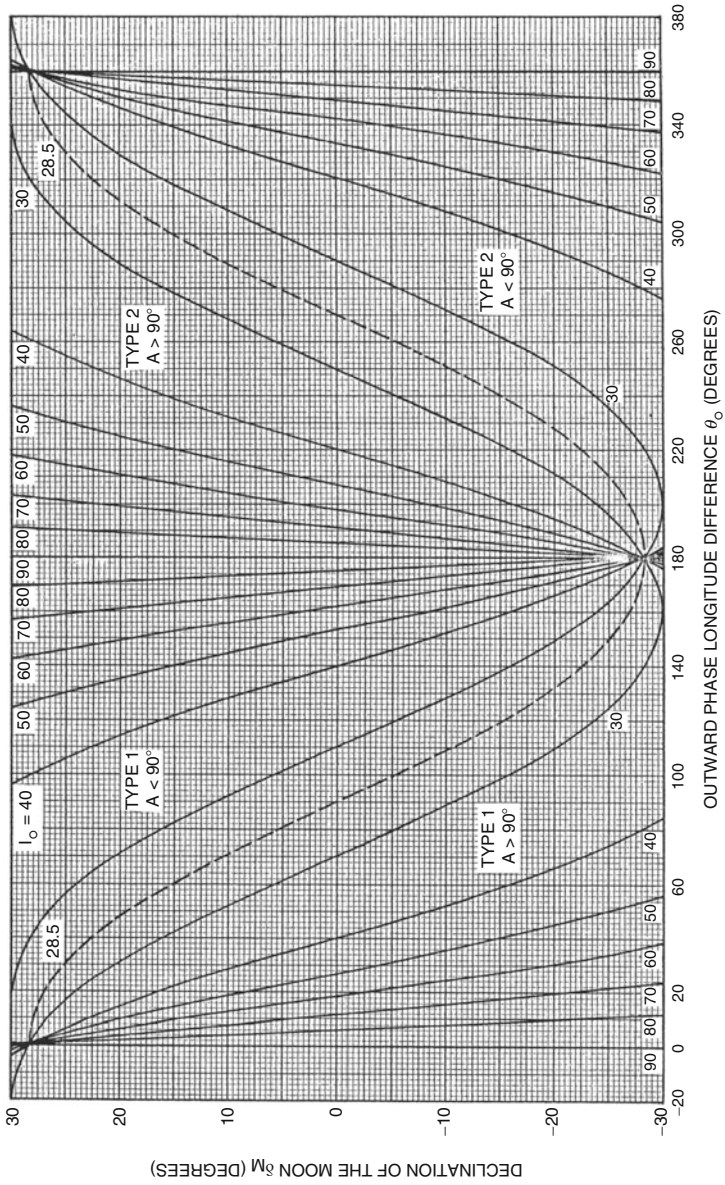

Fig. 7.58 Declination of the moon versus the outward phase longitude difference θ_o for various types and outward phase inclinations wrt the equatorial plane

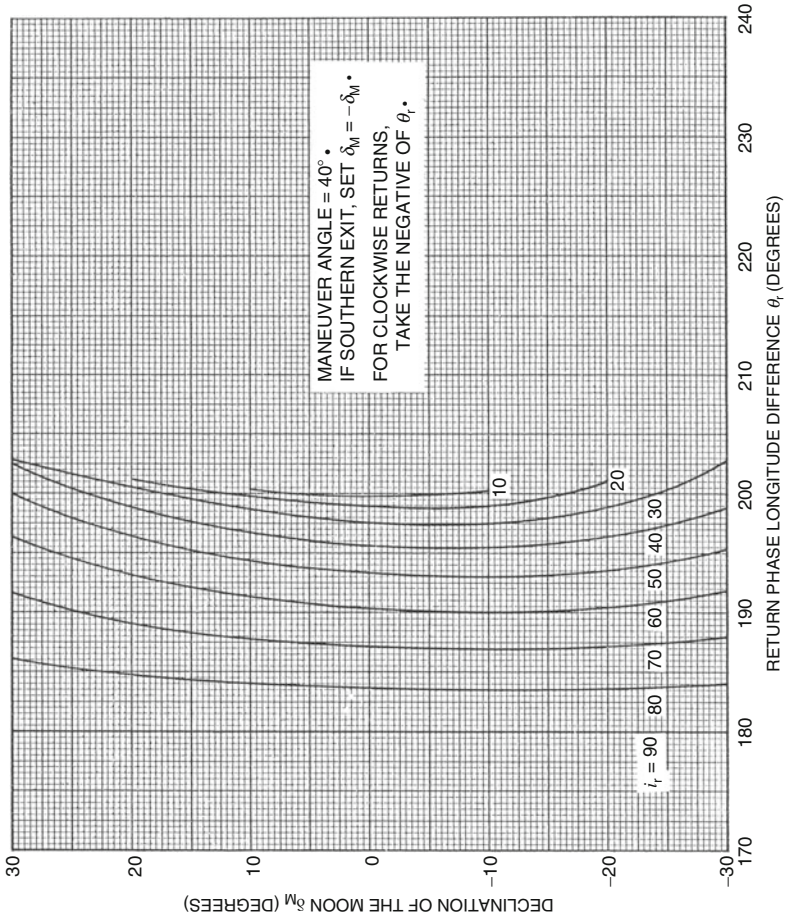

Fig. 7.59 Declination of the moon versus the outward phase longitude difference θ_o for various types and outward phase inclinations wrt the equatorial plane: maneuver angle = 40°

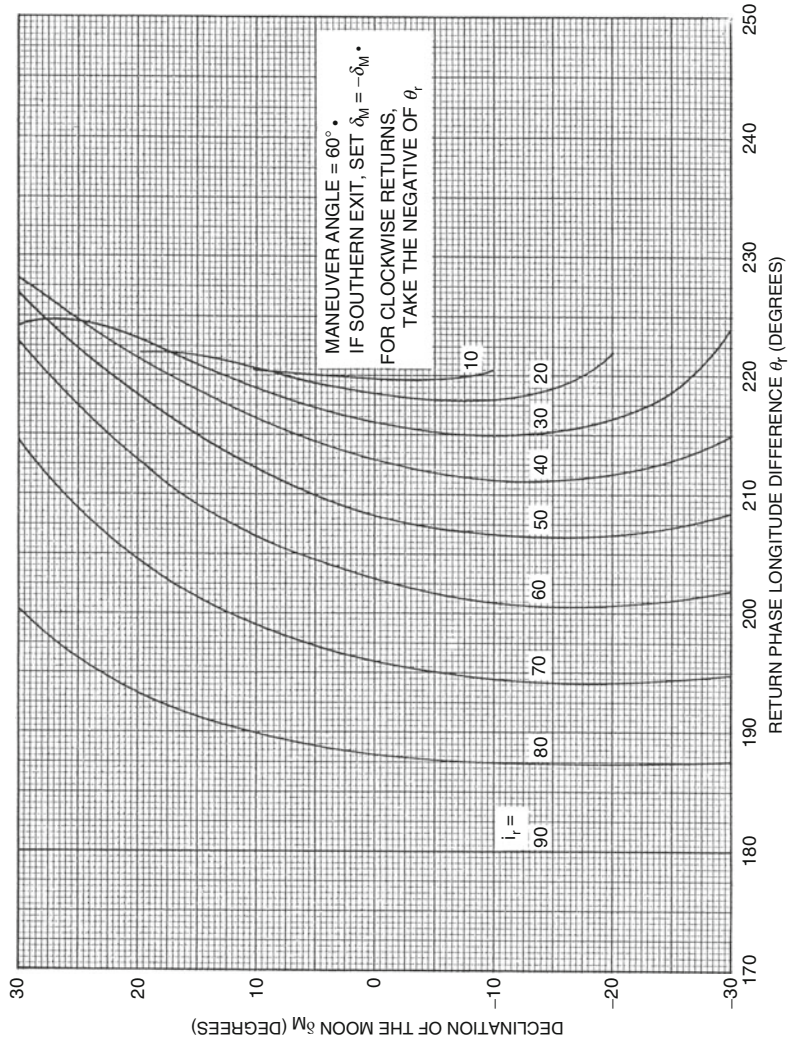

Fig. 7.60 Declination of the moon versus the outward phase longitude difference θ_o for various types and outward phase inclinations wrt the equatorial plane: maneuver angle = 60°

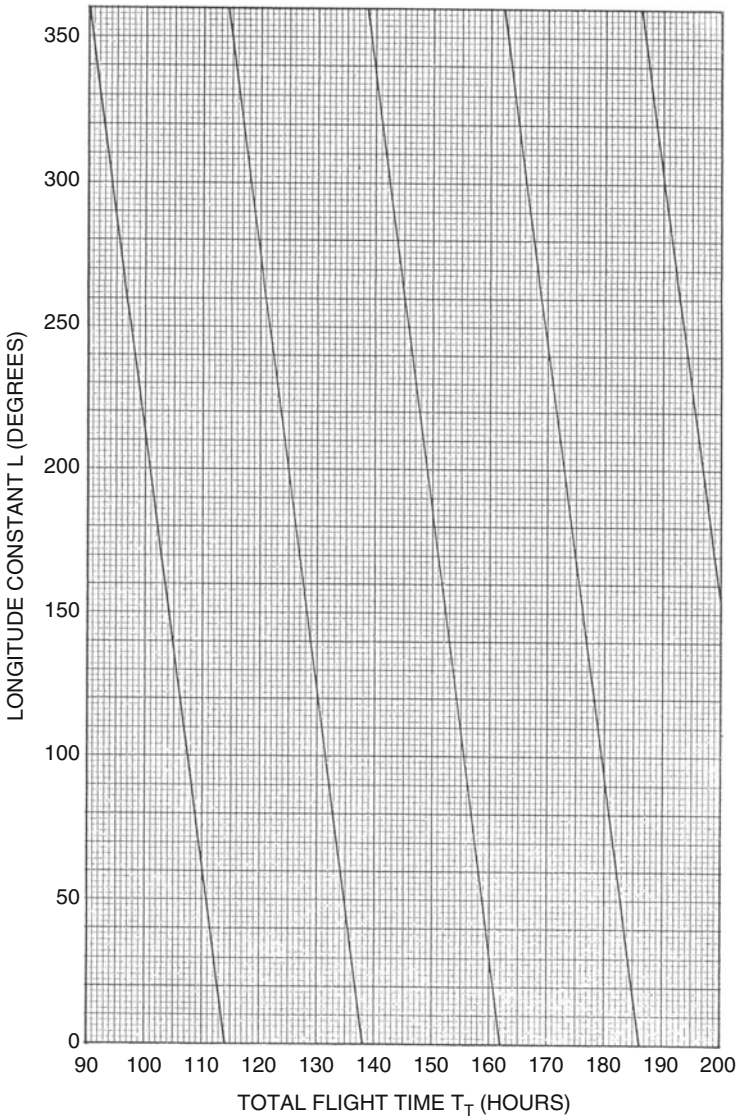

Fig. 7.61 Longitude constant versus the total time of flight

where $L_o = -80.5°$, the longitude of the Cape, and L is defined as the longitude constant. Thus, if $(\theta_o + \theta_r)$ is known, the touchdown longitude can be found by adding this sum to the longitude constant.

Example:
Assume that the spacecraft is launched from the Cape into the moon's orbit plane on a particular day when the moon is at Position A and at a declination of $-15°$. If the spacecraft is to come within 100 nautical miles of the surface of the moon, then the Fixed Pericynthion Altitude condition applies. Further, if the return inclination is to be $-40°$, then Fig. 7.41 indicates that the outward and the return flight times must be 61.5 h and 64.8 h, respectively. The total flight time is 126.3 h. Also, if the re-entry maneuver angle is 40° and the touchdown latitude 30°, then $i_r = -56°$ from Fig. 7.55 and $\theta_r = 198°$ from Fig. 7.59. Figure 7.58 for a Type (2) coast gives $\theta_o = 240°$ for $i_o = 28.5°$ at the Cape. The sum $(\theta_o + \theta_r) = 438°$ (mod 360°) = 78°. Finally, with a flight time of about 126 h, Fig. 7.61 gives $L = 180°$ for the longitude constant. Adding 78° results in 258° (or $-102°$) as the touchdown longitude. This landing site would be somewhere in Texas.

Since the touchdown longitude will most likely be a chosen parameter, it is desirable to solve this problem in reverse.

Example: What position of the moon will produce a specified touchdown latitude?

The total flight time can be chosen by other considerations such as how close the spacecraft is to come to the moon's surface. The longitude constant can then be found and the sum $(\theta_o + \theta_r)$ must then be a definite amount. Figures 7.58, 7.59, and 7.60 can then be used to determine which declination of the moon will result in the correct sum. Note that θ_r will vary only about 25° for $\eta_r = 40°$ and by about 45° for $\eta_r = 60°$. The variation of θ_o is much more extensive: about 180° for the whole range of declinations for the moon and Type (2) coast. Thus, if the declination of the moon, or day of launch, is to be chosen, varying the launch azimuth will result in a wide range of possible touchdown latitudes.

Category (7): Some Additional Parameters
The reference "An Analysis of Free-Flight Circumlunar Trajectories" by Paul A. Penzo gives parametric plots of additional parameters, including the following:

1. Injection velocity versus the outward time of flight for various positions of the moon in its orbit,
2. Parking orbit altitude versus injection velocity for fixed injection energies C_3,
3. Probe–moon–earth angle versus the outward time of flight for various positions of the moon in its orbit,
4. Hyperbolic excess velocity versus the outward time of flight for fixed outward phase inclinations and various positions of the moon in its orbit,
5. Earth–moon–probe angle at exit from the SoI versus the return time of flight for various positions of the moon in its orbit, and
6. Components of the impact vector **B** for constant outward times of flight.

These additional P^2 plots are given in Appendix C.

Application of the P^2 Plots to the Apollo Missions

You will complete this part by working the exercises for this subsection.

References for this chapter: Adamo; Apollo Program; DSN Website; Egorov; Goodman; Hintz, Farless, and Adams; Infoplease/Encyclopedia Website; Kaplan; NEO Website; National Space Science Data Center Website; Penzo; Roncoli; Seidelmann; Simon; ssd Website, Walter; Woolston; Yeomans

Exercises

7.1 (a) Derive Eq. (7.1):

$$\partial\tau/\partial V_M = (3av/\mu)\tau$$

(b) Use this formula to compute $\partial\tau/\partial V_M$ at periapsis and apoapsis for the PVO orbit.

(c) Compare the values obtained from this formula to the values obtained from finite differences as shown in Fig. 7.2.

7.2 Identify the conversion (rotation) process that converts Keplerian elements to Cartesian state coordinates.

7.3 Identify the conversion process that converts the Cartesian state coordinates to Keplerian elements.

7.4 The Pioneer Venus Orbiter (PVO) orbit parameters are:

$$\tau = 24.0 \text{ h}$$
$$r_p = 6{,}252.0 \text{ km}$$
$$i = 105.0^\circ$$
$$\Omega = 33.1^\circ$$
$$\omega = 147.2^\circ$$

with respect to mean ecliptic and equinox of 1950.0 coordinates when the Mission Design Team determines that the period must be decreased to 23.8 h. To avoid interfering with science-data-taking activities, the maneuver may not be scheduled within 1 h, i.e., within 120° in true anomaly, of periapsis.

(a) Compute the magnitude (in m/s) of the minimum Δv maneuver for this period change, subject to the above conditions and constraints.

(b) Determine the value of the parameters r_p, i, Ω, and ω immediately after this maneuver.

7.5 Write a MATLAB program for generating the gradient curves as in Figs. 7.2, 7.3, 7.4, 7.5, and 7.6 and generate these figures for PVO.

7.6 Show that the following statements are valid:

(a) The eccentricity for the lunar Hohmann transfer trajectory is $e \cong 0.97$.

(b) The eccentricity of a transfers that has higher energy than the Hohmann transfer is

$$e \cong \sqrt{0.932 + 0.033v_r^2}$$

for any radial velocity v_r at the lunar distance.

7.7 A sightseeing space shuttle is sent on a round trip to the moon from a low earth orbit.
   (a) Use the Michielsen Chart to obtain the deflection angle δ by the lunar flyby for a direct outward leg of 3 days and a direct return to a low earth orbit of 3 days.
   (b) Should the craft pass in front of or behind the moon?
   (c) What is the radial distance of closest approach to the moon?
   (d) What is the pericynthion altitude ?

7.8 Apollo 17 performed a maneuver to leave its initial free-return translunar trajectory to provide an opportunity for a more precise landing on the lunar surface. The point of closest approach where the Lunar Orbit Insertion (LOI) maneuver was to be performed was $r_{p/M} = 1{,}849$ km. (Note that the subscript "M" refers to the moon.) Apollo 17 passed in front of the moon.
   (a) Use the Michielsen chart to determine the distance of the hyperbolic asymptote from the moon and the eccentricity of the hyperbolic approach trajectory for a direct outward transfer of 3.4 days.
   (b) Assuming the initial circular earth parking orbit had an altitude of 200 km, determine (estimate) the Δv needed to reach the moon.
   (c) Assume that the spacecraft performed an impulsive LOI maneuver to insert from its flyby hyperbolic trajectory into a lunar orbit having a perilune altitude of 111 km and apolune altitude of 314 km without rotating the line of apsides. Determine the Δv at the LOI point if this point is the perilune position.
   (d) Assume that the astronauts performed a maneuver to move the spacecraft into a circular orbit with altitude 111 km and compute the (impulsive) Δv for that maneuver.

7.9 Apollo 13 had the same translunar trajectory as Apollo 17. But Apollo 13 experienced a major failure en route to the moon after leaving the free-return trajectory and before arriving at the moon.
   (a) If all of Apollo 13's rockets had then been inoperable, determine its orbit after the flyby of the moon and the fate of the three astronauts, Lovell, Haise, and Swigert. In particular, how close would the spacecraft have come to the earth and how far would the spacecraft have travelled from the earth? If the orbit is closed, what is the period of that orbit? It is not necessary to consider subsequent gravity assists from the moon or collision with the moon.
   (b) Fortunately, the astronauts were able to use the propulsion systems of the Lunar Module (LM) to perform trajectory correction maneuvers (TCMs) to return safely to the earth. The first of the TCMs returned the spacecraft, consisting of the Command Module (CM) and the Lunar Module, to a free-return trajectory. For mass data, use the value of the mass of the CM as 28,945 kg and the mass of the LM as 15,235 kg. The LM propulsion systems used nitrogen tetroxide as the oxidizer and unsymmetrical dimethyl hydrazine (UDMH) hypergolic as the propellant. For this first recovery TCM, the $\Delta v = 0.0115$ km/s. Compute the amount of propellant used in this maneuver.

7.10 Consider the Apollo free-return trajectories with a 3-day outward trajectory from the parking orbit about the earth to the moon and a 3-day direct return trajectory from the moon to the earth. Compute the gravity assist Δv (denoted as Δv_{GA}) from the hyperbolic trajectory about the moon.

7.11 In studying the Free-Return Circumlunar Trajectory Selection Procedure, we learned that the two moon-centered velocity vectors at entrance and exit of the sphere of influence at the moon completely determine the moon-phase hyperbolic orbit.

(a) Show how to determine the hyperbolic parameters a and e from these data.

(b) Draw a figure for use in explaining how you derived the formula for computing the eccentricity e.

7.12 Consider the free-return trajectory designed for Apollo 11.

(a) Assume that Apollo 11 was launched in the moon's orbit plane with an outward flight time (from injection into the translunar free-return trajectory to pericynthion) $T_o = 72$ h and that it had continued into a 40° return inclination with respect to the moon's orbit plane without stopping at the moon. Assume the moon was at apogee with a 15° declination at the time of the spacecraft's pericynthion and 28° inclination with respect to the earth's equatorial plane. Use the appropriate Penzo parametric plot(s) to determine the return flight time T_r from pericynthion to re-entry and the spacecraft's altitude at pericynthion. Show your work on a copy of the Penzo parametric plot(s).

(b) Will the Apollo 11 trajectory examined in part (a) be direct or retrograde?

(c) What was the distance between the moon's center of mass and the earth's center of mass in km?

7.13 Assume the moon is at apogee and a spacecraft is launched in the moon's orbit plane into a free-return trajectory.

(a) Let the spacecraft's outward flight time $T_o = 68$ h.
For which return inclinations i_r can this spacecraft travel in a counter-

clockwise trajectory? For which return trajectories can it travel in a clockwise trajectory? Give answers in degrees.

(b) Let $T_o = 70$ h and answer the same questions as in part (a). Give answers in degrees.

(c) If $T_o = 74$ h and the spacecraft travels in a return orbit having inclination $i_r = 60°$, what was the altitude above the moon at pericynthion and what is the return flight time?

(d) Show your results on a copy of the appropriate Penzo parametric plot.

7.14 A spacecraft is on a free-return lunar trajectory with a 100-nautical mile altitude at pericynthion.

(a) If the spacecraft was launched in the moon's orbit plane and its return inclination $i_r = 0°$, what are the outward and inward flight times if the moon was at the maximum perigee (Position A) and if the moon was at its apogee (Position C)?

(b) Answer the same question as in part (a) if the spacecraft was launched normal to the moon's orbit plane from the south.
(c) Use the data obtained in parts (a) and (b) to compute the difference in T_o and T_r between the values for $i_o = 0°$ and $i_o = -90°$ at maximum perigee and apogee.
(d) Construct a table showing the 12 values obtained in parts (a), (b), and (c).

7.15 In Exercise 7.12, we considered the free-return trajectory designed for Apollo 11. We made the following assumptions:
(i) Apollo 11 was launched in the moon's orbit plane with an outward flight time (from injection into the translunar free-return trajectory to pericynthion) $T_o = 72$ h
(ii) Apollo 11 continued into a 40° return inclination with respect to the moon's orbit plane without stopping at the moon.
(iii) Assume the moon was at apogee with a 15° declination at the time of the spacecraft's pericynthion and had a 28° inclination with respect to the earth's equatorial plane.

Now also assume that the spacecraft and the moon were both on an upward swing with respect to the earth's equator. Use the appropriate Penzo parametric plots to answer the following questions and include the plots with your results highlighted.

(a) What was the launch azimuth from Cape Canaveral?
(b) What was the inclination of the return trajectory with respect to the earth's equatorial plane?

7.16 Assume a spacecraft has a re-entry maneuver angle $\eta_r = 60°$.
(a) What are the spacecraft's available touchdown (landing site) latitudes, if the declination δ_M of the moon when the spacecraft is at pericynthion is 20°.
(b) What are the spacecraft's possible return-phase inclinations measured in degrees with respect to the earth's equatorial plane?
(c) Highlight your results on a copy of the appropriate Penzo parametric plot.

Further Study

8

8.1 Introduction

A student of Orbital Mechanics and Astrodynamics can now pursue further study in related topics. Several such topics are considered at a high level in this section, together with appropriate references for such continuing study.

8.2 Additional Navigation, Mission Analysis and Design, and Related Topics

Mission Analysis and Design

Mission analysis and design begins with one or more broad objectives and constraints and then proceeds to define a space mission that will meet them at the lowest possible cost. The Space Mission Analysis and Design (SMAD) process is an iterative one consisting of the following steps:

1. Define Objectives
   (a) Define broad objectives and constraints
   (b) Estimate quantitative mission needs and requirements
2. Characterize the Mission
   (a) Define alternative mission concepts
   (b) Define alternative mission architectures
   (c) Identify system drivers for each
   (d) Characterize mission concepts and architectures
3. Evaluate the Mission
   (a) Identify critical requirements
   (b) Evaluate mission utility
   (c) Define baseline mission concept

© Springer International Publishing Switzerland 2015

G.R. Hintz, *Orbital Mechanics and Astrodynamics*,
DOI 10.1007/978-3-319-09444-1_8

4. Define Requirements
   (a) Define system requirements
   (b) Allocate requirements to system elements

   Reference: SMAD3, pp 1–2
   References for Mission Analysis and Design:

1. Charles D. Brown, *Spacecraft Mission Design,* Second Edition, AIAA Education Series, American Institute of Aeronautics and Astronautics, Inc., 1998.
2. James R. Wertz and Wiley J. Larson, eds., *Space Mission Analysis and Design,* Third Edition, Space Technology Library, Published Jointly by Microcosm Press, El Segundo, California and Kluwer Academic Publishers, Dordrecht, The Netherlands, 1999.
   For errata, go to http://www.astrobooks.com and click on "STL Errata" (on the right-hand side) and scroll down to and click on the book's name.
3. James Wertz, David Everett, and Jeffery Puschell, eds., and 65 authors, *Space Mission Engineering: The New SMAD,* Space Technology Library, Vol. 28.

Orbit Determination

Orbit determination is the statistical estimation of where a spacecraft is and where it is going. A syllabus for a course of study in this field is:

- Navigating the solar system: an overview
- Required mathematical background
- Orbit determination problem
- Error sources included in statistical analyses
- Least squares and weighted least squares solutions
- Minimum variance and maximum likelihood solutions
- Computational algorithms for batch, sequential (Kalman filter), and extended Kalman processing
- State noise and dynamic model compensation and the Gauss-Markov process
- Information filter
- Smoothing
- Elementary illustrative examples
- Square-root filter algorithms
- Consider covariance analyses
- Optical navigation
- Autonomous optical navigation (AutoNav)
- Space Navigation: The Practice or Meeting the Challenges of Space Navigation: Guidance, Navigation and Control (GN&C)
- Suggestions for topics for further study such as nonlinear filters

An excellent textbook for studying orbit determination is:

Byron D. Tapley, Bob E. Schutz, and George H. Born, *Statistical Orbit Determination,* Elsevier Academic Press, Burlington, MA, 2004.
Numerous other references are cited in the bibliography for this textbook.

Launch

A syllabus for studying spacecraft launch is:

- Launch considerations and concepts
- Rocket payloads
- World Launch vehicles
- Optimal staging or maximizing performance by shedding dead weight
- World-wide launch sites
- Launch vehicle selection
- Launch Integration and Operations
- Launch Schedules

References include:

1. Steven Isakowitz, Joshua Hopkins, and Joseph P. Hopkins Jr, *International Reference Guide to Space Launch Systems*, Fourth Edition, Revised, American Institute of Aeronautics and Astronautics, Washington, DC, 2004.
2. John E. Prussing and Bruce A. Conway, *Orbital Mechanics,* Oxford University Press, New York, 1993.

Spacecraft Attitude Dynamics

A syllabus for a course on spacecraft attitude dynamics is:

- Preliminaries: reference frames, coordinate systems, rotations, quaternions
- Kinematics and Dynamics: yo-yo despin
- Stability of motion: polhodes; body cone and space cone
- Spinning spacecraft: large angular defections, energy dissipation, nutation dampers
- Dual-spin spacecraft: gyrostats, reaction wheels, thrusting maneuvers
- Environmental and disturbance torques: gravitational torque
- Gravity gradient and momentum bias spacecraft: gravitational torque

This syllabus is for a graduate course taught by Troy Goodson in the Department of Astronautical Engineering at the University of Southern California.

References for this topic include:

1. Vladimir A. Chobotory, *Spacecraft Attitude Dynamics and Control*, Krieger Publishing Company, Malabar, Florida, 1991.
2. Peter C. Hughes, *Spacecraft Attitude Dynamics*, John Wiley & Sons, New York, 1986.
3. Thomas R. Kane, Peter W. Likins, David A. Levinson, *Spacecraft Dynamics*, McGraw-Hill Book Co., New York, 1983.
4. Marshall H. Kaplan, *Modern Spacecraft Dynamics & Control*, John Wiley & Sons, Inc., New York, 1976.
5. Malcolm D. Shuster, "A Survey of Attitude Representations," *The Journal of the Astronautical Sciences*, Vol. 41, No. 4, pp. 439–517, October–December 1993.
6. William Tyrrell Thomson, *Introduction to Space Dynamics,* Dover Publications, Inc. (originally published by John Wiley & Sons, Inc. in 1961), 1986.
7. James R. Wertz with contributions by Hans F. Meissinger, Lauri Kraft Newman, and Geoffrey N. Smit, *Mission Geometry; Orbit and Constellation Design and Management*, Space Technology Library, Published Jointly by Microcosm Press, El Segundo, CA and Kluwer Academic Publishers, Dordrecht, The Netherlands, 2001.
8. William E. Wiesel, *Spaceflight Dynamics*, Second Edition, Irwin McGraw-Hill, Boston, 1997.

Spacecraft Attitude Determination and Control

The Introduction of reference (3) by James R. Wertz, ed. states:

> Attitude analysis may be divided into determination, prediction, and control. *Attitude determination* is the process of computing the orientation of the spacecraft relative to either an inertial frame or some object, such as the Earth...
>
> *Attitude prediction* is the process of forecasting the future orientation of the spacecraft by using dynamical models to extrapolate the attitude history...
>
> *Attitude control* is the process of orientating the spacecraft in a specified, predetermined direction. It consists of two areas—*attitude stabilization* and *attitude maneuver control*...

References include:

1. Marcel J. Sidi, *Spacecraft Dynamics and Control: A Practical Engineering Approach*, Cambridge Aerospace Series, Cambridge University Press, 2001.
2. Marshall H. Kaplan, *Modern Spacecraft Dynamics & Control*, John Wiley & Sons, Inc., New York, 1976.
3. James R. Wertz, ed., *Spacecraft Attitude Determination and Control*, Dordrecht: Kluwer Academic Publishers, 2002.

Constellations

Def.: A collection of spacecraft operating without any direct onboard control of relative positions or orientation is a constellation.

Earth-Orbiting Constellations

References:

1. Chia-Chun "George" Chao, *Applied Orbit Perturbation and Maintenance*, The Aerospace Press, El Segundo, CA, 2005.
2. Bradford W. Parkinson and James J. Spilker, Jr., eds., Penina Axelrad and Per Enge, assoc. eds. *Global Positioning System: Theory and Applications*, Progress in Astronautics and Aeronautics Series, Vol. 163, AIAA, 1996.

Mars Network

References:
Fundamental constellation design approaches for circular orbits:

(a) Streets of Coverage technique:
L. Rider, "Analytic Design of Satellite Constellations for Zonal Earth Coverage Using Inclined Circular Orbits," *The Journal of the Astronautical Sciences*, Vol. 34, No. 1, January–March 1986, pages 31–64.
(b) Walker technique:
1. A. H. Ballard, "Rosette Constellations of Earth Satellites," *IEEE Transactions on Aerospace and Electronic Systems*, Vol. AES-16, No. 5, September 1980.
2. J. G. Walker, "Circular Orbit Patterns Providing Continuous Whole Earth Coverage," *Royal Aircraft Establishment*, *Tech. Rep. 70211* (UDC 629.195:521.6), November 1970.
Website for information on constellations;
http://www.ee.surrey.ac.uk/Personal/L.Wood/constellations/

Formation Flying

A collection of spacecraft operating without any direct onboard control of relative positions or orientation is a constellation. Formation flying (FF) requires the distributed spacecraft to exert collaborative control of their mutual positions and orientations.

The spacecraft FF problem of maintaining the relative orbit of a cluster of satellites that must continuously orbit each other is sensitive to relative orbit modeling errors. Making linearization assumptions, for example, can potentially lead to a substantial fuel cost. The reason is that this formation must be maintained over the entire life span of the satellites, not for a short duration in the life span as, for example, in rendezvous and docking. If a relative orbit is designed using a very simplified orbit model, then the formation stationkeeping control law will need to continuously compensate for these modeling errors by burning fuel. Depending on

the severity of the modeling errors, this fuel consumption could drastically reduce the lifetime of the spacecraft formation.

Selecting the cluster of satellites in formation flying to have equal type and build insures that each satellite ideally has the same ballistic coefficient. Thus each orbit will decay nominally at the same rate from atmospheric drag. For this case, it is possible to find analytically closed relative orbits. These relative orbits describe a fixed geometry as seen in a rotating spacecraft reference frame. Thus the relative drag has only a secondary effect on the relative orbits. The dominant dynamical effect is then the gravitational attraction of the central body, particularly the J_2 perturbations of an oblate body, which cause secular drift in the mean Ω, mean ω, and mean anomaly.

The reference by Schaub and Junkins provides a set of relative orbit control methods:

1. Mean Orbit Element Continuous Feedback Control Laws
2. Cartesian Coordinate Continuous Feedback Control Law
3. Impulsive Feedback Control Law
4. Hybrid Feedback Control Law.

References include:

1. Hanspeter Schaub and John L Junkins, *Analytical Mechanics of Space Systems*, AIAA, Inc, Reston, VA, 2009, Chapter 14.
2. Richard H. Battin, *An Introduction to the Mathematics and Methods of Astrodynamics*, AIAA Education Series, AIAA, New York, 1999.
3. Hanspeter Schaub and K.T. Alfriend, "J_2 Invariant Reference Orbits for Spacecraft Formations," *Celestial Mechanics and Dynamical Astronomy*, Vol. 79, 2001, pp 77–95.

Aerogravity Assist (AGA)

Use the atmosphere of a celestial body such as Venus, Mars, Earth, or Titan to increase the bending of the line of asymptotes experienced during a gravity assist. The V_∞ at departure will then be less than the V_∞ at arrival. An adaptive ΔV can also be executed while still in the gravity well after exiting the atmosphere to modify the velocity if necessary.

For more information on aero-gravity assist, see the following references:

1. M. R. Patel, J. M. Longuski, and J. A. Sims, "A Uranus-Neptune-Pluto Opportunity," *Acta Astronautica*, Vol. 36, No. 2., July 1995, pp. 91–98.
2. Jon A. Sims, James M. Longuski, and Moonish R. Patel, "Aerogravity-Assist Trajectories to the Outer Planets and the Effect of Drag," *Journal of Spacecraft and Rockets*, Vol. 37, No. 1, January–February 2000, pp. 49–55.

3. Wyatt R. Johnson and James M. Longuski, "Design of Aerogravity-Assist Trajectories," *Journal of Spacecraft and Rockets*, Vol. 39, No. 1, January–February 2002, pp. 23–30.

Lagrange Points and the Interplanetary Superhighway

Our solar system is connected by a vast network of an interplanetary superhighway (IPS). This network is generated by Lagrange points of all planets and moons and is a critical, natural infrastructure for space travel. Lagrange points are locations in space where gravitational forces and the orbital motion of a body balance each other.

References:

1. ESA Space Science Website at http://www.esa.int/Our_Activities/Operations/What_are_Lagrange_points [accessed 12/24/2013]
2. G. Gomez, A. Jorba, C. Simo, and J. Masdemont, *Dynamics and Mission Design Near Libration Points*, Vol. I-IV, World Scientific, Singapore, 2001.
3. M. Lo, "The Interplanetary Superhighway and the Origins Program," IEEE Space 2002 Conference, Big Sky, MT, March 2002.
4. M. Lo and S. Ross, "The Lunar L1 Gateway: Portal to the Stars and Beyond," AIAA Space 2001 Conference, Albuquerque, NM, August 28–30, 2001.
5. Ulrich Walter, *Astronautics: The Physics of Space Flight*, 2nd Edition, WILEY-VCH Verlag GmbH & Co. KGaA, 2012.
6. W. Koon, M. Lo, J. Marsden, and S. Ross, "Heteroclinic Orbits between Periodic Orbits and Resonance Transitions in Celestial Mechanics," *Chaos*, Vol. 10, No. 2, June 2000.
7. W. Koon, M. Lo, J. Marsden, and S. Ross, "Shoot the Moon," AAS/AIAA Astrodynamics Conference, Clear-water, Florida, Paper AAS 00-166, January 2000.
8. W. Koon, M. Lo, J. Marsden, and S. Ross, "Constructing a Low Energy Transfer Between Jovian Moons," *Contemporary Mathematics*, Vol. 292, 2002.

References 6–8 describe the technical details of how the pieces of the IPS work. References 7 and 8 give explicit construction of how transferring from one system to another is accomplished.

Solar Sailing

The Planetary Society's Website says, "A solar sail, simply put, is a spacecraft propelled by sunlight." Solar sails gain momentum from an ambient source, viz., photons, the quantum packets of energy of which sunlight is composed. "By changing the angle of the sail relative the Sun it is possible to affect the direction in which the sail is propelled—just as a sailboat changes the angle of its sails to affect its course. It is even possible to direct the spacecraft towards the Sun,

rather than away from it, by using the photon's pressure on the sails to slow down the spacecraft's speed and bring its orbit closer to the Sun.

In order for sunlight to provide sufficient pressure to propel a spacecraft forward, a solar sail must capture as much sunlight as possible. This means that the surface of the sail must be very large. Cosmos 1, a project of The Planetary Society and Cosmos Studios, was to be a small solar sail intended only for a short mission. Nevertheless, once it spread its sails even this small spacecraft would have been 10 stories tall. Its eight triangular blades would have been 15 m (49 ft) in length and have a total surface area of 600 square meters (6500 square feet). This is about one and a half times the size of a basketball court. Unfortunately, the launch of Cosmos 1 failed to achieve orbit.

References:

1. Colin R. McInnes, *Solar Sailing: Technology, Dynamics and Mission Applications*, Springer-Praxis Series in Space Science and Technology, Springer, London in association with Praxis Publishing Ltd, Chichester, UK, 1999.
2. L. Friedman, "Solar Sailing: The Concept Made Realistic," AIAA-78-82, 16th AIAA Aerospace Sciences Meeting, Huntsville, January 1978.
3. The Planetary Society's Website at http://www.planetarysociety.org [accessed 6/1/2014]

Entry, Decent and Landing (EDL)

For example, the Entry, Descent and Landing of the Mars Exploration Rovers (MERs) was harrowing from the sheer number of events that had to occur autonomously on board the vehicle for landing to be accomplished safely. In less than 30 min, MER morphed from a spacecraft to an aeroshell, to a complex two-, then three-body form falling furiously through the Martian atmosphere, to a balloon encased tetrahedron jerked to a standstill and then cut loose to bounce precipitously on the unknown terrain below.

References:

See papers in the special section on planetary entry systems in the *Journal of Spacecraft and Rockets,* Vol. 36, Number 3, May–June 1999.

Cyclers

A future Earth–Mars transportation system will probably use many different kinds of spacecraft trajectories. For example, some trajectories are well suited for human transportation, whereas others are better suited for ferrying supplies. One potentially useful type of trajectory is the Earth–Mars cycler trajectory, or cycler. A spacecraft on a cycler regularly passes close to both Earth and Mars (but never stops at either). The "passenger" vehicle enters or leaves the cycler at the appropriate planet. Cyclers

that require propulsive maneuvers are referred to as powered cyclers, whereas cyclers that rely only on gravitational forces are referred to as ballistic cyclers. There are some variations on cyclers, in which the spacecraft enters a temporary parking orbit at Mars (semi-cyclers), at earth (reverse semi-cyclers), or at both earth and Mars (stop-over cyclers). Reference 2 analyzes all cyclers that repeat every two synodic periods and have one intermediate earth encounter. In the reference, the Earth–Mars synodic period is assumed, at least initially, to be 2 1/7 years.

Buzz Aldrin devised a transit system between Earth and Mars known as the "Aldrin Mars Cycler." "Aldrin's system of cycling spacecraft makes travel to Mars possible using far less propellant than conventional means, with an expected five and a half month journey from the Earth to Mars, and a return trip to Earth of about the same duration on a twin semi-cycler. . . . In each cycle when the Aldrin Cycler's trajectory swings it by the Earth, a smaller Earth-departing interceptor spacecraft ferries crew and cargo up to dock with the Cycler spacecraft."

References:

1. Buzz Aldrin's Website at http://buzzaldrin.com/space-vision/rocket_science/aldrin-mars-cycler/[accessed 5/1/2014]
2. T. Troy McConaghy, Chit Hong Yam, Damon F. Landau, and James M. Longuski, "Two-Synodic-Period Earth-Mars Cyclers With Intermediate Earth Encounter," Paper AAS 03-509, AAS/AIAA Astrodynamics Specialists Conference, Big Sky, Montana, August 3–7, 2003.
3. K. Joseph Chen, T. Troy McConaghy, Damon F. Landau, and James M. Longuski, "A Powered Earth-Mars Cycler with Three Synodic-Period Repeat Time," Paper AAS 03-510, AAS/AIAA Astrodynamics Specialists Conference, Big Sky, Montana, August 3–7, 2003.

Spacecraft Propulsion

A syllabus for spacecraft propulsion is:

- History of space exploration. Types of rockets. Units. Definitions
- Orbital mechanics. Basic orbits, Hohmann transfer, maneuvers, ΔV. Launch sites.
- Thrust. Specific impulse. Rocket equation. Staging. Thermodynamics of fluid flow.
- Combustion. Chemical equilibrium.
- One-dimensional flow.
- Flow in nozzles. Nonideal flow. Shocks. Boundary layer.
- Ideal rocket, thrust coefficient, characteristic velocity. Nozzle types.
- Rocket heat transfer. Liquid rocket systems.
- Starting and ignition. Processes in combustion chamber. Injection. Liquid propellants. Feed systems.
- Solid rocket. Burn rate, erosive burning. Grain design.
- Solid propellants. Hybrid rockets. Thrust vector control.

- Power sources. Electric propulsion.
- Advanced propulsion.

This syllabus is for a graduate course taught by Keith Goodfellow in the Department of Astronautical Engineering at the University of Southern California.

References for this topic include:

1. P. Hill and C. Peterson, *Mechanics and Thermodynamics of Propulsion*, 2nd ed. Addison-Wesley Publishing Company, 1992.

Advanced Spacecraft Propulsion

A syllabus for Advanced Spacecraft Propulsion is:

- Introduction to advanced propulsion. Mission ΔV and orbital mechanics
- Review of rockets. System sizing.
- Review of thermodynamics and compressible gas dynamics.
- Review of thermal rockets. Heat transfer.
- Power systems. Nuclear reactions. Nuclear thermal rockets.
- Solar and Nuclear electric propulsion.
- Electromagnetic theory: electric charges and fields, currents, and magnetic fields, and applications to ionized gases.
- Ionization. Introduction to rarified gases. Charged particle motion. Electrode phenomena.
- Introduction to arc discharges.
- Electrothermal acceleration: 1-D model and frozen flow losses. Resistojet thrusters. Arcjet thrusters.
- Electrostatic acceleration: 1-D space charge model, ion thrusters, ion production, beam optics, beam neutralization. Other thrusters.
- Electromagnetic acceleration: MHD channel flow; Magnetoplasmadynamic (MPD) thrusters, description and thrust derivation, operating limits, and performance calculation.
- Hall thrusters: physics and technology. Unsteady electromagnetic acceleration: pulsed plasma thruster (PPT).
- Overview of advanced concepts. Sails, beamed energy, fusion propulsion, antimatter propulsion. Interstellar missions.
- Special topics: micro-propulsion, tethers, piloted Mars mission.

This syllabus is for a graduate course taught by Keith Goodfellow in the Department of Astronautical Engineering at the University of Southern California.

References:

1. P. Hill and C. Peterson, *Mechanics and Thermodynamics of Propulsion*, 2nd ed. Addison-Wesley Publishing Company, 1992.
2. G. P. Sutton and O. Biblarz, *Rocket Propulsion Elements*, 8th ed., John Wiley & Sons, 2001.
3. R. W. Humble, G. N. Henry and W. J. Larson, *Space Propulsion Analysis and Design*, McGraw-Hill Inc, 1995.
4. W. G. Vincenti and C. H. Kruger, *Introduction to Physical Gas Dynamics*, Krieger Publishing, 1986.
5. M. Mitchner and C. H. Kruger, *Partially Ironized Plasmas*, John Wiley & Sons, 1974.
6. F. F. Chen, *Introduction to Plasma Physics and Controlled Fusion*, 2nd ed., Plenum Press, 1985.
7. R. L. Forward, *Any Sufficiently Advanced Technology is Indistinguishable from Magic*, Baen Publishing, 1995.

Appendix A Vector Analysis

A.1 Vectors and Scalars

We consider column vectors

$$\mathbf{u} = \begin{bmatrix} u_1 \\ u_2 \\ u_3 \end{bmatrix} = [u_1 u_2 u_3]^T = (u_1, u_2, u_3)$$

where u_1, u_2, and u_3 are real numbers.

Def.: Addition of vectors **u** and **v** is defined as

$$\mathbf{u} + \mathbf{v} = (u_1 + v_1, u_2 + v_2, u_3 + v_3)$$

Def.: Multiplication of a vector **u** by a scalar is defined as

$$c\mathbf{u} = (cu_1, cu_2, cu_3)$$

where c is a (scalar) real number.

Notation: The zero vector is $\mathbf{0} = [0\ 0\ 0]^T$.

Properties for any vectors **u**, **v**, and **s**:

(i) $\mathbf{u} + \mathbf{v} = \mathbf{v} + \mathbf{u}$; that is, vector addition is commutative.
(ii) $\mathbf{u} + (\mathbf{v} + \mathbf{s}) = (\mathbf{u} + \mathbf{v}) + \mathbf{s}$; that is, vector addition is associative.

Def.: The magnitude of the vector **u** is

$$|\mathbf{u}| \equiv u \equiv \left(u_1{}^2 + u_2{}^2 + u_3{}^2\right)^{1/2} \tag{A.1}$$

for any vector **u**.

© Springer International Publishing Switzerland 2015

G.R. Hintz, *Orbital Mechanics and Astrodynamics*,
DOI 10.1007/978-3-319-09444-1

A.2 Dot and Cross Product of Vectors

Def.: The dot (scalar or inner) product of two vectors $\mathbf{u}$ and $\mathbf{v}$ is

$$\mathbf{u} \bullet \mathbf{v} = \mathbf{u}^{\mathbf{T}}\mathbf{u} = u_1v_1 + u_2v_2 + u_3v_3 \quad \text{(a scaler number)} \tag{A.2}$$

Notation: $\hat{\mathbf{u}} = \mathbf{u}/u$ (a unit vector)

Properties of the dot product for any vectors $\mathbf{u}$, $\mathbf{v}$, and $\mathbf{s}$:

(i) Commutative law: $\mathbf{u} \bullet \mathbf{v} = \mathbf{v} \bullet \mathbf{u}$

(ii) $\mathbf{u} \bullet \mathbf{u} = u^2$ so the magnitude of the vector $\mathbf{u}$ is $u = (\mathbf{u} \bullet \mathbf{u})^{1/2}$ (A.3)

(iii) Distributive law : $\mathbf{u} \bullet (\mathbf{v} + \mathbf{s}) = \mathbf{u} \bullet \mathbf{v} + \mathbf{u} \bullet \mathbf{s}$ (A.4)

(iv) $\mathbf{u} \bullet \mathbf{v} = uv\cos\theta$ where $\theta = \angle(\mathbf{u}, \mathbf{v})$ from Exercise A-1 (A.5)

(v) For any unit vector $\hat{\mathbf{u}}$, $\mathbf{v} \bullet \hat{\mathbf{u}} = v\cos\theta$ (from property (iv)) for all vectors $\mathbf{v}$ (Fig. A.1).

That is, $\mathbf{v} \bullet \hat{\mathbf{u}} = v\cos\theta$ is the projection of the vector $\mathbf{v}$ along $\hat{\mathbf{u}}$.

Three basis vectors in three dimensions:

$$\begin{aligned} \hat{\mathbf{i}} &= (1, 0, 0) \\ \hat{\mathbf{j}} &= (0, 1, 0) \\ \hat{\mathbf{k}} &= (0, 0, 1) \end{aligned}$$

Def.: The vector set $\left\{\hat{\mathbf{i}}, \hat{\mathbf{j}}, \hat{\mathbf{k}}\right\}$, where $\hat{\mathbf{i}} = (1, 0, 0)$, $\hat{\mathbf{j}} = (0, 1, 0)$, and $\hat{\mathbf{k}} = (0, 0, 1)$, is called the standard basis of all vectors in three-dimensional space.

For simplicity, we omit the "∧" symbol over unit reference vectors and write

$$\begin{aligned} \mathbf{i} \bullet \mathbf{i} &= 1 = \mathbf{j} \bullet \mathbf{j} = \mathbf{k} \bullet \mathbf{k} \\ \mathbf{i} \bullet \mathbf{j} &= 0 = \mathbf{i} \bullet \mathbf{k} = \mathbf{j} \bullet \mathbf{k} \end{aligned}$$

For any vector $\mathbf{u} = (u_1, u_2, u_3)$, $\mathbf{u} \bullet \mathbf{I} = (u_1\mathbf{i} + u_2\mathbf{j} + u_3\mathbf{k}) \bullet \mathbf{i} = u_1\mathbf{i} \bullet \mathbf{i} + u_2\mathbf{j} \bullet \mathbf{i} + u_3\,\mathbf{k} \bullet \mathbf{i} = u_1$.

Similarly, $u_2 = \mathbf{u} \bullet \mathbf{j}$ and $u_3 = \mathbf{u} \bullet \mathbf{k}$.

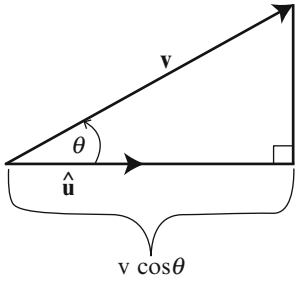

Fig. A.1 Projection of $\mathbf{v}$ along $\hat{\mathbf{u}}$

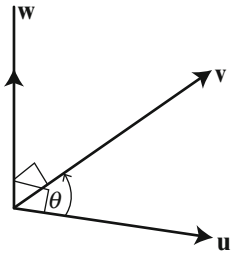

Fig. A.2 Geometric definition of the cross product of two vectors

In general,

$$\mathbf{u} = (u_1, u_2, u_3) = u_1\mathbf{i} + u_2\mathbf{j} + u_3\mathbf{k} = (\mathbf{u} \bullet \mathbf{i})\mathbf{i} + (\mathbf{u} \bullet \mathbf{j})\mathbf{j} + (\mathbf{u} \bullet \mathbf{k})\mathbf{k}$$

Therefore, any vector **u** can be written uniquely as a linear combination of the three basis vectors:

$$\mathbf{u} = u\cos\alpha\mathbf{i} + u\cos\beta\mathbf{j} + u\cos\gamma\mathbf{k} \text{ from property (v)}$$

where α, β, and γ denote the direction angles of the vector **u**, $\alpha = \angle(\mathbf{u}, \mathbf{i})$, $\beta = \angle(\mathbf{u}, \mathbf{j})$, and $\gamma = \angle(\mathbf{u}, \mathbf{k})$ and cosα, cosβ, and cosγ are the direction cosines of the vector **u**.

Remark: The direction of the zero vector is undefined.

Def.: Two vectors **u** and **v** are perpendicular (or orthogonal, $\mathbf{u} \perp \mathbf{v}$) iff $\mathbf{u} \bullet \mathbf{v} = 0$.

Def. (geometric definition): The cross product of **u** and **v** is the vector $\mathbf{w} \equiv \mathbf{u} \times \mathbf{v}$ that is perpendicular to **u** and **v** in the direction shown in Fig. A.2 and has the magnitude

$$w = uv\sin\theta \text{ if } \mathbf{u}, \mathbf{v} \text{ are not zero} \tag{A.6}$$

where $\theta = \angle(\mathbf{u}, \mathbf{v})$. If **u** or $\mathbf{v} = \mathbf{0}$, then $\mathbf{w} = \mathbf{0}$.

Def.: Two vectors **u** and **v** are parallel iff $\mathbf{u} \times \mathbf{v} = 0$.

In particular, two nonzero vectors are parallel iff the angle between them is either 0 or π radians and the zero vector is parallel to every vector in three-dimensional space.

Properties of the cross product of vectors:

(i) $\mathbf{u} \times \mathbf{v} = (u_2v_3 - u_3v_2, u_3v_1 - u_1v_3, u_1v_2 - u_2v_1)$

$$= \left(\begin{vmatrix} u_2 & u_3 \\ v_2 & v_3 \end{vmatrix}, \begin{vmatrix} u_3 & u_1 \\ v_3 & v_1 \end{vmatrix}, \begin{vmatrix} u_1 & u_2 \\ v_1 & v_2 \end{vmatrix} \right) \tag{A.7}$$

(ii) $\mathbf{u} \times \mathbf{v} = -\mathbf{v} \times \mathbf{u}$ (not commutative)

(iii) $\mathbf{u} \times \mathbf{u} = 0$ and $c_1\mathbf{u} \times c_2\mathbf{u} = 0$, where c_1 and c_2 are real numbers (A.8)

(iv) $c\mathbf{u} \times \mathbf{v} = \mathbf{u} \times c\mathbf{v}$ for any real number c (A.9)

(v) Distributive law of the cross product over addition:

$$\mathbf{u} \times (\mathbf{v} + \mathbf{s}) = (\mathbf{u} \times \mathbf{v}) + (\mathbf{u} \times \mathbf{s}) \tag{A.10}$$

$$(\mathbf{v} + \mathbf{s}) \times \mathbf{u} = (\mathbf{v} \times \mathbf{u}) + (\mathbf{s} \times \mathbf{u}) \tag{A.11}$$

(vi) Vector triple product expansions:

$$\mathbf{u} \times (\mathbf{v} \times \mathbf{s}) = (\mathbf{u} \bullet \mathbf{s})\mathbf{v} - (\mathbf{u} \bullet \mathbf{v})\mathbf{s} \tag{A.12}$$

$$(\mathbf{u} \times \mathbf{v}) \times \mathbf{s} = (\mathbf{u} \bullet \mathbf{s})\mathbf{v} - (\mathbf{v} \bullet \mathbf{s})\mathbf{u} \tag{A.13}$$

Therefore, in general,

$$\mathbf{u} \times (\mathbf{v} \times \mathbf{s}) \neq (\mathbf{u} \times \mathbf{v}) \times \mathbf{s}$$

i.e., the associative law does not hold in general for vector triple products so that it is necessary to include parentheses in these expressions.

(vii) Scalar triple product or triple scalar product or box product:

$$\begin{aligned} \mathbf{u} \bullet (\mathbf{v} \times \mathbf{s}) &= \mathbf{s} \bullet (\mathbf{u} \times \mathbf{v}) \\ &= \mathbf{v} \bullet (\mathbf{s} \times \mathbf{u}) = (\mathbf{v} \times \mathbf{s}) \bullet \mathbf{u} \\ &= (\mathbf{u} \times \mathbf{v}) \bullet \mathbf{s} = (\mathbf{s} \times \mathbf{u}) \bullet \mathbf{v} \end{aligned}$$

Therefore,

$$\mathbf{u} \bullet (\mathbf{v} \times \mathbf{s}) = (\mathbf{u} \times \mathbf{v}) \bullet \mathbf{s}. \tag{A.14}$$

That is, we can interchange dot and cross products in the sense shown. Also, the triple scalar product of three vectors is zero if any two of the vectors are parallel or the same.

Def.: A vector **n** is normal to a plane iff it is nonzero, originates at a point P in the plane, and is perpendicular to any two nonparallel vectors in the plane through P.

Given two non-collinear vectors, **u** and **v**, a set of three orthogonal vectors is obtained as

$$\begin{aligned} &\mathbf{u} \\ &\mathbf{u} \times \mathbf{v} \\ &(\mathbf{u} \times \mathbf{v}) \times \mathbf{u} \end{aligned}$$

An orthonormal basis is obtained by unitizing each of these three vectors by dividing them by their length as follows:

$$\begin{aligned}&\mathbf{u}/\mathrm{u}\\&(\mathbf{u}\times\mathbf{v})/|\mathbf{u}\times\mathbf{v}|\\&((\mathbf{u}\times\mathbf{v})\times\mathbf{u})/|((\mathbf{u}\times\mathbf{v})\times\mathbf{u})|\end{aligned}$$

A.3 Derivative of a Vector Function

Let t denote a scalar variable.

Def.: If to each value of t in an interval there corresponds a vector $\mathbf{u}=\mathbf{u}(t)$, we say that $\mathbf{u}$ is a vector function of t.

The vector function may be written as

$$\mathbf{u}=\mathbf{u}(t)=(u_1(t),\ u_2(t),\ u_3(t))=u_1(t)\mathbf{i}+u_2(t)\mathbf{j}+u_3(t)\mathbf{k}$$

Def.: A vector function $\mathbf{u}(t)\equiv(u_1(t), u_2(t), u_3(t)$ is continuous iff the three component scalar functions $u_1(t)$, $u_2(t)$, and $u_3(t)$ are continuous functions of t.

If t changes by Δt, then $\mathbf{u}(t)$ changes in magnitude and direction as

$$\begin{aligned}\Delta\mathbf{u}&=\mathbf{u}(t+\Delta t)-\mathbf{u}(t)=[u_1(t+\Delta t)\mathbf{i}+u_2(t+\Delta t)\mathbf{j}+u_3(t+\Delta t)\mathbf{k}]\\&\quad-[u_1(t)\mathbf{i}+u_2(t)\mathbf{j}+u_3(t)\mathbf{k}]\\&=[u_1(t+\Delta t)-u_1(t)]\mathbf{i}+[u_2(t+\Delta t)-u_2(t)]\mathbf{j}+[u_3(t+\Delta t)-u_3(t)]\mathbf{k}\\&=\Delta u_1\mathbf{i}+\Delta u_2\mathbf{j}+\Delta u_3\mathbf{k}\end{aligned}$$

Therefore, the derivative of a vector function $\mathbf{u}(t)$ is

$$\begin{aligned}\frac{d\mathbf{u}}{dt}&=\lim_{\Delta t\to 0}\frac{\Delta\mathbf{u}}{\Delta t}=\left(\lim_{\Delta t\to 0}\frac{\Delta u_1}{\Delta t}\right)\mathbf{i}+\left(\lim_{\Delta t\to 0}\frac{\Delta u_2}{\Delta t}\right)\mathbf{j}+\left(\lim_{\Delta t\to 0}\frac{\Delta u_3}{\Delta t}\right)\mathbf{k}\\&=\left(\frac{du_1}{dt},\frac{du_2}{dt},\frac{du_3}{dt}\right)\end{aligned}$$

This equation motivates us to make the following definition.

Def.: The differential of a vector function $\mathbf{u}(t)$ is

$$d\mathbf{u}=du_1\mathbf{i}+du_2\mathbf{j}+du_3\mathbf{k}$$

Notation:

$$\dot{\mathbf{u}}=\frac{d\mathbf{u}}{dt}$$

Properties of vector derivatives:

If **u** and **v** are differentiable vector functions of a scalar t and ϕ is a differentiable scalar function of t,

$$\begin{aligned} &\text{(i)}\quad d(\mathbf{u}+\mathbf{v})/dt = d\mathbf{u}/dt + d\mathbf{v}/dt \\ &\qquad\quad d(\mathbf{u}-\mathbf{v})/dt = d\mathbf{u}/dt - d\mathbf{v}/dt \end{aligned} \tag{A.15}$$

$$\text{(ii)}\quad d(\mathbf{u}\bullet\mathbf{v})/dt = \mathbf{u}\bullet d\mathbf{v}/dt + d\mathbf{u}/dt\bullet\mathbf{v} \tag{A.16}$$

In particular, $d(\mathbf{u}\bullet\mathbf{u})/dt = 2\mathbf{u}\bullet d\mathbf{u}/dt$

$$\text{(iii)}\quad d(\mathbf{u}\times\mathbf{v})/dt = \mathbf{u}\times d\mathbf{v}/dt + d\mathbf{u}/dt\times\mathbf{v} \tag{A.17}$$

where the order of the cross products must be maintained.

$$\text{(iv)}\quad d(\phi\mathbf{u})/dt = \phi(d\mathbf{u}/dt) + (d\phi/dt)\mathbf{u} \tag{A.18}$$

Example: Kinematics (the study of motion)

Position vector

$$\mathbf{r} = (r_1, r_2, r_3) = (x,\ y,\ z) = x\mathbf{i} + y\mathbf{j} + z\mathbf{k}$$

$$\mathbf{r} \equiv \mathbf{r}(\mathbf{t}) = (r_1(t), r_2(t), r_2(t)) \tag{A.19}$$

Velocity vector = rate of change of position

$$\begin{aligned} \mathbf{v} = \dot{r} = \frac{d\mathbf{r}}{dt} &= \left(\frac{dr_1}{dt}, \frac{dr_2}{dt}, \frac{dr_3}{dt}\right) = (\dot{r}_1, \dot{r}_2, \dot{r}_3) \\ &= (v_1, v_2, v_3) = (\dot{x}, \dot{y}, \dot{z}) = \dot{x}\mathbf{i} + \dot{y}\mathbf{j} + \dot{z}\mathbf{k} \end{aligned} \tag{A.20}$$

Acceleration vector = rate of change of velocity

$$\mathbf{a} \equiv \frac{d\mathbf{v}}{dt} \equiv \dot{\mathbf{v}} \equiv (\ddot{x}, \ddot{y}, \ddot{z}) \tag{A.21}$$

Def.: The speed of a particle at the time t is the magnitude v of the velocity vector

$$\mathbf{v}(\mathbf{t}) = (\dot{x}, \dot{y}, \dot{z}). \tag{A.22}$$

That is, the speed is $v = |\mathbf{v}|$.

Possible confusion: We often say "velocity" instead of speed for the magnitude of the velocity vector.

A.4 Gradient

Def.: If to each point (x, y, z) of a region R in three-dimensional space there corresponds a number or scalar ϕ (x, y, z), then ϕ is called a scalar function of position and we say that a scalar field ϕ has been defined in the region R.

Def.: A scalar field that is independent of time is called a stationary or steady-state scalar field.

Def.: If to each point (x, y, z) of a region R in three-dimensional space there corresponds a vector $\mathbf{u}(x, y, z)$, then $\mathbf{u}$ is called a vector function of position and we say that a vector field $\mathbf{u}$ has been defined in the region R.

Def.: A vector field that is independent of time is called a stationary or steady-state vector field.

Def.: If $\phi(x, y, z)$ is a scalar function of position possessing first partial derivatives with respect to x, y, and z throughout a region of space, the vector function

$$\frac{\partial \phi}{\partial x}\mathbf{i} + \frac{\partial \phi}{\partial y}\mathbf{j} + \frac{\partial \phi}{\partial z}\mathbf{k}$$

is known as the gradient of ϕ (or gradϕ).

The gradient of a function is often written in operator form as

$$\text{grad}\phi = \left(\mathbf{i}\frac{\partial}{\partial x} + \mathbf{j}\frac{\partial}{\partial y} + \mathbf{k}\frac{\partial}{\partial z}\right)\phi = \nabla\phi$$

The symbol ∇ is called the "del" operator. Note that $\nabla\phi$ defines a vector field. (The definition given here for the ∇ operator is the Cartesian form. This operator can be expressed in more general coordinate systems, but these forms will not be considered in this book.)

Def.: The directional derivative $D_{\hat{\mathbf{u}}}\phi(R_0)$ of a function $\phi(x, y, z)$ at the position $\mathbf{R_0} = (x_0, y_0, z_0)$ in the direction of a unit vector $\hat{\mathbf{u}}$ is

$$D_{\hat{\mathbf{u}}}\phi(\mathbf{R}_0) = \lim_{h\to 0}\frac{\phi(\mathbf{R}_0 + h\hat{\mathbf{u}}) - \phi(\mathbf{R}_0)}{h} \tag{A.23}$$

Properties of the gradient:

(i) If ϕ and ψ are differentiable scalar functions of position (x, y, z), then

$$\nabla(\phi + \Psi) = \nabla\phi + \nabla\Psi \text{ or } \text{grad}(\phi) + \text{grad}(\Psi)$$

(ii) The directional derivative of ϕ in the direction of a unit vector $\hat{\mathbf{u}}$ is $\nabla\phi \bullet \hat{\mathbf{u}}$, i.e., the component of $\nabla\phi$ in the direction of $\hat{\mathbf{u}}$.

(iii) The gradient, $\nabla\phi$, of ϕ extends in the direction of the greatest rate of change of ϕ and has that rate of change for its length.

A.5 Curl

Def.: If $\mathbf{u}(x, y, z)$ is a differentiable vector field, then the curl of $\mathbf{u}$, written $\nabla \times \mathbf{u}$ or curl$\mathbf{u}$, is defined by

$$\nabla \times \mathbf{u} = \left(\frac{\partial}{\partial x}\mathbf{i} + \frac{\partial}{\partial y}\mathbf{j} + \frac{\partial}{\partial z}\mathbf{k}\right) \times (u_1\mathbf{i} + u_2\mathbf{j} + u_3\mathbf{k})$$

Alternate expressions:

$$\nabla \times \mathbf{u} = \begin{vmatrix} \hat{\mathbf{i}} & \hat{\mathbf{j}} & \hat{\mathbf{k}} \\ \frac{\partial \bullet}{\partial x} & \frac{\partial \bullet}{\partial y} & \frac{\partial \bullet}{\partial z} \\ u_1 & u_2 & u_3 \end{vmatrix} = \left(\frac{\partial u_3}{\partial y} - \frac{\partial u_2}{\partial z}\right)\hat{\mathbf{i}} + \left(\frac{\partial u_1}{\partial z} - \frac{\partial u_3}{\partial x}\right)\hat{\mathbf{j}} + \left(\frac{\partial u_2}{\partial x} - \frac{\partial u_1}{\partial y}\right)\hat{\mathbf{k}} \tag{A.24}$$

Note that, in the expansion of the determinant, the operators $\frac{\partial}{\partial x}$, $\frac{\partial}{\partial y}$, and $\frac{\partial}{\partial z}$ must precede the components u_1, u_2, and u_3.

Properties:

(i) For differentiable vector functions $\mathbf{u}$ and $\mathbf{s}$,

$$\nabla \times (\mathbf{u} + \mathbf{s}) = \nabla \times \mathbf{u} + \nabla \times \mathbf{s} \text{ or } \text{curl}(\mathbf{u} + \mathbf{s}) = \text{curl}\mathbf{u} + \text{curl}\mathbf{s} \tag{A.25}$$

(ii) For a differentiable vector function $\mathbf{u}$ and differentiable scalar function ϕ of position,

$$\nabla \times (\phi\mathbf{u}) = (\nabla\phi) \times \mathbf{u} + \phi(\nabla \times \mathbf{u}) \tag{A.26}$$

(iii) If ϕ is a differentiable scalar function with continuous second partial derivatives, then

$$\nabla \times (\nabla\phi) = 0 \tag{A.27}$$

i.e., the curl of the gradient of ϕ is zero (from an exercise).

Note that if ϕ is a function of x, y, and z and has continuous second partial derivatives, then the order of differentiation is immaterial so that

$$\frac{\partial^2}{\partial y \partial x}\phi = \frac{\partial^2}{\partial x \partial y}\phi, \frac{\partial^2}{\partial z \partial x}\phi = \frac{\partial^2}{\partial x \partial z}\phi, \frac{\partial^2}{\partial z \partial y}\phi = \frac{\partial^2}{\partial y \partial z}\phi$$

For a physical interpretation of the curl of a vector, see Fig. 15.12 in the reference by Wylie and Barrett.

A.6 Integral of a Vector Function

$$\int \mathbf{u}(t)dt = \hat{\mathbf{i}} \int u_1(t)dt = \hat{\mathbf{j}} \int u_2(t)dt = \hat{\mathbf{k}} \int u_3(t)dt + \mathbf{c} \tag{A.28}$$

where $\mathbf{u}(t) = u_1(t)\hat{\mathbf{i}} + u_2(t)\hat{\mathbf{j}} + u_3(t)\hat{\mathbf{k}}$ and $c = c_1\hat{\mathbf{i}} + c_2\hat{\mathbf{j}} + c_3\hat{\mathbf{k}}$ denotes a constant vector.

References for Appendix A: Arfken and Weber, BMW, Bond and Allman, Lass, Spiegel, Wylie and Barrett

Exercises

A.1. Derive a formula for the cosine of the angle between two vectors:

$$\mathbf{r}_1 = (x_1, y_1, z_1) \quad \text{and } \mathbf{r}_2 = (x_2, y_2, z_2)$$

That is, prove that

$$\cos\theta = \frac{\mathbf{r}_1 \bullet \mathbf{r}_2}{\mathbf{r}_1 \mathbf{r}_2}$$

where θ denotes the angle between $\mathbf{r}_1$ and $\mathbf{r}_2$. This equation is property (iv) for the dot product. (Do not use property (iv) in doing this exercise.)

A.2. Let $\mathbf{r}_1 = \mathbf{i} + 2\mathbf{j} + 2\mathbf{k}$ and $\mathbf{r}_2 = 4\mathbf{i} - 3\mathbf{k}$.
- (a) Determine the unit vector along $\mathbf{r_1}$.
- (b) Determine the dot product of the vectors $\mathbf{r}_1$ and $\mathbf{r}_2$.
- (c) Determine the angle between $\mathbf{r}_1$ and $\mathbf{r}_2$.

A.3. Let $\mathbf{r_1} = 3\mathbf{i} - \mathbf{j} + 2\,\mathbf{k}$, $\mathbf{r_2} = 2\mathbf{i} + \mathbf{j} - \mathbf{k}$, and $\mathbf{r_3} = \mathbf{i} - 2\mathbf{j} + 2\,\mathbf{k}$.
- (a) Compute $(\mathbf{r_1} \times \mathbf{r_2}) \times \mathbf{r_3}$.
- (b) Compute $\mathbf{r_1} \times (\mathbf{r_2} \times \mathbf{r_3})$.
  Note that $(\mathbf{r_1} \times \mathbf{r_2}) \times \mathbf{r_3} \neq \mathbf{r_1} \times (\mathbf{r_2} \times \mathbf{r_3})$, showing the need for parentheses in $\mathbf{r_1} \times \mathbf{r_2} \times \mathbf{r_3}$ to avoid ambiguity.
- (c) Compute $\mathbf{r_1} \bullet (\mathbf{r_2} \times \mathbf{r_3})$.
- (d) Compute $(\mathbf{r_1} \times \mathbf{r_2}) \bullet \mathbf{r_3}$.
  Note that $\mathbf{r_1} \bullet (\mathbf{r_2} \times \mathbf{r_3}) = (\mathbf{r_1} \times \mathbf{r_2}) \bullet \mathbf{r_3}$.
  In general, the dot and cross product are interchangeable in the sense shown.

A.4. Let $\mathbf{r_1} = 2\mathbf{i} + \mathbf{j}$ and $\mathbf{r_2} = \mathbf{i} + 3\mathbf{j}$.
- (a) Compute $\mathbf{r_3} = \mathbf{r_1} \times \mathbf{r_2}$.
- (b) Compute $\mathbf{r_4} = \mathbf{r_3} \times \mathbf{r_1}$.
- (c) Sketch the vectors $\mathbf{r_1}$, $\mathbf{r_2}$, and $\mathbf{r_4}$ in the x,y plane.
- (d) Where is the $\mathbf{r_3}$ vector and where is it pointing?
- (e) Show that $\mathbf{r_4}$ is perpendicular to $\mathbf{r_1}$.

A.5. Let $\mathbf{R} = \sin(t)\mathbf{i} + \cos(t)\mathbf{j} + t\mathbf{k}$.
Find:
(a) $d\mathbf{R}/dt$
(b) $d^2\mathbf{R}/dt^2$
(c) $|d\mathbf{R}/dt|$
(d) $|d^2\mathbf{R}/dt^2|$
(e) R = magnitude of $\mathbf{R}$
(f) dR/dt
(g) d^2R/dt^2

A.6. Determine the derivative with respect to time t of the cross product $\mathbf{r}_1 \times \mathbf{r}_2$ where

$$\mathbf{r}_1 = 2t\mathbf{i} - 3t^2\mathbf{j} \quad \text{and } \mathbf{r}_2 = -4\mathbf{i} + 2t\mathbf{j}$$

and compare the result to the derivative determined by the equation given in property (iii) in the subsection entitled "Derivative of a Vector Function."

A.7. Prove Lagrange's identity:

$$(\mathbf{a} \times \mathbf{b}) \bullet (\mathbf{c} \times \mathbf{d}) = (\mathbf{a} \bullet \mathbf{c})(\mathbf{b} \bullet \mathbf{d}) - (\mathbf{a} \bullet \mathbf{d})(\mathbf{b} \bullet \mathbf{c})$$

for any vectors **a**, **b**, **c**, and **d**.

A.8. Prove that, for any differentiable vector $\mathbf{u} = \mathbf{u}(t)$,

$$\mathbf{u} \bullet \frac{d\mathbf{u}}{dt} = u\frac{du}{dt}$$

A.9. A particle moves along a curve whose parametric equations are

$$x = 2t^2, y = t^2 - 4t, z = 3t - 5,$$

where t denotes time. Find the particle's velocity and acceleration in the direction of the vector $\mathbf{i} - 3\mathbf{j} + 2\mathbf{k}$ at time t = 1.

A.10. Consider the curve which is defined parametrically by the equations

$$x = t^2 + 1, y = 4t - 3, z = 2t^2 - 6t$$

(a) Find the unit tangent vector at any point on this curve as a function of t.
(b) Determine the unit vector that is tangent to this curve at t = 2.

A.11. A particle moves so that its position vector is given by the equation

$$\mathbf{r} = \cos(\omega t)\mathbf{i} + \sin(\omega t)\mathbf{j}$$

where ω is a constant.
(a) Show that the velocity **v** of the particle is perpendicular to the position **r**.
(b) Show that $\mathbf{r} \times \mathbf{v}$ is a constant vector.

A.12. (a) What is the directional derivative of the function

$$\phi(x, y, z) = x^2yz + 4xz^2$$

at the point (1, −2, −1) in the direction of the vector $\mathbf{u} = 2\mathbf{i} - \mathbf{j} - 2\,\mathbf{k}$?

(b) Is ϕ increasing or decreasing in the direction of the vector **u** at the point given? Explain.

A.13. Prove that if ϕ is a differentiable scalar function with continuous second partial derivatives, then

$$\nabla \times (\nabla \phi) = 0$$

i.e., the curl of the gradient of ϕ is zero.

A.14. A particle moves along a curve whose parametric equations are

$$x = e^{-t},\ y = 2\cos(3t), z = 2\sin(3t)$$

where t denotes time.

(a) Determine the velocity and acceleration vectors of the particle at any time t.

(b) Compute the magnitude of the velocity and acceleration vectors at time $t = 0$.

(c) Compute the rate of change dr/dt of the magnitude r of the position vector at any time t.

(d) Compute dr/dt at $t = 0$.

(e) Note that $|d\mathbf{r}/dt| \neq dr/dt$. Why?

A.15. Let $\phi = 1/r$, where r denotes the magnitude of the vector $\mathbf{r} = (x, y, z)$. Find $\nabla\phi$.

A.16. The acceleration of a particle at any time $t \geq 0$ is given by

$$\mathbf{a} = \frac{d\mathbf{v}}{dt} = 12\cos(2t)\mathbf{i} - 8\sin(2t)\mathbf{j} + 16t\mathbf{k}$$

If the velocity vector **v** and position **r** are zero at $t = 0$, find the vectors **v** and **r** at any time $t \geq 0$.

Appendix B Projects

The following projects have been designed to build on and strengthen the student's grasp of the material contained in Chaps. 1–8 by combining several of the topics studied in those chapters in useful exercises.

B.1 Trajectory Propagation Project

MATLAB References

Selected MATLAB references are:

1. Brian D. Hahn and Daniel T. Valentine, *Essential MATLAB For Engineers and Scientists,* Fifth Edition, Elsevier Ltd., Burlington, 2013.
2. Duane Hanselman and Bruce Littlefield, *Mastering Matlab 8,* Prentice Hall, 2011.
3. The MathWorks URL for online MATLAB documentation at http://www.mathworks.com/access/helpdesk/help/helpdesk.html [accessed 6/1/2014]
4. MATLAB Tutorial website at http://www.cyclismo.org/tutorial/matlab/ [accessed 6/1/2014]

However, the reader may already own and be accustomed to using a satisfactory alternative reference or tutorial.

Project Statement

Let initial values $\mathbf{r_0}$ (position vector) and $\mathbf{v_0}$ (velocity vector) be given at the initial time t_0. Write a MATLAB computer program to do the following:

1. Determine the type of orbit.
2. Compute Keplerian elements at the initial time t_0 as follows:
   (a) For elliptical orbits: e, p, a, τ, r_p, r_a, i, Ω, ω, θ, E, M, t_p
   (b) For parabolic orbits: p, r_p, i, Ω, ω, θ
   (c) For hyperbolic orbits: e, p, a, V_∞, r_p, i, Ω, ω, θ

© Springer International Publishing Switzerland 2015

G.R. Hintz, *Orbital Mechanics and Astrodynamics*,
DOI 10.1007/978-3-319-09444-1

3. Determine whether the spacecraft will or will not impact the central body.
4. Compute the position vector $\mathbf{r} = \mathbf{r}(t)$ and velocity vector $\mathbf{v} = \mathbf{v}(t)$ at a specified time t, where $t > t_0$.

Rules for Completing This Project

1. It is acceptable to use mathematical subroutines such as those used to compute the dot or cross product of vectors.
2. It is not acceptable to call a subroutine that converts Cartesian coordinates to classical (Keplerian) elements or vice versa unless you have written the subroutine yourself.
3. It is not acceptable to call a subroutine that you have not written yourself to solve an equation such as Kepler's equation.
4. You may not copy or use someone else's code, including other students, colleagues, any textbooks, references, or online sources.
5. It is okay to discuss the project with others.
6. You may not give your code to anyone, except your instructor or assistant, during this course or later.
7. Show angles in degrees.

Programming Guidelines

1. Construct MATLAB M-file(s) as you did in Exercise 4.4 for the patched conic model.
2. Use input commands to supply the input data as you did for Exercise 4.4.
3. Provide comments that:
   (a) Give the name of each variable and describe it when it is initialized and give its unit(s).
   (b) Describe the input and output with units.
   (c) Describe what the program does and the computations.
   (d) Describe the logic and functional flow of the program.
4. In general, follow the programming guidelines given in the reference by Hahn and Valentine or an equivalent MATLAB text.
5. Then submit your well-commented code.

Final Report

Turn in all of the following:

1. Your computer printout from the command window for each of the five data cases defined below.
2. Your well-commented code.

3. A table of your answers for each of the data cases defined below. Submit one table for each of the five data cases.
4. Data that verify that the final vectors **r**(t) and **v**(t) are correct. Do not just make a generic statement such as "I made a lot of computations to verify the results." Give specific examples and explain how the data you provide verify that your final vectors **r**(t) and **v**(t) are correct.
5. Something extra that is related to the project (an interesting, related, nontrivial task), but not required by the above statement of the project. That is, do something extra and explain it in your write-up. Do not just discuss a topic. Then identify the extra task in your report.

Input for Computer Project

Add other input as required. Also, see the explanation below for the data cases.

Case I: Spacecraft at Earth

$$\mathbf{r_0} = (-14192.498,\ -16471.197,\ -1611.2886) \quad (\text{km})$$

$$\mathbf{v_0} = (-4.0072937,\ -1.2757932, 1.9314620) \quad (\text{km/s})$$

in an earth-centered inertial coordinate system

$$\Delta t = 8.0 \text{ h}$$

Case II: Heliocentric Orbit

$$\mathbf{r_0} = (148204590.0357, 250341849.5862, 72221948.8400) \quad (\text{km})$$

$$\mathbf{v_0} = (-20.5065125006,\ 7.8793469985,\ 20.0718337416) \quad (\text{km/s})$$

$$\Delta t = 10 \text{ days}$$

in the heliocentric, ecliptic of J2000 coordinate system.

Case III: Cassini Spacecraft at Saturn
On June 30, 2004, at 14:00:00 ET, the Cassini spacecraft was at the position

$$\mathbf{r_0} = (-321601.0957,\ -584995.9962,\ -78062.5449) \quad (\text{km})$$

with the velocity vector

$$\mathbf{v_0} = (8.57101142, 7.92783797, 1.90640217) \quad (\text{km/s})$$

in Saturn-centered, Earth mean equator and equinox of J2000.0 coordinates. What were the spacecraft's position and velocity vectors in this inertial coordinate system when the spacecraft crossed the ring plane on July 1, 2004, at 00:47:39.30 ET?

Case IV: Huygens Probe at Titan*
On January 14, 2005, at 09:00:00 ET, Cassini's Huygens probe was at the position

$$\mathbf{r_0} = (8193.2875, -21696.2925, 7298.8168) \quad (\text{km})$$

with the velocity vector

$$\mathbf{v_0} = (-2.29275936, 4.94003573, -1.67537281) \quad (\text{km/s})$$

in Titan-centered*, Earth mean ecliptic and equinox of J2000.0 coordinates. Determine the probe's position and velocity vectors 1 h 4 min and 1.18 s later in this inertial coordinate system.

Where was the probe at this time? As an approximation, ignore all forces other than the gravity of Titan, i.e., use the two-body mechanics model, in answering this question.

*Titan is a moon of Saturn with mean radius of 2,575 km, making it larger than the planet Mercury.

Case V: Spacecraft at Earth

$$\mathbf{r_0} = (5492.00034, 3984.00140, 2.95581) \quad (\text{km})$$

$$\mathbf{v_0} = (-3.931046491, 5.498676921, 3.665980697) \quad (\text{km/s})$$

$$\Delta t = 5.0 \text{ h}$$

in ECI coordinates

Explanations for these data cases:

1. Case III gives the times t_0 and t as dates and epochs. It is not necessary to make your computer project convert $t - t_0$ from date/epoch to Δt. It is okay to do this conversion off-line and input Δt. However, be careful in making off-line computations. Remember GIGO (garbage in, garbage out).
2. Case IV gives $\Delta t = 1$ h. 4 min. 1.18 s. It is okay to convert this value of $t - t_0$ to Δt in hours off-line and input Δt in hours as for the other data cases.
3. It is not necessary to compute the answer to the extra question ("Where was the probe at this time?") for Case IV in your program. You may perform required computations off-line and give your answer with explanation in the text of your report.

B.2 Online Ephemeris Project for an Asteroid

Background for Asteroids

Events for asteroids are:

1. Discovery
2. Reacquisition for Confirmation
3. Provisional (Temporary) Name, e.g., 1999 TL10
4. Number and name designation, e.g., 1 Ceres, 4 Vesta, 9007 James Bond (Closest approach to earth at 1.516 AU on 1/22/08), and 13070 Seanconnery (Closest approach to earth at 1.980 AU on 1/24/08)

Some facts about asteroids are:

1. The first asteroid, 1 Ceres, was discovered by Giuseppe Piazzi in January 1801.
2. The Dawn spacecraft was launched on 9/27/07 to orbit Vesta and then Ceres, the only dwarf planet in the inner solar system.
3. Spacecraft flybys include, e.g., Galileo of Gaspra and Ida (and Ida's satellite Dactyl), NEAR-Shoemaker of Mathilde and landing on Eros, and Stardust of Annefrank.

Example (Temporary Asteroid Name): 1999 TL10
In this name "1999" is the year of discovery; "T" denotes the half-month of its discovery, which is the first half of October (after skipping "I" because it looks too much like a "one"); and "L10" denotes the number of the asteroid in the half-month of its discovery. In determining the half-month, "A" covers January 1–15, "B" January 16–31, "C" February 1–15, "D" February 16–28 or 29, etc. skipping I as noted. The first letter of the pair of letters for a given month denotes the first 15 days of the month and the second of the pair denotes the rest of the month. Thus, "1999 TA" is the temporary name of the first asteroid discovered in October, "1999TB" the second discovered in October, etc., skipping I, etc., 1999 TZ is the 25th, 1999 TA1 the 26th, etc., 1999 TZ1 the 50th, 1999 TZ2 the 51st, etc. Therefore, 1999 TL10 is the $(10 \times 25) + 11 = 261$st asteroid discovered in the first half of October 1999.

Reference: Cunningham

Project Statement

Use the web-interface option (method) in HORIZONS, JPL's Online Solar System Data and Ephemeris Computation Service, to answer the questions in Part 1. HORIZONS is available on the solar system dynamics website at
http://ssd.jpl.nasa.gov/

Include select printout from HORIZONS as part of your answers and "highlight" (draw a box around) the appropriate data. Also, complete Part 2 as indicated below.

Part 1: Questions About Asteroid 2012 DA14

The asteroid 2012 DA14, which made a closest approach (encounter) to the earth in 2013, is cited as an example for the Online Ephemeris Project, but a different small body can be substituted by the instructor in its place.

1. What is the solution date and epoch for your data?
2. What are the period, eccentricity, perihelion distance, and aphelion distance of the heliocentric orbit of the asteroid 2012 DA14?
3. What is the closest this asteroid came to the earth in 2013? (You need to do a calculation off-line using data obtained from HORIZONS.)
4. On what date and at what time (to the nearest minute) did this encounter occur?
5. In which constellation did the asteroid appear at the time of its closest approach to the earth? (Give the full name of the constellation, not an abbreviation.)
6. What was the asteroid's velocity with respect to the sun at closest approach to the earth?
7. What was the asteroid's greatest distance from the earth in the period between 1/1/13 and 3/26/13 and when was it at this greatest distance?
8. What was the asteroid's velocity with respect to an observatory in Los Angeles at the time of the asteroid's closest approach to the earth?
9. What are the coordinates of the observatory in Los Angeles?
10. Find something interesting in the ssd website.

Part 2: Other Questions/Problems Related to Course Material

11. Convert the closest distance found in response to question 3 to LD (lunar distances). That is, convert the distance to a fraction of the distance between the earth and the moon.
12. Calculate the V_∞ of the asteroid's hyperbolic trajectory at its passage of the earth, using data available from the ssd website.
13. When was the asteroid 2012 DA14 discovered?
14. How many asteroids were discovered before 2012 DA14 in the half-month of its discovery?

B.3 Online Ephemeris Project on PHAs, NEOs, and Other Celestial Objects

Project Statement

Use the ssd and neo websites to answer the following questions. Dates below are given as examples. Different dates may be specified by the instructor as appropriate for this exercise if desired.

Part 1: Questions About PHAs, NEOs, and the Torino Scale

1. What is a potentially hazardous asteroid (PHA)? How many PHAs are known?
2. Which near-earth objects (NEOs) came within a nominal miss distance of 0.5 LD (lunar distance) of the earth since 12/12/12? What was the nominal closest approach (CA) distance of each of these objects? What was the date of each of these closest approaches? Include a copy of the one page in the table from the website with the appropriate information "highlighted."
3. Which NEO discovered in 2012 came within the closest nominal miss distance of the earth since 11/10/12? What was the nominal CA distance of this object and what was the date of its CA? Highlight the appropriate information in the page from the website supplied in your answer to question 2.
4. Which of the known PHAs will come closest to the earth, considering the nominal miss distance, in the next 25 years? What date will this object make its CA to the earth and how close will this object approach the earth? Include a copy of the one page in the table from the website with the appropriate information (asteroid name, date of CA, and nominal miss distance) "highlighted."

5a. What is the Torino scale?

5b. Which asteroids have a value on the Torino scale greater than zero?

6. Explore the ssd and neo websites to find something else that is interesting. What is one interesting item that you found?

Part 2: Computation of Rise, Transit, and Set Times for Earth-Based Observatories

1. At what time UT did Mars rise as seen from an observatory in Los Angeles, CA, on 12/11/2013?
2. Was Mars optically observable from a site in Los Angeles, CA, as it set on 12/11/2013? Explain why or why not.
3. What constellation was Mars in when it set on 12/11/2013?
4. What are the latitude and longitude of Los Angeles, CA?

Part 3: Questions About Trojan Asteroids

1. Which Trojan asteroids have a semimajor axis that satisfies the conditions

$$5.328 \text{ AU} \leq a < 5.3305 \text{ AU}?$$

2. What are the semimajor axis, eccentricity, inclination, and argument of perihelion of each of these asteroids?

   For these two questions, include a copy of the one page in the table from the website with the appropriate information (object full name, e, a, *i*, and peri) "highlighted."
3. Which of the asteroids found in the answer to question 1 of Part 3 has an IAU name? What is the IAU name for each one?

Part 4: Use of Orbit Diagrams in the Neo Website

Follow the procedure for visualizing the orbit of a comet or asteroid via an orbit diagram in the neo website to answer the following questions with respect to the comet Lulin (2007N3), nicknamed the "green comet."

1. On what date did comet Lulin pass through perihelion and what was its distance from the sun at that point?
2. When (approximate date) did comet Lulin make its closest approach to Mars?
3. What is the eccentricity of comet Lulin's orbit? Make a copy of the table that gives this value, "highlight" the appropriate entry in the table, and submit the table with your answer. Note how close comet Lulin's orbit is to being parabolic.
4. Is comet Lulin's orbit posigrade or retrograde? Note how close comet Lulin's orbit is to being in the ecliptic plane.

References for Appendix B: Cunningham, MathWorks website, MATLAB Tutorial website, neo website, ssd website.

Appendix C Additional Penzo Parametric Plots

C.1 Objectives

The P^2 parameters discussed so far are either constraints or have been directly connected with a parametric representation of these constraints. They were chosen to minimize the parametric representation required and to enhance intuitive knowledge of free-return circumlunar trajectories.

The reference "An Analysis of Free-Flight Circumlunar Trajectories" by Paul A. Penzo gives parametric plots of additional parameters, including the following:

1. Injection velocity versus the outward time of flight for various positions of the moon in its orbit (Fig. C.1).
2. Parking orbit altitude versus injection velocity for fixed injection energies C_3 (Fig. C.2).
3. Probe-moon-earth angle versus the outward time of flight for various positions of the moon in its orbit (Fig. C.3).
4. Hyperbolic excess velocity versus the outward time of flight for fixed outward-phase inclinations and various positions of the moon in its orbit (Fig. C.4).
5. Earth-moon-probe-angle at the spacecraft's exit from the SoI versus the return time of flight for various positions of the moon in its orbit (Figs. C.5 and C.6).
6. Components of the impact vector **B** for constant outward times of flight (Fig. C.7).

These parameters provide velocity information at the earth and at the moon and information about entrance and exit angles at the moon's sphere of influence.

C.2 Injection Velocities and the PME Angle

Figure C.1 presents the injection velocities required for specified outward times of flight. The injection altitude is fixed at 600,000 ft (183 km). This velocity is essentially a function of only the time of flight and distance of the moon. Figure C.2 can be used to convert these injection velocities to other altitudes while holding the energy fixed.

© Springer International Publishing Switzerland 2015

G.R. Hintz, *Orbital Mechanics and Astrodynamics*,
DOI 10.1007/978-3-319-09444-1

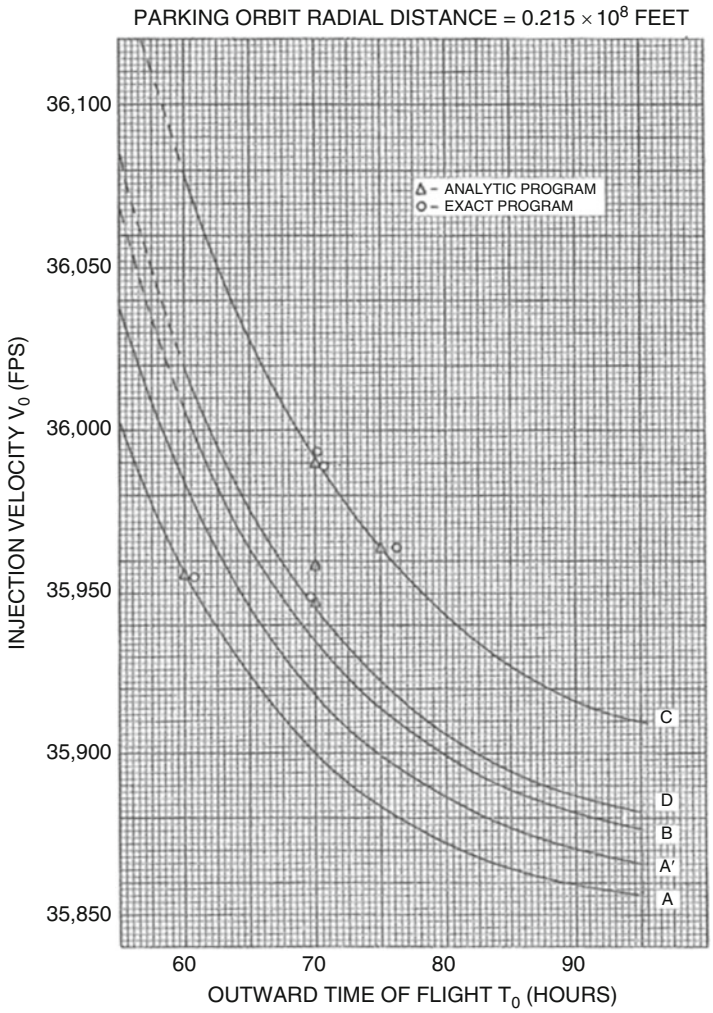

Fig. C.1 Injection velocity versus outward time of flight for various positions of the moon in its orbit

Considering parameters in the moon phase, Fig. C.3 presents the probe-moon-earth (PME) angle of the asymptotic velocity vector with the moon-to-earth line at the time of pericynthion passage for various positions of the moon in its orbit. We consider two specific types of launch trajectories:

Case I for all trajectories in which the spacecraft is launched ccw wrt the earth and so that the outward-phase conic lies in the moon's orbit plane.

Case II for which the spacecraft is launched normal to the moon's orbit plane. The symmetry relationship makes it immaterial as to whether the spacecraft approaches the moon from above or below the moon's orbit plane.

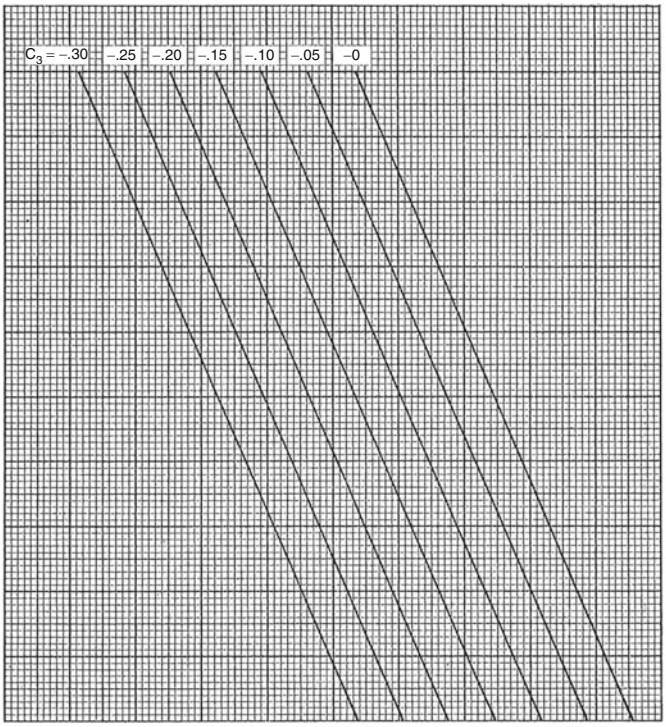

Fig. C.2 Parking orbit altitude versus the injection velocity for fixed injection energies C_3

Case I and Case II represent outward-phase launches in the moon's orbit plane and normal to the moon's plane, respectively. Qualitatively, we can deduce that the longer the flight time is to the moon the larger the PME angle. Also, from Fig. C.1, since shorter distances of the moon require lower injection velocities for a given flight time, the PME angle will increase for these shorter distances.

C.3 Moon-Phase Parameters: v_∞, EMP Angle at SoI Exit, and the B-Plane

Figure C.4 presents the moon-phase hyperbolic excess velocity as a function of the outward time of flight and the distance of the moon. The injection velocity is essentially independent of the outward inclination, but the v_∞ is not. For Case II, this velocity is from 400 to 800 fps greater than that for Case I. Exact integration (precision) software was run to provide a comparison with the analytic software. The exact integration software consistently produced a higher value for v_∞ than the analytic program.

An estimate for the earth-moon-probe (EMP) angle at exit from the SoI is given in Figs. C.5 and C.6. The behavior of this angle is similar to the PME angle. Three

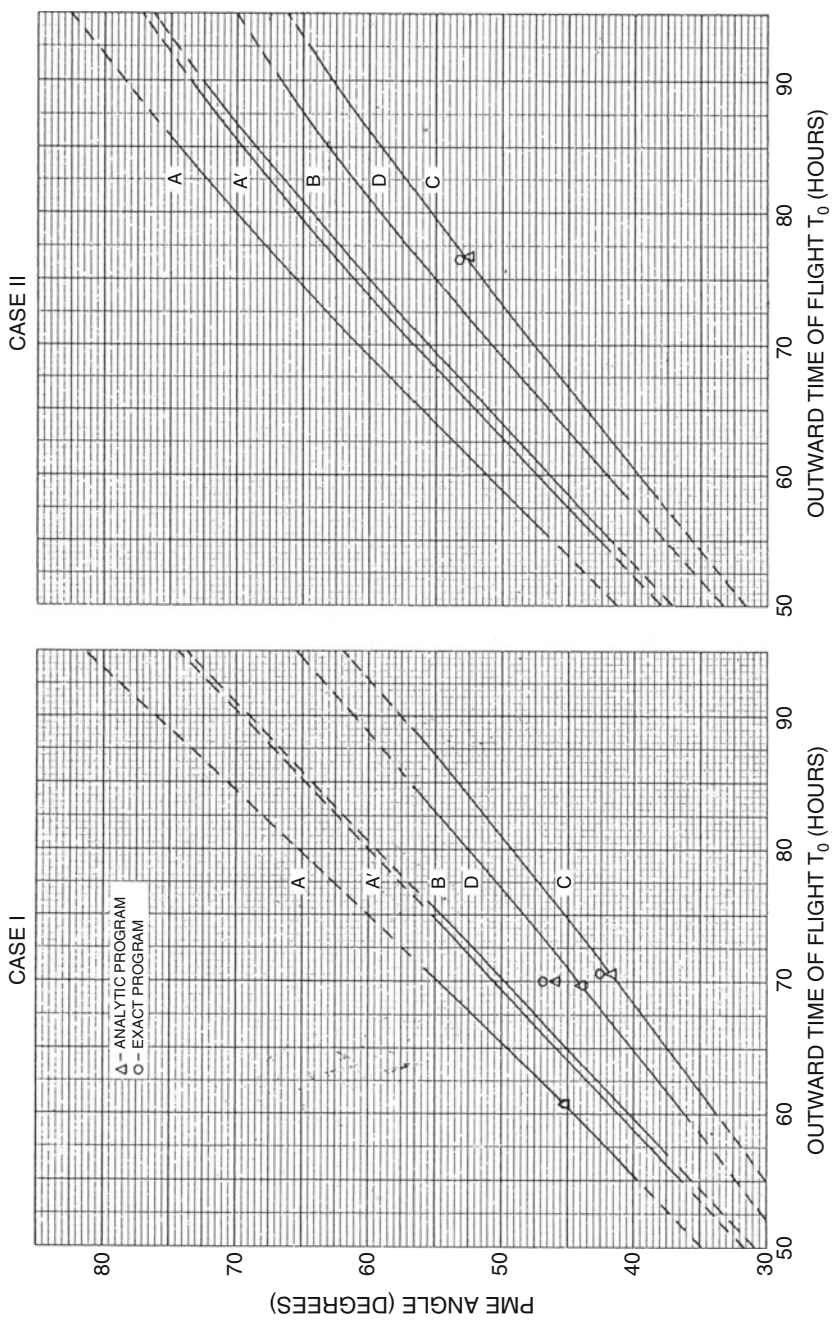

Fig. C.3 Probe-moon-earth angle versus the outward time of flight for various positions of the moon in its orbit

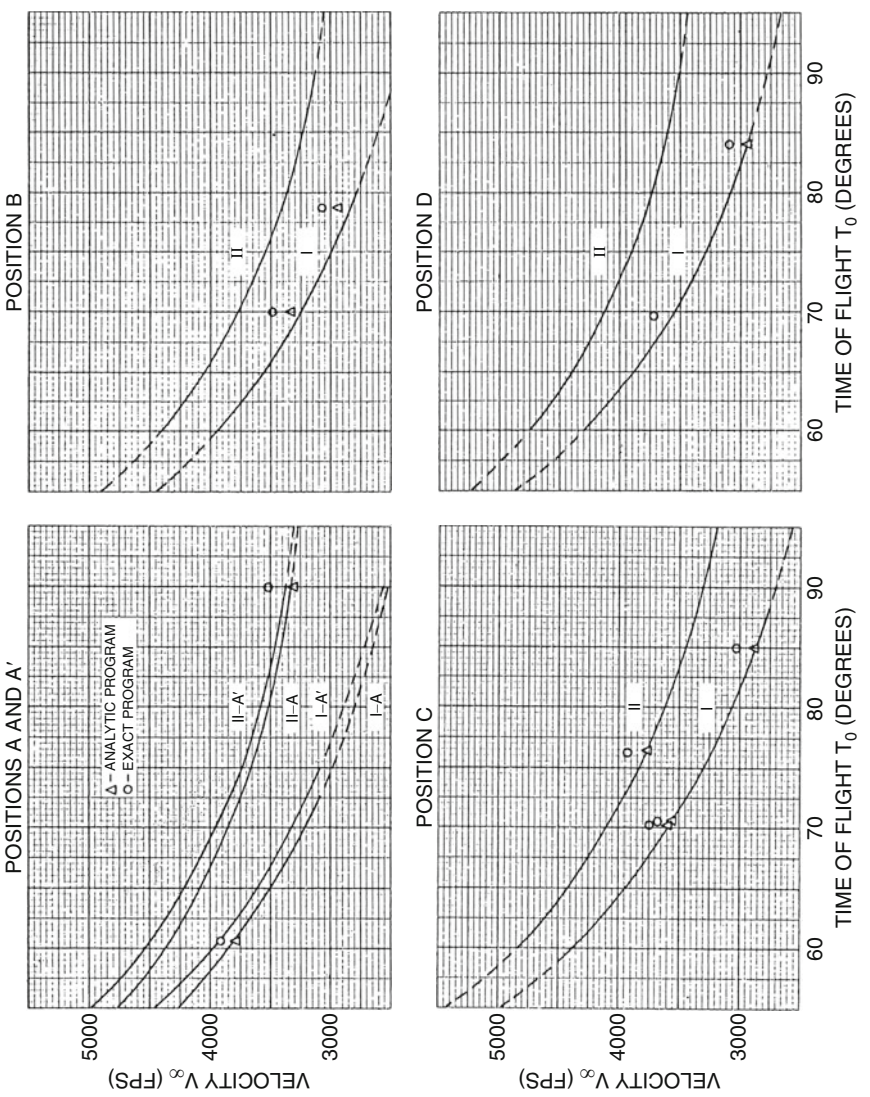

Fig. C.4 Hyperbolic excess velocity versus the outward time of flight for fixed outward-phase inclinations and various positions of the moon in its orbit

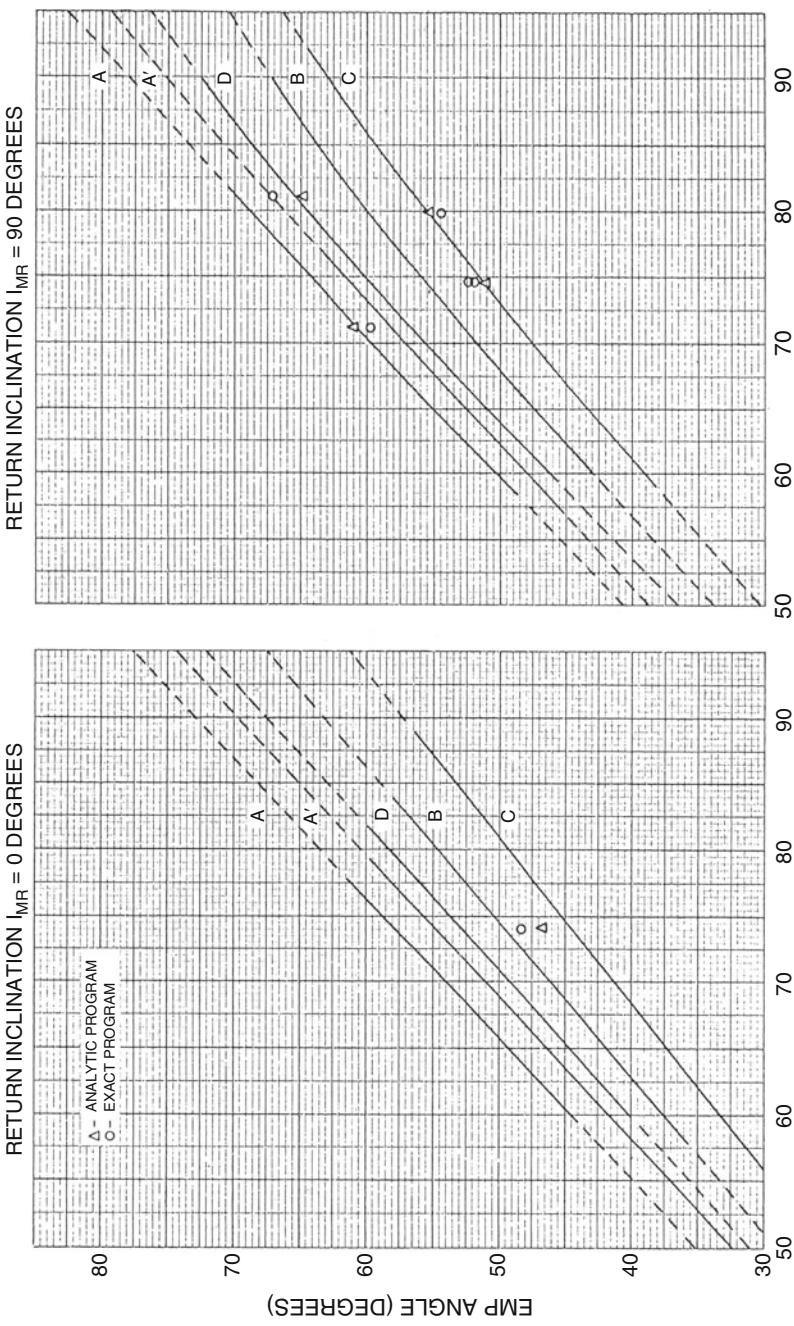

Fig. C.5 Earth-moon-probe angle versus the return time of flight for various positions of the moon in its orbit at the spacecraft's exit from the SoI

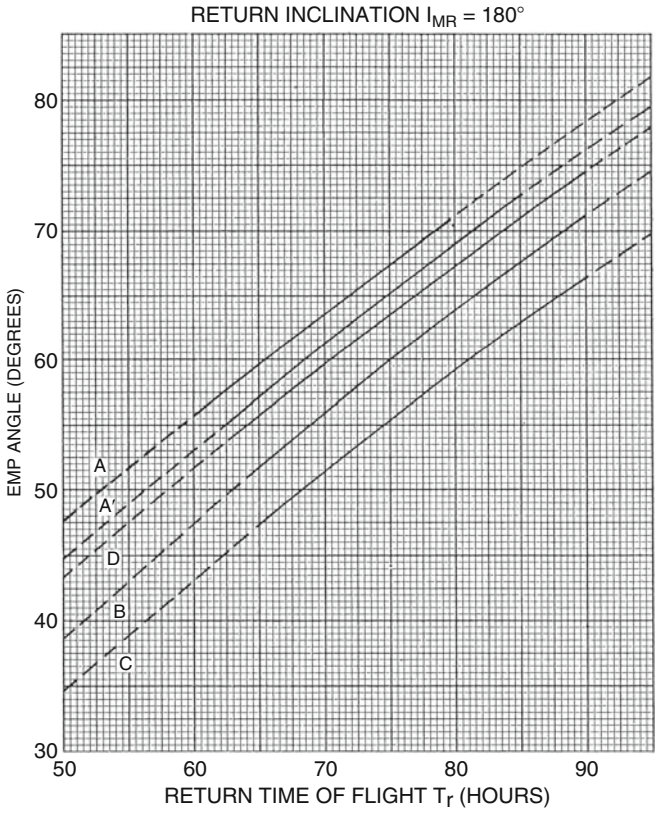

Fig. C.6 Earth-moon-probe angle versus the return time of flight for various positions of the moon in its orbit at the spacecraft's exit from the SoI (continued)

return inclinations are considered. Note that the EMP angle increases as the return inclination rotates from ccw to cw.

Finally, traces of the (impact) B-vector measured in the (impact) B-plane are presented in Fig. C.7. The B-plane is defined to be perpendicular to the incoming hyperbolic asymptote. The horizontal or B•T axis lies in the moon's orbit plane and is directed positively opposite the moon's direction of motion. The vertical or B•R axis is directed positively below the moon's orbit plane. The origin is fixed to the center of the moon. For all circumlunar trajectories considered here, the asymptote is inclined only $\pm 10^\circ$ to the moon's orbit plane. The PME angle, which indicates the position of the asymptote wrt the earth-moon line, also indicates the position of the impact parameter plane. Since this angle varies greatly with time of flight, outward inclination, and position of the moon, the impact parameter plane is oriented differently from the earth-moon line for each point in Fig. C.7.

Both graphs in Fig. C.7 are drawn for the maximum distance of the moon. The outward flight time and the return inclination wrt the moon's orbit plane are

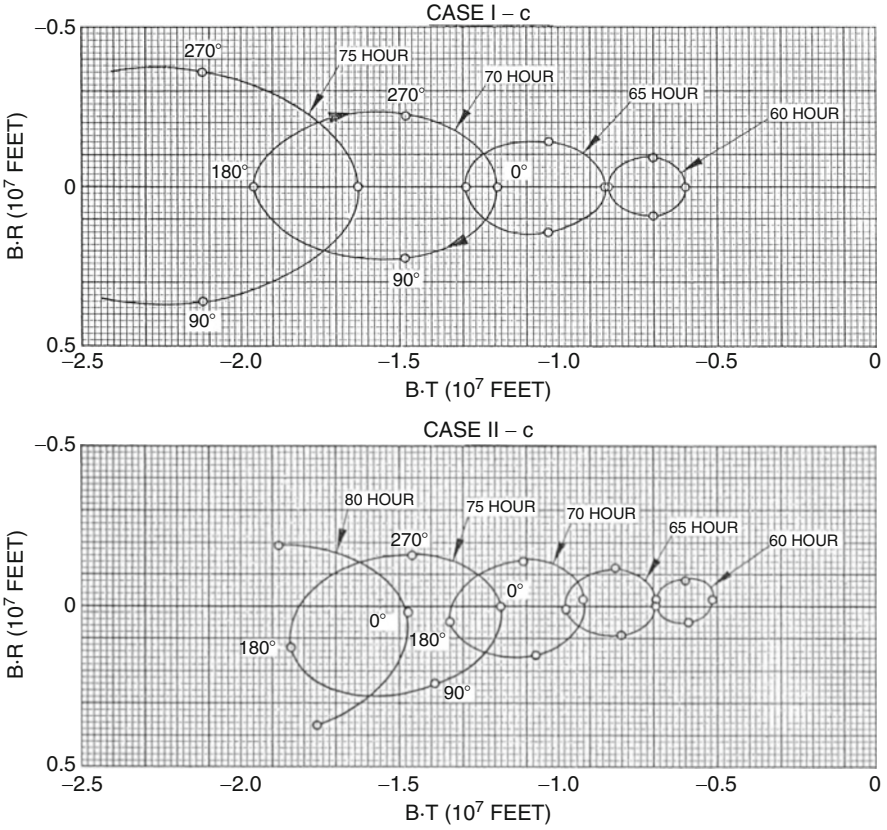

Fig. C.7 Components of the impact vector **B** for constant outward times of flight

indicated. The larger magnitude of the impact parameter for a fixed time of flight implies a greater pericynthion distance. A greater time of flight produces a greater impact parameter since the incoming asymptote must be further from the moon for lower moon-centered energies and the same turning of the spacecraft's velocity vector.

Answers to Selected Exercises

Chapter 1

1.3. α, β
1.5. (2.0164, −1.9377, 18.4981)
1.6. (17.9610, 4,7662, 2.1651) (km)

Chapter 2

2.9. (a) ellipse
(b) 286.83°
2.11. (e) $(\pi/2 - e)/(2\pi)$
2.16. (a) $\beta_0 = 45.17°$
$\dot{r} = 1.41045\,\text{km/s}$
$\dot{r}\theta = 1.40229\,\text{km/s}$
(b) radial component vector = (−1.17271992, −0.72798589, 0.29004357)
transverse component vector = (0.77502268, −1.02438770, 0.56248357)
(c) $a = 970375.5$ km
$e = 0.8495$
$p = 540145.94$ km
$r_p = 292046.76$ km
$r_a = 3589455.02$ km
$\tau = 31.92$ days
(d) $\theta = 168.57°$
$E = 141.35°$
$M = 110.94°$
(e) $t_p = 9.8371$ days
Time to next periapsis = 22.0833 days

© Springer International Publishing Switzerland 2015

G.R. Hintz, *Orbital Mechanics and Astrodynamics*,
DOI 10.1007/978-3-319-09444-1

Chapter 3

3.1. (c) $\mathscr{E} = -12.65\ \text{km}^2/\text{s}^2$
$a = 15{,}759$ km
$p = 11430.6$ km
$h = 67500\ \text{km}^2/\text{s}$

3.3. (a) $e = 0.34$
$\theta_0 = 110^\circ$
$\mathscr{E} = -28.4417\text{km}^2/\text{s}^2$
$a = 7007.3$ km
$r_p = 4624.8$ km
$r_a = 9389.8$ km
$E = 90^\circ$

(b) $\beta = 30^\circ$
$v = 7.91$ km/s

3.9. (a) 6.305 km/s

(b) 116.07°

3.14. (a) $e = 0.1179$
$\theta = 119.48^\circ$
$h = 5.338 \times 10^9\ \text{km}^2/\text{s}$
$r_p = 1.9207 \times 10^8$ km
$a = 2.1775 \times 10^8$ km
$\tau = 641.41$ days

(b) $e = 0.1179$
$\theta = 240.52^\circ$
$h = 5.338 \times 10^9\ \text{km}^2/\text{s}$
$r_p = 1.9207 \times 10^8$ km
$a = 2.1775 \times 10^8$ km
$\tau = 641.41$ days

3.16. $\Delta v_{SOI} = 0.624$ km/s

3.20. (a) Thrust = 96,500 N

(b) $\Delta v = 0.6152$ km/s

3.21. $\Delta m = 9924.72$ kg

3.22. $\Delta m = 850.9$ kg

Chapter 4

4.8. $i = 26.8^\circ$, $\Omega = 187.2^\circ$, $\omega = 341.9^\circ$

4.9. (a) $\theta = 207.23^\circ$

(b) $\mathbf{r} = (-174663897.0, 74685964.6, 49660154.5)$ km
$\mathbf{v} = (-5.44426, -21.66724, -3.38179)$ km/s

4.12. (a) $a = 5.112$ AU
$e = 0.8045$

4.20. (a) 48,214,824 km
(b) 112,378 km
(c) 43,317 km

Chapter 5

5.3. (a) $i = 63.43^\circ$ or 116.57°
(b) $63.43^\circ < i < 116.57^\circ$
5.7. 2.0×10^{-5}

Chapter 6

6.1. $\Delta V_{TOTAL} = 3.932$ km/s
6.2. (b) $\phi = 1.76$ rad $= 100.9^\circ$
(c) $\phi = 0.725$ rad $= 41.5^\circ$
6.5. (b) $\Delta V_{TOTAL} = 0.2428$ m/s

Chapter 7

7.1. (b)
$$\left.\frac{\partial \tau}{\partial V_M}\right|_{\theta=0^\circ} = 5.133 \text{ min/mps}$$
$$\left.\frac{\partial \tau}{\partial V_M}\right|_{\theta=180^\circ} = 0.442 \text{ min/mps}$$

7.7. (a) $\delta = 80.3^\circ$
(c) $r_p = 2{,}292$ km
7.9. (a) $r_p = 75{,}121$ km
$r_a = 700{,}546.2$ km
$\tau = 27.82$ days
(b) $\Delta m = 186.64$ kg
7.13. (c) $h_p = 639$ km
$T_r = 80$ h
7.15. (a) $Az = 90^\circ$
(b) $i_{req} = 65^\circ$

Acronyms and Abbreviations

AAS	American Astronomical Society
ACM	Attitude correction maneuver
AD	Arrival date
AGA	Aerogravity assist
AIAA	American Institute of Aeronautics and Astronautics
aka	Also known as
APS	Ascent Propulsion System
A Train	Afternoon constellation of spacecraft
AU	Astronomical unit
ATV	Automated Transfer Vehicle
AutoNav	Autonomous (optical) navigation
BMW	Text entitled *Fundamentals of Astrodynamics* by Roger R. Bate, Donald D. Mueller, and Jerry E. White
C3, C_3	Launch energy
CA	Closest approach
ccw	Counterclockwise
cw	Clockwise
cm	Center of Mass
CM	Command Module
CNES	Centre National d'Etudes Spatiales (French Space Agency)
Co.	Company
CONAE	Comision Nacional de Actividades Espaciales (Space Agency of Argentina)
CSM	Command and Service Module
CW	Clohessy-Wiltshire (equations or reference frame)
EDT	Eastern Daylight Time
DLA	Declination of launch azimuth
DSM	Deep Space Maneuver
DOF	Degrees of freedom
DPS	Descent Propulsion System
DS1	Deep Space 1 (spacecraft or space mission)
DSM	Deep Space Maneuver
DSN	Deep Space Network

© Springer International Publishing Switzerland 2015

G.R. Hintz, *Orbital Mechanics and Astrodynamics*,
DOI 10.1007/978-3-319-09444-1

ECI	Earth-centered inertial
EDL	Entry, descent, and landing
EGA	Earth gravity assist
EI	Entry interface
EMP	Earth-moon-probe (angle at exit of the moon's sphere of influence)
EOM	Equation of motion
ERT	Earth-received time
ESA	European Space Agency
ET	Ephemeris Time
FAQ	Frequently asked question
FF	Formation flying
FOM	Figure of merit
FPVS	Flight Plane Velocity Space
FT	Flight time
GEO	Geostationary orbit, geosynchronous orbit
Glonass	Global Navigation Satellite System aka Global Orbiting Navigation satellite system
GNC, GN&C	Guidance, navigation, and control
GPS	Global Positioning System (aka NAVSTAR)
GRB	Gamma ray bursts
GSFC	Goddard Space Flight Center
GTO	Geosynchronous transfer orbit
HCA	Heliocentric angle
HEO	High earth orbit, highly elliptical orbit
IAU	International Astronomical Union
IEEE	Institute of Electrical and Electronics Engineers
IERS	International Earth Rotation Service (formerly the Bureau International L'Heure, BIH)
I/P	Interplanetary
ISS	International Space Station
J2	Oblateness coefficient in spherical harmonic expansion
JAXA	Japanese Aerospace Exploration Agency (Japanese Space Agency)
JD	Julian Date
JPL	Jet Propulsion Laboratory
KI	Kepler's first law
KII	Kepler's second law
KIII	Kepler's third law
KE	Kinetic energy
LAT	Latitude
LD	Launch date
LEO	Low earth orbit
LEM	Lunar Excursion Module
LM	Lunar Module
LOI	Lunar Orbit Insertion

LOX	Liquid oxygen
LTF	Linearized time of flight
LV	Launch vehicle
MATLAB	Matrix Laboratory (computing system)
MCC	Midcourse correction
MER	Mars Explorer Rover
MEO	Medium earth orbit
MOI	Mars orbit insertion, Mercury orbit insertion
MSL	Mars Science Laboratory
NASA	National Aeronautics and Space Agency
NAVSTAR	Navigation Satellite Timing and Ranging (aka GPS)
NEAR	Near-Earth Asteroid Rendezvous (mission or spacecraft)
NEO	Near-earth object
NEXT	NASA's Evolutionary Xeon thruster
NI	Newton's first law of motion
NII	Newton's second law of motion
NIII	Newton's third law of motion
No.	Number
NPOESS	National Polar-orbiting Operational Environmental Satellite System
NPP	NPOESS Preparatory Project
NTO	Nitrogen tetroxide
OCM	Orbit correction maneuver
OD	Orbit determination
OIM	Orbit insertion maneuver
OTM	Orbit trim maneuver
OWLT	One-way light time
p	Page
pp	Pages
P^2	Penzo parametric (plot)
P&C	Text entitled *Orbital Mechanics* by John E. Prussing and Bruce A. Conway
PDT	Pacific Daylight Time
PE	Potential energy
PHA	Potentially hazardous asteroid
PL	Payload
PME	Probe-moon-earth (angle of the asymptotic velocity vector with the moon-to-earth line at the time of pericynthion passage)
PQF	Triangle in Lambert's problem
PVO	Pioneer Venus Orbiter
P&W	Pratt and Whitney
QED	*Quod erat demonstrandtum,* used to indicate the end of a proof
RCS	Reaction Control System
RPM	Rendezvous pitch maneuver
RTN	Radial-Transverse-Normal (coordinate system)

SAC-D	Satelite de Aplicaciones Cientificas-D (Satellite for Scientific Applications-D)
S/C	Spacecraft
SCET	Spacecraft Event Time
SEP	Sun-earth-probe angle
SI	Systeme International
sl	Sea level
SM	Service Module
SMAD	Space Mission Analysis and Design
SMAD3	*Space Mission Analysis and Design,* Third Edition
SoI	Sphere of Influence
SOI	Saturn orbit insertion
SRP	Solar radiation pressure
SS	Solar system
SSD, ssd	Solar System Dynamics
SSO	Sun synchronous orbit
TAI	International Atomic Time
TB	Target body
TD	Touchdown
TI	Terminal initiation
TCG	Geocentric Coordinate Time
TCM	Trajectory correction maneuver
TDB	Barycentric Dynamical Time
TDT	Terrestrial Dynamical Time
TFL	Time of flight
TSB	Orbit Determination text entitled *Statistical Orbit Determination* by Byron D. Tapley, Bob E. Schutz, and George H. Born
TPS	Thermal Protection System
TTIME	Time of flight
UCLA	University of California at Los Angeles
UDMH	Unsymmetrical dimethyl hydrazine
US	United States
USC	University of Southern California
USSR	Union of Soviet Socialist Republics
UT	Universal Time (Greenwich Mean Time)
UTC	Coordinated Universal Time
VEEGA	Venus-Earth-Earth gravity assist
VHP	Arrival V_∞ at the target body
VVEJGA	Venus-Venus-Earth-Jupiter gravity assist
VOI	Venus orbit insertion
Vol.	Volume
wolog	Without loss of generality
wrt	With respect to

References[1]

1. Adamo DR (2008) Apollo 13 trajectory reconstruction via state transition matrices. J Guid Control Dynam 31(6):1772–1781
2. Buzz Aldrin's Website at http://buzzaldrin.com/space-vision/rocket_science/aldrin-mars-cycler/. Accessed 1 May 2014
3. The Apollo Program (1963–1972). http://nssdc.gsfc.nasa.gov/planetary/lunar/apollo.html. Accessed 12 Jun 2012
4. Arfken GB, Weber HJ (1995) Mathematical methods for physicists, 4th edn. Academic, San Diego
5. Aura website at http://aura.gsfc.nasa.gov/. Accessed 10 Jan 2014
6. Barber TJ, Crowley RT (2002) Initial Cassini propulsion system in-flight characterization, Paper Number 2002-4152. 38th AIAA/ASME/SAE/ASEE Joint Propulsion Conference & Exhibition, Indianapolis, IN, 7 July 2002. [This paper won the AIAA's Best Liquid Propulsion Paper Award for 2002.]
7. Barrar RB (1963) An analytic proof that the Hohmann-type transfer is the true minimum two-impulse transfer. Astronaut Acta 9(1):1–11
8. Bate RR, Mueller DD, White JE (1971) Fundamentals of astrodynamics. Dover Publications, New York
9. Battin RH (1964) Astronautical guidance. McGraw-Hill, New York
10. Battin RH (1999) An introduction to the mathematics and methods of astrodynamics, Rev edn. AIAA Education Series. American Institute of Aeronautics and Astronautics, New York
11. Battin RH, Vaughan RM (1984) An elegant Lambert algorithm. J Guid Control Dynam 7:662–670
12. Bell ET (1988) The prince of mathematicians. In: The world of mathematics, 1, Part II, Chapter 11. Tempus Books, Stroud
13. Bennett FV (1970) Apollo Lunar descent and ascent trajectories. Paper presented at the AIAA 8th Aerospace Sciences meeting, New York, NY, 19–21 Jan 1970. NASA Technical Memorandum, NASA TM X-58040, pp 13–14 and 25
14. Bergam MJ, Prussing JE (1982) Comparison of starting values for iterative solutions to a Universal Kepler's Equation. J Astronaut Sci XXX(1):75–84
15. Bills BJ, Ferrari AJ (1977) A harmonic analysis of lunar topography. Icarus 31:244–259
16. Blitzer L (1971) Satellite orbit paradox: a general view. Am J Phys 39:882–886
17. Boain RJ (2004) A-B-Cs of sun-synchronous orbit mission design, Paper No. AAS04-108. 14th AAS/AIAA Spaceflight Mechanics Conference, Maui, Hawaii, 8–12 Feb 2004
18. Bond VR, Allman MC (1996) Modern astrodynamics: Fundamentals and perturbation methods. Princeton University Press, Princeton, NJ

[1] In addition to the references in this list, several references are cited in Chap. 8 as sources for further study. The complete bibliographic information for these sources is given in Sect. 8.2.

© Springer International Publishing Switzerland 2015

G.R. Hintz, *Orbital Mechanics and Astrodynamics*,
DOI 10.1007/978-3-319-09444-1

19. Branley FM (1971) Weight and weightlessness. Let's-Read-And-Find-Out Science Books, Thomas Y. Crowell Company, New York
20. Breakwell JV, Gillespie RW, Ross S (1961) Researches in interplanetary travel. ARS J 31:201–208
21. Broucke R (1980) On Kepler's equation and strange attractors. J Astronaut Sci 28:255–265
22. Broucke RA, Cefola PJ (1972) On the equinoctial orbit elements. Celest Mech 5:303–310
23. Brouke R (2001) On the history of the slingshot effect and cometary orbits. AAS/AIAA Astrodynamics Specialist Conference, AAS Paper 01-435, Quebec City, Quebec, July–August 2001
24. Broucke RA, Prado AFBA (1993) Optimal N-impulse transfer between coplanar orbits. Paper AAS 93-66, AAS/AIAA Astrodynamics Specialist Conference, Victoria, BC, Canada, 16–19 Aug
25. Brown CD (1992) Spacecraft mission design, AIAA Education Series. American Institute of Aeronautics and Astronautics, Washington, DC
26. Brown D, Morone J (2007) Spacecraft reveals new insights about the origin of solar wind. Release 07-264, 6 Dec 2007
27. Burns JA (1976) Elementary derivation of the perturbation equations of celestial mechanics. Am J Phys 44(10):944–949
28. Cassini Equinox Mission Website at http://saturn.jpl.nasa.gov/mission/saturntourdates/saturntime/. Accessed 10 Jan 2014
29. Cassini Solstice Mission Website as http://saturn.jpl.nasa.gov/news/newsreleases/newsrelease1998042. Accessed 18 Feb 2014
30. Cesarone RJ (1989) A gravity assist primer. AIAA Stud J 27:16–22
31. Chamberlin AB webmaster, Solar System Dynamics website. http://ssd.jpl.nasa.gov
32. Chao C-C "G" (2005) Applied orbit perturbation and maintenance. The Aerospace Press, El Segundo, CA
33. Chobotov VA (ed) (2002) Orbital mechanics, 3rd edn, AIAA Education Series. American Institute of Aeronautics and Astronautics, Reston, VA
34. Clohessy WH, Wiltshire RS (1960) Terminal guidance systems for satellite rendezvous. J Aerospace Sci 27(9):653–658
35. Cunningham CJ (1988) Introduction to asteroids. Willman-Bell, Richmond, VA
36. Cutting E, Born GH, Frautnick JC (1978) Orbit analysis for SEASAT-A. J Astronaut Sci 26 (4):315–342
37. Deep Space Network website at http://deepspace.jpl.nasa.gov/dsn/. Accessed 24 Dec 2013
38. Diehl RE, Nock KT (1979) Galileo Jupiter encounter and satellite tour trajectory design, Paper 79-141. AAS/AIAA Astrodynamics Specialist Conference, Provincetown, MA, 25–27 Jun, 1979.
39. Doody D Site Manager, Basics of Space Flight Website at http://www.jpl.nasa.gov/basics/
40. Edelbaum TN (1967) How many impulses? Astronaut Aeronaut 5:64–69
41. Egorov VA (1958) Certain problems of moon flight dynamics, Russian literature of satellites, part I. International Physical Index, New York
42. Epperson JF (2002) An introduction to numerical methods and analysis. Wiley, New York
43. Escobal PR (1965) Methods of orbit determination. Wiley, New York (Republished by R. E. Krieger Pub. Co., NY, 1976)
44. Federation of American Scientists at www.fas.org/spp/military/program/launch/centaur.hlm. Accessed 20 May 2014
45. Fehse W (2003) Automated rendezvous and docking of spacecraft, Cambridge Aerospace Series. Cambridge University Press, Cambridge
46. Gannon M (2013) NASA's Quest for Green Rocket Fuel Passes Big Test, 7/11/2013. http://www.livescience.com/38120-nasa-green-rocket-fuel-test.html. Accessed 2 Jan 2014
47. Gates CR (1963) A simplified model of midcourse maneuver execution errors. Tech. Rep., 32-504, JPL, Pasadena, CA, 1 Oct 1963

48. Glasstone S (1965) Sourcebook on the space sciences. D Van Nostrand Company, Inc., Princeton, NJ
49. Goodman JL (2009) Apollo 13 guidance, navigation, and control challenges, Paper Number AIAA 20. AIAA Space 2009 Conference & Exposition, Pasadena, CA, 14–17 Sep 2009
50. Hahn BD, Valentine DT (2013) Essential MATLAB for engineers and scientists, 5th edn. Elsevier, Burlington
51. Hanselman D, Littlefield B (2011) Mastering Matlab 8. Prentice Hall, Upper Saddle River, NJ
52. Harwood W (2009) Space shuttle's heat shield cleared for entry, story written for CBS News and appeared in Spaceflight Now.com
53. Heavens Above website at http://www.heavens-above.com/ Accessed 8/4/2014
54. Hill GW (1878) Researches in the lunar theory. Am J Math 1:5–26
55. Hintz GR (1982) An interplanetary targeting and orbit insertion maneuver design technique. J Guid Control Dynam 5(2):210–217
56. Hintz GR (2008) Survey of orbit elements sets. J Guid Control Dynam 31(3):785–790
57. Hintz GR, Chadwick C (1985) A design technique for trajectory correction maneuvers. J Astronaut Sci 33(4):429–443
58. Hintz GR, Farless DL, Adams MJ (1980) Viking orbit trim maneuvers. J Guid Control 3:193–194
59. Hintz GR, Longuski JM (1985) Error analysis for the delivery of a spinning probe to Jupiter. J Guid Control Dynam 8(3):384–390
60. Hobson EW (1965) The theory of spherical and ellipsoidal harmonics. Chelsea, New York
61. Hoelker RE, Silber R (1961) The bi-elliptical transfer between coplanar circular orbits. Proceedings of the 4th Symposium on Ballistic Missiles and Space Technology, Pergamon Press, New York, pp 164–175
62. Hohmann W (1925) Die Erreichbarkeit der Himmelskörper. Oldenbourg, Munich (NASA, Technical Translations F-44, 1960)
63. Infoplease/Encyclopedia website at http://www.infoplease.com/ce6/sci/A0849473.html. Accessed 10 Jan 2014
64. Isakowitz S, Hopkins J, Hopkins JP Jr (2004) International reference guide to space launch systems, 4th edn, revised. American Institute of Aeronautics and Astronautics, Washington, DC
65. Jesperson J, Fitz-Randolph J (1999) From sundials to atomic clocks: understanding time and frequency. 2nd revised edn. Dover Publications, Mineola, New York
66. Jones JB (1980) A solution of the variational equations for elliptic orbits in rotating coordinates, Paper Number AIAA-80-1690. AIAA/AAS Astrodynamics Conference, Danvers, MA, 11–13 Aug 1980
67. Kamel OM (2009) Optimization of bi-elliptical transfer with plane change—part 1. Asta Astronaut 64(5):514–517
68. Kane TR, Levinson DA (1985) Dynamics: theory and applications. McGraw-Hill, New York
69. Kaplan MH (1976) Modern spacecraft dynamics and control. Wiley, New York
70. Kaula WM (1966) Theory of satellite geodesy: applications of satellites to geodesy. Blaisdell, Waltham, MA
71. Kechichian JA (1992) Techniques of accurate analytic terminal rendezvous in near-circular orbit. Acta Astronaut 26(6):377–394
72. Kechichian JA (1998) The algorithm of the two-impulse time-fixed noncoplanar rendezvous with drag and oblateness. J Astronaut Sci 46(1):47–64
73. Kizner W (1959) A method of describing miss distances for lunar and interplanetary trajectories. JPL External Publication No. 674, 1 Aug 1959
74. Konopliv AS, Banerdt WB, Sjogren WL (1999) Venus gravity: 180th degree and order model. Icarus 139:3–18
75. Konopliv S, Asmar SW, Carranza E, Sjogren WL, Yuan DN (2001) Recent gravity models as a result of the lunar prospector mission. Icarus 150:1–18

76. Lancaster ER, Blanchard RC (1969) A unified form of Lambert's theorem, NASA technical note, NASA TN D-5368. National Aeronautics and Space Administration, Washington, DC
77. Lass H (1950) Vector and tensor analysis. McGraw-Hill, New York
78. Lawden DF (1963) Optimal trajectories for space navigation. Butterworth & Co, London
79. Lee W (2000) To rise from earth: an easy-to-understand guide to spaceflight, 2nd edn. Checkmark Books, New York
80. Linn A (1983) Oh, what a spin we're in, thanks to the Coriolis effect. Smithsonian, Feb 1983, vol. 13, pages 66ff
81. Llanos PJ, Miller JK, Hintz GR (2012) Mission and navigation design of integrated trajectories to $L_{4,5}$ in the sun-earth system. AAS/AIAA astrodynamicist specialist conference, Minneapolis, MN, Aug 2012
82. Lloyd's Satellite Constellations Website at http://www.ee.surrey.ac.uk/Personal/L.Wood/constellations/tables/overview.html. Accessed 1/10/2014
83. Logsdon T (1998) Orbital mechanics: theory and applications. Wiley, New York
84. The MathWorks URL for online MATLAB documentation at http://www.mathworks.com/access/helpdesk/help/helpdesk.html. Accessed 8/4/2014
85. MATLAB Tutorial website at http://www.cyclismo.org/tutorial/matlab/. Accessed 8/4/2014
86. Mecham M (2004) The big sniff. In: Aviation week and space technology. McGraw-Hill, New York
87. Montenbruck O, Gill E (2000) Satellite orbits: models, methods and applications. Springer, Berlin
88. Murray CD, Dermott SF (1999) Solar system dynamics. Cambridge University Press, Cambridge, p 184. ISBN 0-521-57295-9
89. Nacozy PE, Dallas SS (1977) The geopotential in nonsingular orbital elements. Celest Mech 15:453–466
90. NASA Website at http://www.NASA.gov/
91. NASA'S Mars Exploration Website at mars.jpl.nasa.gov/spotlight/porkchopAll.html for article ""porkchop" in the first menu item on a Trip to Mars Accessed 8/1/2014
92. National Space Science Data Center Website at nssdc.gsfc.nasa.gov. Accessed 5 Feb 2014
93. Near-Earth Objects website at http://neo.jpl.nasa.gov/. Accessed 2 Feb 2014
94. Nelson WC, Loft EE (1962) Space mechanics. Prentice-Hall, Englewood Cliffs, NJ
95. The Official U.S. Time Website at http://www.time.gov/. Accessed 2 Feb 2014
96. Penzo PA (1962) An analysis of free-flight circumlunar trajectories, STL Report No. 8976-6010-RU-000. Space Technology Laboratories, Redondo Beach, CA
97. Phoenix Mars Mission Website at http://phoenix.lpl.arizona.edu/. Accessed 6 Feb 2014
98. Pierce BO (1956) Short table of integrals. 4th edn (revised by Ronald Foster). Ginn and Co., Boston
99. Pisacane VL, Moore RC (eds) (1994) Fundamentals of space systems, JHU/APL series in science and engineering. Oxford University Press, Oxford
100. Prussing JE (1977) The mean radius in Kepler's third law. Am J Phys 45(12):1216
101. Prussing JE (1979) Geometrical interpretation of the angles α and β in Lambert's problem. J Guid Control 2(5):442–443
102. Prussing JE (1985) Kepler's laws of planetary motion. In: The encyclopedia of physics, 3rd edn. Van Nostrand Reinhold Co, New York
103. Prussing JE (1992) Simple proof of the optimality of the Hohmann transfer. J Guid Control Dynam 15(4):1037–1038
104. Prussing JE, Conway BA (1993) Orbital Mechanics. Oxford University Press, New York. Errata are available at https://netfiles.uiuc.edu/prussing/www/
105. Rocket & Space Technology Website at http://www.braeunig.us/space/propuls.htm Subject: Rocket Propulsion. Accessed 13 Feb 2014
106. Rocket & Space Technology Website at http://www.braeunig.us/space/propel.htm Subject: Rocket Propellants. Accessed 2 Jan 2014

107. Roncoli RB (2005) Lunar constants and models document. JPL Technical Document D-32296, 23 Sep 2005
108. Roth HL (1965) Bi-elliptic transfer with plane change. The Aerospace Corporation, El Segundo, CA, Technical Report Number TDR-469(5540-10)-5, May 1965
109. Roy AE (1988) Orbital motion, 3rd edn. Institute of Physics Publishing, Bristol
110. Scharr J (2013) New rocket fuel helps NASA 'Go Green', 16 May 2013. http://www.technewsdaily.com/18090-new-rocket-fuel-helps-nasa-go-green.html. Accessed 2 Jan 2014
111. Schaub H, Junkins JL (2003) Analytical mechanics of space systems, AIAA Education Series. AIAA, Reston, VA. ISBN 1-56347-563-4
112. Seidelmann PK (ed) (1992) Explanatory supplement to the astronomical almanac. University Science, Mill Valley, CA
113. Seidelmann PK et al (2007) Report of the IAU/IAG Working Group on cartographic coordinates and rotational elements: 2006. Celest Mech Dyn Astr 98:155–180
114. Sidi MJ (2001) Spacecraft dynamics and control: a practical engineering approach, Cambridge Aerospace Series. Cambridge University Press, Cambridge
115. Simon T (1972) The moon explorers, Scholastic Book Series. New York
116. Smith GR (1979) A simple, efficient starting value for the iterative solution of Kepler's equation. Celest Mech 19:163–166
117. Solar System Dynamics Website at http://ssd.jpl.nasa.gov/. Accessed 2/2/2014
118. Spaceflight Now Website at http://www.spaceflightnow.com/news/n0403/25messenger/. Posted: 25 Mar 2004. Accessed 9/16/2014
119. Spiegel MR (1959) Schaum's outline of theory and problems of vector analysis and an introduction to tensor analysis. Schaum Publishing Company, New York
120. Strange NJ, Longuski JM (2002) Graphical method for gravity-assist trajectory design. J Spacecraft Rockets 39(1):9–16
121. Stricherz V (2004) New propulsion concept could make 90-day Mars round trip possible. http://www.washington.edu/newsroom/mars.htm. 14 Oct 2004
122. Tapley BD, Schutz BE, Born G (2004) Statistical orbit determination. Elsevier Academic Press, Amsterdam
123. Tholen DJ, Buie MW (1990) Further analysis of Pluto-Charon mutual event observations. Bull Am Astron Soc 22(3):1129
124. Thomson WT (1986) Introduction to Space Dynamics. Dover Publications, New York (originally published by Wiley in 1961)
125. Ting L (1960) Optimum orbital transfer by several impulses. Astronaut Acta 6(5):256–265
126. Uphoff C, Roberts PH, Friedman LD (1974) Orbit Design concepts for Jupiter orbiter missions. AIAA mechanics and control conference, AIAA Paper 74-781, Anaheim, CA, Aug 1974
127. Vallado DA (1997) Fundamentals of astrodynamics and applications. McGraw-Hill, New York
128. Vallado DA with contributions by Wayne D. McClain (2007). Fundamentals of astrodynamics and applications, 3rd edn. Space Technology Library, Published Jointly by Microcosm Press, El Segundo, CA and Kluwer Academic Publishers, Dordrecht, The Netherlands. For errata, go to http://www.astrobooks.com and click on "STL Errata" (on the right-hand side) and scroll down to and click on the book's name
129. Van Domelen D (2008) A (Hopefully) simple explanation of the coriolis force. Available at http://www.dvandom.com/coriolis/. Accessed 2 Feb 2014
130. Van Domelen DJ Getting around the coriolis force. Available at http://www.eyrie.org/~dvandom/Edu/newcor.html. Accessed 2 Feb 14
131. Wagner SV, Goodson TD (2008) Execution-error modeling and analysis of the Cassini-Huygens Spacecraft through 2007. Paper Number AAS 08-113. Proceedings of the AAS/AIAA space flight mechanics meeting, Galveston, TX, 27–31 Jan, 2008
132. Walker MJH, Ireland B, Owens J (1985) A set of modified equinoctal orbit elements. Celest Mech 36:409–419

133. Walker MJH, Ireland B, Owens J (1986) Errata. Celest Mech 38:391–392
134. Walter U (2012) Astronautics: the physics of space flight, 2nd edn. Wiley, Weinheim
135. Weisstein EW Eric Weisstein's "World of Scientific Biography". http://scienceworld.wolfram.com/biography. *There are instances where we have been unable to trace or contact the copyright holder. If notified the publisher will be pleased to rectify any errors or omissions at the earliest opportunity*
136. Wertz J, Everett D, Puschell J (eds) and 65 authors, Space mission engineering: the new SMAD, vol 28. Space Technology Library
137. Wertz JR, Larson WJ (eds) (1999) Space mission analysis and design, 3rd edn. Space Technology Library, Published Jointly by Microcosm Press, El Segundo, CA and Kluwer Academic Publishers, Dordrecht, The Netherlands. For errata, go to http://www.astrobooks.com and click on "STL Errata" (on the right-hand side) and scroll down to and click on the book's name
138. Wiesel WE (1997) Spaceflight dynamics, 2nd edn. Irwin McGraw-Hill, Boston
139. Woolston DS (1961) Declination, radial distance, and phases of the moon for the years 1961 to 1971 for use in trajectory considerations. NASA T.N.D-911, Aug 1961
140. Wylie R, Barrett LC (1995) Advanced engineering mathematics, 6th edn. McGraw-Hill, New York
141. Yeomans DK, Site Manager, Solar system dynamics Website at http://ssd.jpl.nasa.gov. Accessed 1 May 2014
142. Zee H (1963) Effect of finite thrusting time in orbital maneuvers. AIAA J 1(1):60–64

Index

© Springer International Publishing Switzerland 2015

G.R. Hintz, *Orbital Mechanics and Astrodynamics*,
DOI 10.1007/978-3-319-09444-1